

The Roles of Sirtuins and Polyphenols in Brain Ageing and Neurodegeneration

Author:

Jayasena, Tharusha

Publication Date:

2017

DOI:

<https://doi.org/10.26190/unsworks/20071>

License:

<https://creativecommons.org/licenses/by-nc-nd/3.0/au/>

Link to license to see what you are allowed to do with this resource.

Downloaded from <http://hdl.handle.net/1959.4/58889> in <https://unsworks.unsw.edu.au> on 2024-05-02

The Roles of Sirtuins and Polyphenols in Brain Ageing and Neurodegeneration

Tharusha Jayasena

A thesis submitted for the degree of Doctor of Philosophy

School of Psychiatry

Faculty of Medicine

University of New South Wales

December 2016



Supervisors

Professor Perminder Sachdev

Dr Anne Poljak

PLEASE TYPE

THE UNIVERSITY OF NEW SOUTH WALES

Thesis/Dissertation Sheet

Surname or Family name: JAYASENA

First name: THARUSHA

Other name/s:

Abbreviation for degree as given in the University calendar: PhD

School: Psychiatry

Faculty: Medicine

Title: The roles of sirtuins and polyphenols in brain ageing and neurodegeneration

Abstract 350 words maximum: (PLEASE TYPE)

Alzheimer's disease is a neurodegenerative disease characterised by progressive decline in memory. Sirtuins proteins have been shown to deacetylate numerous proteins that regulate pathways implicated in neurodegeneration. However, relatively little is known about the role of sirtuins in the central nervous system and methods for quantification are limited. In this thesis (chapter 2), I describe a targeted mass spectrometric assay developed and validated for the quantification of all mammalian sirtuins (SIRT1-7). All sirtuins were detected in the human brain, with SIRT2 being the most abundant. In chapter 3, I report a significant drop in SIRT1 levels in AD plasma and an increase in SIRT2 in the occipital AD brain. Interestingly, completion of binding partner work for SIRT2 showed association with a number of energy metabolism associated proteins. Increased protein, lipid and nucleic acid oxidation and reduced activities of antioxidants have been reported in AD plasma. In chapter 4, I investigated the effect of plasma from controls, individuals with mild cognitive impairment and AD, on a microglial cell line. I found that AD plasma significantly decreased cell viability and enhanced glycolytic flux in microglia compared to plasma from healthy controls. Proteomic methods found altered levels of complement and other acute phase proteins, in MCI and AD plasma and an upregulation of glycolytic enzymes in cells exposed to AD plasma. It is well established that amyloid aggregation is enhanced by the presence of metals and various polyphenols are thought to have both antioxidant and anti-aggregation properties. In chapter 5, I investigated the ability of copper and iron to enhance amyloid aggregation and the ability of polyphenols such as resveratrol, curcumin and epigallocatechin gallate to prevent aggregation as well as modulate energy metabolism and attenuate cell toxicity in a neuronal cell culture model. In conclusion, I have successfully applied mass spectrometry for the quantification of sirtuins in the CNS. I have also shown that altered expression of acute phase reactants in AD plasma may alter the energy metabolism of glia. Finally, neurons treated with polyphenols were shown to prevent energy deficits and cell toxicity caused by the A β peptide aggregates.

Declaration relating to disposition of project thesis/dissertation

I hereby grant to the University of New South Wales or its agents the right to archive and to make available my thesis or dissertation in whole or in part in the University libraries in all forms of media, now or here after known, subject to the provisions of the Copyright Act 1968. I retain all property rights, such as patent rights. I also retain the right to use in future works (such as articles or books) all or part of this thesis or dissertation.

I also authorise University Microfilms to use the 350 word abstract of my thesis in Dissertation Abstracts International (this is applicable to doctoral theses only).

Signature

Witness Signature

13/1/17

Date

The University recognises that there may be exceptional circumstances requiring restrictions on copying or conditions on use. Requests for restriction for a period of up to 2 years must be made in writing. Requests for a longer period of restriction may be considered in exceptional circumstances and require the approval of the Dean of Graduate Research.

FOR OFFICE USE ONLY

Date of completion of requirements for Award:

COPYRIGHT STATEMENT

'I hereby grant the University of New South Wales or its agents the right to archive and to make available my thesis or dissertation in whole or part in the University libraries in all forms of media, now or here after known, subject to the provisions of the Copyright Act 1968. I retain all proprietary rights, such as patent rights. I also retain the right to use in future works (such as articles or books) all or part of this thesis or dissertation.

I also authorise University Microfilms to use the 350 word abstract of my thesis in Dissertation Abstract International (this is applicable to doctoral theses only).

I have either used no substantial portions of copyright material in my thesis or I have obtained permission to use copyright material; where permission has not been granted I have applied/will apply for a partial restriction of the digital copy of my thesis or dissertation.'

Signed

Date 18/10/17 ..

AUTHENTICITY STATEMENT

'I certify that the Library deposit digital copy is a direct equivalent of the final officially approved version of my thesis. No emendation of content has occurred and if there are any minor variations in formatting, they are the result of the conversion to digital format.'

Signed

Date 18/10/17 ..

Abstract

Alzheimer's disease (AD) is a complex multi-factorial neurodegenerative disease characterised by progressive decline in memory and other cognitive abilities. Sirtuins are a family of NAD-dependent histone deacetylase proteins that have been recently associated with longevity. Sirtuins have been shown to deacetylate numerous proteins which regulate multiple biological pathways implicated in neurodegeneration. However, relatively little is known about the role of the seven mammalian sirtuins in the central nervous system (CNS). At present, quantitative western blotting, PCR and ELISA are the main techniques used to quantify sirtuin protein and mRNA levels. However, these methodologies are limited due to low sensitivity and selectivity in a multiplex-format.

In this thesis (chapter 2), I describe a novel, more robust, targeted mass spectrometric assay developed and validated for the quantification of all seven mammalian sirtuins (SIRT1-7). Quantification of all peptides was performed by multiple reaction monitoring (MRM) using three mass transitions per protein-specific peptide, two specific peptides for each sirtuin and a stable isotope labelled internal standard. All sirtuin peptides were detected in the human brain, with SIRT2 being the most abundant. Sirtuins were also detected in human CSF and plasma, and guinea pig and mouse tissues. I applied (chapter 3) the assay to a variety of samples including cultured brain cells, human control and AD *post mortem* brain tissue, CSF and plasma. I found a significant drop in SIRT1 levels in AD plasma and an increase in SIRT2 in the occipital AD brain tissue. Interestingly, completion of binding partner work for SIRT2 using immunoprecipitation and mass spectrometry based techniques showed that SIRT2 is associated with a number of energy metabolism associated proteins such as ATP synthase and enolase.

Increased protein, lipid and nucleic acid oxidation and reduced activities of antioxidant enzymes have also been reported in AD plasma, and are associated with sirtuin function. Amyloid plaques in the AD brain elicit a range of reactive inflammatory responses including complement activation and acute phase reactions, which may also be reflected in plasma. In chapter 4, I investigated the effect of pooled plasma (n=20 each) from healthy controls, individuals with amnesic mild cognitive impairment (aMCI) and AD, on a cultured microglial cell line. I found that AD plasma significantly decreased cell viability and enhanced glycolytic flux in microglial cells compared to plasma from healthy controls. This effect was prevented by heat inactivation of complement protein. Proteomic methods and

isobaric tags (iTRAQ) were used to identify the expression level of complement and other acute phase proteins, which were found to be altered in MCI and AD plasma and an upregulation of key enzymes involved in the glycolysis pathway in cells exposed to AD plasma.

It is well established that amyloid beta ($A\beta$) aggregation is enhanced by the presence of redox-active metals and various polyphenols are thought to have both antioxidant and anti-aggregation properties. Furthermore, polyphenolic compounds such as resveratrol are known to affect sirtuin expression and activity. In chapter 5, I investigated the ability of transition metals, copper and iron to enhance amyloid aggregation and the ability of polyphenols such as resveratrol, curcumin and epigallocatechin gallate to prevent aggregation as well as modulate energy metabolism and attenuate cell toxicity in a neuronal cell culture model.

In conclusion, I have successfully applied MRM mass spectrometry for the detection and quantification of sirtuin proteins in the CNS, paving the way for more quantitative and functional studies. I have also shown that altered expression levels of acute phase reactants in AD plasma may alter the energy metabolism of glia. Finally, neurons treated with polyphenols were shown to prevent energy deficits and cell toxicity caused by the $A\beta$ peptide aggregates, and with future work investigating these compounds efficacy in activating sirtuins could provide promising results for the development of combination therapies targeting various pathways involved in AD such as oxidative stress, sirtuin activation, mitochondrial dysfunction and energy metabolism for use in transgenic animal models and/or human pilot clinical trials.

ORIGINALITY STATEMENT

‘I hereby declare that this submission is my own work and to the best of my knowledge it contains no materials previously published or written by another person, or substantial proportions of material which have been accepted for the award of any other degree or diploma at UNSW or any other educational institution, except where due acknowledgement is made in the thesis. Any contribution made to the research by others, with whom I have worked at UNSW or elsewhere, is explicitly acknowledged in the thesis. I also declare that the intellectual content of this thesis is the product of my own work, except to the extent that assistance from others in the project's design and conception or in style, presentation and linguistic expression is acknowledged.’

Signed

Date

13/1/17

Acknowledgements

I would like to thank my primary supervisor Professor Perminder Sachdev who provided a high level of guidance, support and mentorship during my candidature.

I sincerely thank my co-supervisor Dr Anne Poljak, for her expert advice and guidance in all aspects of my experimental work and support in editing my thesis and manuscripts. I am also extremely grateful for her encouragement and personal support during the years of my PhD.

Many thanks and appreciation to Dr Nady Braidy for his constant support and assistance with many aspects of my experimental work and editing of my thesis and manuscripts as well as his valuable friendship.

I wish to thank A/Prof Mark Raftery for providing me with desk and lab space during my candidature which was very convenient for me to complete all my mass spectrometry work.

I would also like to extend many thanks to all other members of the Bioanalytical Mass Spectrometry Facility at the Mark Wainwright Analytical Centre, UNSW, in particular Dr Ling Zhong, Ms Sonia Bustamante, Mr Lewis Adler and Dr Sarowar Chowdhury for their help and training in many aspects of mass spectrometry instrumentation and sample preparation as well as for their kind encouragement, friendship and support during my PhD.

Thanks also to Dr Ross Grant and Dr Jade Guest for the collection and donation of CSF samples and patient data.

Finally I would like to extend my deepest gratitude to my friends and family, in particular my sister and parents who have been a great source of understanding, compassion, love and encouragement during the highs and lows of my PhD.

Publications and Presentations

First Author Peer Reviewed Publications

Jayasena T, Poljak A, Braidy N, Zhong L, Rowlands B, Muenchhoff J, Grant R, Smythe G, Teo C, Raftery M, Sachdev P (2016). Application of Targeted Mass Spectrometry for the Quantification of Sirtuins in the Central Nervous System. Scientific Reports 2016 Oct 20;6:35391.

Jayasena T, Poljak A, Braidy N, Smythe G, Raftery M, Hill M, Brodaty H, Trollor J, Kochan N, Sachdev P (2015). Upregulation of glycolytic enzymes, mitochondrial dysfunction and increased cytotoxicity in glial cells treated with Alzheimer's disease plasma. PLoS One 10(3):e0116092.

Jayasena T, Poljak A, Smythe G, Braidy N, Münch G, Sachdev P (2013). The role of polyphenols in the modulation of sirtuins and other pathways involved in Alzheimer's disease. Ageing Research Reviews 12(4):867-883

Collaborative Peer Reviewed Publications

Braidy N, Jugder BE, Poljak A, **Jayasena T**, Mansour H, Nabavi SM, Sachdev P, Grant R (2016). Resveratrol as a potential therapeutic candidate for the treatment and management of Alzheimer's disease. Current Topics in Medicinal Chemistry 16(17):1951-60.

Braidy N, Poljak A, Grant R, **Jayasena T**, Mansour H, Chan-Ling T, Smythe G, Sachdev P and Guillemin GJ (2015). Differential expression of sirtuins in the ageing rat brain. Frontiers in Cellular Neuroscience 9:167

Braidy N, Poljak A, **Jayasena T**, Mansour H, Inestrosa NC, Sachdev PS (2015). Accelerating Alzheimer's disease research through 'natural' animal models. Current Opinions in Psychiatry 28(2):155-64.

Braidy N, Poljak A, Marjo C, Rutledge H, Rich A, **Jayasena T**, Inestrosa NC, Sachdev P (2014). Metal and complementary molecular bioimaging in Alzheimer's disease. Frontiers in Aging Neuroscience 6:138.

Braidy N, Poljak A, Grant R, **Jayasena T**, Mansour H, Chan-Ling T, Guillemin GJ, Smythe G, Sachdev P (2014). Mapping NAD(+) metabolism in the brain of ageing Wistar rats: potential targets for influencing brain senescence. Biogerontology 15(2):177-98

Braidy N, **Jayasena T**, Poljak A, Sachdev P (2012). Sirtuins in cognitive ageing and Alzheimer's disease. Current Opinions in Psychiatry 25(3):226-30.

Book Chapters

Braidy N, Poljak A, **Jayasena T**, Sachdev P (2014). Ionotropic Receptors in the Central Nervous System and Neurodegenerative Disease. R.M. Kostrzewa GJ (ed.), *Handbook of Neurotoxicity*, pg1071-1092; Springer Science. ISBN 978-1-4614-5835-7.

Braidy N, Poljak A, **Jayasena T**, Sachdev P (2014). Drug Treatments for Alzheimer's Disease: Hopes and Challenges. R.M. Kostrzewa GJ (ed.), *Handbook of Neurotoxicity*, pg 1173-1190; Springer Science. ISBN 978-1-4614-5835-7.

Braidy N, Poljak A, **Jayasena T**, Adams S, Sachdev P (2014). Glutamate in the Pathogenesis of Gliomas. R.M. Kostrzewa GJ (ed.), *Handbook of Neurotoxicity*, pg 1287-1299; Springer Science. ISBN 978-1-4614-5835-7.

Conference Presentations

Alzheimer's Association International Conference 2013, Boston, USA

Title: Development of a Targeted Mass Spectrometry Method for the Quantification of Human Sirtuins in Biological Samples

17th Lorne Proteomics Symposium, Victoria, Australia 2012

Title: The role of sirtuins in Alzheimer's disease and Ageing

6th Alzheimer's and Parkinson's Disease Symposium, Sydney, Australia

2012 Title: Sirtuin Expression in Alzheimer's disease

Prizes and Grants

The McConaghy Prize for Postgraduate Research 2013 (\$500)

Mark Wainwright Analytical Centre Research Grant 2016 (\$2,000)

Title: Development of a Quantitative Mass Spectrometry based method to Investigate Metabolic Changes in Astrocytes and Brain Tissue

Alzheimer's Australia Dementia Research Foundation Project Grant 2016 (\$50,000)

Title: Involvement of SIRT3 and related energy metabolite changes in the AD brain

Table of Contents

Title.....	i
Thesis Dissertation Sheet	ii
Abstract	iii-iv
Originality Statement.....	v
Acknowledgements	vi
Publications, Presentations, Prizes and Grants	vii-viii
Table of Contents	ix-xiii
List of Tables	xiv
List of Figures	xv-xvi
Abbreviations	xvii-xix
Chapter 1 General Introduction	1
1.1 Alzheimer's Disease	2-5
1.2 Cholinergic hypothesis	5
1.3 Oxidative stress	5-8
1.4 Amyloid cascade theory	9-12
1.5 Neuroinflammation	12-14
1.6 Mitochondrial dysfunction and energy metabolism	14-17
1.7 Metal homeostasis	17-20
1.8 Plasma biomarkers and AD	20-22
1.9 Polyphenols	22-26
1.10 Involvement of sirtuins in ageing and neurodegeneration	27-34
1.11 Polyphenols, sirtuins and ageing	34-39
1.12 Protective effects of polyphenols against inflammation	40
1.13 Protective effects of polyphenols on mitochondrial dysfunction	40-41
1.14 Involvement of polyphenols in telomere maintenance	41-42
1.15 Therapeutic potential of polyphenols and sirtuin modulation	43-44

1.16 Aims and rationale	44-45
Chapter 2: Application of targeted mass spectrometry for the quantification of sirtuins in the central nervous system.....	46
2.1 Introduction	47-49
2.2 Methods	49
2.2.1 Selection of target sirtuin peptides	49-51
2.2.2 Targeted mass spectrometry.....	51-54
2.2.3 Sirtuin peptide standards	54-55
2.2.4 Cell culture	55-56
2.2.5 Sample preparation of cell cultures, tissues, CSF and plasma	56-58
2.2.6 Sirtuin mRNA expression in human brain tissue using PCR	58-59
2.2.7 Sirtuin expression in human brain cells and tissue using immunohistochemical staining.....	59
2.2.8 Sirtuin protein expression in human control brain tissue using western blotting	59-60
2.2.9 Statistics	60
2.2.10 Ethics	60-61
2.3 Results	61
2.3.1 Peptide standards	61-71
2.3.2 Quantification of sirtuin expression in cells and tissues	72-76
2.3.3 Sirtuin isoforms	77-81
2.3.4 Validation of MRM method with established protocols	81-82
2.3.5 Quantification of sirtuins in CSF and immunodepleted plasma	83
2.3.6 Sirtuin standard recoveries and matrix effects	83-92
2.4 Discussion	92-96
Chapter 3: Sirtuin changes during ageing and Alzheimer's disease.....	97
3.1 Introduction	98-100
3.2 Methods	100
3.2.1 Plasma, CSF and brain tissue samples	100-101
3.2.2 Western blotting and PCR validation.....	102

3.2.3 Immunoprecipitation of SIRT2 interacting proteins	102-103
3.2.4 Mass spectrometry for identification of SIRT2 interacting proteins	103-104
3.3 Results	104
3.3.1 Sirtuin expression in pooled control, MCI and AD immunodepleted plasma	104-105
3.3.2 Sirtuin expression in control and AD <i>post mortem</i> brain tissues	106-107
3.3.3 Sirtuin expression in control CSF in younger and elderly age groups	107
3.3.4 Sirtuin expression in the ageing <i>Octodon Degus</i> rodent brain	108
3.3.5 Validation of SIRT2 changes in AD occipital lobe tissue using western blotting and PCR	108-112
3.4 Discussion	113
3.4.1 Sirtuin levels in control, MCI and AD plasma and young vs old plasma	113
3.4.2 Changes in sirtuin levels in control vs AD brain tissue	114-116
3.4.3 Binding partners of SIRT2	116-117
Chapter 4: Effect of AD plasma on cultured glia: metabolic and cytotoxic effects	118
4.1 Introduction	119-120
4.2 Methods	120
4.2.1 Subjects	120
4.2.2 Cell culture	121
4.2.3 MTT cell proliferation assay	121
4.2.4 NAD(H) assay	121-122
4.2.5 Lactate dehydrogenase (LDH) leakage	122
4.2.6 XF24 microplate-based respirometry as a measure of mitochondrial function	122
4.2.7 Fractionation of plasma	122-123
4.2.8 Proteomics analysis of human control, MCI and AD plasma	123
4.2.9 iTRAQ proteomics of cell lysates treated with control, MCI and AD plasma	124
4.2.10 Proteomic analysis of cell lysates treated with control, MCI and AD plasma	124-126
4.2.11 Statistics	126
4.3 Results	126

4.3.1 Cell proliferation	126-127
4.3.2 NAD levels and LDH leakage.....	127-129
4.3.3 The effect of complement proteins on cellular viability.....	130-131
4.3.4 Effects of plasma metabolites vs proteins on cell proliferation and viability.....	132-133
4.3.5 Plasma fractionation and 1D gel electrophoresis.....	134-135
4.3.6 Proteomics of MCI and AD plasma.....	135-136
4.3.7 Mitochondrial function and cellular bioenergetics.....	137-138
4.3.8 iTRAQ proteomic analysis of cell lysates treated with Control, MCI and AD plasma	139-147
4.4 Discussion.....	148-156
Chapter 5: Effects of polyphenols on cell viability, mitochondrial dysfunction, and amyloid aggregation	157
5.1 Introduction	158-163
5.2 Methods	163
5.2.1 Preparation of A β peptides	163
5.2.2 Cell culture.....	163-164
5.2.3 MTT cell proliferation assay.....	164
5.2.4 XF24 microplate-based respirometry as a measure of mitochondrial function	164-165
5.2.5 Transmission electron microscopy.....	165
5.2.6 Polyphenol metal complexes using mass spectrometry	165-166
5.3 Results.....	166
5.3.1 Effect of aggregation of cell viability in astrocytes	166-168
5.3.2 Effect of polyphenols on oxidative stress in astrocytes	168-171
5.3.3 Effect of polyphenols on mitochondrial function in astrocytes.....	172-173
5.3.4 Amyloid aggregation in the presence of polyphenols	173-177
5.3.5 Chelating properties of polyphenols with iron	178-181
5.4 Discussion.....	182-185
Chapter 6: General Discussion and Future Directions.....	186
6.1 Introduction	187-188

6.2 Distribution of sirtuins across CNS cell types and tissues	188-190
6.3 Sirtuins in ageing and Alzheimer's disease	190-193
6.4 Inflammation and metabolism in AD pathology	193-195
6.5 Brain pathology in AD: offense vs defence	196-198
6.6 Future studies	199-200
6.7 Conclusions	200-202
References	203-235
Appendix (Publications)	236

List of Tables

Table 1.1 Influence of polyphenols on sirtuins and pathways involved in ageing and AD	25-26
Table 1.2 The role of the sirtuin family in calorie restriction, ageing and neurodegeneration.....	28-29
Table 1.3: Influence of polyphenols on sirtuins and pathways involved in ageing and AD	36-38
Table 2.1: Expression of sirtuins in the CNS and current methods used for analysis	48
Table 2.2 List of 14 unique sirtuin peptides selected for sirtuin protein quantification.....	51
Table 2.3 List of product and transition ions with collision energies used for all 14 selected sirtuin peptides.....	52-54
Table 2.4 Human frontal lobe brain tissue sample and subject details	56
Table 2.5 Real-time primer sequences used for PCR analysis	58-59
Table 2.6 Antibodies and dilutions used for western blotting	60
Table 2.7 Human sirtuin peptide homology with guinea pig and mouse	75
Table 2.8 Sirtuin recoveries	91-92
Table 3.1 List of SIRT2 putative binding protein partners	111-112
Table 4.1: Cell viability of microglial cells exposed to MCI and AD plasma.....	127-128
Table 4.2: Cell viability of microglial cells after 48 hour incubation with human complement components	131
Table 4.3: Average normalised spectral counts and emPAI values of significantly deregulated proteins identified in pooled plasma samples between the Control, MCI and AD groups	136
Table 4.4: Dysregulated proteins in glial cells treated with human control, MCI and AD plasma compared to FBS following iTRAQ analysis	140-143
Table 4.5 STRING v9.1 analysis of the 27 proteins deregulated only in glia exposed to AD plasma for enrichment in gene ontology biological processes	147
Table 4.6 Summary of previous studies showing changes in acute phase proteins in Alzheimer's disease	150-151

List of Figures

Figure 1.1 Histological hallmarks of AD	2
Figure 1.2 Brain Atrophy in AD.....	4
Figure 1.3 Evidence of OS in AD and its prevention.....	6
Figure 1.4 Production of the hydroxyl radical via Fenton chemistry	8
Figure 1.5 APP processing by secretase enzymes.....	10
Figure 1.6: Influence of SIRT1 and polyphenols on APP processing and amyloid formation	32
Figure 1.7 Cellular roles/potential roles and mechanisms of action of SIRT1-7	34
Figure 2.1 Sirtuin peptide standard curves, variance and limits of detection.....	62-64
Figure 2.2 Representative chromatograms for all 14 sirtuin peptides	65-71
Figure 2.3 Sirtuin expression in primary cultured brain cells and cell lines.....	72
Figure 2.4: Sirtuin expression in human frontal lobe brain tissue	73
Figure 2.5 SIRT1-3 protein expression in animal organs	74
Figure 2.6 Sample fractionation and MRM workflow.....	76
Figure 2.7 Sequences for all seven human sirtuins and their isoforms	77-81
Figure 2.8 Sirtuin expression in human brain cells and tissue.....	81-82
Figure 2.9 SIRT1 levels in CSF and depleted plasma.....	83
Figure 2.10 A typical colloidal coomassie stained SDS/PAGE gel used to assess matrix effects on standard curves	84
Figure 2.11 Sirtuin peptide standard curves.....	85-89
Figure 2.12 Colloidal coomassie stained SDS/PAGE gel used for sirtuin recovery experiments.....	90-91
Figure 3.1 Sirtuin expression in pooled control, MCI and AD plasma.....	104
Figure 3.2 Representative chromatograms of SIRT1 peptides in control and AD plasma samples for SIRT1	105
Figure 3.3 Sirtuin expression in occipital <i>post mortem</i> control and AD brain tissue	106
Figure 3.4 Sirtuin expression in temporal <i>post mortem</i> control and AD brain tissue.....	106
Figure 3.5 Sirtuin expression in frontal <i>post mortem</i> control and AD brain tissue	107
Figure 3.6 SIRT1 and SIRT2 levels in younger and older age groups.....	107

Figure 3.7 Brain sirtuin levels in <i>Octodon Degus</i> cortex	108
Figure 3.8 SIRT2 protein levels in control and AD occipital lobe	108-109
Figure 3.9 Workflow of immunoprecipitation experiment to target SIRT2 binding partner proteins.....	110
Figure 4.1 Fractionation of non heat inactivated control plasma into protein and metabolite fractions and the effect of these fractions on cell proliferation	132-133
Figure 4.2 Representative chromatogram of separation of plasma into low and high abundant fractions and 1D SDS NuPage gel of these protein fractions	135
Figure 4.3 Effects of human plasma on cellular bioenergetics in a microglial cell line	138
Figure 4.4 Glycolysis Pathway highlighting enzymes which were shown to be upregulated in cells treated with AD plasma.....	144
Figure 4.5 Protein associations of proteins deregulated in AD plasma treated glia	145-146
Figure 5.1 Chemical structures of the polyphenols EGCG, Curcumin and Resveratrol	160
Figure 5.2 Effect of amyloid, metal ion and EGCG treatment on astrocyte viability.....	167
Figure 5.3 Effect of amyloid, metal ion and curcumin treatment on astrocyte viability.....	167
Figure 5.4 Effect of amyloid, metal ion and resveratrol treatment on astrocyte viability ...	168
Figure 5.5 Effect of EGCG to prevent cell toxicity caused by oxidative stressed initiated by Fenton chemistry to astroglial cells	169
Figure 5.6 Effect of curcumin to prevent cell toxicity caused by oxidative stressed initiated by Fenton chemistry to astroglial cells	170
Figure 5.7 Effect of resveratrol to prevent cell toxicity caused by oxidative stressed initiated by Fenton chemistry to astroglial cells	171
Figure 5.8 Effect of amyloid, metal and polyphenol treatment on mitochondrial basal control ratio in cultured astrocytes	172
Figure 5.9 Effect of amyloid, metal and polyphenol treatment on mitochondrial uncoupling ratio in cultured astrocytes	173
Figure 5.10 Representative transmission electron microscopy images of soluble A β 42 after co-incubation with metals and polyphenols	174-177
Figure 5.11 Mass spectrometry chromatogram of EGCG and Fe	179
Figure 5.12 Mass spectrometry chromatogram of resveratrol and Fe	180-181
Figure 6.1 Summary of main findings from thesis.....	187

List of Abbreviations

The following abbreviations have been used in the text and diagrams of this thesis:

4-HNE	4-hydroxynonenal
α KGDH	α -ketoglutarate dehydrogenase
A β	amyloid beta
ABAD	A β -binding alcohol dehydrogenase
ABC	avidin-biotin-complex
AD	Alzheimer's disease
ADP	adenosine diphosphate
aMCI	amnesic mild cognitive impairment
APOE	apolipoprotein E
APP	amyloid precursor protein
ATP	adenosine triphosphate
BBB	blood brain barrier
BCA	bicinchoninic acid
BCR	basal control ratio
C4BP	complement 4 binding protein
CNS	central nervous system
CR	calorie restriction
CSF	cerebrospinal fluid
Cu ²⁺	cupric copper
CV	coefficient of variance
DDA	data dependent acquisition
ECAR	extracellular acidification rate
EGCG	epigallocatechin gallate

FBA A/C	fructose biphosphate aldolase A/C
FCS	fetal calf serum
FDR	false discovery rate
Fe ²⁺	ferrous iron
Fe ³⁺	ferric iron
GAPDH	glyceraldehyde 3-phosphate dehydrogenase
GSEP	grape seed extract polyphenols
H ⁺	proton
H ₂ O ₂	hydrogen peroxide
HA	high abundance fraction
HDTIC	4-Hydroxy-5-hydroxymethyl-[1,3]dioxolan-2,6'-spirane-5',6',7',8'-tetrahydro-indolizine-3'-carbaldehyde
HSP	heat shock protein
IDA	information dependent acquisition
iTRAQ	isobaric tags for relative and absolute quantitation
LA	low abundance fraction
LAP	low abundance plasma
LDH	lactate dehydrogenase
LOD	limit of detection
LOQ	limit of quantification
M-CSF	macrophage colony-stimulating factor
MCI	mild cognitive impairment
MDH	malate dehydrogenase
MnSOD	manganese superoxide dismutase
mPTP	mitochondrial permeability transition pore

MRM	multiple reaction monitoring
MTT	3-[4,5-dimethylthiazol-2-yl]-2,5-diphenyl tetrazolium bromide
NAD	nicotinamide adenine dinucleotide
NFT	neurofibrillary tangles
NSAIDs	non-steroidal anti-inflammatory drugs
OCR	oxygen consumption rate
OH [•]	hydroxyl radical
OS	oxidative stress
PARP-1	poly (ADP-ribose) polymerase-1
PDH	pyruvate dehydrogenase
PDI	protein disulphide isomerase
PET	positron emission tomography
PGM1	phosphoglucomutase 1
PK	pyruvate kinase
PSEN1	presenilin 1
PSEN2	presenilin 2
RAR β	retinoic acid receptor β
ROS	reactive oxygen species
SIRT	sirtuin
TCEP	tris-(2-carboxyethyl) phosphine
TNF α	tumour necrosis factor-alpha
TPI	triose-phosphate isomerase
UCR	uncoupling ratio
ZnT3	zinc transporter 3

Chapter 1

General Introduction

The majority of this chapter has been published as a review article:

Jayasena T, Poljak A, Smythe G, Braidy N, Münch G, Sachdev P (2013). *The role of polyphenols in the modulation of sirtuins and other pathways involved in Alzheimer's disease*. Ageing Research Reviews 12(4):867-883.

Please see Appendix for full publication

1.1 Alzheimer's Disease

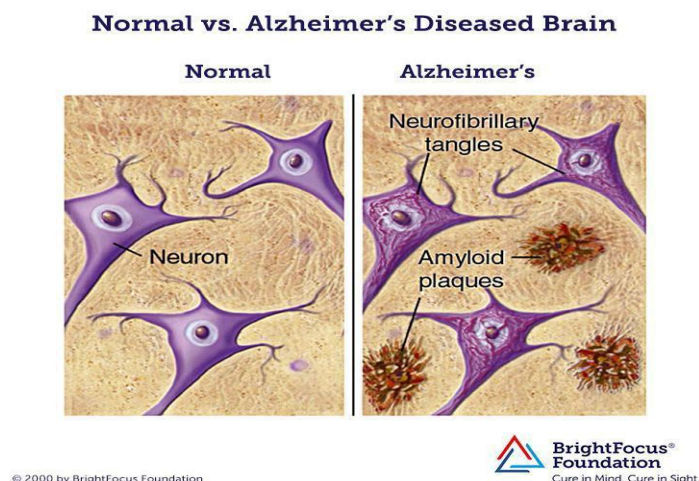
Alzheimer's disease (AD) is a neurodegenerative disease characterised by decline in cognitive and functional abilities ¹. Pathologically AD presents with progressive and irreversible neuronal and synaptic loss, particularly in the hippocampus ².

Neurodegenerative diseases are the most common cause of senile dementia with incidence doubling every five years after the age of sixty. The current ageing boom of most developed societies is predicted to translate into an increase in the incidence of AD in coming decades, creating substantial financial and social burdens however there are still no disease modifying therapies available to stop or reverse the decline in patients with AD.

The disease was first defined by psychiatrist Alois Alzheimer in 1907 describing the case of 55 year old Mrs Auguste Deter who presented with memory impairment, aphasia, psychosocial incompetence and disorientation, which progressed to worsening cognitive function ³⁻⁵. From microscopic analysis of her brain, Alzheimer observed and described the presence of 'fibrillary bundles' and 'small miliary foci,' nowadays recognised as neurofibrillary tangles (NFT) and amyloid beta ($A\beta$) plaques, the two main histological hallmarks of AD ⁴. Neurofibrillary tangles are intracellular lesions found within the cytoplasm of neurons and $A\beta$ plaques are extracellular lesions consisting of an $A\beta$ peptide core surrounded by activated microglia (Figure 1.1) ^{2,6,7}. These plaques also contain high levels of divalent metals such as iron and copper sequestered within them ⁶⁻⁸.

Figure 1.1 Histological hallmarkers of AD – Amyloid Plaques and Neurofibrillary Tangles

(image taken from <http://www.brightfocus.org/alzheimers/infographic/amyloid-plaques-and-neurofibrillary-tangles>)



However AD itself wasn't considered a disease distinct from dementia until decades later when research by Blessed et al in 1968 showed that there was a connection between the plaques and tangles and cognitive decline^{4,9}. Additionally other researchers also established AD as a condition differing from normal ageing, and genetic mutations involved in the hereditary form of the disease were also discovered^{4,10-13}.

The most consistent and strongest genetic predisposition for the late onset form of AD (the most prevalent form, affecting about 95% of individuals with AD) to the disease comes from the gene for apolipoprotein E (*APOE*), with an increase in the risk of developing AD reported to be up to 30 times higher for individuals carrying two copies of the *APOE* ϵ 4 allele^{14,15}. By contrast, evidence suggests that the *APOE* ϵ 2 allele is protective from AD pathology¹⁶. Other genes have also been implicated as disease risk factors including those involved with inflammation, cholesterol metabolism, transport/trafficking proteins, neurotransmission and signalling^{15,17}.

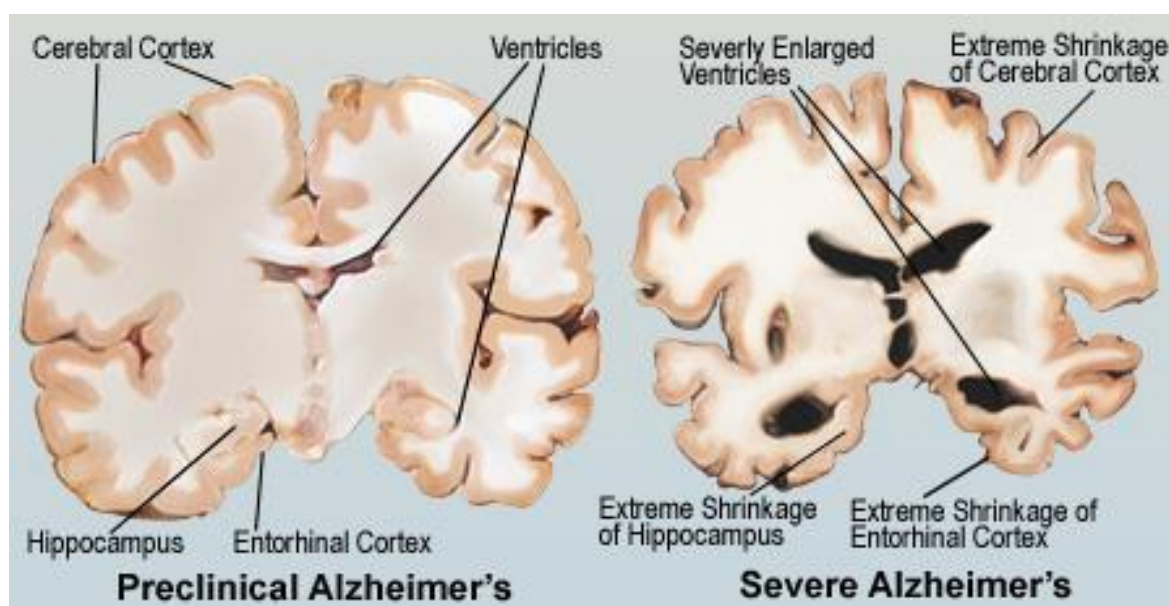
AD remains a difficult disease to study due to its long preclinical phase and the inability to reliably detect the initial stages of the disease. Today, brain scans and improving imaging techniques have provided insight to the aetiopathology of the disease, but reaching agreement on the pathological aspects and causes of AD, in addition to the lack of ways to confirm these, have caused impediments to treatments and cures for the disorder.

Although AD is characterised by the progressive cognitive deterioration of a patient, each individual advances through the course of the disease uniquely. Initial symptoms are often mistaken for age-related problems or stress-induced indicators, including the inability to form new memories and recall recently learnt facts¹⁸. These subtle problems in the pre-dementia stage usually go unnoticed or may be identified as mild cognitive impairment (MCI)¹⁸. Early stages of the disease are characterised by behavioural and psychological changes, as well as a gradual inability to handle normal daily activities, including newly learned skills. Usually a patient is able to manage their own affairs, although their vocabulary and language fluency tend to be noticeably affected at this point of the disease¹⁸. Later phases of AD require full-dependency on a caregiver, leading in some cases to a complete loss of speech and accompanied by a loss in muscle mass due to lack of mobility, ultimately causing the patient to become bedridden¹⁸. Delusional symptoms and irritability, confusion, aggression and wandering tend to become less common than in the intermediate stages of the disease¹⁸.

Postmortem analyses of AD patients' brains show losses of neurons and synapses in the cerebral cortex, atrophy of the hippocampi, temporal and parietal lobes, parts of the frontal cortex and cingulate gyrus, leading to brain atrophy (Figure 1.2), as well as a presentation of large numbers of plaques (in the cortex) and NFT (beginning in the hippocampal region and extending into the cerebral cortex), providing the basis for a confirmed diagnosis of AD^{2,19}.

Figure 1.2 Brain Atrophy in AD

(Image taken from: <http://memory.ucsf.edu/education/diseases/alzheimer>)



There are two main types of AD: familial and sporadic. The familial form accounts for less than 5% of cases. These are caused by mutations in one of three genes and have an early age onset, before 65 years. Most mutations within the three genes - amyloid precursor protein (*APP*), presenilin 1 (*PSEN1*) and presenilin 2 (*PSEN2*) increase brain and CSF levels of the A β peptide. Excess levels of toxic forms of the A β peptide (particularly the longer A β 1-42 version, β -pleated sheet conformers and A β oligomers), which over time may aggregate into plaques, disrupt neuronal messaging, and ultimately cause the death of neurons^{15,17}.

The more common sporadic version of AD has no commonly acknowledged genetic causes (though the *APOE* ϵ 4 gene allele is a recognised risk factor) and is thought to be a multifactorial disease with many risk factors adding up to the dysfunction and disease

pathogenesis. These factors include: acetylcholine decline, increased oxidative stress, amyloid aggregation, mitochondrial dysfunction and divalent metal ion imbalance.

1.2 Cholinergic Hypothesis

The cholinergic hypothesis was theorised because investigations showed that AD brains had lower levels of acetylcholine – a major neurotransmitter in the brain – than non-demented elderly cases²⁰. As one of the oldest causal theories of AD, the disturbances in the cholinergic system have also been the focus of most treatments available on the market, although they provide relatively modest postponement of clinical symptoms and fail to alter the course of the pathology^{20,21}. Treatments of AD based on the cholinergic hypothesis (donepezil, rivastigmine and tacrine etc.) are cholinesterase inhibitors, which act simply by inhibiting cholinesterase – an enzyme which breaks down the neurotransmitter acetylcholine. By reducing cholinesterase activity, the brain retains higher levels of acetylcholine and therefore neurotransmission^{20,21}. However these drugs provide only a temporary reprieve, and do not alter plaque or tangle formation or neuronal cell death.

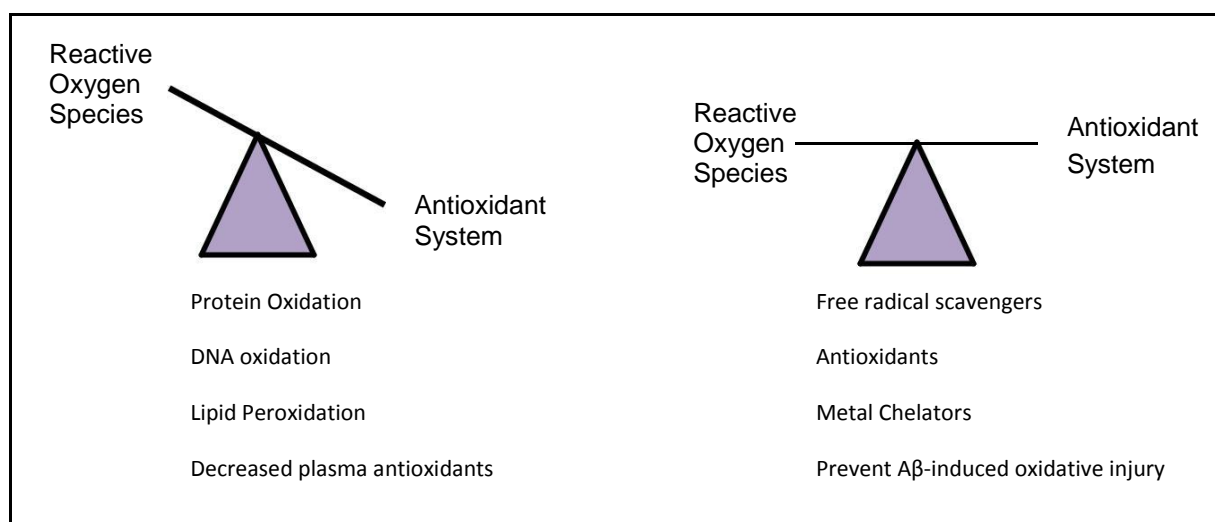
1.3 Oxidative Stress

The accumulation of oxidative damage from free radical production during normal oxidative metabolism increases with age and is known as the free radical theory of ageing. Originally proposed by Denham Harman, it is thought to be linked to age-related diseases such as AD²²⁻²⁴. In fact, one of the earliest pathological events in AD is oxidative damage to the brain cells of affected individuals¹. Oxidative stress results when pro-oxidant and anti-oxidant activities in the body are not occurring at a balanced rate, resulting in dyshomeostasis (Figure 1.3) and generation of toxic reactive species (ROS), such as hydrogen peroxide, superoxide and the highly reactive hydroxyl radical²⁵. The generation of free radicals is catalysed by redox-active metals such as copper and iron. For example, hydrogen peroxide in the presence of copper or iron produces hydroxyl radicals via the Fenton reaction (Figure 1.4). Brain tissue is particularly vulnerable to oxidative damage due to its high oxygen consumption, relatively low antioxidant levels, high content of redox-active metals (copper and iron), and limited regenerative capacity. Thus free radicals have been hypothesised to play an important role in the brain ageing process²⁶. Increased oxidative stress due to free radical damage, and the

resulting cellular dysfunction are widely believed to be responsible for the neuronal degeneration that occurs in AD²⁶.

Oxidative stress results in impaired cellular functions and the formation of toxic species, such as peroxides, alcohols, aldehydes and ketones²⁷. The oxidatively modified lipids acrolein and HNE induce toxicity by crosslinking to cysteine, lysine and histidine. Acrolein down regulates the uptake of glutamate and glucose from cell culture. Modifications to proteins result in the impairment of enzymes, whereas ROS interaction with DNA potentially leads to mutations²⁷. The excess generation of ROS leads to dysregulation of intracellular calcium signalling. Such dysregulation has been widely observed in neurodegenerative diseases in which aberrant calcium levels stimulate multiple pathways that ultimately induce an apoptotic cascade^{1,27}.

Figure 1.3 Evidence of Oxidative Stress in AD and its prevention



Markers of free-radical damage such as increased protein and DNA oxidation, increased levels of lipid peroxidation, advanced glycation end products, carbonyls, dityrosine,

malondialdehyde, and peroxynitrite damage have all been reported to occur in AD²⁸⁻³⁰.

Furthermore, decreased levels of plasma antioxidants are reported in AD patients.

Peroxidation of cellular membrane lipids generates highly reactive aldehydes such as 4-hydroxynonenal (4-HNE). This product is elevated in multiple AD brain regions compared to nondemented elderly controls³¹. 4-HNE is also increased in the plasma and CSF of AD patients³¹. Elevated isoprostanes have also been observed in the plasma, CSF and urine of

AD individuals^{29,32} and protein carbonyls are significantly increased in the AD hippocampus³³. Increased levels of protein carbonyls are observed in both in NFTs as well as in the cytoplasm of tangle free neurons^{23,34}. AD patients have higher dityrosine in plasma³⁵ and increased nucleic acids oxidation. A significant increase in the oxidised purine 8-OH guanosine (a signal product of hydroxyl radical attack), was found in the cortex and cerebellum of AD brains relative to controls³⁶. Elevated levels of this marker were also found in lymphocytes of AD patients³⁷.

DNA damage by ROS, particularly the hydroxyl radical is a key feature of neuronal cell death in AD patients and in experimental models of this disease^{38,39}. Studies demonstrating increased oxidative DNA damage, and helicase activity especially the activity of 8-oxoguanine glycosylase with a concomitant decrease in base excision repair have been reported in the AD brain⁴⁰. DNA damage induced by free radicals or enzymatic modifications can be a trigger that initiates the cell death cascade. These observations have been interpreted to suggest that in addition to the brain being subject to increased oxidative stress in AD, there is a compounding effect of decreased repair of oxidative damage leading to an accumulation of DNA errors, which may be an important factor in the progression of neuronal loss in AD⁴⁰.

The increased oxidative modification of cellular and lesion macromolecules seen in AD may originate from multiple sources, including: increased intracellular production of the membrane permeable oxidant, hydrogen peroxide by abnormal or stressed mitochondria, increased extra-neuronal production of hydrogen peroxide from activated microglia, and by A β deposits^{1,26,41}. These A β plaques are another source of oxidative stress in AD as they sequester divalent metals such as copper and iron, which have the potential to catalyse free radical formation⁴². Copper and iron in abnormally high concentrations and markers representing the endproduct of oxidative stress have been found in amyloid plaques, and are elevated in the neocortex of the AD brain^{25,43}. Iron has been shown to facilitate the aggregation and deposition of A β and to induce aggregation of the major constituent of neurofibrillary tangles, hyperphosphorylated tau^{44,45}. Reaction of hydrogen peroxide with available redox active metal ions via Fenton chemistry leads to the generation of the hydroxyl radical (see figure 1.4). This highly reactive and non-selective free radical has the potential to induce many oxidative modifications to a variety of macromolecules.

Figure 1.4 Production of the hydroxyl radical via Fenton chemistry



As the body ages, increasing levels of oxidative stress markers are produced and the efficient functioning of molecules to clean up and repair these errors also deteriorates with time⁴⁶.

This in turn leads to further oxidation and the destructive spiral continues⁴⁶. These processes themselves are reported to cause inflammation and the hallmarks of AD – amyloid plaques and tangles. How and why are still unanswered questions in this debate, although some researchers suggest that these lesions are the end result of a malfunctioning repair system that ineffectually manages oxidative stress within the brain. The creation of ROS with age results from dyshomeostasis of multiple pathways: – from energy production to the replication of DNA and cellular growth and repair⁴⁶. During ageing, the efficiency of processes that maintain protein integrity and cleanup systems are compromised and numerous errors accumulate. These in turn cause further mistakes to occur and the system suffers with the build-up of dysfunctional proteins and the vicious oxidative stress cycle continues. ROS themselves can directly oxidise and damage DNA, lipids and proteins and induce stress-responses, as well as facilitate apoptosis through mitochondrial pathways⁴⁷. Levels of oxidative stress have been linked with AD, which has lead to clinical trials utilising anti-oxidant therapies¹. These trails have in general been disappointing. For example trials with vitamin E and curcumin have been inconclusive. However it may be that the window of treatment has been surpassed in patients who have converted to late stages of AD^{48,49}. This point has been raised for most failed AD treatments and it is proposed that late stage AD patients have exceeded the threshold for resolving the disease and its causes. It is difficult to determine whether oxidation is causative in AD, since oxidative stress is also a normal part of ageing, and it may just be a matter of degree. It is difficult to determine which individuals will be affected, and also challenging to undo years of cumulative damage. To optimise their efficacy, it is likely that measures to reduce excess levels of ROS and oxidation should be initiated early and ideally at preclinical stages.

1.4 Amyloid Cascade Theory

The main therapeutic approaches for AD are linked to the amyloid cascade hypothesis. This theory highlights the importance of A β , the major component of plaques, as an upstream factor in AD pathogenesis, and suggests that A β initiates a cascade of toxicity, which recruits tau, the major component of tangles in AD pathology and consequently causes neuronal dysfunction, neurotransmitter deficits, and ultimately neuronal cell death^{20,50}. A β has normal physiological activity and is present in the brain, cerebrospinal fluid (CSF) and plasma of healthy individuals throughout life. These peptides do, however, have the ability to aggregate and generate the amyloid that is found in the brain parenchyma and around blood vessels⁵¹.

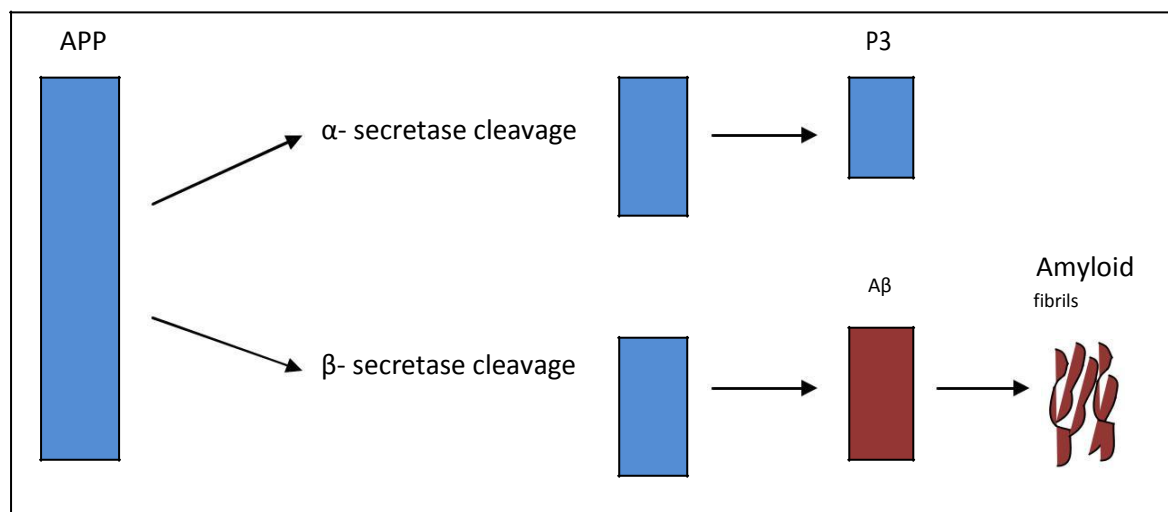
A β possesses physiochemical properties that are consistent with both an antioxidant and a prooxidant. Several studies have shown that A β exhibits neurotrophic and neuroprotective properties when present at physiological (nM) concentrations. A β 1-40 and to a lesser extent A β 1-42 prevents lipoprotein oxidation in CSF and plasma⁵². Evidence that A β has antioxidant activity comes from studies showing that increased production of A β by mutant PS1 fibroblasts is accompanied by a decrease in the production of ROS, particularly the hydroxyl radical formation⁵³. There is a positive correlation between CSF resistance to oxidation and its levels of A β ⁵⁴.

Evidence supporting a neurotoxic role for A β in AD comes primarily from experiments on cultures of primary neuronal cells from neonatal rodents or cultures of neuroblastoma cell lines. Such studies typically report neurotoxic effects from the addition of micromolar concentrations of A β peptide (particularly the longer A β 1-42 variant prevalent in AD) to the culture media⁵⁵⁻⁵⁷. The role of A β in disease is not therefore completely understood. It is possible that it has a dual role in AD pathogenesis. At low nM concentrations it may play a protective role against oxidative stress, however, as the burden of oxidative stress becomes excessive it may become complicit by exacerbating free radical damage⁴¹.

A β is generated by cleavage of amyloid precursor protein (APP) which can occur via 2 sequential pathways: the non amyloidogenic and amyloidogenic pathways⁵⁸ (see figure 1.5). The first cleavage event initiated by either α -secretase or β -secretase, determines whether A β is generated. The next cleavage by γ -secretase determines the species of A β generated⁵⁸. Although its function is not completely understood, APP is suggested to be critical for neuronal growth, signalling, and may also function as an antioxidant and a metalloprotein,

modulating copper transport and metabolism⁵⁸. Cleavage of the APP protein can occur at many sites within the cell, including the trans-Golgi network, mitochondrial membrane and plasma membrane, with location and reactants present said to dictate which pathway is followed.

Figure 1.5 APP processing by secretase enzymes. Top showing non amyloidogenic pathway and bottom showing amyloidogenic pathway producing A β peptides.



The non-amyloidogenic pathway results in the production of the P3 peptide fragment, which consists of 16 amino acids and involves α -secretase cleavage followed by a γ -secretase cut within the A β domain of the APP protein (Figure 1.5). The amyloidogenic version of the pathway involves cleavage by β -secretase followed by the γ -secretase (Figure 1.5), releasing the 40-43 amino acid A β peptide, thought to cause the neurodegenerative disease.⁵⁸ The enzymatic action of β -secretase leaves a C-terminal fragment known as APP-CTF β or C99, within the membrane and releases APPs β into the extracellular space. After A β peptide generation by γ -secretase from the C99 fragment, the A β peptide is extracellularly secreted⁵⁸.

Most of the A β peptides produced are 40 amino acids long, however it is thought in the diseased state A β 42 peptide production increases, causing havoc within the cell and the surrounding environment. This longer form (A β 42) is more hydrophobic and forms β -pleated sheets and fibrils more easily, and is also thought to be more neurotoxic than the A β 40 peptide⁵⁰. Various A β species exist within the brain, including A β 1-39, A β 1-40, A β 1-42 and

A β 1-43. These peptides can be found as monomers, oligomers, protofibrils and fibrils and in the latter stages form the amyloid plaques seen in the brains of AD patients⁵⁹. Much debate has surrounded the identification of the actual toxic form of A β , ranging from the aggregation of the plaques themselves, to the newer idea that soluble forms, specifically oligomers of the peptide, are the detrimental form⁶⁰. It is believed that A β 1-42 is predominantly responsible for toxicity observed in AD. Mainly because familial AD mutations in APP elevate the expression of A β 1-42 and that A β 1-42 is more prone to aggregation and is more toxic than

A β 1-40⁶⁰. In AD, A β exists in both soluble and insoluble forms, with the later associated with plaques. Plaques were initially thought to be the toxic A β source however it is now suggested that soluble A β oligomers are more likely to be the source of A β toxicity, while fibers are inert⁶⁰. This is supported by studies indicating the neurotoxicity of A β oligomers

⁶¹. Research has confirmed the difficulty in identifying the toxic form of A β , due to its different assembly states, with this ability in itself being a potential mechanism of toxicity⁶⁰.

The implication of the amyloid cascade hypothesis is that targeting A β should prevent the molecular pathology of AD and alter the course of the disease. Accordingly, A β -based therapies have been investigated in preclinical models and clinical trials⁶². However to date these clinical trials have been disappointing⁶². For example the ELAN immunotherapy trial was halted due to development of encephalitis in approximately 6% of patients⁶³. However, subsequent studies have also reported some positive effects on plaque clearance⁶⁴. While the amyloid cascade hypothesis of AD has broad support, the failure of drugs that target A β indicates possible limitations of this explanation. Furthermore positron emission tomographic (PET) imaging data have shown that while amyloid can be removed from the brain by immunotherapy, but this does not result in improved clinical outcomes⁶⁵, possibly due to treatment being applied too late in the course of the disease. This supports the possibility that amyloid plaques reflect the presence of disease but are not directly causative of neurodegeneration. Another possibility is that amyloid plaques are a protective response to underlying disease processes, acting as a storage mechanism to contain neurotoxic oligomers, as the presence of plaque inversely correlates with oxidative burden and synaptic loss⁴¹.

Copper enhances A β cytotoxicity to cultured cells, which is ameliorated by co-incubation with zinc. By chelating divalent metals, plaques may confer protection against ROS damage⁴¹.

Apart from a suggested increase in A β peptide production, the accumulation of the peptide in older age can be attributed to the malfunction or ineffectiveness of A β peptide clearance from

the brain^{19,66}. Elimination of A β peptide can be instigated by phagocytosis of the peptide by the resident immune cells – microglia and astrocytes – said to be capable of degrading limited amounts and also transporting A β peptide from the brain into blood or CSF⁶⁷. Other mechanisms of reducing A β peptide include enzymatic degradation such as that by neprilysin and insulin-degrading enzyme. Additionally, removal of the peptide across the blood brain barrier (BBB) can be mediated by proteins such as low-density lipoprotein receptor related protein and P-glycoprotein. Traditional consensus indicates that A β peptide accumulations occur extracellularly and that this is the cause of AD degeneration, comprising the basis of the amyloid theory of pathogenesis²⁶. While validity of the amyloid hypothesis has been questioned due to the failure of A β immunotherapy approaches to improve cognition, further research to identify the actual component or form of the peptide that is neurotoxic may still lead to successful treatments.

1.5 Neuroinflammation

Whilst plaques and tangles are hallmark features of AD, there are other processes which contribute to disruption of brain function and neurodegeneration. Inflammation, seen in many diseases of the elderly, is observed in AD brains and has long been thought to trigger the pathology⁶⁸. In addition, an important AD risk factor is head/brain injury, suggesting that chronic inflammation could initiate or at least contribute to the course of AD⁶⁹.

Epidemiological studies in the early 1990's suggested that exposure to anti-inflammatory drugs (more specifically non-steroidal anti-inflammatory drugs – NSAIDs) reduced the risk of developing AD in later life⁷⁰. Whilst contradictory results have stemmed from this, including failed clinical trials of NSAID use in AD patients, it is evident that inflammation plays some part in the disease⁷⁰.

Much discussion surrounds the type of effect that inflammation plays and there is evidence for both beneficial and detrimental roles in the disease aetiology. Multiple inflammatory markers are observed in *postmortem* AD brains, including pro-, anti- and post-acting molecules, as well as activation of resident immune cells (glia) in the central nervous system – microglia and astrocytes⁷¹⁻⁷³. These have been found in the AD-affected regions of the brain and also localised with plaques and NFT⁷³. Throughout the progression of A β peptide accumulation, plaques are described as having particular immunoreactive elements. Studies have identified various inflammatory components in AD brains and plaques, including ApoE,

tau protein, ubiquitin, protein kinase C, complement proteins, fibroblast growth factor, advanced glycation end products, prostaglandins, cytokines, proteases, free radicals, redox metal ions, and chemokines⁷⁴⁻⁷⁷. These in turn can initiate further inflammatory pathways and indicate that inflammation participates in disease progression, although to what extent and in what pathways is still to be determined.

Microglia make up 12% of brain cells and fully activated microglia are essential for brain development and maintenance, although once activated, they can remain in this state and exacerbate neuronal damage in affected regions⁷³. Activated microglia increase in number throughout AD progression and studies suggest that A β peptide deposits are capable of stimulating this activation, and microglia cluster around A β peptide aggregation sites⁷³. Microglia reportedly produce, or signal other cells to produce pro-inflammatory molecules such as interleukin-1, interleukin-6 and tumour necrosis factor-alpha (TNF α), which recruits lymphocytes to inflamed areas⁷³.

In addition to triggering apoptosis, the excretion of neurotoxins and excitatory neurotransmitters can escalate and spiral out of control in the AD brain. Astroglia are major players in the maintenance of the BBB, including regulating its permeability⁷⁸.

Compromised BBB integrity is key to AD progression, as it regulates clearance of waste and metabolic by-products, influx of important nutrients and is a barrier against potential neurotoxic elements. However permeability changes may not be solely the effect of astroglial actions, and factors such as cerebral amyloid angiopathy may have a contributory role⁷⁸.

Whilst microglia and astrocytes are the resident immune cells within the brain, the neurons also respond to inflammatory signals, and may participate in pathology⁷⁹.

Additional regulatory molecules involved in inflammatory responses such as the COX enzymes, which produce prostaglandins by conversion of arachidonic acid, may link inflammation to increased production of A β peptide through increased prostaglandin E2⁸⁰. Prostaglandin E2 has been shown to increase cleavage of APP, producing A β 40 and A β 42 and can be reduced with COX inhibitors^{80,81}. The mechanism/s by which inflammation contributes to AD pathology and/or progression is complex and probably includes multiple pathways. Genes or polymorphisms that enhance an individual's inflammatory response or susceptibility to a particular disease(s), in addition to compromised homeostasis of biological systems in old age, potentially give rise to chronic inflammatory activation and increase vulnerability to additional comorbidities. The ageing immune system with enhanced innate

immune responses has been suggested by those backing the ‘inflammaging’ theory^{82,83}.

Whilst a substantial body of evidence supports an important role for inflammation in AD, it is still unclear as to whether abnormal immune functioning is a causative, or secondary event in the development of AD pathology.

1.6 Mitochondrial dysfunction and energy metabolism

Mitochondria are the energy production “powerhouses” of the cell and any defects within these usually causes serious disorders, including many neurodegenerative diseases^{84,85}. In dealing with large amounts of energy generation, including ATP and NAD^+ production, mitochondria have developed ways of managing the vast amounts of waste that are created. During ageing however, these systems become less efficient and can break down potentially initiating AD through mitochondrial dysfunction⁸⁶⁻⁸⁸. The ROS generated by dysfunctional mitochondria as well as other oxidised molecules generated by ROS, such as lipids and glucose, can become taxing to the cellular machinery, and increasingly difficult to clear with advancing age, with adverse implications for both individual cells and the body as a whole^{86,87,89,90}.

The main portion of ATP consumed by the brain is produced in mitochondria by oxidative phosphorylation. ATP production occurs within the inner mitochondrial membrane, and involves electron transport through a chain of protein complexes (I-IV)⁸⁸. These complexes transfer electrons from electron donors (NADH, FADH) to O_2 . During the electron carrying steps, protons (H^+) are transferred through the inner membrane against the chemiosmotic concentration gradient. The potential energy stored in this H^+ gradient is utilized to synthesize ATP from ADP and inorganic phosphate, as the protons are released through the ATP synthase⁸⁸. Neurons require large amounts of energy for continuously operating processes such as: action potentials, resting membrane potential maintenance, active transport, receptor function, vesicle release, and neurotransmitter recycling⁹¹. Mitochondria can also mediate apoptosis and programmed cell death⁸⁶. Therefore, the number and functionality of mitochondria play a significant role in neuronal function, proliferation and death, and have an impact on health and disease of the central nervous system⁸⁸.

Since mitochondria are central to cellular metabolism, findings of metabolic impairment have led to extensive investigation of the role of mitochondria in AD and other neurodegenerative

diseases. Early studies of AD brain tissue demonstrated that bioenergetic deficits occur at early stages of the disease⁹²⁻⁹⁴. For example, cerebral glucose metabolic rate observed via positron emission tomography scan in AD patients showed region-specific deficits in energy metabolism that preceded clinical impairments in attention, abstract reasoning, and language and visuospatial functions⁹⁵. This was corroborated by evidence of reduced cerebral glucose metabolism prior to onset of clinical AD symptoms in patients carrying familial AD mutant genes and healthy elderly adults who were later diagnosed with AD⁹⁵. Patients with MCI and patients with sporadic AD associated with the apolipoprotein E ϵ 4 allele who subjectively complained of memory loss also exhibited reduced brain metabolism⁹⁶. This coincides with reduced activity of pyruvate dehydrogenase (PDH) and α -ketoglutarate dehydrogenase (α KGDH) complexes, components of the tricarboxylic acid cycle, in the AD brain^{97,98}. While abnormal activity of TCA cycle proteins were sometimes found concurrent with the presence of A β plaques, NFTs, and neuronal loss, they also occurred in the absence of these histological markers of AD neurodegeneration⁹². This suggests that altered PDH and α KGDH activities are not simply side effects of neurodegeneration^{97,99} and further supports the possibility that metabolic deficiency occurs early and may contribute to AD progression.

Mitochondrial uncoupling occurs in tissue homogenates from patients with AD, frontotemporal dementia and Pick's disease, and may underlie the hypometabolism seen in AD¹⁰⁰. In addition, the expression and activity of mitochondrial proteins are compromised in tissues and cells derived from AD patients¹⁰¹⁻¹⁰³. Deregulation of mitochondrial fission/fusion proteins also occurs in AD brain⁹⁴, and in *post mortem* studies, fragmented mitochondria are observed in several areas of AD patient brains⁹³. It has been suggested that highly functional, mature neurons require elongated highly connected mitochondrial networks to reduce the amount of mitochondrial movement necessary to handle the energy demand of the cell. This may explain why mitochondrial fragmentation coincided with their mislocalisation away from synapses in AD brain⁹⁴. Taken together, this suggests that the energy demands of neurons are not being met in AD, which may contribute to the slow, progressive synaptic dysfunction and neuronal death observed in the disease. Cellular and animal models of AD exhibiting A β and tau pathologies replicate the metabolic and mitochondrial impairment observed in human AD patients^{104,105}.

In addition to generating energy for the cell, mitochondria regulate subcellular calcium signalling and homeostasis as well as subserving neuroplasticity. Distributed throughout the cell, including presynaptic terminals and the axons of neurons, mitochondria also have the ability to undergo fusion and fission, move rapidly between subcellular compartments, function as signalling platforms and respond to electrical, neurotransmitter and growth factor receptor stimuli. Mitochondrial fission and fusion pertains to the regulation of location, number, function and morphology of these organelles. Changes in mitochondrial dynamics have been associated with the processes of learning and memory such as long term potentiation and recovery of synapses in phases of high synaptic activity. When these processes malfunction, oxidised DNA and RNA and structural mitochondrial abnormalities are observed. Additionally, mitochondrial DNA mutations accumulated over the cell's lifecycle may contribute to ageing and disease aetiology as suggested by animal studies. Evidence of the presence of deformed mitochondria, including abnormal shapes and sizes and age related decrease in numbers of mitochondria have all been reported¹⁰⁶⁻¹⁰⁹.

Glucose is essential for healthy brain function and is a primary source of energy in the brain. PET scanning shows a consistent reduction of cerebral glucose consumption in the brain of AD patients¹¹⁰. These observations support the notion that AD is linked to metabolic disorders among which diabetes is currently considered one of the highest risk factors for development of cognitive decline and AD^{111,112}. These findings have led to preclinical studies aimed at establishing the efficacy of anti-diabetic treatments in animal models of the disease¹¹³.

Redox proteomics studies on AD brain have demonstrated the oxidation of pyruvate kinase (PK), Phosphoglucomutase 1 (PGM1), Eno1, Triose-phosphate isomerase (TPI), fructose bisphosphate aldolase A/C (FBA A/C), ATP synthase, glyceraldehyde 3-phosphate dehydrogenase (GAPDH) and Malate dehydrogenase (MDH)¹. Similarly, ATP synthase, PK, MDH, Eno1 and FBA C were found increasingly oxidized in amnesic MCI brain¹¹⁴. All these proteins are directly or indirectly involved in ATP synthesis in the brain; the inactivation of these proteins induced by oxidation might reduce glucose metabolism. In agreement with this view, CK, Eno1, PGM1, GAPDH, and ATPase activities are reportedly diminished in AD brain¹¹⁰. ATP synthase is an essential enzyme in the inner mitochondrial membrane, is the last complex (complex V) of the electron transport chain and is responsible for ATP synthesis. ATP synthase is oxidatively modified at different stages of AD¹¹⁵ leading to inactivation of the complex. Moreover, it has been shown that ATP synthase activity is

decreased in the cortex of an AD mouse model¹¹⁵. Failure of ATP synthase activity significantly contributes to lower ATP levels, and possibly results in electron leakage and increased ROS production, suggesting an alternate rationale for the oxidative stress observed in AD. Thus, the reduced glucose utilization, mitochondrial deficits and decreased production of ATP seen in AD may be contributing factors to the neurodegenerative process and its progression culminating in AD pathology.

1.7 Metal Homeostasis

Metals are required in the body, especially in the brain, in order to perform redox reactions and also as components of some enzymes. An imbalance in metals can cause oxidative stress and neurodegeneration⁷⁷. Metal chelators are capable of disrupting plaques and oxidative stress, although their toxicity and inability to cross the BBB has limited their use as therapeutic treatments for the disease^{116,117}. Research on the metal chelator clioquinol has proven to be at least partially successful in both animal and human studies¹¹⁸. Metals that are in dyshomeostasis in AD brains include divalent ions of iron, zinc, and copper. These metals instigate aggregation of A β peptides, and A β peptides, bind the divalent metal ions of copper, iron and zinc¹¹⁹. Whether peptide accumulation is a compensatory response to sequester excess metal or if the presence of metals causes A β aggregation in AD is still yet to be determined. Zinc is distributed ubiquitously in the brain, and its level significantly increases in the brain and serum of patients with AD^{120,121}. Synaptic zinc levels are regulated by the zinc transporter 3 (ZnT3), which is essential for memory and normal cognitive function^{122,123}. In AD, there is a redistribution of zinc into extracellular plaques and surrounding neuropil. Zinc binds A β residues 6-28 causing rapid aggregation and precipitation of the protein; thus co-deposition of zinc with A β could initiate plaque formation in the disease.

Zinc-induced plaque formation in disease is also supported by the anatomic distribution of plaque and zinc in the brain¹²⁴. Plaque formation only occurs in neocortical regions of AD-affected brains, but A β is expressed in all brain regions¹²⁴. The distribution of plaque closely aligns with the expression of ZnT3 prevalent in glutamatergic neurons¹²⁵. This protein trafficks zinc into synaptic vesicles and zinc is released into the synapse upon exocytosis¹²⁵. APP transgenic mice crossed with mice lacking ZnT3 were shown to have reduced plaque burden. Zinc also interferes with A β processing, the α -secretase involved in the processing of

APP is a zinc-dependent enzyme and zinc increases APP proteolysis, while zinc inhibits γ -secretase activity¹²⁶.

Copper is thought to interact with A β in two ways significant to AD pathology. First copper mediates the aggregation of A β under slightly acidic conditions¹²⁷. Second and more importantly, copper and A β act synergistically to cause oxidative stress. A study of synthetic A β found that submicromolar concentrations of copper induced the aggregation of low nanomolar concentrations of A β under slightly acidic conditions *in vitro*¹²⁷. The study also found that the aggregating effects of copper were reversible upon addition of a copper-chelating agent or with an increase in pH¹²⁷. More importantly, another study established that A β in the presence of a catalytic quantity of copper produces hydrogen peroxide¹²⁸. Toxicity due to the generation of hydrogen peroxide was confirmed by the addition of catalase which reduced A β toxicity by 75%¹²⁸. Copper is also a redox active metal that can catalyse the formation of the hydroxyl radical via the Fenton reaction, and can cause free radical mediated damage and cell death in the same way as iron (Figure 1.4).

In the presence of amyloid, copper undergoes redox cycling, which enhances the potential for copper induced toxicity in AD. This is important because copper is increased in amyloid plaques, however, copper levels are decreased in AD neuronal tissue, which could deprive copper-binding proteins such as superoxide dismutase and ceruloplasmin of their metal cofactor, and consequently impair their function^{121,129}. Superoxide dismutase is a major copper binding protein and antioxidant in neurons, which utilises copper to convert the superoxide free radical into hydrogen peroxide. Ceruloplasmin is another major copper-binding protein, which functions as a ferroxidase to promote iron export. Copper also accelerates A β aggregation, but unlike zinc, copper induces oligomer rather than fibril structures¹²⁹. Toxicity of A β oligomers can be attenuated in cultures by copper chelation^{43,130}. The binding of copper to A β is likely to be a factor in AD because copper, too, is enriched in amyloid plaques.

Serum copper levels are elevated in patients with AD. In the brain, copper is concentrated in the extracellular compartment and in the amyloid plaques¹²⁹. In a mouse model of AD, copper accumulates in the brain capillaries and parenchyma, and this accumulation is related to increased A β production, neuroninflammation, and reduced A β clearance¹³¹. Furthermore, oxidative stress and neuronal toxicity, induced by hydrogen peroxide and toxic hydroxyl radicals, reduce Cu(II) to Cu(I) through copper and A β interactions⁷. Therefore copper

affects A β production, clearance, aggregation and fibrillisation through diverse mechanisms, either directly or indirectly.

Iron is the most abundant transition metal in the body and in the brain. It exists in two forms: ferrous (Fe²⁺) and ferric (Fe³⁺). Its strong redox potential affords it versatile functions as a cofactor and biocatalyst in many vital as well as potentially damaging reactions in the cell⁴³. In AD patients, accumulation of iron in the hippocampus and cerebral cortex colocalises with the lesions, NFTs and A β plaques⁴⁴. Abnormal iron deposition in senile plaques can associate with A β and may promote increased formation of oxygen radicals²⁵. The ability of iron to interact with oxygen is critical for energy production in the cell, but the same property makes it capable of producing damaging free radicals via the Fenton reaction. ROS resulting from this reaction, such as the hydroxyl radical, nonselectively damage intracellular structures via lipid peroxidation, protein cross-linking and carboxylation, and DNA mutation¹³². A β itself can also be a substrate for hydroxyl radical production¹³³. Deposition of A β fragment and APP cleavage and synthesis are promoted by the presence of iron¹³⁴. Several MRI studies have shown a positive correlation between ageing and iron accumulation in the brain^{135,136}. As a consequence of iron accumulation, especially if ferritin does not also increase in parallel, the brain becomes increasingly vulnerable to iron-catalysed oxidative stress. Hence the age-related accumulation of iron may underlie or at least contribute to the commonly accepted theory that age is the biggest risk factor for most neurodegenerative diseases.

In vitro studies using synthetic A β have shown that iron induces the aggregation and potentiates the neurotoxicity of A β . A β binds to and reduces Fe³⁺ to Fe²⁺, which is followed by formation of hydrogen peroxide⁴¹. The generation of Fe²⁺ and hydrogen peroxide creates conditions ideal for the Fenton reaction, which leads to the formation of the highly reactive hydroxyl radical.

Iron elevation in affected areas of the brain is a feature of a number of neurodegenerative diseases including AD¹³⁷. Neuronal iron deposition causes oxidative stress via the Fenton reaction, which may contribute to elevated oxidative stress observed in AD⁷⁷. Iron-induced oxidative stress has been shown to initiate several apoptotic pathways in neurons and damages proteins⁷⁷. Oxidative damage to proteins and lipids by iron can cause synaptic dysfunction and neuronal cell death. The overload of iron in AD may also lead to increased A β production by increasing the expression of APP, and altering its processing. High iron

conditions lead to increased processing of APP, which in turn leads to accelerated degeneration in a mouse model of AD¹³⁸.

1.8 Plasma Biomarkers and AD

Although clinical manifestations of cognitive dysfunction and impairment of activities of daily living are the current standard for the diagnosis of AD, neurochemical and neuroimaging biomarker candidates are receiving increasing attention as potential objectively measurable diagnostic tools. Biochemical biomarkers in CSF have been extensively studied and are already a well-established diagnostic markers at least for the last stages of diagnostic validation¹³⁹. Measurement of A β 42, tau protein, and hyperphosphorylated tau protein (p-tau) in CSF of AD patients, as well as patients with other dementias and normal elderly controls revealed sensitivity and specificity levels between 80% and 90% for detecting AD versus normal elderly¹⁴⁰. CSF is known to act as a valuable source of biomarkers, as being in direct contact with the brain and spinal cord it provides a complete representation of various biochemical and metabolic profiles of the brain. However, this fluid is obtained by lumbar puncture in patients which is invasive, more painful for patients, and carries a small risk of serious side effects. Thus obtaining CSF, especially repeatedly, on large numbers of elderly individuals in the community is inherently challenging, risky, and is not likely to be accepted world-wide as routine approach for AD diagnosis. Thus, it is essential to identify new biomarkers in other sources such as plasma and urine, which are cheaper, less invasive, easily collectable and allow follow-up and tracking of patients over time. Blood samples are easy to obtain and offer a rich source of disease biomarkers, as approximately 500 mL of CSF are absorbed daily into the circulating blood. Furthermore, damage to the blood brain barrier which occurs in the course of AD may enhance exchange of proteins between CSF and blood in either direction¹⁴¹.

Previous studies have revealed some potential AD biomarkers in plasma. One such biomarker are miRNAs, which belong to the class of non-coding RNA molecules which regulate more than 60% of all known genes through post-transcriptional gene silencing¹⁴². The dysregulation of miRNA expression in peripheral blood can serve as a potential source of diagnosis of Alzheimer's disease. Schipper et al identified a number of downregulated miRNAs in sporadic AD patients¹⁴³. The targets of these miRNAs were interestingly found to be part of p53, Notch and Bcl-2 pathways which are already known to be involved in AD

pathogenesis¹⁴³. Other studies have also found decreased levels of miRNA in the brain and blood of AD patients^{144,145}. It has been suggested that specific miRNAs can regulate important cellular functions in the brain. Thus the contribution of miRNAs to functions such as redox defences and DNA repair mechanisms highlight the potential of miRNAs as therapeutic biomarkers for AD.

Although the efficiency of amyloid beta as a highly sensitive and specific biomarker from CSF for AD has already been established, studies focussing on evaluating A β as a potential biomarker from blood serum have been undertaken as well. A meta-analysis performed by Koyama et al showed a highly statistical and clinically significant decrease in A β ₁₋₄₂ ratio to predict cognitive impairment¹⁴⁶.

Neuroinflammation is a critical and invariable component of many neurodegenerative diseases. Indeed, the co-occurrence of inflammatory markers such as interleukins, cytokines, chemokines, growth factors and acute phase reactant proteins in plasma, CSF and *post-mortem* brain tissue has become a hallmark feature of AD^{72,147-151}. The complement system may also have a role in the clearance of amyloid¹⁵².

Oxidative stress is another area being explored for biomarkers in AD. The parts of brain affected by neurodegeneration show increased ROS levels. In such conditions, proteins undergo post-translation modifications, leading to formation of mixed disulphides, nitration of tyrosine residues, and formation of lipid peroxides. Protein oxidation besides causing toxic cell damage also results in fragmentation and aggregation, leading to proteolysis. The most common known markers for oxidative stress reported in AD include protein DNA oxidation, isoprostane formation, 4-Hydroxy 2 trans nonenal (HNE), lipid peroxidation and advanced glycation end products^{37,153,154}.

There is also growing evidence of the positive effects of parabiosis experiments, in which circulatory systems of young and aged animals are connected. These studies show that blood from young animals can have rejuvenating and disease modifying effects on older animals^{155,156}, however the specific components of blood responsible for this effect are not well understood.

Conboy et al hypothesized that there are systemic factors that support the robust regeneration of tissues in young animals and/or inhibit regeneration in old animals, and that these factors act to modulate the key molecular pathways that control regenerative properties¹⁵⁵.

Exposing old mice to factors present in young serum restored the activation of Notch signalling as well as the proliferation and regenerative capacity of aged satellite cells¹⁵⁵. Villeda et al showed that exposure of an aged animal to young blood can counteract and reverse pre-existing effects of brain ageing at the molecular, structural, functional and cognitive level^{156,157}. That blood can have such potent disease attenuating effects in the CNS also indicates that there is important information exchange between blood and the CNS. Synaptic plasticity-related transcriptional changes in the hippocampus of aged mice was found, dendritic spine density of mature neurons increased and synaptic plasticity improved in the hippocampus of aged heterochronic parabionts¹⁵⁶. At the cognitive level, systemic administration of young blood plasma into aged mice improved age-related cognitive impairments in both contextual fear conditioning and spatial learning and memory¹⁵⁶.

1.9 Polyphenols

Polyphenols may hold potential therapeutic benefits in age-related disorders due to their potent free-radical scavenging and antioxidant effects, thus promoting cell longevity through preventing oxidative damage¹⁵⁸. Polyphenols are secondary plant metabolites that are involved in plant defence against pathogens and ultraviolet damage¹⁵⁹. They are found in many fruits, herbs and vegetables and thus serve as important dietary micronutrients. Chemically, polyphenols include a wide variety of biomolecules which contain several hydroxyl groups on one or more aromatic rings. They can be divided into various groups according to chemical structure – including flavonoids, stilbenes and lignans^{160,161}. Natural phenolics are compounds which contain hydroxyl groups on only a single aromatic ring and therefore are smaller in size than polyphenols. They include phenolic acids and phenolic alcohols (see Table 1.1 for further details). Recently, the potential role of polyphenols in ageing and neurodegeneration has widened with discoveries that they can modulate various important pathways in the pathogenesis of AD by reducing amyloid aggregation and inflammation and by modulating sirtuins which are involved in longevity and cell survival.

Polyphenols are well known as antioxidants and direct scavengers of free radicals^{158,162,163}. In addition, polyphenols can act as metal chelators¹⁶⁴⁻¹⁶⁶, which adds to the antioxidant effects of these compounds through inhibition of transition metal-catalysed free radical formation⁷⁷. Chelation of transition metals such as Fe^{2+} can directly reduce the rate of the Fenton reaction thus preventing oxidation caused by highly reactive hydroxyl radicals^{167,168}. Epigallocatechin

gallate (EGCG), a green tea polyphenol, for examples has also been shown to be a potent chelator of transition metals such as copper and iron¹⁶⁹, and inhibits over 90% of iron-mediated DNA damage caused by Fe^{2+} and H_2O_2 ¹⁷⁰. It has also been found that polyphenols are involved in the regeneration of essential vitamins^{171,172}. Polyphenols can activate antioxidant enzymes such as glutathione peroxidase, catalase, superoxide dismutase, as well as hydrogen peroxide and superoxide anions, and inhibit the expression of enzymes such as xanthine oxidase, which is involved in the generation of free radicals^{170,173-180}. These multiple antioxidant effects prevent oxidative damage to important cellular components and have lead to investigation of polyphenols as therapeutic agents for the treatment of AD, to combat the increase in oxidative stress seen in this disease.

Several studies have suggested that polyphenols may have anti-amyloidogenic effects. A number of polyphenols including tannic acid, quercetin, kaempferol, curcumin, catechin and epicatechin were shown to dose-dependently inhibit the formation of $\text{A}\beta$ fibrils as well as their elongation^{181,182}. In addition, polyphenols can bind directly to $\text{A}\beta$ or mature aggregates and impair their stability, as all the compounds tested destabilised pre-formed $\text{A}\beta$ fibrils¹⁸². EGCG significantly inhibits $\text{A}\beta$ aggregation and has the ability to remodel large $\text{A}\beta$ fibrils into smaller aggregates which displayed no toxic effects¹⁸³ (Figure 1.5). Fish oil has a synergistic effect in combination with EGCG, leading to reduction in $\text{A}\beta$ plaque formation and levels of $\text{A}\beta(1-40)$ and $\text{A}\beta(1-42)$ in AD transgenic Tg2576 mice¹⁸⁴.

Tannic acid was shown to reduce $\text{A}\beta$ deposits as well as $\text{A}\beta$ species including oligomers in the transgenic AD mouse brain^{182,185}. Tannic acid decreased cleavage of the β -carboxyl-terminal APP fragment, lowered APP- β production, and attenuated neuroinflammation¹⁸⁵. It is thought to inhibit amyloidogenic APP metabolism by reducing β -site APP cleaving enzyme 1 expression and lowering β -secretase activity¹⁸⁵. EGCG also down-regulates APP levels and cerebral amyloidosis in Alzheimer transgenic mice¹⁸⁶.

Curcumin, found in the spice turmeric, has been shown to prevent brain lipid peroxidation in rats and increase glutathione levels and the activity of other detoxifying enzymes^{187,188}. Curcumin has also been shown to protect cells against $\text{A}\beta$ -induced oxidative insult¹⁸⁹. When administered to AD transgenic mice, curcumin was found to prevent protein oxidation and inflammation and reduce the formation of soluble and insoluble $\text{A}\beta$ by up to 50%¹⁹⁰.

Luteolin, a citrus polyphenol was found to reduce $\text{A}\beta$ peptide production in cultured neurons and was also found to decrease amyloidogenic γ -secretase APP processing¹⁹¹. In the AD

mouse model Tg2576 mice, this compound along with a structurally similar compound, diosim, were both shown to reduce soluble A β levels¹⁹¹. In a recent study anthocyanin-enriched fractions of bilberry and blackberry extracts were found to modulate APP processing and significantly alter A β 40 and A β 42 levels. Both compounds also alleviated spatial working memory deficits in a mouse model of AD¹⁹².

Abnormal folding of the microtubule-associated protein tau leads to aggregation of tau into neurofibrillary tangles, another major pathological hallmark of AD. It has been shown that polyphenols derived from grape seed extract reduce tau pathology in mouse models of AD¹⁹³⁻¹⁹⁵. These polyphenols also enhanced disaggregation of neurofibrillary filaments, and improved structural stability^{193,195}. EGCG also modulates tau pathology in a mouse model of Alzheimer's disease¹⁹⁶. Tannic acid dose-dependently inhibits tau aggregation and polymerisation through formation of a hairpin binding motif¹⁹⁷.

Table 1.1 Influence of Polyphenols on Sirtuins and Pathways involved in Ageing and AD

Polyphenol	Fruit/Vegetable	Effect on Sirtuins	Influence on AD	Influence in Ageing	Reference
Resveratrol	Red Grapes (1.5-7.8ug/g), Red wine (1.98-7.13mg/L),	Increased SIRT1,SIRT2, SIRT3, SIRT4 and SIRT7	Selectively remodels toxic amyloid aggregates; reduces A β plaques in animal models;	CR mimetic; increases longevity in a variety of organisms from yeast to mammals;	198-205
Quercetin	Black and Green Tea (2-2.5ug/g) Apples (0.4ug/g) Red Onion (0.2ug/g)	Increased SIRT1	Reduces A β -mediated cytotoxicity and OS	Extends life span in worms and yeast	206-210
Curcumin	Tumeric (50mg/g)	Increased SIRT1	Reduces A β levels in AD mice; enhances memory in AD rat model	Extends life span in flies and mice	211-215
Kaempferol	Tea, Broccoli, Cabbage, Beans, Leek, Tomato, Berries, Grapes, Apple	Increased SIRT3	Reversed A β -induced impaired performance of mice in a maze test; inhibit A β formation and toxicity	Protective effects against OS-induced cytotoxicity;	182,216-219
Catechin, gallic acid, gentisic acid, chlorogenic acid, epicatechin	Bitter Melon	Increased SIRT1 and SIRT3	Attenuates OS and neuroinflammation		220,221
Procyanidins, phloridzin and other unidentified phenolics	Apple	No extension of lifespan in worms lacking Sir2.1; increase Sirt1 activity in yeast	Not known	Extend lifespan of Drosophila flies and in worms; upregulates superoxide dismutase and catalase genes	222-224
Astragaloside, astragalus saponin I	Astragalus root	Not known	Prevents amyloid induced memory and neuronal loss in AD mouse model	Reduced DNA damage after OS, increased telomere length in mice fibroblasts	225-229
EGCG, Catechins	Green tea	Increase Sir2 activity in yeast	Neuroprotective; Inhibits formation of fibrillar A β ;	Increases lifespan in worms, flies and mice and	171,186,196,230-235

			metal chelating properties	delays memory regression in mice models of ageing	
Quercetin, kaempferol, catechin, rutin, naringin	Centella Asiatica	Not known	Cognitive enhancing effects; reduces brain A β levels; protective against A β -induced neurotoxicity;	reduced markers of oxidative stress in the brain, increases activity of antioxidant enzymes	236-242
Ginsenoside Rbl	Ginseng	Not known	Inhibit β -secretase activity; protect against A β toxicity, reduce ROS production and apoptosis; reduced tau phosphorylation; anti-inflammatory effect in the brain of AD rat model	Improves cognition in senescence-accelerated mice; improves memory loss in mice; ginseng intake decreased mortality in older males	243-249
Proanthocyanidins	Blueberry	Not known	Suppress OS; improves learning and memory in mice;	Increase lifespan in worms	250-255
Catechins, Proanthocyanidins, Tannins, Resveratrol	Grape seed	Not known	Inhibit abnormal protein aggregation and enhance cognition	Increases telomere length in mice; increase lifespan in Drosophila and mice	256-260
Procyanidins	Cocoa	Not known	Increased resistance to oxidative stress in yeast and worms; improved cognition	Increase lifespan of worms and rats	261,262
α -mangostin	Mangosteen	Not known	Inhibits A β aggregation and A β -induced cytotoxicity ²⁶³ 264		

1.10 Involvement of Sirtuins in Ageing and Neurodegeneration

Sirtuins are a class of proteins that possess deacetylase or mono-ribosyltransferase activity and play critical roles in cell survival in response to oxidative stress and caloric restriction (CR) regimes^{265,266}. The reversible acetylation of proteins controls their activity, and deacetylation leads to their activation or inactivation. Sirtuins are orthologues of yeast Sir2 protein, where SIR stands for silent information regulator, because in yeast, where Sir2 was first discovered, the protein silences certain genes and results in the extension of replicative lifespan. Sirtuins are NAD^+ dependent lysine deacetylases. The sirtuin-mediated deacetylation reaction couples lysine deacetylation to nicotinamide adenine dinucleotide (NAD) hydrolysis. The NAD^+/NADH ratio affects sirtuin activity; at times of low energy availability, this ratio increases, leading to higher sirtuin activity and deacetylation of other proteins.

During the deacetylation catalysed by sirtuins, a cleavage of the chemical bond between nicotinamide and ribose in NAD is coupled with the transfer of an acetyl group from the substrate (acetylated lysine residue) to ribose within the remaining ADP-ribose molecule. The final products of the reaction are: deacetylated lysine residue, O-acetyl-ADP-ribose, and nicotinamide. Thus sirtuin activity may be determined by the quantity of sirtuin molecules, availability of NAD as a co-substrate, and local concentration of nicotinamide which is a product inhibitor of sirtuin activity.

In mammals, seven sirtuins (SIRT1-7) have been identified. All mammalian sirtuins contain a conserved NAD-binding and catalytic domain, but differ in their N and C-terminal domains²⁶⁵. They have different specific substrates including histones, transcriptional regulators and enzymes²⁶⁶. They also have various biological functions, are localised in specific cell compartments, and play various roles in health and disease including ageing and neurodegeneration²⁶⁶ (Table 1.2).

Sirtuins can affect ROS production and increase resistance to its damaging effects. Oxidative stress has been shown to decrease SIRT1 expression in the rat hippocampus and cortex²⁶⁷. SIRT1 overexpression prevents oxidative stress-induced apoptosis and increases resistance to oxidative stress through regulation of the FOXO family of forkhead transcription factors²⁶⁸. The only cytoplasmic sirtuin protein SIRT2, has been shown to increase in response to oxidative stress but promotes cell death through FOXO proteins²⁶⁹. SIRT3, a mitochondrial

protein, reduces oxidative stress through activation of superoxidase dismutase activity²⁷⁰. In a recent study it was found that SIRT3 mRNA expression is elevated in response to increased mitochondrial ROS production in primary mouse hippocampal cells and the SIRT3 over-expression increases neuronal lifespan²⁷¹. In AD transgenic mice SIRT3 expression was shown to mirror the pattern of A β deposition²⁷¹. The study also showed a significant increase in SIRT3 expression in the AD temporal cortex of human *post-mortem* brain tissue²⁷¹. SIRT6, like the founding member of the sirtuin family SIRT1, is a nuclear protein which is involved in oxidative-stress induced DNA repair through its activation of the PARP-1 DNA repair enzyme²⁷², (for a summary see Table 1.2 and Figure 1.6).

Table 1.2 The Role of the Sirtuin family in Calorie Restriction, Ageing and Neurodegeneration

Name	Location	Involvement in Calorie Restriction, Ageing and Neurodegeneration
SIRT1	Nucleus	<p>Suppresses amyloid production by promoting α-secretase cleavage of APP.²⁷³</p> <p>Ameliorates learning impairment and neurodegeneration in mouse models.²⁷⁴</p> <p>Induces the Notch pathway, involved in repair of neuronal damage in the brain.²⁷³</p> <p>Regulates proteins and genes involved in antioxidant response (FOXO3), apoptosis (p53) and anti-inflammatory response (NFκB)^{268 275 276 277 278}</p> <p>Modulates memory formation and synaptic plasticity. Activation of SIRT1 in brain enhances, and its deletion impairs, memory function and synaptic plasticity in mice²⁷⁹</p> <p>Reduction in SIRT1 is associated with accumulation of Aβ and tau in the cerebral cortex of AD patients^{280 281}</p> <p>Promotes feeding behaviour during dietary limited conditions including calorie restriction or fasting²⁸²</p> <p>Mouse KO: impaired cognitive abilities, decreased dendritic branching, length and complexity, reduced oxidised proteins and lipids in the brain, lower growth hormone levels, shortened lifespan^{279,283,284}</p>
SIRT2	Cytoplasm	<p>Appears to promote neurodegeneration as SIRT2 inhibition prevents α-synuclein-mediated toxicity in a Parkinson's disease model²⁸⁵</p> <p>A tubulin deacetylase which regulates cell division and differentiation and accumulates with age²⁸⁶</p> <p>Impairs neurite outgrowth and oligodendrocyte differentiation and promotes axonal degeneration^{287 288 289}</p> <p>Small molecule inhibitor of SIRT2 showed neuroprotection via cholesterol-reducing properties in a Huntington's disease model^{290 291}</p> <p>Upregulates in response to calorie restriction and oxidative stress, and</p>

		<p>promotes cell death under severe stress conditions via interaction with FOXO3a.²⁶⁹</p> <p>Involved in myelin formation²⁹²</p>
SIRT3	Mitochondria	<p>Protects against excitotoxic injury in neurons²⁹³</p> <p>Plays a role in CR-mediated reduction in oxidative stress and decreases reactive oxygen species by increasing activity of superoxide dismutase 2^{294 295}</p> <p>Variability of the SIRT3 gene may have a role in human longevity^{297 298}</p> <p>SIRT3 upregulates fatty acid oxidation and lowers ATP levels during fasting²⁹⁹</p> <p>Involved in the maintenance of mitochondrial function by preventing premature opening of the mitochondrial permeability transition pore³⁰⁰</p>
SIRT4	Mitochondria I Matrix	<p>Downregulates glutamate dehydrogenase activity, and controls insulin secretion in response to calorie restriction³⁰¹</p> <p>Negatively regulates fatty acid oxidation in combination with SIRT1³⁰²</p>
SIRT5	Mitochondria I Matrix	<p>SIRT5 promoter polymorphism is associated with a higher brain molecular ageing³⁰³</p> <p>Involved in regulation of the urea cycle during fasting and calorie restriction^{304,305}</p>
SIRT6	Nucleus	<p>Neuronal SIRT6 is involved in regulation of somatic growth and obesity prevention in mice³⁰⁶</p> <p>Involved in DNA double strand break repair following oxidative stress by inducing PARP1 activity³⁰⁷</p> <p>SIRT6 associates with telomeric chromatin and depletion of SIRT6 results in premature cellular senescence and telomere dysfunction^{308 309}</p> <p>Prevention of transforming growth factor-β-induced cell senescence in human epithelial cells³¹⁰</p> <p>SIRT6 genes suppress NF-kappaB signalling and thus can delay the ageing process and extend lifespan³¹¹</p> <p>SIRT6-knockout mice exhibit genomic instability, ageing-like phenotypes and die from hypoglycaemia by 4-5 weeks. Stem cells that are deficient in SIRT6 show genomic instability³¹²</p>
SIRT7	Nucleus	<p>SIRT7 overexpression in fibroblasts inhibits cell growth and proliferation and promotes cell cycle arrest³¹³</p> <p>Positive regulator of RNA polymerase I transcription³¹⁴</p> <p>SIRT7 deficient mice exhibit heart hypertrophy, inflammatory cardiomyopathy and a reduced lifespan³¹⁵</p>

Interest in sirtuins increased greatly after the discovery that the sirtuin gene, Sir2 (SIRT1 being the equivalent in mammals) extends yeast lifespan up to 30 %³¹⁶. A similar effect was found in nematodes and flies and it was thought the effect may occur through a pathway related to caloric restriction^{317,318}. Recent work however suggest that the effects on longevity may not be as strong as were observed in the early studies, as controlling for genetic background removed any effects on longevity³¹⁹. The sirtuin system is strongly influenced by caloric restriction (CR), which refers to a reduction in calorie intake without malnutrition³²⁰. CR has a wide range of benefits in humans³²¹⁻³²³ and life span extension in many species from yeast, fruit flies, nematodes, rodents to primates³²⁴⁻³²⁷. Furthermore, CR for 3 months was found to improve memory functions in the elderly³²⁸. CR is also known to modulate neuroinflammation and oxidative stress in various animal models³²⁹⁻³³¹.

The mechanism by which CR increases life span is still unclear. Some theories include reduced cellular divisions, reduced metabolic rate, reduced production of ROS and hormesis³³²⁻³³⁵. Hormesis is used to describe the beneficial actions resulting from the response of an organism to a low-intensity biological stressor³³⁴. The hormesis theory of CR proposes that diet imposes a low-intensity biological stress on the organism, which causes a defence response that helps protect it against the causes of ageing³³⁴. Therefore, it is highly likely that CR places the organism in a defensive state, and enables it to survive adversity, leading to improved health and life span.

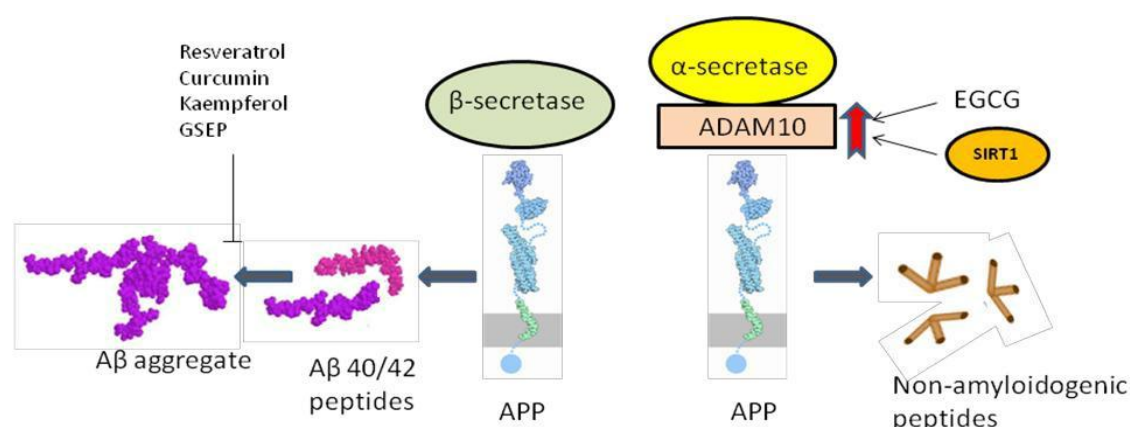
Evidence suggests that some of the beneficial effects of CR occur through its influence on sirtuins. The functions of mitochondrial sirtuins suggest that they control activity of several metabolic enzymes and play a crucial role in metabolic adaptation to dietary conditions, such as CR and fasting³³⁶ (Table 1.2). CR does not extend lifespan in SIRT1-deficient mice, suggesting that CR works via activation of SIRT1^{327,337}. Conversely, transgenic mice overexpressing SIRT1 display a number of phenotypic features, such as increased metabolic activity, glucose tolerance, and reduced body weight and cholesterol levels³³⁷. The ability of SIRT1 to mimic the anti-ageing effects of CR is most likely linked to its regulation of various proteins and genes involved in oxidative stress, inflammation, amyloidogenesis and synaptic plasticity (Table 1.2 and Figure 1.6).

CR prevents A β neuropathology in animal models of AD and modulation of SIRT1 expression or activity may be a mechanism by which CR influences AD-type neuropathology^{281,327,338}. In one study 30% CR resulted in significantly lower levels of A β (1-40) and A β (1-

42) in the temporal cortex of Squirrel monkeys relative to control fed monkeys. The cortical A β levels were inversely correlated with SIRT1 protein concentrations in the same brain region, and there was also a selective elevation of α - but not β - or γ -secretase activity³²⁷. As mentioned previously, the cleavage of the membrane-bound APP leads to a range of protein fragments that have a role in AD pathogenesis³³⁹. Cleavage of APP by β -secretase leads to the formation of APPs- β , and together with γ -secretase leads to the generation of the A β peptides (1-40) and (1-42). The latter is thought to be the main toxic component in AD³³⁹. If

APP is processed by α -secretase, then the formation of these pathogenic peptides is prevented, and instead a fragment APPs- α that is associated with a neuroprotective effect is generated^{340,341}. SIRT1 is able to modulate APP processing by activating the expression of the α -secretase gene ADAM10, thereby reducing brain levels of A β (1-42) as well as A β (1-40)³⁴⁰ (Figure 1.5). Moreover, deacetylation of the retinoic acid receptor β (RAR β) by SIRT1 can induce transcription of the ADAM10 gene and suppress the production of the neurotoxic A β (1-42) peptide³⁴⁰. There is however, no published literature to date on the effects of CR or sirtuin activation in AD using human clinical trials.

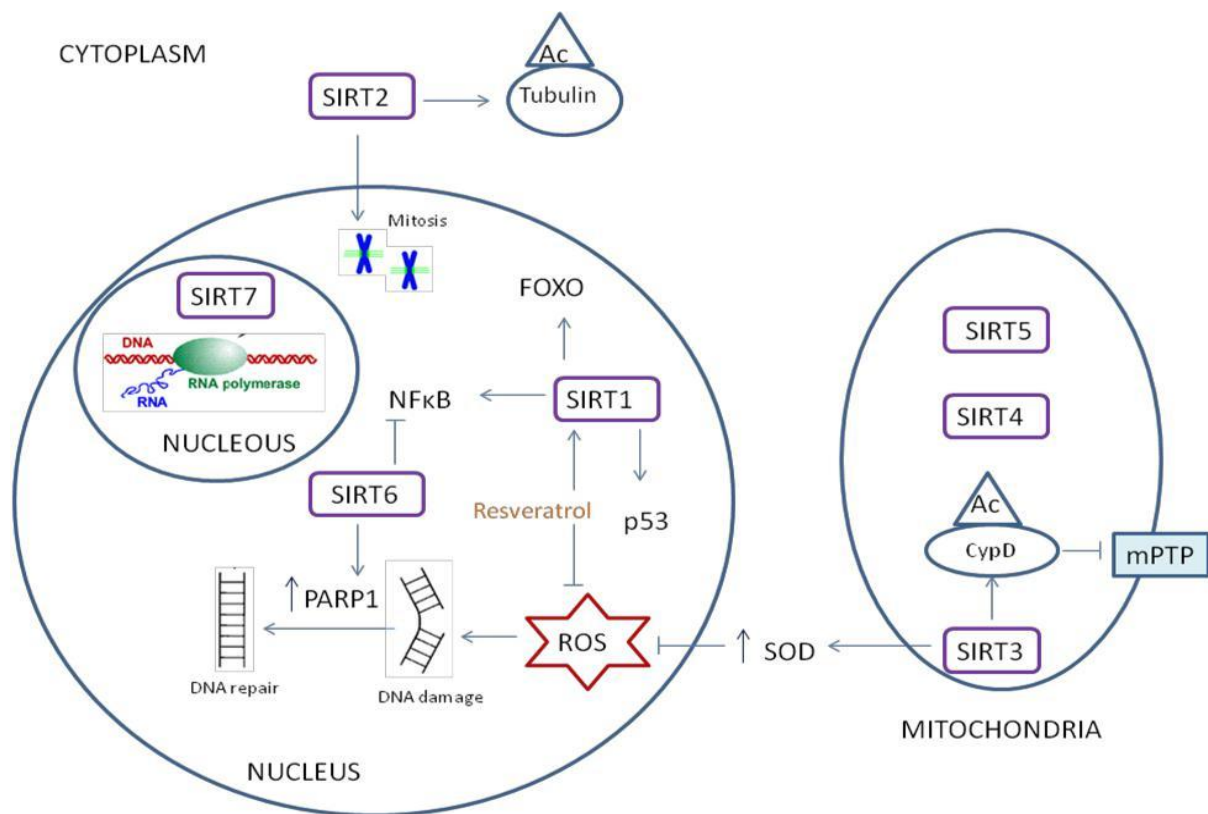
Figure 1.6: Influence of SIRT1 and polyphenols on APP processing and amyloid formation. SIRT1 and the green tea polyphenol (-)-epigallocatechin-3-gallate (EGCG) activate ADAM10 and thus enhance α -secretase APP processing leading to the generation of non-amyloidogenic peptides. Resveratrol is able to selectively remodel toxic amyloid aggregates into non-toxic species. Other polyphenols such as curcumin, kaempferol and grape seed extract polyphenols (GSEP) also have the ability to reduce A β levels in the brain.



SIRT1 induces a neuroprotective effect through its interaction with FOXO proteins, p53 and NF κ B^{268,275,277}. SIRT1 is also directly activated by resveratrol. SIRT2 is involved in regulation of the cell cycle as well as neurite outgrowth and axonal degeneration, possibly through its ability to deacetylate tubulin^{269,286}. The cellular effects of mammalian sirtuins are broad-ranging since they are found in multiple organelles, can translocate across membranes and between organelles and are likely involved in active responses to changing cellular environments. However the mitochondria have more sirtuins than any other cellular compartment, which may reflect an important link between cellular energy metabolism and longevity since mitochondria are the primary cellular organelles responsible for energy production. SIRT3, 4, and 5 are expressed only in mitochondria. SIRT3 appears to be the predominant mitochondrial deacetylase and to play an important role in several mitochondrial pathways in all tissues³³⁶. The targets of SIRT3 include proteins involved for example in substrate utilization, electron transfer, and redox homeostasis³⁴². SIRT3 reduces oxidative stress by increasing superoxidase dismutase activity. It also deacetylates cyclophilin D (which regulates opening of the mPTP) and thus prevents age-related increase in mitochondrial swelling due to increased opening of the mPTP. In response to caloric restriction or fasting, SIRT3 deacetylates a set of mitochondrial proteins, resulting in

activation, inhibition, and allosteric modification of protein functioning²⁷⁰. Unlike other sirtuins, SIRT4 does not possess deacetylase activity, but it is instead an ADP-ribosyltransferase³⁴³. It is activated in response to amino acids, downregulating insulin secretion by inhibiting mitochondrial glutamate dehydrogenase 1 activity. SIRT4 is also involved in regulation of fatty acid oxidation and mitochondrial gene expression in liver and muscle³⁴⁴. SIRT5 is found in the cytosol and mitochondria however, the targets of SIRT5 are not yet well identified. It has been shown to regulate energetic flux through glycolysis and also protein malonylation³⁴⁵. The deacetylase activity of SIRT5 is weak, and its main targets are succinyl and malonyl groups. In addition to glycolysis, it is likely involved in many other metabolic pathways, including the urea cycle, where it activates detoxification of excess ammonia that may accumulate during fasting³⁰⁴. In a recent study using a SIRT3-/- mouse knockout model relevant for neurological disease, hippocampal SIRT3 expression was found to be enhanced by running wheel exercise³⁴⁶. The striatal and hippocampal neurons of mice lacking SIRT3 showed increased vulnerability in pathological conditions. Another study showed that overexpression of SIRT3 protected against age-related hearing loss in mice via enhancing the mitochondrial glutathione antioxidant defense system, suggesting a neuroprotective role for SIRT3³⁴⁷. SIRT6 is involved in DNA repair following oxidative stress through activation of the DNA repair enzyme PARP-1³⁰⁷. SIRT7 is thought to be involved in RNA transcription as it activates RNA polymerase 1 transcription³¹⁴.

Figure 1.7 Cellular Roles/Potential Roles and mechanisms of action of Sirt1-7



1.11 Polyphenols, sirtuins and ageing

The most studied polyphenol which shows effects on the sirtuin family of proteins is resveratrol which is found in its highest levels in grape seed and skin as well as in red wine (see Table 1.3 for details). Apart from its free radical scavenging and antioxidant properties, resveratrol has many of the same benefits as calorie restriction. Resveratrol is associated with neuroprotective effects³⁴⁸⁻³⁵⁰, and other beneficial effects such as: maintenance of mitochondrial integrity, reduction of insulin-like growth factor-1 expression, activation of SIRT1, and increased longevity in some animals models^{207,351-358}, though life span effects are controversial³⁵⁹⁻³⁶¹. Epidemiological evidence suggests that moderate red wine consumption, which is rich in resveratrol, reduces the risk of dementia³⁶².

Resveratrol has also been shown to improve outcomes after ischemic episodes in the heart and brain of mice by a SIRT1-mediated process^{363,364}. Resveratrol strongly stimulates SIRT1 deacetylase activity in a dose-dependent manner by increasing its binding affinity to both the acetylated substrate and NAD^+ ³⁶⁵. Whether resveratrol is a direct or indirect activator of SIRT1 remains controversial^{366,367}. Resveratrol and CR have also been shown to modulate

mitochondrial sirtuins^{270,347,367,368}. Resveratrol-fed rats showed increased expression of SIRT3 and SIRT4 in the heart compared to control-fed mice³⁶⁹, however the opposite effect was seen in the liver of a zebrafish model³⁷⁰. Resveratrol also increased expression of SIRT3 in adipocytes³⁷¹. Resveratrol mediated changes to sirtuin expression in the brain have yet to be intensively studied. Investigation of polyphenolic sirtuin-activating compounds are thought to hold promise for enhancing longevity^{207,372}.

Table 1.3: Influence of Polyphenols on Sirtuins and Pathways involved in Ageing and AD

Polyphenol	Fruit/Vegetable	Effect on Sirtuins	Influence on AD	Influence in Ageing	Reference
Resveratrol	Red Grapes (1.5-7.8ug/g), Red wine (1.98-7.13mg/L),	Increased SIRT1,SIRT2, SIRT3, SIRT4 and SIRT7	Selectively remodels toxic amyloid aggregates; reduces A β plaques in animal models;	CR mimetic; increases longevity in a variety of organisms from yeast to mammals;	198-205
Quercetin	Black and Green Tea (2-2.5ug/g) Apples (0.4ug/g) Red Onion (0.2ug/g)	Increased SIRT1	Reduces A β -mediated cytotoxicity and OS	Extends life span in worms and yeast	206-210
Curcumin	Tumeric (50mg/g)	Increased SIRT1	Reduces A β levels in AD mice; enhances memory in AD rat model	Extends life span in flies and mice	211-215
Kaempferol	Tea, Broccoli, Cabbage, Beans, Leek, Tomato, Berries, Grapes, Apple	Increased SIRT3	Reversed A β -induced impaired performance of mice in a maze test; inhibit A β formation and toxicity	Protective effects against OS-induced cytotoxicity;	182,216-219
Catechin, gallic acid, gentisic acid, chlorogenic acid,	Bitter Melon	Increased SIRT1 and SIRT3	Attenuates OS and neuroinflammation		220,221

epicatechin					
Procyanidins, phloridzin and other unidentified phenolics	Apple	No extension of lifespan in worms lacking Sir2.1; increase Sirt1 activity in yeast	Not known	Extend lifespan of <i>Drosophila</i> flies and in worms; upregulates superoxide dismutase and catalase genes	222-224
Astragaloside, astragalus saponin I	Astragalus root	Not known	Prevents amyloid induced memory and neuronal loss in AD mouse model	Reduced DNA damage after OS, increased telomere length in mice fibroblasts	225-229
EGCG, Catechins	Green tea	Increase Sir2 activity in yeast	Neuroprotective; Inhibits formation of fibrillar A β ; metal chelating properties	Increases lifespan in worms, flies and mice and delays memory regression in mice models of ageing	171,186,196,230-235
Quercetin, kaempferol, catechin, rutin, naringin	Centella Asiatica	Not known	Cognitive enhancing effects; reduces brain A β levels; protective against A β -induced neurotoxicity;	reduced markers of oxidative stress in the brain, increases activity of antioxidant enzymes	236-242
Ginsenoside Rbl	Ginseng	Not known	Inhibit β -secretase activity; protect against A β toxicity, reduce ROS production and apoptosis; reduced tau phosphorylation; anti-inflammatory effect in the brain of AD rat model	Improves cognition in senescence-accelerated mice; improves memory loss in mice; ginseng intake decreased mortality in older males	243-249
Proanthocyanidins	Blueberry	Not known	Suppress OS; improves learning and memory in	Increase lifespan in worms	250-255

mice;				
Catechins, Proanthocyanidins, Tannins, Resveratrol	Grape seed	Not known	Inhibit abnormal protein aggregation and enhance cognition	Increases telomere length in mice; increase lifespan in Drosophila and mice ²⁵⁶⁻²⁶⁰
Procyanidins	Cocoa	Not known	Increased resistance to oxidative stress in yeast and worms; improved cognition	Increase lifespan of worms and rats ^{261,262}
α-mangostin	Mangosteen	Not known	Inhibits Aβ aggregation and Aβ-induced cytotoxicity ²⁶³ ²⁶⁴	

A variety of polyphenols (or foods rich in polyphenolic compounds) have been investigated for their effects on AD and longevity (Table 1.3). Interestingly, many of these compounds influence sirtuins through direct or indirect pathways. For example, in a recent study, the functional food, bitter melon was found to attenuate oxidative stress and neuroinflammation in mice on a high fat diet³⁷³. Functional foods are foods or food components which beyond providing basic nutritional needs, also have physiological/pharmacological benefits or reduce the risk of chronic diseases³⁷⁴. Bitter melon was also found to regulate sirtuin protein and mRNA expression. A high fat diet significantly reduced SIRT1 mRNA expression by 20%, and brain SIRT1 protein levels were reduced by 25% in C57BL/6 female mice³⁷³. Feeding of bitter melon normalised both. Interestingly, bitter melon not only normalised SIRT3 levels but also up-regulated SIRT3 mRNA by 20%³⁷³. Bitter melon also attenuated oxidative stress and neuroinflammatory marker levels caused by the high fat diet. The bitter melon extract contains a variety of polyphenols including gallic acid, gentistic acid, chlorogenic acid and epicatechin, but the most abundant polyphenol isolated was catechin³⁷³. Catechins are also most abundant in tea, cocoa and berries and daily consumption of catechin increases life span and delays memory regression in animal models of ageing^{375,376}.

Another traditional food, the herb, *Centella asiatica* has been reported to have a variety of beneficial effects on A β -mediated toxicity, and to promote longevity²³⁷. It contains numerous polyphenols including quercetin, kaempferol, catechin, rutin and naringin, some of which are potent antioxidants and have demonstrated effects on sirtuins (Table 1.3). Therefore *C.asiatica* may have the ability to modulate the effects of oxidative stress in the brain directly, and through regulation of sirtuin activity since several of its polyphenols influence the activity and expression of sirtuins. Most of the work to date has focused on SIRT1 as it is the mammalian homolog of yeast Sir2, which was the first organism in which sirtuin functions were studied. SIRT1 was also the first sirtuin which was shown to be activated by a polyphenol, namely resveratrol. Future investigation into the interaction between sirtuins (especially SIRT2-7) and polyphenols may help determine which polyphenols are specific to which sirtuin and which if any have a general effect on the whole family of proteins.

1.12 Protective effects of polyphenols against inflammation

Excessive inflammation is considered a critical factor in the pathogenesis of AD. The AD brain has an increased expression of pro-inflammatory cytokines such as interleukin-1 and tumour necrosis factor and evidence of microglial activation³⁷⁷. Several inflammatory genes are associated with an increased risk of AD, and epidemiological studies on AD patients using non-steroidal anti-inflammatory drugs suggest some benefits³⁷⁸. Inflammation is also another source of oxidative stress as superoxide and nitric oxide are released.

The anti-inflammatory activity of phenolic compounds has been demonstrated in a number of *in vitro* and *in vivo* studies³⁷⁹. *Polyphenols* may affect inflammation not only as antioxidants, but also as modulators of inflammatory redox signalling pathways. Polyphenols can work as modifiers of signal transduction pathways to elicit their beneficial effects³⁷⁹. These compounds express anti-inflammatory activity by modulating the expression of pro-inflammatory genes such as cyclooxygenase, lipoxygenase, nitric oxide synthases and several important cytokines, mainly acting through nuclear factor-kappaB and mitogen-activated protein kinase signalling³⁷⁹⁻³⁸⁴.

In a transgenic mouse model of AD, treatment with pomegranate extract was found to reduce microgliosis and A β deposition. Significant behavioural improvements were also seen and collated with decreased tumor necrosis factor α concentration and lower nuclear factor of activated T-cell activity in the pomegranate-fed mice. Pomegranate polyphenols punicalagin and ellagic acid were also shown to decrease A β -induced tumor necrosis factor α in cultured mouse microglia³⁸⁵.

Polyphenols may also modulate programmed cell death pathways. Resveratrol, EGCG and luteolin have been shown to significantly inhibit the activation of caspase-3 and are able to modulate mitogen-activated protein kinases known to play an important role in neuronal apoptosis³⁸⁶.

1.13 Protective effects of polyphenols on mitochondrial dysfunction

Changes to the mitochondria seem to be another pathological characteristic of AD. The AD brain shows a reduction in mitochondrial enzyme activities including dehydrogenase enzymes such pyruvate dehydrogenase, and cyclooxygenase enzymes³⁸⁷. The cause is

unknown, although OS is thought to play a role. Furthermore the number of intact, normal appearing mitochondria has been shown to decline in the AD brain, particularly in hippocampal neurons³⁸⁷. Elevation of intracellular A β levels may also potentially alter mitochondrial function and lead to increased reactive oxygen species generation³⁸⁸.

Polyphenols have also been proposed to protect mitochondrial function, as has been shown for quercetin, rutin and resveratrol³⁸⁹. Apple peel polyphenols have similar protective effects by preventing mitochondrial complex 1 inhibition³⁹⁰. Grape seed extract has been shown to protect the enzyme activities of the mitochondrial respiratory electron transport chain (complexes I and II) and pyruvate dehydrogenase against oxidative stress³⁹¹. EGCG and luteolin have been found to restore amyloid-induced mitochondrial dysfunction by reducing reactive oxygen species production and normalising mitochondrial membrane potential and cellular ATP levels³⁹². Moreover, polyphenols have also been reported to exert their anti-apoptotic action by inhibiting apoptosis-inducing factor release from mitochondria, thus providing a new mechanism of action for polyphenols³⁹³.

1.14 Involvement of polyphenols in telomere maintenance

The role of a number of polyphenols in the maintenance of telomere length has been investigated (Table 1.3). Telomeres are specialised nucleoprotein structures that protect the end of eukaryotic chromosomes from unscheduled DNA repair reactions and degradation. Due to the intrinsic inability of the DNA replication machinery to copy the end of linear molecules, and the endogenous DNA end-degrading activity, telomeres become progressively shorter after every cell division cycle. When a critical number of replications are reached, the cells enter senescence³⁹⁴ or the end of their replicative ability (Hayflick limit).

In humans, several studies have described an inverse correlation between telomere length and age or age-related disease³⁹⁵⁻³⁹⁷. Telomere length shortens with normal ageing, life stress, inflammation and chronic diseases³⁹⁴ and telomere dysfunction is linked to the pathogenesis of age-related diseases including AD^{396,398}. Various nutrients such as nicotinamide and vitamins A, D, C and E are positively associated with telomere length³⁹⁹⁻⁴⁰² via mechanisms that reflect their role in cellular functions, including DNA repair and chromosome maintenance, DNA methylation, inflammation, oxidative stress modulation and activity of the enzyme telomerase which repairs chromosome ends by adding telomeric repeat subunits.

Healthy lifestyles and diets are positively correlated with telomere length. Changes in diet and lifestyle can modulate telomerase activity in peripheral blood mononuclear cells, although it is not yet clear if this translates to changes in telomere length⁴⁰³.

Resveratrol has been shown to induce telomere maintenance factor WRN helicase⁴⁰⁴. Another study showed that habitual tea drinkers have longer telomeres in peripheral blood cells than those who drink tea less often⁴⁰⁵. This may possibly be due to the anti-inflammatory effect of tea polyphenols⁴⁰⁶. Similarly, the dietary administration of grape seed polyphenols to mice resulted in a trend for longer telomeres compared with controls²⁵⁸. It is clear that diet and lifestyle can together play a pivotal role in influencing inflammation, oxidative stress and psychological stress, all of which cause telomere attrition. A healthy lifestyle with a diet rich in fruits and vegetables combined with exercise and lower body mass index is indeed associated with longer telomeres⁴⁰⁷. EGCG, quercetin and carvediol were shown to prevent telomere shortening and oxidative stress markers in rat cardiomyocytes after cardiac hypertrophy⁴⁰⁸. Two isomers, 4-Hydroxy-5-hydroxymethyl-[1,3]dioxolan-2,6'-spirane-5',6',7',8'-tetrahydro-indolizine-3'-carbaldehyde (HDTIC-1 and HDTIC-2) extracted from *Astragalus membranaceus* root have been shown to extend lifespan of human fetal lung fibroblasts⁴⁰⁹. Cells pre-treated with these compounds show a significant reduction in DNA damage after exposure to oxidative stress. The authors hypothesised that the *Astragalus* root extract related delay in replicative senescence was due to the combined effects of: (1) reduction in telomere shortening rate, (2) reduced DNA damage and (3) improvement in DNA repair⁴⁰⁹. A small-molecule activator of telomerase known as TA-65 has been purified from the root of the *Astragalus*, and is capable of increasing average telomere length and decreasing the percentage of critically short telomeres, and attenuating DNA damage in mouse fibroblasts⁴¹⁰.

More recently, SIRT1 was reported to be a positive regulator of telomere length *in vivo* and to attenuate age related telomere shortening, an effect dependent on telomerase activity⁴¹¹. By contrast, another study found that SIRT1 inhibition was associated with increased telomerase activity in human cells⁴¹². These findings link SIRT1 to telomere biology and global DNA repair. Furthermore this effect does not appear to be specific to SIRT1 alone. SIRT6 is associated with telomeric chromatin, and depletion of SIRT6 has been shown to result in premature cellular senescence and telomere dysfunction³⁰⁸.

1.15 Therapeutic Potential of Polyphenols and Sirtuin Modulation

As the human population continues to age, interventions that improve the quality of life and delay the onset of age-related diseases are highly desirable. Polyphenols are candidates for such interventions through their diverse biochemical roles including free radical scavenging, protein homeostasis, metal chelation, telomere maintenance and stimulation of sirtuins. Their potent effects in combination with little or no known toxicity may give them a therapeutic advantage. In the past, clinical trials using vitamins and antioxidants have frequently had equivocal outcomes in the treatment of AD. One explanation for the failure of single drugs or natural compounds in AD is that this disorder has multiple aetiologies, involving various pathological and molecular events occurring in parallel or sequentially. This has lead to the assumption that a single drug targeting two or more active neuroprotective moieties or a combination of compounds, targeting multiple pathological aspects of the disease, may offer a superior therapeutic benefit over a drug targeting one pathway alone. For example, a treatment regime using a mixture of polyphenols which together exhibit antioxidant, metal chelating, anti-amyloidogenic and sirtuin activation properties may prove to be superior. Initial studies using polyphenol combination therapy or “cocktails” have shown some promising preliminary results^{413,414}.

Another important issue is the bioavailability of such compounds. Most polyphenols have poor bioavailability following oral ingestion⁴¹⁵. Those found in food take the form of glycosides, esters or polymers which cannot be absorbed directly and therefore must be hydrolysed by microflora or enzymes of the small intestine¹⁵⁹. A further confounder for the central nervous system is that polyphenols cannot pass easily through the blood brain barrier. There are however, various strategies currently under investigation to improve bioactivity. It has been found that some polyphenols can specifically modify metabolic and transport processes that govern bioavailability⁴¹⁵. Therefore, specific synergistic combinations and interactions could be designed to improve entry into the brain. Another promising method is the use of nanoparticle carriers coupled to polyphenols⁴¹⁶. Brain permeable nanoparticles may be used to enhance entry of poorly absorbed phenolic compounds into the brain^{117,417,418}. Creation and administration of EGCG nanolipidic complexes were found to double the oral bioavailability of EGCG in male Spague-Dawley rats and also improved the EGCG’s ability to enhance α -secretase activity *in vitro*⁴¹⁹. Cocrystallisation is another technique which could increase solubility and thus bioavailability of polyphenols. This procedure used

with quercetin has shown promising results with cocrystals of quercetin showing significant increases in solubility and oral bioavailability⁴²⁰.

AD is a multifactorial disease involving a variety of different pathways including oxidative stress, inflammation, amyloid aggregation and mitochondrial dysfunction. Furthermore the emerging view that polyphenols may exert a variety of modulatory actions which influence the pathogenesis of AD has brought attention to functions beyond their usual antioxidant activities. Sirtuins are a class of proteins that have been linked to longevity, ageing and neurodegeneration. Investigating the role of sirtuins and other related pathways may lead to the development of effective treatment regimes for AD.

1.16 Aims and Rationale

The overall aim was to gain insight into mechanisms, risk and protective factors for MCI and AD. Sirtuins have been shown to play important roles in ageing and neurodegeneration however the quantification of these proteins in the CNS is limited. Parabiosis experiments show that plasma carries factors which vary with age and disease, and can have an impact when introduced into other living systems. Here we have explored: (1) the role of mammalian sirtuins in ageing and AD, since these proteins may have a role in cellular health and longevity, (2) the impact of MCI and AD plasma on neuronal cell line health, viability and proteomic expression, (3) how the constituents of MCI and AD plasma vary from controls and (4) the effect of polyphenols on a specific hallmark mechanisms in AD such as A β 1–42 aggregation and oxidative stress.

The specific foci of each chapter were as follows:

Mass spectrometry has been used to successfully assay metabolites of SIRT1 activator drugs in plasma and urine, but to date has not been used to quantify protein levels directly. Mass spectrometry has a great advantage over the conventionally used antibody based methods, such as western blotting, in that it offers greater specificity, linearity, reproducibility and typical limits of quantification down to the low fmol range. It also removes some of the antibody specificity issues that are associated with methods such as western blotting and ELISA, as peptides unique to each protein are measured. Targeted mass spectrometry may provide a more specific and sensitive method to detect and quantify sirtuin expression at the protein level, providing a tool

for comprehensive sirtuin protein expression analysis. Therefore one of the aims of this project was to develop a targeted mass spectrometry method using multiple reaction monitoring (MRM) to quantify the seven human sirtuins at the protein level and to apply the assay to CNS biological samples.

The second aim was to apply this mass spectrometry based assay to quantify levels of sirtuins in a variety of biological samples such as primary and cancer brain cells, animal tissues, human *post mortem* brain tissue, CSF and plasma.

The third aim was to investigate changes to sirtuin levels during ageing and neurodegeneration by measuring sirtuins in CSF from control patients over an age range of 30-65yrs and also in control and AD *post mortem* brain tissues.

Since previous studies indicate that AD plasma may contain oxidative stress markers as well as cytotoxic factors, the fourth aim of the project was to investigate the effect of the addition of pooled control, MCI and AD plasma from 20 individuals each on a microglial cell line by measuring cell viability, proliferation and mitochondrial function following 48 hour treatment with non heat-inactivated plasma and plasma in which complement proteins had been deactivated.

The fifth aim was to complete a proteomic analysis using iTRAQ quantitative proteomic analysis of cell extracts exposed to plasma from each group to investigate possible plasma protein alterations unique to MCI or AD, and to detect any protein aberrations within the cells treated with the plasma and to correlate these finding to cell viability and mitochondrial function assays measured *in vitro*.

It has previously been shown that transition metal ions such as iron, zinc and copper have the ability to enhance aggregation of A β and polyphenols such as resveratrol, curcumin and EGCG can disrupt this process. Therefore the final aim was to investigate the effect of various polyphenols and metals on amyloid aggregation using electron microscopy, and also to detect any neuroprotective effects of polyphenol treatment on cell viability and mitochondrial energy metabolism using a neuronal cell line treated with aggregated “aged” amyloid.

Chapter 2

Application of Targeted Mass Spectrometry for the Quantification of Sirtuins in the Central Nervous System

Majority of the content of this chapter has been published:

Jayasena T, Poljak A, Braidy N, Zhong L, Rowlands B, Muenchhoff J, Grant R, Smythe G, Teo C, Raftery M, Sachdev P (2016). *Application of Targeted Mass Spectrometry for the Quantification of Sirtuins in the Central Nervous System. Scientific Reports 2016 Oct 20;6:35391.*

See Appendix for full publication

2.1 Introduction

Sirtuins are a class of proteins that possess histone deacetylase or mono-ribosyltransferase activity and play critical roles in cell survival in response to oxidative stress and caloric restriction (CR) regimes⁴²¹. In mammals, seven sirtuins (SIRT1-7) have been identified. All mammalian sirtuins contain a conserved NAD-binding and catalytic domain, but differ in their N and C-terminal domains. They have different specific substrates including histones, transcriptional regulators and enzymes. They localise to cell compartments which regulate cellular structure, metabolism and gene expression, including the cytoskeleton (SIRT2), mitochondria (SIRT3, SIRT4 and SIRT5) and nucleus/nucleolus (SIRT1, SIRT6 and SIRT7), and play important roles in health and disease^{421,422}. SIRT1 is the best characterized and has the broadest substrate specificity. Sirtuins have emerged as critical modulators of metabolic adaptive responses, and their activities have been linked to ageing and multiple diseases, from metabolic abnormalities to neurodegeneration.

Sirtuins can affect reactive oxygen species (ROS) production and promote resistance to their damaging effects. Oxidative stress has been shown to decrease SIRT1 expression in the hippocampus and cortex, possibly by direct degradation by ROS⁴²³. SIRT1 overexpression prevents oxidative stress-induced apoptosis and increases resistance to oxidative stress through regulation of the FOXO family of forkhead transcription factors⁴²⁴. The cytoplasmic sirtuin protein SIRT2, has been shown to increase in response to oxidative stress but promotes cell death through FOXO proteins²⁶⁹. SIRT3, a mitochondrial protein, reduces oxidative stress through activation of superoxidase dismutase²⁷⁰. SIRT6 and SIRT7, like the founding member of the sirtuin family SIRT1, are nuclear proteins involved in oxidative-stress induced DNA repair through activation of the PARP-1 DNA repair enzyme.

SIRT1 is expressed in the adult brain, in the cortex, hippocampus, cerebellum, and hypothalamus, and in lower levels in the white matter⁴²⁵. Among the brain cell types, SIRT1 is predominantly expressed in neurons and viewed as a nuclear protein⁴²⁵. The mRNAs for all seven sirtuins have been identified in mouse brain tissue and also neural stem cells⁴²⁶. SIRT1, SIRT2 and SIRT3 have also been detected in human serum, and levels were shown to decline with age and were linked to frailty^{427,428}. SIRT3 is elevated at both the mRNA and protein levels in Alzheimer's disease (AD) *post mortem* brain tissue compared to controls²⁷¹.

The most common techniques currently utilised for detecting a change in sirtuin levels at the mRNA or protein level are PCR and western blotting, respectively (Table 2.1). Other studies

have used methods such as immunohistochemistry, surface plasmon resonance and ELISA assays (Table 2.1). The majority of these methods are only semi-quantitative with moderate sensitivity, use antibodies which may not have sufficient specificity or detect expression at the mRNA level which may not reflect protein expression. Furthermore, there is no current assay which detects multiple sirtuins simultaneously.

Table 2.1: Expression of sirtuins in the CNS and current methods used for analysis

Name	Areas detected in CNS	Function in CNS	Techniques used
SIRT1	Human hippocampus and cortex ⁴²⁵ . Has also been detected in human serum at approx 8.16ng/μl ⁴²⁷ . Mouse neural stem cells and adult mouse brain ^{42b} . Porcine brain ⁴²⁹ .	Modulates memory formation and synaptic plasticity. Reduces with age in mice. Metabolic sensor.	TR-qPCR ⁴²⁵ , immunohistochemistry ⁴³⁰ , western blotting, surface plasmon resonance and ELISA ⁴²⁷ .
SIRT2	Mouse neural stem cells and adult mouse brain ^{42b} . Porcine brain ⁴²⁹ . Human serum ⁴²⁸ .	Inhibitor of microglia-mediated inflammation and neurotoxicity ⁴³¹ . Impairs neurite outgrowth and oligodendrocyte differentiation. Involved in myelin formation.	Mouse knockouts ⁴³¹ , western blotting.
SIRT3	Cortex, Hippocampus and Cerebellum ²⁷¹ . Mouse neural stem cells and adult mouse brain ^{42b} . Porcine brain ⁴²⁹ . Rat brain. Human serum ⁴²⁸ .	Responses to oxidative stress and involved in maintenance of mitochondrial function.	Western blotting and qPCR ²⁷¹ .
SIRT4	Mouse neural stem cells and adult mouse brain ⁴²⁶ . Porcine brain ⁴²⁹ . Rat cortical cells and brain tissue ⁴³² .	Regulation of glial development ⁴³² ; involved in glutamate transport and protective role against excitotoxicity ⁴³³ .	qPCR, western blotting and immunofluorescence ^{429,432}
SIRT5	Mouse neural stem cells and adult mouse brain ⁴²⁶ . Porcine brain ⁴²⁹ .	SIRT5 gene polymorphism may promote molecular brain ageing and be a risk factor for mitochondrial dysfunction-related diseases ⁴³⁴ .	qPCR ⁴²⁹
SIRT6	Mainly localised in the nucleus in the cortical layers ⁴³⁵ . Mouse neural stem cells and adult mouse brain ^{42b,43b,437} . Rat brain. Porcine brain ⁴²⁹ .	Regulator of somatic growth by modulating neural chromatin and gene activity ^{43b} . Modulated DNA repair in the brain ⁴³⁸ . Suppresses proinflammatory gene expression.	Brain specific mouse knockout models and primary brain cell models ^{436,438,439} ; immunohistochemistry ⁴³⁵ ; western blotting, immunofluorescence ⁴³⁷ .
SIRT7	Mouse neural stem cells and adult mouse brain ^{42b} . Porcine brain ⁴²⁹ .	Positive regulator of RNA polymerase I transcription.	Mouse knockout ^{43b} .

Quantitative expression analysis of mammalian sirtuin proteins (especially SIRT2-7), across cell and tissue types is limited in the current literature. Previous studies have shown an increase in SIRT3 in AD *post-mortem* brain tissue using western blotting for protein expression and multiplex qPCT to assay SIRT3 mRNA levels²⁷¹. Both SIRT3 protein and mRNA were shown to be significantly elevated in the AD group²⁷¹. Another recent paper detected SIRT1 in human serum samples using western blotting, surface plasmon resonance and ELISA to measure SIRT1 protein levels⁴²⁷. SIRT1 declines with age and is more dramatically reduced in MCI and AD patients compared to age matched controls, suggesting that SIRT1 may warrant further investigation as a potential plasma biomarker for AD⁴²⁷. SIRT1 and SIRT3 levels in serum were found to be significantly lower in frail subjects as compared to the non-frail⁴²⁸. Another study reported a decrease in SIRT1 and SIRT2 mRNA levels using quantitative real time PCR in the primary motor cortex of human *post-mortem* amyotrophic lateral sclerosis brain tissue⁴⁴⁰.

Mass spectrometry has been used to successfully assay metabolites of SIRT1 activator drugs in plasma and urine⁴⁴¹, but to date has not been used to quantify protein levels directly.

Mass spectrometry has a great advantage over the conventionally used antibody based methods, such as western blotting, in that it offers greater specificity, linearity, reproducibility and typical limits of quantification down to the low fmol range. It also removes some of the antibody specificity issues that are associated with methods such as western blotting and ELISA, as peptides unique to each protein are measured. Targeted MRM based mass spectrometry may provide a more specific and sensitive method to detect and quantify sirtuin expression at the protein level, providing a tool for comprehensive sirtuin protein expression analysis. The aim of this study was to develop a targeted mass spectrometry method using multiple reaction monitoring (MRM) to quantify the seven human sirtuins at the protein level and to apply the assay to CNS biological samples.

Methods

Selection of target sirtuin peptides

Recombinant protein standards were purchased for seven human sirtuins (Cayman Chemical, USA), and 5 µg of each was run by 1D SDS-PAGE gel and colloidal coomassie stained. Sirtuin bands were excised, trypsin digested overnight followed by LC-MS/MS analysis on a

QToF Ultima API hybrid tandem mass spectrometer (Micromass, UK) as previously described⁴⁴²⁻⁴⁴⁴.

Digested peptides were separated by nano-LC using a Cap-LC autosampler system (Waters, USA). Samples (5 μ l) were concentrated and desalted onto a micro C18 precolumn (500 μ m x 2 mm, Michrom Bioresources, Auburn, CA) with H₂O:CH₃CN (98:2, 0.05% HFBA) at 15 μ l/min. After a 4 min wash, the pre-column was automatically switched (Valco 10 port valve, Houston, TX) into line with a fritless nano column (75 μ m x ~12 cm) containing Magic C18 (~10cm, 200 \AA , Michrom). Peptides were eluted using a linear gradient of H₂O:CH₃CN (98:2, 0.1% formic acid) to H₂O:CH₃CN (55:45, 0.1% formic acid) at ~300 nl/min over 30 min. The precolumn was connected via a fused silica capillary (10 cm, 25 μ) to a low volume tee (Upchurch Scientific) where high voltage (2400 V) was applied and the column tip positioned ~1 cm from the Z-spray inlet of an QToF Ultima API hybrid tandem mass spectrometer (Micromass, UK). Positive ions were generated by electrospray and the QToF operated in data dependent acquisition mode (DDA). A ToF MS survey scan was acquired (m/z 350-1700, 1 s) and the two largest multiply charged ions (counts > 20) were sequentially selected by Q1 for MS-MS analysis. Argon was used as collision gas and an optimum collision energy chosen (based on charge state and mass). Tandem mass spectra were accumulated for up to 2 s (m/z 50-2000). Peak lists were submitted to the database search program Mascot (Matrix Science, UK) to confirm identification of sirtuin peptides.

The two peptides with the highest signal intensity for each sirtuin were cross-referenced with Skyline software (MacCoss Lab Software, USA). Peptide sequences were checked to ensure no overlap with other sirtuins. Sirtuin standards were run using MRM LC-MS/MS on a 4000 Q TRAQ (SCIEX, USA) mass spectrometer to ensure good signals were detected for all 14 peptides selected for the final list (two unique peptides for each sirtuin).

Table 2.2 List of 14 unique sirtuin peptides selected for sirtuin protein quantification.

Arg and Lys amino acids highlighted in bold used in ‘heavy’ peptides, labelled with a stable isotope (^{13}C and ^{15}N). Precursor charge state for all peptides was 2⁺.

Sirtuin	Peptide	Light Precursor Ion <i>m/z</i>	Heavy Precursor Ion <i>m/z</i>
SIRT1	DINTIEDAVK	559.2904	563.2975
	TSVAGTVR	395.7245	400.7286
SIRT2	LLDEELTLEGVAR	664.8746	669.8788
	IFSEVTPK	460.758	464.7651
SIRT3	LYTQNIDGLER	661.341	666.3451
	VSGIPASK	379.724	383.7311
SIRT4	RPIQHGDVFR	612.8334	617.8376
	FILTAWEK	504.2817	508.2888
SIRT5	VVITQNIDELHR	512.6229	515.9589
	NLLEIHGSLFK	635.8613	639.8613
SIRT6	FLVSQNV DGLHVR	742.4044	747.4086
	LVIVNLQPTK	562.8555	566.8626
SIRT7	LLAESADLVTELQGR	807.9385	812.9426
	DTIVHFGER	537.2724	542.2765

2.2.2 Targeted mass spectrometry

MRM analyses were performed on a 4000 Q TRAP hybrid triple quadrupole linear ion trap mass spectrometer (SCIEX, USA) interfaced with a nanospray ion source, operating in positive ion mode and controlled by Analyst 1.5 software. Peptides were concentrated and desalted onto a micro C18 precolumn (500 μm x 2 mm, Michrom Bioresources, USA) with $\text{H}_2\text{O}:\text{CH}_3\text{CN}$ (98:2, 0.05% TFA) at 15 $\mu\text{l}/\text{min}$. After a 4 min wash, the pre-column was automatically switched (10 port valve, Valco, USA) into line with a nano column (as described in the previous section). Peptides were eluted using a linear gradient of $\text{H}_2\text{O}:\text{CH}_3\text{CN}$ (98:2, 0.1% formic acid) to $\text{H}_2\text{O}:\text{CH}_3\text{CN}$ (36:64, 0.1% formic acid) at ~300 nl/min over 30 minutes. Samples were analyzed with an ion spray voltage of 2.4 kV, curtain gas flow of 12 and nebulizing gas flow of 5 L/min. Quadrupoles were operated in the low resolution mode, and the dwell time was 50 ms. For validation runs, the MRM experiment triggered MS/MS spectrum acquisition. MS/MS spectra were acquired in the trap mode (enhanced product ion) with dynamic fill time, Q1 was operated using low resolution. Each sirtuin protein (SIRT1-7, 2 peptides per protein) was run with 12 transition ions per run, per

protein and with a 50ms dwell time. See Table 2.3 for a full list of transitions for each peptide and corresponding collision energies (estimated using Skyline software).

Table 2.3 List of product and transition ions with collision energies used for all 14 selected siruin peptides. Each siruin protein (SIRT1-7, with 2 peptides per protein) was run with 12 transition ions per run, per protein and with a 50ms dwell time. Precursor charge state for all peptides was 2⁺.

Precursor Ion <i>m/z</i>	Transition Ion	Peptide	Declustering Potential	Collision Energy
559.2904	889.4625	SIRT1.DINTIEDAVK.y8.light	71.9	27.6
559.2904	775.4196	SIRT1.DINTIEDAVK.y7.light	71.9	27.6
559.2904	674.3719	SIRT1.DINTIEDAVK.y6.light	71.9	27.6
563.2975	897.4767	SIRT1.DINTIEDAVK.y8.heavy	71.9	27.6
563.2975	783.4338	SIRT1.DINTIEDAVK.y7.heavy	71.9	27.6
563.2975	682.3861	SIRT1.DINTIEDAVK.y6.heavy	71.9	27.6
395.7245	602.362	SIRT1.TSVAGTVR.y6.light	60	18.3
395.7245	503.2936	SIRT1.TSVAGTVR.y5.light	60	18.3
395.7245	432.2565	SIRT1.TSVAGTVR.y4.light	60	18.3
400.7286	612.3703	SIRT1.TSVAGTVR.y6.heavy	60	18.3
400.7286	513.3019	SIRT1.TSVAGTVR.y5.heavy	60	18.3
400.7286	442.2648	SIRT1.TSVAGTVR.y4.heavy	60	18.3
664.8746	858.5043	SIRT2.LLDELTLEGVAR.y8.light	79.6	33.6
664.8746	745.4203	SIRT2.LLDELTLEGVAR.y7.light	79.6	33.6
664.8746	644.3726	SIRT2.LLDELTLEGVAR.y6.light	79.6	33.6
669.8788	868.5126	SIRT2.LLDELTLEGVAR.y8.heavy	79.6	33.6
669.8788	755.4285	SIRT2.LLDELTLEGVAR.y7.heavy	79.6	33.6
669.8788	654.3809	SIRT2.LLDELTLEGVAR.y6.heavy	79.6	33.6
460.758	807.4247	SIRT2.IFSEVTPK.y7.light	64.7	22
460.758	660.3563	SIRT2.IFSEVTPK.y6.light	64.7	22
460.758	573.3243	SIRT2.IFSEVTPK.y5.light	64.7	22
464.7651	815.4389	SIRT2.IFSEVTPK.y7.heavy	64.7	22
464.7651	668.3705	SIRT2.IFSEVTPK.y6.heavy	64.7	22
464.7651	581.3385	SIRT2.IFSEVTPK.y5.heavy	64.7	22
661.341	944.4796	SIRT3.LYTQNIDGLER.y8.light	79.3	33.4
661.341	816.421	SIRT3.LYTQNIDGLER.y7.light	79.3	33.4
661.341	702.3781	SIRT3.LYTQNIDGLER.y6.light	79.3	33.4
666.3451	954.4879	SIRT3.LYTQNIDGLER.y8.heavy	79.3	33.4
666.3451	826.4293	SIRT3.LYTQNIDGLER.y7.heavy	79.3	33.4

666.3451	712.3863	SIRT3.LYTQNIDGLER.y6.heavy	79.3	33.4
379.724	659.3723	SIRT3.VSGIPASK.y7.light	58.8	17.4
379.724	572.3402	SIRT3.VSGIPASK.y6.light	58.8	17.4
379.724	515.3188	SIRT3.VSGIPASK.y5.light	58.8	17.4
383.7311	667.3865	SIRT3.VSGIPASK.y7.heavy	58.8	17.4
383.7311	580.3544	SIRT3.VSGIPASK.y6.heavy	58.8	17.4
383.7311	523.333	SIRT3.VSGIPASK.y5.heavy	58.8	17.4
612.8334	1068.559	SIRT4.RPIQHGDVFR.y9.light	75.8	30.7
612.8334	971.5057	SIRT4.RPIQHGDVFR.y8.light	75.8	30.7
612.8334	858.4217	SIRT4.RPIQHGDVFR.y7.light	75.8	30.7
617.8376	1078.567	SIRT4.RPIQHGDVFR.y9.heavy	75.8	30.7
617.8376	981.514	SIRT4.RPIQHGDVFR.y8.heavy	75.8	30.7
617.8376	868.4299	SIRT4.RPIQHGDVFR.y7.heavy	75.8	30.7
504.2817	747.4036	SIRT4.FILTAWEK.y6.light	67.9	24.5
504.2817	634.3195	SIRT4.FILTAWEK.y5.light	67.9	24.5
504.2817	533.2718	SIRT4.FILTAWEK.y4.light	67.9	24.5
508.2888	755.4178	SIRT4.FILTAWEK.y6.heavy	67.9	24.5
508.2888	642.3337	SIRT4.FILTAWEK.y5.heavy	67.9	24.5
508.2888	541.286	SIRT4.FILTAWEK.y4.heavy	67.9	24.5
512.6229	896.4585	SIRT5.VVVITQNIDELHR.y7.light	68.5	23
512.6229	782.4155	SIRT5.VVVITQNIDELHR.y6.light	68.5	23
512.6229	669.3315	SIRT5.VVVITQNIDELHR.y5.light	68.5	23
515.9589	906.4667	SIRT5.VVVITQNIDELHR.y7.heavy	68.5	23
515.9589	792.4238	SIRT5.VVVITQNIDELHR.y6.heavy	68.5	23
515.9589	679.3397	SIRT5.VVVITQNIDELHR.y5.heavy	68.5	23
635.8613	930.5043	SIRT5.NLLEIHGSLFK.y8.light	77.5	32
635.8613	801.4618	SIRT5.NLLEIHGSLFK.y7.light	77.5	32
635.8613	688.3777	SIRT5.NLLEIHGSLFK.y6.light	77.5	32
639.8684	938.5185	SIRT5.NLLEIHGSLFK.y8.heavy	77.5	32
639.8684	809.4759	SIRT5.NLLEIHGSLFK.y7.heavy	77.5	32
639.8684	696.3919	SIRT5.NLLEIHGSLFK.y6.heavy	77.5	32
742.4044	1124.581	SIRT6.FLVSQNVDGLHVR.y10.light	85.2	38.1
742.4044	909.4901	SIRT6.FLVSQNVDGLHVR.y8.light	85.2	38.1
742.4044	696.3787	SIRT6.FLVSQNVDGLHVR.y6.light	85.2	38.1
747.4086	1134.589	SIRT6.FLVSQNVDGLHVR.y10.heavy	85.2	38.1
747.4086	919.4984	SIRT6.FLVSQNVDGLHVR.y8.heavy	85.2	38.1
747.4086	706.387	SIRT6.FLVSQNVDGLHVR.y6.heavy	85.2	38.1
562.8555	912.5513	SIRT6.LVIVNLQPTK.y8.light	72.1	27.8
562.8555	799.4672	SIRT6.LVIVNLQPTK.y7.light	72.1	27.8
562.8555	700.3988	SIRT6.LVIVNLQPTK.y6.light	72.1	27.8

566.8626	920.5655	SIRT6.LVIVNLQPTK.y8.heavy	72.1	27.8
566.8626	807.4814	SIRT6.LVIVNLQPTK.y7.heavy	72.1	27.8
566.8626	708.413	SIRT6.LVIVNLQPTK.y6.heavy	72.1	27.8
807.9385	915.5258	SIRT7.LLAESADLVTELQGR.y8.light	90	41.8
807.9385	802.4417	SIRT7.LLAESADLVTELQGR.y7.light	90	41.8
807.9385	703.3733	SIRT7.LLAESADLVTELQGR.y6.light	90	41.8
812.9426	925.5341	SIRT7.LLAESADLVTELQGR.y8.heavy	90	41.8
812.9426	812.45	SIRT7.LLAESADLVTELQGR.y7.heavy	90	41.8
812.9426	713.3816	SIRT7.LLAESADLVTELQGR.y6.heavy	90	41.8
537.2724	958.5105	SIRT7.DTIVHFGER.y8.light	70.3	26.4
537.2724	857.4628	SIRT7.DTIVHFGER.y7.light	70.3	26.4
537.2724	744.3787	SIRT7.DTIVHFGER.y6.light	70.3	26.4
542.2765	968.5188	SIRT7.DTIVHFGER.y8.heavy	70.3	26.4
542.2765	867.4711	SIRT7.DTIVHFGER.y7.heavy	70.3	26.4
542.2765	754.387	SIRT7.DTIVHFGER.y6.heavy	70.3	26.4

2.2.3 Sirtuin Peptide Standards

Multiple point calibration was used where a series of standard ‘light’ peptides with known concentrations together with fixed amounts of stable isotope-labelled ‘heavy’ peptides (100fmol/μl) were used to generate calibration curves for each sirtuin. The curves were expressed as ratios of light/heavy peak area versus concentration of light peptide for each of the 14 peptides selected. A commercially available stable isotope-labelled peptide standard (AQUA peptide, Sigma, USA) was used for absolute quantification of proteins. This heavy surrogate of each of the peptide standards is added at a constant level to all samples and standards and is used for correction of sample losses during workup and normalisation across runs, allowing accurate quantification of the target protein in samples. Peptides labelled with a stable isotope (^{13}C and ^{15}N) are chemically identical to their native counterparts and have identical chromatographic behaviour but can be distinguished from the calibration standards based on a small specific mass difference.

Isotopically labelled internal standards are excellent tools to normalise the variability in sample handling, injection volume and the performance of the mass spectrometer. Synthetic light and heavy peptides were purchased from GL Biochem (China) and Sigma-Aldrich (USA) respectively. Calibration curves in the range of 1-200 fmol/μl (three replicates using

three transitions) were prepared. Heavy peptide (100 fmol/μl) was added to all standards and peptide ratios (light/heavy) were obtained using Skyline MRM analysis software. Average inter- and intra- assay %CV values (n=3) were calculated for each of the seven sirtuins at the 100fmol/ul concentration point. The linear range, limit of detection (LOD) and limit of quantification (LOQ) were determined. A signal-to-noise ratio of >3:1 and >10:1 were used to define LOD and LOQ respectively. Sirtuin standard curves can be seen in Figure 2.1.

2.2.4 Cell Culture

Cells were cultured in medium RPMI 1640 supplemented with 10% foetal bovine serum, 1% 1-glutamax, 1% antibacterial/antifungal, and 0.5% glucose. Cells were maintained at 37°C in a humidified atmosphere containing 95% air/5% CO₂. Cells were seeded into 24-well tissue culture plates to a density of 1×10^5 cells 24 hours prior to experimentation. Neurons were prepared from the same mixed brain cell cultures as previously described⁴⁴⁵. Briefly, cells were plated in 24-well culture plates coated with Matrigel (1/20 in Neurobasal) and maintained in Neurobasal medium supplemented with 1% B-27 supplement, 1% Glutamax, 1% antibiotic/antifungal, 0.5% HEPES buffer, and 0.5% glucose. Microglia were prepared from the mixed brain cell cultures using a published protocol⁴⁴⁶. Briefly, the original mixed brain cell culture was shaken at 220 rpm for 2 h, floating cells were centrifuged, transferred to Permanox chamber slides (NUNC) at a density of 5×10^5 cells/ml and grown in DMEM supplemented with 10% fetal calf serum (FCS), 1% L-glutamax, 0.5% glucose, IL-3 (300 IU/ml), macrophage colony-stimulating factor (M-CSF) (50 IU/ml), and 1% antibiotic/antifungal. Oligodendrocytes were prepared from the mixed brain cell cultures using a published protocol⁴⁴⁶. Briefly, cells were seeded and grown in flasks coated with poly-L-lysine to confluence at 34°C, the permissive temperature, in DMEM/F12 supplemented with 10% FBS, 1% antibiotic/antifungal, 1% of G418 (Invitrogen, Melbourne, Australia) and then shifted to 39°C, the non-permissive temperature that leads to the 'differentiated' state for 72 hours. Cells were cultured in medium RPMI supplemented with 1% myelin binding protein, 1% 1-glutamax, and 1% antibacterial/antifungal. CNS cell lines of neurons (SKNSH), astrocytes (U251), oligodendrocytes (M310) and microglia (CHM5) were cultured in medium RPMI supplemented with 10% foetal bovine serum, 1% 1-glutamax, 1% antibacterial/antifungal, and 0.5% glucose. All cells were maintained at 37°C in a humidified atmosphere containing 95% air/5% CO₂. Cells were seeded into 24-well

tissue culture plates (3 wells per cell type) to a density of 1×10^5 cells 24 hours prior to experimentation. Wells were pooled prior to cell lysis and probe sonication and all measurements were performed in triplicate.

2.2.5 Sample Preparation of Cell Cultures, Tissues, CSF and Plasma

Cells: Adult human primary microglia, astrocytes, neurons and oligodendrocytes were cultured from resected normal adult brain tissue following removal of brain tumour with informed consent at the Minimally Invasive Cancer Centre, Prince of Wales Hospital, Sydney, Australia. Astrocytes were prepared from the mixed brain cell cultures using a protocol previously described by Guillemín et al.⁴⁴⁶. All cells and cell lines were lysed using RIPA buffer followed by probe sonication and cell debris removed by centrifugation at 10,000RPM for 5 min. Total protein concentration was assayed in the supernatant using the Pierce BCA protein assay kit (Life Technologies, Australia), and three 10 µg replicates were run by 1D SDS-PAGE followed by colloidal coomassie staining.

Human Tissues: 20 µg of protein from five individual control *post mortem* brain tissue samples were extracted as described for cells in the previous section, and run on a 1D SDS-PAGE gel and coomassie stained. Brain tissue samples included both gray and white matter and were frozen and stored at -80°C. Detailed patient information including age, sex and *post-mortem* delay of frontal lobe brain tissue collection times are summarised in Table 2.4.

Table 2.4 Human frontal lobe brain tissue sample and subject details

Patient	Sex	Age at death	Post mortem tissue collection time
1	Male	72	24h
2	Female	71	24h
3	Male	72	24h
4	Male	71	29h
5	Male	54	24h

For the fractionated samples, 200 mg of frontal lobe brain tissue from five control subjects were pooled and differential detergent fractionation performed to obtain cytosol, nucleus,

cytoskeletal and membrane protein fractions⁴⁴⁷. Each fraction (20ug) was run on a 1D SDS-PAGE gel and coomassie stained.

Animals: Female guinea pigs (Dunkin–Hartley) and C57Bl6 mice were housed in temperature-controlled rooms (21-22°C; 49-55% humidity) with 12 h light-dark cycle (lights on 7:00-19:00). Food and water was available *ad libitum*. Wild type mice and guinea pig organs were lysed (RIPA buffer) by probe sonication. Protein (20µg/lane) were run by 1D SDS-PAGE and coomassie stained. Protein concentrations were determined using the Pierce BCA protein assay kit (Life Technologies, Australia).

CSF and plasma: CSF samples were collected by standard lumbar puncture from five patients assessed as clinically well after investigation for suspected meningitis, returning normal results for routine CSF pathology markers (white cell count, protein, glucose and bacterial sterility). Aliquots (50 µl) for each patient were obtained for the study. Control human plasma from a healthy individual was immunodepleted of the six most abundant plasma proteins using the Hu6 column (Agilent, USA) according to manufacturer's instructions⁴⁴⁸. For immunodepletion using the Multiple Affinity Removal System Hu6 column and buffer kit (Agilent, Santa Clara, CA, USA), 24 µl EDTA plasma was diluted into 120 µl Buffer A. Diluted EDTA plasma (100 µL) was injected onto the Hu6 column connected to a HP 1090 HPLC system (Agilent, Santa Clara, CA, USA) and the low abundance protein fraction was collected following the manufacturer's instructions. The low abundance protein fractions from six injections were pooled, buffer exchanged and concentrated into 45 mM NaHCO₃ using Amicon 3 kDa centrifugal devices (Millipore, Billerica, MA, USA). CSF protein (5 µg) and depleted plasma protein (20 µg), as determined by a BCA protein assay, were run on a 1D SDS-PAGE gel and colloidal coomassie stained.

For all samples, the band corresponding to the molecular weight for each sirtuin was excised, de-stained and trypsin digested overnight with heavy sirtuin peptides added as internal standards to all samples prior to digestion (the internal standard was constant for all samples and standards and added at a level at about the midrange of the standard curve). The tryptic peptides were dried under vacuum (Savant Speedvac, Thermo Scientific, USA), reconstituted in 0.1% formic acid (5 µl) injected into the mass spectrometer (1uL) and analysed using MRM. Peak area ratios (light/heavy) were calculated for each endogenous peptide (light)

relative to the spiked isotope-labelled (heavy) peptide using Skyline MRM analysis software. Protein concentrations were determined using calibration curves. All samples were fractionated by 1D-SDS-PAGE to reduce sample complexity. A workflow of the sample preparation procedure can be found in Figure 2.6.

2.2.6 Sirtuin mRNA Expression in Human Brain Tissue using PCR

For the gene expression studies RNA was extracted from human brain cells using RNeasy mini kits (Qiagen, Germany). The cDNA was prepared using SuperScript III First-Strand Synthesis System and random hexamers (Invitrogen Corporation, USA) as previously described⁴⁴⁹.

Briefly, for each reaction 2 µl of diluted cDNA, 10 µL of SYBR green master mix, 0.15 µL of 10 µM forward and reverse primers and 7.7 µl of nuclease-free water was used making a total volume of 20 µl. Q-PCR was carried out using the Mx3500P Real-Time PCR system (Stratagene, Australia). The primer sequences are shown in Table 2.5. The relative expression levels of sirtuin transcripts were calculated using a mathematical model based on the individual Q-PCR primer efficiencies and the quantified values were normalized against the housekeeping gene 18S. From these values, fold-differences in the levels of transcripts between individual cell cultures were calculated according to the formula $2^{-\Delta\Delta Ct}$

Table 2.5 Real-time primer sequences used for PCR analysis

Primer name	Oligo name	Sequence (5'→3')
SIRT1-Forw	NM_012238-Forw	CAC-CAG-AAA-GAA-CTT-CAC-CAC-CAG
SIRT1-Rev	NM_012238-Rev	ACC-ATC-AAG-CCG-CCT-ACT-AAT-CTG
SIRT2-Forw	AJ505014-Forw	AGG-GAC-AAG-GAG-CAG-GGT-TC
SIRT2-Rev	AJ505014-Rev	GAA-GAG-AGA-CAG-CGG-CAG-GAC
SIRT3-Forw	NM_12239-Forw	GAG-GTT-CTT-GCT-GCA-TGT-GGT-TG
SIRT3-Rev	NM_12239-Rev	AGT-TTC-CCG-CTG-CAC-AAG-GTC
SIRT4-Forw	NM_012240-Forw	TTG-TGC-CAG-CAA-GTC-CTC-CTC
SIRT4-Rev	NM_012240-Rev	GTC-TCT-TGG-AAA-GGG-TGA-TGA-AGC
SIRT5-Forw	NM_12241-Forw	TCC-AGC-GTC-CAC-ACG-AAA-CC
SIRT5-Rev	NM_12241-Rev	AAC-ACC-AGC-TCC-TGA-GAT-GAT-GAC
SIRT6-Forw	NM_016539-Forw	GCT-GGA-GCC-CAA-GGA-GGA-ATC
SIRT6-Rev	NM_016539-Rev	AGT-AAC-AAA-GTG-AGA-CCA-CGA-GAG

SIRT7-Forw	NM_016538-Forw	GAG-CCA-ACC-CTC-ACC-CAC-ATG
SIRT7-Rev	NM_016538-Rev	ACG-CAG-GAG-GTA-CAG-ACT-TCA-ATG
GAPDH-Forw	NM_017008-Forw	TGG-AGT-CTA-CTG-GCG-TCT-T
GAPDH –Rev	NM_017008-Rev	TGT-CAT-ATT-TCT-CGT-GGT-TCA

2.2.7 Sirtuin Expression in Human Brain Cells and Tissue using immunohistochemical staining

Post mortem brain tissue from a control male aged 63 years was obtained from the Sydney Brain Bank. Individual had no evidence of neurological disease. Immunohistochemical staining was performed using a previously published procedure⁴⁵⁰. Anti-human sirtuin (1:250) primary antibodies (raised in rabbit) were used.

Formalin fixed blocks from the hippocampal region were embedded in paraffin and cut into 5 µm sections on superfrost plus slides. For sirtuin staining, sections were deparaffinised in xylene for 20 min and rehydrated through graded alcohol treatment. Antigen retrieval was performed through the use of Target Retrieval solution pH 6 (DAKO, Denmark) and autoclaving at 121°C for 20 min. Endogenous peroxidase was blocked using 3% w/v hydrogen peroxide for 5 min and endogenous biotin was blocked as described previously. After incubation with 10% horse serum for 30 min to block non-specific binding, sections were incubated with anti-human sirtuin (1:250) primary antibodies (raised in rabbit), for 2 hours at ambient temperature. After three rinses, sections were incubated with secondary antibodies–biotinylated goat-anti rabbit or mouse (Vector Laboratories, USA, 1:200) for 30 min at ambient temperature followed by 30 min treatment with avidin-biotin-complex (ABC) elite (Vector). Labelling was visualized with liquid DAB and sections were counterstained and mounted. Negative controls for non-specific staining included replacement of the primary antibody by normal rabbit or mouse IgG.

2.2.8 Sirtuin Protein Expression in human control brain tissue using western blotting

Protein from three individual control *post mortem* frontal brain tissue samples were extracted as described in the previous section, and run on a 1D SDS-PAGE gel (20 µg protein per lane), and western blotted with antibodies for SIRT1, SIRT2 and SIRT3.

The gel was electroblotted (20V, 110mA, 90mins) onto a nitrocellulose membrane in transfer buffer of 50mM tris, 40mM glycine, 1.3mM SDS, 20% methanol, pH 9.2. After transfer of proteins, the membrane was incubated in 10% skim milk powder solution containing primary sirtuin antibody. SIRT1, SIRT2 and SIRT3 rabbit polyclonal antibodies were used (1:1000 dilution, Abcam, UK), followed by a secondary antibody (1:100,000 dilution of anti-mouse IgG, Pierce, USA). See Table 2.6 for antibody details and dilutions. Chemiluminescence blots were developed using 1:1 solution of Super Signal West Femto luminol and peroxide buffer (Pierce, USA) according to manufacturer's instructions.

Table 2.6 Antibodies and dilutions used for western blotting

Antibody	Dilution	Manufacturer
Rabbit Polyclonal SIRT1	1:1000	Abcam (Cambridge, UK)
Rabbit Polyclonal SIRT2	1:1000	Abcam (Cambridge, UK)
Rabbit Polyclonal SIRT3	1:1000	Abcam (Cambridge, UK)

2.2.9 Statistics

Sirtuin concentrations are presented as means \pm SEM using peak area ratios of light and heavy peptides obtained from Skyline MRM Proteomics software v3.1 (MacCoss Lab, USA). Sirtuins were quantified based on an average of data from both peptides used for each sirtuin where possible. Statistical comparisons were performed using two-tailed student *t*-tests assuming equal variance. Differences between groups were considered statistically significant at the $p \leq 0.05$ level.

2.2.10 Ethics

All human and animal brain tissue samples were obtained and experiments conducted in accordance with the guidelines of the National Health and Medical Research Council of Australia and were approved by the University of New South Wales Human Research Ethics Committee (human brain tissue reference number HC12563) and the University of New South Wales Animal Care Ethics Committee (guinea pig tissue reference number 14/40B and mice 13/39B). Adult human primary microglia, astrocytes, neurons and oligodendrocytes

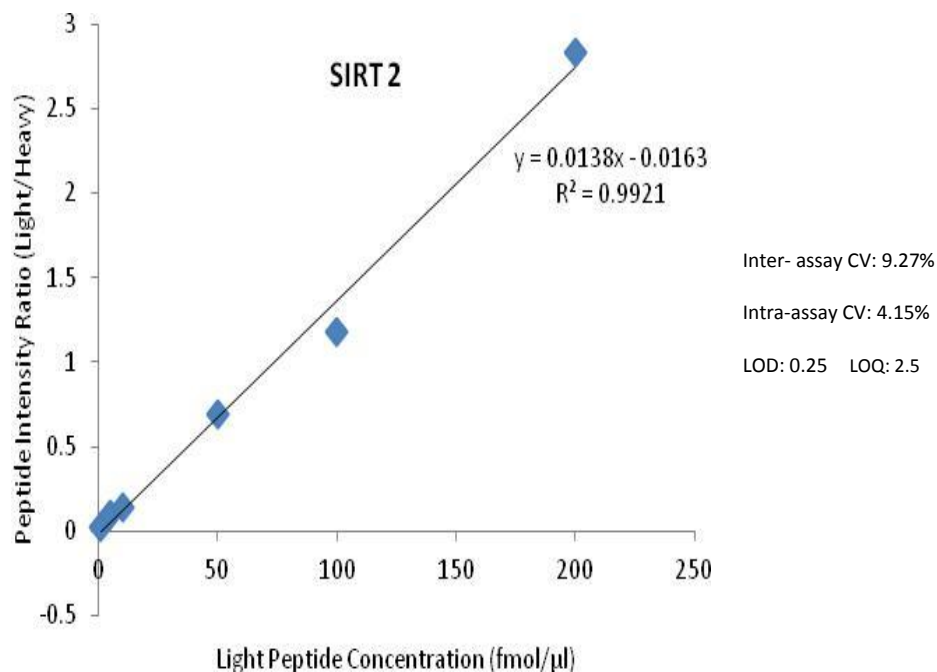
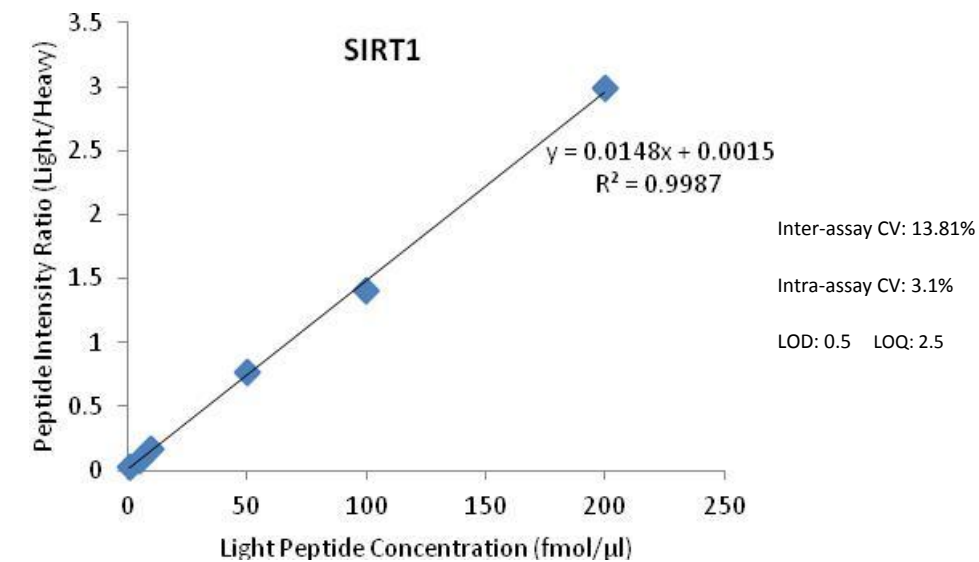
were cultured from resected normal adult brain tissue following removal of brain tumour with informed consent at the Minimally Invasive Cancer Centre, Prince of Wales Hospital, Sydney, Australia (reference number X12-0314 and HREC/12/RPAH/481). All control CSF samples were obtained with ethics approval from the Sydney Adventist Hospital, Sydney Australia, with informed consent obtained from all subjects (reference number SAHHREC #13-02).

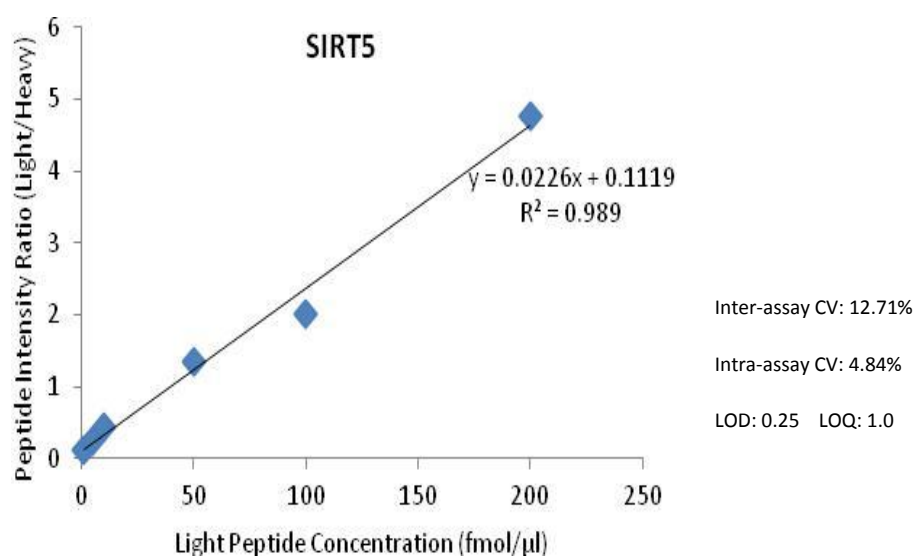
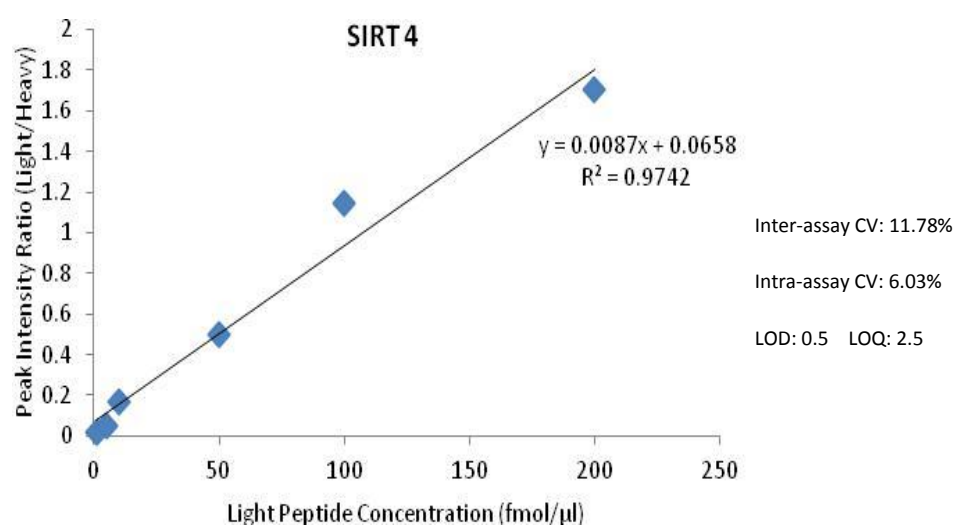
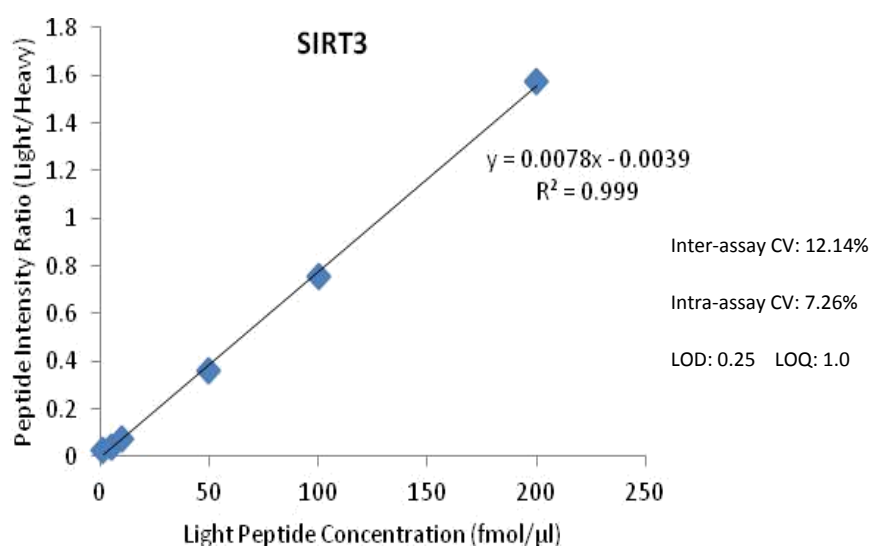
Results

Peptide standards

Standard curves for sirtuin peptides are shown in Figure 2.1. The LOD and LOQ were determined when the signal to noise ratio of the transition with the highest intensity was approximately 3:1 and 10:1 respectively. All peptides had good linearity in the 1-200 fmol/ μ l range and intra- and inter- assay coefficients of variance (CV %) were <10% and less than <14% respectively.

Figure 2.1 Sirtuin peptide standard curves, variance and limits of detection and quantification. Sirtuin peptide standard curves (average of two peptides, in triplicate for each sirtuin, with heavy peptide spike of 100fmol/μl). Both inter- and intra-assay CV% were calculated for three replicates and the LOD and LOQ are shown in fmol/ul. CVs calculated using peptide intensity ratios (light/heavy) at the 100fmol/μl peptide concentration level.





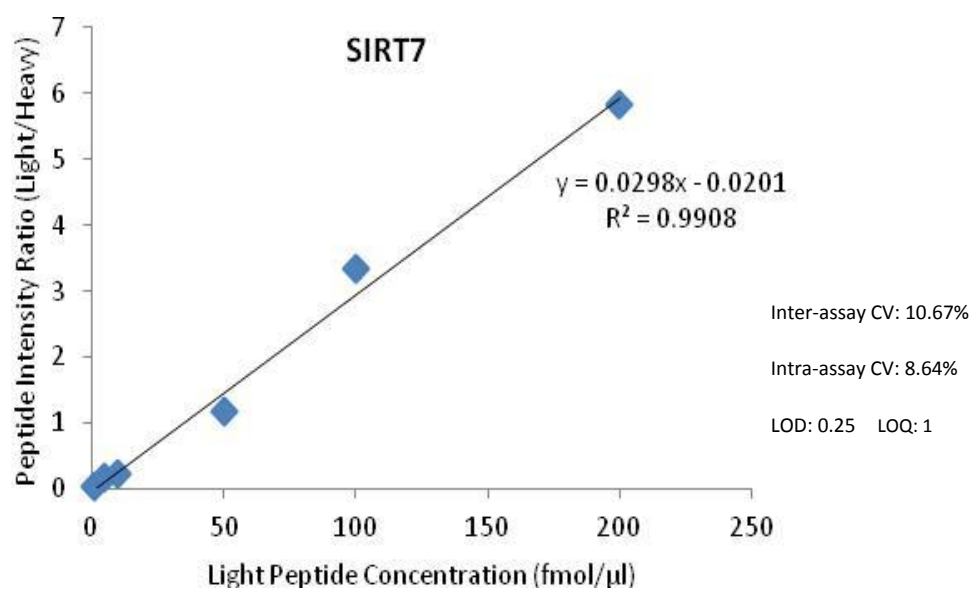
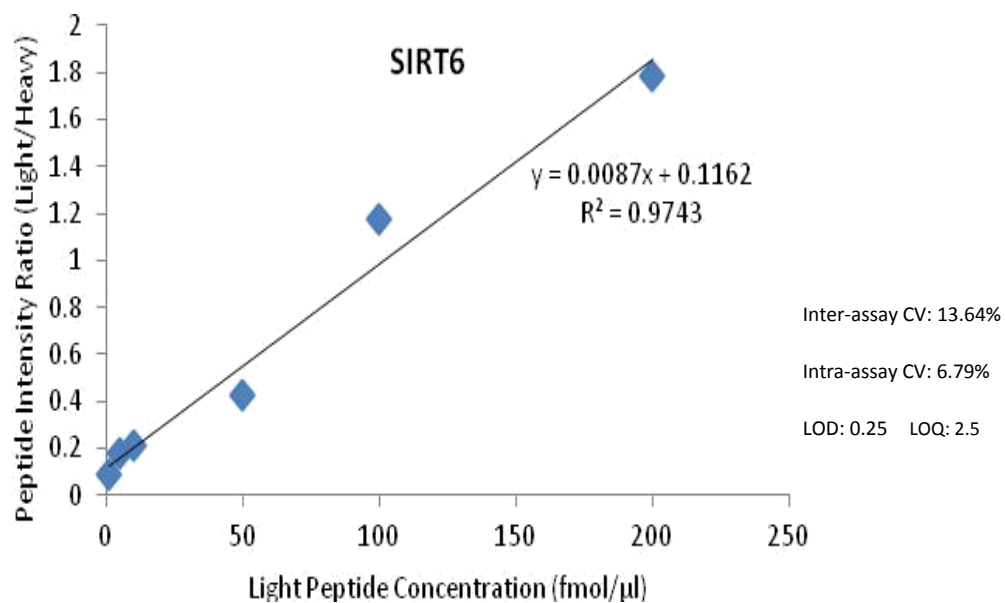
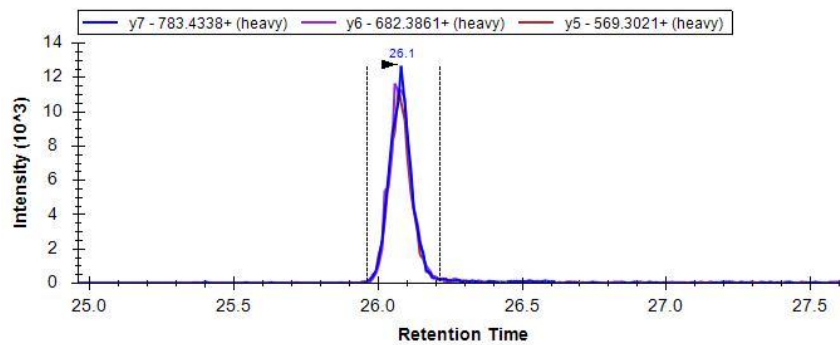
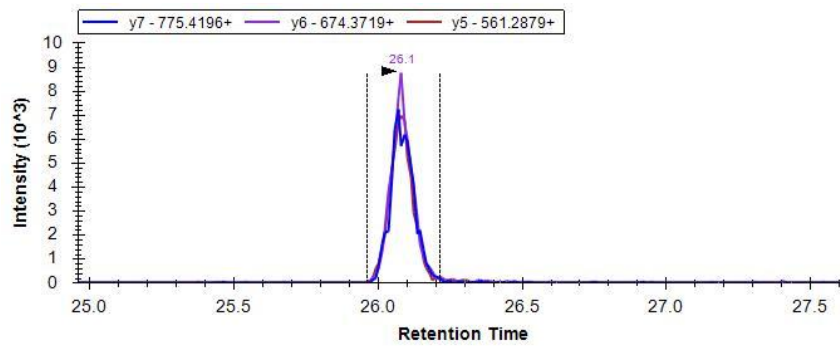
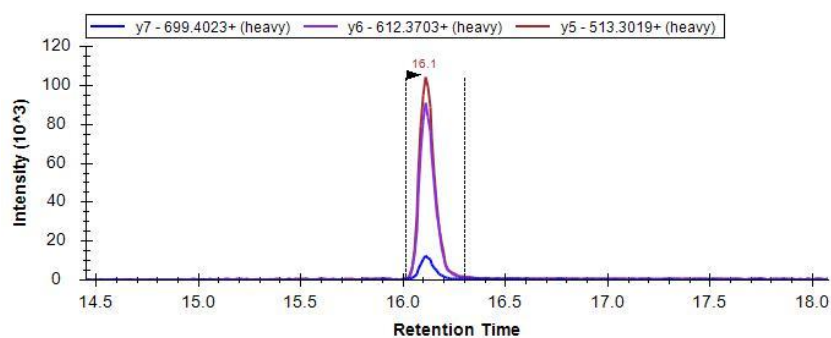
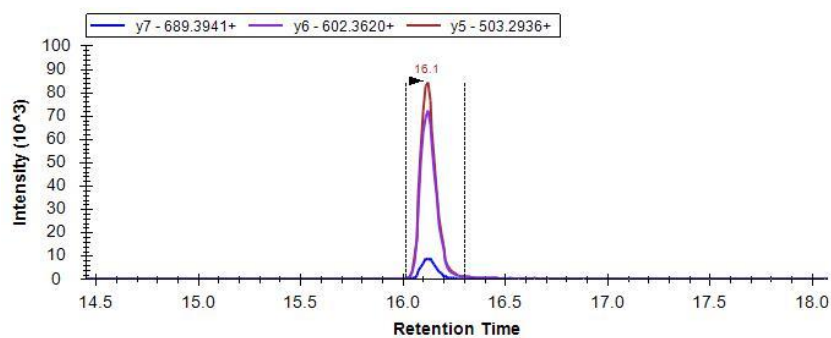


Figure 2.2 Representative chromatograms for all 14 sirtuin peptides used in the MRM method. Showing transition ions, retention times and signal intensities. The vertical dotted lines either side of the peak clusters indicate the boundaries for peak area integration.

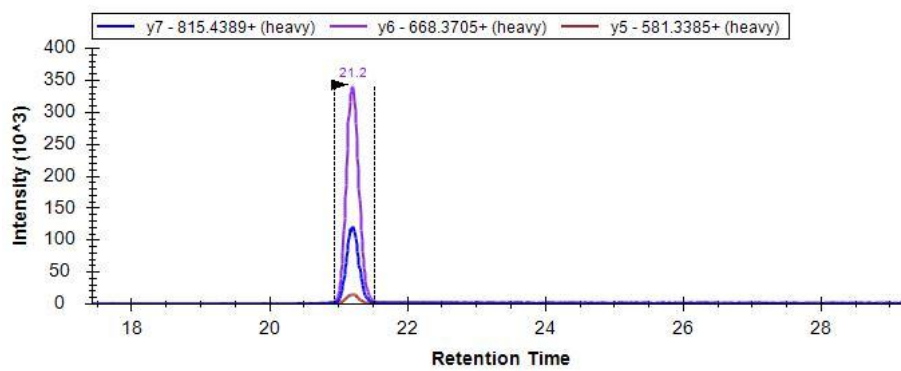
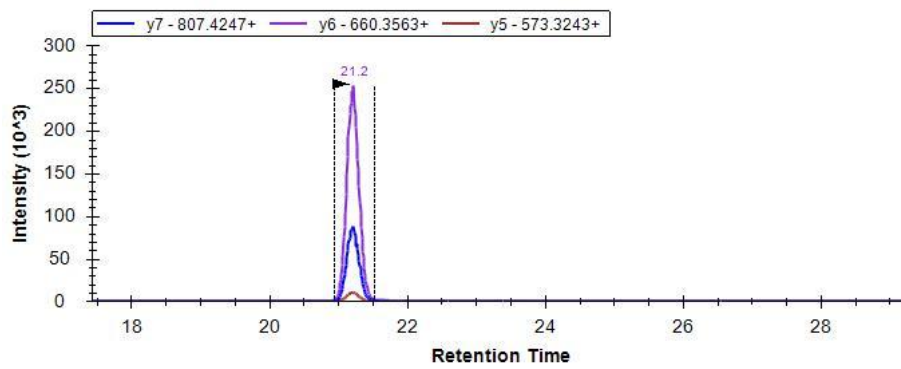
SIRT1 DINTIEDAVK (precursor mass, 2^+ m/z = 559.2904)



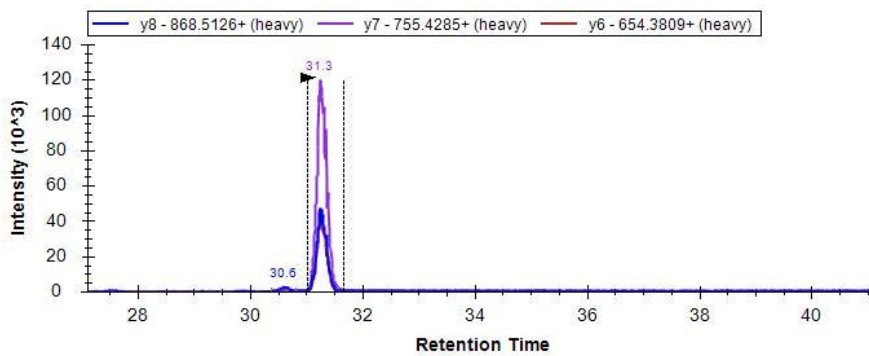
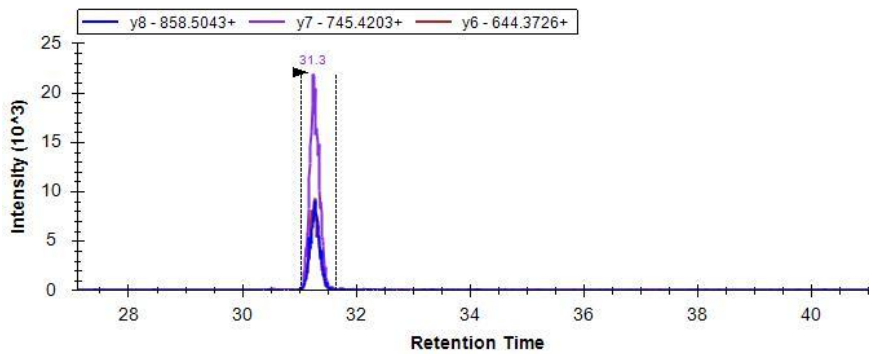
SIRT1 TSVAGTVR (precursor mass, 2^+ m/z = 395.7245)



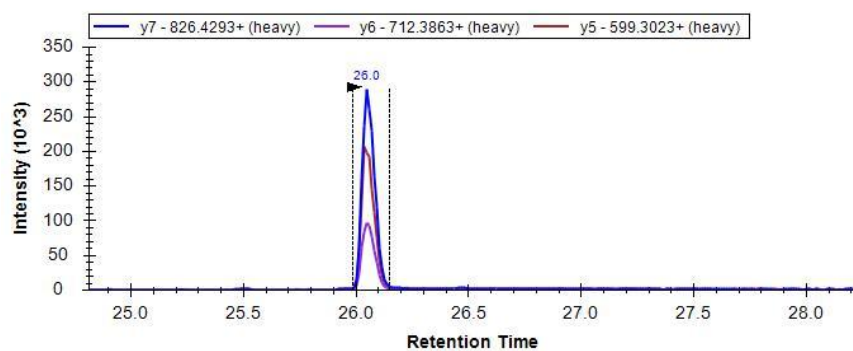
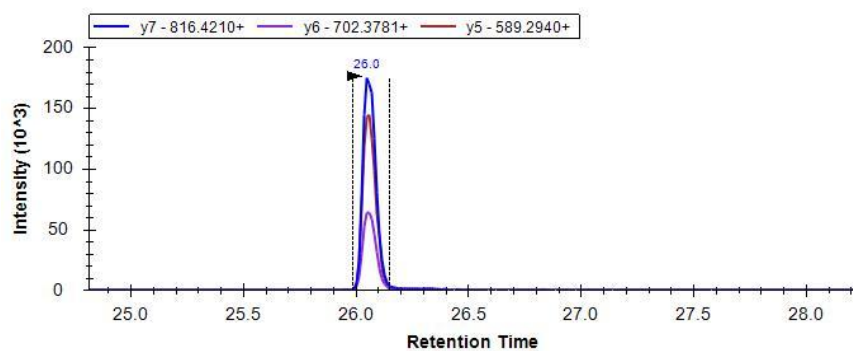
SIRT2 IFSEVTPK (precursor mass, 2^+ $m/z = 460.758$)



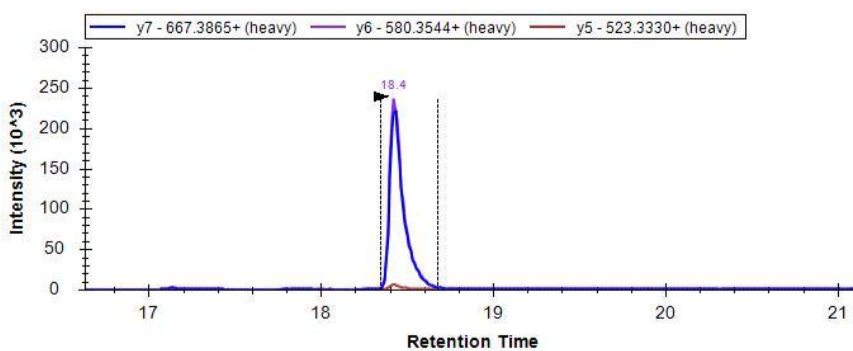
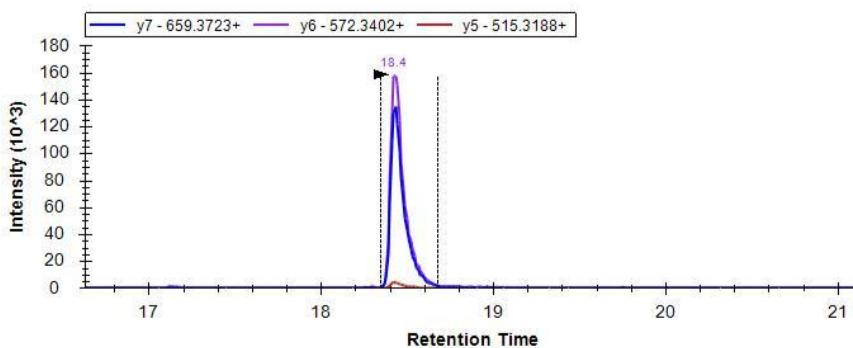
SIRT 2 LLDELTLEGVAR (precursor mass, 2^+ $m/z = 664.8746$)



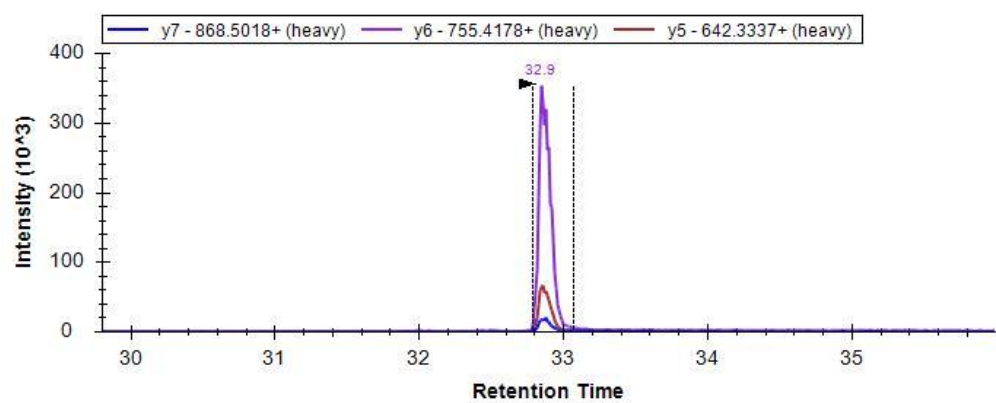
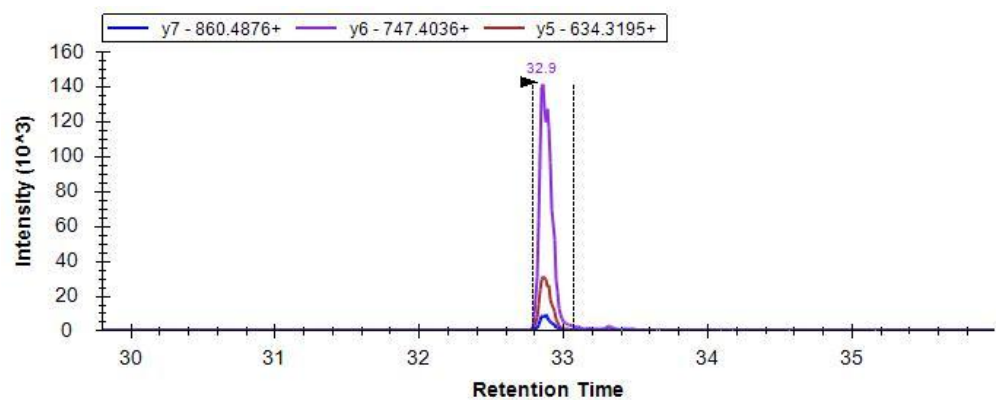
SIRT3 LYTQNIIDGLER (precursor mass, 2^+ $m/z = 661.341$)



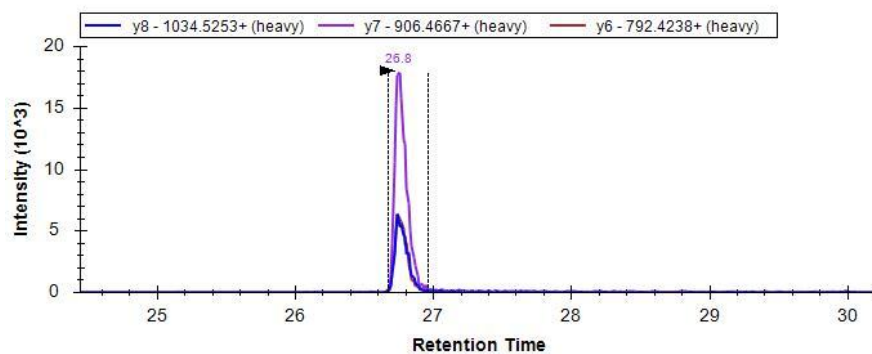
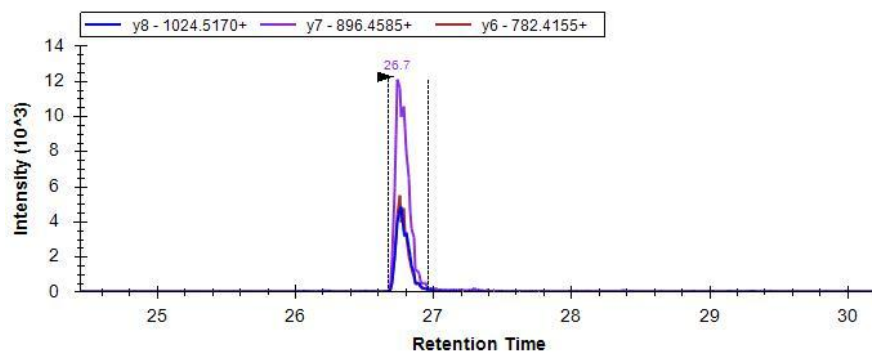
SIRT3 VSGIPASK (precursor mass, 2^+ $m/z = 379.24$)



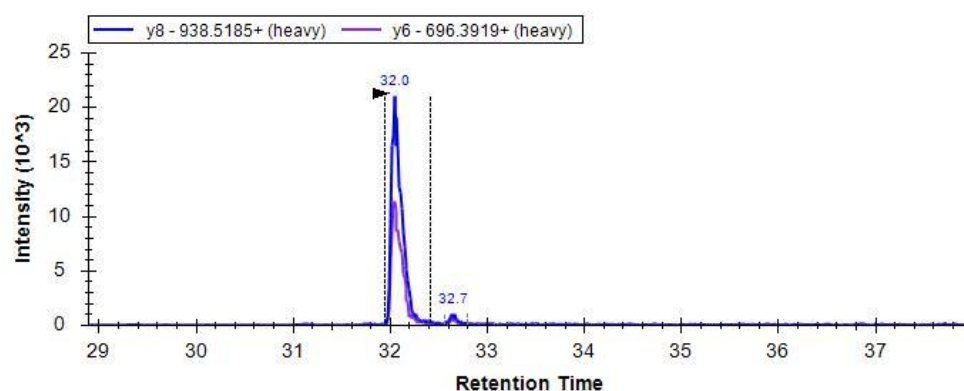
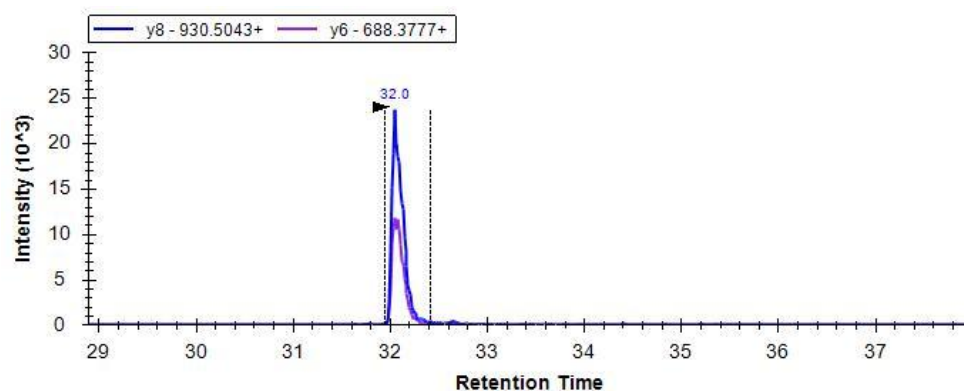
SIRT4 FILTAWEK (precursor mass, 2^+ m/z = 612.8334)



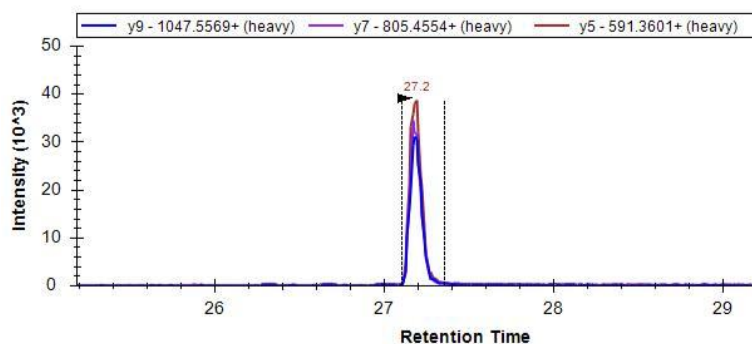
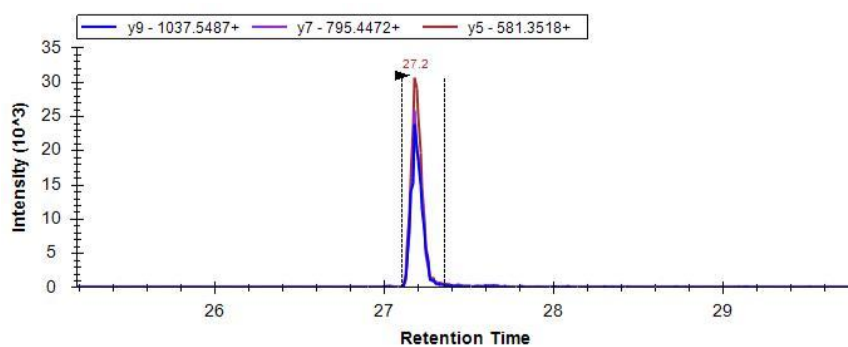
SIRT5 VVVITQNIDELHR (precursor mass, 2^+ m/z = 512.6229)



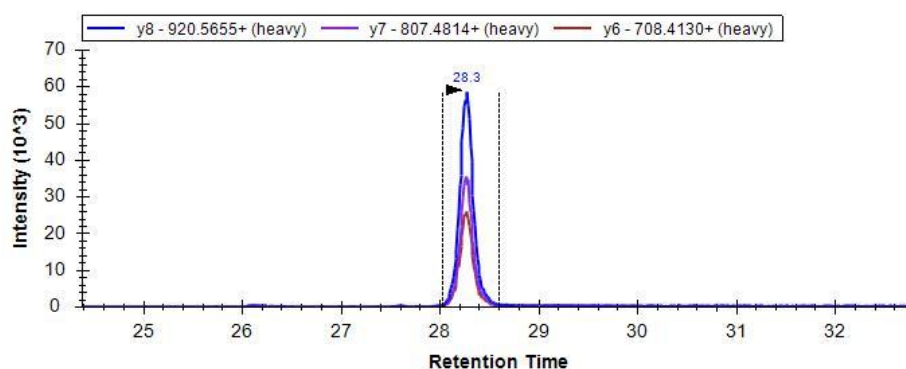
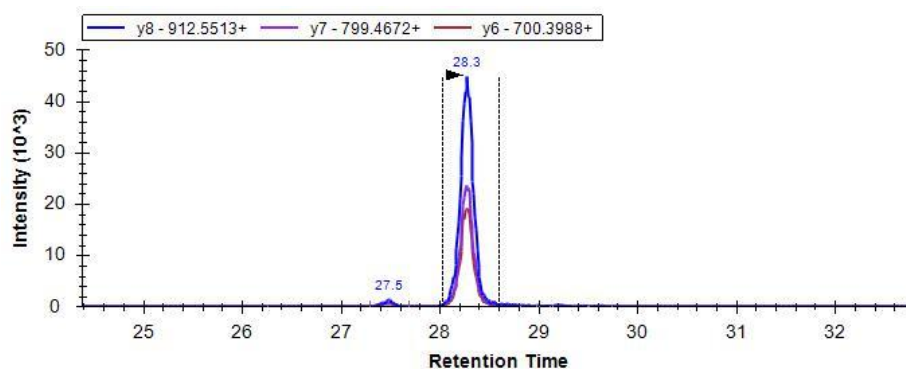
SIRT5 NLLIEHGSFLK (precursor mass, 2^+ $m/z = 635.8613$)



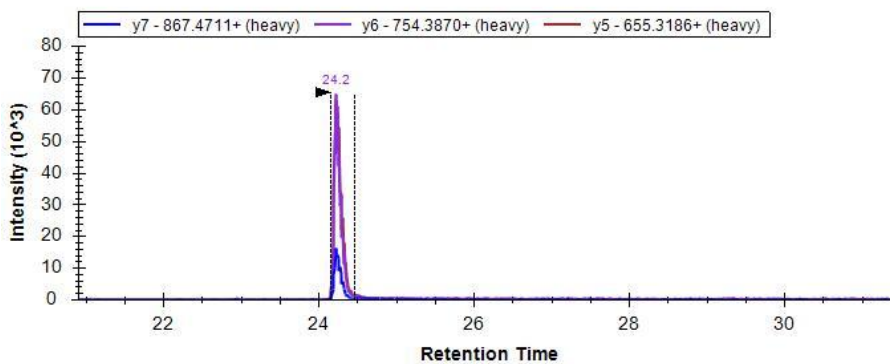
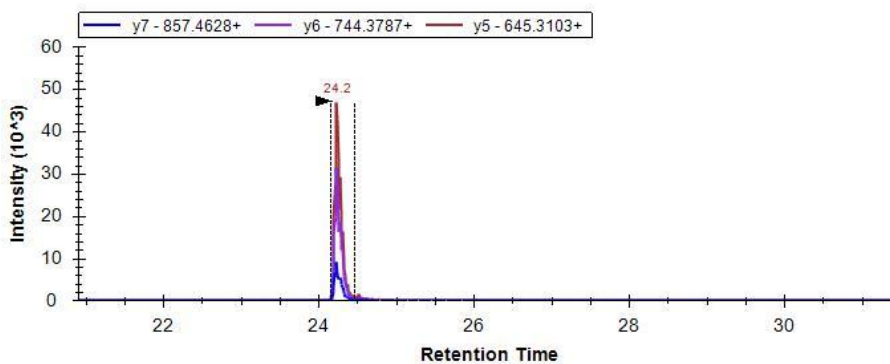
SIRT6 FLVSQNVDGLHVR (precursor mass, 2^+ $m/z = 742.4044$)



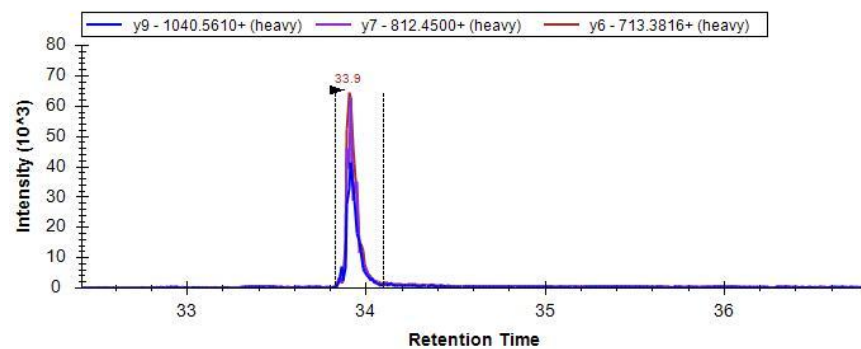
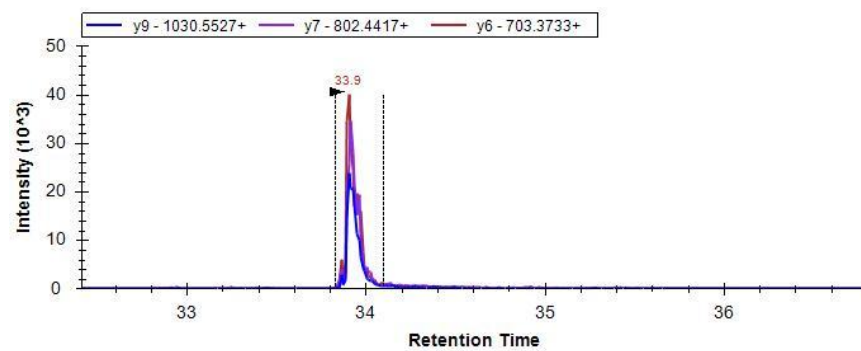
SIRT6 LVIVNLQPTK (precursor mass, 2^+ $m/z = 562.8555$)



SIRT7 DTIVHFGER (precursor mass, 2^+ $m/z = 537.2724$)



SIRT7 LLAESADLVTELQGR (precursor mass, 2^+ $m/z = 807.9385$)

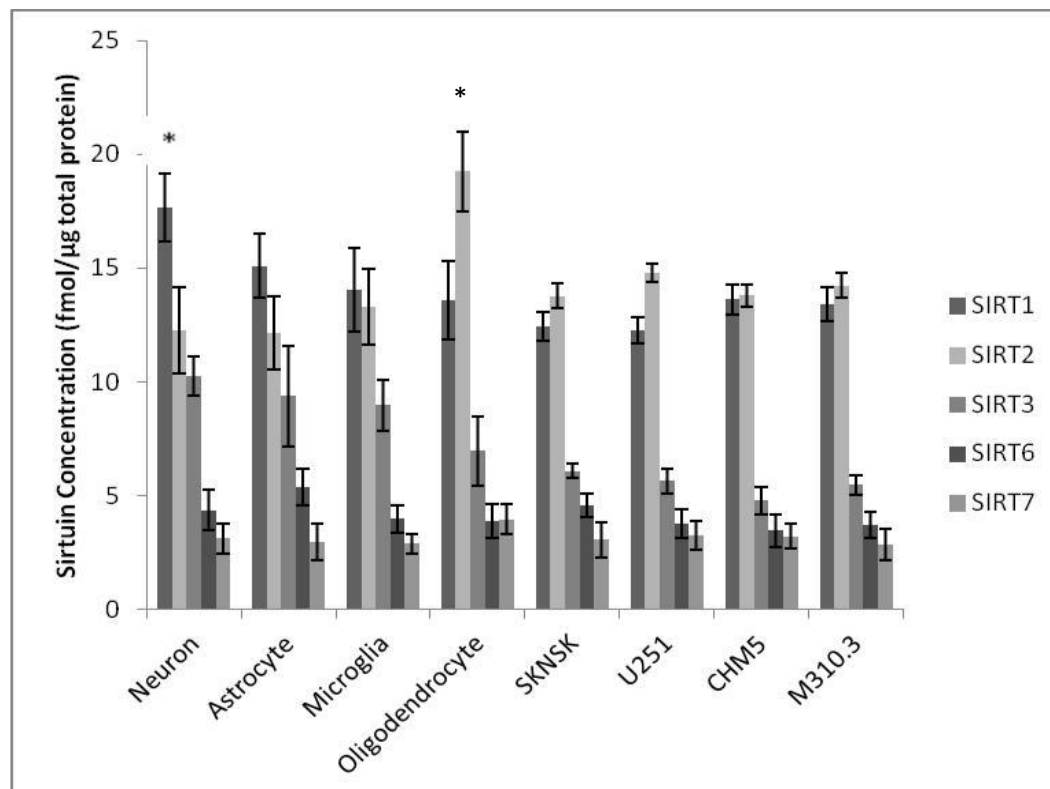


2.3.2 Quantification of sirtuin expression in cells and tissues

In all the human primary brain cell types and human brain cell lines SIRT1, 2, 3, 6 and 7 were detected and quantified (Figure 2.3).

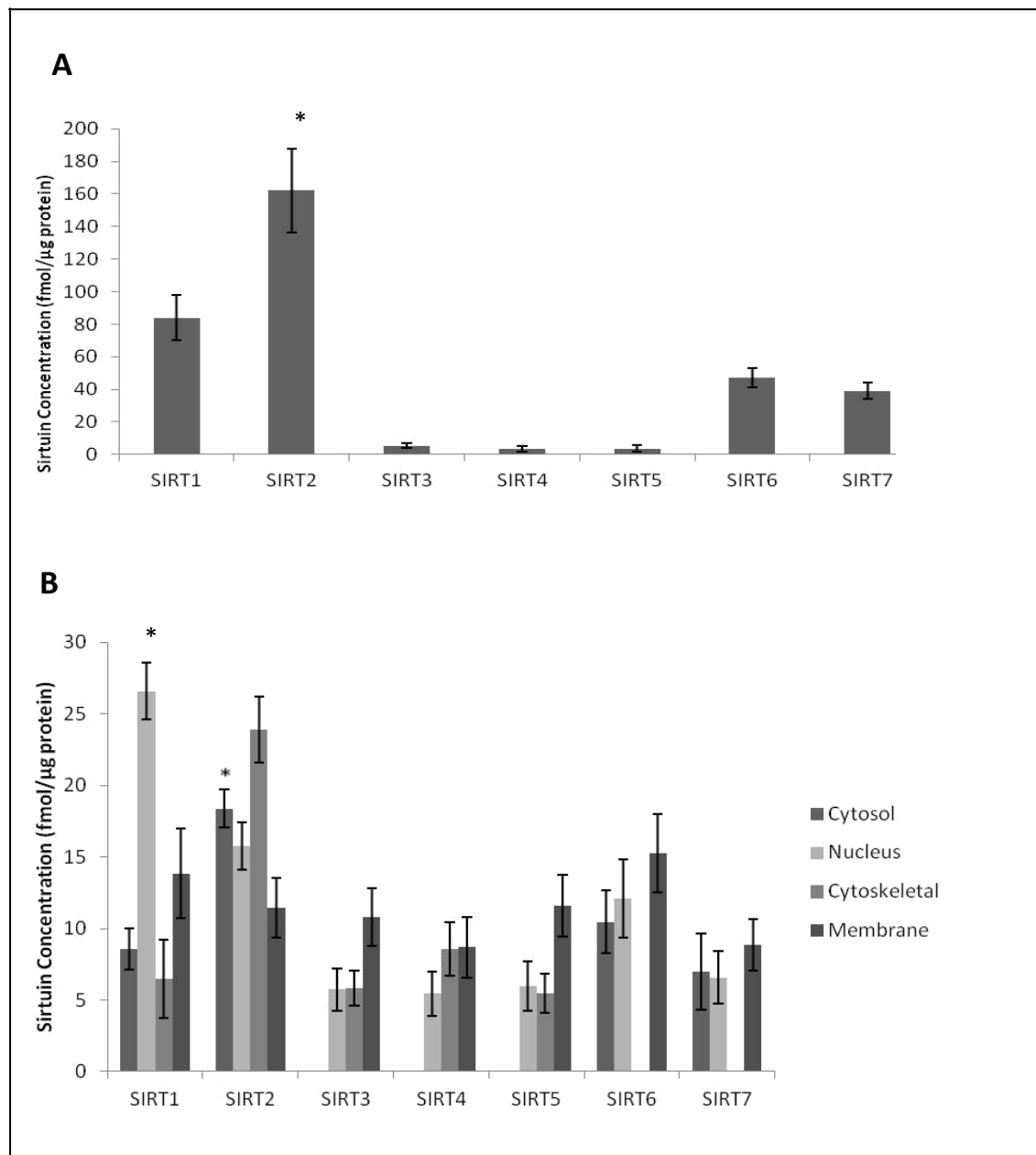
Figure 2.3 Sirtuin expression in primary cultured brain cells and cell lines.

In primary neurons SIRT1 was found to be the most abundant sirtuin (* $p < 0.05$) compared to other neuronal sirtuins ($n=3$). SIRT2 was found to be abundant in primary oligodendrocytes (* $p < 0.05$) compared to other cell types ($n=3$). SIRT1 and SIRT2 were the most abundant in all the cell cultures. SIRT4 and SIRT5 were below the detection limits and only small amounts of SIRT6 and SIRT7 were detected.



All seven sirtuins were detected in human control brain tissue, with SIRT2 highly expressed (Figure 2.4, Panel A). Detergent fractionation into subcellular groups improved identification of mitochondrial sirtuins (SIRT3-5) (Figure 2.4, Panel B).

Figure 2.4: Sirtuin expression in human frontal lobe brain tissue. Sirtuin expression in unfractionated (Panel A) and fractionated (Panel B) human frontal lobe brain tissue. All seven sirtuins were detected in unfractionated human frontal lobe brain tissue with SIRT2 the most abundant ($*p<0.05$) compared to all other sirtuins (Panel A). The mitochondrial sirtuins (SIRT3-5) were found to be close to the LOQ, but their signals improved following fractionation of the tissue into cytosolic, nuclear, cytoskeletal and membrane fractions (Panel B). Fractionation showed SIRT1 and SIRT2 expressed in all fractions, whereas SIRT3-5 were below the LOD in the cytosol and SIRT6 and SIRT7 were below the LOD in the cytoskeletal fraction. SIRT1 was most abundant in the nucleus and SIRT2 in the cytoskeletal fraction ($*p<0.05$, Panel B). In the cytosol, SIRT2 was the most abundant sirtuin ($*p<0.05$), and all sirtuins were captured in the membrane fraction.



Quantification of some sirtuins was possible in guinea pig and mouse tissue due to their common sequences with human sirtuin peptides. SIRT1-3 levels in the guinea pig (Figure 2.5 Panel A) and SIRT 1 and 3 levels in mouse organs (Figure 2.5 Panel B) were quantified. Furthermore the method could be adapted for all sirtuins from other species with purchase of the appropriate synthetic peptides and their heavy internal standards.

Figure 2.5 SIRT1-3 protein expression in animal organs. SIRT1-3 protein expression in guinea pig (Panel A) and mouse organs (Panel B). SIRT2 was found to be the most abundant sirtuin in guinea pig, with higher levels expressed in the brain (* $p < 0.01$, $n = 2$) compared to liver and kidney. SIRT2 in mouse was not quantified due to peptide sequence difference with the human peptide standards.

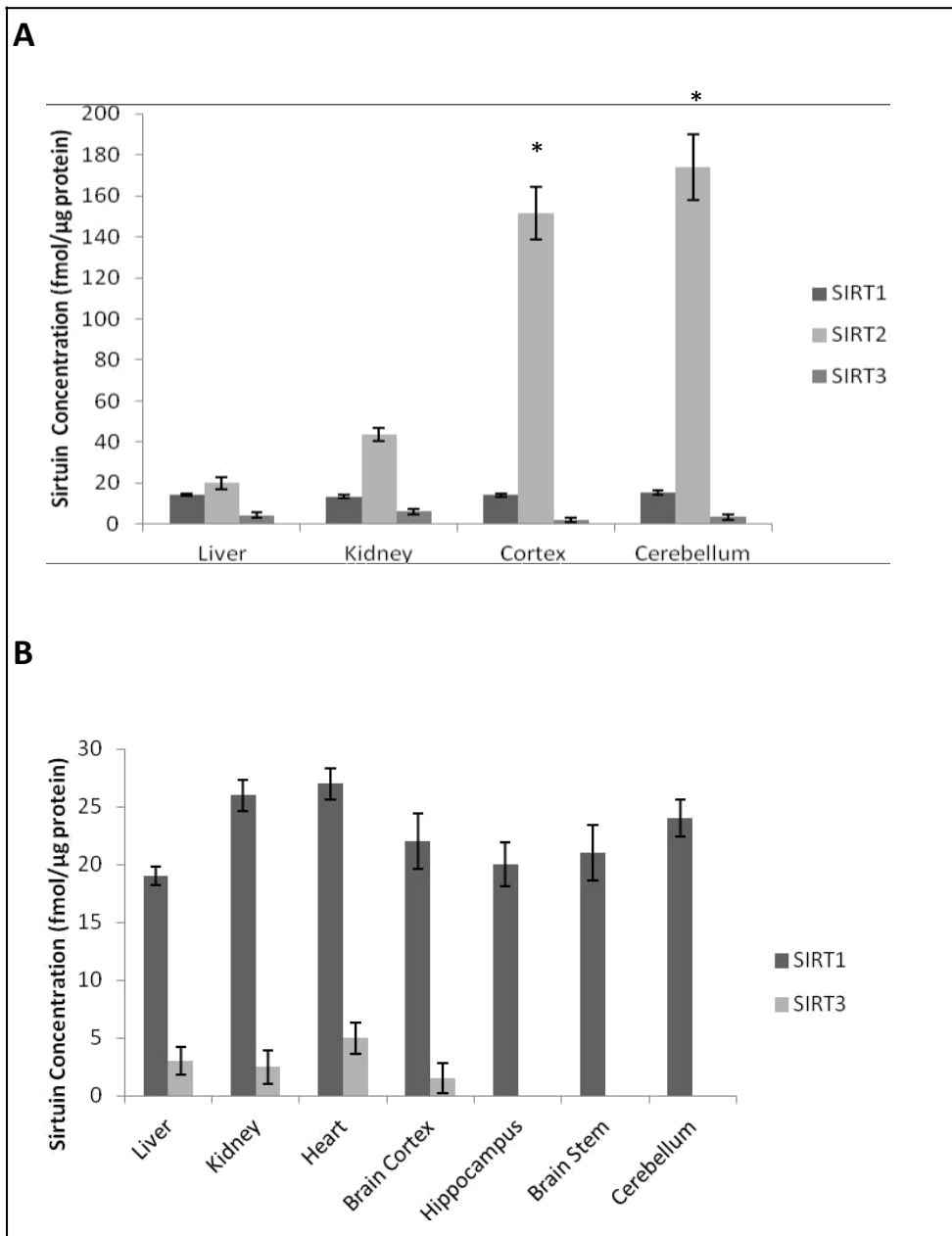


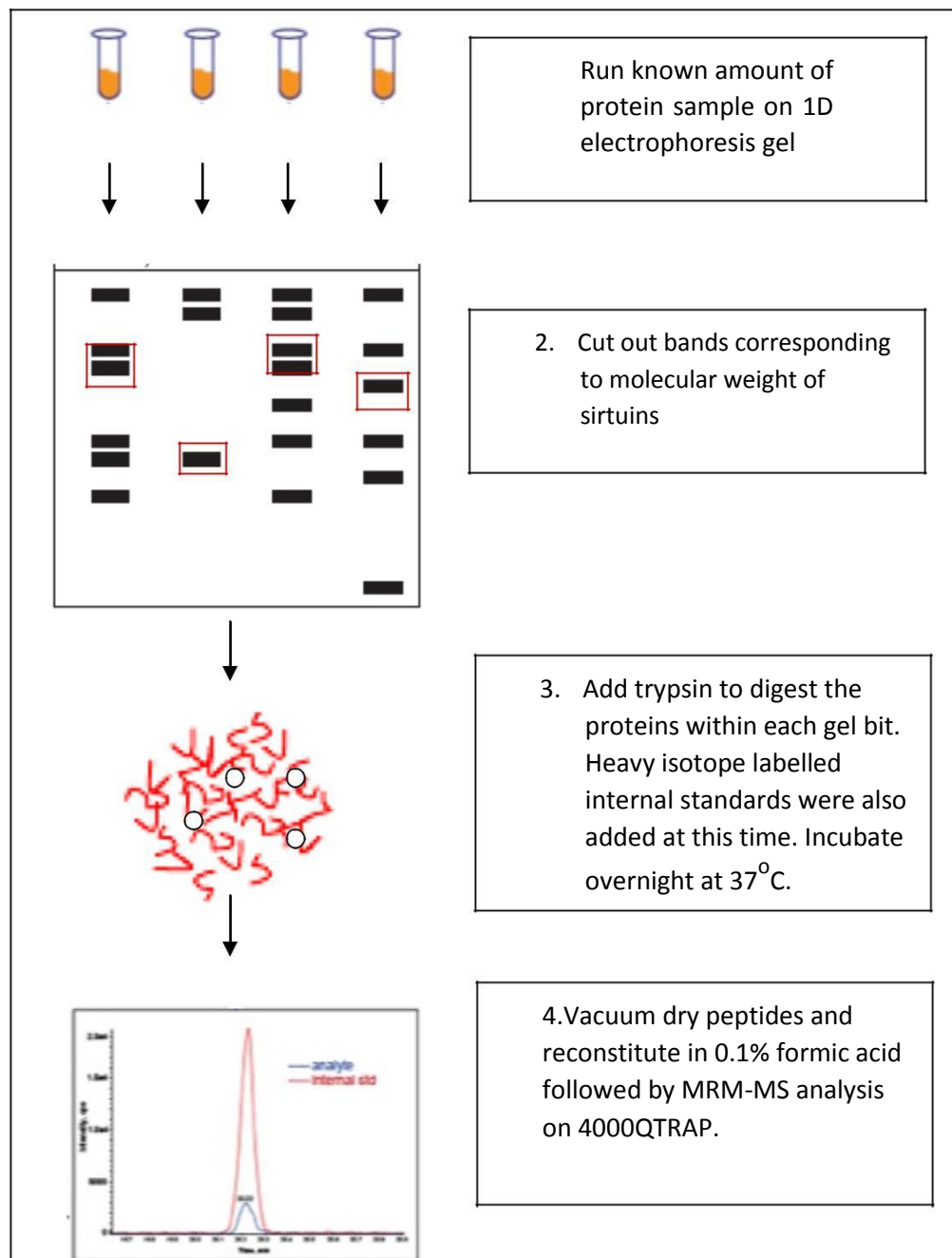
Table 2.7 shows the level of homology (or identity) of human SIRT1-7 peptide sequences with mouse and guinea pig.

Table 2.7 Human sirtuin peptide homology with guinea pig and mouse. Sequence variations from the human are highlighted in red.

Sirtuin	Human Peptide	Homology in Guinea Pig and Mice
SIRT1	DINTIEDAVK	Identical sequence found in both Guinea Pig and Mouse
	TSVAGTVR	In Mice: TSVA E TVR In GP: TSVA E TVR
SIRT2	LLDELTLEGVAR	Identical sequence found in Guinea Pig In Mice: LLDELTLEGV T R
	IFSEVTPK	In mice: IFSE A TP R In GP: L FS D VTPK
SIRT3	LYTQNIDGLER	Identical sequence found in both Guinea Pig and Mouse
	VSGIPASK	In mice: A SGIPASK In GP: A SGIPASK
SIRT4	RPIQHGDFVR	In mice: RPIQH I DFVR In GP: RPIQH S DFVR
	FILTAWEK	In mice: FILT A RE Q In GP: F TL A Q D K
SIRT5	VVVITQNIDELHR	Identical sequence found in Mouse In GP: V AVITQNIDEL H L R
	NLLEIHGSLFK	In mice: NLLEIHG T L F K In GP: NL V EIHG T IFK
SIRT6	FLVSQNV DGLHVR	Identical sequence found in both Guinea Pig and Mouse
	LVIVNLQPTK	Identical sequence found in both Guinea Pig and Mouse
SIRT7	LLAESADLVTELQGR	In mice: LLAES E DLVTELQGR In GP: LLAES E DLVTELQGR
	DTIVHFGER	Identical sequence found in both Guinea Pig and Mouse

All samples were fractionation on a 1D-SDS-PAGE to reduce sample complexity and a workflow of the sample preparation procedure can be found in Figure 2.6 below.

Figure 2.6 Sample Fractionation and MRM Workflow



2.3.3 Sirtuin Isoforms

Another important issue is the existence of splice variants or isoforms of the sirtuin proteins. Sequences of all 7 human sirtuins and their isoforms (obtained from UniProt). The peptides used for MRM quantification experiments are highlighted in red and in larger font size in Figure 2.7. All sirtuin isoforms contain at least one of the peptides used for quantification, and both peptides are represented in the majority of isoforms.

Figure 2.7 Sequences for all seven human sirtuins and their isoforms

SIRT1 Isoform 1	>sp Q96EB6 SIR1_HUMAN NAD-dependent protein deacetylase sirtuin-1 OS=Homo sapiens GN=SIRT1 PE=1 SV=2 MADEAALALQPGGSPAAGADREAASSPAGEPLRKRRRDGPGGLERSPGEPGGAAPER EVPAAARGCPGAAAAALWREAEAEAAAAGGEQEAQATAAAGEGDNGPGLQGPSREP PLADNLYDEDDDDDEGESEEEEEAAAAAIGYRDNLLFGDEIITNGFHSCESDEEDRASHASSS DWTPRPRIGPYTFVQQHLMIGTDPRTILKDLLPETIPPPPELDDMTLWQIVINILSEPPKRRK KRK DINTIEDAVK LLQECKKIIVLTGAGVSVSCGIPDFRSRDGIYARLAVDFPDLPDPQA MFDIEYFRKDPRPFFKFAKEIYPGQFQPSLCHKFIALSDKEGKLLRNYTQNIDTLEQVAGIQ RIIQCHGSFATASCLICKYKVDCEAVRGDIFNQVVPRCPRCPADEPLAIMKPEIVFFGENL PEQFHRAMKYDKDEVDLLIVIGSSLKVRPVALIPSSIPHEVPQILINREPLPHLHFDVVELLD CDVIINELCHRLGGEYAKLCCNPVKLSEITEKPPRTQKELAYLSELPTPLHVSEDSSSPERT SPPDSSVIVTLLDQAASNDLDLVSESKGCMECKPQEVQTSRNVESIAEQMENPDLKNV GSSTGEKNER TSVAGTVR KCWPNRVAKEQISRRLDGNQYLFLPPNRYIFHGAEVYSDS EDDLSSSSCGSNSDSGTCQSPSLEEPMEDESEIEEFYNGLEDEPDVPERAGGAGFGTDG DDQEAINEAISVKQEVTDMMNYPNSKS
------------------------	--

SIRT1 Isoform 2	>sp Q96EB6-2 SIR1_HUMAN Isoform 2 of NAD-dependent protein deacetylase sirtuin-1 OS=Homo sapiens GN=SIRT1 MADEAALALQPGGSPAAGADREAASSPAGEPLRKRRRDGPGGLERSPGEPGGAAPER EVPAAARGCPGAAAAALWREAEAEAAAAGGEQEAQATAAAGEGDNGPGLQGPSREP PLADNLYDEDDDDDEGESEEEEEAAAAAIGYRDNLLFGDEIITNGFHSCESDEEDRASHASSS DWTPRPRIGPYTFVQQHLMIGTDPRTILKDLLPETIPPPPELDDMTLWQIVINILSEPPKRRK KRK DINTIEDAVK LLQECKKIIVLTGAGVSVSCGIPDFRSRDGIYARLAVDFPDLPDPQA MFDIEYFRKDPRPFFKFAKEIYPGQFQPSLCHKFIALSDKEGKLLRNYTQNIDTLEQVAGIQ RIIQCHGSFATASCLICKYKVDCEAVRGDIFNQVVPRCPRCPADEPLAIMKPEIVFFGENL PEQFHRAMKYDKDEVDLLIVIGSSLKVRPVALIPSNQYLFLPPNRYIFHGAEVYSDSEDDV LSSSSCGSNSDSGTCQSPSLEEPMEDESEIEEFYNGLEDEPDVPERAGGAGFGTDGDDQ EAINEAISVKQEVTDMMNYPNSKS
------------------------	---

SIRT2 Isoform 1	>sp Q8IXJ6 SIR2_HUMAN NAD-dependent protein deacetylase sirtuin-2
------------------------	---

OS=Homo sapiens GN=SIRT2 PE=1 SV=2
MAEPDPSHPLETQAGKVQEAQSDSDSEGGAGGEADMDFLRNLSQTLSLGSQKER
LLDELTLEGVARYMQSERCRRVICLVGAGISTSAGIPDFRSPSTGLYDNLEKYHLPYPE
AIFEISYFKKHPEPFFALAKELYPGQFKPTICHYFMRLKDKGLLRCYTQNIDTLERAGLE
QEDLVEAHGTFYTSHCVSASCRHEYPLSWMKEK**IFSEVTPK**CEDCQSLVKPDIVFFGES
LPARFFSCMQSDFLKVDLLLVMGTSLQVQPFASLISKAPLSTPRLLINKEKAGQSDPFLG
MIMGLGGGMDFDSSKAYRDVAWLGECDQGCLALAEELLGWKKELEDLVRREHASIDAQ
SGAGVNPSTSPKKSPPPAKDEARTTEREKPQ

SIRT2 Isoform 2 >sp|Q8IXJ6-2|SIR2_HUMAN Isoform 2 of NAD-dependent protein deacetylase
sirtuin-2 OS=Homo sapiens GN=SIRT2
MDFLRNLSQTLSLGSQKER**LLDELTLEGVAR**YMQSERCRRVICLVGAGISTSAGIPDF
RSPSTGLYDNLEKYHLPYPEAIFEISYFKKHPEPFFALAKELYPGQFKPTICHYFMRLKDKG
LLRCYTQNIDTLERAGLEQEDLVEAHGTFYTSHCVSASCRHEYPLSWMKEK**IFSEVTPK**
KCEDCQSLVKPDIVFFGESLPARFFSCMQSDFLKVDLLLVMGTSLQVQPFASLISKAPLST
PRLLINKEKAGQSDPFLGMIMGLGGGMDFDSSKAYRDVAWLGECDQGCLALAEELLGW
KKELEDLVRREHASIDAQSGAGVNPSTSPKKSPPPAKDEARTTEREKPQ

SIRT2 Isoform 3 >sp|Q8IXJ6-3|SIR2_HUMAN Isoform 3 of NAD-dependent protein deacetylase
sirtuin-2 OS=Homo sapiens GN=SIRT2
MPLAECPSRCCLSSFRSVDFLRNLSQTLSLGSQKER**LLDELTLEGVAR**YMQSERCRR
VICLVGAGISTSAGIPDFRSPSTGLYDNLEKYHLPYPEAIFEISYFKKHPEPFFALAKELYPGQ
FKPTICHYFMRLKDKGLLRCYTQNIDTLERAGLEQEDLVEAHGTFYTSHCVSASCRHE
YPLSWMKEK**IFSEVTPK**CEDCQSLVKPDIVFFGESLPARFFSCMQSDFLKVDLLLVMGT
SLQVQPFASLISKAPLSTPRLLINKEKAGQSDPFLGMIMGLGGGMDFDSSKAYRDVAWL
GECDQGCLALAEELLGWKKELEDLVRREHASIDAQSGAGVNPSTSPKKSPPPAKDEA
RTTEREKPQ

SIRT2 Isoform 4 >sp|Q8IXJ6-4|SIR2_HUMAN Isoform 4 of NAD-dependent protein deacetylase
sirtuin-2 OS=Homo sapiens GN=SIRT2
MAEPDPSHPLETQAGKVQEAQSDSDSEGGAGGEADMDFLRNLSQTLSLGSQKER
LLDELTLEGVARYMQSERCRRVICLVGAGISTSAGIPDFRSPSTGLYDNLEKYHLPYPE
AIFEISYFKKHPEPFFALAKELYPGQFKPTICHYFMRLKDKGLLRCYTQNIDTLERAGLE
QEDLVEAHGTFYTSHCVSASCRHEYPLSWMKEK**IFSEVTPK**CEDCQSLVKPDIVFFGES
LPARFFSCMQSDFLKVDLLLVMGTSLQGRGLAG

SIRT2 Isoform 5 >sp|Q8IXJ6-5|SIR2_HUMAN Isoform 5 of NAD-dependent protein deacetylase
sirtuin-2 OS=Homo sapiens GN=SIRT2
MAEPDRRRVICLVGAGISTSAGIPDFRSPSTGLYDNLEKYHLPYPEAIFEISYFKKHPEPFFA
LAKELYPGQFKPTICHYFMRLKDKGLLRCYTQNIDTLERAGLEQEDLVEAHGTFYTSHC
VSASCRHEYPLSWMKEK**IFSEVTPK**CEDCQSLVKPDIVFFGESLPARFFSCMQSDFLKV
DLLLVMGTSLQVQPFASLISKAPLSTPRLLINKEKAGQSDPFLGMIMGLGGGMDFDSSK
AYRDVAWLGECDQGCLALAEELLGWKKELEDLVRREHASIDAQSGAGVNPSTSPKK

	SPPPAKDEARTTEREKPQ
SIRT3 Isoform 1	<p>>sp Q9NTG7 SIR3_HUMAN NAD-dependent protein deacetylase sirtuin-3, mitochondrial OS=Homo sapiens GN=SIRT3 PE=1 SV=2</p> <p>MAFWGWRAAAALRLWGRVVERVEAGGGVGPFQACGCRLVLGGRDDVSAGLRGSHG ARGEP LDPARPLQRPPRPEVPRAFRRQPRAAAPSTFFSSIKGRRSISFSVGASSVVGSGGSSDKG KLSLQDVAELIRARACQRVVVMVGAGISTPSGIPDFRSPGSGLYSNLQQYDLPYPEAIFEL PFFFHNPKPFFTLAKELYPGNYKPNVTHYFLRLLHDKGLLLRLYTQNIIDGLERVSGIPA SKLVEAHGTFASATCTVCQRPFPGEDIRADVMADRVPRCPVCTGVVKPDIVFFGEPLPQ RFLHVVDFPMADLLLILGTSLEVEPFASLTEAVRSSVPRLLINRDLVGPLAWHPRSRDVA QLGDVVHGVESLVELLGWTEEMRDLVQRETGKLDGPDK</p>
SIRT3 Isoform 2	<p>>sp Q9NTG7-2 SIR3_HUMAN Isoform 2 of NAD-dependent protein deacetylase sirtuin-3, mitochondrial OS=Homo sapiens GN=SIRT3</p> <p>MVGAGISTPSGIPDFRSPGSGLYSNLQQYDLPYPEAIFELPFFFHNPKPFFTLAKELYPGNY KPNVTHYFLRLLHDKGLLLRLYTQNIIDGLERVSGIPASKLVEAHGTFASATCTVCQRPFP GEDIRADVMADRVPRCPVCTGVVKPDIVFFGEPLPQRFLLHVVDFPMADLLLILGTS LEVEPFASLTEAVRSSVPRLLINRDLVGPLAWHPRSRDVAQLGDVVHGVESLVELLGWT EEMRDLVQRETGKLDGPDK</p>
SIRT4	<p>>sp Q9Y6E7 SIR4_HUMAN NAD-dependent protein lipoamidase sirtuin-4, mitochondrial OS=Homo sapiens GN=SIRT4 PE=1 SV=1</p> <p>MKMSFALTFRSAKGRWIANPSQPCSKASIGLFPASPPLDPEKVKELQRFITLSKRLLVM TGAGISTESGIPDYRSEKVGLYARTDRRPIQHGDVFRSAPIRQRYWARNFVGWPQFS SHQPNPAHWALSTWEKLGKLYWLVTQNVDAHLTKAGSRRLTELHGCMDRVLCCLDCGE QTPRGVLQERFQVLNPTWSAEAHGLAPDGDVFLSEEQVRSFQVPTCVQC GGHLKPDV VFFGDTVNPDKVDFVHKRVKEADSLLVVGSSLQVYSGYRFILTAWEKKLPIAILNIGPTR SDDLACLKLNSRCGELLPLIDPC</p>
SIRT5 Isoform 1	<p>>sp Q9NXA8 SIR5_HUMAN NAD-dependent protein deacylase sirtuin-5, mitochondrial OS=Homo sapiens GN=SIRT5 PE=1 SV=2</p> <p>MRPLQIVPSRLISQLYCGLKPPASTRNQICLKMARPSSSMADFRKFFAKAKHIVIISGAGV SAESGVPTFRGAGGYWRKWQAQDLATPLAFAHNPSRVWEFYHYRREVMGSKEPNAG HRAIAECETRLGKQGRRVVITQNIIDELHRKAGTKNLLEIHGSLFKTRCTSCGVVA ENYKSPICPALSGKGAPEPGTQDASIPVEKLPRCEEAGCGGLLRPHVVWFGENLDPAILE EVDRELAHCDLCLVVGTSVVYPAAAMFAPQVAARGVPVAEFNTETTPATNRFHFHQG PCGTTLPEALACHENETVS</p>
SIRT5 Isoform 2	<p>>sp Q9NXA8-2 SIR5_HUMAN Isoform 2 of NAD-dependent protein deacylase sirtuin-5, mitochondrial OS=Homo sapiens GN=SIRT5</p> <p>MRPLQIVPSRLISQLYCGLKPPASTRNQICLKMARPSSSMADFRKFFAKAKHIVIISGAGV SAESGVPTFRGAGGYWRKWQAQDLATPLAFAHNPSRVWEFYHYRREVMGSKEPNAG HRAIAECETRLGKQGRRVVITQNIIDELHRKAGTKNLLEIHGSLFKTRCTSCGVVA ENYKSPICPALSGKGAPEPGTQDASIPVEKLPRCEEAGCGGLLRPHVVWFGENLDPAILE</p>

	EVDRELAHCDLCLVVGTSVVYPAAMFAPQVAARGVPVAEFNTETTPATNRFSHLISISS LIIKN
SIRT5 Isoform 3	>sp Q9NXA8-3 SIR5_HUMAN Isoform 3 of NAD-dependent protein deacylase sirtuin-5, mitochondrial OS=Homo sapiens GN=SIRT5 MRPLQIVPSRLISQLYCGLKPPASTRNQICLKMARPSSSMADFRKFFAKAKHIVIISGAGV SAESGVPTFRGAGGYWRKWQAQDLATPLAFAHNPSRVWEFYHYRREVMGSKEPNAG HRAIAECETRLGKQGR VVVITQNIDELHR KAGTK NLLEIHGSLFK TRCTSCGVVA ENYKSPICPALSGKGCEEAGCGLLRPHVWVWFGENLDPAILLEEVDRELAHCDLCLVVGTS SVVYPAAMFAPQVAARGVPVAEFNTETTPATNRFHFQGPCGTTLPEALACHENETV S
SIRT5 Isoform 4	>sp Q9NXA8-4 SIR5_HUMAN Isoform 4 of NAD-dependent protein deacylase sirtuin-5, mitochondrial OS=Homo sapiens GN=SIRT5 MGSKEPNAGHRAIAECETRLGKQGR VVVITQNIDELHR KAGTK NLLEIHGSLFK T RCTSCGVVAENYKSPICPALSGKGAPEPGTQDASIPVEKLPRCEEAGCGLLRPHVWVWF GENLDPAILLEEVDRELAHCDLCLVVGTSVVYPAAMFAPQVAARGVPVAEFNTETTPAT NRFHFQGPCGTTLPEALACHENETVS
SIRT6 Isoform 1	>sp Q8N6T7 SIR6_HUMAN NAD-dependent protein deacetylase sirtuin-6 OS=Homo sapiens GN=SIRT6 PE=1 SV=2 MSVNYAAGLSPYADKGKCGLPEIFDPPEELERKVVWELARLVWQSSSVFHTGAGISTAS GIPDFRGPHGVWTMEERGLAPKFDTTFESARPTQTHMALVQLERVGLLR FLVSQNV DGLHVR SGFPRDKLAELHGNMFVEECAKCKTQYVRDTPVVGTMGLKATGRLCTVAKA RGLRACRGELRDTILDWEDSLPDRDLALADEASRNADLSITLGTSIQIRPSGNLPLATKRR GGR LVIVNLQPTK HDRHADLRIHGYVDEVMTRLMKHLGLEIPAWDGPRVLERALPPL PRPPTPKLEPKESPTRINGSIPAGPKQEPCAQHNGSEPA SPKRERPTSPAPHRPPKRVKA KAVPS
SIRT6 Isoform 2	>sp Q8N6T7-2 SIR6_HUMAN Isoform 2 of NAD-dependent protein deacetylase sirtuin-6 OS=Homo sapiens GN=SIRT6 MSVNYAAGLSPYADKGKCGLPEIFDPPEELERKVVWELARLVWQSSSVFHTGAGISTAS GIPDFRGPHGVWTMEERGLAPKFDTTFESARPTQTHMALVQLERVGLLR FLVSQNV DGLHVR SGFPRDKLAELHGNMFVEECAKCKTQYVRDTPVVGTMGLKATGRLCTVAKA RGLRACRNADLSITLGTSIQIRPSGNLPLATKRRGGR LVIVNLQPTK HDRHADLRIHGY VDEVMTRLMKHLGLEIPAWDGPRVLERALPPLPRPPTPKLEPKESPTRINGSIPAGPKQ EPCAQHNGSEPA SPKRERPTSPAPHRPPKRVKAKAVPS
SIRT7 Isoform 1	>sp Q9NRC8 SIR7_HUMAN NAD-dependent protein deacetylase sirtuin-7 OS=Homo sapiens GN=SIRT7 PE=1 SV=1 MAAGGLSRSERKAAERVRLREEQQRERLRQVSRILRKAASAEGR LLAESADLV TELQGR SRRREGKRRQEEVCDDPEELRGKVRERLASAVRNAKYLVVYTGAGISTAASIP DYRGPNGVWTLQKGRSVSAADLSEAEPTLTHMSITRLHEQKLQHVVSQNCGLHLR SGLPRTAISELHGNMYIEVCTSCVPNREYVRVFDVTERTALHRHQTGR TCHKCGTQLR D

TIVHFGERGTLGQPLNWEAATEAASRADTILCLGSSLKVLKKYPRLWCMTKPPSRRPKL
YIVNLQWTPKDDWAALKLHGKCDDVMRLLMAELGLEIPAYSRWQDPIFSLATPLRAGE
EGSHSRKSLCRSREEAPPGDRGAPLSSAPILGGWFGRGCTKRTRKKVT

SIRT7 Isoform 2 >sp|Q9NRC8-2|SIR7_HUMAN Isoform 2 of NAD-dependent protein
deacetylase sirtuin-7 OS=Homo sapiens GN=SIRT7

MAAGGLSRSEKAAERVRLREEQQRERLRQVSRLRKAASAEGR**LLAESADLV**
TELQGRSRRREGLKRRQEEVCDDPEELRGKVELASAVRNAKYLVVYTGAGISTAASIP
DYRGPNGVWTLQKGRSVSAADLSEAEPTLTHMSITRLHEQKLVRLGGWYTCQGPGR
APWCPVGN

SIRT7 Isoform 3 >sp|Q9NRC8-3|SIR7_HUMAN Isoform 3 of NAD-dependent protein
deacetylase sirtuin-7 OS=Homo sapiens GN=SIRT7

MPGPRRRSPSACPQVSRILRKAASAEGR**LLAESADLVTELQGR**SRRREGLKRR
QEEVCDDPEELRGKVELASAVRNAKYLVVYTGAGISTAASIPDYRGPNGVWTLQKGR
SVSAADLSEAEPTLTHMSITRLHEQKLVQHVSQNCGLHLRSLPRTAISELHGNMYIE
VCTSCVPNREYVRVFDVTERTALHRHQTGRTCHKCGTQLRDTIVHFGERTLGQPLNW
EAATEAASRADTILCLGSSLKVLKKYPRLWCMTKPPSRRPKLYIVNLQWTPKDDWAALKL
HGKCDDVMRLLMAELGLEIPAYSRVL

2.3.4 Validation of MRM method with established protocols

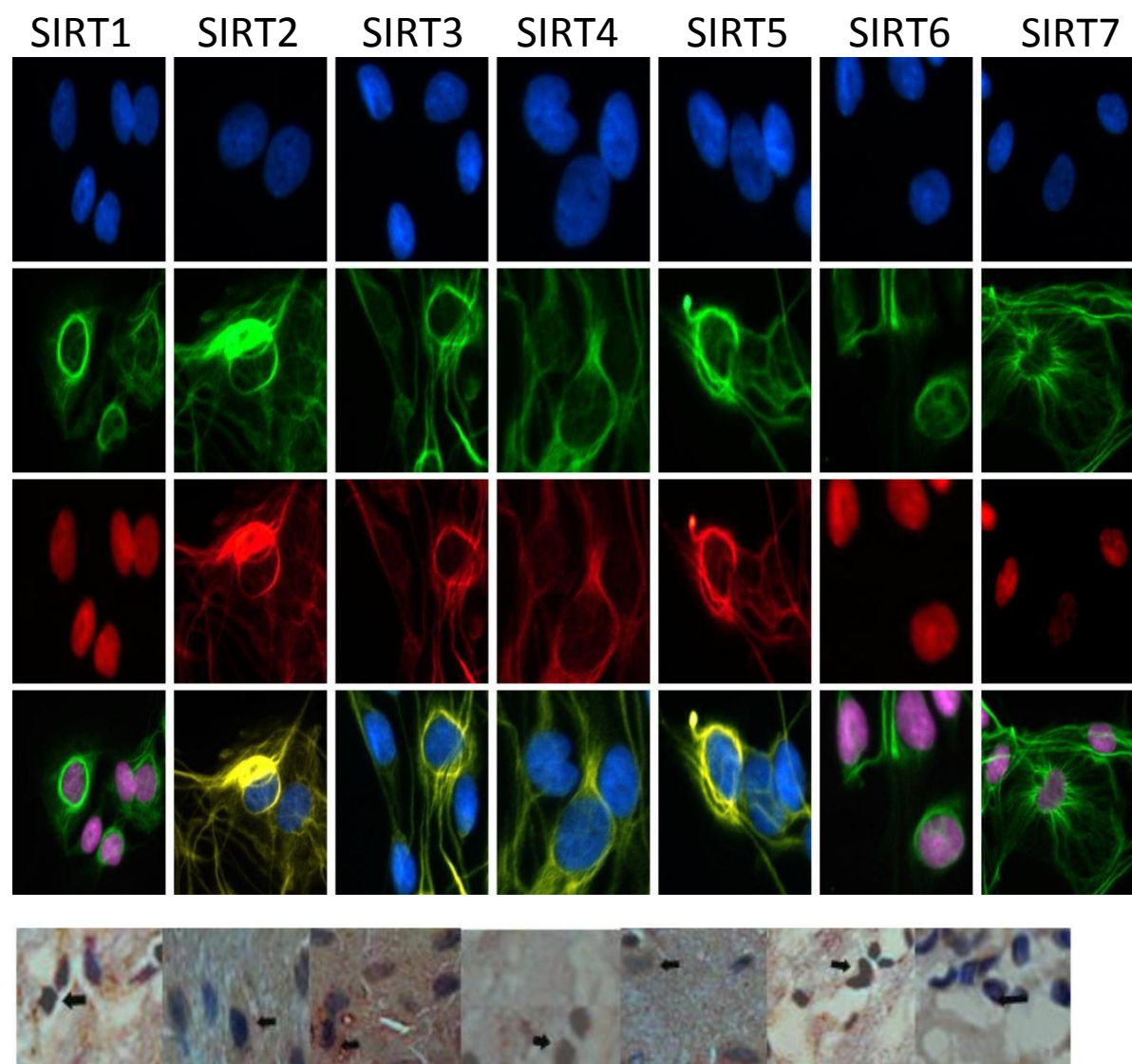
Human brain cells and tissue samples were compared with established protocols for sirtuin detection such as immunohistochemical staining, PCR and western blotting.

Immunohistochemical staining showed that all seven sirtuins are expressed in astrocytes (Figure 2.8, Panel A, rows 1-4) and control human frontal lobe brain tissue (Panel A, row 5).

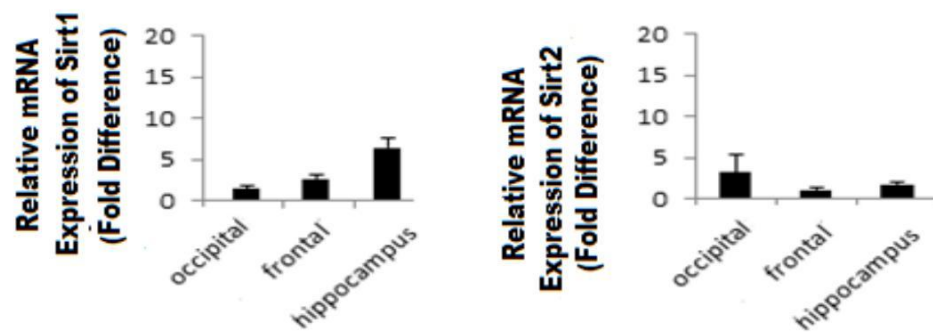
PCR identified SIRT1 and SIRT2 mRNA in control human frontal, occipital and hippocampus brain tissue (Figure 2.8 Panel B). Western blotting confirmed the identification of SIRT1, 2 and 3 in control human frontal lobe brain tissue.

Figure 2.8 Sirtuin expression in human brain cells and tissue. Immunohistochemical staining of astrocytes (Panel A row 1-4) and human frontal brain tissue (Panel A, row 5). Row 1 is blue (DAPI) staining of nuclei, row 2 is green cell marker for GFAP, row 3 is red stain for sirtuin and row 4 is a merge of above three stains. Row 5 shows brown staining (highlighted with arrows) for sirtuin and pruple haemoatoxylin staining. PCR of SIRT1 and SIRT2 mRNA in occipital, frontal and hippocampal human control brain (Panel B) and cropped images of western blotting of SIRT1-3 protein expression in human control frontal brain tissue (n=3) at molecular weights of approximately 40kDa, 50kDa and 30kDa respectively (Panel C).

A



B



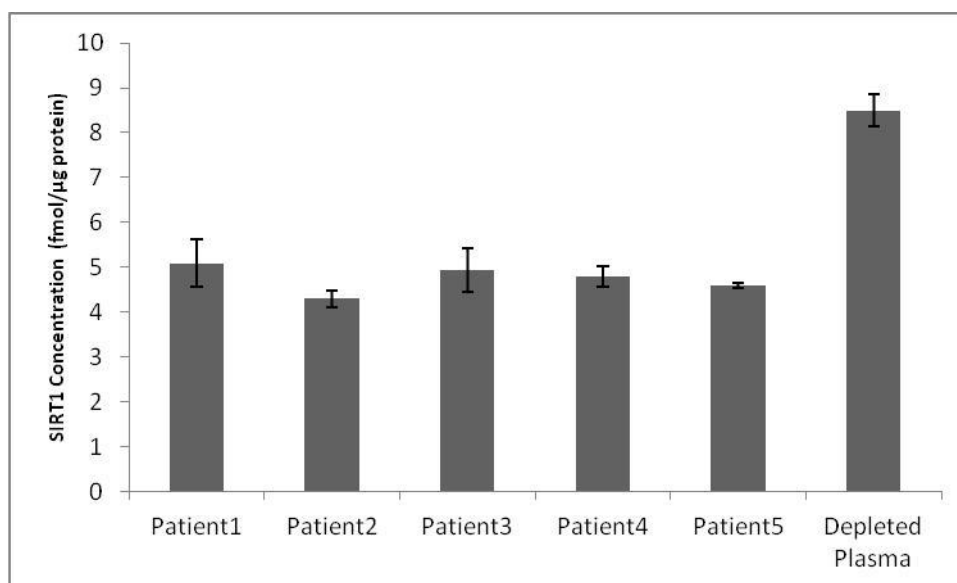
C



2.3.5 Quantification of sirtuins in CSF and immunodepleted plasma

SIRT1 was quantified in five control CSF patients and in control plasma immunodepleted of the six most abundant proteins. SIRT1 was the only sirtuin detected and was found to range from 4.30 ± 0.19 to 5.09 ± 0.53 fmol/ μ g protein in CSF and 8.68 ± 0.35 fmol/ μ g protein in plasma (Figure 2.9). SIRT2-7 in CSF and immunodepleted plasma were found to be below the detection limits of the assay. All samples were fractionation by 1D-SDS-PAGE to reduce sample complexity and a workflow of the sample preparation procedure can be found in Figure 2.6.

Figure 2.9 SIRT1 levels in CSF and depleted plasma. SIRT1 levels in CSF (n=5) samples and a plasma sample depleted of the six most abundant plasma proteins (high abundance protein removal was achieved using an Agilent Hu6 affinity column).



Sirtuin Standard Recoveries and Matrix Effects

The sirtuin levels presented in samples tested are the amounts after the in-gel extraction. Additional experiments to determine the recovery of peptides after this SDS/PAGE step were completed as were experiments to determine matrix effects.

Standard curves were prepared in 3 different matrices and recoveries compared after spiking known amounts of commercially obtained standard sirtuin proteins (Abcam, UK) into depleted human plasma samples.

For the experiments investigating matrix effects, standard curves using buffer only (0.1% formic acid), gel control (blank gel bits) and depleted plasma protein (LAP) were completed using gel bits cut from the appropriate sections of gel lanes containing 20ug of depleted plasma. For the blank and LAP gel matrix work, the various concentrations of light synthetic peptide were added after the gel bits were excised, followed by tryptic digestion and then MRM analysis. Standard curves for SIRT1, 2, 3, 5 and 6 with a seven point standard curve for each were completed. The gel image can be seen in Figure 2.10 (each label representing one point on the standard curve) and the standard curves for each of the individual peptides across the 3 matrices can be seen in Figure 2.11

Figure 2.10 A typical colloidal coomassie stained SDS/PAGE gel used to assess matrix effects on standard curves. Bands were cut from positions at which intact sirtuin proteins would typically be expected, and used to test matrix effects on the synthetic peptide standards. In addition to this, intact commercial recombinant sirtuin preparations were spiked into depleted plasma and run by SDS/PAGE (see Figure 2.11).

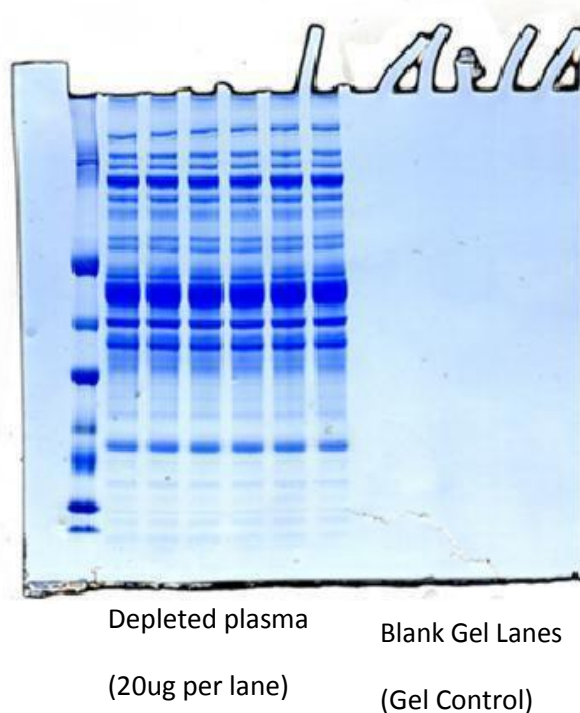
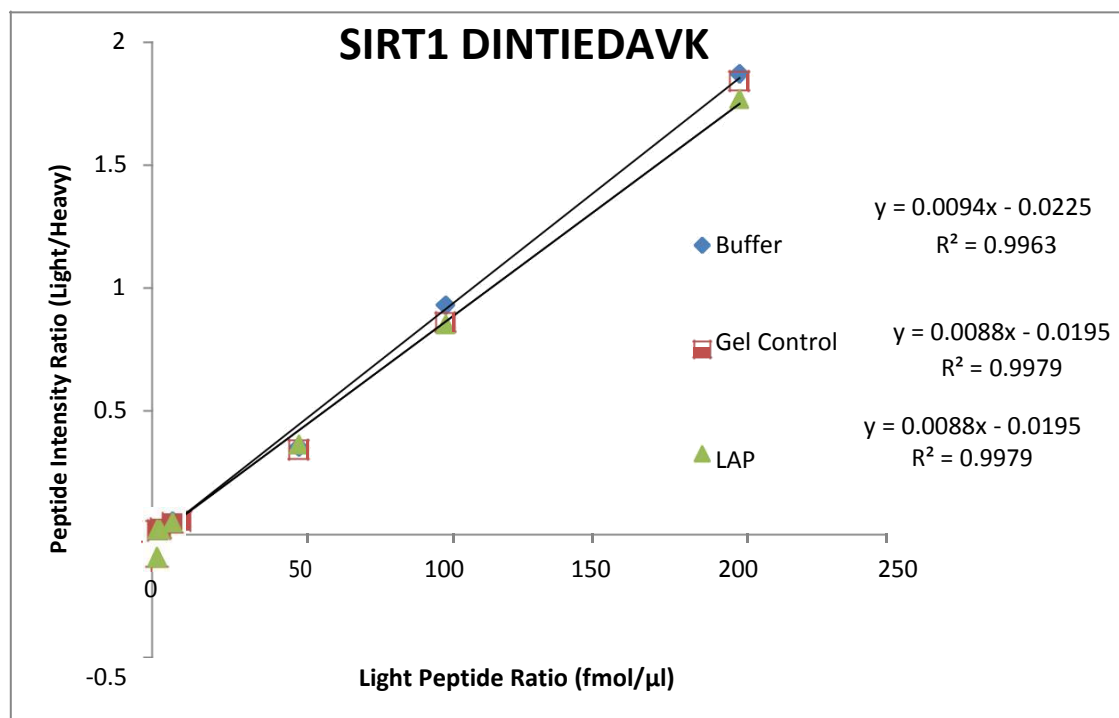
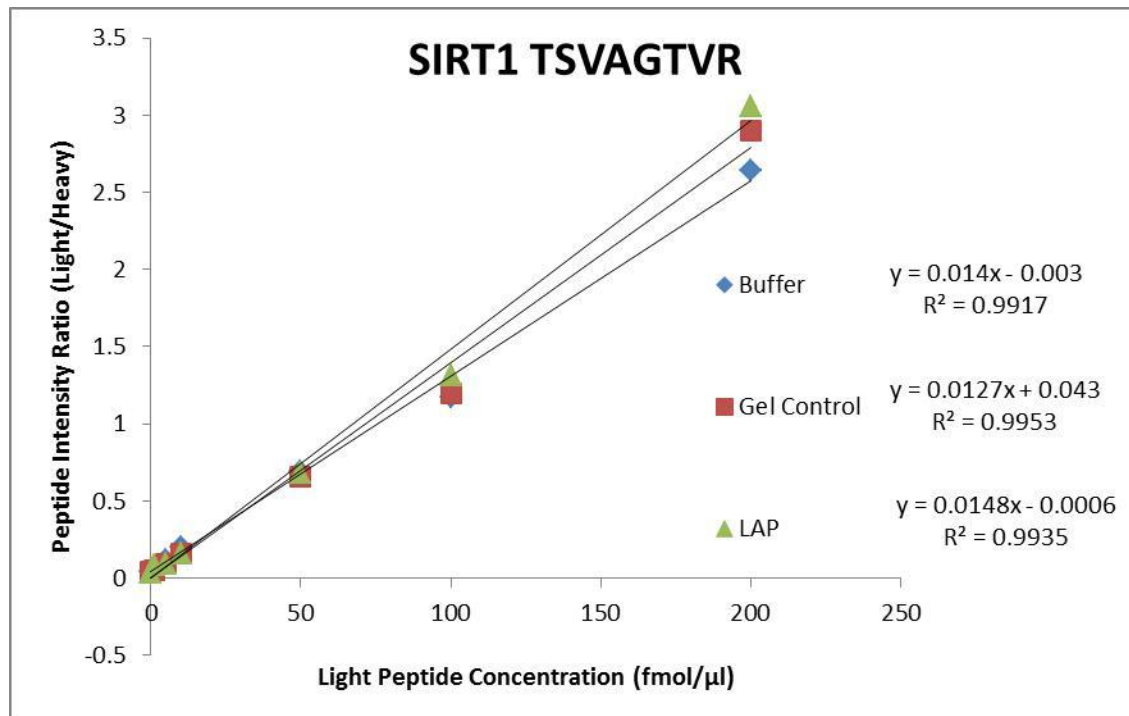
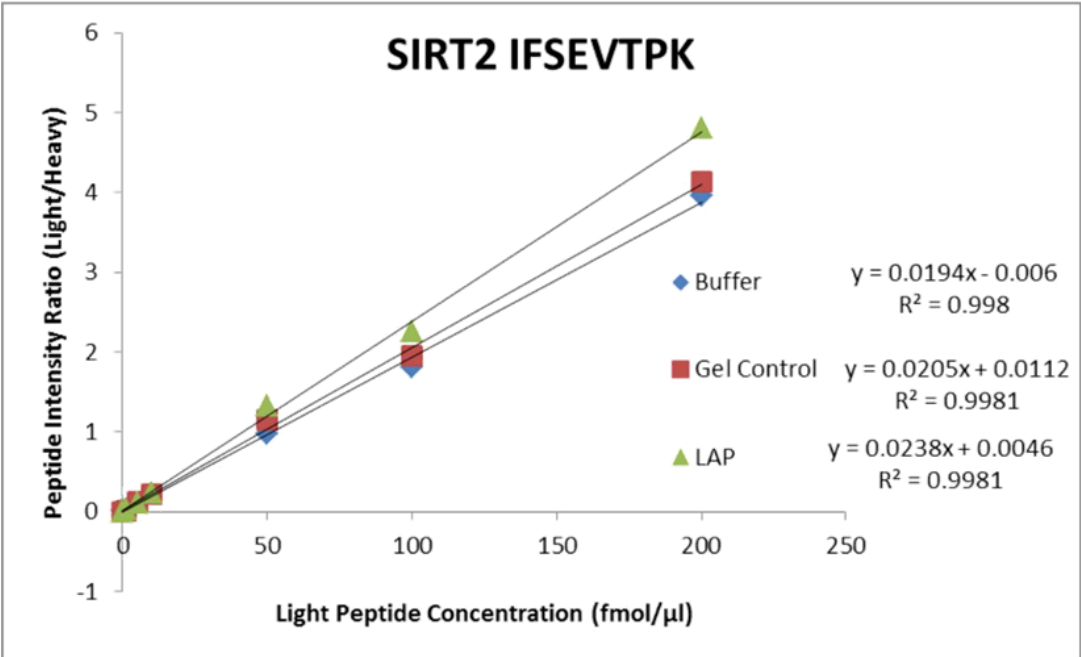
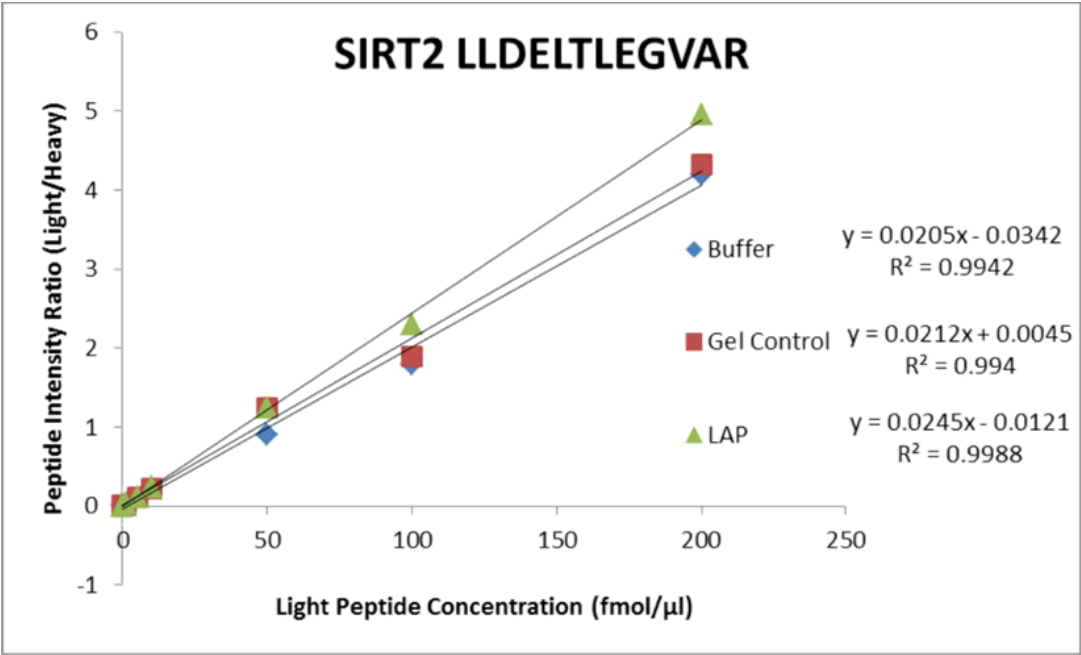
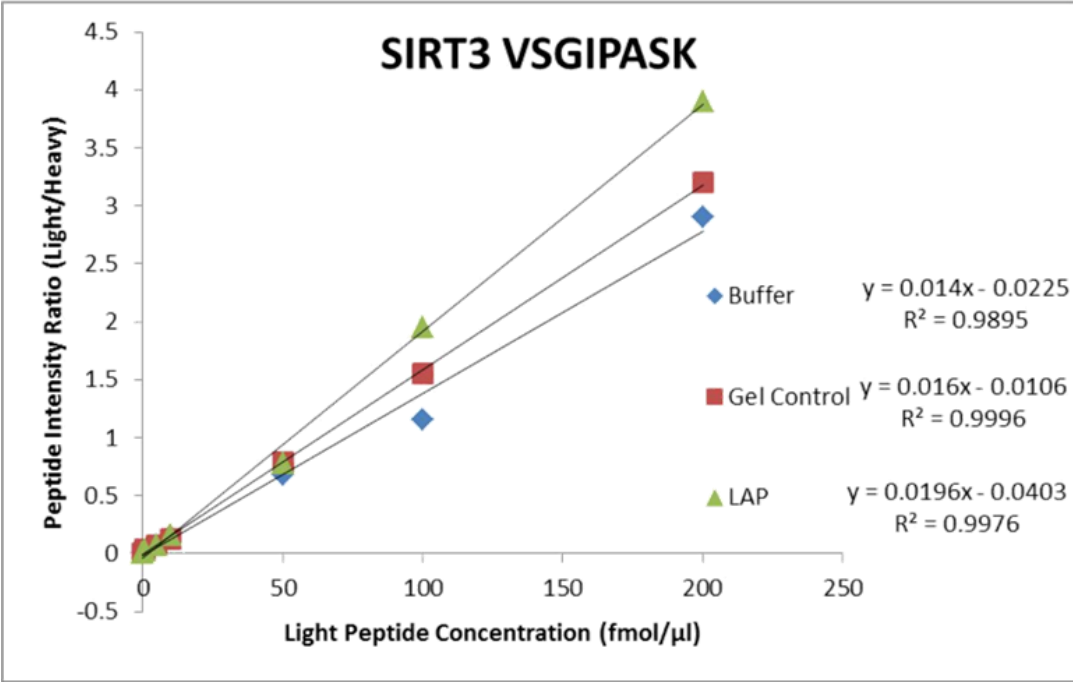
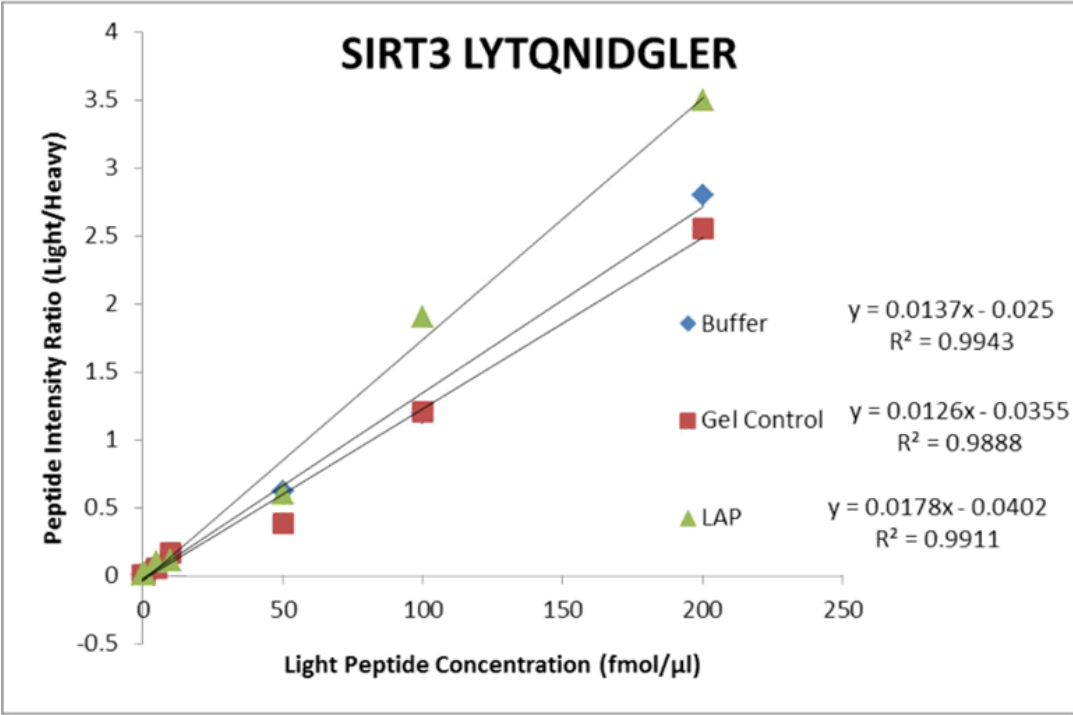
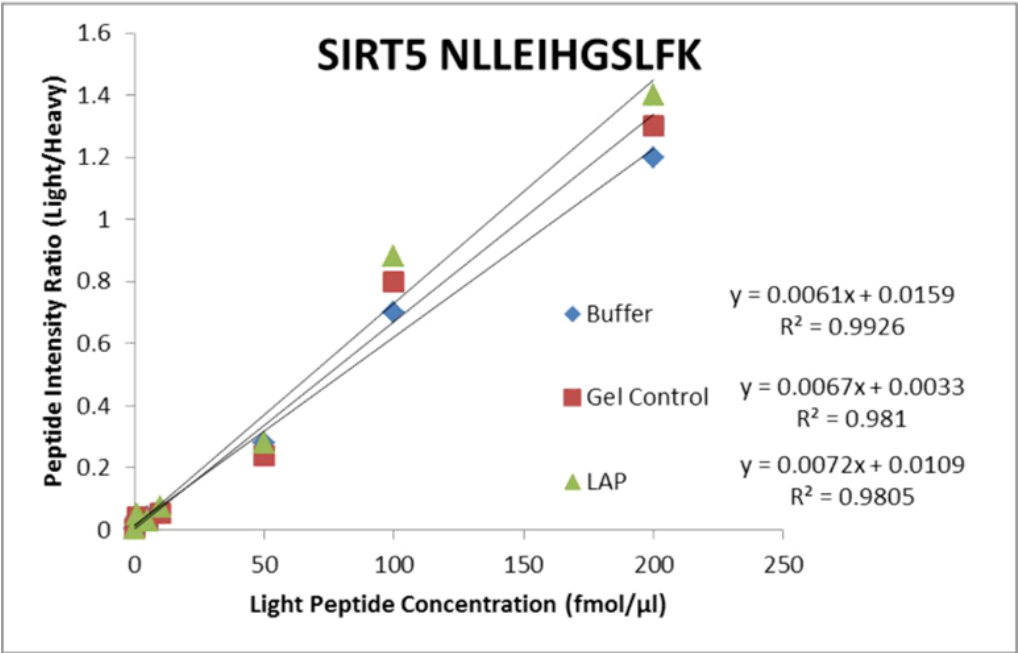
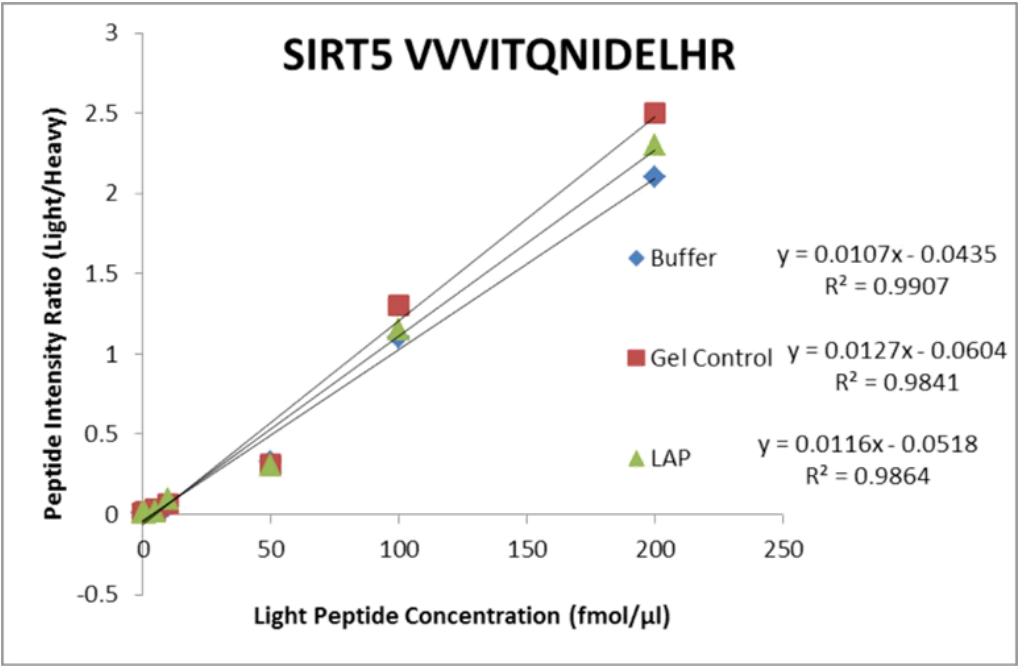


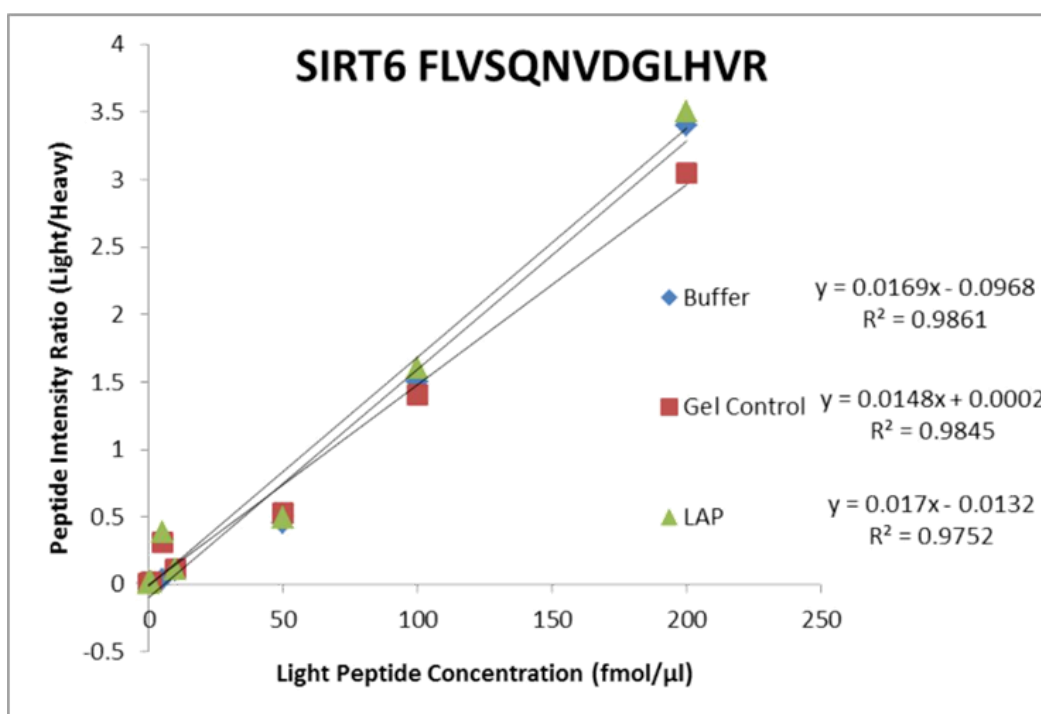
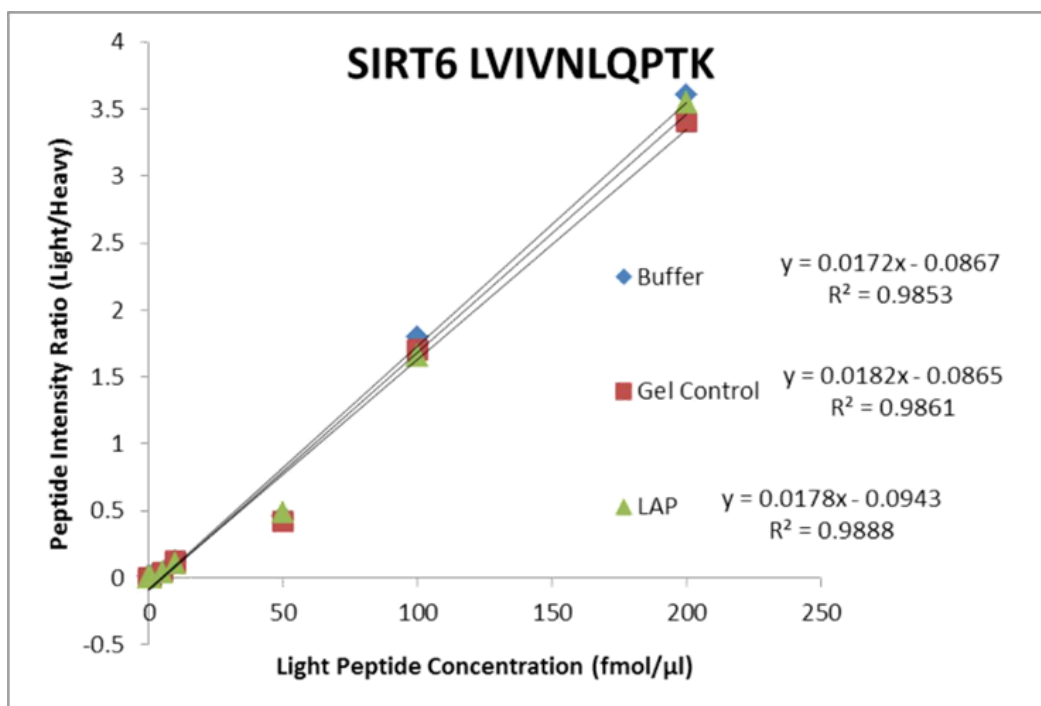
Figure 2.11 Sirtuin peptide standard curves. Prepared in several matrices, including buffer only, a blank gel control, a gel containing low abundance plasma (LAP) proteins (see figure 2.10 for the gel used for the gel matrices).











Our results show that the introduction of the gel bits (blank and LAP) did not affect the linearity of the standard curves produced, and the regression equations are similar.

For further validation of extraction efficiency, intact recombinant sirtuin protein standards were purchased (SIRT1,2,3,5 and 6) and were spiked into depleted control plasma and recoveries calculated after gel fractionation, and in-gel digestion of the recombinant sirtuins.

To determine recoveries of sirtuin proteins, commercial intact sirtuin standards were run by SDS PAGE (5 µg per lane). Hu6 high abundance depleted plasma spiked with 2 ug and 5 µg of the sirtuin standard for SIRT1, 2, 3, 5 and 6 were also run on the same gel (Figure 2.12). Sirtuin 5 µg spike recoveries were calculated in the LAP spike relative to the sirtuin 5 µg standard protein in buffer only samples. The sirtuin 2 µg spike recoveries were calculated in the LAP spike relative to values extrapolated from the results of the sirtuin 5 µg standard protein in buffer only samples (Table 2.8).

The main issue confronted with this approach was that the highest quality commercial sirtuin standards were not highly pure as can be seen by the multiple bands stained on the gel (Figure 2.12). Consequently it is likely that there is an overestimation of the amount of sirtuin loaded on the gel, and therefore a concomitant underestimation of sirtuin peptide recovery.

However, even with the below ideal standards, the majority of sirtuin peptides had reasonable recovery estimates from the samples after gel bit digestion, relative to buffer only preparations. Sirtuin recoveries (from the gel spike experiment, Figure 2.12), relative to sirtuin run in buffer only achieved 61–96% recovery and 58–131% recovery for the 5 µg and 2 µg sirtuin levels respectively, all recoveries are shown in Table 2.8.

Figure 2.12 Colloidal coomassie stained SDS/PAGE gel used for sirtuin recovery experiments. Lane 1: prestained molecular weight markers; Lanes 2-6: commercial SIRT1, 2, 3, 5 and 6 recombinant sirtuin protein standards (5ug per lane); Lanes 8-12: 20ug Depleted plasma spiked with 5ug of sirtuin standards 1, 2, 3, 5 and 6; Lanes 14-18: Depleted plasma spiked with 2ug of sirtuin standards 1, 2, 3, 5 and 6. Sirtuins 4 and 7 were not used for this experiment as the SIRT4 yield was very low, and SIRT7 was particularly impure.

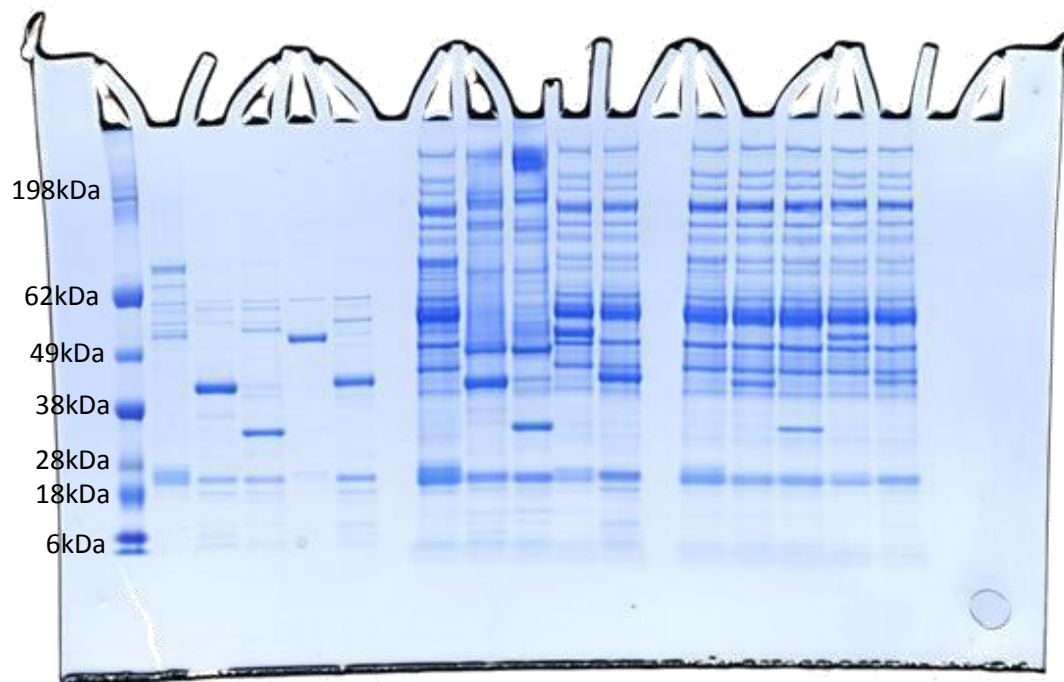


Table 2.8 Sirtuin Recoveries

Sirtuin recovery using the full protocol (sirtuins run by SDS/PAGE) with spiking into matrices consisting of either buffer only (5 μ g sirtuin) or low abundance plasma (LAP) proteins with either 5 μ g or 2 μ g sirtuin spiked. Sirtuin 5 μ g spike recoveries were calculated in the LAP spike relative to sirtuin 5 μ g standard protein in buffer only samples. Sirtuin 2 μ g spike recoveries were calculated in the LAP spike relative to values extrapolated from the results of the sirtuin 5 μ g standard protein in buffer only samples. The peak ratios and percentage recovery values is from three transitions used for each of the two sirtuin peptides per sirtuin protein and were obtained from one gel lane per sirtuin protein. The gel on which these samples were run is shown in Figure 2.12.

	Avg Peak Intensity Ratio (Light/Heavy)	Avg Peak Intensity Ratio (Light/Heavy)	% Recovery	%Recovery
	DINTIEDAVK	TSVAGTVR	DINTIEDAVK	TSVAGTVR
SIRT1 Std 5 μ g	0.0106	0.0196		
SIRT1 Std 2 μ g (extrapolated)	0.0042	0.0078		
SIRT1 Std 5 μ g + 20 μ g LAP	0.0080	0.0178	76.10	90.79
SIRT1 Std 2 μ g + 20 μ g LAP	0.0046	0.0101	108.50	128.83

	LLDELTLEGVAR	IFSEVTPK	LLDELTLEGVAR	IFSEVTPK
SIRT2 Std 5µg	0.0656	0.0514		
SIRT2 Std 2µg (extrapolated)	0.0262	0.0206		
SIRT2 Std 5µg + 20µg LAP	0.0523	0.0496	79.70	96.34
SIRT2 Std 2µg + 20µg LAP	0.0245	0.0219	93.51	106.31
	LYTQNIDGLER	VSGIPASK	LYTQNIDGLER	VSGIPASK
SIRT3 Std 5µg	0.1015	0.0085		
SIRT3 Std 2µg (extrapolated)	0.0406	0.0034		
SIRT3 Std 5µg + 20µg LAP	0.0620	0.0067	61.08	78.80
SIRT3 Std 2µg + 20µg LAP	0.0236	0.0035	58.13	102.9
	VVVITQNIDELHR	NLLEIHGSLFK	VVVITQNIDELHR	NLLEIHGSLFK
SIRT5 Std 5µg	0.0224	0.0271		
SIRT5 Std 2µg (extrapolated)	0.00896	0.01084		
SIRT5 Std 5µg + 20µg LAP	0.01812	0.0198	80.89	73.33
SIRT5 Std 2µg + 20µg LAP	0.0093	0.0104	103.80	95.94
	FLVSQNV DGLHVR	LVIVNLQPTK	FLVSQNV DGLHVR	LVIVNLQPTK
SIRT6 Std 5µg	0.0789	0.0837		
SIRT6 Std 2µg (extrapolated)	0.0316	0.0335		
SIRT6 Std 5µg + 20µg LAP	0.0571	0.0743	72.37	88.76
SIRT6 Std 2µg + 20µg LAP	0.0326	0.0459	103.16	131.14

2.4 Discussion

The rapid expansion of instruments and software in the field of targeted protein quantification by MRM is expected to have vast applications in quantitative protein biochemistry^{451,452}.

Most of the currently used protocols to measure sirtuin changes in the CNS have utilised methods such as ELISA, surface Plasmon resonance, western blotting and fluorescent staining. Mass spectrometry provides a platform that overcomes some of the limitations of antibody based approaches for protein quantification. Isotopically labelled peptide standards allow for the quantification of protein levels and also provide the ability to monitor stability

of analytes throughout the sample processing steps. This greatly simplifies the development of assays from standard immunological formats such as ELISA where well-characterised antibodies are needed. Furthermore MRM facilitates multiplexed analysis, identifying several proteins in a single run, thereby maximising information obtained per sample, and minimising assay time. It measures several transitions per quantified protein, thus generating several independent measurements, and with the use of heavy peptide standards allows for generation of standard curves and accurate quantification, thus having advantages over methods such as western blotting and staining techniques which are semi-quantitative at best and sometimes lack specificity. The MRM approach is also complementary to PCR which targets mRNA levels only.

Perhaps the major limitation to mass spectrometry based protein quantification is throughput and cost. Immunological assays can be performed in 96 well formats and plate readers allow measurement of an entire plate in a single run. Mass spectrometry requires each sample to be run individually with longer run times. Future developments in mass spectrometer detectors may help address this limitation. However one of the main advantages of mass spectrometry is its ability to accurately distinguish different isoforms or modified forms of proteins, even in complex samples. The sensitivity of mass spectrometry is very high and limitations to sensitivity of quantitative assays are often caused by the dynamic range of the proteins in the sample. Thus improved sample purification procedures are often needed for better sensitivity. For example in this study all samples were fractionation on a 1D-SDS-PAGE gel and gel bands excised and tryptic digested prior to MRM analysis to reduce sample complexity. A workflow of the sample preparation procedure can be found in Figure 2.6.

MRM mass spectrometry was successfully utilised in this study to quantify seven mammalian sirtuins in human brain cells, tissues and fluid. Furthermore the method can be used to measure sirtuin expression in animal tissues, such as mouse and guinea pig, in cases where peptide sequences are identical to the human standards. In line with previous data, our results affirm that there is significant divergence in abundance amongst members of the sirtuin family of proteins in the brain. We report SIRT1 and SIRT2 to be the most abundant sirtuins in cultured brain cells with SIRT1 highest in neurons and SIRT2 highest in oligodendrocytes, validating previous studies showing SIRT2 to be highly expressed in oligodendrocytes⁴⁵³. Our study and others have also found SIRT2 expressed in neurons and glial cells^{454,455}. Further validation with higher sample numbers and across a wider range of cell lines may help elucidate differences between cell types for the lower abundant sirtuins.

We found SIRT2 to be the most abundant sirtuin in the adult human frontal lobe and cortex and cerebellum homogenates from the guinea pig. SIRT2 is known to co-localise with microtubules and functions as a tubulin-deacetylase. It is a suppressor of microglial activation and brain inflammation, with reduced levels of SIRT2 leading to increased production of free radicals and neurotoxicity, while its overexpression inhibits brain inflammation⁴³¹. In other studies, however, it has been shown to increase in cells with oxidative stress and promote death cell²⁶⁹. In addition, SIRT2 inhibition has been shown to protect against Parkinson's disease and Huntington's disease^{285,456}. Previously published results have shown SIRT2 to be abundant in the brain and serum^{428,429,440,457} and our study provides further evidence for this and extends its abundance to the guinea pig brain.

SIRT1 was the second-most abundant sirtuin in the brain and the only sirtuin detected in the CSF and plasma using our method. SIRT1 is a neuroprotective factor in a variety of models for neurodegenerative diseases, including Huntington's disease, Multiple Sclerosis and AD^{458,459}. It increases following exposure to cellular stressors, including energy/nutrient depletion and has been linked to increased lifespan in animal models⁴⁶⁰. We were only able to detect SIRT1 in both CSF and plasma while Kumar *et al* have recently identified SIRT1, SIRT2 and SIRT3 in human serum using surface plasmon resonance⁴²⁸. The use of more sensitive mass spectrometry instrumentation, and/or fractionation or enrichment of plasma proteins, may improve sensitivity for the other sirtuins in plasma.

The mitochondrial sirtuins SIRT3-5 were found at lower levels in human brain but detection was improved after detergent fractionation. Further fractionation of samples or purification of mitochondria may facilitate improved mitochondrial sirtuin quantification. Our data also show that SIRT6 and SIRT7 are the third and fourth most abundant members of the sirtuins family in the adult human frontal lobe. Both SIRT6 and SIRT7 have been associated with the maintenance of DNA stability and promotion of DNA repair following exposure to cellular stressors^{461,462}.

We also confirm that mammalian sirtuins are localised to several subcellular compartments. While SIRT1, SIRT6 and SIRT7 are predominantly found in nuclear fractions, they are also detected in cytosol, cytoskeleton and membrane fractions, albeit at much lower levels. Similarly, although SIRT2 is the only human sirtuin primarily localised in the cytoplasm, it may also be found at lower levels in the nucleus and cellular membrane. Our data confirm that SIRT1 and SIRT2 may interact with both the nuclear and cytoplasmic subcellular

compartments. Similarly, while the mitochondrial sirtuins (SIRT3-5) have been previously reported to be exclusively localised to the mitochondria, other studies have reported the localisation of several variants in the nucleus as well as the cytoplasm, in line with our study⁴⁶³. SIRT5 has recently been found to have both desuccinylase and de-malonylase activities in both the mitochondria and cytosol^{345,464}. The expression patterns of sirtuins in brain cells remains controversial and it is unclear whether certain sirtuins are specific to cell types. Our MRM study indicates that the majority of sirtuins (SIRT1, 2, 6 and 7) are present across all the main brain cell types.

For validation, analyses of the samples by immunohistochemical staining confirmed that all seven sirtuins are found in human primary astrocytes (Figure 2.8, Panel A row 1-5). PCR detected SIRT1 and SIRT2 mRNA in frontal, occipital and hippocampal brain tissue. Western blotting identified protein levels in frontal brain tissue with SIRT2 showing the strongest bands, corresponding well with the results from our MRM assay (Figure 2.8, Panel C).

Various studies have demonstrated that abnormal changes to sirtuin proteins occur during disease states as well as ageing. SIRT2 accumulates with age in the mouse brain and spinal cord⁴⁵⁷. Other recent studies have shown that SIRT1 decreases with age in the rat brain⁴⁶⁵ and SIRT2 is upregulated in brain tumours⁴⁶⁶. Hence, there is great value in developing robust quantitative assays such as MRM mass spectrometry to accurately quantify these proteins in control vs disease states. Another important aspect of sirtuin biology is that their deacetylase activity is nicotinamide and NAD⁺ dependent, establishing a direct link between their function and energy metabolism. To improve sensitivity, we found our fractionation method of running the samples on SDS PAGE and excising gel bands corresponding to the molecular weights of the intact sirtuin proteins to improve detection. The use of more sensitive mass spectrometers with high resolution MRM capability may improve detection of low abundant sirtuins and/or allow removal of the gel fractionation step. This would allow for sample lysates to be digested and analysed directly and increase sample throughput. Using hybrid mass spectrometers capable of high resolution and accurate mass measurements such as the quadrupole-orbitrap may overcome these issues and yield better sensitivity for high-complexity samples. This will help future validation of levels in large cohorts which may be useful for the identification of sirtuins as potential biomarkers.

Collectively, our results add further insights to the limited data which currently exist regarding the expression of sirtuins in the human CNS. This technique provides a powerful tool and helps improve upon the limitations of current protocols. While mass spectrometry based assays for protein quantification may still have some barriers to overcome before they can be used in a clinical setting due to low throughput and expense compared to methods such as ELISA, it has great value in investigating lower abundance proteins such as sirtuins in complex samples such as the brain with great sensitivity and specificity. MRM mass spectrometry can also be utilised for the quantification of sirtuin related metabolites and thus targeted mass spectrometry methodologies have the potential to not only validate and complement currently established methods for investigation of sirtuin protein expression changes but can also help build a larger view of sirtuin biology in the normal brain and in disease conditions by linking sirtuin protein expression with metabolism.

Chapter 3

Sirtuin Changes During Ageing and Alzheimer's Disease

Introduction

Sirtuins have generated considerable interest as important players in ageing biology. It is generally agreed that sirtuins have a role in extending lifespan, in laboratory model organisms, by mediating the anti-ageing effects of a low-calorie diet (calorie restriction)⁴²¹. In mammals, there are seven sirtuin homologues (SIRT1 to SIRT7), each having diverse locations and multiple targets, and affecting a broad range of cellular processes. Of these seven, the biological activities of SIRT1 has been studied the most extensively. SIRT1 is a nuclear protein in most cell types. It deacetylates transcription factors and cofactors that regulate several metabolic pathways in energy metabolism, lipid metabolism and glucose homeostasis and also targets proteins related to DNA repair and inflammation^{288,421,467}.

SIRT2 is predominantly a cytoplasmic protein and can deacetylate several cytoskeletal proteins, including α -tubulin, histones, and forkhead proteins and suppresses inflammation^{431,468}. SIRT2 is protective against neurodegenerative pathology in mouse models of Alzheimer's disease, with overactivation of SIRT2 protecting against axonopathy and neurodegeneration in a mouse model of Wallerian degeneration⁴⁶⁹. Small-molecule inhibitors targeting SIRT2 have been shown to attenuate several models of neurodegeneration^{456,470,471}.

Mitochondria represent the primary site for the production of ROS through one-electron carriers in the respiratory chain and this organelle is highly vulnerable to the cytotoxic effect of oxidative stress. Interestingly, three mammalian sirtuins localize to mitochondria: SIRT3, SIRT4 and SIRT5. SIRT3 responds to changes in mitochondrial redox status by altering the enzymatic activity of specific downstream targets, including manganese superoxide dismutase (MnSOD)⁴⁷². MnSOD is the primary mitochondrial ROS scavenging enzyme which modulates ROS levels as well as metabolic homeostatic poise⁴⁷².

SIRT4 may be involved in brain ageing, and controls glutamate metabolism through glutamate dehydrogenase, an enzyme which converts glutamate to α -ketoglutarate in the mitochondria in an NAD^+ dependent manner³⁰¹. Over expression of SIRT4 has been shown to alter synaptic activity⁴⁷³. In addition, serotonin1b (5-HT1b) receptor knockout mice, up-regulate SIRT5 in adult male mice, causing early onset of brain ageing⁴⁷⁴. SIRT4 has also been shown to regulate fatty acid oxidation and mitochondrial gene expression in liver and muscle cells³⁴⁴. SIRT4 knockdown in hepatocytes increases SIRT1 mRNA and protein levels both *in vitro* and *in vivo*, suggesting that the effect of SIRT4 on fatty acid oxidation may be

SIRT1 dependent³⁴⁴. A significant increase in fatty acid oxidation in the ageing rat brain has been reported with a reduction in SIRT4 expression⁴⁶⁵.

SIRT6, is another nuclear sirtuin protein which promotes longevity^{308,475,476}. SIRT6 knockout mice display premature ageing, including excessive loss of subcutaneous fat, a significant reduction in bone density, and die within 4 weeks of birth³¹². Another less characterized sirtuin, SIRT7, is localized to the nucleolus of mammalian cells. SIRT7 protein expression levels correlate with tissue proliferation and its expression is reduced in non-proliferating tissue, such as the heart, brain and muscle³¹⁴. SIRT7 has been associated with rDNA and interacts with RNA polymerase I (Pol I), suggesting a role in NAD-dependent regulation³¹⁴. Recently SIRT7 has been shown to be a histone desuccinylase which is recruited to DNA double-strand breaks in a PARP1-dependent manner and promotes chromatin condensation and DNA repair⁴⁷⁷.

Several reports have been published on the association between sirtuins and diseases, such as diabetes, metabolic diseases, cardiovascular diseases, cancer and neurodegenerative diseases^{265,421,478}. Of the seven mammalian sirtuins, SIRT1 is the best characterized and is considered to be responsible for delaying ageing in animal models⁴²¹. SIRT1 has also been credited with neuro-protective action in response to stress, in cell culture models. It is also believed to mediate the lifespan extending effects of calorie restriction, which protects experimental animals from neurodegenerative diseases such as AD^{281,327,479}. In AD transgenic mouse models SIRT1 overexpression is neuroprotective against amyloid and tau pathologies, and more recently has been shown to improve cognitive performance^{340,480}. Since SIRT-1 is a deacetylase that regulates several neuroprotective cellular pathways promoting neuron survival, by deacetylating a broad spectrum of molecules it has been hypothesized that the loss of SIRT-1 protein in the brain contributes to the pathogenesis of AD.

Although a number of sirtuins have promising effects in cellular and animal models of AD, mammalian distribution and functional roles in the central nervous system are still not well understood. In the present study we aimed to investigate changes to sirtuin protein expression during normal human ageing and also changes occurring in AD. We examined sirtuin levels in control, MCI and AD plasma, in the CSF of both a younger and elderly age group, in control and AD *post-mortem* brain tissue and finally in young and older samples of a potential new natural AD animal model – the *Octogon Degus*. To further investigate the functional role of SIRT2, which we found to be the most abundant in the human brain (see

Chapter 2), we completed an immunoprecipitation pulldown followed by mass spectrometry detection of potential binding partners. Owing to the importance of mammalian sirtuins in neurodegeneration and ageing, we hypothesized that they may be differentially expressed in the plasma, CSF and brain and may regulate various targets involved in metabolic processes and neurodegenerative diseases.

3.2 Methods

3.2.1 Plasma, CSF and brain tissue samples

CSF and plasma: CSF samples were collected by standard lumbar puncture from 13 patients during epidural and 13 patients assessed as clinically well after investigation for suspected meningitis, returning normal results for routine CSF pathology markers (white cell count, protein, glucose and bacterial sterility). Aliquots (50 µl) from each patient were obtained for our study. Pooled plasma from MCI, AD, and cognitively normal control subjects, balanced for age, sex and level of education, were obtained from the Sydney Memory and Ageing Study (261 MCI subjects, 24 AD subjects, 411 controls). Demographics of the subjects have previously been published by our group. Plasma was immunodepleted of the six most abundant plasma proteins using the Hu6 column (Agilent, USA) according to manufacturer's instructions⁴⁴⁸. For immunodepletion using the Multiple Affinity Removal System Hu6 column and buffer kit (Agilent, Santa Clara, CA, USA), 24 µl EDTA plasma was diluted into 120 µl Buffer A. Diluted EDTA plasma (100µL) was injected onto the Hu6 column connected to a HP 1090 HPLC system (Agilent, Santa Clara, CA, USA) and the low abundance protein fraction was collected, following manufacturer's instructions. The low abundance protein fractions from six injections were pooled, and buffer exchanged and concentrated into 45 mM NaHCO₃ using Amicon 3 kDa centrifugal devices (Millipore, Billerica, MA, USA). CSF protein (5 µg) and depleted plasma protein (20 µg), as determined by a BCA protein assay, were run on a 1D SDS-PAGE gel and colloidal coomassie stained.

Human Tissues: Protein (20 µg) from 5 individual control and AD *post mortem* brain tissue samples across 3 brain regions (occipital, frontal and temporal lobes) were extracted. Tissue was lysed using RIPA buffer followed by probe sonication and cell debris removed by centrifugation at 10,000RPM for 5 min. Total protein concentration was assayed in the supernatant using the Pierce BCA protein assay kit (Life Technologies, Australia), and three

10 µg replicates were run by 1D SDS-PAGE followed by colloidal coomassie staining.
Detailed patient information can be found in Chapter 2, Table 2.4.

Animal Tissues: Brain tissue from the *O. degus* were from the laboratory of Professor Nibaldo C. Inestrosa, to whom we are greatly appreciative for his provision of these samples. The *O. degus* were bred at the animal facility of the University of Valparaiso, Chile and maintained in a controlled temperature room (23 ± 1 °C), under a 12:12 light/dark cycle, with water and food provided *ad libitum*. At the time of this study, 16 Male *O. degus* were grouped by age, from 12 to 36 months of age ($n = 8$ per group). Ages were selected to represent the development of AD-like pathology (36 months). All efforts were made to minimize animal discomfort and stress while also limiting the number of animals used. Aged animals were anesthetized with Equitesin (2.5 ml/kg, i.p.) and injected with heparin (4 USP/kg, i.p.). Afterwards, brains were surgically removed from their skulls and frozen in isopentane at -78.5°C . All procedures were conducted according to animal protocols approved by the Institutional Animal Care and Use Committee at the University of Valparaiso and Pontifical Catholic University of Chile. Tissue was lysed using RIPA buffer followed by probe sonication and cell debris removed by centrifugation at 10,000RPM for 5 min. Total protein concentration was assayed in the supernatant using the Pierce BCA protein assay kit (Life Technologies, Australia), and three 10 µg replicates were run by 1D SDS-PAGE followed by colloidal coomassie staining.

For all samples, the band corresponding to the molecular weight for each sirtuin was excised, de-stained and trypsin digested overnight with heavy sirtuin peptides added as internal standards to all samples prior to digestion (the internal standard was constant for all samples and standards and added at a level at about the midrange of the standard curve). The tryptic peptides were dried under vacuum (Savant Speedvac, Thermo Scientific, USA), reconstituted in 0.1% formic acid (5 µl) injected into the mass spectrometer (1µL) and analysed using the MRM approach described in Chapter 2. Peak area ratios (light/heavy) were calculated for each endogenous peptide (light) relative to the spiked isotope-labelled (heavy) peptide using Skyline MRM analysis software. Protein concentrations were determined using calibration curves. All samples were fractionated by 1D-SDS-PAGE to reduce sample complexity. Full details of the SIRT MRM targeted mass spectrometry quantification protocol is provided in Chapter 2 (section 2.2.2) and has been published⁴⁸¹.

3.2.2 Western Blotting and PCR validation

Protein from five individual control and AD *post mortem* occipital brain tissue samples were extracted as described in section 2.1, and run on a 1D SDS-PAGE gel (20 µg protein per lane), and western blotted with antibody against SIRT2. The gel was electroblotted (20V, 110mA, 90mins) onto a nitrocellulose membrane in transfer buffer of 50mM tris, 40mM glycine, 1.3mM SDS, 20% methanol, pH 9.2. After transfer of proteins, the membrane was incubated in 10% skim milk powder solution containing primary SIRT2 antibody. SIRT2 rabbit polyclonal antibody was used (1:1000 dilution, Abcam, UK), followed by a secondary antibody (1:100,000 dilution of anti-mouse IgG, Pierce, USA). Chemiluminescence blots were developed using 1:1 solution of Super Signal West Femto luminol and peroxide buffer (Pierce, USA) according to manufacturer's instructions.

For the PCR studies RNA was extracted from control and AD *post mortem* tissue using RNeasy mini kits (Qiagen, Germany). The cDNA was prepared using SuperScript III First-Strand Synthesis System and random hexamers (Invitrogen Corporation, USA) as previously described⁴⁴⁹.

Briefly, for each reaction 2 µl of diluted cDNA, 10 µL of SYBR green master mix, 0.15 µL of 10 µM forward and reverse primers and 7.7 µl of nuclease-free water was used, making a total volume of 20 µl. Q-PCR was carried out using the Mx3500P Real-Time PCR system (Stratagene, Australia). The SIRT2 primer sequences are shown in Chapter 2, Table 2.5. The relative expression levels of SIRT2 transcripts were calculated using a mathematical model based on the individual Q-PCR primer efficiencies and the quantified values were normalized against the housekeeping gene 18S. From these values, fold-differences in the levels of transcripts between individual subjects were calculated according to the formula $2^{-\Delta\Delta Ct}$

3.2.3 Immunoprecipitation of SIRT2 interacting proteins

Immunoprecipitation is a method that enables the purification of a protein, together with any binding partners that it may have. An antibody for the protein of interest is incubated with a cell extract enabling the antibody to bind to the protein in solution. The antibody/antigen/binding partner complex is then pulled out of the sample using protein A/G-coupled agarose beads. This isolates the protein of interest (and its specific binding partners)

from the rest of the sample. The sample can then be separated by SDS-PAGE followed by tryptic digestion and identification of bound proteins using mass spectrometry.

Occipital lobe tissue (mix of white and grey matter) from five control subjects (1mg each) were pooled and homogenised in 1ml of lysis buffer containing 20 mM Tris HCl pH 8, 137mM NaCl, 1% Nonidet P-40 and 2mM EDTA and homogenised using a probe sonicator. The sample was then centrifuged for 20min at 10,000RPM at 4°C. The supernatant was removed and placed in a fresh polypropylene tube. Proteins were immunoprecipitated with SIRT2 antibody in solution according to manufacturer's instructions. Briefly, 50 µg of occipital tissue lysate plus SIRT2 antibody were mixed and incubated overnight at 4°C with gentle rotation. Protein A-coupled human IgG1 Sepharose beads were prepared, 1mL PBS, 0.1% BSA added and the solution mixed for 1hr with rotation. The supernatant was removed and 400 µL lysis buffer added. This slurry was mixed well and then 100 µL of beads were added to the lysate sample. The sample was incubated at 4°C with rotation for 4hrs. Tubes were centrifuged, supernatant removed and beads washed three times to remove non-specifically bound proteins. The specific binding-partner proteins were then eluted from the beads and samples run by 1D SDS PAGE. The procedural workflow and representative gel is shown in Figure 3.9.

3.2.4 Mass Spectrometry for Identification of SIRT2 Interacting Proteins

A one dimensional SDS 4-12% NuPage (Thermo Fisher Scientific Inc, MA, USA) gel was run using the elute, unbound and wash fractions from the immunoprecipitation experiments. The gel was colloidal coomassie stained⁴⁸², and the lanes uniformly cut into 7-8 bits using a gridcutter and mount from The Gel Company, CA, USA. The gel bits were trypsin digested and then analysed using mass spectrometry as outlined below.

Digested peptides were separated by nano-LC using a Cap-LC autosampler system (Waters, Milford MA). Samples (5 µl) were concentrated and desalted onto a micro C18 precolumn (500 µm x 2 mm, Michrom Bioresources, Auburn, CA) with H₂O:CH₃CN (98:2, 0.05 % HFBA) at 15 ul/min. After a 4 min wash the precolumn was automatically switched (Valco 10 port valve, Houston, TX) into line with a fritless nano column (75 µm x ~12 cm) containing Magic C18 (~10cm, 200Å, Michrom) manufactured according to Gatlin [35]. Peptides were eluted using a linear gradient of H₂O:CH₃CN (98:2, 0.1 % formic acid) to H₂O:CH₃CN (55:45, 0.1 % formic acid) at ~300 nl/min over 30 min. The precolumn was connected via a fused silica capillary (10 cm, 25 µ) to a low volume tee (Upchurch Scientific)

where HV (2400 V) was applied and the column tip positioned ~ 1 cm from the Z-spray inlet of a QToF Ultima API hybrid tandem mass spectrometer (Micromass, Manchester, UK). Positive ions were generated by electrospray and the QToF operated in data dependent acquisition mode (DDA). A ToF MS survey scan was acquired (m/z 350-1700, 1 s) and the 2 largest multiply charged ions (counts > 20) were sequentially selected by Q1 for MS-MS analysis. Argon was used as collision gas and an optimum collision energy chosen (based on charge state and mass). Tandem mass spectra were accumulated for up to 2 s (m/z 50-2000).

Peak lists were generated by MassLynx (version 4.0 SP1, Micromass) using the Mass Measure program and submitted to the database search program Mascot (version 2.2, Matrix Science, London, England). Search parameters were: Precursor and product ion tolerances \pm 0.25 and 0.2 Da respectively; Met(O) and Cys-carboxyamidomethyl were specified as variable modification, enzyme specificity was trypsin, one missed cleavage was allowed on the UniProtKB/Swiss-Prot database.

3.3 Results

3.3.1 Sirtuin expression in pooled Control, MCI and AD immunodepleted plasma

SIRT1-3 and SIRT6 were all detected in pooled human control, MCI and AD plasma. A significant drop in SIRT1 levels was found in the AD plasma samples compared to controls.

Figure 3.1 Sirtuin expression in pooled control, MCI and AD plasma. * $p < 0.01$ vs control plasma.

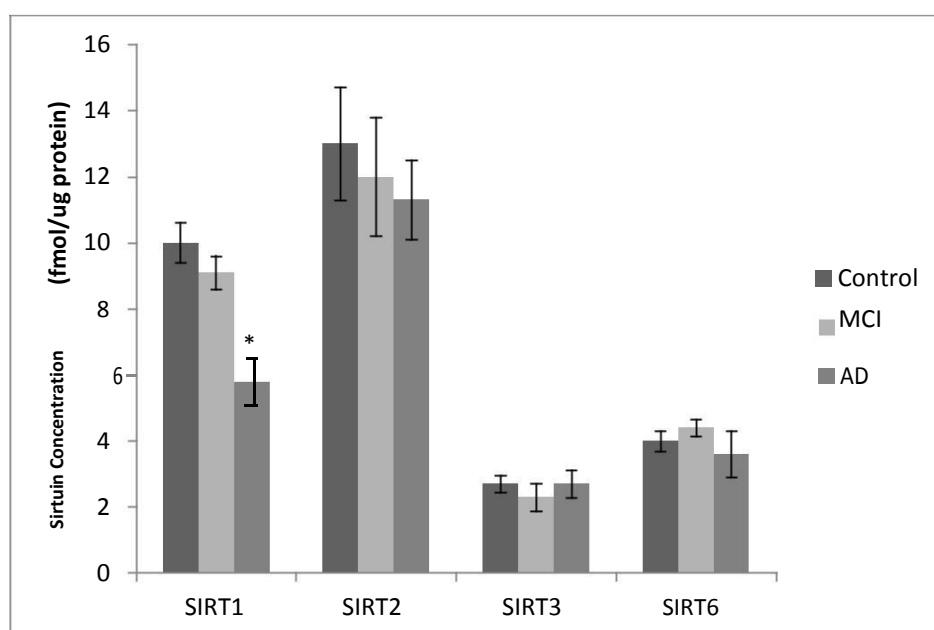
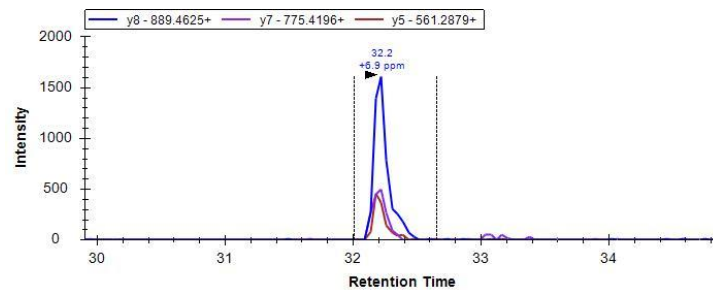
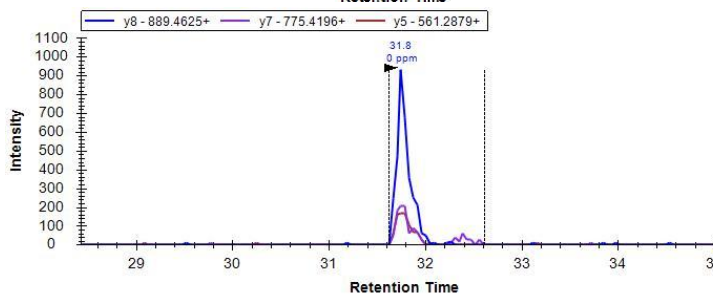
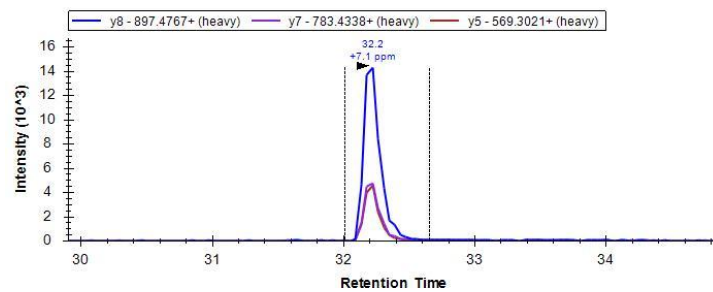


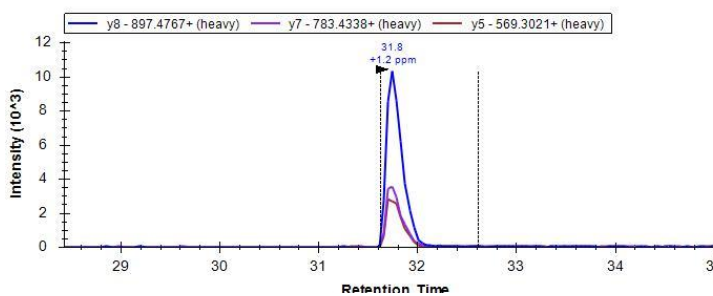
Figure 3.2 Representative chromatograms of SIRT1 peptides in control and AD plasma samples for SIRT1. Showing analyte peptide transitions (top) and the internal standards (bottom) for each sample.



SIRT1 in Control plasma



SIRT1 in AD plasma



3.3.2 Sirtuin Expression in control and AD *post mortem* brain tissues

SIRT1-3, 6 and 7 were quantified in various brain regions of control and AD *post mortem* brain tissues. A significant increase in SIRT2 was found in AD brain tissues of the occipital lobe (Figure 3.3). SIRT1 and SIRT3 were elevated in the temporal lobe (Figure 3.4). There was also a trend upwards in SIRT2 in the temporal lobe. No significant differences were found in frontal lobe tissue (Figure 3.5).

Figure 3.3 Sirtuin expression in occipital *post mortem* control and AD brain tissue, n=5; *p<0.05 vs control.

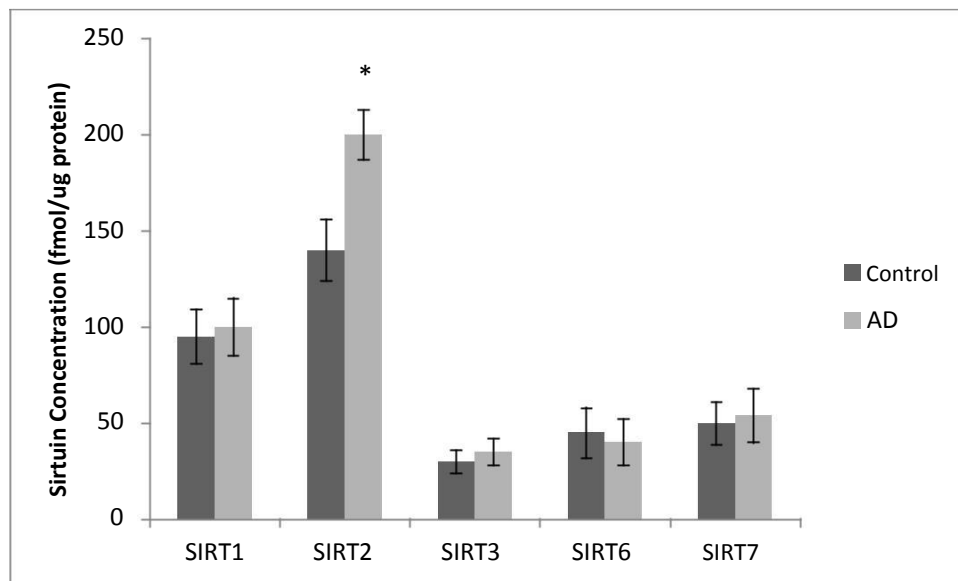


Figure 3.4 Sirtuin expression in temporal *post mortem* control and AD brain tissue, n=5; *p<0.05 vs control.

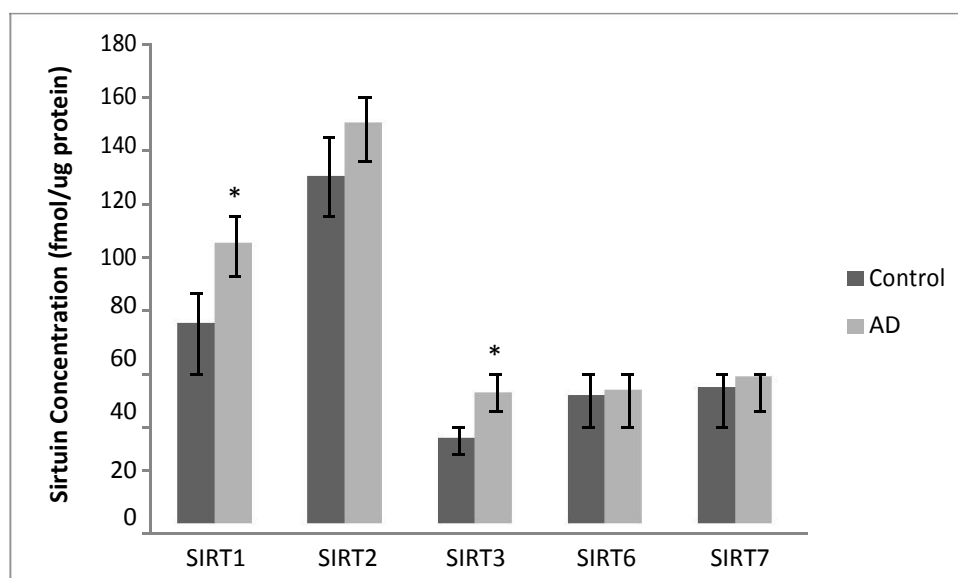
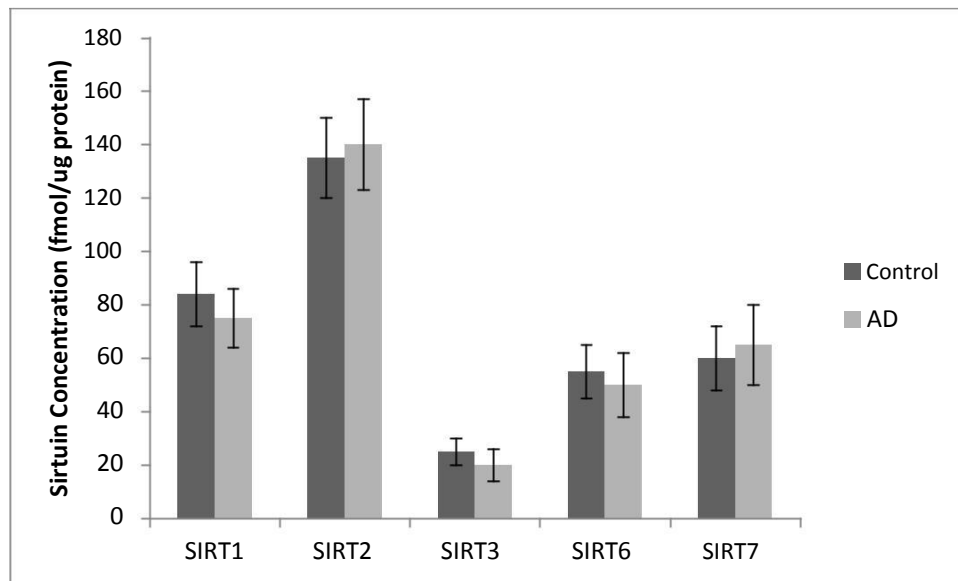


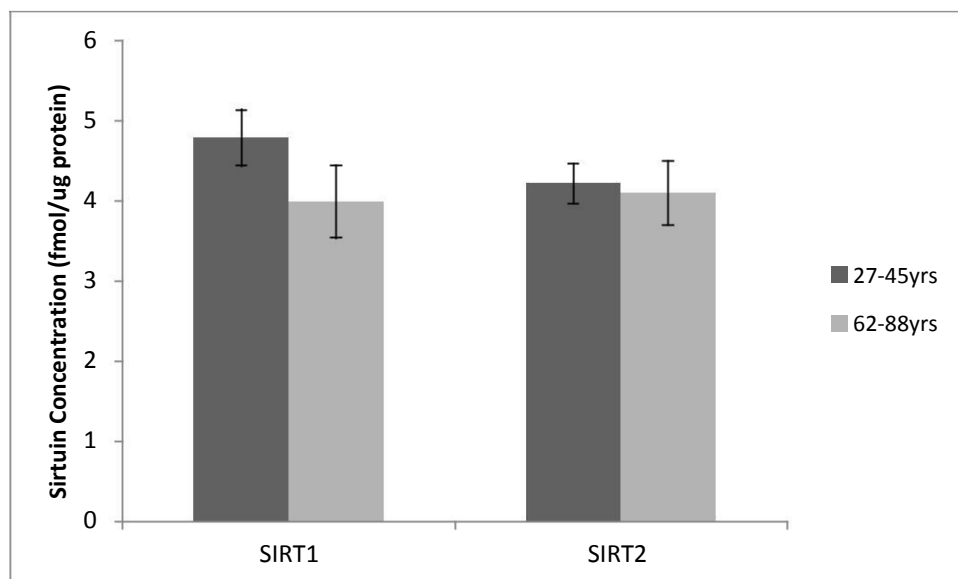
Figure 3.5 Sirtuin expression in frontal *post mortem* control and AD brain tissue, n=5.



3.3.3 Sirtuin expression in control CSF in younger and elderly age groups

SIRT1 and SIRT2 levels were compared between a younger age group (27-45yrs) and a older age group (62-88yrs). SIRT1 and SIRT2 were found in control CSF and though there was a downward trend in SIRT1 in the older age group, there were no statistically significant differences between the two groups.

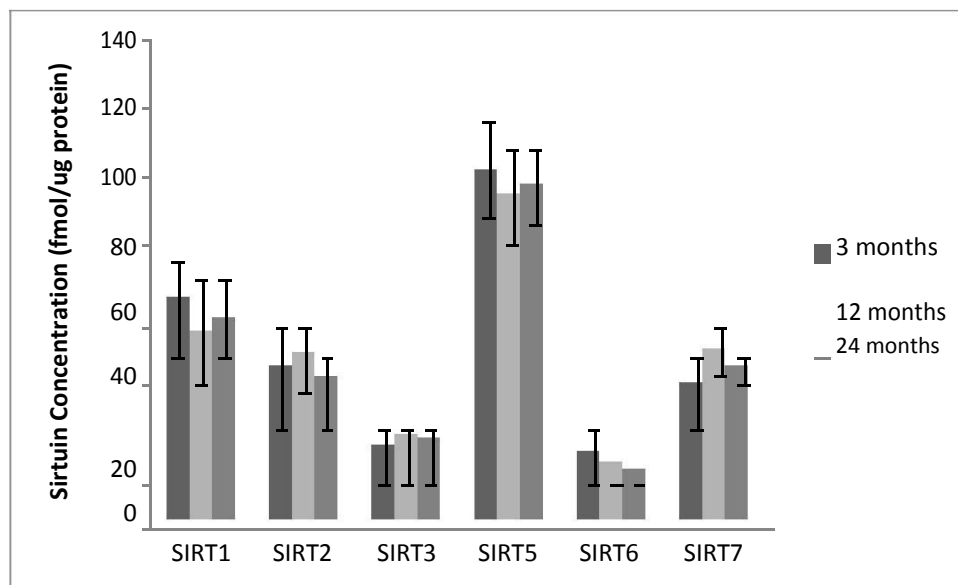
Figure 3.6 SIRT1 and SIRT2 levels in younger and older age groups (n=12 in each group).



3.3.4 Sirtuin expression in the ageing *Octodon Degus* rodent brain

SIRT1-3 and SIRT5-7 were detected in the *O. Degus* rodent brain. No marked age related changes within the cortex of the ageing brain were observed in this small sample set. However SIRT5 was found to be the most abundant brain sirtuin.

Figure 3.7 Brain sirtuin levels in *Octodon Degus* cortex, n=2.

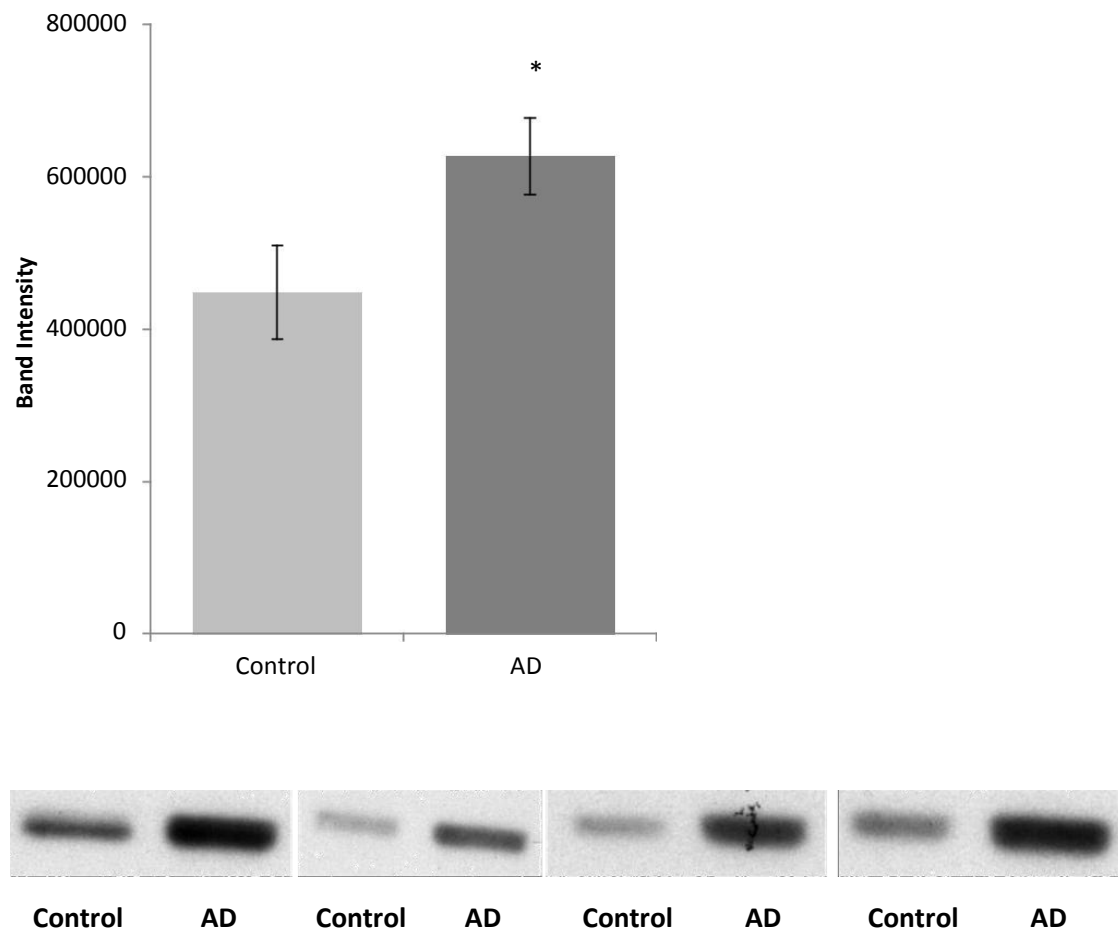


3.3.5 Validation of SIRT2 changes in AD occipital lobe tissue using western blotting and PCR

The significant elevation seen in SIRT2 in the AD occipital lobe using the MRM method was validated using orthogonal methods. In this case western blotting was used to validate SIRT2 protein expression and PCR to measure SIRT2 mRNA changes. These methods identified both upregulation of SIRT2 protein and mRNA expression in AD occipital lobe, validating the MRM quantification.

Figure 3.8 SIRT2 protein levels in control and AD occipital lobe. Using western blotting (panel A) and SIRT2 mRNA in control and AD *post mortem* brain tissue of various brain regions (panel B) both showing a significant elevation of SIRT2 protein and mRNA in the occipital lobe of AD brain, n=5, *p<0.05 vs control.

A



B

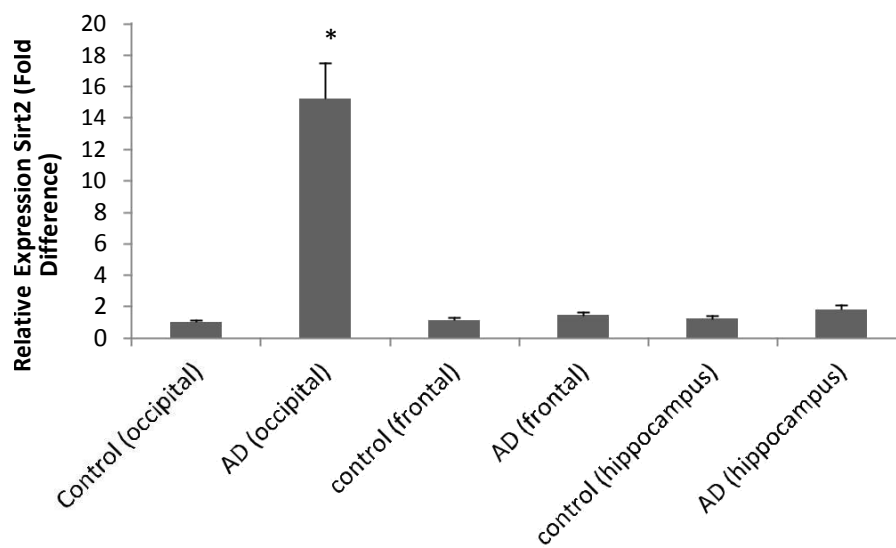
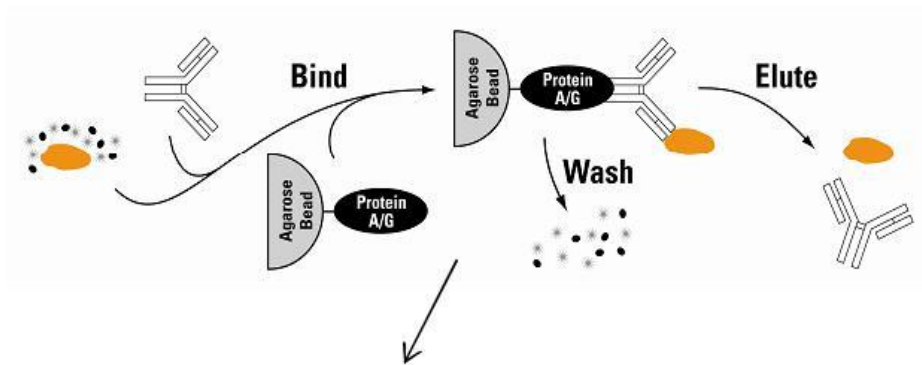
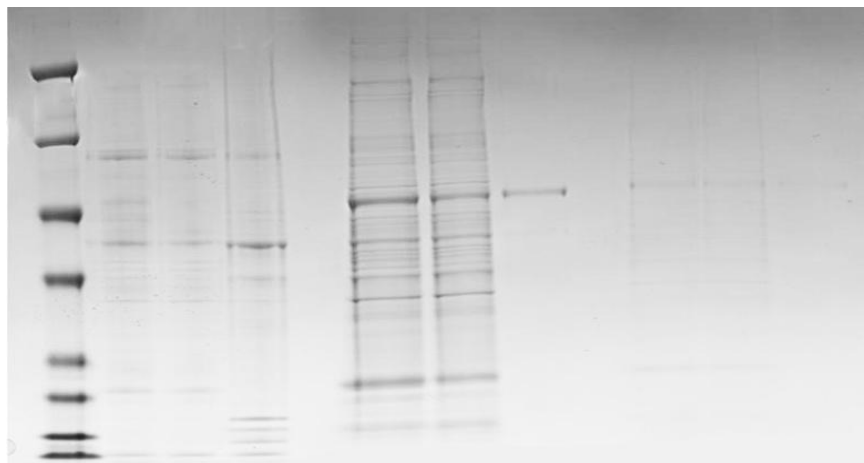


Figure 3.9 Workflow of immunoprecipitation experiment to target SIRT2 binding partner proteins. Using in gel digestion followed by mass spectrometry analysis showing fractions collected after pulldown. Gel lanes 2-4: Elute fraction triplicates, lanes 6-8: Unbound fraction triplicates, lanes 9-11: Wash fraction triplicates.



1D SDS-PAGE Gel of fractions collected



Elute fractions
(potential SIRT2
binding partners)

Unbound fractions

Wash fractions

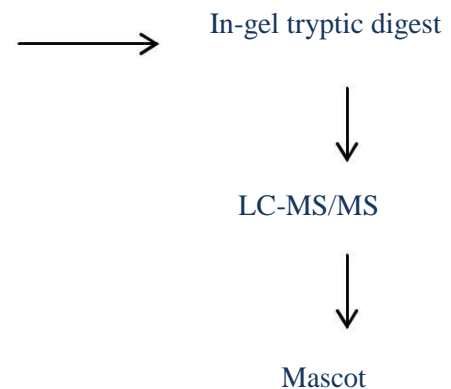


Table 3.1 List of SIRT2 putative binding protein partners identified by immunoprecipitation pulldown and mass spectrometry and their functions.

Accession #	Protein Name	emPAI	Protein Sequence Coverage	Peptide Sequences	Function
Q13885	Tubulin beta-2A	5.38	64	26	polymerize into dynamic microtubules; one of the major components of the cytoskeleton ⁴⁸³
P60709	Actin, cytoplasmic 1	4.64	55	24	form microfilaments, one of the three major components of the cytoskeleton ⁴⁸⁴
O60814	Histone H2B	2.71	55	10	one of the main histone proteins involved in chromatin structure ⁴⁸⁵
P04075	Fructose-bisphosphate aldolase A	2.07	46	16	enzyme catalyzing a reversible reaction that splits the aldol, fructose 1,6-bisphosphate, into the triose phosphates, dihydroxyacetone phosphate and glyceraldehydes 3-phosphate in gluconeogenesis and glycolysis ⁴⁸⁶
P02686	Myelin basic protein	1.57	44	20	provide structural integrity to the myelin sheath of nerves ⁴⁸⁷
P00441	Superoxide dismutase 1	1.56	68	5	an important constituent in apoptotic signaling and oxidative stress, most notably as part of the mitochondrial death pathway ⁴⁸⁸
P62805	Histone H4	0.87	24	2	proteins involved in the structure of chromatin in eukaryotic cells ⁴⁸⁹
P40926	Malate dehydrogenase, mitochondrial	0.77	39	9	is an enzyme that reversibly catalyzes the oxidation of malate to oxaloacetate using the reduction of NAD ⁺ to NADH. This reaction is part of many metabolic pathways and is involved in the citric acid cycle and gluconeogenesis ⁴⁹⁰
P04406	Glyceraldehyde-3-phosphate dehydrogenase	0.67	39	12	catalyzes the sixth step of glycolysis and thus serves to break down glucose for energy and carbon molecules and can also initiate apoptosis ⁴⁹¹
P06576	ATP synthase, subunit beta,	0.62	26	11	important enzyme that creates the energy storage molecule adenosine triphosphate (ATP). ATP is the most commonly

	mitochondrial				used "energy currency" of cells for most organisms ⁴⁹²
P09936	Ubiquitin	0.52	25	5	functions through covalent attachment to other cellular proteins, thereby changing the stability, localization, or activity of the target protein ⁴⁹³
Q06830	Peroxiredoxin 1	0.51	25	5	ubiquitous family of antioxidant enzymes that also control cytokine-induced peroxide levels and thereby mediate signal transduction in mammalian cells ⁴⁹⁴
P09104	Gamma-enolase	0.45	24	7	responsible for the catalysis of the ninth and penultimate step of glycolysis ⁴⁹⁵
P07900	Heat shock protein 90-alpha	0.34	18	14	a chaperone protein that assists other proteins to fold properly, stabilizes proteins against heat stress, and aids in protein degradation ⁴⁹⁶
P14618	Pyruvate kinase	0.25	20	10	catalyzes the final step of glycolysis. It catalyzes the transfer of a phosphate group from phosphoenolpyruvate to adenosine diphosphate, yielding one molecule of pyruvate and one molecule of ATP ⁴⁹⁷
P09211	Glutathione s-transferase	0.14	14	2	catalyses the conjugation of the reduced form of glutathione to xenobiotic substrates for the purpose of detoxification ⁴⁹⁸

3.4 Discussion

Ageing is the strongest risk factor for developing MCI and AD in epidemiological studies. There is a progressive increase in the prevalence of AD with increasing age (doubling every 5 to 6 years after the age of 60 up to the 9th decade of life), therefore it is worth considering whether anti-ageing interventions could be of preventive value in dealing with AD in an ageing population. The sirtuin family of proteins has been associated with lifespan extension in lower organisms. Since mammals contain multiple sirtuins, we explored the expression of these in ageing and AD, using a variety of sample types, including brain tissue, CSF and plasma.

3.4.1 Sirtuin levels in control, MCI and AD plasma and young vs old plasma

We investigated sirtuin expression in immunodepleted plasma from pooled control, MCI and AD subjects and found a significant drop in SIRT1 levels in the plasma of AD patients (figure 3.1 and figure 3.2). We also investigated sirtuin CSF concentrations in younger and elderly controls. We found a downward trend in SIRT1 levels in the elderly group (62-88yrs) compared to the younger group (27-45yrs) but statistical significance was not reached (Figure 3.6). In general changes to most sirtuin levels with age appear to be quite modest in the mammalian tissues we assayed.

Recently the first study investigating sirtuin levels in serum have been reported. The study investigated serum SIRT1 concentration in patients with AD and MCI as well as in young and elderly controls. A significant decline in SIRT1 with age in serum and a larger drop in patients with MCI and AD was found. Thus the authors suggest that SIRT1 may be a promising biomarker for AD. This data also suggests that sirtuin activators may potentially have a preventive role in AD. Another study by the same group examined the association of sirtuins to a major geriatric syndrome, frailty. Serum levels of SIRT1, 2 and 3 were found to be significantly lower in frail patients compared to nonfrail controls.

3.4.2 Changes in sirtuin levels in control vs AD brain tissue

Interestingly when control and AD *post mortem* brain tissue were compared, we found a significant elevation of a number of sirtuins. In the occipital lobe we found an elevation of SIRT2 (Figure 3.3), this result was further confirmed using both western blotting and PCR (Figure 3.8) as both these techniques also showed a significant increase in SIRT2 both at the protein and mRNA level in the AD occipital lobe. In the temporal lobe we found an increase in both SIRT1 and SIRT3 in the AD brain (Figure 3.4). No significant differences in sirtuin expression was found in the frontal lobe (Figure 3.5).

Previous studies from our group have identified the *Octodon degus* (*O. degus*), a South American rodent endemic to Central Chile, as a “natural” rodent model for AD. The *O. degus* is a diurnal, visual, and highly social rodent that “naturally” develops several features linked to the neuropathology of AD. This caviomorph rodent lives up to an average of 7 years in captivity, making it a useful model for use in longitudinal studies, including those related to the neurobiology of AD. The amino acid sequence of wild-type *O. degus* A β shares a high degree (97.5%) of genetic homology with humans and it has been reported that age-related changes in A β oligomers and *tau* phosphorylation in *O. Degus* correlates with a decrease in both spatial and object recognition memory, and impaired postsynaptic and neural plasticity. In the *octodon degus* model of AD we found no changes to sirtuins during normal ageing (3 months to 24 months). However interestingly we found the largest amounts of SIRT5 in the brain of this rodent model (Figure 3.7), which was quite a different pattern of expression to the other mammalian tissues we examined (this chapter and in Chapter 2).

Sirtuin expression levels have not been very well investigated in AD, a few recent studies have reported significant changes. One of the first papers to report change to sirtuin in AD was published by Weir et al showing a significant increase in SIRT3 in the temporal cortex of AD *post mortem* brain tissue using western blotting²⁷¹. Progressive mitochondrial dysfunction contributes to neuronal degeneration in age-mediated disease and SIRT3 is an essential regulator of mitochondrial function⁴⁹⁹. Pharmacological augmentation of mitochondrial ROS was shown to increase SIRT3 expression in hippocampal cells with SIRT3 over-expression being neuroprotective. SIRT3 expression was also found to correlate with the deposition of β -amyloid in an AD mouse model and SIRT3 was also upregulated in AD patient temporal neocortex²⁷¹. Our results are consistent with these previous findings, confirming an elevation of SIRT3 in the AD temporal lobe. This suggests a possible role for

SIRT3 in mechanisms sensing and protecting against ROS and AD-mediated mitochondrial stress.

Another recent study has reported changes to SIRT1, 3 and 5 expression in the entorhinal cortex and hippocampal subregions and white matter of 45 cases grouped according to Braak and Braak stages of neurofibrillary degeneration using western blotting and immunohistochemistry analysis⁵⁰⁰. They report a decline in SIRT1 and SIRT3, and an elevation of SIRT5 with AD progression in these brain regions⁵⁰⁰. SIRT3 decline has also been reported in an AD transgenic mouse model. The expression of SIRT3 was significantly lower in the cortex of APP/PS1 double transgenic mice than in wild types at both the

protein and mRNA level⁵⁰¹. These results suggest that mitochondrial SIRT3 might participate in the development of AD via mitochondrial dysfunction. The elevation we see in the temporal lobe may therefore be a compensatory mechanism by the brain to induce these neuroprotective proteins to boost neuronal longevity. SIRT1 and SIRT3 are also upregulated in response to fasting and calorie restriction and have been shown to reduce ROS levels and reduce oxidative damage. SIRT3 also enhances the mitochondrial glutathione antioxidant defense system in cochlear neurons³⁴⁷. The decline reported by others in the hippocampus where the highest level of AD pathology is seen may indicate loss of these neuroprotective activities and metabolic dysfunction reported in this vulnerable region may thus, in part be due to reduction of SIRT1 and SIRT3 levels. Kim et al have reported that mitochondrial SIRT3 protects neurons against excitotoxic injury⁵⁰². Excitotoxic injury was induced by exposure of primary cultured mouse cortical neurons to NMDA resulting in a rapid decrease of cytoplasmic NAD⁺ in neurons through poly (ADP-ribose) polymerase-1 (PARP-1) activation⁵⁰². Mitochondrial SIRT3 was increased following PARP-1 mediated NAD⁺ depletion, which was reversed by either inhibition of PARP-1 or exogenous NAD⁺⁵⁰². The large amount of ROS produced under this NAD⁺ depleted condition mediated the increase in mitochondrial SIRT3⁵⁰². SIRT3 overexpression confirmed that SIRT3 is required for neuroprotection against excitotoxicity⁵⁰². Thus SIRT3 seems to play an essential role in protecting neurons against excitotoxic injury. As AD is associated with significant increases in neuronal ROS production and previous studies have shown that SIRT3 mRNA expression is regulated by mitochondrial ROS levels, it seems likely that the SIRT3 upregulation in AD we see in the temporal lobe may be a consequence of A β -related oxidative stress. Given that SIRT3 upregulation has been shown to increase neuronal lifespan, it is tempting to speculate that upregulation of SIRT3 in response to A β -induced oxidative stress might prolong neuronal function by decreasing ROS, maintaining ATP-levels and sustaining synaptic activity. However this possibility will need further investigation. Furthermore, due to inevitable inter-individual variations in protein expression, as well as potentially variable tissue quality, human AD *post mortem* studies will need to be expanded to include a larger cohort of control and AD samples to validate these findings.

SIRT1 increases the expression of the ADAM10 gene encoding α secretase. In AD the down regulation of SIRT1 reduces the expression of α -secretase and as a result increases the accumulation of pathogenic A β peptide formed by β and γ secretase³⁴⁰. Serum A β 1–40 levels were shown to be higher in the AD group than both controls and MCI³⁴⁰. Transgenic

over-expression of SIRT1 in the brain markedly reduced amyloid plaque formation, gliosis and decline in learning and memory capabilities, while brain SIRT1 specific knock-out greatly attenuated lifespan likely due to juvenile onset of an AD-like disease³⁴⁰. Resveratrol, a SIRT1 activator, has proved to be beneficial in models of AD (*in vitro* and *in vivo*), reducing amyloid- β protein accumulation and also a variety of other neuroprotective effects

355,389,479,503.

A significant decrease in SIRT1 concentration in parietal cortex of AD brain has been reported and a strong correlation was established between tissue SIRT1 concentration, duration of symptoms and tau accumulation²⁸⁰, but the exact relationship and its role in the sequence of events leading to development of AD remains unclear.

3.4.3 Binding partners of SIRT2

This work has mainly highlighted SIRT2 as the most abundant sirtuin in the brain and we also see a substantial elevation of this protein in the AD occipital lobe. This may be a homeostatic response to pathology, and as the most significant change relative to other sirtuins, it was of interest to explore potential mechanisms of action, by identifying some putative SIRT2 binding partners. We therefore aimed to gain further insights into its biological functions through investigating its binding partners. Using immunoprecipitation pulldown and protein identification using mass spectrometry we identified a list of potential binding partners for SIRT2 (Table 3.1). Interestingly our results reveal a novel potential role of SIRT2 as a regulator of mitochondrial function and metabolism. To date SIRT1, 3, 4 and 5 are the only sirtuins directly shown to be involved in mitochondrial function. However interestingly, many of the binding partners identified in our SIRT2 binding partner study are mitochondrial and involved in energy metabolism (Table 3.1). These include superoxide dismutase, which is also a known target of the mitochondrial sirtuin SIRT3, aldolase, ATP synthase, enolase, pyruvate kinase and glucose-6-phosphate isomerase which are all involved in energy metabolism and glycolysis. Our pulldown also highlights other binding partners which have already been validated as being associated with SIRT2 function such as myelin, histones, tubulin and actin. A recently published study has also suggested SIRT2 may regulate the activity of mitochondria. Liu et al found that SIRT2 can localise to mitochondria and directly interact with mitochondrial proteins⁵⁰⁴. In addition, the depletion of SIRT2 was

shown to increase markers of oxidative stress and reduce ATP production in the mouse brain⁵⁰⁴. In SIRT2 knockout mice 20 mitochondrial proteins were found to have changes in acetylation including protein targets also found in our study such as ATP synthase⁵⁰⁴. ATP synthase has also been identified as a SIRT3 target in a previous study which also used mass spectrometry to identify SIRT1 and SIRT3 interacting proteins⁵⁰⁵. Taken together our data and previous studies suggest that SIRT2 is not only a cytosolic protein but can interact with mitochondrial proteins and appears to have multiple mitochondrial targets and may have an emerging role in regulating mitochondrial function, oxidative stress and energy metabolism, all of which has been well established as important factors in the pathogenesis of AD.

Sirtuins represent a unique class of enzymes that not only regulate protein acetylation and metabolism, but also play prominent roles in promoting longevity, preventing neurodegeneration and improving cell survival. Our present study helps add further insight into the changes and distribution of mammalian sirtuins in the CNS during ageing and AD and some potential targets of SIRT2 within the brain, revealing evidence of novel roles for these proteins in the brain and revealing new pathways for future research and validation.

Chapter 4

Effect of AD Plasma on Cultured Glia: Metabolic and Cytotoxic Effects

Majority of the content of this chapter has been published:

Jayasena T, Poljak A, Braidy N, Smythe G, Raftery M, Hill M, Brodaty H, Trollor J, Kochan N, Sachdev P (2015). *Upregulation of glycolytic enzymes, mitochondrial dysfunction and increased cytotoxicity in glial cells treated with Alzheimer's disease plasma*. PLoS One 10(3):e0116092.

See Appendix for full publication

Introduction

A variety of inflammatory markers are increased with the onset of AD pathology, including cytokines and chemokines, coagulation factors and acute-phase reactive proteins as well as reactive astrocytes and activated microglial cells, the main cells involved in the neuroinflammation process^{506,507}. Whether accumulation of cytokines and acute phase reactants within the brain is reflected in plasma has not been elucidated as many of these proteins do not easily cross the blood brain barrier. Alternatively, AD may be associated with a more widespread immune dysregulation, detectable in plasma.

Evidence from parabiosis experiments has shown that blood from young, old or diseased animals can have phenotypic effects when introduced into test animals^{155,156}. Previous studies investigating the effects of human AD plasma on cells in culture have found differential effects on protein expression and cell biology. One study aimed to determine if exposure to serum from AD patients would affect markers for AD brain lesions⁵⁰⁸, and found that 24 hour exposure to AD serum increased four molecular markers characteristic of AD senile plaques and neurofibrillary tangles (NFTs) in rat hippocampal neurons⁵⁰⁸. These markers were Alz-50, beta-amyloid, MAP2 and ubiquitin⁵⁰⁸. This stimulation of AD markers by human serum suggests that the genesis of both neuronal plaques and tangles may arise from exposure of susceptible neurons to toxic serum factors and/or failure to detoxify these factors. Another study found that antibodies in serum of patients with AD caused immunolysis of cholinergic nerve terminals from the rat cerebral cortex, supporting the hypothesis that autoimmune mechanisms may operate in the pathogenesis of AD⁵⁰⁹.

Other studies have shown that serum of multiple sclerosis patients causes demyelination in rat CNS explant cultures and also induces cytotoxicity in rat oligodendrocytes in culture^{510,511}. Demyelination was present not only in multiple sclerosis sera but was also found in sera from patients with other neurological diseases and complement was shown to be a factor involved in the effect^{512,513}. In yet another study, human serum from patients with septic shock was shown to induce apoptosis in human cardiac myocytes⁵¹⁴. This work demonstrates the utility of examining effects of disease plasma on cell culture systems, to facilitate the study of both disease markers and disease mechanisms. These potent biological effects of blood highlight the likelihood that disease and ageing biomarkers and risk factors are present and could potentially be identified in blood.

Previous studies indicate that AD plasma may contain oxidative stress markers as well as cytotoxic factors, and because there is growing evidence from parabiosis experiments of the impact of blood factors, we aimed to investigate the effect of pooled control, MCI and AD plasma from 20 individuals each on a microglial cell line. Cell viability, proliferation and mitochondrial function were investigated following 48 hour treatment with non heat-inactivated plasma and plasma in which complement proteins had been deactivated. We also tested the effect of commercially purchased complement factors alone and in combination on cultured glia. We then undertook proteomic analysis of the plasma from each group and iTRAQ quantitative proteomic analysis of cell extracts exposed to plasma from each group to investigate possible plasma protein alterations unique to MCI or AD, to detect any protein aberrations within the cells treated with the plasma and to correlate these findings with cell viability and mitochondrial function assays measured *invitro*.

4.2 Methods

4.2.1 Subjects

Age matched healthy control (n = 20), amnesic mild cognitive impairment (aMCI, n = 20), and probable AD (n = 20) fasting EDTA plasmas were aliquoted with a minimum of freeze-thaw cycles (generally ≤ 2) and stored at -80°C . Plasmas were pooled and used in both the cell culture and plasma proteomics experiments. AD patients were recruited from the Memory Clinic of the Department of Old Age Psychiatry of the Prince of Wales Hospital and participants in a clinical drug trial of donepezil (Aricept[®]). All met the NINCDS-ADRDA criteria⁵¹⁵ for probable AD. The aMCI subjects were recruited from the Memory and Ageing Study, a longitudinal study of community dwelling individuals aged 70-90⁵¹⁶. The diagnosis of aMCI was determined using the Petersen Criteria as follows⁵¹⁷: (i) subjective complaint of memory impairment, (ii) objective impairment in memory (performance >1.5 SD below normal for age on a standardised memory test) (iii) essentially preserved general cognitive function (MMSE ≥ 24) (iv) intact functional activities as indicated by instrumental activities of daily living; and (v) not meeting DSM-IV criteria for dementia. Healthy control subjects had a normal performance for age on a range of neuropsychological tests and intact functional activities. Ethics committee approval was obtained from the University of New South Wales (UNSW) and the South Eastern Sydney Illawarra Area Health Service (SESAHS) ethics committees and written informed consent was obtained from all participants.

4.2.2 Cell Culture

CHME-5 cells are a human microglial cell line obtained from embryonic fetal human microglia through transformation with SV-40 virus^{518,519} and were a generous gift of Prof Gilles Guillemin (Macquarie University, Sydney, Australia). These cells express antigens present on adult human microglia, secrete pro-inflammatory cytokines upon activation, exhibit properties of primary human microglia and have been successfully used as a model of microglial activation by others^{518,520}. Cells were maintained in RPMI1640 cell culture medium, supplemented with 10% heat inactivated foetal bovine serum, 2 mM l-glutamine, and 1% penicillin/streptomycin, at 37°C in a humidified atmosphere containing 95% air/5% CO₂. Before experimentation, cells were seeded into 24 or 96 well culture plates to a density of approximately 1×10^4 or 2×10^3 cells respectively. Cells were left overnight and then supplemented with up to 20% (by volume) heat-inactivated and non heat-inactivated control, MCI or AD plasma for 48 hours. For the cell viability and iTRAQ proteomic analyses cells were washed to remove all plasma, and lysed in RIPA buffer (Thermo Fisher Scientific, IL, USA) followed by sonication. For the complement factor experiments cells were seeded into plates and treated with 1, 5 or 10 µg of each complement factor or the complement standard (in a total volume of 200µL cell culture media) and then incubated for 48hrs. These concentrations are within the physiological range of these proteins in plasma⁵²¹.

4.2.3 MTT Cell Proliferation Assay

In actively proliferating cells, an increase in 3-[4,5-dimethylthiazol-2-yl]-2,5-diphenyl tetrazolium bromide (MTT) conversion in cells relative to controls represents an increase in cellular proliferative activity. Conversely, in cells that are undergoing apoptosis, MTT conversion, and thus biological activity, decreases. Cell proliferation was analysed using established protocols^{522,523}.

4.2.4 NAD(H) Assay

Damaged cells show mitochondrial dysfunction, which results in decreased cellular nicotinamide adenine dinucleotide (NAD) levels. Intracellular NAD(H) concentration was quantified using the thiazolyl blue microcycling assay established by Bernofsky and Swan

and adapted here for the 24 well plate format⁵²⁴.

4.2.5 Lactate Dehydrogenase (LDH) Leakage

Cytoplasmic enzyme leakage has been shown to be a useful tool for measuring early cellular damage or impairment⁵²⁵, and has also been used as a sign of cytotoxicity^{526,527}. LDH is released from cells due to loss of membrane integrity. Therefore LDH was measured in the cell culture medium as well as in cell homogenates as another measure of cell viability.

4.2.6 XF24 Microplate-Based Respirometry as a measure of mitochondrial function

To determine the effect of human control, MCI and AD plasma on oxygen consumption rates (OCRs; an indicator of mitochondrial respiration) and extracellular acidification rates (ECARs; a measure of glycolytic flux) in the microglial cell line, the Seahorse XF24, extracellular flux analyzer (Seahorse Bioscience, North Billerica, MA, USA) was employed and assays performed as previously described⁵²⁸⁻⁵³⁰. Briefly, culture plates were incubated in a CO₂-free incubator at 37°C for 1 hr to equilibrate temperature and pH. The microplate was then loaded into the XF24 and further incubated for 15 min with 3 min mix, 2 min wait cycles before commencement of the assay. After determination of the basal respiration in the cell culture, oligomycin (2 µM), carbonylcyanide-p-trifluoromethoxy-phenylhydrazone (FCCP, 500 nM), and antimycin (3 µM) were sequentially added and the OCRs and ECARs for each culture well were quantified for 2 minutes. The basal control ratio (BCR) and the uncoupling ratio (UCR) were determined as previously described⁵³¹. Essentially, the BCR is a measure of how close the basal level of respiration is to the maximum level of respiration. The closer this ratio is to 1, the greater the mitochondrial malfunction. The UCR is a measurement of mitochondrial functional integrity and measures the ratio of uncoupled to physiologically normal respiration levels. The greater the maximum level of respiration, the greater the mitochondrial functional integrity.

4.2.7 Fractionation of Plasma

Control, MCI and AD plasma from 20 subjects was pooled and fractionated by two methods. For analysis of effects of plasma protein vs metabolite fractions on cultured glia, a PD10

column separation method was used. The PD10 column was washed with MilliQ water before the addition of 500 μ L of plasma. The flow-through was collected as 750 μ L fractions topping the column with MilliQ water. In total 20 fractions were collected and the absorbances read at 280nm.

For the proteomics analysis of plasma proteins, fractionation into low and high abundant protein fractions was undertaken using an MARS-Hu6 column (Agilent Technologies, CA, USA) according to the manufacturer's instructions. The MARS-Hu6 column depletes the top 6 highest abundance proteins (albumin, IgG, IgA, transferrin, haptoglobin and antitrypsin) from plasma. This eliminates the masking effect of highly abundant proteins so that lower-abundant proteins can be more easily detected by the mass spectrometer. The low abundance fraction was used for the proteomic analysis experiments.

4.2.8 Proteomics Analysis of Human Control, MCI and AD plasma

A one dimensional SDS 4-12% NuPage (Thermo Fisher Scientific Inc, MA, USA) gel was run using the low abundance fraction from each of the three groups. The gel was colloidal coomassie stained⁴⁸², and the lanes uniformly cut into 7-8 bits using a gridcutter and mount from The Gel Company, CA, USA. The gel bits were trypsin digested and then analysed using mass spectrometry as outlined in Chapter 3, under section 3.2.4.

Peak lists were generated by MassLynx (version 4.0 SP1, Micromass) using the Mass Measure program and submitted to the database search program Mascot (version 2.2, Matrix Science, London, England). Search parameters were: Precursor and product ion tolerances \pm 0.25 and 0.2 Da respectively; Met(O) and Cys-carboxyamidomethyl were specified as variable modification, enzyme specificity was trypsin, one missed cleavage was possible on the NCBI database.

Scaffold Q+ (version 4.3.4), Proteome Software, Portland, OR, USA) was used to identify any altered proteins between the groups. The Scaffold programme uses mass spectrometric data to identify protein changes in biological samples by collating Mascot data and using the ProteinProphet algorithm⁵³². We compared the normalised total spectral count values from Scaffold⁵³³ with the emPAI values from Mascot⁵³⁴, which uses a different algorithm for spectral counting.

4.2.9 iTRAQ Proteomics of Cell Lysates Treated with Human Control, MCI and AD Plasma

Two biological replicates of cells treated with 10% (by volume) non-heat inactivated fetal bovine serum, human control, MCI or AD plasma were washed to remove all plasma/serum and then lysed using RIPA buffer and probe sonicated. Total protein concentrations were determined using the Bicinchoninic acid (BCA) protein assay kit (Pierce, IL, USA). The total protein (120 µg) from each sample was reduced with 2 µl of 5mM tris-(2-carboxyethyl) phosphine (TCEP) for 60 min at 60°C followed by alkylation with 200 mM iodoacetamide (1 µL) for 10 min at room temperature. To remove any buffer components incompatible with mass spectrometry a buffer exchange was performed with 50 mM NaHCO₃ using Microcon centrifugal filter devices with a 3,000 Da nominal molecular weight limit membrane (Millipore, MA, USA) to give a final protein concentration of 1 µg/µl.

For tryptic digestion 100 µg total protein from each sample was incubated overnight at 37°C with 4µg of trypsin. Samples were labelled using the 8-plex iTRAQ kit (Applied Biosystems, CA, USA). Each iTRAQ reporter label was mixed with a biological replicate of cell lysate sample, pH adjusted to basic (*ca* pH = 9) with 2 µl of 50 mM of Na₂CO₃ and incubated for 2 hours. The reporter masses for the samples were labelled as follows: fetal bovine serum; 113 and 117, human control plasma; 114 and 118, human MCI plasma; 115 and 119, human AD plasma; 116 and 121.

Sample clean-up was performed using a strong cation exchange cartridge (Applied Biosystems, CA, USA) and a syringe pump at a flow rate of 9.5 ml/hr, and using the manufacturer's protocol. Sample was then passed through a C18 Peptide Macrotrap (Michrom Bioresources, CA, USA). The flow-through from the C18 step was passed through an Oasis cartridge (Waters, MA, USA) to maximise peptide recovery and the two eluants pooled and dried under vacuum. Dried peptide pellets were resuspended in 0.2% heptafluorobutyric acid and then analysed using mass spectrometry as described below.

4.2.10 Proteomic Analysis of Cell Lysates Treated with Human Control, MCI and AD Plasma

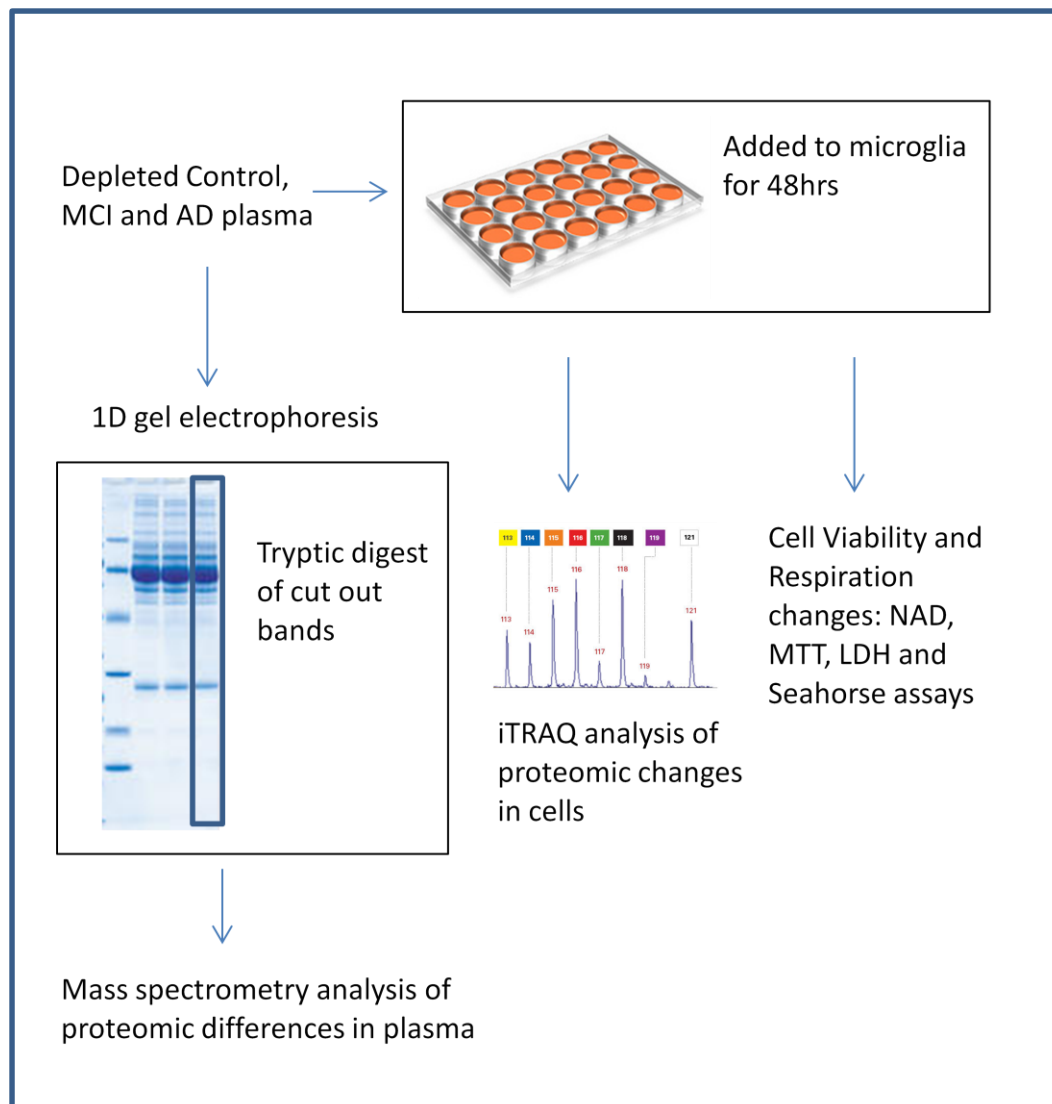
Chromatography was performed using an LC Packings capillary HPLC system (Dionex, Amsterdam, Netherlands), comprised of an Ultimate pump system, Switchos valve unit and

Famos autosampler. Samples (iTRAQ labelled peptide mixtures) were captured onto a C18 pre-column cartridge (500 μm x 2 mm, Michrom Bioresources, Auburn, CA). After a 10 min wash to remove any residual buffers or salts, the pre-column was automatically switched into line with a capillary column (75 μm x ~12 cm) containing C18 reverse phase packing material (ReproSil-Pur 120 C18-AQ, 1.9 μM , Dr Maisch, Ammerbuch-Entringen, Germany). Peptides were eluted using a 240 min linear gradient of $\text{H}_2\text{O}:\text{CH}_3\text{CN}$ (98:2, 0.1 % formic acid) to $\text{H}_2\text{O}:\text{CH}_3\text{CN}$ (20:80, 0.1 % formic acid) at ~300 nl/min. The precolumn was connected via a fused silica capillary (10 cm, 25 μ) to a low volume tee (Upchurch Scientific, WA, USA) where high voltage (2300 V) was applied and the column tip positioned ~ 1 cm from the spray inlet of a TripleTOF 5600⁺ hybrid tandem mass spectrometer (ABSciex, CA, USA). Positive ions were generated by electrospray and the instrument operated in information dependent acquisition (IDA) mode. A TOF MS survey scan was acquired (m/z 350-1700, 0.75 s) and the three largest multiply charged ions (counts > 20, charge state ≥ 2 and ≤ 4) were sequentially selected by Q1 for MS-MS analysis. Nitrogen was used as collision gas and an optimum collision energy automatically chosen (based on charge state and mass). Tandem mass spectra were accumulated for up to 2.5 s (m/z 65-2000).

Protein identification and quantification was performed using the MS/MS data (WIFF files) and the Paragon algorithm as implemented in Protein Pilot v4.0 software (Applied Biosystems, CA, USA) using the NCBIInr database. Only proteins identified with a ProteinPilot unused score of ≥ 1.3 (greater than 95% confidence in sequence identity) were accepted, as previously described^{535,536}. The unused score is a ProteinPilot generated value for the level of confidence in protein sequence identification. As an approximate guide, ProteinPilot unused scores give the following percentage levels of confidence: score ≥ 1.3 ($\geq 95\%$ confidence), score ≥ 2 ($\geq 99\%$ confidence), score ≥ 3 ($\geq 99.9\%$ confidence)⁵³⁵. The only fixed modification used was iodoacetamide alkylation of cysteine residues. Mass tolerances were set to 50ppm for the precursor and 0.2 Da for the fragment ions. Autobias correction was applied to correct for any systematic bias in total protein concentration during sample pooling. Both biological replicates for the three human plasma types (control, MCI and AD) were compared to the fetal bovine serum control (iTRAQ reporter 117) and data exported to Microsoft Excel software (Microsoft, WA, USA).

Protein interactions between dysregulated proteins were determined using the WEB-based bioinformatics tool STRING v9.1 (<http://string-db.org>). STRING has a database that collates information on protein-protein interactions and associations. It scores and weights connections and provides predicted interaction network maps from literature mining searches. The 27 proteins which were significantly dysregulated in glia treated with AD plasma, but not dysregulated in either control or MCI plasma treated glia (shown in Table 4.4) were analysed in STRING v9.1. MCL clustering was used with the 2 clusters option picked and with the confidence view selected to display the strength of evidence for protein associations. Analysis of enrichment was also performed.

Figure 4.1 Schematic workflow of methodological procedures



4.2.11 Statistics

All cell viability values are presented as means \pm SEM. Statistical comparisons were performed using two-tailed student *t*-tests assuming equal variance. Differences between treatment groups were considered statistically significant at the $p \leq 0.05$ level. Scaffold values are represented as normalised total spectral counts and p-values for significantly altered proteins were obtained using the ProteinProphet algorithm of the Scaffold Q⁺ software (Proteome Software, OR, USA). All iTRAQ quantitative data are presented as iTRAQ tag peak area ratios of cells treated with human plasma to cells treated with fetal bovine serum control. Ratios and p-values for significantly altered proteins were obtained through the Paragon algorithm of the Protein Pilot v4.0 software (Applied Biosystems, CA, USA).

Results

4.3.1 Cell Proliferation

Cells treated with non heat-inactivated AD plasma for 48 hours showed a significant decrease in cell proliferation compared to controls (Table 4.1). The addition of MCI plasma to the cells also caused a similar drop in cell proliferation, though not reaching statistical significance (Table 4.1). Mild heat treatment of the plasma at 56°C for 30 minutes is an established approach for inactivating complement proteins^{537,538}. Such heat treatment eliminated the

effects of MCI and AD plasma on cell proliferation (Table 4.1). Even with heat treatment there was a slight, though not statistically significant downward trend in cell proliferation.

4.3.2 NAD levels and LDH Leakage

Incubation with non heat inactivated plasma caused a significant drop in cell viability as reflected in lower NAD levels, for cells treated with both MCI and AD plasma, compared to controls (Table 4.1). This result was again prevented by plasma heat inactivation (Table 4.1). A significant increase in LDH leakage into the cell culture medium was seen in cells incubated with non heat inactivated AD plasma (Table 4.1). A concurrent decrease was seen in the amount of intracellular LDH in these same cells (Table 4.1).

Table 4.1: Cell viability of microglial cells exposed to MCI and AD plasma. Measured by MTT absorbance, LDH release and intracellular NAD levels of microglial cells after 48 hour incubation in pooled, non heat inactivated and heat inactivated control, MCI and AD plasma. Cell viability was determined by measurement of cell proliferation, intracellular NAD levels and LDH activity in cell culture media and cell homogenates. n=9 (nine replicates) for cell proliferation measurements, n=6 (six replicates) for NAD concentration and LDH activity. Plasma used for the measurements were obtained from the pooled plasma of 20 patients from each of the three groups (Control, MCI and AD).

		Non Heat Inactivated Plasma									Heat Inactivated Plasma					
		Control			MCI			AD			Control		MCI		AD	
		MTT assay Cell Proliferat -ion (abs at 570nm)	NAD (ng)	LDH Activity (U/L)	MTT assay Cell Proliferat -ion (abs at 570nm)	NAD (ng)	LDH Activity (U/L)	MTT assay Cell Proliferat -ion (abs at 570nm)	NAD (ng)	LDH Activity (U/L)	MTT assay Cell Proliferat -ion (abs at 570nm)	NAD (ng)	MTT assay Cell Proliferat -ion (abs at 570nm)	NAD (ng)	MTT assay Cell Prolifera -tion (abs at 570nm)	NAD (ng)
plasma	volume	Mean	0.21	10.71	0.23	10.84		0.14	10.3							
		S.E.M	0.05	3.84	0.05	1.26		0.03*	1.82							
10% of plasma	volume	Mean	0.13	3.61	0.09	2.35		0.04	0.89		0.13		0.11		0.11	
	media	S.E.M	0.03	1.25	0.02	0.85		0.01**	1.3*		1.05* (media)		0.04		0.02	

plasma represents 20% of media volume	Mean	0.06	0.79	0.06	0.56	0.03	0	14.02	12.3	12.1
	S.E.M	0.01	0.14	0.004	0.07	0.004**	0**	1.15	0.60	0.65

* $p \leq 0.05$ vs Control, ** $p \leq 0.01$ vs Control

4.3.3 The effect of complement proteins on cellular proliferation and viability

Since heat inactivation seemed to ameliorate the effect of plasma, we hypothesised that the complement protein family may be responsible. Treatment of cells with complement factors C1q, C1 inhibitor, C4, C5 and C9 effected a downward trend in cell proliferation with increasing concentration, but did not reach significance (Table 4.2). In combination, the factors were found to reduce cell proliferation at the highest concentration tested. The human complement standard which contains the factors C1q, C2, C3, C4, C5, C6, C7, C8, C9 and factor B was found to be the most potent at minimising cell proliferation (Table 4.2). The addition of human complement standard containing C1q, C2, C3, C4, C5, C6, C7, C8, C9 and factor B was found to significantly reduce NAD levels in the microglia (Table 4.2).

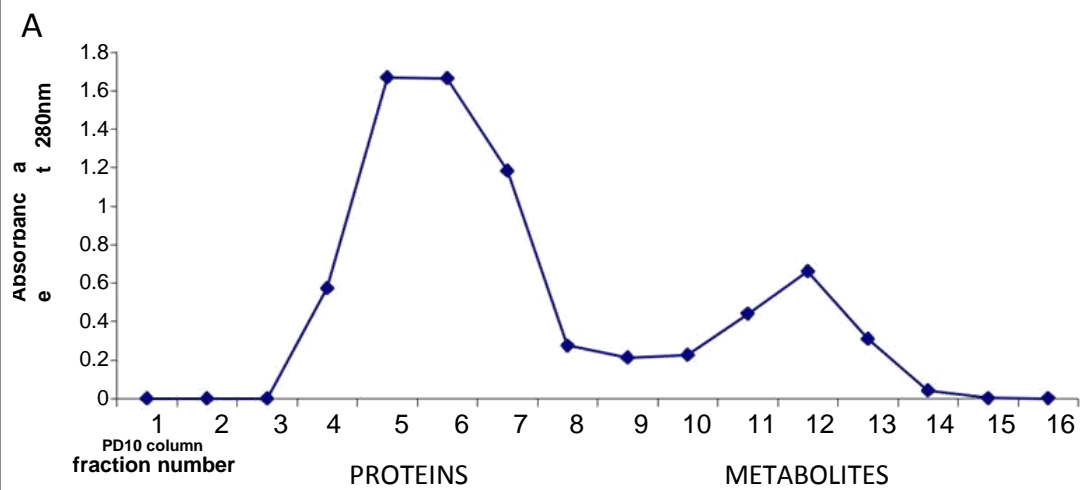
Table 4.2: Cell viability of microglial cells after 48 hour incubation with human complement components (C1q, C1 inhibitor, C4, C5 and C9), both individually and in combination with each other; and a human complement standard containing complement components C1q, C2, C3, C4, C5, C6, C7, C8, C9 and factor B. Cell viability was determined by MTT assay of cell proliferation and intracellular NAD levels (for complement standard samples). Replicates included n=6 for cell proliferation measurements and, n=3 for NAD concentrations. * $p \leq 0.05$ vs Control, ** $p \leq 0.01$ vs Control

	Cell Proliferation (abs at 570nm)	Complement C1q	Complement C1 inhibitor	Complement C4	Complement C5	Complement C9	C1q + C4	C5 + C9	Complement C1q, C1inhib, C4, C5, + C9	Complement Standard	Complement Standard (NAD, ng)
Control	Avg	0.317	0.609	0.454	0.375	0.324	0.384	0.356	0.378	0.511	0.114
(0µg/µl)	SEM	0.019	0.07	0.025	0.031	0.014	0.025	0.018	0.013	0.004	0.003
0.005µg/µl	Avg	0.3	0.593	0.458	0.382	0.333	0.377	0.371	0.377	0.426	0.104
	SEM	0.042	0.02	0.019	0.028	0.0098	0.019	0.025	0.019	0.031	0.010
0.025µg/µl	Avg	0.31	0.571	0.461	0.364	0.336	0.366	0.359	0.331*	0.210**	0.094
	SEM	0.018	0.03	0.02	0.025	0.0096	0.025	0.021	0.015	0.036	0.063
0.05µg/µl	Avg	0.267	0.49	0.435	0.355	0.344	0.289*	0.265*	0.292*	0.129**	0.063*
	SEM	0.0075	0.05	0.019	0.03	0.021	0.027	0.013	0.024	0.018	0.0024

4.3.4 Effects of plasma metabolites vs proteins on cell proliferation and viability

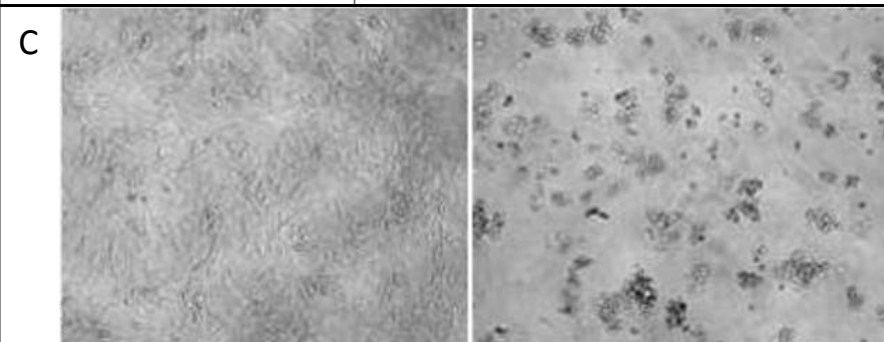
To determine whether the effect on cell proliferation was due to the protein or metabolite component of plasma (or both), the protein and low molecular weight components of plasma were separated. Plasma was fractionated using a PD10 column (GE Healthcare Life Science, UK) into its protein and metabolite portions to determine which portion of the plasma was causing the cytotoxic effect (Figure 4.1). Addition of these two fractions to the cells showed that it was exclusively the protein portion which was initiating the reduction in cell proliferation (Figure 4.1). Protein fractions of both MCI and AD plasma were found to significantly reduce cell proliferation (Figure 4.1). The metabolite fraction of the plasma had no significant effect on microglial proliferation (Figure 4.1).

Figure 4.2: Fractionation of non heat inactivated control plasma into protein and metabolite fractions using PD10 column, and the effect of these fractions on cell proliferation. Three replicates were performed. Plasma used for the measurements were obtained from the pooled plasma of 20 patients from each of the three groups (Control, MCI and AD). Effect on cell proliferation at a plasma concentration of 10% and 20% of total media volume are shown. * $p \leq 0.01$ vs Control, ** $p \leq 0.001$ vs Control. **Panel A:** Fractionation of non heat inactivated control plasma into protein and metabolite fractions using PD10 column **Panel B:** Effect of these fractions on cell proliferation. **Panel C:** Images of microglia after 48 hour incubation with non heat inactivated 20% control plasma (left) and non heat inactivated 20% AD plasma (right), showing increased toxicity and reduced cell proliferation in the AD plasma treated cells.



B

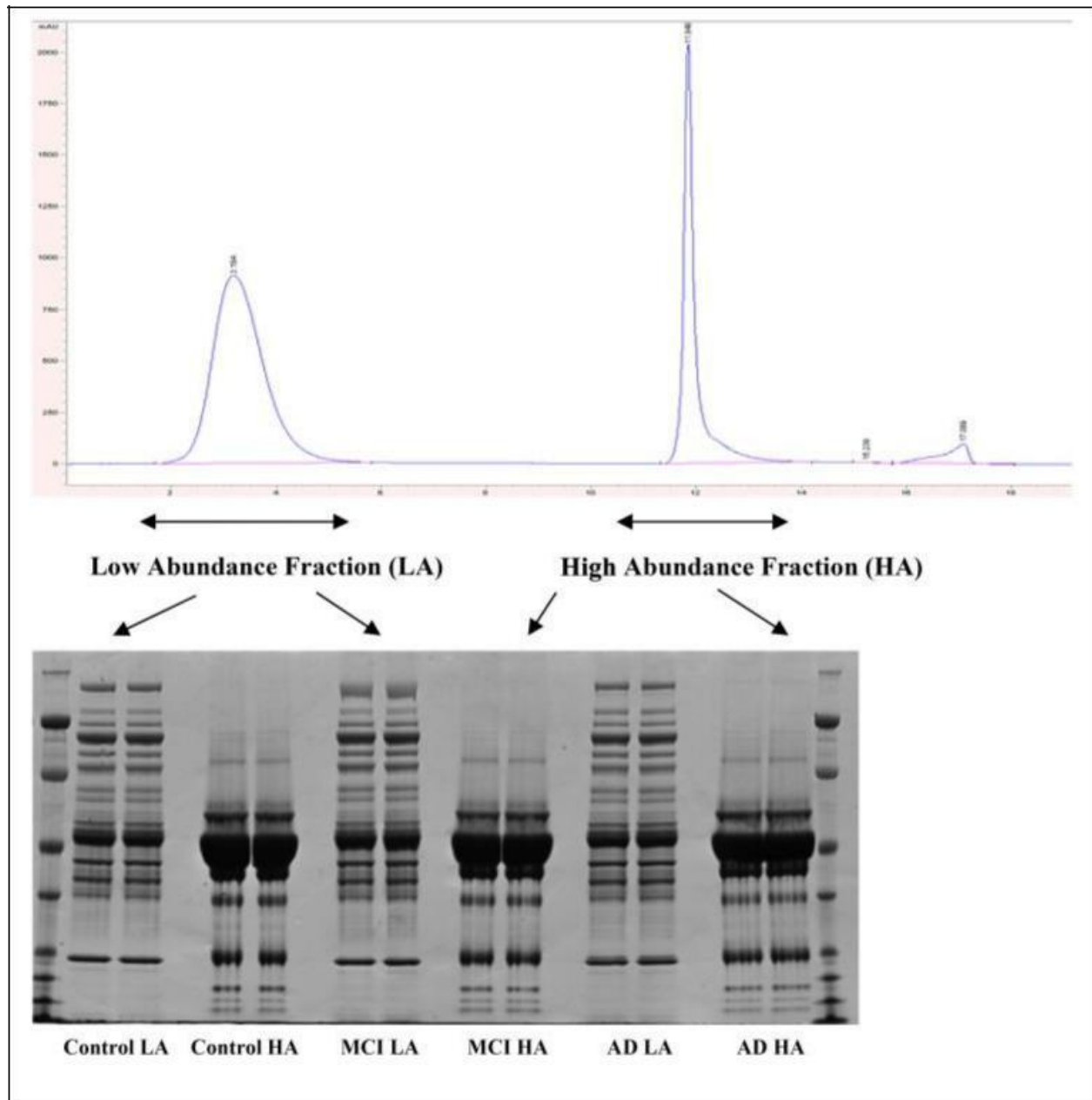
	Protein Fraction				Metabolite Fraction			
	MCI		AD		MCI		AD	
Fraction Volume added (% of total media volume)	10%	20%	10%	20%	10%	20%	10%	20%
Average Cell Proliferation (% of Control)	90.77	75.96*	53.37**	37.39**	111.57	103.78	99.19	101.18
S.E.M	3.65	0.92	1.88	1.84	9.36	10.02	3.37	7.59



4.3.5 Plasma fractionation and 1D gel electrophoresis

Chromatogram using the MARS-Hu6 column provided a baseline separation of low and high abundant proteins (Figure 4.2). Low abundant proteins are eluted first (first peak on chromatogram) and high abundant proteins are eluted after (second peak, containing the six highest abundance plasma proteins including: albumin, IgG, IgA, transferrin, haptoglobin and antitrypsin). These fractions were run on a 1D SDS NuPAGE gel and proteins were shown to be effectively separated with a substantial depletion of high abundant proteins, revealing many lower abundant protein bands in the low abundant fraction (Figure 4.2). Loading was 50 µg/lane. First and last lanes contained molecular weight markers. Each fraction was run in duplicate.

Figure 4.3 Representative chromatogram of separation of plasma into low and high abundant fractions and 1D SDS NuPage gel of these protein fractions.



4.3.6 Proteomics of MCI and AD plasma

We used an unbiased label free proteomics approach to explore the MCI and AD plasma proteomes, to identify any dysregulated proteins. Following proteomic analysis of pooled control, MCI and AD plasma, normalised total spectral counts using Scaffold software and emPAI values from Mascot showed complement component 2, fibronectin and fibrinogen to be significantly increased in the AD group compared to the control group (Table 4.3).

Thrombin was decreased in the MCI and AD patients compared to controls (Table 4.3).

Table 4.3: Average normalised spectral counts (obtained from Scaffold) and emPAI values (obtained from Mascot) of significantly deregulated proteins identified in pooled plasma samples between the Control, MCI and AD groups. Values are averages from 4 replicates. Plasma used was obtained from the pooled plasma of 20 patients from each of the three groups (Control, MCI and AD) with depletion of high abundance proteins.

		Complement component 2 (gi 14550407)			Complement component 1 inhibitor (gi 114642584)			Complement component 4 binding protein (gi 4502503)			Fibronectin (gi 109658664)			Thrombin (gi 119588383)			Fibrinogen (gi 70906435)			Alpha-1B-glycoprotein (gi 46577680)		
		C	MCI	AD	C	MCI	AD	C	MCI	AD	C	MCI	AD	C	MCI	AD	C	MCI	AD	C	MCI	AD
Normalised Spectral Count	Average	0	0.82	2.77	9.98	7.45	11.30	4.18	3.38	4.51	18.9	15.1	32.2	10.34	5.57	6.29	39.78	35.93	43.19	6.08	8.32	7.64
	S.E.M	0	0.50	0.29	1.0	0.46	2.10	0.51	0.46	0.83	0.18	2.55	2.29	1.18	0.50	0.88	5.58	2.42	7.25	0.49	0.70	1.01
	p-value		0.015#	0.000074**		p = 0.06 vs AD						0.0025##	0.0012**		0.098*	0.033*					0.040*	
emPAI value	Average	0.08	0.06	0.145	0.74	0.62	0.95	0.35	0.18	0.26	0.39	0.30	0.64	0.83	0.46	0.48	5.40	4.74	7.87	0.78	0.86	0.75
	S.E.M	0.010	0.020	0.014	0.090	0.06	0.13	0.027	0.037	0.029	0.068	0.065	0.033	0.068	0.055	0.033	0.48	0.62	0.71	0.10	0.032	0.029
	p-value		0.014#	0.025*		p = 0.06 vs AD				0.013*		0.0071##	0.0018**		0.0057*	0.0034*		0.016#	0.036*		0.050#	

* p ≤ 0.05 vs Control, ** p ≤ 0.01 vs Control

p ≤ 0.05 vs AD, # #p ≤ 0.01 vs AD

4.3.7 Mitochondrial Function and Cellular Bioenergetics

Since changes in NAD and LDH were seen in response to cells exposed to AD plasma, we explored the possibility that cellular energy generating pathways were affected more broadly. To determine whether mitochondrial bioenergetic mechanisms are associated with AD pathogenesis, we assessed mitochondrial function in glial cells treated with human plasma using the Seahorse XF24 bioanalyzer (Seahorse Bioscience, MA, USA). We observed a significant decrease in oxygen consumption rates (OCRs) and an increase in extracellular acidification rates (ECARs) for cells treated with AD plasma. MCI plasma effected similar trends though did not achieve statistical significance (Figure 4.3). We also observed a significant increase in the basal control ratio (BCR) and a decline in the uncoupling ratio (UCR) in microglial cells after 48 hr incubation with AD plasma (Figure 4.3), consistent with impaired mitochondrial function and increased shift towards glycolysis.

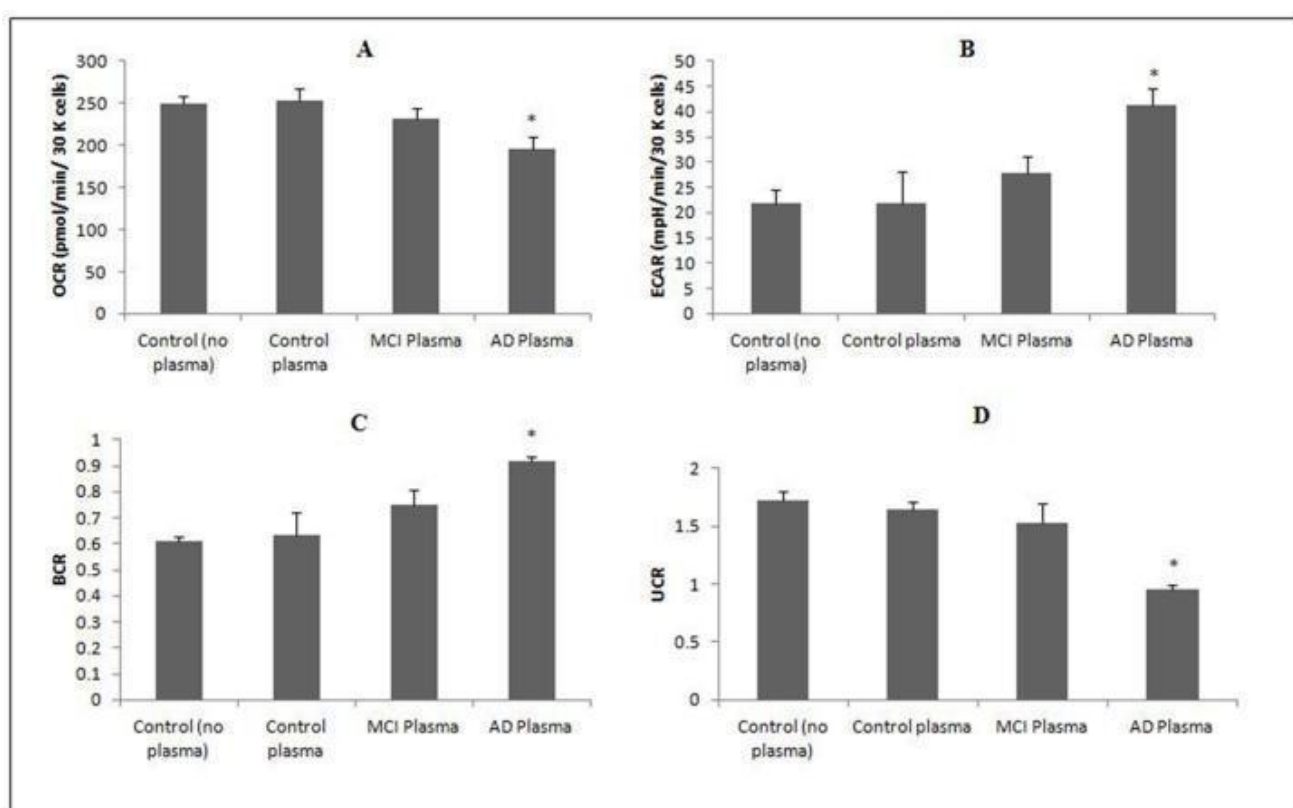
Figure 4.4: Effects of human plasma on cellular bioenergetics in a microglial cell line.

Effect of human plasma on oxygen consumption rates (OCR) in a microglial cell line for 48 hours. * $p < 0.05$ compared to non-treated cells (control); (n=4 for each treatment group).

Effect of human plasma on extracellular acidification rates (ECAR) in a microglial cell line for 48 hours. * $p < 0.05$ compared to non-treated cells (control); (n=4 for each treatment group).

(C) Effect of human plasma on the basal control ratio (BCR) in a microglial cell line for 48 hours. * $p < 0.05$ compared to non-treated cells (control); (n=4 for each treatment group).

(D) Effect of human plasma on the uncoupling ratio (UCR) in a microglial cell line for 48 hours. * $p < 0.05$ compared to non-treated cells (control); (n=4 for each treatment group).



4.3.8 iTRAQ proteomic analysis of cell lysates treated with Control, MCI and AD plasma

Differential protein expression in glial cells treated with fetal bovine serum (control) or human plasma from control, MCI and AD subjects were analysed with two biological replicates performed using an 8-plex iTRAQ experimental design. In total, 791 proteins were identified with 95% or greater confidence in correct protein sequence identification and 750 proteins with a false discovery rate of 5%. Forty-nine proteins were found significantly altered between the three groups of cellular lysates (Table 4.4). The highest number of dysregulated proteins were found in the cells treated with AD plasma (Table 4.4, 27 proteins highlighted in bold).

Interestingly quite a few proteins involved in the glycolysis cycle were shown to be upregulated in this group, namely glyceraldehyde-3-phosphate dehydrogenase, phosphoglycerate kinase, enolase, aldolase and pyruvate kinase. These enzymes catalyse five of the ten enzyme reactions of the pathway and their functions are shown in Figure 4.4.

Transketolase was also shown to be significantly elevated in both the AD plasma treated cell sample replicates. This enzyme is part of the pentose phosphate pathway and connects this pathway to glycolysis. Analysis of protein interactions of the 27 dysregulated glial proteins treated with AD plasma using the online STRING v9.1 tool confirmed a significant enrichment of proteins involved in glucose metabolism (Figure 4.5 and Table 4.5).

Table 4.4: Dysregulated proteins in glial cells treated with human control, MCI and AD plasma compared to FBS (non human serum control) following iTRAQ analysis. Cells were incubated with plasma in two 24 well plates, 3 wells for each of the plasma types were pooled from each plate to obtain two biological replicates for the 8-plex iTRAQ experiment. iTRAQ reporter ratios and p-values for altered proteins are shown for both replicates. Proteins found to be dysregulated in MCI and AD treated cells are shown in the table in bold: upregulation in red and downregulation in blue.

Protein Function	Accession #	Name	Replicate 1		Replicate 2		Replicate 1		Replicate 2		Replicate 1		Replicate 2	
			Ctrl:FBS	PVal	Ctrl:FBS	PVal	MCI:FBS	PVal	MCI:FBS	PVal	AD:FBS	PVal	AD:FBS	PVal
Glycolysis	gi 7669492	glyceraldehyde-3-phosphate dehydrogenase	0.97	0.524	1.02	0.603	0.98	0.676	0.98	0.655	1.27	3.4E-5*	1.32	1.0E-4*
	gi 4505763	phosphoglycerate kinase 1	1.07	0.175	1.05	0.322	1.05	0.279	1.06	0.207	1.2	7.0E-5*	1.31	1.1E-4*
	gi 4503571	alpha-enolase isoform 1	0.93	0.12	0.98	0.753	0.99	0.719	0.98	0.553	1.19	2.7E-4*	1.22	1.0E-4*
	gi 342187211	fructose-bisphosphate aldolase A	0.99	0.829	1	0.989	1.02	0.836	1	0.991	1.2	0.004*	1.22	0.001*
	gi 33286418	pyruvate kinase isozymes M1/M2	0.98	0.746	1.02	0.726	1.01	0.869	1.03	0.6	1.22	0.008*	1.22	0.002*
	gi 4507521	transketolase isoform 1	0.98	0.686	1.01	0.881	1.04	0.323	0.99	0.749	1.13	0.022*	1.16	0.002*
Chaperone	gi 20070125	protein disulfide-isomerase precursor	0.98	0.566	0.96	0.352	0.93	0.057	1.01	0.821	0.93	0.026*	0.98	0.478
	gi 153792590	heat shock protein HSP 90-alpha	1.03	0.679	1.05	0.601	1.06	0.512	1.06	0.473	1.3	0.036*	1.2	0.059

Cytoskeletal	gi 66933005	calnexin precursor	1	0.942	0.98	0.7	0.94	0.315	0.93	0.149	0.92	0.266	0.88	0.010*
	gi 5031973	protein disulfide-isomerase A6 precursor	0.97	0.429	0.98	0.662	0.94	0.134	1	0.952	0.96	0.546	0.91	0.019*
	gi 21361657	protein disulfide-isomerase A3 precursor	0.96	0.427	0.98	0.653	0.9	0.013*	1	0.871	0.92	0.117	0.89	0.06
	gi 16507237	78 kDa glucose-regulated protein precursor	0.99	0.806	0.97	0.729	0.92	0.038*	0.98	0.643	0.91	0.101	0.91	0.108
	gi 4505257	moesin	1.08	0.265	1.14	0.243	1.12	0.106	1.03	0.721	1.22	0.021*	1.2	0.028*
	gi 21614499	ezrin	1.06	0.498	0.95	0.718	1.05	0.555	1.13	0.446	1.31	0.033*	0.9	0.712
	gi 38176300	nestin	0.99	0.773	1	0.984	0.97	0.518	1.04	0.354	0.94	0.173	0.85	0.004*
	gi 44680105	caldesmon isoform 1	0.91	0.154	0.97	0.773	0.9	0.174	0.94	0.478	0.87	0.085	0.86	0.027*
	gi 19920317	cytoskeleton-associated protein 4	0.85	0.049*	0.77	0.012*	0.92	0.229	0.79	0.032*	0.74	1.0E-4*	0.77	0.019*
	gi 62414289	vimentin	0.97	0.23	1	0.965	0.9	2.4E-4*	0.99	0.778	0.97	0.261	0.96	0.277
Proteolysis	gi 4506713	ubiquitin-40S ribosomal protein S27a	0.98	0.738	0.82	0.159	1.06	0.286	1.04	0.594	0.84	0.066	0.77	0.022*
	gi 66346681	plasminogen activator inhibitor 1	1.04	0.587	0.99	0.922	1	0.999	0.93	0.476	0.97	0.612	0.79	0.023*
	gi 54792069	small ubiquitin-related modifier 2	1.15	0.291	1.02	0.948	1.46	0.083	1.41	0.052	1.23	0.26	1.29	0.043*
	gi 109637759	calpastatin isoform f	0.86	0.228	0.75	0.138	0.81	0.24	0.88	0.46	0.82	0.206	0.74	0.045*
Translation	gi 4503471	elongation factor 1-alpha 1	0.97	0.493	1.02	0.76	0.93	0.225	0.97	0.563	1.13	0.024*	1.24	0.014*
	gi 17158044	40S ribosomal protein S6	0.95	0.62	0.54	0.063	0.83	0.091	0.7	0.172	0.74	0.041*	0.72	0.178

Transcription	gi 15431288	60S ribosomal protein L10a	1.14	0.206	1.31	0.037*	1.19	0.098	1.27	0.048*	1.41	0.079	1.06	0.732
	gi 214010226	40S ribosomal protein S24 isoform d	0.68	0.062	0.66	0.015*	0.75	0.011*	0.66	0.085	0.6	0.063	0.64	0.022*
	gi 124494254	proliferation-associated protein 2G4	0.97	0.897	0.99	0.974	1.36	0.040*	1.22	0.194	1.24	0.276	1.15	0.146
	gi 4885379	histone H1.4	0.86	0.158	0.78	0.053	0.79	0.063	0.96	0.61	0.58	0.006*	0.79	0.349
	gi 4885377	histone H1.3	1.04	0.538	1.21	0.386	0.94	0.438	1.18	0.369	0.75	0.012*	0.96	0.613
	gi 4885381	histone H1.5	0.83	0.011*	0.77	0.057	0.79	0.006*	0.9	0.164	0.65	3.4E-4*	0.85	0.205
	gi 4885375	histone H1.2	0.87	0.059	0.73	0.002*	0.74	0.002*	0.95	0.468	0.54	0.001*	0.76	0.102
Immune response	gi 4502101	annexin A1	1	0.999	0.99	0.848	0.93	0.161	1.02	0.794	0.87	0.023*	0.83	0.042*
	gi 50845388	annexin A2 isoform 1	1.04	0.339	1.1	0.021*	0.89	8.0E-4*	0.99	0.647	0.95	0.192	0.93	0.1
	gi 48255891	glucosidase 2 subunit beta	1.04	0.679	1.13	0.292	1.14	0.081	1.16	0.012*	1.01	0.914	1.05	0.584
Antioxidant	gi 32189392	peroxiredoxin-2 isoform a	1.34	0.096	1.2	0.268	1.28	0.15	1.16	0.454	1.19	0.026*	1.28	0.146
	gi 4505591	peroxiredoxin-1	1.01	0.871	0.95	0.379	1.01	0.871	0.96	0.479	1.07	0.223	1.17	0.021*
Cell Growth Regulation	gi 4503057	alpha-crystallin B chain	1.04	0.429	1.02	0.718	1.04	0.45	0.99	0.931	1.24	0.002*	1.26	0.043*
Fatty Acid Metabolism	gi 19743823	integrin beta-1 isoform 1A precursor	1.32	0.102	1.05	0.81	1.14	0.259	1.52	0.038*	1.35	0.069	1.08	0.829
	gi 4557585	fatty acid-binding protein, brain	0.85	0.22	0.84	0.176	0.8	0.228	0.87	0.353	0.9	0.247	0.83	0.049*
	gi 4758504	3-hydroxyacyl-CoA dehydrogenase	1.17	0.445	1.09	0.795	1.33	0.097	1.57	0.015*	1.18	0.49	1.14	0.381

Energy														
Metabolism	gi 19923437	GTP:AMP phosphotransferase	1.4	0.083	1.27	0.371	1.46	0.047*	1.14	0.44	1.43	0.052	1.43	0.149

* p ≤ 0.05 vs Fetal Bovine Serum Control

Figure 4.5 Glycolysis Pathway highlighting enzymes which were shown to be upregulated in cells treated with AD plasma.

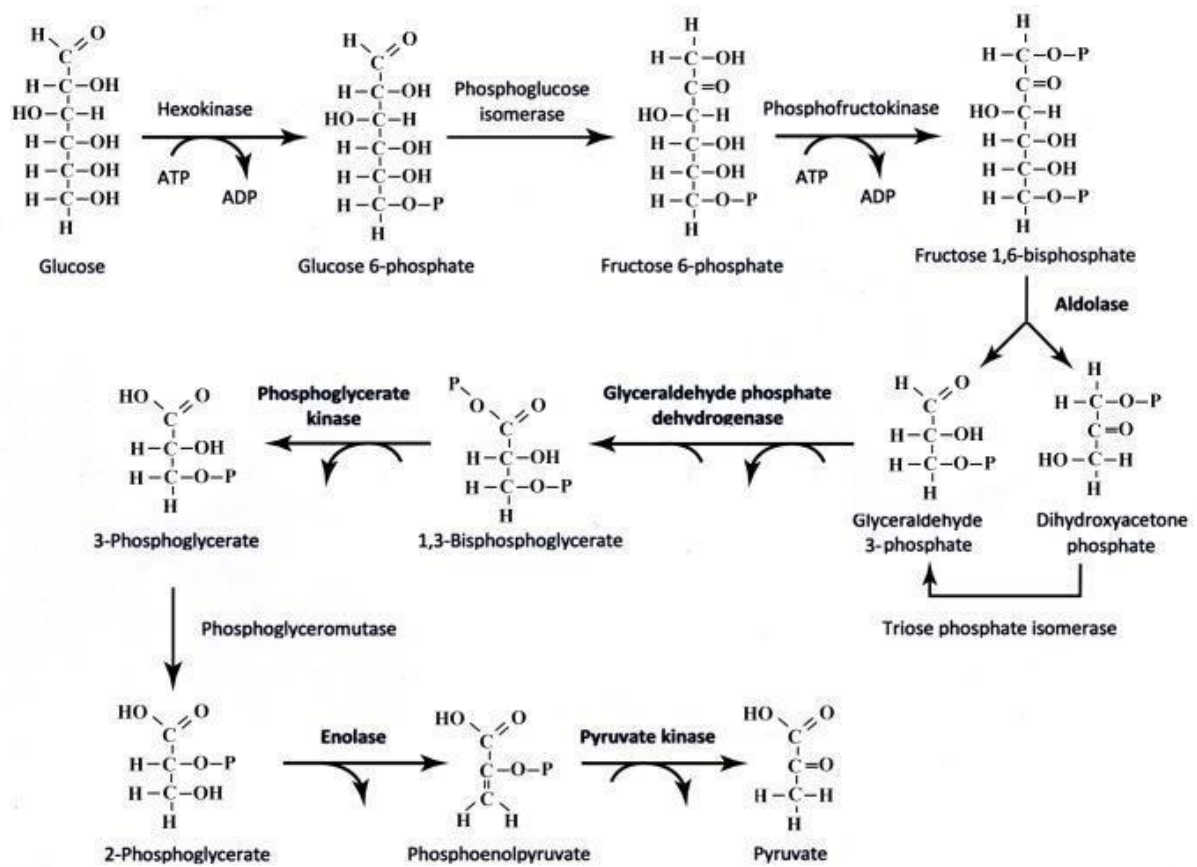


Figure 4.6: Protein associations of proteins dysregulated in AD plasma treated glia. The 27 proteins which were significantly dysregulated in glia treated with AD plasma, but not dysregulated in either control or MCI plasma treated glia (shown in Table 4.4) were analysed in STRING v9.1. MCL clustering was used with the 2 clusters option picked and with the confidence view selected to display the strength of evidence for protein associations (panel A). Analysis of enrichment was also performed and the most significantly enriched biological process was glucose metabolic process (FDR p-value = 1.759×10^{-8} , with the 9 proteins involved in this process shown in panel B). Other distinct biological processes which were also significantly enriched included response to hydrogen peroxide (FDR p-value = 3.559×10^{-2} with 4 proteins involved; ANXA1, PRDX1, PRDX2, CRYAB) and membrane to membrane docking (FDR p-value = 4.299×10^{-2} with 2 proteins involved; MSN, EZR). Several molecular functions were also enriched, the most significant being RNA binding (FDR p-value = 5.340×10^{-9} with 17 proteins involved shown in panel C). Another distinct and significantly enriched molecular function is thioredoxin peroxidase activity (FDR p-value = 9.220×10^{-3} with 4 proteins involved; PRDX1, PRDX2). Several cellular components were also enriched, the most significant of these being extracellular vesicle exosome (FDR p-value = 5.019×10^{-9} with 17 proteins involved as shown in panel D). Multiple other significantly enriched cellular components were also observed, and all enriched protein groups are shown in Table 4.5.

Table 4.5 STRING v9.1 analysis of the 27 proteins dysregulated only in glia exposed to AD plasma (shown in Table 4.4) for enrichment in gene ontology biological processes. Glucose metabolism was found to be the most significant biological process, and is also highlighted in the STRING network map (Figure 4.5).

molecular function enrichment					
GO_id	Term	Number of Proteins	p-value	p-value_fdr	p-value_bonferroni
GO:0003723	RNA binding	17	1.94E-12	5.34E-09	7.51E-09
GO:0044822	poly(A) RNA binding	16	2.75E-12	5.34E-09	1.07E-08
GO:0008379	thioredoxin peroxidase activity	2	8.88E-06	9.22E-03	3.45E-02
GO:0003676	nucleic acid binding	16	9.50E-06	9.22E-03	3.69E-02
GO:0051920	peroxiredoxin activity	2	2.95E-05	2.29E-02	1.15E-01
biological process enrichment					
GO_id	Term	Number of Proteins	p-value	p-value_fdr	p-value_bonferroni
GO:0006006	glucose metabolic process	9	1.42E-12	1.76E-08	1.76E-08
GO:0019318	hexose metabolic process	9	7.28E-12	4.51E-08	9.02E-08
GO:0005996	monosaccharide metabolic process	9	3.63E-11	1.50E-07	4.49E-07
GO:0046364	monosaccharide biosynthetic process	6	2.23E-10	6.89E-07	2.75E-06
GO:0016051	carbohydrate biosynthetic process	7	7.56E-10	1.87E-06	9.35E-06
GO:0006094	gluconeogenesis	5	5.43E-09	1.12E-05	6.73E-05
GO:0019319	hexose biosynthetic process	5	9.29E-09	1.64E-05	1.15E-04
GO:0042542	response to hydrogen peroxide	4	2.30E-05	3.56E-02	2.85E-01
GO:0022614	membrane to membrane docking	2	3.13E-05	4.30E-02	3.87E-01
GO:0016584	nucleosome positioning	2	6.56E-05	8.12E-02	8.12E-01
Cellular component enrichment					
GO_id	Term	Number of Proteins	p-value	p-value_fdr	p-value_bonferroni
GO:0070062	extracellular vesicular exosome	17	1.04E-11	5.02E-09	1.51E-08
GO:0044421	extracellular region part	18	1.23E-09	4.44E-07	1.77E-06
GO:0005576	extracellular region	18	1.08E-07	3.06E-05	1.57E-04
GO:0031988	membrane-bounded vesicle	15	1.27E-07	3.06E-05	1.84E-04
GO:0031982	vesicle	15	1.83E-07	3.77E-05	2.64E-04
GO:0043233	organelle lumen	16	2.50E-07	4.32E-05	3.62E-04
GO:0042470	melanosome	5	2.98E-07	4.32E-05	4.32E-04
GO:0005829	cytosol	15	1.22E-06	1.47E-04	1.77E-03
GO:0070013	intracellular organelle lumen	13	5.33E-05	5.93E-03	7.71E-02
GO:0031254	cell trailing edge	2	7.00E-05	6.76E-03	1.01E-01
GO:0001931	uropod	2	7.00E-05	6.76E-03	1.01E-01
GO:0030016	myofibril	4	1.41E-04	1.28E-02	2.05E-01
GO:0016323	basolateral plasma membrane	4	1.51E-04	1.29E-02	2.19E-01
GO:0043292	contractile fiber	4	1.66E-04	1.33E-02	2.40E-01
GO:0060205	cytoplasmic membrane-bounded vesicle lumen	3	2.64E-04	1.91E-02	3.82E-01
GO:0031983	vesicle lumen	3	2.64E-04	1.91E-02	3.82E-01
GO:0031528	microvillus membrane	2	2.98E-04	2.05E-02	4.31E-01
GO:0016023	cytoplasmic membrane-bounded vesicle	7	3.68E-04	2.42E-02	5.32E-01
GO:0005719	nuclear euchromatin	2	5.70E-04	3.43E-02	8.24E-01
GO:0000791	euchromatin	2	7.98E-04	4.62E-02	1.00E+00

4.4 Discussion

There is growing evidence from parabiosis experiments on the positive effects of young blood in ageing, in which circulatory systems of young and aged animals are connected. These studies show that blood from young animals can rejuvenate older animals and ameliorate disease^{155,156}. A variety of studies have looked at the effects of plasma on cell cultures in different diseases. For example, Brewer *et al* found that 24 hr exposure of human serum from AD patients to rat hippocampal neurons increased four molecular markers characteristic of Alzheimer senile plaques and neurofibrillary tangles⁵⁰⁸. Another study has shown that Parkinsonian serum has complement-dependent toxicity to rat dopaminergic neurons⁵³⁹. A study using a differentiated neuronal cell line investigated the susceptibility of neuronal cells to human complement. It was found that human serum caused lysis of the neurons by complement, as tested by cell viability. The effect was lost when cells were treated with complement-depleted serum by heat inactivation⁵⁴⁰.

Our cell culture results also showed that the loss of cell viability and reduction in cell proliferation caused by AD plasma can be prevented by heat inactivation, which inhibits the activity of plasma complement proteins. Alterations to the expression of peripheral proteins may reflect changes in the brain, possibly through a compromised blood brain barrier. Damage to the blood-brain-barrier resulting in increased permeability has been reported in MCI and AD^{141,541}. Together these data suggests that complement may have the capacity to contribute to cell loss seen in AD. Complement factors may work synergistically to cause loss in cell viability. We observed reduced cell viability when cells were exposed to the complement standard mixture, as compared to addition of single complement factors (Table 4.2). However in all cases we observed a downward trend in cell viability as complement concentration levels increased regardless of the number of complement proteins present. The data achieved statistical significance with exposure to as few as two complement factors (Table 4.2), indicating that the full spectrum of complement proteins are not necessary for cytotoxicity. Indeed it has been found that treatment of a transgenic mouse model with an agonist to a single complement receptor, C5aR, decreased pathology and improved behavioural performance⁵⁴².

There is significant evidence for the involvement of inflammation in the pathogenesis of Alzheimer's disease. In the AD brain, damaged neurons and highly insoluble A β peptide deposits and NFTs provide stimuli for inflammation^{506,507}. Various neuroinflammatory mediators including complement activators and inhibitors, chemokines, cytokines, radical oxygen species and inflammatory enzymes have been shown to be altered in AD^{506,507}. Another prominent feature of AD neuropathology is the association of activated proteins of the classical complement pathway with the lesions. The full-range of classical pathway complement proteins from C1q to C5b-9, known as the membrane attack complex, have been found localised with A β deposits in neuritic plaques^{543,544}. Complement proteins are also present in dystrophic neurites in AD. The fact that complement activation has progressed until the final membrane attack complex stage and the observation that complement regulators are associated with AD lesions suggests a disturbance in the regulatory mechanisms controlling complement activation in this disease⁵⁴⁵⁻⁵⁴⁸.

A β itself can induce complement-mediated toxicity against neurons in culture, suggesting that A β -induced complement activation may contribute to the neuropathogenesis of AD^{544,549}. Hyperphosphorylated tau protein, the main component of NFTs, is also a potent stimulator of the complement cascade. Purified NFTs have been shown to activate the complement system in plasma, resulting in a significant increase in the level of membrane attack complex⁵⁵⁰. Tau and A β are both able to increase inflammatory responses and cytokine production. Since the complement system is strongly activated in AD, it could possibly participate either in the exacerbation or amelioration of the pathology. Because A β deposits and extracellular NFTs are present during early preclinical until terminal stages of AD, their ability to activate complement provides a mechanism for initiating and sustaining chronic, low-level inflammatory responses that may have cumulative effects over the disease course. This supports the idea that complement system cascade intervention might be a useful pharmacological approach to treat early stages of AD.

Proteomic analysis of MCI and AD plasma in this study revealed a number of proteins which were significantly altered between the three groups. The majority of these proteins were acute phase reactants, including proteins which were related to the complement system (Table 4.3). This data is consistent with a number of other published proteomics studies, which have

shown changes in complement protein levels and other acute phase proteins in AD plasma^{536,551-553}. A summary of proteins found altered in such studies is provided in Table 4.6 and some of the proteins found in our study overlap with those found by other groups using larger cohorts of patients. Furthermore, one study has also shown a correlation between brain hippocampal volume changes and plasma levels of acute phase proteins, including complement⁵⁵¹, suggesting a mechanistic link.

Table 4.6 Summary of previous studies showing changes in acute phase proteins in Alzheimer's disease.

Name	Site of effect	Function	Modification	Reference
Alpha-2-macroglobulin	plasma	Inhibitor of coagulation; inhibitor of fibrinolysis	Increased in MCI and AD	536,552
Complement C3	plasma	Most abundant protein of the complement system, enhances response	Increased in AD	554-557
Complement C4	plasma	Protein involved in the complement system and undergoes cleavage	Increased in AD	552,558
C4b-binding protein	plasma	Inhibits C4 and binds necrotic cells	Decreased in MCI and AD	536
Complement C5	plasma	Fifth component of the complement pathway	Increased in MCI	536
Complement C9	mRNA and protein levels, vascular amyloid deposits	Involved in MAC formation	Increased in AD brain areas, increased deposition in vascular plaques	554,555,559

Complement factor H	plasma	Regulation of alternative pathway of the complement system, ensuring no damage to host tissue	Increased in AD	552,560
Fibrinogen	plasma	Involved in blood clotting	Decreased in AD	536,557,561,562
Haptoglobin	Plasma, CSF	Binds free haemoglobin thereby reducing its oxidative activity	Increased in AD plasma, decreased in CSF of MCI and AD patients Other studies show increase in CSF of AD	563,564
Hemopexin	plasma and CSF	Binds heme, preserves iron levels in the body	Increased in AD	558,565,566
Thrombin	Brain tissue, amyloid plaques, neurofibrillary tangles	Coagulation protein that converts fibrinogen into fibrin, also catalyses other coagulation related reactions	Increased in AD	567-569
Transthyretin	Plasma, CSF	Carrier of the thyroid hormone thyroxine	Decreased in AD	536,565,570,571

Interestingly one of the complement proteins that was downregulated in the AD plasma, complement 4 binding protein (C4BP), is a complement inhibitor which is detected in A β plaques and on apoptotic cells in the AD brain⁵⁷². *In vitro*, C4BP binds apoptotic and necrotic but not viable brain cells. It also binds to A β (1-42) peptide directly and limits the extent of complement activation by A β ⁵⁷². C4BP levels in CSF of dementia patients and controls were low compared to levels in plasma and correlated with CSF levels of other

inflammation-related factors⁵⁷². Therefore it possibly protects against excessive complement activation in AD brains.

Fibronectin is present in plaques of AD brains and may modify biosynthesis of APP in microglia⁵⁷³. Addition of A β to cultured astrocytes has been shown to induce a marked increase in the production of fibronectin⁵⁷⁴. This suggests that *in vivo* fibronectin accumulation in senile plaques may be the result, at least in part, of the response of reactive astrocytes to the presence of A β . Fibrinogen is associated with an increased risk of AD and vascular dementia⁵⁷⁵. Our study found fibronectin and fibrinogen to be significantly increased in the AD group compared to controls (Table 4.3).

Furthermore, we have also shown that treatment with AD plasma can affect cellular bioenergetics in a microglial cell line, by increasing glycolysis to compensate for declining oxygen consumption and mitochondrial respiration (Figure 4.3). The reduction in cerebral glucose metabolism, as measured by FDG-PET, is a common diagnostic tool for AD. Positron emission tomography (PET) imaging has identified a strong correlation between the spatial distribution of increased glycolysis, and A β plaques in the AD brain⁵⁷⁶. It is estimated that aerobic glycolysis accounts for up to 90% of glucose consumed⁵⁷⁷. By contrast, a recent neuroimaging study which correlated multimodal neuronal parameters including glucose metabolism and hippocampal volume with A β deposition in cognitively normal older individuals, did not find any association between the multimodal neurodegenerative biomarkers⁵⁷⁸. However, diminished neuronal integrity and cognitive function correlated with an increased A β burden in brain regions that are most affected by AD pathology⁵⁷⁸. Increased glycolysis was associated with better verbal episodic memory in individuals with elevated amyloid levels in another study⁵⁷⁹. The increased shift towards glycolysis may occur in regions of the brain most vulnerable to insult, or may occur in response to A β accumulation during ageing. Loss of this protective mechanism may increase the vulnerability of certain brain regions to A β -induced neurotoxicity.

Quantitative iTRAQ analysis of glial cells treated with human AD plasma showed the highest number of dysregulated proteins (Table 4.4). The most significantly enriched biological

process was glucose metabolism (Figure 4.5 and Table 4.5), and a significant number of upregulated glycolytic proteins were found (highlighted in bold in Figure 4.4), which is in agreement with the ECAR effect we found in cellular biogenetics using mitochondrial function assays (Figure 4.3). Increased expression of glyceraldehyde-3-phosphate dehydrogenase, phosphoglycerate kinase, enolase, aldolase and pyruvate kinase may increase glycolytic flux leading to the accumulation of pyruvate and thus stimulating anaerobic metabolism to lactic acid. We found an increased level of LDH activity in the cell culture media and an increase in extracellular acidification, as indicated by the increase in ECAR in the microglial cells exposed to human AD plasma (Figure 4.3). These findings suggest a role for mitochondrial bioenergetic deficits in AD pathogenesis. Our study is consistent with

previous PET metabolic analyses in individuals with AD, MCI, or incipient to late AD⁵⁸⁰.

Our findings are also consistent with microarray analyses and activity assays of ageing, incipient AD, and AD human samples and rodent models which indicate that genes and the catalytic activity of several glycolytic enzymes are altered in AD or MCI patients^{581,582}.

Similarly, increased amyloid production and nerve cell atrophy, have been shown to induce mitochondrial dysfunction⁵⁸³. Overexpression of pyruvate dehydrogenase kinase and lactate dehydrogenase in neurons has been shown to provide resistance to A β toxicity and reduces mitochondrial respiration and oxidative stress⁵⁸⁴. Previous proteomic studies have also revealed that enzymes involved in energy metabolism show altered oxidative modification in the AD brain⁵⁸⁵. A recent study has also shown a number of proteins significantly oxidised in the Down syndrome brain with and without AD pathology⁵⁸⁶. A significant number of proteins involved in energy metabolism were identified including some of the glycolysis enzymes which we found altered in this study.

We also report an increase in the protein expression of the enzyme transketolase in microglial cells in response to human AD plasma. Transketolase is a thiamine-dependent enzyme which catalyses the first reaction in the pentose phosphate pathway. Transketolase alterations have been previously identified in (i) several probable AD patients regardless of age-of-onset and severity of disease; (ii) all early-onset AD patients and APOE ϵ 4/4 carriers; and (iii) nearly half of asymptomatic AD relatives⁵⁸⁷. Increased transketolase activity has been correlated with increased levels of BACE1, the key rate-limiting enzyme for the production of the A β peptide⁵⁸⁷.

Increased oxidative stress, mitochondrial dysfunction and alterations to energy metabolism have all been identified as early events in the pathogenesis of AD. Cellular models for AD display functional impairment of the mitochondrial respiratory chain, and a decrease in oxygen respiration and ATP production⁵⁸⁸. All functional measures highlight biogenetic impairment in AD cells and correlation with amyloid peptide accumulation⁵⁸⁸.

Factors which induce the upregulation of glycolysis in glial cells treated with AD plasma remain unclear. However, aerobic glycolysis has been correlated spatially with amyloid deposition in AD brains⁵⁷⁶. Furthermore, elevated levels of the enzymes pyruvate dehydrogenase kinase and lactate dehydrogenase provide resistance to amyloid and other neurotoxins⁵⁸⁴. The ability of the brain to maintain expression of these enzymes involved in mitochondrial energy metabolism may explain why some individuals show high levels of amyloid deposition without neurodegeneration^{584,589-591}. In our study, the indicators of increased glycolysis in microglia may be a compensatory response to the loss of cell viability and mitochondrial function following exposure to AD plasma, very possibly triggered by complement and/or other inflammatory factors. Altered activities of key glycolytic enzymes have been found in hippocampal, frontal and temporal cortex of AD brains and thought to possibly be due to the astrogliosis that occurs in AD⁵⁸¹.

A number of chaperone proteins such as protein disulfide isomerases were found to be downregulated in cells treated with MCI and AD plasma. Protein disulfide isomerases can inhibit the aggregation of misfolded proteins and are also involved in modulating apoptosis and endoplasmic reticulum redox balance⁵⁹². It has been shown that the proinflammatory activation of microglia suppresses mitochondrial function and increases glycolysis and overexpression of the mitochondrial chaperone mortalin can attenuate this effect⁵⁹³. Heat shock proteins are chaperone proteins which have an important impact on the proteotoxic effects of tau and A β accumulation. Immunohistochemical studies and expression analyses in AD brain tissue have shown that expression levels of a number of heat shock proteins are upregulated and it has been hypothesised that this effect may be due to a hybridisation of activated glia and dysregulated/stressed neurons^{594,595}. Dysregulated chaperone proteins in

the cells in our study may reflect a homeostatic attempt to clear toxic plasma proteins and protect mitochondrial function. Some chaperone proteins such as heat shock proteins were upregulated whereas other chaperones, such as several protein disulphide isomerase (PDI) isoforms were found to be downregulated. It is known that HSP90α expression is induced when a cell experiences proteotoxic stress. Since it, and several other HSPs, are upregulated, in the iTRAQ results, it could be inferred that it is a homeostatic response to such stress induced by the addition of AD/MCI plasma. So perhaps it is not just complement, but also proteotoxicity of the AD plasma which is inducing the proteomic changes in the glia. It has been shown that PDIs can be anti-apoptotic, but they can also have toxic effects, particularly when nitrosylated, in which case they are associated with protein misfolding⁵⁹⁶⁻⁵⁹⁸.

Therefore, in a high oxidative stress environment it may be advantageous to downregulate PDI expression to minimise the potential unwanted side effects of exacerbated proteotoxicity. There is evidence from the proteomic data that oxidative stress is indeed at play, because several peroxidases are upregulated. Therefore the dual oxidoreductase and chaperone roles of PDI may not always act synergistically.

Cytoskeletal proteins are another group of proteins with altered expression level identified in our iTRAQ proteomics data (Table 4.5). Nestin expression is seen during pathological situations and is a marker of cell proliferation and is reduced in the cells treated with AD plasma, supporting our MTT data (Table 4.1 and Figure 4.1). Ezrin and moesin are involved in crosslinking actin filaments with plasma membranes and stabilising microtubules respectively^{599,600} and both were found to be upregulated in cells treated with AD plasma. The antioxidant proteins peroxiredoxins were also found to be elevated in cells exposed to AD plasma which may be another indication of a compensatory mechanism triggered to attenuate the toxic effects of AD plasma.

In conclusion, this study shows that plasma expression levels of acute phase proteins are altered in AD and MCI, supporting a role for increased inflammatory activity in this disease which is detectable in the plasma. Cells exposed to AD plasma show an upregulation of glycolysis possibly as a compensatory mechanism in response to compromised mitochondrial function. Together our observations support an emerging body of evidence that inflammation and metabolism are closely linked processes, which are regulated by transcriptional and

protein translation events^{601,602}. In the CNS, complement proteins are synthesised by a variety of cells including neurons, microglia, astrocytes, oligodendrocytes and endothelial cells⁶⁰³. Since disruptions in the blood-brain-barrier have been reported in AD there is a possible source of increased complement levels in the AD brain from plasma. It is however likely that there may be other thermolabile factors in disease plasma which facilitate the cytotoxic and glycolytic effects in microglia, one example may be micro RNAs as they are emerging as important factors in neurogenesis, synaptic plasticity and AD^{604,605}. Other yet to be characterised substances may also make a significant contribution. This study shows that the use of biological assays in combination with proteomic analysis may help uncover possible mechanisms of disease and may be complementary techniques to validate cellular changes and effects in a range of biological samples.

Chapter 5

Effects of Polyphenols on Cell Viability, Mitochondrial Dysfunction, and Amyloid Aggregation

Introduction

Alzheimer's disease is a multifactorial neurodegenerative condition with a complex pathology including oxidative stress, metal deposition, formation of aggregates of amyloid and tau and enhanced inflammatory responses⁶⁰⁶. Drugs targeted toward reduction of amyloid load have been identified, and some have been trialed^{607,608}, but there is no effective pharmacological treatment for combating the disease so far. Early intervention, or preventative measures targeting risk factors may be a better approach than treatment once the disease and neuronal death have substantially progressed. Attempts at disease reversal are likely to be both more challenging and have less certain outcomes than bypassing or at least decelerating disease progression. However this approach requires early intervention, well before substantial neuronal damage, and ideally at preclinical stages. Such intervention is likely to be most efficacious if sustained over a long period of time, and should therefore carry no or low risk of side effects. Consequently natural products may be an important potential avenue for disease intervention. Many are components of foods or indigenous medicines which have been used in human communities for aeons, and therefore substantial knowledge is available about safety or potential side effects (in a sense a natural clinical trial). Furthermore such natural substances can be selected to target multiple risk factors and pathways dysregulated in AD, such as oxidative stress, metal ion accumulation, and most importantly the hallmark protein aggregates which define the disease. AD is characterized by the progressive loss of cholinergic neurons in the cortex and hippocampus along with global cognitive decline and by the accumulation A β deposits in the form of extracellular senile plaques⁶⁰⁹. A β is produced by the aberrant cleavage of APP, by the sequential action of β - and γ -secretases, that gives rise to a 39–42 amino acid residue polypeptide which is part of the α -helical transmembrane segment of APP⁶⁰⁹. A β released extracellularly after the catalytic activity of secretases, undergoes conformational modifications and becomes prone to aggregation⁶⁰⁹. The mechanisms by which the self-assembly of A β 1-42 leads to toxicity, are not well understood. This is because all transient intermediates and oligomers preceding fibrils comprise a very large number of conformations. A β aggregates can exist in multiple forms, from soluble oligomers or protofibrils to insoluble large fibrils, which are responsible for various pathological effects⁶¹⁰. Amyloid fibrils range in size from nanometers to microns and are composed of aggregated peptide β -sheets formed from parallel or anti-parallel alignments of peptide β -strands⁶¹⁰. The fibrillogenesis process proceeds with the deposition of oligomers into

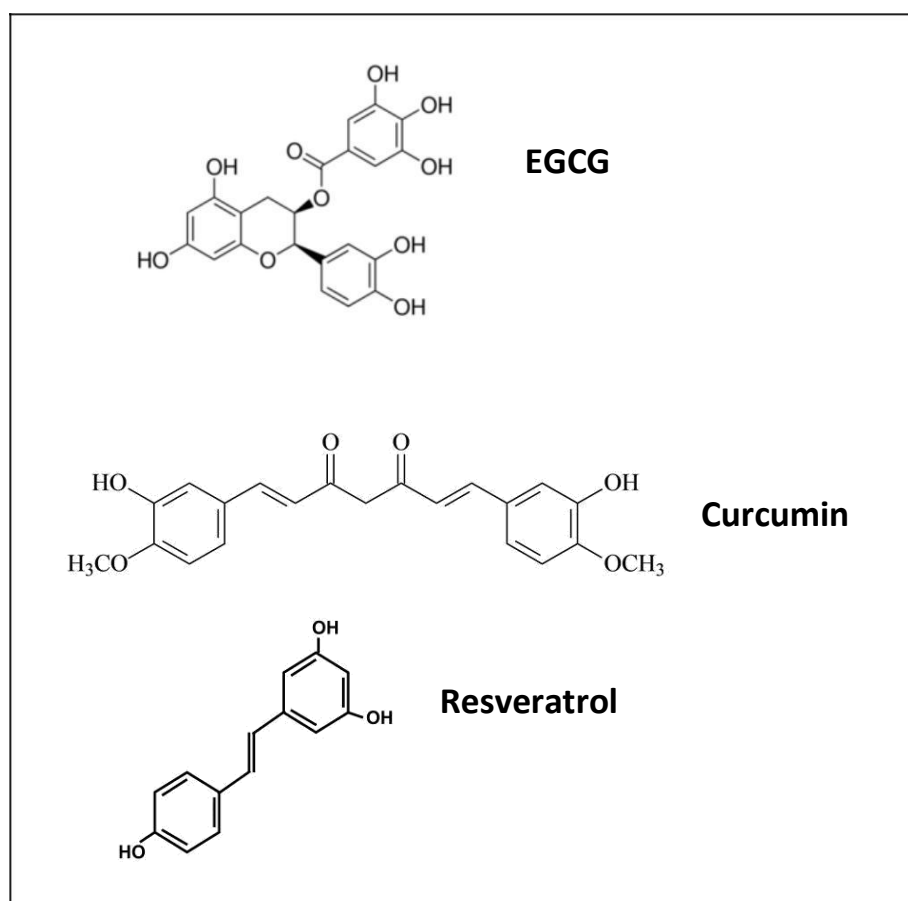
protofibrils, characterized by a 2–5 nm diameter observed by electron microscopy, and then in protofilaments or fibrillar aggregates larger in size (7–13 nm wide up to 30 nm)⁶¹⁰. At present, the biological role of different aggregation states of A β protein remains unclear. Indeed, whether the accumulation of these large fibrils is the cause or rather the consequence of the disease remains to be elucidated. It is noteworthy that numerous inherited forms of AD display mutations of the APP gene that increases susceptibility to β - and γ -secretase cleavage and the aggregation properties of A β , unequivocally linking the production of A β to the disease⁶¹¹. Moreover, several studies using a variety of cellular and animal models have shown that A β neuronal toxicity may depend on soluble oligomeric fractions rather than on mature fibrils⁶¹²⁻⁶¹⁴. Therefore, preventing oligomer formation is an attractive approach as a potential treatment for preventing or delaying the onset of sporadic and familial AD.

Mitochondria, which are abundant in synapses and neurons, are a target site for amyloid oligomer complexes. Mitochondria are critical regulators of neuronal survival and death, and there is strong evidence that mitochondrial dysfunction might represent an important initiator of the pathophysiological cascade in AD⁸⁵. Mitochondria are important targets of the A β peptide, and disturbances of membranes and bioenergetics may be key triggers of neuritic damage leading to dementia⁶¹⁵. Recognised mitochondrial targets of A β include the translocase import machinery, enzymes involved in the Krebs cycle, respiratory chain enzymes, the mitochondrial permeability transition pore (mPTP), the mitochondrial matrix protein A β -binding alcohol dehydrogenase (ABAD), and mitochondrial DNA⁶¹⁵⁻⁶¹⁷.

Polyphenols are the most abundant micronutrients of our daily food, occupying the major portion of naturally occurring phytochemicals in plants⁶¹⁸. They are produced in plants as a protective response to various stress stimuli, including bacterial and viral infections, and UV-light⁶¹⁸. They are well known for their antioxidant capacity and the ability to scavenge the free radicals formed during pathological processes such as cancer, cardiovascular diseases and neurodegenerative disorders⁶¹⁸. Dietary intake of polyphenols is known to attenuate the progression of AD by showing strong potential to tackle the alterations and reduce the risk of AD⁶¹⁹. A number of polyphenolic compounds showing promising results against AD pathologies have been identified⁶¹⁹. Recent research is unravelling novel molecular mechanisms and elucidating specific interactions of polyphenols with their targets in a variety of pathways involved in neurodegeneration.

Numerous polyphenols from natural products such as turmeric, grapes, red wine and green tea, have been reported to inhibit A β aggregation and toxicity and show promise *in vivo*, including epigallocatechin gallate (EGCG), curcumin and resveratrol^{183,190,620-626}. The major tea polyphenol, EGCG, shows neuroprotective activity against neurological disorders, and inhibits toxicity induced by A β and α -synuclein oligomers¹⁸³. Moreover, using isothermal titration calorimetry at different EGCG and salt concentrations, it has been shown that the interactions between A β 1-42 and EGCG are mainly hydrogen bonds in the region 1–16 and hydrophobic in the region 17–42^{621,627}. Experimentally, EGCG has been reported to generate unstructured, off-pathway A β 1-42 oligomers, and by this means offsets formation of the structured toxic forms⁶²⁰.

Figure 5.1: Chemical structures of the polyphenols EGCG, Curcumin and Resveratrol



Polyphenols exhibit remarkable antioxidant and anti-inflammatory activities that may exert a leading role in reducing age-related oxidative stress and inflammation, thereby hampering the

onset and progression of degenerative diseases. Oxidative stress is a key hallmark in AD. It occurs early in disease pathogenesis and can exacerbate its progression²⁶. Several causes of oxidative stress have been determined, which point to both mitochondrial dysfunction and neuroinflammation⁵⁰. Based on these observations, various neuroprotective strategies against reactive oxygen species-mediated damage have been proposed for the treatment of AD. Epidemiological studies have suggested associations between lack of consumption of phenolic-rich foods or beverages and various diseases, such as stroke, cardiovascular diseases, cancer, and neurodegenerative diseases^{618,628}. Conversely polyphenolic and flavenoid rich diets (such as the Mediterranean diet) have documented health benefits^{618,628}. For example, cognitive performance in elderly subjects is associated with the consumption of polyphenol-rich foods such as chocolate, red wine, and tea⁶²⁸⁻⁶³². As a modifiable lifestyle factor, diet is an important target, since (1) the benefits of calorie restriction on longevity have been well documented^{322,325,633}, and (2) the disease preventive benefits of specific dietary nutrients, such as the multitude of polyphenolic constituents, are emerging. Therefore a diet with a high polyphenolic/calorie ratio is likely to be both disease preventative and longevity promoting.

A very important feature of polyphenols is their multiple modes of action. Firstly, their well known antioxidant capacity may counteract oxidative stress induced by A β , thus hampering neurodegeneration and blunting the self-propagating effect of the vicious cycle between A β generation and oxidative stress^{634,635}. Secondly, these compounds may competitively interact with aromatic residues in amyloidogenic proteins and block the self-assembly process⁶³⁵. Furthermore, they may modulate A β production by stimulating the α -secretase pathway and inhibiting the β -and γ -secretase pathways⁶³⁵. Some phenolics show a strong enzymatic inhibition of the cascade of A β generation and other phenolics show a much pronounced physico-chemical effect against amyloid aggregation and fibrillogenesis. Polyphenols also have metal chelating properties⁶³⁶. Copper, iron or zinc are present in A β deposits and induce the production of hydrogen peroxide, which may mediate oxidative damage in AD^{77,128}. Therefore another therapeutic approach for preventing AD pathogenesis may be linked to metal chelation. These important chemical characteristics of polyphenols might be harnessed to ameliorate multiple pathological processes and pathways and prevent or postpone the onset of neurodegeneration.

EGCG is a member of a family of plant-derived flavan-3-ols, and is the major polyphenolic component of green tea¹⁸³. EGCG directly binds to natively unfolded A β , reduces thioflavin T fluorescence, and promotes the assembly of large, spherical oligomers which seem to be off-pathway species (non-toxic or low toxicity variants), as they are unable to seed fibrillogenesis⁶²⁰. Importantly, EGCG-stabilized oligomers are not toxic to cells, and are not recognized by the A11 antibody, which binds to pathologically relevant high-molecular weight oligomers formed by numerous amyloid peptides⁶²⁰. It has also been demonstrated that EGCG is able to remodel A β mature fibrils into smaller, amorphous protein aggregates that are nontoxic to mammalian cells, by direct binding to the β -sheet-rich aggregates and mediating a conformational change without generating potentially toxic monomers or oligomers^{606,637}. Notably, *in vivo* administration of EGCG improves spatial cognition in rats and reduces A β levels and plaque by as much as 50% in Tg2576 transgenic mice^{186,196,638}. This effect may be due to its ability to counteract A β fibrillogenesis.

Curcumin is the main constituent of the spice turmeric, whose extensive use is thought to account for the significantly lower prevalence of AD in the Indian population⁶³⁹. *In vitro* studies have shown that curcumin can inhibit fibril formation and destabilizes preformed fibrils⁶⁴⁰. Curcumin also binds to plaques and reduces amyloid levels *in vivo*⁶²⁴. The ability of curcumin to bind A β and to inhibit its aggregation is due to its biphenolic structure that mimics congo red. Curcumin comprises three structural features: a hydroxyl substitution on the aromatic endgroup, a rigid linker region between 8 and 16 Å in length, and a second terminal phenyl group⁶⁰⁶. *In vitro* studies have revealed that curcumin can only bind to the fibrillar conformer of A β , and not to shorter, aggregation-incompetent A β fragments⁶⁰⁶. Tg2576 transgenic mice fed with curcumin for six months showed decreased levels of A β and inflammatory cytokines in the brain⁶²⁴. The ability of curcumin to cross the blood–brain barrier, to bind to A β and to induce rapid dissolution of plaques was verified using multi-photon microscopy in APPsw/PS1dE9 mice⁶⁴¹. Furthermore, curcumin was found to reduce the levels of interleukin-1 β and isoprostanes (an index of oxidative stress) in the central nervous system and ameliorated amyloid plaque burden in transgenic mice¹⁹⁰.

Resveratrol is a stilbene polyphenol which holds great promise as a therapeutic agent. Many studies have demonstrated its beneficial effects, though some doubts still remain regarding its clinical efficacy^{202,642,643}. Epidemiological studies have suggested that moderate red wine consumption may protect against the development of AD and other studies have revealed that

certain components of red wine, including resveratrol, reduce A β production and toxicity by a number of different mechanisms^{202,626,644}. Recent studies on the effects of grape seed polyphenolic extracts revealed that these compounds prevent β -structural transitions, thereby reducing formation of oligomers and protofibrils, and attenuate A β -induced cellular toxicity⁶⁰⁶.

In this chapter, we explored the ability of three common polyphenols to prevent the neurotoxicity caused by amyloid and Fenton chemistry on astrocytes using a brain cell model for oxidative stress and amyloid toxicity. We also investigated the effects of polyphenol treatment on amyloid aggregation and the metal chelating properties of these compounds using electron microscopy and mass spectrometry respectively.

5.2 Methods

5.2.1 Preparation of A β peptides

Recombinant A β (1-42) peptides were reconstituted in HFIP, vortexed, aliquoted and the HFIP evaporated in a fume hood. The resulting peptide films were dried under vacuum in a Speed Vac for 2 hours and the desiccated peptides stored at -20 degrees until use. 5 μ M concentration of peptides were resuspended in neat DMSO followed by bath sonication for 10 minutes and stored at -20°C freezer until required. 10mM HCL was added to peptides and samples incubated at 37°C for 48 hours to initiate fibril formation for TEM experiments. For cell culture experiments soluble aliquots were added to cells and incubated for at 37°C for 48 hours to initiate fibril formation.

5.2.2 Cell Culture

U251 cells are a human astroglial cell line obtained from embryonic fetal human astrocytes following viral transformation^{518,519} and were a generous gift of Prof Gilles Guillemain (Macquarie University, Sydney, Australia). These cells express antigens present on adult human astrocytes, secrete pro-inflammatory cytokines upon activation, exhibit properties of primary human astrocytes and have been successfully used as a model of microglial activation by others^{518,520}. Cells were maintained in RPMI1640 cell culture medium, supplemented with 10% heat inactivated foetal bovine serum, 2 mM l-glutamine, and 1%

penicillin/streptomycin, at 37°C in a humidified atmosphere containing 95% air/5% CO₂. Before experimentation, cells were seeded into 24 or 96 well culture plates to a density of approximately 1x10⁴ or 2x10³ cells respectively.

5.2.3 MTT Cell Proliferation Assay

In actively proliferating cells, an increase in 3-[4,5-dimethylthiazol-2-yl]-2,5-diphenyl tetrazolium bromide (MTT) conversion in cells relative to controls represents an increase in cellular proliferative activity. Conversely, in cells that are undergoing apoptosis, MTT conversion, and thus biological activity, decreases. Cell proliferation was analysed using established protocols in a 96 well plate format⁶⁴⁵. Briefly MTT substrate was prepared at a final concentration of 0.5mg/ml, added to cells in culture and incubated for 2 hours. The quantity of formazan (proportional to the number of viable cells) is measured by recording changes in absorbance at 570 nm using a Amersham Biosciences Biotrak II plate reading spectrophotometer (Buckinghamshire, UK). When cells die, they lose the ability to convert MTT into formazan, thus color formation serves as a useful and convenient marker of only the viable cells. The formazan product of the MTT tetrazolium accumulates as an insoluble precipitate inside cells as well as being deposited near the cell surface and in the culture medium. Acidified isopropanol was added to all wells prior to obtaining absorbance readings to solubilize the formazan product, stabilize the color, avoid evaporation, and reduce interference by phenol red and other culture medium components.

5.2.4 XF24 Microplate-Based Respirometry as a Measure of Mitochondrial Function

A mitochondrial function assay was used to determine the effect of selected polyphenols on oxygen consumption rates (OCRs; an indicator of mitochondrial respiration) and extracellular acidification rates (ECARs; a measure of glycolytic flux) following co-treatment with redox active metals and/or aggregated A β in the microglial cell line. The Seahorse XF24, extracellular flux analyzer (Seahorse Bioscience, North Billerica, MA, USA) was employed and assays performed as previously described⁵²⁸⁻⁵³⁰. Briefly, culture plates were incubated in a CO₂-free incubator at 37°C for 1 hr to equilibrate temperature and pH. The microplate was then loaded into the XF24 and further incubated for 15 min with 3 min and 2 min wait cycles before commencement of the assay. After determination of the basal respiration in the cell

culture, oligomycin (2 μ M), carbonylcyanide-p-trifluoromethoxy-phenylhydrazone (FCCP, 500 nM), and antimycin (3 μ M) were sequentially added and the OCRs and ECARs for each culture well were quantified for 2 minutes. This allowed the basal control ratio (BCR) and the uncoupling ratio (UCR) to be determined as previously described⁵³¹. Essentially, the BCR is a measure of how close the basal level of respiration is to the maximum level of respiration. The closer this ratio is to 1, the greater the mitochondrial malfunction. The UCR is a measurement of mitochondrial functional integrity and measures the ratio of uncoupled to physiologically normal respiration levels. The greater the maximum level of respiration, the greater the mitochondrial functional integrity.

5.2.5 Transmission Electron Microscopy

An aliquot (5 μ l) of A β and polyphenol samples were spotted onto copper mesh electron microscopy grids (Sigma-Aldrich, USA) for 1min and blot dried. The grids were subsequently stained using 5 μ l of 2% uranyl acetate for 1min followed by blot drying. Samples were imaged using a Hitachi JEOL 1400 transmission electron microscope, which operates at accelerating voltages up to 120kV. The microscope is equipped with a high contrast lens configuration especially suited to imaging biological, medical or polymer specimens that lack electron density and inherent contrast. Specimens undergo preparation procedures to ensure they are 100 nm or thinner in order to transmit the electron beam. Dense regions within the specimen cause electrons to scatter and an aperture, positioned near the specimen in the electron column, prevents the scattered electrons from reaching the imaging plane. This results in light and dark regions or ‘contrast’ within the TEM image. The microscope is equipped with a Gatan digital camera and Digital Micrograph software to facilitate acquisition of digital images.

5.2.6 Polyphenol Metal Complexes using Mass Spectrometry

Polyphenol:metal samples (0.5mg/ml:1mg/ml ratio) using copper (II) sulphate and iron (II) sulphate were prepared in methanol and run on an Orbitrap LTQ XL (Thermo Fisher Scientific, San Jose Ca, USA) ion trap mass spectrometer using a nanospray (nano-electrospray) ionization source to generate ions from the analyte in solution. The instrument was calibrated with the manufacturer’s standard calibration solution on the day of analysis

using direct infusion into the ESI source. The instrument conditions were optimized for sensitivity of the compounds using the XCalibur LC tune software. The analysis was carried out in positive ion mode using the orbitrap FTMS analyser at a resolution of 60000. Samples (5µL of 1mg/ml polyphenol in methanol) were transferred into a conductive glass needle and inserted into the nanospray source. Ions generated were measured over a 150 to 2000 Da mass range. Data was acquired in full scan mode over 30 seconds and visualised using the Qual Browser feature in Xcaliber 2.1 (Thermo Fisher Scientific, San Jose, Ca, USA).

5.3 Results

5.3.1 Effect of Aggregation on Cell Viability in Astrocytes

Treatment of astroglial cultures with 5µM of fresh soluble amyloid followed by 48hr incubation at 37^oC (to initiate aggregation) caused a significant drop in cell proliferation. This was prevented by co-incubation with EGCG (Figure 5.2). A further drop was seen with the addition of transition metals iron and copper in which a ~50% drop in cell viability was observed relative to controls. Again EGCG was shown to prevent the toxicity caused by the addition of these metals and amyloid (Figure 5.2). Curcumin and resveratrol did not significantly prevent the toxicity caused by amyloid alone but were shown to significantly prevent the toxic effects of metal addition to amyloid in the same astroglial model (Figures 5.3 and 5.4).

Figure 5.2: Effect of amyloid, metal ion and EGCG treatment on astrocyte viability. 5 μ M A β 42 and/or 5 μ M metals were used for all treatments *p<0.05 vs Control, **p<0.05 vs A β 42 + 5 μ M Fe/Cu, n=6.

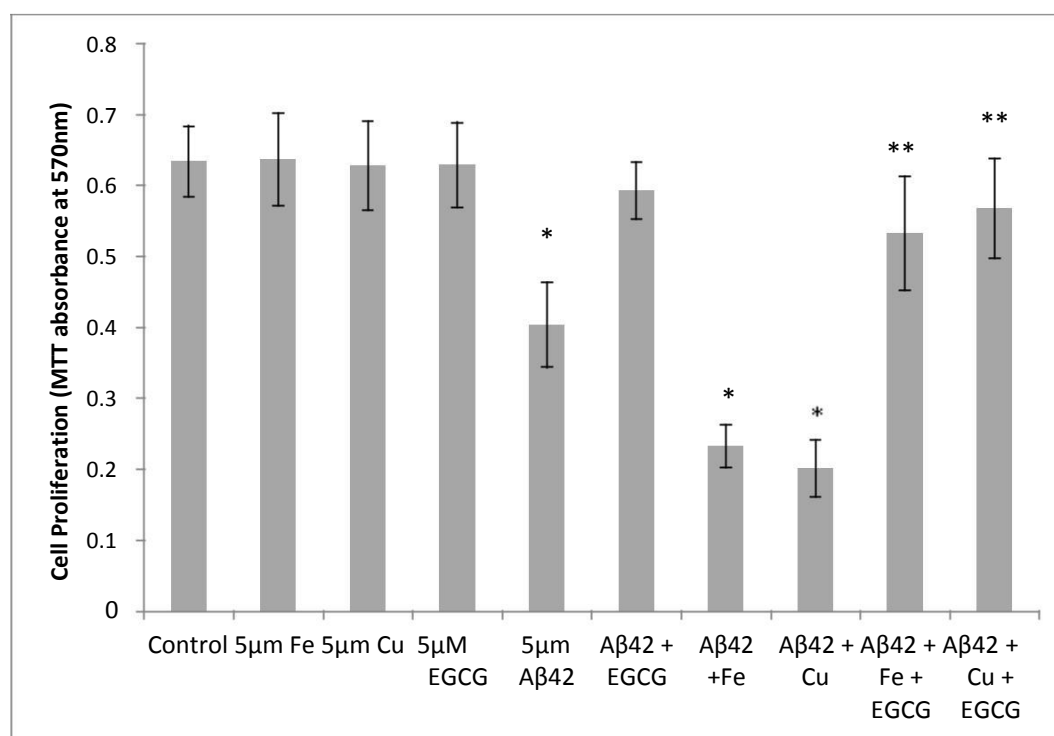


Figure 5.3: Effect of amyloid, metal ion and curcumin treatment on astrocyte viability. 5 μ M A β 42 and/or 5 μ M metals were used for all treatments *p<0.05 vs Control, **p<0.05 vs 5 μ M A β 42 + 5 μ M Fe/Cu, n=6.

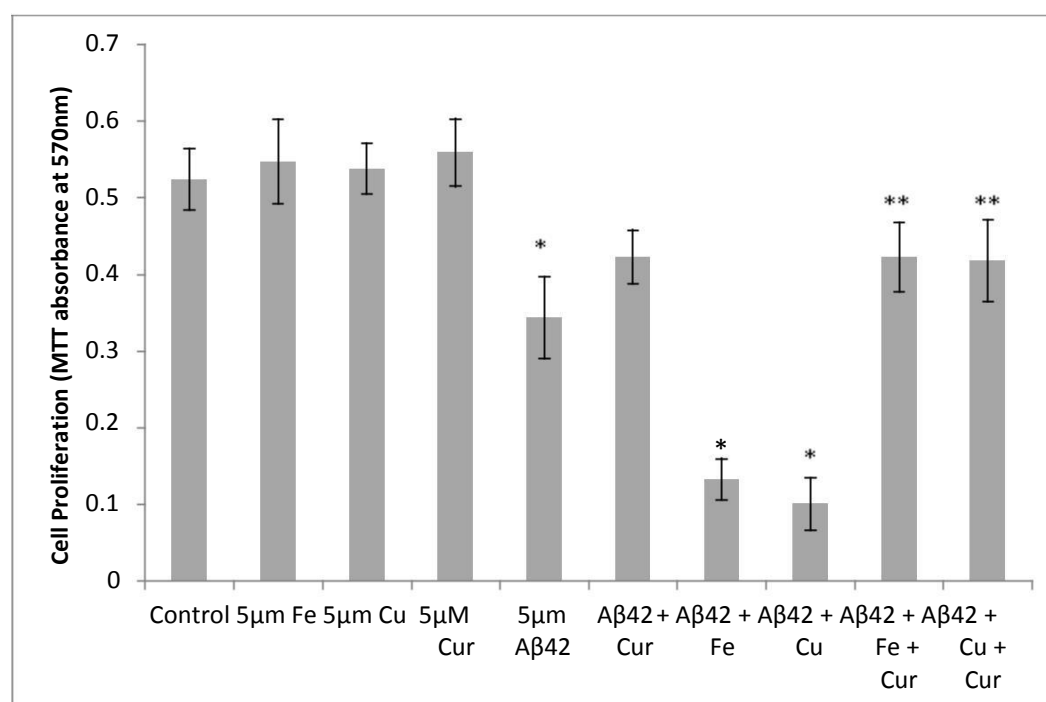
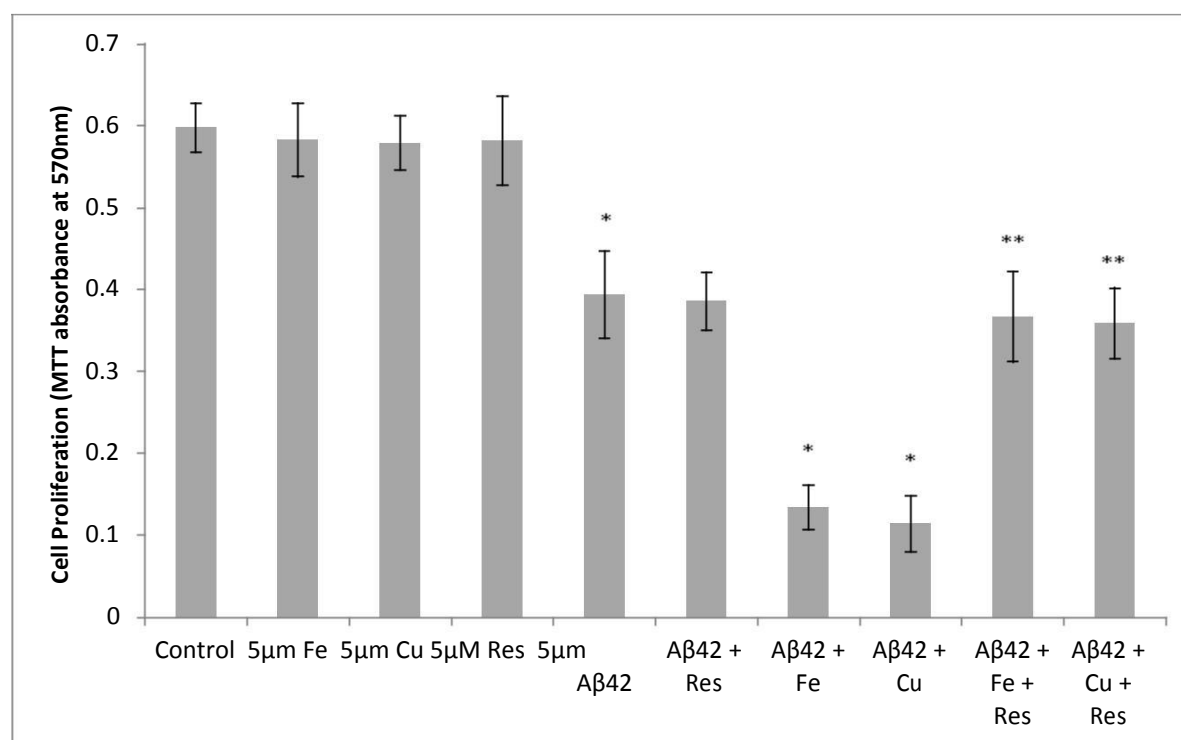


Figure 5.4: Effect of amyloid, metal ion and resveratrol treatment on astrocyte viability. 5µM Aβ42 and/or 5 µM metals were used for all treatments *p<0.05 vs Control, **p<0.05 vs 5µM Aβ42 + 5µM Fe/Cu, n=6.



Effect of Polyphenols on Oxidative Stress in Astrocytes

Oxidative stress was modelled in an astrocyte cell line by the addition of hydrogen peroxide (H₂O₂), iron and copper, followed by 24hr incubation at 37°C. The resulting initiation of Fenton chemistry caused a drop in cell proliferation by approximately 75%. All three polyphenols were found to be effective in preventing this toxicity in a dose dependent fashion with 50uM concentrations restoring neurons to control levels (Figures 5.5, 5.6 and 5.7).

Figure 5.5: Effect of EGCG to prevent cell toxicity caused by oxidative stressed initiated by Fenton chemistry (addition of H_2O_2 and Fe^{2+}/Cu^{2+} for 24hrs) to astroglial cells. * $p < 0.05$ vs Control, ** $p < 0.05$ vs $5\mu M A\beta_{42} + 5\mu M Fe/Cu$, $n=6$.

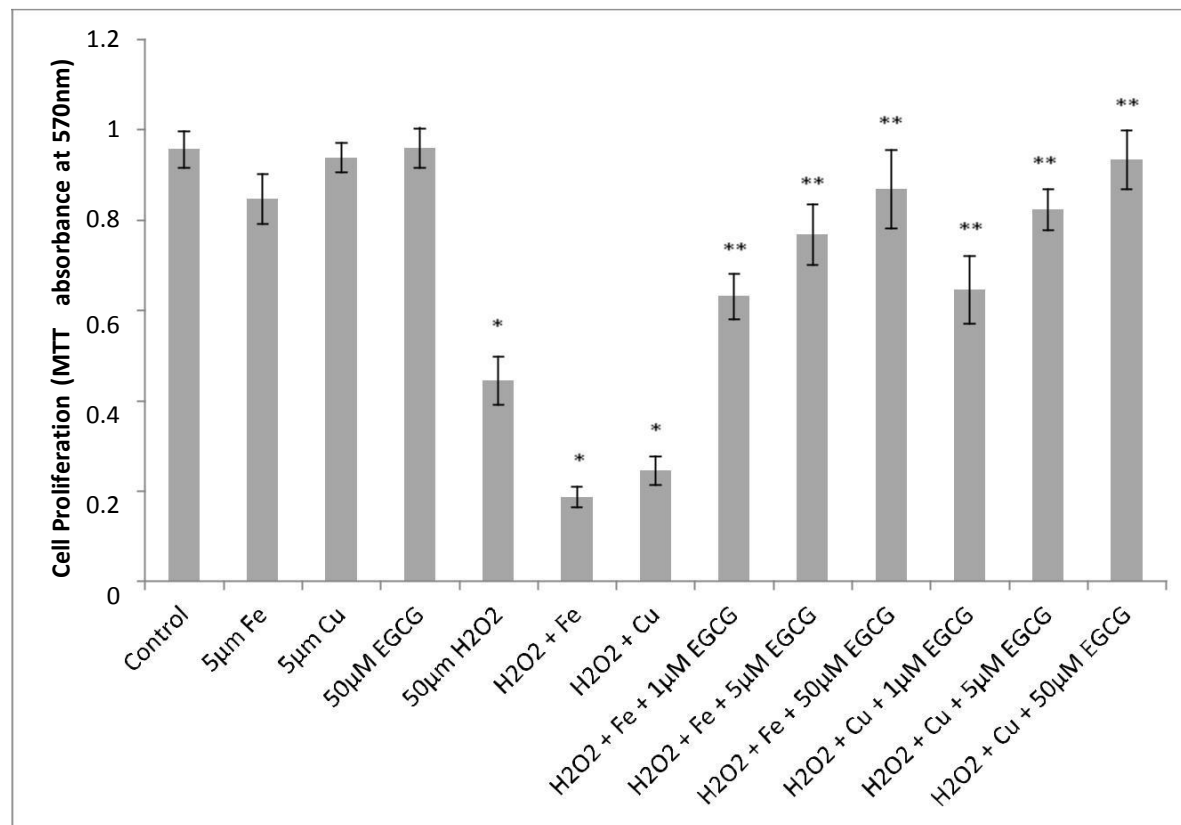


Figure 5.6: Effect of curcumin to prevent cell toxicity caused by oxidative stressed initiated by Fenton chemistry (addition of H_2O_2 and $\text{Fe}^{2+}/\text{Cu}^{2+}$ for 24hrs) to astroglial cells. * $p < 0.05$ vs Control, ** $p < 0.05$ vs $\text{A}\beta_{42} + \text{Fe}/\text{Cu}$, $n=6$.

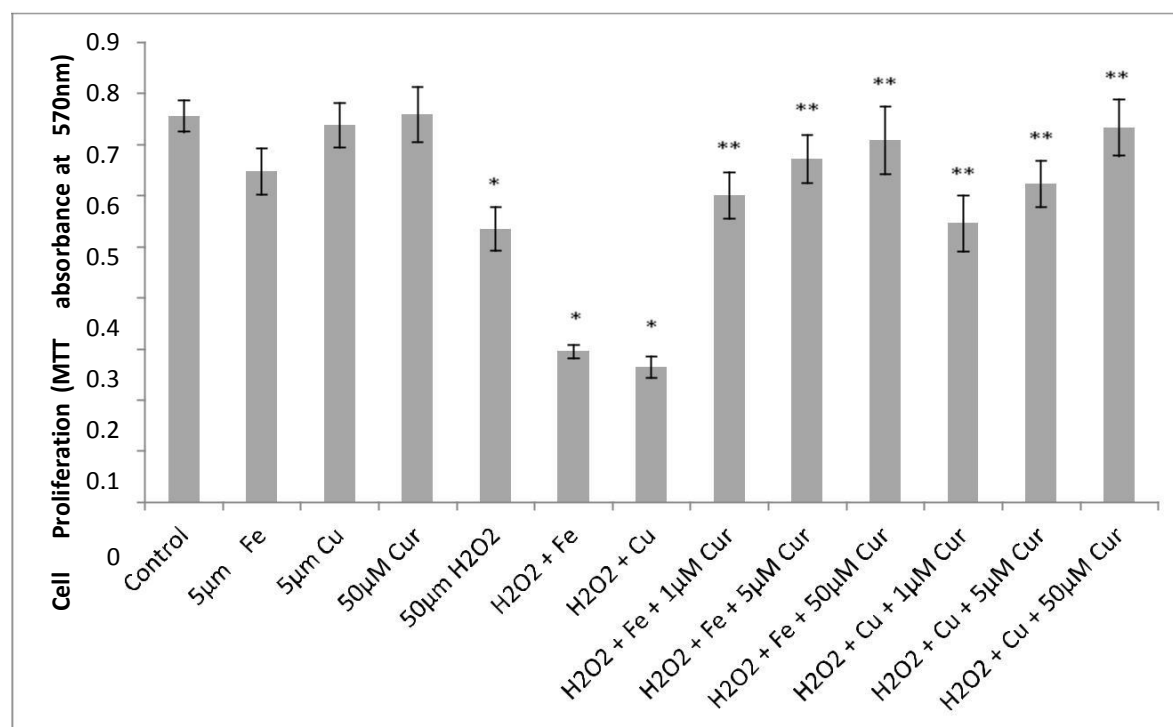
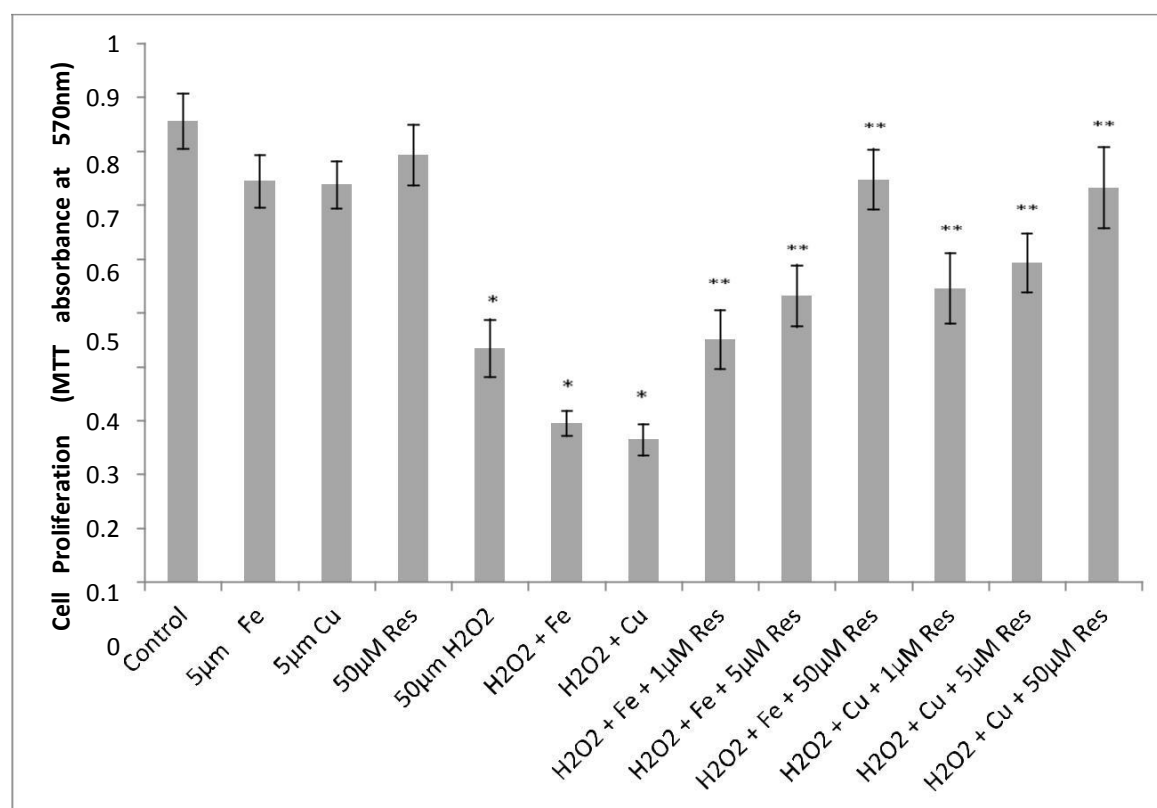


Figure 5.7: Effect of resveratrol to prevent cell toxicity caused by oxidative stressed initiated by Fenton chemistry (addition of H_2O_2 and $\text{Fe}^{2+}/\text{Cu}^{2+}$ for 24hrs) to astroglial cells. * $p < 0.05$ vs Control, ** $p < 0.05$ vs $\text{A}\beta 42 + \text{Fe}/\text{Cu}$, $n=6$.



Effect of Polyphenols on Mitochondrial Function in Astrocytes

Using the Seahorse XF24 assay, we observed a significant increase in basal control ratio (BCR), Figure 5.8 and a decline in uncoupling ratio (UCR), Figure 5.9, in astrocytes after 48 hr incubation with soluble A β 42 (resulting in aggregated A β 42, and in combination with iron, and copper, consistent with impaired mitochondrial function. Co-treatment with selected polyphenols attenuated mitochondrial function and restored the BCR and UCR to control levels.

Figure 5.8: Effect of amyloid, metal and polyphenol treatment on mitochondrial basal control ratio in cultured astrocytes. *p<0.05 vs Ctrl, **p<0.05 vs A β 42+Fe/Cu, n=3.

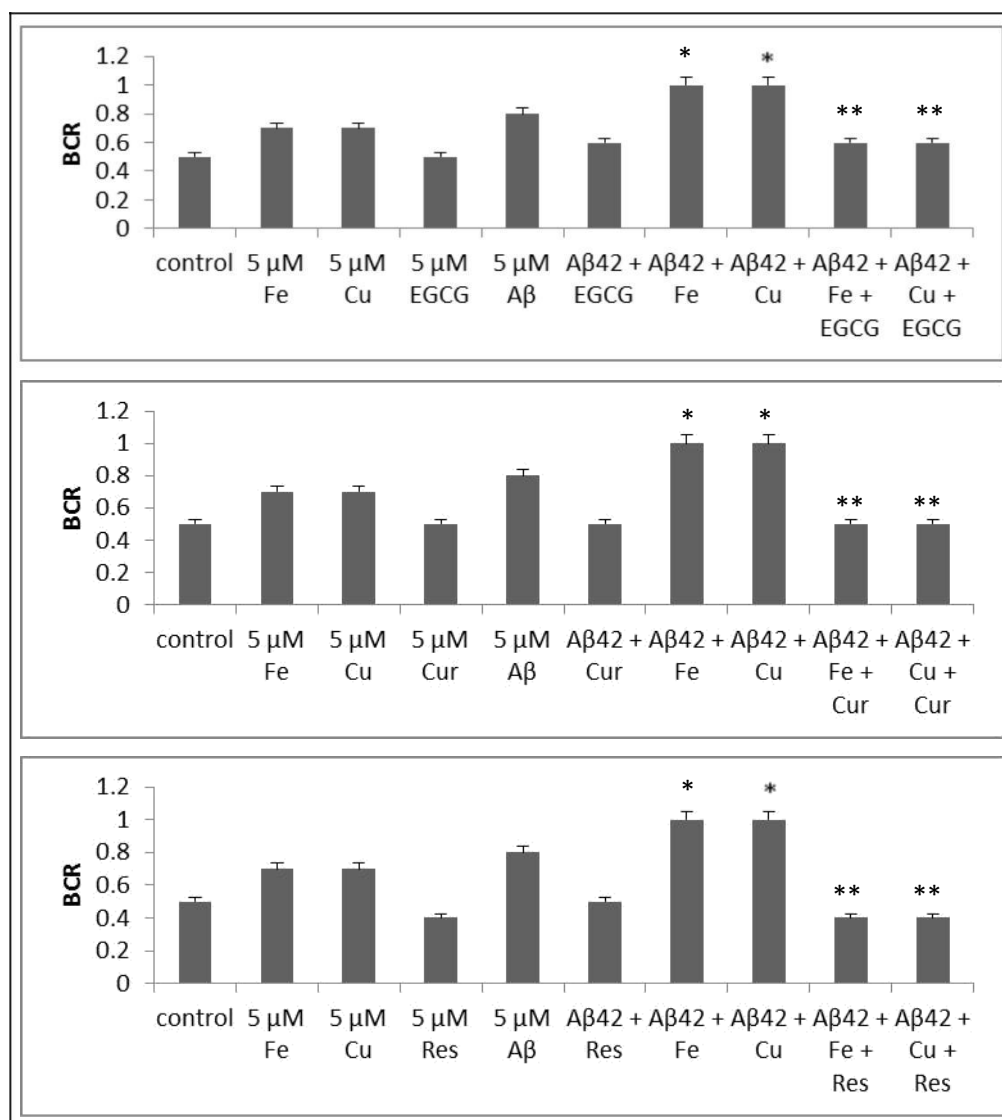
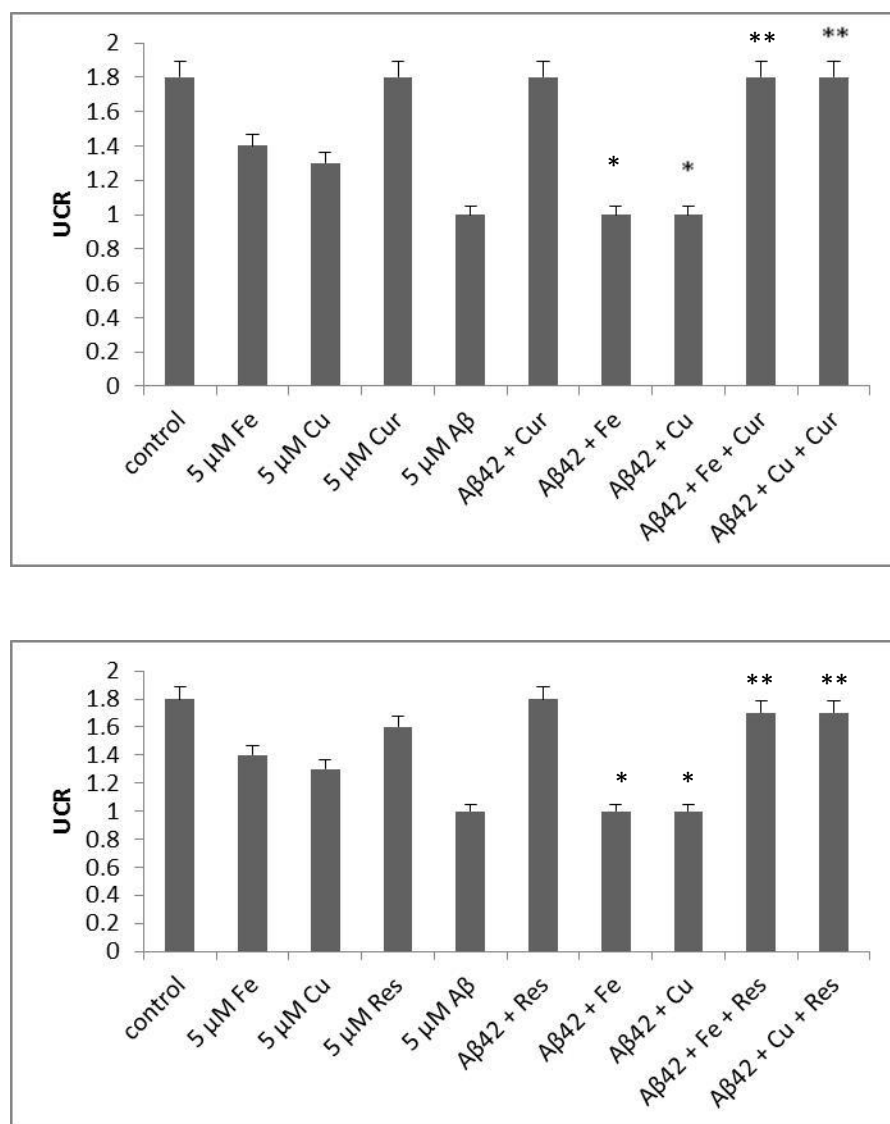


Figure 5.9: Effect of amyloid, metal and polyphenol treatment on mitochondrial uncoupling ratio in cultured astrocytes. * $p < 0.05$ vs Control, ** $p < 0.05$ vs A β 42+Fe/Cu, $n=3$.

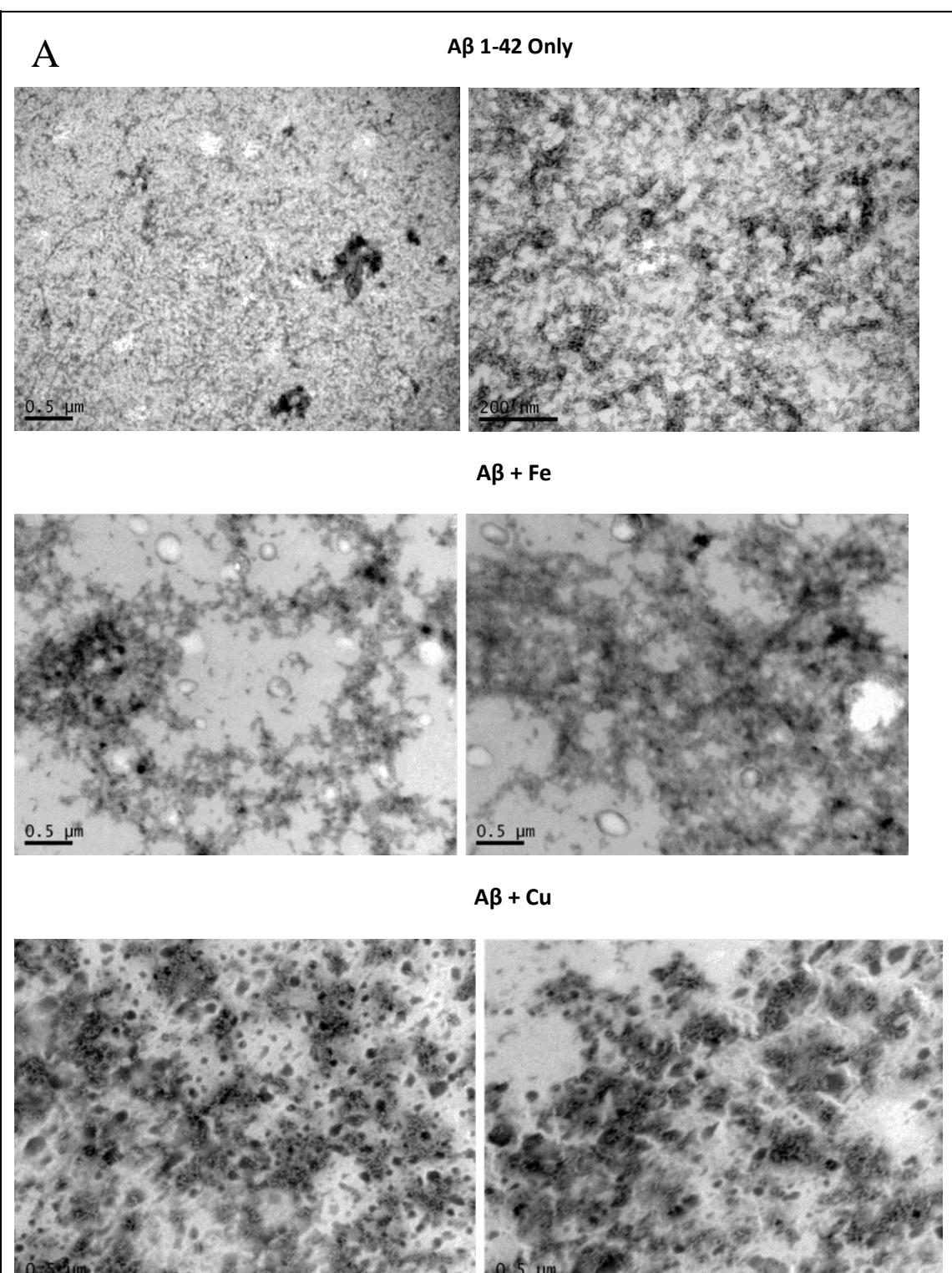


5.3.4 Amyloid Aggregation in the Presence of Polyphenols

Electron microscopy of amyloid samples co-incubated metals showed that both iron and copper enhanced aggregation of the peptide with iron seeming to be the more potent of the two (Figure 5.10). Addition of EGCG, curcumin and resveratrol created structures distinct from those formed in the presence of metal ions (Figure 5.10). Structures formed in the presence of amyloid peptide and of the polyphenolics with the addition of iron and copper to enhance aggregation, resembled those in amyloid peptide and polyphenolics alone more so

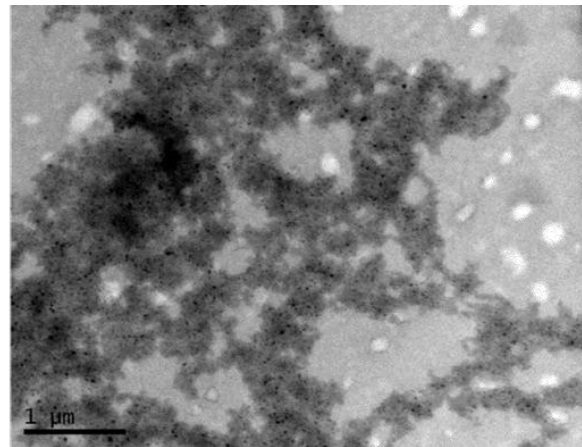
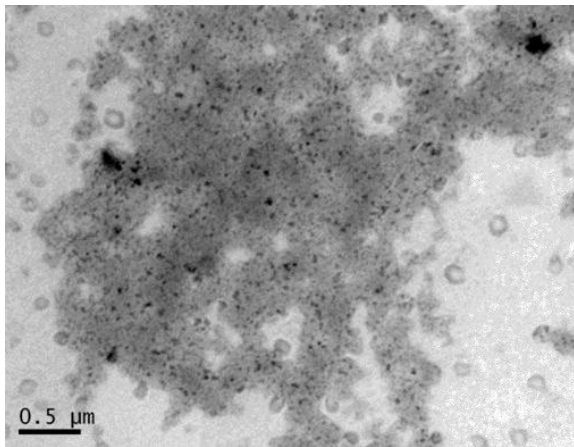
than those with amyloid peptide and metal ion alone (Figure 5.10). This was particularly true for the ECGC and curcumin samples.

Figure 5.10: Representative transmission electron microscopy images of soluble A β 42 after co-incubation with metals (Panel A) and polyphenols, EGCG (Panel B), Curcumin (Panel C) and Resveratrol (Panel D) for 48hrs at 37°C. A β 1-42 alone was shown to form some fibril clusters (Panel A), however in the presence of metal, more complex, larger fibril networks were observed (Panel A). Polyphenols both with and without metals were found to produce more pronounced dense amorphous aggregates with not much fibril structures found (Panel B-D).

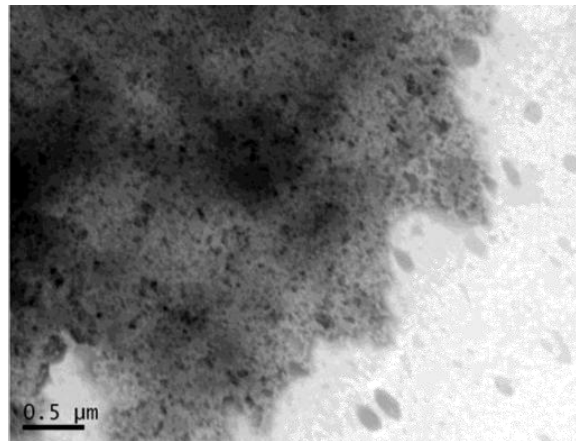
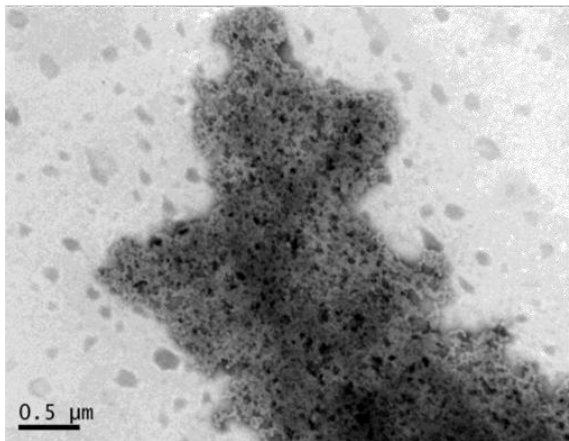


B

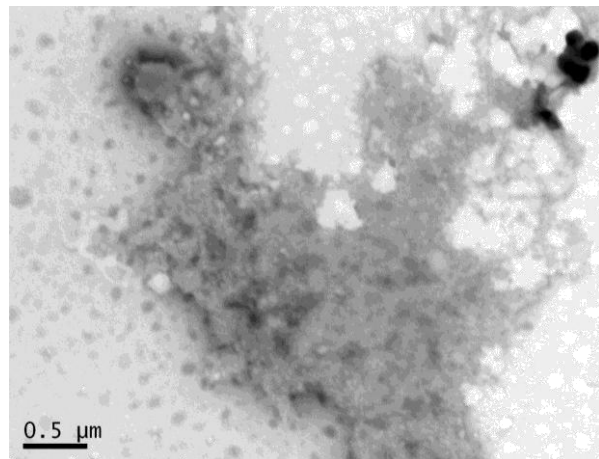
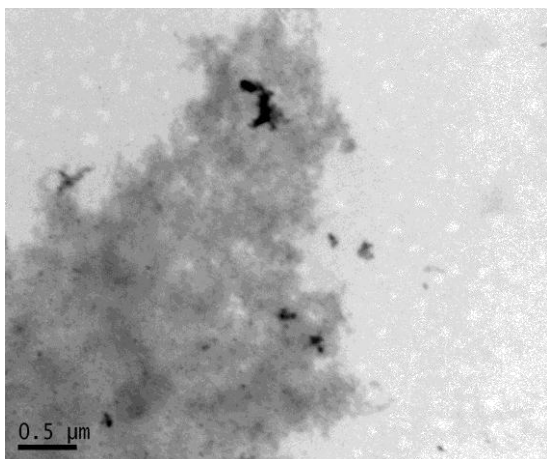
A β + EGCG



A β + Fe + EGCG

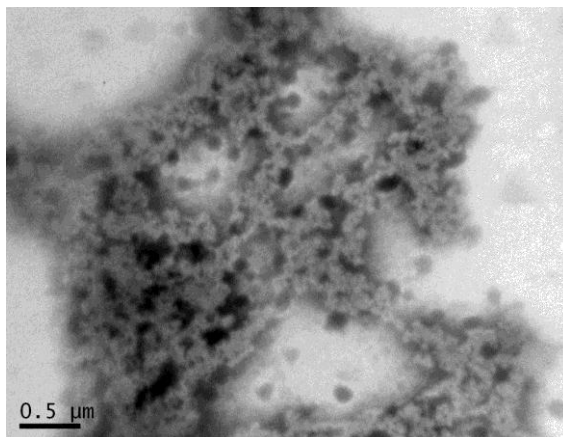
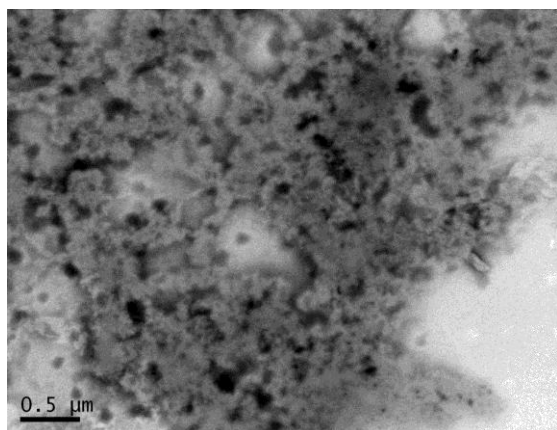


A β + Cu + EGCG

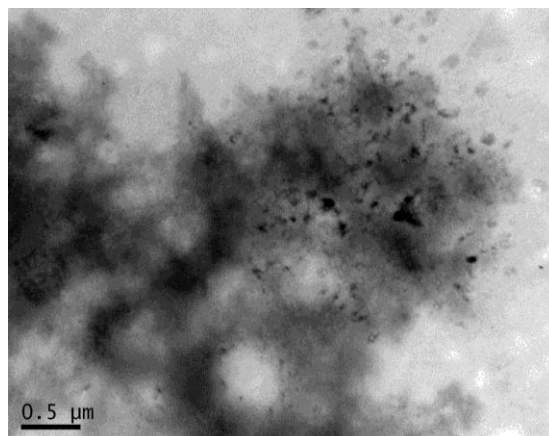
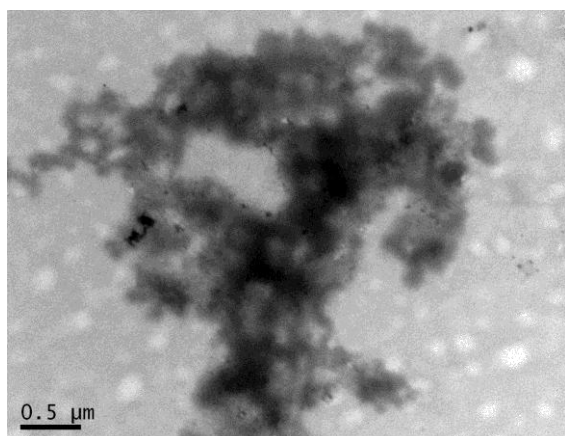


C

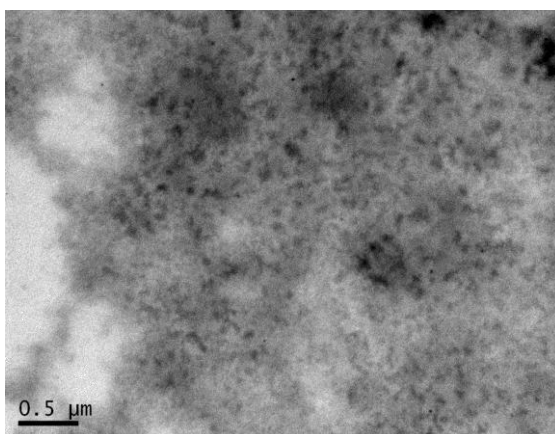
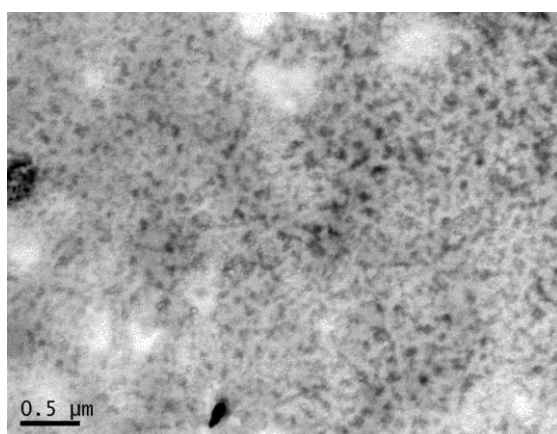
A β + Cur



A β + Fe + Cur

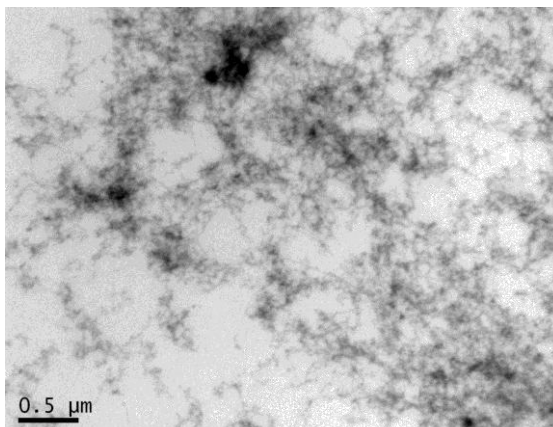
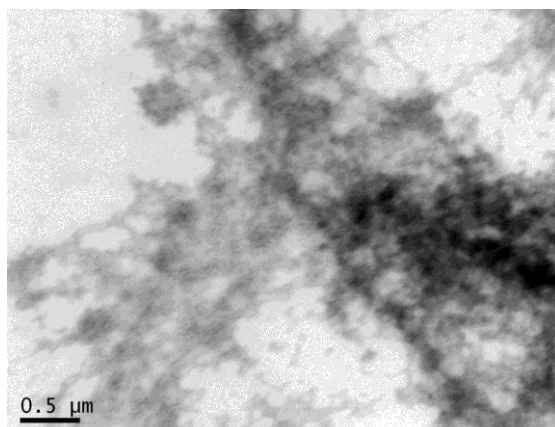


A β + Cu + Cur

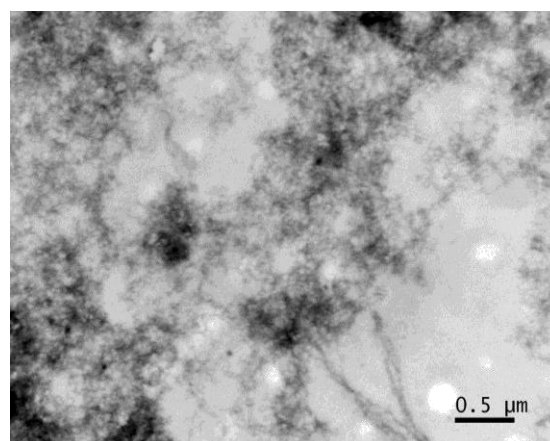
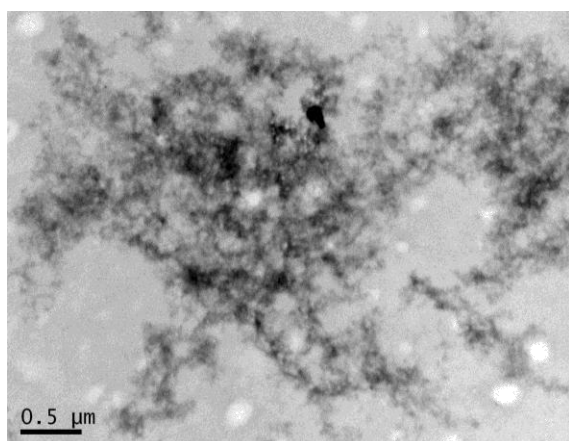


D

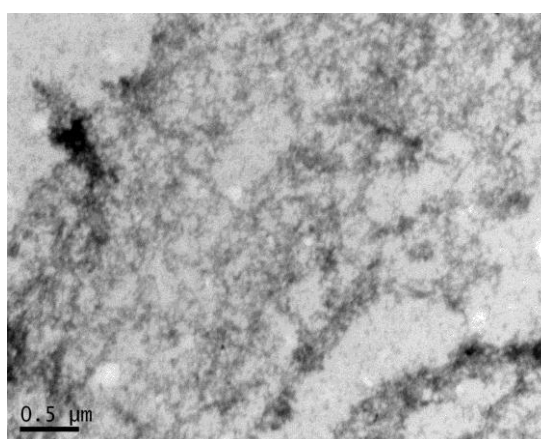
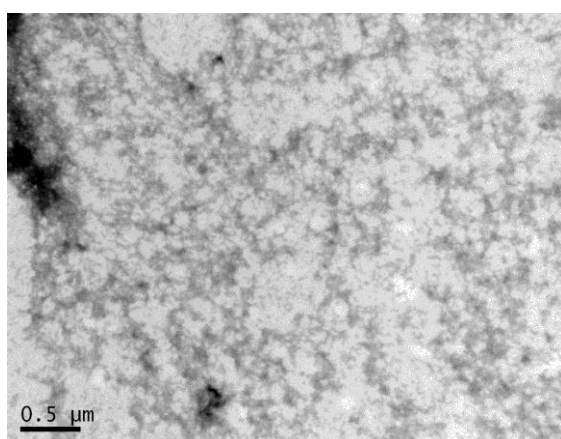
A β + Res



A β + Fe + Res



A β + Cu + Res



Chelating Properties of Polyphenols with Iron

Mass spectrometry was used to look at the ability of EGCG and Resveratrol to bind to iron. Both polyphenols were found to form metal chelate complexes with iron (see Figures 5.11 and 5.12). These data are not conclusive regarding solution phase chemistry, since gas phase adducts with metals such as sodium and potassium are known to form readily in the gas phase and are common in mass spectra. However it should be noted that the metal ion adducts with EGCG and resveratrol, both $[M+\text{metal}]^+$ and the $[2M+\text{metal}]^+$ species, are quite intense relative to the protonated species. This extent of adduct formation, is much stronger than the more common 10-20% relative to the protonated ion, which is typically observed in MALDI-TOF. This outcome may therefore reflect an inherently stronger association with metals which may well be recapitulated in solution phase properties and would be worth further investigation.

Figure 5.11: Mass spectrometry chromatogram of EGCG and Fe (1:2 ratio). Top chromatogram showing sodium adduct of EGCG and bottom spectrum showing iron chelate.

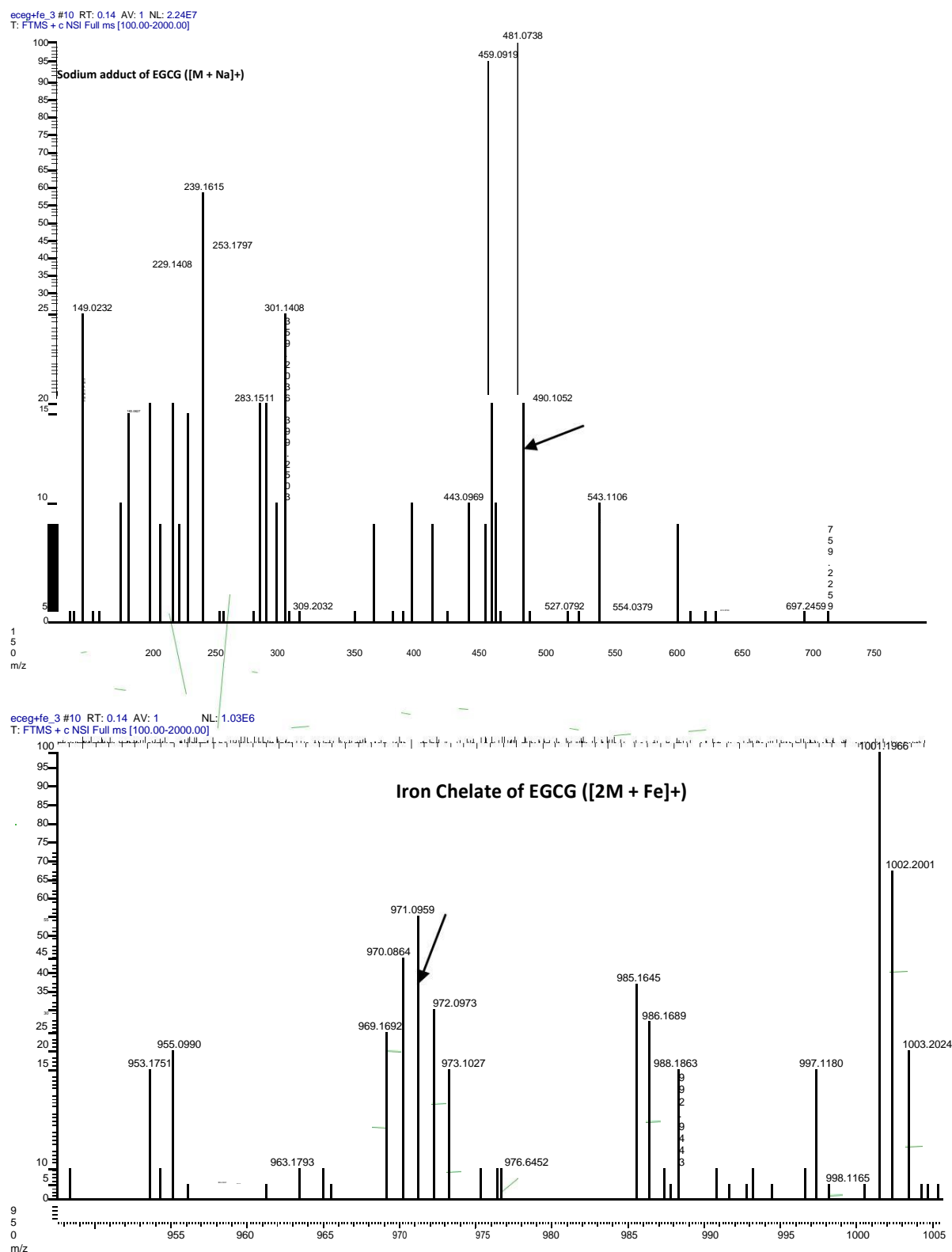
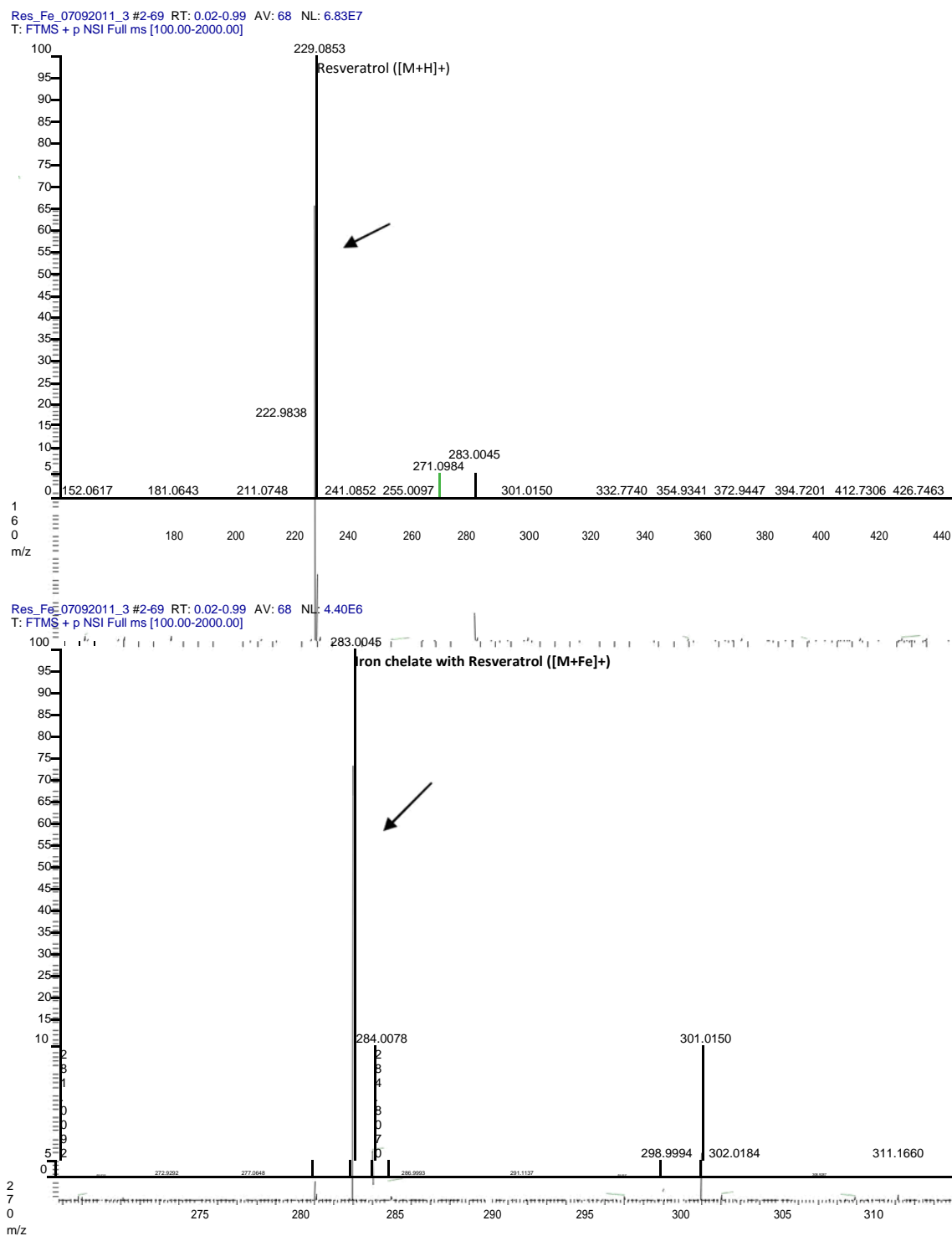


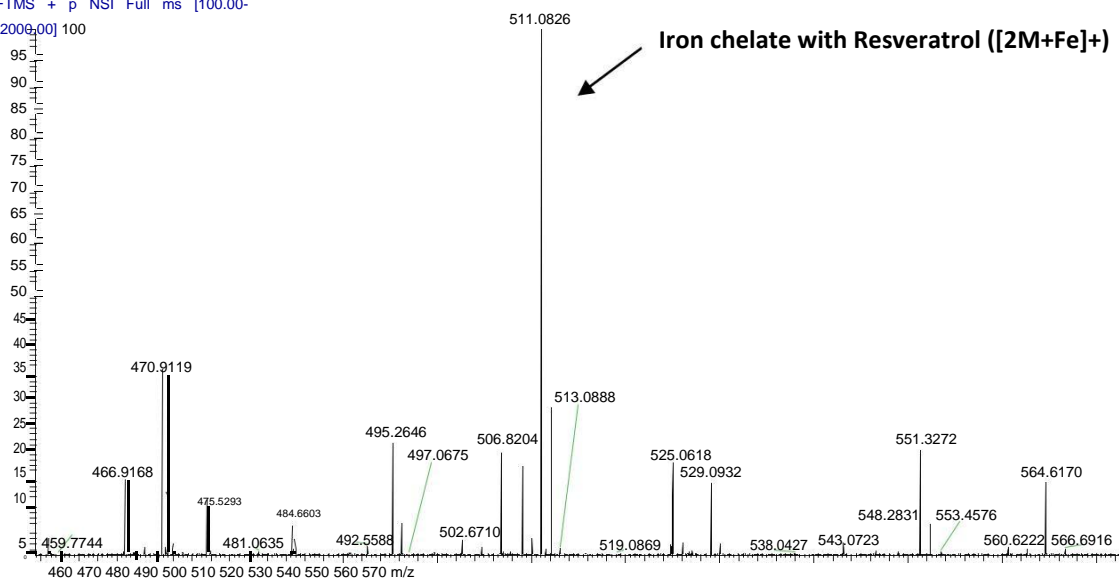
Figure 5.12: Mass spectrometry chromatogram of Resveratrol and Fe (1:2 ratio). Top chromatogram showing resveratrol only, middle and bottom showing formation of iron chelates with resveratrol.



Res_Fe_07092011_3 #2-69 RT: 0.02-0.99 AV: 68 NL: 8.10E5
FTMS + p NSI Full ms [100.00-

2006.00] 100

Relative Abundance



Iron chelate with Resveratrol ([2M+Fe]+)

5.4 Discussion

AD is the most prevalent neurodegenerative disorder of ageing. It is a multifactorial disease with several pathology related pathways. Therefore, therapy or preventative strategies may be more efficacious if they target multiple pathological processes simultaneously. In this regard, cumulative data have demonstrated that polyphenols can display neuroprotective effects through a variety of mechanisms⁶¹⁹.

Protein aggregation is a feature of a number of human diseases including many age related neurodegenerative diseases such as Alzheimer's and Parkinson's diseases. The underlying mechanism/s explaining how amyloidoses cause cell death in neurodegenerative diseases still evades our knowledge. Even the process of amyloid formation, its endogenous triggers and its mechanism/s of proliferation and propagation are incompletely understood. Amyloid fibrils exhibit a common molecular architecture in which arrays of β -strands are connected by hydrogen bonds oriented parallel to the fiber long axis, into an array known as a cross- β structure⁶²¹. The substructure of mature fibrils consists of one or more protofilament units, which can assemble laterally or intertwine in various ways as rope-like or ribbon-like modifications to the common fibrillar framework⁶²¹. The finding that amyloid fibrils are stabilized primarily by hydrogen bonds involving the polypeptide main chain explains why fibrils formed from polypeptides of different sequence are morphologically and structurally similar. The toxic effects of amyloid aggregates to exposed cells, includes nonspecific membrane permeabilization, oxidative stress, mitochondrial impairment and eventually apoptosis^{26,610,621}. The use of polyphenols is promising, as agents that are capable to protect cells against oxidative stress or inhibit amyloid formation at its earliest stages and disrupt the toxic fibrillar structures.

Studies of the interaction of polyphenols such as EGCG and resveratrol with A β lead to the proposal, that polyphenols function as amyloid aggregation inhibitors by diverting polypeptides from their normal amyloid formation pathway into nonproductive off-pathway states⁶²⁰.

Polyphenols are characterized by the presence of several phenolic hydroxyl groups with acidic properties and with their planar structures form hydrogen bonds with peptides⁶⁴⁶.

The various types of damage seen in AD including glycation, protein oxidation, lipid peroxidation and nucleic acid oxidation, almost all result directly or indirectly from metal catalysed hydroxyl radical production^{43,128}. Redox active metals therefore play a primary role in the oxidative damage associated with AD^{43,128}. Importantly redox active metals such as

copper and iron also accumulate in the neuropil of the AD brain at concentrations 3-5 fold higher than age-matched controls^{129,130}. An increase in the concentration of CSF copper and an accompanying increase in ceruloplasmin, iron and iron-binding proteins have been observed in AD^{130,647}.

Evidence for the link between this metal dyshomeostasis, free radical production and A β plaques is abundant. Accumulation of iron in the hippocampus and cerebral cortex of AD patients colocalises with the lesions, NFTs and A β and may promote increased formation of oxygen radicals²⁵. Several MRI studies have found positive correlations between ageing and iron accumulation in the brain^{135,648}. As a consequence, with increased free iron accumulation the brain becomes increasingly vulnerable to the iron-catalysed oxidative stress. It is possible that age-related accumulation of iron may underlie or at least contribute to age being the most significant risk factor for most neurodegenerative diseases.

In vitro studies using synthetic A β have shown that iron induces the aggregation and potentiates the neurotoxicity of A β ⁶⁴⁹. A β binds to and reduces Fe³⁺ to Fe²⁺, which is followed by formation of H₂O₂⁶⁴⁹. The generation of Fe²⁺ and H₂O₂ creates conditions ideal for the Fenton reaction, leading to the formation of the highly reactive hydroxyl radical⁶⁴⁹. The hydroxyl radical can then initiate lipid peroxidation, protein modifications and damage to DNA. Copper in the presence of A β , has been observed to facilitate the generation of oxidative stress. Synthetic A β in the presence of catalytic quantities of copper has been shown to produce significant quantities of H₂O₂ via similar mechanisms to iron and suggests a possible mechanism for A β -mediated neurotoxicity⁶⁴⁹.

Since metals such as iron and copper induce aggregation of A β and facilitate free radical-mediated oxidative stress reactions, metal chelation has gained increasing popularity as a means of reducing cell damage in AD. Metal chelation involves introducing compounds to bind metal ions, making them nonbioavailable and facilitating their elimination⁶⁵⁰.

Consequently the redox active metals are no longer available to bind other larger ligands such as A β , promoting its deposition, nor to promote oxidative stress reactions, through participation in Fenton type reactions⁶⁵⁰. Thus, chelating agents have the potential to inhibit the copper and iron-dependent neurotoxicity in the AD brain.

We have found that the polyphenols, EGCG, resveratrol and curcumin displayed neuroprotective properties against amyloid and metal ion toxicity in cultured astrocytes by protecting cell viability (Figures 5.2 – 5.4) and preventing the effects of oxidative stress via

Fenton chemistry (Figures 5.5 – 5.7). Electron microscopy images of the amyloid:polyphenol complexes showed that they have the ability to bind directly to amyloid, and look similar regardless of whether metal ions are present (Figure 5.10, Panels B-D), and differ in appearance to the aggregates where there are no polyphenolics present (Figure 5.10, Panel A). This suggests that the different structures formed in the presence of polyphenols may be a mechanism of preventing the neurotoxic properties of A β 42 aggregates. This may also explain the protective effects of the polyphenolics toward glial cells and mitochondrial function (Figures 5.2 – 5.9). Our data are consistent with studies which have shown that EGCG binds to amyloid, forming highly stable structures which are not in the β -sheet conformation⁶⁵¹. TEM images showed that curcumin had a similar effect to EGCG. Resveratrol however displayed slightly different structure to EGCG and curcumin in the TEM images but was none-the-less neuroprotective as shown via the cell viability effects in the amyloid and oxidative stress cellular model.

EGCG and resveratrol may also chelate iron as suggested from the mass spectrometry results (Figures 5.11 and 5.12). Further investigation using methods such as iTTC will help further validate the binding stoichiometry and kinetics of these polyphenolic compounds. Thus these compounds may have the dual ability to provide neuroprotection by binding to amyloid directly and also preventing the effects of metal ions to promote oxidative stress via chelation.

The soluble aggregates of amyloid seen in Alzheimer's disease have been shown to disrupt mitochondrial function, initiating a pathophysiological cascade leading to synaptic and neuronal degeneration⁶⁵². Treatment with EGCG, resveratrol and curcumin mitigated the mitochondrial dysfunction caused by incubation of cells with amyloid and metals (Figures 5.8 and 5.9). Polyphenols have been shown to affect the mitochondria-related redox parameters by acting either directly or indirectly upon the organelle. Santos et al.⁶⁵³ showed that quercetin or its metabolite 3'-O-methyl-quercetin (50 μ M each for 30 min) did suppress Fe²⁺/ADP-induced lipid peroxidation in mitochondria isolated from rat liver, demonstrating a direct antioxidant action in that experimental model. Furthermore, quercetin at 50 μ M (but not its metabolite) prevented potassium phosphate or mefenamic acid-induced protein thiol group oxidation in isolated mitochondria (incubation for 15 min). Quercetin was the most potent compound tested, inhibiting mitochondrial permeability transition pore (MPTP) and, consequently, swelling of the organelle, when compared to other flavonoids. Some authors stated that the enolic 3-OH group in the quercetin structure (C-ring) is responsible for

enhancing the antioxidant activity of quercetin. Additionally, this 3-OH group would exhibit an ability to chelate Fe^{2+} , decreasing its availability to react with H_2O_2 through Fenton chemistry reaction⁶⁵⁴. Devienne et al.⁶⁵⁵ found that quercetin (1-50 μM) scavenged superoxide anion radicals ($\text{O}_2^{\cdot-}$) (and strongly inhibited hydrogen peroxide generation) in mitochondrial suspensions, leading to decreased rates of lipid peroxidation through a mechanism involving a Fe^{2+} -chelating activity. Dorta et al.⁶⁵⁶ reported that quercetin (5-50 μM for 5 min) was the most potent agent in scavenging $\text{O}_2^{\cdot-}$ and preventing Fe^{2+} /citrate-induced lipid peroxidation in mitochondria isolated from rat liver when compared to taxifolin, galangin, and catechin. In spite of this, there are controversial data regarding the chelating capacity of quercetin and other flavonoids^{657,658}.

Thus, the protective ability of quercetin upon isolated mitochondria is apparent, but the exact mechanism by which this flavonoid elicits beneficial effects on the organelle still remains a matter of debate. Polyphenols have been shown to elicit antioxidant effects upon mitochondria by mechanisms that involve its chemical structure and/or its direct action on components of the mitochondrial electron transport chain, the main source of free radicals in this organelle. Moreover, polyphenols interact with other proteins located in the mitochondrial matrix, causing alterations in redox-related parameters. On the other hand the mode of action of polyphenolic compounds is not without contradictory findings. Consequently this area needs further research to determine the mechanisms by which polyphenols modulate mitochondria-related redox parameters.

As with many other drugs developed to counteract AD, the role of these compounds in ameliorating disease progression is still to be clinically verified. First of all, bioavailability of polyphenols is in general low, and concerns still remain regarding their capacity to bypass the blood brain barrier. Studies conducted on cell cultures demonstrate that in most cases the concentration able to exert a protective effect range from 5 to 50 μM , levels that are seldom if ever reached *in vivo* after oral ingestion⁶⁰⁶. To date, clinical trials conducted with these compounds have failed to demonstrate the efficacy of this family of molecules to slow disease progression in patients affected by AD^{659,660}. Although many attempts have been made to elucidate the molecular mechanism of natural polyphenols against amyloidogenesis, the structure-activity relationship is still obscure and remains to be further explored. Considerable work remains before the potential clinical benefits of polyphenolic compounds can be fully realised. Nonetheless the advantages of polyphenol rich diets warrants further research.

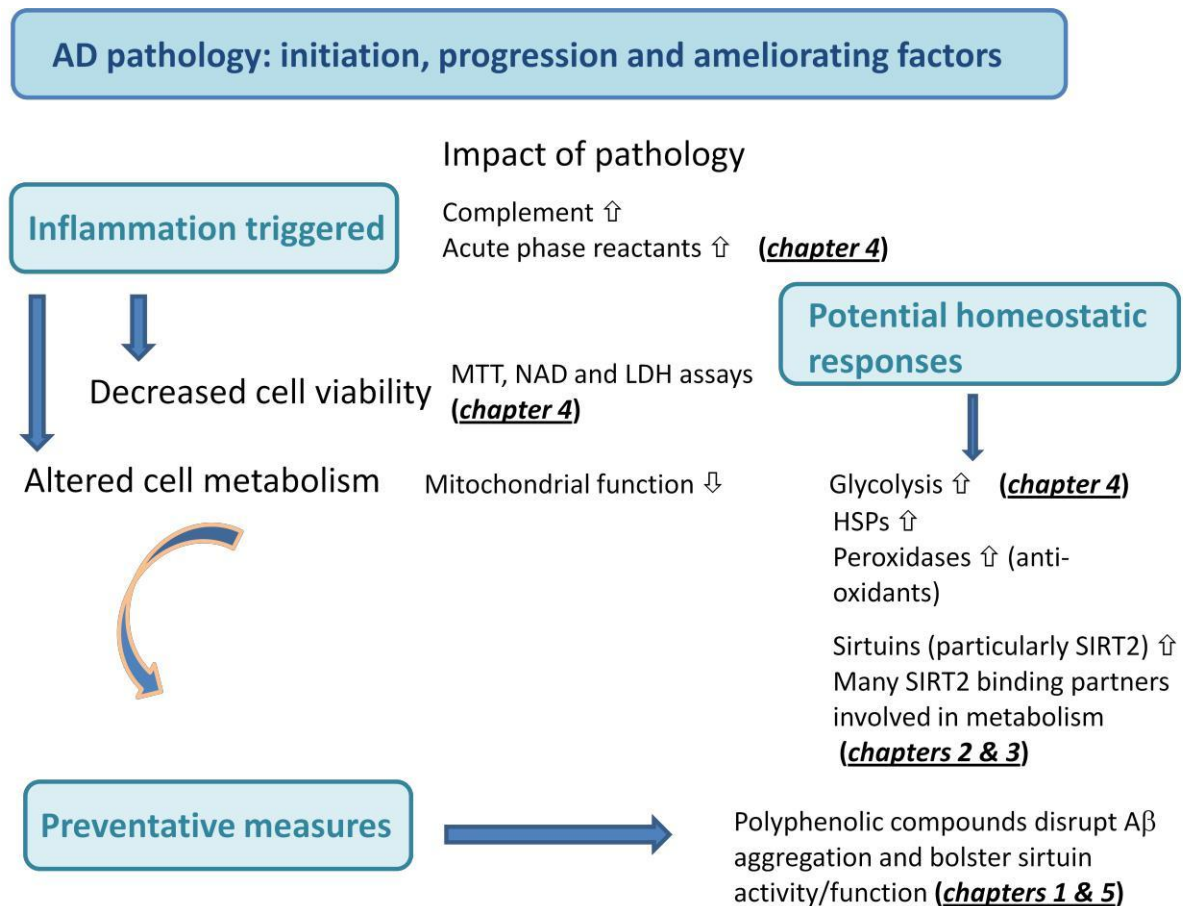
Chapter 6

General Discussion and Future Directions

6.1 Introduction

AD is a multifactorial disease on several levels: (a) it has a wide variety of risk factors, (b) multiple cell types are affected (neurons, glia, astrocytes, oligodendrocytes, endothelial cells), (c) both intracellular and extracellular changes are observed, and (d) there are both genetic and environmental factors in the aetiology of the disease (autosomal dominant AD, Down's syndrome, late onset AD). Ageing is the strongest risk factor for AD, yet most researchers would agree that ageing and AD are not synonymous. This thesis has explored some common pathways which affect both ageing and AD, to better understand what ageing and AD have in common, and also how they are different, a summary of findings is shown in Figure 6.1.

Figure 6.1 Summary of main findings from thesis.



In chapter 3 the role of the longevity associated sirtuins family was explored in ageing and AD, showing that while the sirtuins in general are on a downward trajectory with age, in AD

there appears to be a homeostatic upregulation of specific sirtuins, particularly SIRT1 and SIRT2. In exploring potential mechanisms by which SIRT2 might mediate its effect/s, a variety of binding partners were identified. About 50% were metabolism related, particularly several glycolysis pathway enzymes. The remainder were from diverse cellular locations known to be affected in AD, including histones, cytoskeletal proteins, antioxidant proteins and regulators of protein structure and folding. In chapter 4, the effect of AD vs age matched control plasma on glial cells was explored, with effects on the complement pathway and metabolism (particularly glycolysis) differentiating ageing from AD. In chapter 5, the question of how AD pathology might be modulated was explored. For a multifactorial disease, perhaps disease modifying approaches also need to be multifactorial. Polyphenolic compounds can potentially impact multiple aspects of AD pathology, including: (a) ROS and oxidative stress, (b) function of sirtuins (e.g., resveratrol), (c) protein structure and activity, and (d) metabolism/mitochondrial function.

6.2 Distribution of Sirtuins across CNS cell types and tissues

Sirtuin proteins have a variety of intracellular targets, regulating multiple biological pathways, and could be considered pleiotropic mediators of cellular homeostasis. Both ageing and neurodegenerative conditions such as AD impact multiple cellular pathways. Consequently, proteins with pleiotropic effects such as the sirtuin family may be ideal targets for modulating some of the deleterious effects of both ageing and AD. Relatively little is currently known about the role or expression of the 7 mammalian sirtuins in the central nervous system. Quantitative expression analysis of mammalian sirtuin proteins (especially SIRT2-7), in the CNS is limited in the current literature. SIRT1 has been reported to be expressed in the cortex, hippocampus, cerebellum, and hypothalamus, and in lower levels in the white matter⁴²⁵. Among the brain cell types, SIRT1 is predominantly expressed in neurons and viewed as a nuclear protein⁴²⁵. The mRNAs for all seven sirtuins have been identified in mouse brain tissue and also neural stem cells⁴²⁶. SIRT1, SIRT2 and SIRT3 have also been detected in human serum, and levels were shown to decline with age and were linked to frailty^{427,428}. SIRT3 has been shown to be elevated at both the mRNA and protein levels in Alzheimer's disease (AD) *post mortem* brain tissue compared to controls²⁷¹.

The most common techniques currently utilised for detecting a change in sirtuin levels at the mRNA or protein level are PCR and western blotting, respectively. Other studies have used

methods such as immunohistochemistry, surface plasmon resonance and ELISA assays. The majority of these methods are only semi-quantitative with moderate sensitivity, use antibodies which may not have sufficient specificity or detect expression at the mRNA level which may not reflect protein expression. Furthermore, there is no current assay which detects multiple sirtuins simultaneously.

Mass spectrometry has a great advantage over the conventionally used antibody based methods, such as western blotting, in that it offers greater specificity, linearity, reproducibility and typical limits of quantification down to the low fmol range. It also removes some of the antibody specificity issues that are associated with methods such as western blotting and ELISA, as peptides unique to each protein are measured. Thus in Chapter 2, I focus on the development of a targeted mass spectrometry method using multiple reaction monitoring (MRM) to quantify the seven human sirtuins at the protein level. To achieve sufficient sensitivity and selectivity in a multiplex-format, a targeted mass spectrometric assay was developed and validated for the quantification of all seven mammalian sirtuins (SIRT1-7). The assay was applied to a variety of samples including cultured brain cells, mammalian brain tissue, CSF and plasma. In line with previous data, my results affirm that there is significant divergence in abundance amongst members of the sirtuin family of proteins in the brain. SIRT1 and SIRT2 are the most abundant sirtuins in cultured brain cells with SIRT1 highest in neurons and SIRT2 highest in oligodendrocytes, validating previous studies showing SIRT2 to be highly expressed in oligodendrocytes⁴⁵³. My study and others have also found SIRT2 expressed in neurons and glial cells^{454,455}. Further validation with higher sample numbers and across a wider range of cell lines may help elucidate differences between cell types for the lower abundant sirtuins.

SIRT2 was found to be the most abundant sirtuin in the adult human frontal lobe and cortex and cerebellum homogenates from the guinea pig. Previously published results have shown SIRT2 to be abundant in the brain and serum^{428,429,440,457} and my study provides further evidence for this and extends its abundance to the guinea pig brain. The mitochondrial sirtuins SIRT3-5 were found at lower levels in human brain but detection was improved after detergent fractionation. Further fractionation of samples or purification of mitochondria may facilitate improved mitochondrial sirtuin quantification. I also confirmed that mammalian sirtuins are localised to several subcellular compartments. While SIRT1, SIRT6 and SIRT7 are predominantly found in nuclear fractions, they are also detected in cytosol, cytoskeleton and membrane fractions, albeit at much lower levels. Similarly, although SIRT2 is the only

human sirtuin primarily localised in the cytoplasm, it may also be found at lower levels in the nucleus and cellular membrane. My data confirm that SIRT1 and SIRT2 may interact with both the nuclear and cytoplasmic subcellular compartments. Similarly, while the mitochondrial sirtuins (SIRT3-5) have been previously reported to be exclusively localised to the mitochondria, other studies have reported the localisation of several variants in the nucleus as well as the cytoplasm, in line with my study⁴⁶³. The expression patterns of sirtuins in brain cells remains controversial and it is unclear whether certain sirtuins are specific to cell types. My MRM study indicates that the majority of sirtuins (SIRT1, 2, 6 and 7) are present across all the main brain cell types. Sirtuins were also detected in human CSF and plasma, and guinea pig and mouse tissues.

6.3 Sirtuins in Ageing and Alzheimer's disease

Although a number of sirtuins have been found to be promising in boosting longevity and neuroprotection in cellular and animal models of AD, mammalian distribution and functional roles in the central nervous system are still not well studied. There is a paucity of information about the role of CNS sirtuins in ageing brain and neurodegenerative diseases. Previous studies have shown an increase in SIRT3 in AD *post-mortem* brain tissue using western blotting for protein expression and multiplex qPCT to assay SIRT3 mRNA levels²⁷¹. Both

SIRT3 protein and mRNA were shown to be significantly elevated in the AD group²⁷¹.

Another recent paper detected SIRT1 in human serum samples using western blotting, surface plasmon resonance and ELISA to measure SIRT1 protein levels⁴²⁷. SIRT1 declines with age and is more dramatically reduced in MCI and AD patients compared to age matched controls, suggesting that SIRT1 may warrant further investigation as a potential plasma biomarker for AD⁴²⁷. SIRT1 and SIRT3 levels in serum were found to be significantly lower in frail subjects as compared to the non-frail⁴²⁸. Another study reported a decrease in SIRT1 and SIRT2 mRNA levels using quantitative real time PCR in the primary motor cortex of human *post-mortem* amyotrophic lateral sclerosis brain tissue⁴⁴⁰.

In AD transgenic mouse models SIRT1 overexpression has been reported to be neuroprotective against amyloid and tau pathologies as well as more recently also shown to induce cognitive enhancement^{340,480}. Since SIRT-1 is a deacetylase that regulates several neuroprotective cellular pathways promoting neuron survival by deacetylating a broad spectrum of molecules, it has been hypothesized that the loss of SIRT-1 protein in the brain

contributes to the pathogenesis of AD. A significant decrease in SIRT1 concentration in parietal cortex of AD brain has been reported and a strong correlation was established between tissue SIRT1 concentration, duration of symptoms and tau accumulation²⁸⁰, but the exact relationship and its role in the sequence of events leading to development of AD remains unclear.

Recently the first study investigating sirtuin levels in serum has been reported. The study investigated serum SIRT1 concentration in patients with AD and MCI as well as in young and elderly controls⁴²⁷. A significant decline in SIRT1 with age in serum and a larger drop in patients with MCI and AD was found⁴²⁷. The authors suggest that SIRT1 may be a promising biomarker for AD. These data also suggest that sirtuin activators may potentially have a preventive role in AD. Another study by the same group examined the association of sirtuins to a major geriatric syndrome, frailty⁴²⁸. Serum levels of SIRT1, 2 and 3 were found to be significantly lower in frail patients compared to nonfrail controls⁴²⁸.

Thus, in Chapter 3, I investigated changes to sirtuin protein expression during normal human ageing and also changes occurring in AD. I examined sirtuin levels in control, MCI and AD plasma, in the CSF of both a younger and elderly age group, in control and AD *post-mortem* brain tissue and finally in young and older samples of a potential new natural AD animal model – the *Octodon Degus*. To further investigate the functional role of SIRT2, which I found to be the most abundant in the human brain, I completed an immunoprecipitation pulldown followed by mass spectrometry detection of potential binding partners. Owing to the potential importance of mammalian sirtuins in neurodegeneration and ageing, I hypothesized that they may be differentially expressed in the plasma, CSF and brain and may regulate various targets involved in metabolic processes and neurodegenerative diseases. I investigated sirtuin expression in immunodepleted plasma from pooled control, MCI and AD subjects and found a significant drop in SIRT1 levels in the plasma of AD patients, in line with other studies in the literature^{427,428}. My data and the work of others suggest the possibility that SIRT1 may be a useful clinical biomarker of AD. However, further validation in larger cohorts is needed with longitudinal samples and non-AD dementia controls.

I also investigated sirtuin CSF concentrations in younger and elderly controls and found a downward trend in SIRT1 in the elderly group but not reaching significance. It would be interesting to further valid these results by looking at sirtuin expression in matched plasma samples and to also investigate levels in larger cohorts of subjects. Evaluation of sirtuin

levels in the CSF, plasma and *post mortem* brain tissue of centenarians would also provide greater insights into how sirtuins may change in those who have “super aged” brains and may provide clues as to how these individuals stay healthy during exceptional longevity.

Interestingly, when comparing control and AD *post mortem* brain tissue, I found a significant elevation of a number of sirtuins. In the occipital lobe, I found a higher level of SIRT2 and in the temporal lobe an increase in both SIRT1 and SIRT3 in the AD brain. Published reports on sirtuin expression in the AD brain are limited in the current literature, though a few recent studies have reported significant changes. One study showed a significant increase in SIRT3 in the temporal cortex of AD *post mortem* brain²⁷¹. SIRT3 expression was found to correlate with the deposition of β -amyloid in an AD mouse model²⁷¹. My results also confirmed an elevation of SIRT3 in the AD temporal lobe. This suggests a possible role for SIRT3 in mechanisms of sensing and protecting against ROS and AD-mediated mitochondrial stress. Another recent study has reported changes to SIRT1, 3 and 5 expression, reporting a decline in SIRT1 and SIRT3, and an elevation of SIRT5 in the cortex and hippocampus, with AD progression⁵⁰⁰. SIRT3 decline has also been reported in an AD transgenic mouse model⁵⁰¹. These results suggest that mitochondrial SIRT3 might participate in the development of AD via mitochondrial dysfunction. The elevation we see in the temporal lobe may therefore be a compensatory mechanism by the brain to induce these neuroprotective proteins and bolster neuronal longevity. SIRT1 and SIRT3 are also upregulated in response to fasting and calorie restriction and have been shown to reduce ROS levels and reduce oxidative damage. The decline reported by others in the hippocampus where the highest level of AD pathology is seen may indicate loss of these neuroprotective activities and metabolic dysfunction reported in this vulnerable region may be thus, in part due to reduction of SIRT1 and SIRT3 levels. As AD is associated with significant increases in neuronal ROS production and previous studies have shown that SIRT3 mRNA expression is regulated by mitochondrial ROS levels, it seems likely that the SIRT3 upregulation in AD we see in the temporal lobe may be a consequence of A β -related oxidative stress. Given that others have shown that SIRT3 upregulation subsequently increases neuronal lifespan, it is tempting to speculate that upregulation of SIRT3 in response to A β -induced oxidative stress might prolong neuronal function by decreasing ROS, maintaining ATP-levels and sustaining synaptic activity. These possibilities will need further investigation, and will no doubt yield important information about mechanistic links between metabolism, longevity and defence against the impacts of pathology.

This work has identified SIRT2 as the most abundant sirtuin in the brain and we also see an elevation of SIRT2 in the AD occipital lobe, one of the least AD pathology susceptible brain regions. I therefore aimed to gain further insights into its biological functions by identifying its binding partners. Using immunoprecipitation pulldown and protein identification using mass spectrometry, I identified a list of potential binding partners for SIRT2. Interestingly, our results reveal a novel potential role of SIRT2 as a regulator of mitochondrial function and metabolism with many of the binding partners identified being involved in energy metabolism. These include aldolase, ATP synthase, enolase, pyruvate kinase and glucose-6-phosphate isomerase which are all involved in energy metabolism and glycolysis. A recently published study has also suggested SIRT2 may regulate the activity of mitochondria. Liu et al found that SIRT2 can localise to mitochondria and directly interact with mitochondrial proteins⁵⁰⁴. Furthermore, the depletion of SIRT2 was shown to increase markers of oxidative stress and reduce ATP production in the mouse brain⁵⁰⁴. Thus taken together my data shown in Chapter 3 and previous studies suggest that SIRT2 is not only a cytosolic protein but may translocate to mitochondria, appears to have many mitochondrial targets and a new role for SIRT2 in mitochondrial function, oxidative stress and energy metabolism may be emerging. All of these processes are established as important factors in the pathogenesis of AD, and as a modulator, SIRT2 may represent a potential target for disease prevention and/or amelioration.

6.4 Inflammation and Metabolism in AD Pathology

Markers of increased protein, lipid and nucleic acid oxidation and reduced activities of antioxidant enzymes have been reported in AD plasma⁶⁶⁴⁻⁶⁶⁶. Amyloid plaques in the AD brain elicit a range of reactive inflammatory responses including complement activation and acute phase reactions, which may also be reflected in plasma. Previous studies have shown that human AD plasma may be cytotoxic to cultured cells^{508,509,511}. In Chapter 4, I investigated the effect of pooled plasma from healthy controls and individuals with MCI and AD, on cultured microglial cells. Since previous studies indicate that AD plasma may contain oxidative stress markers as well as cytotoxic factors, in Chapter 4, I investigated the effect of the addition of pooled control, MCI and AD plasma from 20 age matched older individuals on a microglial cell line. Cell viability, proliferation and mitochondrial function were investigated following 48 hour treatment with non-heat-inactivated plasma and plasma in

which complement proteins had been deactivated. I also tested the effect of commercially purchased complement factors alone and in combination on cultured glia. I then undertook proteomic analysis of the plasma from each group and iTRAQ quantitative proteomic analysis of cell extracts exposed to plasma from each group to investigate possible plasma protein alterations unique to MCI or AD, to detect any protein aberrations within the cells treated with the plasma and to correlate these findings to cell viability and mitochondrial function assays measured *in vitro*.

AD plasma was found to significantly decrease cell viability and increase glycolytic flux in microglia compared to plasma from healthy controls. This effect was prevented by heat inactivation. Proteomic methods and isobaric tags showed expression levels of complement and other acute phase proteins to be altered in MCI and AD plasma and an upregulation of key enzymes involved in the glycolysis pathway in cells exposed to AD plasma. The increased expression of glyceraldehyde-3-phosphate dehydrogenase, phosphoglycerate kinase, enolase, aldolase and pyruvate kinase may increase glycolytic flux leading to the accumulation of pyruvate and thus stimulating anaerobic metabolism to lactic acid. I found an increased level of LDH activity in the cell culture media and an increase in extracellular acidification, as indicated by the increase in ECAR in the microglial cells exposed to human AD plasma. These findings suggest a role for mitochondrial bioenergetic deficits in AD pathogenesis, and a possible homeostatic response through upregulation of glycolysis. Thus my data suggested that altered expression levels of acute phase reactants in AD plasma may alter the energy metabolism of glia.

Damage to the blood-brain barrier is thought to occur in AD, and this may increase movement of proteins between the brain and the vasculature⁵⁵². A variety of inflammatory markers are increased with the onset of AD pathology, including cytokines and chemokines, coagulation factors and acute-phase reactive proteins as well as reactive astrocytes and activated microglial cells, the main cells involved in the neuroinflammation process^{506,507}. Whether accumulation of cytokines and acute phase reactants within the brain is reflected in plasma has not been elucidated as many of these proteins do not easily cross the blood brain barrier. Alternatively, AD may be associated with a more widespread immune dysregulation, detectable in plasma.

Previous studies investigating the effects of human AD plasma on cells in culture have found differential effects on protein expression and cell biology. One study aimed to determine if exposure to serum from AD patients would affect markers for AD brain lesions⁵⁰⁸, and found

that 24 hour exposure to AD serum increased four molecular markers characteristic of AD senile plaques and neurofibrillary tangles in rat hippocampal neurons⁵⁰⁸. This stimulation of AD markers by human serum suggests that the genesis of both neuronal plaques and tangles may arise from exposure of susceptible neurons to toxic serum factors and/or failure to detoxify these factors. Another study found that antibodies in serum of patients with AD caused immunolysis of cholinergic nerve terminals from the rat cerebral cortex, supporting the hypothesis that autoimmune mechanisms may operate in the pathogenesis of AD⁵⁰⁹. This work demonstrated the utility of examining effects of disease plasma on cell culture systems, to facilitate the study of both disease markers and disease mechanisms. The role of blood factors in ageing and disease is underscored by recent experiments using the parabiosis technique and showing the rejuvenating and pathology ameliorating effects of young blood in older animals^{667,668}.

Factors which induce the upregulation of glycolysis in glial cells treated with AD plasma remain unclear. However, aerobic glycolysis has been correlated spatially with amyloid deposition in AD brains⁵⁷⁶. It has also been shown that elevated levels of the enzymes pyruvate dehydrogenase kinase and lactate dehydrogenase provide resistance to amyloid and other neurotoxins⁵⁸⁴. The ability of the brain to maintain expression of these enzymes involved in mitochondrial energy metabolism may explain why some individuals could show high levels of amyloid deposition without neurodegeneration^{584,589-591}. Interestingly I found some of these glycolytic proteins overlapped with the SIRT2 binding partner proteins we found in Chapter 3. In my study, the indicators of increased glycolysis in microglia may be a compensatory action caused by the loss of cell viability and mitochondrial function following exposure to AD plasma. Altered activities of key glycolytic enzymes have also been found in hippocampal, frontal and temporal cortex of AD brains and thought to possibly be related to the astrogliosis that occurs in AD⁵⁸¹.

Interestingly I have found that SIRT2 is upregulated in the AD brain and that many of the SIRT2 binding partners identified in Chapter 3 are involved in metabolism (including glycolysis). Also in Chapter 4, I show that glycolysis is upregulated when glia are exposed to AD plasma. Therefore this data, taken together, suggests the possibility that some of the metabolic changes observed upon exposure to AD plasma may be mediated by SIRT2 and perhaps also other sirtuins as well.

6.5 Brain pathology in AD: offense vs defence

In the pathogenesis of AD, there is a strong interplay between how much of the disease is due to pathological processes and stressors and how much might be due to insufficient defensive strategies. Therefore, reinforcing defensive strategies such as preventing amyloid aggregation via the use of compounds such as polyphenols, might prove a potent way to avoid/postpone disease onset.

A β , the product of the proteolytic cleavage of the APP into 38, 40, or 42 amino acid peptides, is generally viewed as a toxic mediator of AD⁶⁶⁹. The generation of A β is orchestrated by the β - and γ -secretases in a sequential manner such that inhibition of either secretase prevents A β generation. The oligomerisation of A β is toxic to neurons *in vitro* and *in vivo* and produces synaptic dysfunction, calcium dysregulation, oxidative stress, and neuroinflammation.

Additionally, A β (specifically A β ₄₂) is the primary component of the senile plaques that become deposited in the brains of AD patients and are a hallmark pathological feature of the disease⁶⁶⁹. Alternative processing of APP, through α -secretase cleavage (followed by that of γ -secretase), produces a soluble segment of APP that may be neuroprotective. This “non-amyloidogenic” pathway deters the processing of APP through the β - and γ -secretases and thus inhibits the formation of toxic A β species. Interestingly, recent evidence indicates that SIRT1, along with its varied role in the regulation of ageing, is also a key regulator of α -secretase, and thus of amyloidogenic processing^{340,669}. SIRT1 hyperactivity is capable of reducing AD pathologies both *in vitro* and *in vivo* through upregulation of the ADAM10 gene³⁴⁰. Laboratory upregulation of the sirtuin pathway, via sirtuin-activating compounds like resveratrol, have also effectively reversed the ageing process and its comorbidities in animal models^{200,202,479}. SIRT1 was upregulated in AD temporal lobe (Chapter 3, Figure 3.4), which may be a homeostatic response to the pathology. Consequently SIRT1 upregulation may provide a possible therapeutic (or preventative) avenue for age-related diseases such as AD, and polyphenolic compounds are potential modulators of sirtuin activity.

Polyphenols, which include resveratrol, epigallocatechin gallate and curcumin, have gained considerable interest in AD research for their ability to reduce many of the main pathological hallmarks of AD and their potential to slow down cognitive decline^{252,389,634}. Polyphenols exhibit remarkable antioxidant and anti-inflammatory activities that may exert a leading role in reducing age-related oxidative stress and inflammation, and thus hampering the onset and progression of degenerative diseases^{379,635}. Oxidative stress is a key hallmark in AD. More

recently polyphenols have been shown to produce other important effects including anti-amyloidogenic activity, metal chelation and modulation of the sirtuin proteins^{365,619,634}. Numerous polyphenols from natural products such as turmeric, grapes, red wine and green tea, have been reported to inhibit A β aggregation and toxicity and show promise *in vivo*, including EGCG, curcumin and resveratrol^{183,190,620-626}. The major tea polyphenol, EGCG, shows neuroprotective activity against neurological disorders, and inhibits toxicity induced by A β and α -synuclein oligomers¹⁸³. Moreover, using isothermal titration calorimetry at different EGCG and salt concentrations, it has been shown that the interactions between A β 1-42 and EGCG are mainly H-bonds in the region 1–16 and hydrophobic in the region 17–42^{621,627}. Experimentally, EGCG has been reported to generate unstructured, off-pathway A β 1-42 oligomers⁶²⁰.

Brain accessible polyphenols with multiple effects on pathways involved in neurodegeneration and ageing may therefore prove efficacious in the treatment of age-related diseases such as AD, although the evidence for this so far is limited. The toxic effects of amyloid aggregates to exposed cells, includes nonspecific membrane permeabilization, oxidative stress, mitochondria impairment and eventually apoptosis^{26,610,621}. Polyphenols are characterized by the presence of several phenolic hydroxyl groups with acidic properties and their planar structure forms hydrogen bonds with peptides⁶⁴⁶. Thus the use of polyphenols is promising, as agents that are capable to protect cells against oxidative stress, inhibit amyloid formation at its earliest stages and disrupt the fibrillar structures.

The various types of damage seen in AD including glycation, protein oxidation, lipid peroxidation and nucleic acid oxidation, almost all result directly or indirectly from metal catalysed hydroxyl radical production^{43,128}. Redox active metals therefore play a primary role in the oxidative damage associated with AD^{43,128}. Considering that metals such as iron and copper induce aggregation of A β and facilitate free radical-mediated oxidative stress reactions, metal chelation has gained increasing popularity as a means of reducing cell damage in AD. Metal chelation involves introducing compounds to bind metal ions, making them nonbioavailable and facilitating their elimination⁶⁵⁰. Consequently the redox active metals are no longer available to bind other larger ligands such as A β , promoting its deposition, nor to promote oxidative stress reactions, through participation in Fenton type reactions⁶⁵⁰.

Therefore, in Chapter 5, I explored the ability of three common polyphenols to prevent the neurotoxicity caused by amyloid and Fenton chemistry on astrocytes using a brain cell model for oxidative stress and amyloid toxicity. I also investigated the effects of polyphenol treatment on amyloid aggregation using electron microscopy and the metal chelating properties of these compounds using mass spectrometry. The polyphenols, EGCG, resveratrol and curcumin displayed neuroprotective properties against amyloid toxicity in cultured astrocytes by preventing the loss of cell viability caused by amyloid in the presence of transition metals iron and copper and preventing the effects of oxidative stress via Fenton chemistry. Electron microscopy images of the amyloid:polyphenol complexes showed that they have the ability to bind directly to amyloid forming non-structured, non-toxic aggregates. Other studies have also shown this effect and found EGCG to bind to amyloid and form highly stable structures which are not in the β -sheet formation⁶⁵¹. TEM analysis also showed that curcumin also had a similar effect as EGCG. Resveratrol however displayed slightly different structure to the other two TEM images, but was also neuroprotective as shown via the cell viability effects in my amyloid and oxidative stress cellular model. EGCG and resveratrol were also able to chelate iron as seen from the mass spectrometry results. Thus these compounds have the dual ability to provide neuroprotection by binding to amyloid directly and by chelation of metal ions minimizing oxidative stress. I found treatment with EGCG, resveratrol and curcumin also minimised mitochondrial dysfunction caused by incubation of cells with amyloid and metals.

As for many other drugs developed to counteract AD, the role of these compounds in ameliorating disease progression is still to be clinically verified. First of all, bioavailability of polyphenols is in general low, and some concerns still remain regarding their capacity to bypass the blood brain barrier. Clinical trials conducted with these compounds have also failed to demonstrate efficacy in slowing the progression of the disease in patients affected by AD^{659,660}. Furthermore, although many attempts have been made to elucidate the molecular mechanism of natural polyphenols against amyloidogenesis, the structure-activity relationship is still obscure and remains to be further explored.

6.6 Future Studies

An important aspect of sirtuin biology is that their deacetylase activity is nicotinamide and NAD^+ dependent, establishing a direct link between their function and energy metabolism. MRM mass spectrometry can not only be utilised for the quantification of sirtuin proteins as demonstrated in Chapter 2, but MRM can also be applied to measure sirtuin and energy related metabolites such as metabolites of the NAD salvage pathway and ATP. Thus targeted mass spectrometry methodologies have the potential to not only validate and complement currently established methods for investigation of sirtuin protein expression changes but can also help build a larger view of sirtuin biology in the normal brain and in disease conditions by linking sirtuin protein expression with NAD^+ metabolism. It has been shown that NAD^+ declines with age, reducing sirtuin activity⁶⁷⁰. This could potentially contribute to the pathogenesis of age-related diseases. Further exploration of sirtuin related metabolites such as the metabolites of the NAD salvage pathway will enhance our understanding of the interplay between energy metabolism and sirtuin function in the process of ageing and neurodegeneration. It can also serve to investigate the efficacy of potential treatments such as polyphenols and NAD^+ intermediates such as nicotinamide mononucleotide and nicotinamide riboside, which are currently under study for their longevity promoting effects.

My preliminary data showing changes to SIRT1 and SIRT2 in AD *post mortem* brain tissues will need to be expanded to include a larger cohort of control and AD samples to validate these findings. This is to overcome any inevitable inter-individual variations in protein expression, as well as potentially variable tissue quality. Future work investigating sirtuin changes in the hippocampus of control and AD subjects would also be interesting as it will highlight how sirtuins change in this especially vulnerable part of the brain. Looking at brain tissue samples from younger, middle aged, older, and exceptionally old individuals would also be helpful in discovering changes that happen during normal ageing versus those that occur more specifically during neurodegenerative diseases such as AD. Combining my proteomics data with metabolomics data would be another avenue to explore in order to gain further insights into the biological effects and importance of sirtuins. Sirtuin proteins are linked to NAD and thus energy metabolism. By looking at changes to NAD and other related metabolites in the same samples quantifying sirtuin protein will validate corresponding metabolite changes that are occurring as a result of differential sirtuin protein expression. Finally it would also be important to look at sirtuin activation by polyphenols, both

individually and also to investigate combination therapy using polyphenols and possibly NAD related metabolites to protect CNS cells against oxidative stress.

My SIRT2 binding partner work revealed some interesting proteins for further investigation. iTC methodology will help confirm the binding properties of some of these novel proteins such as ATP synthase with SIRT2. It would also be ideal to repeat the pulldowns and analysis for the other 6 sirtuins as this may uncover further new or overlapping roles for these sirtuins and novel sites of action.

The use of SIRT2 knock out mouse models would be another possible avenue to explore biological functions of this abundant brain sirtuin. These animals would allow us to further investigate metabolic and proteomic changes that occur as a result of the loss of SIRT2 in the brain. I predict that such a knockout would leave the brain more vulnerable to pathology, particularly to oligodendrocytes, where SIRT2 is most abundant.

Results from the work on the effects of AD plasma on cell viability, mitochondrial function and glycolysis can also be further explored, using neuronal cells to investigate toxicity differences between different cell types. It would also be interesting to measure the metabolites of some of the glycolytic enzymes we found upregulated to validate the proteomics data using measures that reflect functional changes. Further fractionation of the AD plasma would also allow deeper investigation into the toxic proteins/factors involved in the loss of cell viability seen in the cultured cells.

The next step in connecting to my polyphenolics work, would be to look at sirtuin activation following treatment of CNS cell lines with various polyphenols, alone and in combination. The combination of polyphenols along with NAD precursors would also be an interesting avenue to explore. With the use of transgenic AD mouse models, the neuroprotective role of polyphenol and/or sirtuin activation could be further explored. Animal models would also allow us to investigate how treatment with polyphenols and sirtuins may affect amyloid deposition and aggregation.

6.7 Conclusions

In conclusion, I have successfully applied MRM mass spectrometry for the detection and quantification of sirtuin proteins in the central nervous system, paving the way for more quantitative and functional studies. Collectively, my results add further insights to the limited

data which currently exist regarding the expression of sirtuins in the human CNS. I found differential expression of SIRT1 in plasma and brain tissue, SIRT2 being the most abundant sirtuin and elevated in the occipital lobe of AD brain. This technique provides a powerful tool and helps improve upon the limitations of current protocols. While mass spectrometry based assays for protein quantification may still have some barriers to overcome before they can be used in a clinical setting due to low throughput and expense compared to methods such as ELISA, MS has great value in investigating lower abundance proteins such as sirtuins in complex samples such as the brain with great sensitivity and specificity.

This work has also demonstrated the utility of examining effects of disease plasma on cell culture systems, to facilitate the study of both disease markers and disease mechanisms. I found AD plasma caused loss of cell viability and mitochondrial function (Figure 6.1). I showed that plasma expression levels of acute phase proteins are altered in AD and MCI, supporting a role for increased inflammatory activity in this disease which is detectable in the plasma (Figure 6.1). Cells exposed to AD plasma show an upregulation of glycolysis possibly as a compensatory response to compromised mitochondrial function. I also found SIRT2 to be elevated in the AD brain and having the ability to interact with a number of proteins involved in metabolism (particularly glycolysis). Together these observations support an emerging body of evidence that inflammation and metabolism are closely linked processes, which are regulated by transcriptional and protein translation events^{601,602}. This study showed that the use of biological assays in combination with proteomic analysis may help uncover possible mechanisms of disease and may be complementary techniques to validate cellular changes and effects in a range of biological samples.

Finally I have investigated the anti-oxidant, anti-aggregation and chelation properties of a number of common polyphenols (Figure 6.1) and with future work investigating these compounds efficacy in activating sirtuins could provide promising results for the development of combination therapies targeting various pathways involved in AD such as oxidative stress, sirtuin activation, mitochondrial dysfunction and energy metabolism for use in transgenic animal models and/or human pilot clinical trials.

Ultimately, an efficient harnessing of the beneficial effects of the sirtuin pathway will certainly be of great therapeutic importance in the general population, where AD and ageing both suffer a lack of preventative measures. This work helps add further insight to the changes and distribution of mammalian sirtuins in the CNS during ageing and AD and some

of their potential targets within the brain, revealing evidence for novel roles for these proteins in the brain and revealing new pathways for future research.

References

Swomley, A. M. & Butterfield, D. A. Oxidative stress in Alzheimer disease and mild cognitive impairment: evidence from human data provided by redox proteomics. *Archives of toxicology* **89**, 1669-1680 (2015).

Serrano-Pozo, A., Frosch, M. P., Masliah, E. & Hyman, B. T. Neuropathological alterations in Alzheimer disease. *Cold Spring Harbor perspectives in medicine* **1**, a006189 (2011).

About a peculiar disease of the cerebral cortex. By Alois Alzheimer, 1907 (Translated by L. Jarvik and H. Greenson). *Alzheimer Dis Assoc Disord* **1**, 3-8 (1987).

Cipriani, G., Dolciotti, C., Picchi, L. & Bonuccelli, U. Alzheimer and his disease: a brief history. *Neurol Sci* **32**, 275-279 (2011).

Alzheimer, A., Stelzmann, R. A., Schnitzlein, H. N. & Murtagh, F. R. An English translation of Alzheimer's 1907 paper, "Über eine eigenartige Erkrankung der Hirnrinde". *Clinical anatomy* **8**, 429-431 (1995).

Maynard, C. J., Bush, A. I., Masters, C. L., Cappai, R. & Li, Q. X. Metals and amyloid-beta in Alzheimer's disease. *Int J Exp Pathol* **86**, 147-159 (2005).

Sayre, L. M. *et al.* In situ oxidative catalysis by neurofibrillary tangles and senile plaques in Alzheimer's disease: a central role for bound transition metals. *J Neurochem* **74**, 270-279 (2000).

Braid, N. *et al.* Metal and complementary molecular bioimaging in Alzheimer's disease. *Frontiers in aging neuroscience* **6**, 138 (2014).

Blessed, G., Tomlinson, B. E. & Roth, M. The association between quantitative measures of dementia and of senile change in the cerebral grey matter of elderly subjects. *The British journal of psychiatry : the journal of mental science* **114**, 797-811 (1968).

West, M. J., Coleman, P. D., Flood, D. G. & Troncoso, J. C. Differences in the pattern of hippocampal neuronal loss in normal ageing and Alzheimer's disease. *Lancet* **344**, 769-772 (1994).

Wang, J., Dickson, D. W., Trojanowski, J. Q. & Lee, V. M. The levels of soluble versus insoluble brain Abeta distinguish Alzheimer's disease from normal and pathologic aging. *Experimental neurology* **158**, 328-337 (1999).

Hyman, B. T., Van Hoesen, G. W., Damasio, A. R. & Barnes, C. L. Alzheimer's disease: cell-specific pathology isolates the hippocampal formation. *Science* **225**, 1168-1170 (1984).

Morris, J. C. & Price, J. L. Pathologic correlates of nondemented aging, mild cognitive impairment, and early-stage Alzheimer's disease. *Journal of molecular neuroscience : MN* **17**, 101-118 (2001).

Riedel, B. C., Thompson, P. M. & Brinton, R. D. Age, APOE and sex: Triad of risk of Alzheimer's disease. *The Journal of steroid biochemistry and molecular biology* **160**, 134-147 (2016).

Giri, M., Zhang, M. & Lu, Y. Genes associated with Alzheimer's disease: an overview and current status. *Clinical interventions in aging* **11**, 665-681 (2016).

Benjamin, R. *et al.* Protective effect of apoE epsilon 2 in Alzheimer's disease. *Lancet* **344**, 473 (1994).

Song, F. *et al.* Alzheimer's Disease: Genomics and Beyond. *International review of neurobiology* **121**, 1-24 (2015).

Lindbergh, C. A., Dishman, R. K. & Miller, L. S. Functional Disability in Mild Cognitive Impairment: A Systematic Review and Meta-Analysis. *Neuropsychology review* **26**, 129-159 (2016).

Raskin, J., Cummings, J., Hardy, J., Schuh, K. & Dean, R. A. Neurobiology of Alzheimer's Disease: Integrated Molecular, Physiological, Anatomical, Biomarker, and Cognitive Dimensions. *Curr Alzheimer Res* **12**, 712-722 (2015).

Barage, S. H. & Sonawane, K. D. Amyloid cascade hypothesis: Pathogenesis and therapeutic strategies in Alzheimer's disease. *Neuropeptides* **52**, 1-18 (2015).

Kulshreshtha, A. & Piplani, P. Current pharmacotherapy and putative disease-modifying therapy for Alzheimer's disease. *Neurol Sci* (2016).

Harman, D. Aging: a theory based on free radical and radiation chemistry. *J Gerontol* **11**, 298-300 (1956).

Smith, M. A. *et al.* Oxidative damage in Alzheimer's. *Nature* **382**, 120-121 (1996).

Harman, D. Free radical theory of aging: an update: increasing the functional life span. *Ann N Y Acad Sci* **1067**, 10-21 (2006).

Smith, M. A., Harris, P. L., Sayre, L. M. & Perry, G. Iron accumulation in Alzheimer disease is a source of redox-generated free radicals. *Proc Natl Acad Sci U S A* **94**, 9866-9868 (1997).

Butterfield, D. A. Amyloid beta-peptide (1-42)-induced oxidative stress and neurotoxicity: implications for neurodegeneration in Alzheimer's disease brain. A review. *Free Radic Res* **36**, 1307-1313 (2002).

Zambrano, C. A., Egana, J. T., Nunez, M. T., Maccioni, R. B. & Gonzalez-Billault, C. Oxidative stress promotes tau dephosphorylation in neuronal cells: the roles of cdk5 and PP1. *Free Radic Biol Med* **36**, 1393-1402 (2004).

Sultana, R., Perluigi, M. & Butterfield, D. A. Protein oxidation and lipid peroxidation in brain of subjects with Alzheimer's disease: insights into mechanism of neurodegeneration from redox proteomics. *Antioxid Redox Signal* **8**, 2021-2037 (2006).

Pratico, D. The neurobiology of isoprostanes and Alzheimer's disease. *Biochim Biophys Acta* **1801**, 930-933 (2010).

Pratico, D. & Delanty, N. Oxidative injury in diseases of the central nervous system: focus on Alzheimer's disease. *The American journal of medicine* **109**, 577-585 (2000).

Zarkovic, K. 4-hydroxynonenal and neurodegenerative diseases. *Mol Aspects Med* **24**, 293-303 (2003).

Roberts, L. J., 2nd *et al.* Formation of isoprostane-like compounds (neuroprostanes) in vivo from docosahexaenoic acid. *J Biol Chem* **273**, 13605-13612 (1998).

Hensley, K. *et al.* Brain regional correspondence between Alzheimer's disease histopathology and biomarkers of protein oxidation. *J Neurochem* **65**, 2146-2156 (1995).

Smith, M. A., Richey Harris, P. L., Sayre, L. M., Beckman, J. S. & Perry, G. Widespread peroxynitrite-mediated damage in Alzheimer's disease. *J Neurosci* **17**, 2653-2657 (1997).

Polidori, M. C. *et al.* Plasma antioxidant status, immunoglobulin g oxidation and lipid peroxidation in demented patients: relevance to Alzheimer disease and vascular dementia. *Dementia and geriatric cognitive disorders* **18**, 265-270 (2004).

Mecocci, P., MacGarvey, U. & Beal, M. F. Oxidative damage to mitochondrial DNA is increased in Alzheimer's disease. *Ann Neurol* **36**, 747-751 (1994).

Mecocci, P. *et al.* Oxidative damage to DNA in lymphocytes from AD patients. *Neurology* **51**, 1014-1017 (1998).

Lovell, M. A. & Markesbery, W. R. Oxidative DNA damage in mild cognitive impairment and late-stage Alzheimer's disease. *Nucleic acids research* **35**, 7497-7504 (2007).

Markesbery, W. R. & Lovell, M. A. DNA oxidation in Alzheimer's disease. *Antioxid Redox Signal* **8**, 2039-2045 (2006).

Davydov, V., Hansen, L. A. & Shackelford, D. A. Is DNA repair compromised in Alzheimer's disease? *Neurobiol Aging* **24**, 953-968 (2003).

Atwood, C. S. *et al.* Amyloid-beta: a chameleon walking in two worlds: a review of the trophic and toxic properties of amyloid-beta. *Brain Res Brain Res Rev* **43**, 1-16 (2003).

Roberts, B. R., Ryan, T. M., Bush, A. I., Masters, C. L. & Duce, J. A. The role of metallobiology and amyloid-beta peptides in Alzheimer's disease. *J Neurochem* **120 Suppl 1**, 149-166 (2012).

Perry, G. *et al.* Adventitiously-bound redox active iron and copper are at the center of oxidative damage in Alzheimer disease. *Biometals : an international journal on the role of metal ions in biology, biochemistry, and medicine* **16**, 77-81 (2003).

Connor, J. R. *et al.* Is hemochromatosis a risk factor for Alzheimer's disease? *J Alzheimers Dis* **3**, 471-477 (2001).

Egana, J. T., Zambrano, C., Nunez, M. T., Gonzalez-Billault, C. & Maccioni, R. B. Iron-induced oxidative stress modify tau phosphorylation patterns in hippocampal cell cultures. *Biometals : an international journal on the role of metal ions in biology, biochemistry, and medicine* **16**, 215-223 (2003).

Finkel, T. & Holbrook, N. J. Oxidants, oxidative stress and the biology of ageing. *Nature* **408**, 239-247 (2000).

Selman, C., Blount, J. D., Nussey, D. H. & Speakman, J. R. Oxidative damage, ageing, and life-history evolution: where now? *Trends in ecology & evolution* **27**, 570-577 (2012).

Grundman, M. Vitamin E and Alzheimer disease: the basis for additional clinical trials. *Am J Clin Nutr* **71**, 630S-636S (2000).

Baum, L. *et al.* Six-month randomized, placebo-controlled, double-blind, pilot clinical trial of curcumin in patients with Alzheimer disease. *Journal of clinical psychopharmacology* **28**, 110-113 (2008).

Butterfield, D. A., Griffin, S., Munch, G. & Pasinetti, G. M. Amyloid beta-peptide and amyloid pathology are central to the oxidative stress and inflammatory cascades under which Alzheimer's disease brain exists. *J Alzheimers Dis* **4**, 193-201 (2002).

Huang, X. *et al.* Alzheimer's disease, beta-amyloid protein and zinc. *J Nutr* **130**, 1488S-1492S (2000).

Kontush, A. *et al.* Amyloid-beta is an antioxidant for lipoproteins in cerebrospinal fluid and plasma. *Free Radic Biol Med* **30**, 119-128 (2001).

Gibson, G. E., Zhang, H., Sheu, K. R. & Park, L. C. Differential alterations in antioxidant capacity in cells from Alzheimer patients. *Biochim Biophys Acta* **1502**, 319-329 (2000).

Kontush, A., Donarski, N. & Beisiegel, U. Resistance of human cerebrospinal fluid to in vitro oxidation is directly related to its amyloid-beta content. *Free Radic Res* **35**, 507-517 (2001).

Pike, C. J., Walencewicz, A. J., Glabe, C. G. & Cotman, C. W. Aggregation-related toxicity of synthetic beta-amyloid protein in hippocampal cultures. *Eur J Pharmacol* **207**, 367-368 (1991).

Brera, B., Serrano, A. & de Ceballos, M. L. beta-amyloid peptides are cytotoxic to astrocytes in culture: a role for oxidative stress. *Neurobiol Dis* **7**, 395-405 (2000).

Malouf, A. T. Effect of beta amyloid peptides on neurons in hippocampal slice cultures. *Neurobiol Aging* **13**, 543-551 (1992).

Thinakaran, G. & Koo, E. H. Amyloid precursor protein trafficking, processing, and function. *J Biol Chem* **283**, 29615-29619 (2008).

Dahlgren, K. N. *et al.* Oligomeric and fibrillar species of amyloid-beta peptides differentially affect neuronal viability. *J Biol Chem* **277**, 32046-32053 (2002).

Marshall, K. E., Marchante, R., Xue, W. F. & Serpell, L. C. The relationship between amyloid structure and cytotoxicity. *Prion* **8** (2014).

Jana, M. K., Cappai, R. & Ciccotosto, G. D. Oligomeric Amyloid-beta Toxicity Can Be Inhibited by Blocking Its Cellular Binding in Cortical Neuronal Cultures with Addition of the Triphenylmethane Dye Brilliant Blue G. *ACS chemical neuroscience* (2016).

Godyn, J., Jonczyk, J., Panek, D. & Malawska, B. Therapeutic strategies for Alzheimer's disease in clinical trials. *Pharmacological reports : PR* **68**, 127-138 (2016).

Schenk, D. Amyloid-beta immunotherapy for Alzheimer's disease: the end of the beginning. *Nature reviews. Neuroscience* **3**, 824-828 (2002).

Nicoll, J. A. *et al.* Neuropathology of human Alzheimer disease after immunization with amyloid-beta peptide: a case report. *Nature medicine* **9**, 448-452 (2003).

Lemere, C. A. & Masliah, E. Can Alzheimer disease be prevented by amyloid-beta immunotherapy? *Nature reviews. Neurology* **6**, 108-119 (2010).

Ramanathan, A., Nelson, A. R., Sagare, A. P. & Zlokovic, B. V. Impaired vascular-mediated clearance of brain amyloid beta in Alzheimer's disease: the role, regulation and restoration of LRP1. *Frontiers in aging neuroscience* **7**, 136 (2015).

Ries, M. & Sastre, M. Mechanisms of Abeta Clearance and Degradation by Glial Cells. *Frontiers in aging neuroscience* **8**, 160 (2016).

Calsolaro, V. & Edison, P. Neuroinflammation in Alzheimer's disease: Current evidence and future directions. *Alzheimer's & dementia : the journal of the Alzheimer's Association* **12**, 719-732 (2016).

Roberts, G. W., Gentleman, S. M., Lynch, A. & Graham, D. I. beta A4 amyloid protein deposition in brain after head trauma. *Lancet* **338**, 1422-1423 (1991).

Miguel-Alvarez, M. *et al.* Non-steroidal anti-inflammatory drugs as a treatment for Alzheimer's disease: a systematic review and meta-analysis of treatment effect. *Drugs & aging* **32**, 139-147 (2015).

Teunissen, C. E. *et al.* Inflammation markers in relation to cognition in a healthy aging population. *J Neuroimmunol* **134**, 142-150 (2003).

Tan, Z. S. *et al.* Inflammatory markers and the risk of Alzheimer disease: the Framingham Study. *Neurology* **68**, 1902-1908 (2007).

Lue, L. F., Kuo, Y. M., Beach, T. & Walker, D. G. Microglia activation and anti-inflammatory regulation in Alzheimer's disease. *Molecular neurobiology* **41**, 115-128 (2010).

Strittmatter, W. J. *et al.* Apolipoprotein E: high-avidity binding to beta-amyloid and increased frequency of type 4 allele in late-onset familial Alzheimer disease. *Proc Natl Acad Sci U S A* **90**, 1977-1981 (1993).

Stoltzner, S. E. *et al.* Temporal accrual of complement proteins in amyloid plaques in Down's syndrome with Alzheimer's disease. *Am J Pathol* **156**, 489-499 (2000).

Singh, R., Barden, A., Mori, T. & Beilin, L. Advanced glycation end-products: a review. *Diabetologia* **44**, 129-146 (2001).

Jomova, K., Vondrakova, D., Lawson, M. & Valko, M. Metals, oxidative stress and neurodegenerative disorders. *Mol Cell Biochem* **345**, 91-104 (2010).

Abbott, N. J., Ronnback, L. & Hansson, E. Astrocyte-endothelial interactions at the blood-brain barrier. *Nature reviews. Neuroscience* **7**, 41-53 (2006).

Griffin, W. S. *et al.* Glial-neuronal interactions in Alzheimer's disease: the potential role of a 'cytokine cycle' in disease progression. *Brain pathology* **8**, 65-72 (1998).

Hoshino, T. *et al.* Involvement of prostaglandin E2 in production of amyloid-beta peptides both in vitro and in vivo. *J Biol Chem* **282**, 32676-32688 (2007).

Liang, X. *et al.* Deletion of the prostaglandin E2 EP2 receptor reduces oxidative damage and amyloid burden in a model of Alzheimer's disease. *J Neurosci* **25**, 10180-10187 (2005).

Franceschi, C. & Campisi, J. Chronic inflammation (inflammaging) and its potential contribution to age-associated diseases. *J Gerontol A Biol Sci Med Sci* **69 Suppl 1**, S4-9 (2014).

Franceschi, C. *et al.* Inflammaging and anti-inflammaging: a systemic perspective on aging and longevity emerged from studies in humans. *Mech Ageing Dev* **128**, 92-105 (2007).

Beal, M. F. Mitochondrial dysfunction in neurodegenerative diseases. *Biochim Biophys Acta* **1366**, 211-223 (1998).

Lin, M. T. & Beal, M. F. Mitochondrial dysfunction and oxidative stress in neurodegenerative diseases. *Nature* **443**, 787-795 (2006).

Wang, X. *et al.* Oxidative stress and mitochondrial dysfunction in Alzheimer's disease. *Biochim Biophys Acta* **1842**, 1240-1247 (2014).

Bhat, A. H. *et al.* Oxidative stress, mitochondrial dysfunction and neurodegenerative diseases; a mechanistic insight. *Biomedicine & pharmacotherapy = Biomedecine & pharmacotherapie* **74**, 101-110 (2015).

Cabezas-Opazo, F. A. *et al.* Mitochondrial Dysfunction Contributes to the Pathogenesis of Alzheimer's Disease. *Oxidative medicine and cellular longevity* **2015**, 509654 (2015).

Beal, M. F. Mitochondrial dysfunction and oxidative damage in Alzheimer's and Parkinson's diseases and coenzyme Q10 as a potential treatment. *Journal of bioenergetics and biomembranes* **36**, 381-386 (2004).

Massudi, H., Grant, R., Guillemin, G. J. & Braid, N. NAD⁺ metabolism and oxidative stress: the golden nucleotide on a crown of thorns. *Redox report : communications in free radical research* **17**, 28-46 (2012).

Raichle, M. E. & Gusnard, D. A. Appraising the brain's energy budget. *Proc Natl Acad Sci U S A* **99**, 10237-10239 (2002).

Bubber, P., Haroutunian, V., Fisch, G., Blass, J. P. & Gibson, G. E. Mitochondrial abnormalities in Alzheimer brain: mechanistic implications. *Ann Neurol* **57**, 695-703 (2005).

Baloyannis, S. J. Mitochondrial alterations in Alzheimer's disease. *J Alzheimers Dis* **9**, 119-126 (2006).

Wang, X. *et al.* Impaired balance of mitochondrial fission and fusion in Alzheimer's disease. *J Neurosci* **29**, 9090-9103 (2009).

Grady, C. L. *et al.* Longitudinal study of the early neuropsychological and cerebral metabolic changes in dementia of the Alzheimer type. *Journal of clinical and experimental neuropsychology* **10**, 576-596 (1988).

Mosconi, L., Pupi, A. & De Leon, M. J. Brain glucose hypometabolism and oxidative stress in preclinical Alzheimer's disease. *Ann N Y Acad Sci* **1147**, 180-195 (2008).

Starkov, A. A. An update on the role of mitochondrial alpha-ketoglutarate dehydrogenase in oxidative stress. *Molecular and cellular neurosciences* **55**, 13-16 (2013).

Sheu, K. F., Kim, Y. T., Blass, J. P. & Weksler, M. E. An immunochemical study of the pyruvate dehydrogenase deficit in Alzheimer's disease brain. *Ann Neurol* **17**, 444-449 (1985).

Gibson, G. E., Sheu, K. F. & Blass, J. P. Abnormalities of mitochondrial enzymes in Alzheimer disease. *Journal of neural transmission* **105**, 855-870 (1998).

Sims, N. R., Finegan, J. M. & Blass, J. P. Altered metabolic properties of cultured skin fibroblasts in Alzheimer's disease. *Ann Neurol* **21**, 451-457 (1987).

Gibson, G. E., Park, L. C., Zhang, H., Sorbi, S. & Calingasan, N. Y. Oxidative stress and a key metabolic enzyme in Alzheimer brains, cultured cells, and an animal model of chronic oxidative deficits. *Ann N Y Acad Sci* **893**, 79-94 (1999).

Manczak, M., Park, B. S., Jung, Y. & Reddy, P. H. Differential expression of oxidative phosphorylation genes in patients with Alzheimer's disease: implications for early mitochondrial dysfunction and oxidative damage. *Neuromolecular medicine* **5**, 147-162 (2004).

Kish, S. J. *et al.* Brain cytochrome oxidase in Alzheimer's disease. *J Neurochem* **59**, 776-779 (1992).

Calkins, M. J., Manczak, M., Mao, P., Shirendeb, U. & Reddy, P. H. Impaired mitochondrial biogenesis, defective axonal transport of mitochondria, abnormal mitochondrial dynamics and synaptic degeneration in a mouse model of Alzheimer's disease. *Hum Mol Genet* **20**, 4515-4529 (2011).

Wang, X. *et al.* Amyloid-beta overproduction causes abnormal mitochondrial dynamics via differential modulation of mitochondrial fission/fusion proteins. *Proc Natl Acad Sci U S A* **105**, 19318-19323 (2008).

Ozawa, T. Genetic and functional changes in mitochondria associated with aging. *Physiological reviews* **77**, 425-464 (1997).

Shigenaga, M. K., Hagen, T. M. & Ames, B. N. Oxidative damage and mitochondrial decay in aging. *Proc Natl Acad Sci U S A* **91**, 10771-10778 (1994).

Hirai, K. *et al.* Mitochondrial abnormalities in Alzheimer's disease. *J Neurosci* **21**, 3017-3023 (2001).

Corral-Debrinski, M. *et al.* Marked changes in mitochondrial DNA deletion levels in Alzheimer brains. *Genomics* **23**, 471-476 (1994).

Hoyer, S. Causes and consequences of disturbances of cerebral glucose metabolism in sporadic Alzheimer disease: therapeutic implications. *Advances in experimental medicine and biology* **541**, 135-152 (2004).

Crane, P. K. *et al.* Glucose levels and risk of dementia. *The New England journal of medicine* **369**, 540-548 (2013).

Butterfield, D. A., Di Domenico, F. & Barone, E. Elevated risk of type 2 diabetes for development of Alzheimer disease: a key role for oxidative stress in brain. *Biochim Biophys Acta* **1842**, 1693-1706 (2014).

De Felice, F. G. *et al.* Protection of synapses against Alzheimer's-linked toxins: insulin signaling prevents the pathogenic binding of Abeta oligomers. *Proc Natl Acad Sci U S A* **106**, 1971-1976 (2009).

Sultana, R., Perluigi, M. & Butterfield, D. A. Oxidatively modified proteins in Alzheimer's disease (AD), mild cognitive impairment and animal models of AD: role of Abeta in pathogenesis. *Acta neuropathologica* **118**, 131-150 (2009).

Terni, B., Boada, J., Portero-Otin, M., Pamplona, R. & Ferrer, I. Mitochondrial ATP-synthase in the entorhinal cortex is a target of oxidative stress at stages I/II of Alzheimer's disease pathology. *Brain pathology* **20**, 222-233 (2010).

Jayasena, T., Grant, R. S., Keerthisinghe, N., Solaja, I. & Smythe, G. A. Membrane permeability of redox active metal chelators: an important element in reducing hydroxyl radical induced NAD⁺ depletion in neuronal cells. *Neuroscience research* **57**, 454-461 (2007).

Bonda, D. J. *et al.* Nanoparticle delivery of transition-metal chelators to the brain: Oxidative stress will never see it coming! *CNS Neurol Disord Drug Targets* **11**, 81-85 (2012).

Finkelstein, D. I. *et al.* Clioquinol Improves Cognitive, Motor Function, and Microanatomy of the Alpha-Synuclein hA53T Transgenic Mice. *ACS chemical neuroscience* **7**, 119-129 (2016).

Mantyh, P. W. *et al.* Aluminum, iron, and zinc ions promote aggregation of physiological concentrations of beta-amyloid peptide. *J Neurochem* **61**, 1171-1174 (1993).

Baum, L. *et al.* Serum zinc is decreased in Alzheimer's disease and serum arsenic correlates positively with cognitive ability. *Biometals : an international journal on the role of metal ions in biology, biochemistry, and medicine* **23**, 173-179 (2010).

Deibel, M. A., Ehmann, W. D. & Markesbery, W. R. Copper, iron, and zinc imbalances in severely degenerated brain regions in Alzheimer's disease: possible relation to oxidative stress. *J Neurol Sci* **143**, 137-142 (1996).

Adlard, P. A., Parncutt, J. M., Finkelstein, D. I. & Bush, A. I. Cognitive loss in zinc transporter-3 knock-out mice: a phenocopy for the synaptic and memory deficits of Alzheimer's disease? *J Neurosci* **30**, 1631-1636 (2010).

Sindreu, C., Palmiter, R. D. & Storm, D. R. Zinc transporter ZnT-3 regulates presynaptic Erk1/2 signaling and hippocampus-dependent memory. *Proc Natl Acad Sci U S A* **108**, 3366-3370 (2011).

Bush, A. I. The metallobiology of Alzheimer's disease. *Trends in neurosciences* **26**, 207-214 (2003).

Zhang, L. H. *et al.* Altered expression and distribution of zinc transporters in APP/PS1 transgenic mouse brain. *Neurobiol Aging* **31**, 74-87 (2010).

Hoke, D. E. *et al.* In vitro gamma-secretase cleavage of the Alzheimer's amyloid precursor protein correlates to a subset of presenilin complexes and is inhibited by zinc. *FEBS J* **272**, 5544-5557 (2005).

Atwood, C. S. *et al.* Dramatic aggregation of Alzheimer abeta by Cu(II) is induced by conditions representing physiological acidosis. *J Biol Chem* **273**, 12817-12826 (1998).

Huang, X. *et al.* The A beta peptide of Alzheimer's disease directly produces hydrogen peroxide through metal ion reduction. *Biochemistry* **38**, 7609-7616 (1999).

Lovell, M. A., Robertson, J. D., Teesdale, W. J., Campbell, J. L. & Markesbery, W. R. Copper, iron and zinc in Alzheimer's disease senile plaques. *J Neurol Sci* **158**, 47-52 (1998).

Squitti, R. *et al.* Elevation of serum copper levels in Alzheimer's disease. *Neurology* **59**, 1153-1161 (2002).

Singh, I. *et al.* Low levels of copper disrupt brain amyloid-beta homeostasis by altering its production and clearance. *Proc Natl Acad Sci U S A* **110**, 14771-14776 (2013).

Finefrock, A. E., Bush, A. I. & Doraiswamy, P. M. Current status of metals as therapeutic targets in Alzheimer's disease. *Journal of the American Geriatrics Society* **51**, 1143-1148 (2003).

Dikalov, S. I., Vitek, M. P. & Mason, R. P. Cupric-amyloid beta peptide complex stimulates oxidation of ascorbate and generation of hydroxyl radical. *Free Radic Biol Med* **36**, 340-347 (2004).

Rogers, J. T. *et al.* An iron-responsive element type II in the 5'-untranslated region of the Alzheimer's amyloid precursor protein transcript. *J Biol Chem* **277**, 45518-45528 (2002).

Bartzokis, G. *et al.* MR evaluation of age-related increase of brain iron in young adult and older normal males. *Magnetic resonance imaging* **15**, 29-35 (1997).

Martin, W. R., Ye, F. Q. & Allen, P. S. Increasing striatal iron content associated with normal aging. *Movement disorders : official journal of the Movement Disorder Society* **13**, 281-286 (1998).

Schneider, S. A. Neurodegeneration with Brain Iron Accumulation. *Current neurology and neuroscience reports* **16**, 9 (2016).

Guo, C. *et al.* Intranasal deferroxamine reverses iron-induced memory deficits and inhibits amyloidogenic APP processing in a transgenic mouse model of Alzheimer's disease. *Neurobiol Aging* **34**, 562-575 (2013).

Blennow, K. & Hampel, H. CSF markers for incipient Alzheimer's disease. *Lancet Neurol* **2**, 605-613 (2003).

Hampel, H. *et al.* Core candidate neurochemical and imaging biomarkers of Alzheimer's disease. *Alzheimer's & dementia : the journal of the Alzheimer's Association* **4**, 38-48 (2008).

Zipser, B. D. *et al.* Microvascular injury and blood-brain barrier leakage in Alzheimer's disease. *Neurobiol Aging* **28**, 977-986 (2007).

Ha, M. & Kim, V. N. Regulation of microRNA biogenesis. *Nature reviews. Molecular cell biology* **15**, 509-524 (2014).

Schipper, H. M., Maes, O. C., Chertkow, H. M. & Wang, E. MicroRNA expression in Alzheimer blood mononuclear cells. *Gene regulation and systems biology* **1**, 263-274 (2007).

Geekiyanaage, H., Jicha, G. A., Nelson, P. T. & Chan, C. Blood serum miRNA: non-invasive biomarkers for Alzheimer's disease. *Experimental neurology* **235**, 491-496 (2012).

Villa, C. *et al.* Expression of the transcription factor Sp1 and its regulatory hsa-miR-29b in peripheral blood mononuclear cells from patients with Alzheimer's disease. *J Alzheimers Dis* **35**, 487-494 (2013).

Koyama, A. *et al.* Plasma amyloid-beta as a predictor of dementia and cognitive decline: a systematic review and meta-analysis. *Arch Neurol* **69**, 824-831 (2012).

Sun, Y. X. *et al.* Inflammatory markers in matched plasma and cerebrospinal fluid from patients with Alzheimer's disease. *Dementia and geriatric cognitive disorders* **16**, 136-144 (2003).

Laske, C. *et al.* Immune profiling in blood identifies sTNF-R1 performing comparably well as biomarker panels for classification of Alzheimer's disease patients. *J Alzheimers Dis* **34**, 367-375 (2013).

Weisman, D., Hakimian, E. & Ho, G. J. Interleukins, inflammation, and mechanisms of Alzheimer's disease. *Vitamins and hormones* **74**, 505-530 (2006).

Mastrangelo, M. A., Sudol, K. L., Narrow, W. C. & Bowers, W. J. Interferon- γ differentially affects Alzheimer's disease pathologies and induces neurogenesis in triple transgenic-AD mice. *Am J Pathol* **175**, 2076-2088 (2009).

O'Bryant, S. E. *et al.* Decreased C-reactive protein levels in Alzheimer disease. *Journal of geriatric psychiatry and neurology* **23**, 49-53 (2010).

Fu, H. *et al.* Complement component C3 and complement receptor type 3 contribute to the phagocytosis and clearance of fibrillar A β by microglia. *Glia* **60**, 993-1003 (2012).

Butterfield, D. A., Bader Lange, M. L. & Sultana, R. Involvements of the lipid peroxidation product, HNE, in the pathogenesis and progression of Alzheimer's disease. *Biochim Biophys Acta* **1801**, 924-929 (2010).

Padurariu, M. *et al.* Changes of some oxidative stress markers in the serum of patients with mild cognitive impairment and Alzheimer's disease. *Neurosci Lett* **469**, 6-10 (2010).

Conboy, I. M. *et al.* Rejuvenation of aged progenitor cells by exposure to a young systemic environment. *Nature* **433**, 760-764 (2005).

Villeda, S. A. *et al.* Young blood reverses age-related impairments in cognitive function and synaptic plasticity in mice. *Nature medicine* **20**, 659-663 (2014).

Villeda, S. A. & Wyss-Coray, T. The circulatory systemic environment as a modulator of neurogenesis and brain aging. *Autoimmunity reviews* **12**, 674-677 (2013).

Salah, N. *et al.* Polyphenolic flavanols as scavengers of aqueous phase radicals and as chain-breaking antioxidants. *Arch Biochem Biophys* **322**, 339-346 (1995).

Manach, C., Scalbert, A., Morand, C., Remesy, C. & Jimenez, L. Polyphenols: food sources and bioavailability. *Am J Clin Nutr* **79**, 727-747 (2004).

D'Archivio, M. *et al.* Polyphenols, dietary sources and bioavailability. *Ann Ist Super Sanita* **43**, 348-361 (2007).

Tsao, R. Chemistry and biochemistry of dietary polyphenols. *Nutrients* **2**, 1231-1246 (2010).

Lodovici, M. *et al.* Antioxidant and radical scavenging properties in vitro of polyphenolic extracts from red wine. *European journal of nutrition* **40**, 74-77 (2001).

Robak, J. & Gryglewski, R. J. Flavonoids are scavengers of superoxide anions. *Biochem Pharmacol* **37**, 837-841 (1988).

Brown, J. E., Khodr, H., Hider, R. C. & Rice-Evans, C. A. Structural dependence of flavonoid interactions with Cu²⁺ ions: implications for their antioxidant properties. *The Biochemical journal* **330 (Pt 3)**, 1173-1178 (1998).

Hider, R. C., Liu, Z. D. & Khodr, H. H. Metal chelation of polyphenols. *Methods in enzymology* **335**, 190-203 (2001).

Moridani, M. Y., Pourahmad, J., Bui, H., Siraki, A. & O'Brien, P. J. Dietary flavonoid iron complexes as cytoprotective superoxide radical scavengers. *Free Radic Biol Med* **34**, 243-253 (2003).

Cheng, I. F. & Breen, K. On the ability of four flavonoids, baicilin, luteolin, naringenin, and quercetin, to suppress the Fenton reaction of the iron-ATP complex. *Biometals : an international journal on the role of metal ions in biology, biochemistry, and medicine* **13**, 77-83 (2000).

Lopes, G. K., Schulman, H. M. & Hermes-Lima, M. Polyphenol tannic acid inhibits hydroxyl radical formation from Fenton reaction by complexing ferrous ions. *Biochim Biophys Acta* **1472**, 142-152 (1999).

Mandel, S. A. *et al.* Cell signaling pathways and iron chelation in the neurorestorative activity of green tea polyphenols: special reference to epigallocatechin gallate (EGCG). *J Alzheimers Dis* **15**, 211-222 (2008).

Mandel, S. A., Amit, T., Weinreb, O. & Youdim, M. B. Understanding the broad-spectrum neuroprotective action profile of green tea polyphenols in aging and neurodegenerative diseases. *J Alzheimers Dis* **25**, 187-208 (2011).

Mandel, S. A., Amit, T., Weinreb, O., Reznichenko, L. & Youdim, M. B. Simultaneous manipulation of multiple brain targets by green tea catechins: a potential neuroprotective strategy for Alzheimer and Parkinson diseases. *CNS Neurosci Ther* **14**, 352-365 (2008).

Pedrielli, P. & Skibsted, L. H. Antioxidant synergy and regeneration effect of quercetin, (-)-epicatechin, and (+)-catechin on alpha-tocopherol in homogeneous solutions of peroxidizing methyl linoleate. *J Agric Food Chem* **50**, 7138-7144 (2002).

Alvarez-Suarez, J. M. *et al.* Strawberry polyphenols attenuate ethanol-induced gastric lesions in rats by activation of antioxidant enzymes and attenuation of MDA increase. *PLoS One* **6**, e25878 (2011).

Frei, B. & Higdon, J. V. Antioxidant activity of tea polyphenols in vivo: evidence from animal studies. *J Nutr* **133**, 3275S-3284S (2003).

Lee, K. W. *et al.* Cocoa polyphenols inhibit phorbol ester-induced superoxide anion formation in cultured HL-60 cells and expression of cyclooxygenase-2 and activation of NF-kappaB and MAPKs in mouse skin in vivo. *J Nutr* **136**, 1150-1155 (2006).

Luceri, C., Caderni, G., Sanna, A. & Dolara, P. Red wine and black tea polyphenols modulate the expression of cyclooxygenase-2, inducible nitric oxide synthase and glutathione-related enzymes in azoxymethane-induced f344 rat colon tumors. *J Nutr* **132**, 1376-1379 (2002).

Luczaj, W., Waszkiewicz, E., Skrzydlewska, E. & Roszkowska-Jakimiec, W. Green tea protection against age-dependent ethanol-induced oxidative stress. *J Toxicol Environ Health A* **67**, 595-606 (2004).

Mandel, S. A., Amit, T., Kalfon, L., Reznichenko, L. & Youdim, M. B. Targeting multiple neurodegenerative diseases etiologies with multimodal-acting green tea catechins. *J Nutr* **138**, 1578S-1583S (2008).

Moskaug, J. O., Carlsen, H., Myhrstad, M. C. & Blomhoff, R. Polyphenols and glutathione synthesis regulation. *Am J Clin Nutr* **81**, 277S-283S (2005).

Sanbongi, C., Suzuki, N. & Sakane, T. Polyphenols in chocolate, which have antioxidant activity, modulate immune functions in humans in vitro. *Cellular immunology* **177**, 129-136 (1997).

Ono, K., Hasegawa, K., Naiki, H. & Yamada, M. Anti-amyloidogenic activity of tannic acid and its activity to destabilize Alzheimer's beta-amyloid fibrils in vitro. *Biochim Biophys Acta* **1690**, 193-202 (2004).

Ono, K. *et al.* Potent anti-amyloidogenic and fibril-destabilizing effects of polyphenols in vitro: implications for the prevention and therapeutics of Alzheimer's disease. *J Neurochem* **87**, 172-181 (2003).

Bieschke, J. *et al.* EGCG remodels mature alpha-synuclein and amyloid-beta fibrils and reduces cellular toxicity. *Proc Natl Acad Sci U S A* **107**, 7710-7715 (2010).

Giunta, B. *et al.* Fish oil enhances anti-amyloidogenic properties of green tea EGCG in Tg2576 mice. *Neuroscience letters* **471**, 134-138 (2010).

Mori, T. *et al.* Tannic acid is a natural beta-secretase inhibitor that prevents cognitive impairment and mitigates Alzheimer-like pathology in transgenic mice. *J Biol Chem* **287**, 6912-6927 (2012).

Rezai-Zadeh, K. *et al.* Green tea epigallocatechin-3-gallate (EGCG) modulates amyloid precursor protein cleavage and reduces cerebral amyloidosis in Alzheimer transgenic mice. *J Neurosci* **25**, 8807-8814 (2005).

Jena, S., Dandapat, J. & Chainy, G. B. Curcumin differentially regulates the expression of superoxide dismutase in cerebral cortex and cerebellum of L: -thyroxine (T(4))-induced hyperthyroid rat brain. *Neurol Sci* (2012).

Khurana, S., Jain, S., Mediratta, P. K., Banerjee, B. D. & Sharma, K. K. Protective role of curcumin on colchicine-induced cognitive dysfunction and oxidative stress in rats. *Hum Exp Toxicol* **31**, 686-697 (2012).

Huang, H. C., Chang, P., Dai, X. L. & Jiang, Z. F. Protective effects of curcumin on amyloid-beta-induced neuronal oxidative damage. *Neurochem Res* **37**, 1584-1597 (2012).

Lim, G. P. *et al.* The curry spice curcumin reduces oxidative damage and amyloid pathology in an Alzheimer transgenic mouse. *J Neurosci* **21**, 8370-8377 (2001).

Rezai-Zadeh, K. *et al.* Flavonoid-mediated presenilin-1 phosphorylation reduces Alzheimer's disease beta-amyloid production. *Journal of cellular and molecular medicine* **13**, 574-588 (2009).

Vepsalainen, S. *et al.* Anthocyanin-enriched bilberry and blackcurrant extracts modulate amyloid precursor protein processing and alleviate behavioral abnormalities in the APP/PS1 mouse model of Alzheimer's disease. *J Nutr Biochem* **24**, 360-370 (2013).

Ksiezak-Reding, H. *et al.* Ultrastructural alterations of Alzheimer's disease paired helical filaments by grape seed-derived polyphenols. *Neurobiol Aging* **33**, 1427-1439 (2012).

Santa-Maria, I. *et al.* GSPE interferes with tau aggregation in vivo: implication for treating tauopathy. *Neurobiol Aging* **33**, 2072-2081 (2012).

Wang, J. *et al.* Grape derived polyphenols attenuate tau neuropathology in a mouse model of Alzheimer's disease. *J Alzheimers Dis* **22**, 653-661 (2010).

Rezai-Zadeh, K. *et al.* Green tea epigallocatechin-3-gallate (EGCG) reduces beta-amyloid mediated cognitive impairment and modulates tau pathology in Alzheimer transgenic mice. *Brain Res* **1214**, 177-187 (2008).

Yao, J. *et al.* Molecular hairpin: a possible model for inhibition of tau aggregation by tannic acid. *Biochemistry* **52**, 1893-1902 (2013).

Schirmer, H. *et al.* Modulatory effect of resveratrol on SIRT1, SIRT3, SIRT4, PGC1alpha and NAMPT gene expression profiles in wild-type adult zebrafish liver. *Mol Biol Rep.*

Suzuki, K. & Koike, T. Resveratrol abolishes resistance to axonal degeneration in slow Wallerian degeneration (WldS) mice: activation of SIRT2, an NAD-dependent tubulin deacetylase. *Biochem Biophys Res Commun* **359**, 665-671 (2007).

Fernandez, A. F. & Fraga, M. F. The effects of the dietary polyphenol resveratrol on human healthy aging and lifespan. *Epigenetics* **6**.

Ladiwala, A. R. *et al.* Resveratrol selectively remodels soluble oligomers and fibrils of amyloid Abeta into off-pathway conformers. *J Biol Chem* **285**, 24228-24237.

Karuppagounder, S. S. *et al.* Dietary supplementation with resveratrol reduces plaque pathology in a transgenic model of Alzheimer's disease. *Neurochem Int* **54**, 111-118 (2009).

Mouchiroud, L., Molin, L., Dalliere, N. & Solari, F. Life span extension by resveratrol, rapamycin, and metformin: The promise of dietary restriction mimetics for a healthy aging. *Biofactors* **36**, 377-382.

Chandrashekara, K. T. & Shakarad, M. N. Aloe vera or Resveratrol Supplementation in Larval Diet Delays Adult Aging in the Fruit Fly, *Drosophila melanogaster*. *J Gerontol A Biol Sci Med Sci*.

Agarwal, B. & Baur, J. A. Resveratrol and life extension. *Ann N Y Acad Sci* **1215**, 138-143.

Pietsch, K., Saul, N., Menzel, R., Sturzenbaum, S. R. & Steinberg, C. E. Quercetin mediated lifespan extension in *Caenorhabditis elegans* is modulated by age-1, daf-2, sek-1 and unc-43. *Biogerontology* **10**, 565-578 (2009).

Howitz, K. T. *et al.* Small molecule activators of sirtuins extend *Saccharomyces cerevisiae* lifespan. *Nature* **425**, 191-196 (2003).

Ansari, M. A., Abdul, H. M., Joshi, G., Opii, W. O. & Butterfield, D. A. Protective effect of quercetin in primary neurons against Abeta(1-42): relevance to Alzheimer's disease. *J Nutr Biochem* **20**, 269-275 (2009).

Heo, H. J. & Lee, C. Y. Protective effects of quercetin and vitamin C against oxidative stress-induced neurodegeneration. *J Agric Food Chem* **52**, 7514-7517 (2004).

Belinha, I. *et al.* Quercetin increases oxidative stress resistance and longevity in *Saccharomyces cerevisiae*. *J Agric Food Chem* **55**, 2446-2451 (2007).

Chung, S. *et al.* Regulation of SIRT1 in cellular functions: role of polyphenols. *Arch Biochem Biophys* **501**, 79-90.

Zhang, C., Browne, A., Child, D. & Tanzi, R. E. Curcumin decreases amyloid-beta peptide levels by attenuating the maturation of amyloid-beta precursor protein. *J Biol Chem* **285**, 28472-28480.

Ahmed, T., Enam, S. A. & Gilani, A. H. Curcuminoids enhance memory in an amyloid-infused rat model of Alzheimer's disease. *Neuroscience* **169**, 1296-1306.

Lee, K. S. *et al.* Curcumin extends life span, improves health span, and modulates the expression of age-associated aging genes in *Drosophila melanogaster*. *Rejuvenation Res* **13**, 561-570.

Kitani, K., Osawa, T. & Yokozawa, T. The effects of tetrahydrocurcumin and green tea polyphenol on the survival of male C57BL/6 mice. *Biogerontology* **8**, 567-573 (2007).

Kim, J. K. *et al.* Protective effects of kaempferol (3,4',5,7-tetrahydroxyflavone) against amyloid beta peptide (A β)-induced neurotoxicity in ICR mice. *Biosci Biotechnol Biochem* **74**, 397-401.

Roth, A., Schaffner, W. & Hertel, C. Phytoestrogen kaempferol (3,4',5,7-tetrahydroxyflavone) protects PC12 and T47D cells from beta-amyloid-induced toxicity. *J Neurosci Res* **57**, 399-404 (1999).

Qu, W. *et al.* Kaempferol derivatives prevent oxidative stress-induced cell death in a DJ-1-dependent manner. *J Pharmacol Sci* **110**, 191-200 (2009).

Marfe, G. *et al.* Kaempferol induces apoptosis in two different cell lines via Akt inactivation, Bax and SIRT3 activation, and mitochondrial dysfunction. *J Cell Biochem* **106**, 643-650 (2009).

Nerurkar, P. V. *et al.* Momordica charantia (bitter melon) attenuates high-fat diet-associated oxidative stress and neuroinflammation. *J Neuroinflammation* **8**, 64.

Horax, R., Hettiarachchy, N., Over, K., Chen, P. & Gbur, E. Extraction, fractionation and characterization of bitter melon seed proteins. *J Agric Food Chem* **58**, 1892-1897.

Peng, C., Chan, H. Y., Huang, Y., Yu, H. & Chen, Z. Y. Apple polyphenols extend the mean lifespan of *Drosophila melanogaster*. *J Agric Food Chem* **59**, 2097-2106.

Sunagawa, T. *et al.* Procyanidins from apples (*Malus pumila* Mill.) extend the lifespan of *Caenorhabditis elegans*. *Planta Med* **77**, 122-127.

Xiang, L. *et al.* Anti-Aging Effects of Phloridzin, an Apple Polyphenol, on Yeast via the SOD and Sir2 Genes. *Biosci Biotechnol Biochem* **75**, 854-858.

Wang, P., Zhang, Z., Sun, Y., Liu, X. & Tong, T. The two isomers of HDTIC compounds from Astragali Radix slow down telomere shortening rate via attenuating oxidative stress and increasing DNA repair ability in human fetal lung diploid fibroblast cells. *DNA Cell Biol* **29**, 33-39.

Lei, H. *et al.* Anti-aging effect of astragalosides and its mechanism of action. *Acta Pharmacol Sin* **24**, 230-234 (2003).

Li, W., Yin, Y., Gong, H., Wu, G. & Zhu, F. [Protective effects of AST and ASI on memory impairment and its mechanism in senescent rats treated by GC]. *Zhongguo Zhong Yao Za Zhi* **34**, 199-203 (2009).

de Jesus, B. B. *et al.* The telomerase activator TA-65 elongates short telomeres and increases health span of adult/old mice without increasing cancer incidence. *Aging Cell* **10**, 604-621.

Tohda, C., Tamura, T., Matsuyama, S. & Komatsu, K. Promotion of axonal maturation and prevention of memory loss in mice by extracts of *Astragalus mongholicus*. *Br J Pharmacol* **149**, 532-541 (2006).

Weinreb, O., Mandel, S., Amit, T. & Youdim, M. B. Neurological mechanisms of green tea polyphenols in Alzheimer's and Parkinson's diseases. *J Nutr Biochem* **15**, 506-516 (2004).

Mandel, S., Weinreb, O., Amit, T. & Youdim, M. B. Cell signaling pathways in the neuroprotective actions of the green tea polyphenol (-)-epigallocatechin-3-gallate: implications for neurodegenerative diseases. *J Neurochem* **88**, 1555-1569 (2004).

Zhang, L., Jie, G., Zhang, J. & Zhao, B. Significant longevity-extending effects of EGCG on *Caenorhabditis elegans* under stress. *Free Radic Biol Med* **46**, 414-421 (2009).

Xu, Z. *et al.* Neuroprotective effects of (-)-epigallocatechin-3-gallate in a transgenic mouse model of amyotrophic lateral sclerosis. *Neurochem Res* **31**, 1263-1269 (2006).

Unno, K. *et al.* Daily consumption of green tea catechin delays memory regression in aged mice. *Biogerontology* **8**, 89-95 (2007).

Li, Y. M., Chan, H. Y., Yao, X. Q., Huang, Y. & Chen, Z. Y. Green tea catechins and broccoli reduce fat-induced mortality in *Drosophila melanogaster*. *J Nutr Biochem* **19**, 376-383 (2008).

Kumar, A., Prakash, A. & Dogra, S. Centella asiatica Attenuates D-Galactose-Induced Cognitive Impairment, Oxidative and Mitochondrial Dysfunction in Mice. *Int J Alzheimers Dis* **2011**, 347569.

Dhanasekaran, M. *et al.* Centella asiatica extract selectively decreases amyloid beta levels in hippocampus of Alzheimer's disease animal model. *Phytother Res* **23**, 14-19 (2009).

Veerendra Kumar, M. H. & Gupta, Y. K. Effect of Centella asiatica on cognition and oxidative stress in an intracerebroventricular streptozotocin model of Alzheimer's disease in rats. *Clin Exp Pharmacol Physiol* **30**, 336-342 (2003).

Haleagrahara, N. & Ponnusamy, K. Neuroprotective effect of Centella asiatica extract (CAE) on experimentally induced parkinsonism in aged Sprague-Dawley rats. *J Toxicol Sci* **35**, 41-47.

Mato, L. *et al.* Centella asiatica Improves Physical Performance and Health-related Quality of Life in Healthy Elderly Volunteer. *Evid Based Complement Alternat Med* (2009).

Shinomol, G. K. & Muralidhara. Effect of Centella asiatica leaf powder on oxidative markers in brain regions of prepubertal mice in vivo and its in vitro efficacy to ameliorate 3-NPA-induced oxidative stress in mitochondria. *Phytomedicine* (2008).

Hussin, M. *et al.* Modulation of lipid metabolism by Centella asiatica in oxidative stress rats. *J Food Sci* **74**, H72-78 (2009).

Wang, Y. H. & Du, G. H. Ginsenoside Rg1 inhibits beta-secretase activity in vitro and protects against A β -induced cytotoxicity in PC12 cells. *J Asian Nat Prod Res* **11**, 604-612 (2009).

Wang, Y. *et al.* Anti-neuroinflammation effect of ginsenoside Rb1 in a rat model of Alzheimer disease. *Neurosci Lett* **487**, 70-72.

Zhao, R. *et al.* Implication of phosphatidylinositol-3 kinase/Akt/glycogen synthase kinase-3 β pathway in ginsenoside Rb1's attenuation of beta-amyloid-induced neurotoxicity and tau phosphorylation. *J Ethnopharmacol* **133**, 1109-1116.

Shi, S., Shi, R. & Hashizume, K. American ginseng improves neurocognitive function in senescence-accelerated mice: Possible role of the upregulated insulin and choline acetyltransferase gene expression. *Geriatr Gerontol Int*.

Gong, L., Li, S. L., Li, H. & Zhang, L. Ginsenoside Rg1 protects primary cultured rat hippocampal neurons from cell apoptosis induced by beta-amyloid protein. *Pharm Biol* **49**, 501-507.

Zhao, H. F., Li, Q. & Li, Y. Long-term ginsenoside administration prevents memory loss in aged female C57BL/6J mice by modulating the redox status and up-regulating the plasticity-related proteins in hippocampus. *Neuroscience* **183**, 189-202.

Yi, S. W., Sull, J. W., Hong, J. S., Linton, J. A. & Ohrr, H. Association between ginseng intake and mortality: Kangwha cohort study. *J Altern Complement Med* **15**, 921-928 (2009).

Hurst, R. D. *et al.* Blueberry fruit polyphenolics suppress oxidative stress-induced skeletal muscle cell damage in vitro. *Mol Nutr Food Res* **54**, 353-363.

Papandreou, M. A. *et al.* Effect of a polyphenol-rich wild blueberry extract on cognitive performance of mice, brain antioxidant markers and acetylcholinesterase activity. *Behav Brain Res* **198**, 352-358 (2009).

Lau, F. C., Shukitt-Hale, B. & Joseph, J. A. The beneficial effects of fruit polyphenols on brain aging. *Neurobiol Aging* **26 Suppl 1**, 128-132 (2005).

Joseph, J. A., Shukitt-Hale, B. & Casadesus, G. Reversing the deleterious effects of aging on neuronal communication and behavior: beneficial properties of fruit polyphenolic compounds. *Am J Clin Nutr* **81**, 313S-316S (2005).

Wilson, M. A. *et al.* Blueberry polyphenols increase lifespan and thermotolerance in *Caenorhabditis elegans*. *Aging Cell* **5**, 59-68 (2006).

Joseph, J. A. *et al.* Differential protection among fractionated blueberry polyphenolic families against DA-, Abeta(42)- and LPS-induced decrements in Ca(2+) buffering in primary hippocampal cells. *J Agric Food Chem* **58**, 8196-8204.

Ono, K. *et al.* Effects of grape seed-derived polyphenols on amyloid beta-protein self-assembly and cytotoxicity. *J Biol Chem* **283**, 32176-32187 (2008).

Pfleger, C. M. *et al.* Grape-seed polyphenolic extract improves the eye phenotype in a *Drosophila* model of tauopathy. *Int J Alzheimers Dis* **2010**.

Thomas, P. *et al.* Grape seed polyphenols and curcumin reduce genomic instability events in a transgenic mouse model for Alzheimer's disease. *Mutat Res* **661**, 25-34 (2009).

Wang, J. *et al.* Grape-derived polyphenolics prevent Abeta oligomerization and attenuate cognitive deterioration in a mouse model of Alzheimer's disease. *J Neurosci* **28**, 6388-6392 (2008).

Wang, J. *et al.* Potential Application of Grape Derived Polyphenols in Huntington's Disease. *Transl Neurosci* **1**, 95-100.

Martorell, P. *et al.* Use of *Saccharomyces cerevisiae* and *Caenorhabditis elegans* as model organisms to study the effect of cocoa polyphenols in the resistance to oxidative stress. *J Agric Food Chem* **59**, 2077-2085.

Bisson, J. F. *et al.* Effects of long-term administration of a cocoa polyphenolic extract (Acticoa powder) on cognitive performances in aged rats. *Br J Nutr* **100**, 94-101 (2008).

Moongkarndi, P. *et al.* Protective effect of mangosteen extract against beta-amyloid-induced cytotoxicity, oxidative stress and altered proteome in SK-N-SH cells. *J Proteome Res* **9**, 2076-2086.

Wang, Y. *et al.* alpha-Mangostin, a polyphenolic xanthone derivative from mangosteen, attenuates beta-amyloid oligomers-induced neurotoxicity by inhibiting amyloid aggregation. *Neuropharmacology*.

Horio, Y., Hayashi, T., Kuno, A. & Kunimoto, R. Cellular and molecular effects of sirtuins in health and disease. *Clin Sci (Lond)* **121**, 191-203 (2011).

Yamamoto, H., Schoonjans, K. & Auwerx, J. Sirtuin functions in health and disease. *Mol Endocrinol* **21**, 1745-1755 (2007).

Wu, A., Ying, Z. & Gomez-Pinilla, F. Oxidative stress modulates Sir2alpha in rat hippocampus and cerebral cortex. *Eur J Neurosci* **23**, 2573-2580 (2006).

Brunet, A. *et al.* Stress-dependent regulation of FOXO transcription factors by the SIRT1 deacetylase. *Science* **303**, 2011-2015 (2004).

Wang, F., Nguyen, M., Qin, F. X. & Tong, Q. SIRT2 deacetylates FOXO3a in response to oxidative stress and caloric restriction. *Aging Cell* **6**, 505-514 (2007).

Qiu, X., Brown, K., Hirschey, M. D., Verdin, E. & Chen, D. Calorie restriction reduces oxidative stress by SIRT3-mediated SOD2 activation. *Cell Metab* **12**, 662-667 (2010).

Weir, H. J. *et al.* CNS SIRT3 expression is altered by reactive oxygen species and in Alzheimer's disease. *PLoS One* **7**, e48225 (2012).

Mao, Z. *et al.* SIRT6 promotes DNA repair under stress by activating PARP1. *Science* **332**, 1443-1446 (2011).

Donmez, G., Wang, D., Cohen, D. E. & Guarente, L. SIRT1 suppresses beta-amyloid production by activating the alpha-secretase gene ADAM10. *Cell* **142**, 320-332.

Kim, D. *et al.* SIRT1 deacetylase protects against neurodegeneration in models for Alzheimer's disease and amyotrophic lateral sclerosis. *EMBO J* **26**, 3169-3179 (2007).

Chen, J. *et al.* SIRT1 protects against microglia-dependent amyloid-beta toxicity through inhibiting NF-kappaB signaling. *J Biol Chem* **280**, 40364-40374 (2005).

Kao, C. L. *et al.* Resveratrol protects human endothelium from H₂O₂-induced oxidative stress and senescence via SirT1 activation. *J Atheroscler Thromb* **17**, 970-979.

Langley, E. *et al.* Human SIR2 deacetylates p53 and antagonizes PML/p53-induced cellular senescence. *EMBO J* **21**, 2383-2396 (2002).

Yeung, F. *et al.* Modulation of NF-kappaB-dependent transcription and cell survival by the SIRT1 deacetylase. *EMBO J* **23**, 2369-2380 (2004).

Michan, S. *et al.* SIRT1 is essential for normal cognitive function and synaptic plasticity. *J Neurosci* **30**, 9695-9707.

Julien, C. *et al.* Sirtuin 1 reduction parallels the accumulation of tau in Alzheimer disease. *J Neuropathol Exp Neurol* **68**, 48-58 (2009).

Qin, W. *et al.* Neuronal SIRT1 activation as a novel mechanism underlying the prevention of Alzheimer disease amyloid neuropathology by calorie restriction. *J Biol Chem* **281**, 21745-21754 (2006).

Cohen, D. E., Supinski, A. M., Bonkowski, M. S., Donmez, G. & Guarente, L. P. Neuronal SIRT1 regulates endocrine and behavioral responses to calorie restriction. *Genes Dev* **23**, 2812-2817 (2009).

Akieda-Asai, S. *et al.* SIRT1 Regulates Thyroid-Stimulating Hormone Release by Enhancing PIP5Kgamma Activity through Deacetylation of Specific Lysine Residues in Mammals. *PLoS One* **5**, e11755.

Li, Y., Xu, W., McBurney, M. W. & Longo, V. D. SirT1 inhibition reduces IGF-I/IRS-2/Ras/ERK1/2 signaling and protects neurons. *Cell Metab* **8**, 38-48 (2008).

Outeiro, T. F. *et al.* Sirtuin 2 inhibitors rescue alpha-synuclein-mediated toxicity in models of Parkinson's disease. *Science* **317**, 516-519 (2007).

Maxwell, M. M. *et al.* The Sirtuin 2 microtubule deacetylase is an abundant neuronal protein that accumulates in the aging CNS. *Hum Mol Genet* **20**, 3986-3996.

Suzuki, K. & Koike, T. Mammalian Sir2-related protein (SIRT) 2-mediated modulation of resistance to axonal degeneration in slow Wallerian degeneration mice: a crucial role of tubulin deacetylation. *Neuroscience* **147**, 599-612 (2007).

Li, W. *et al.* Sirtuin 2, a mammalian homolog of yeast silent information regulator-2 longevity regulator, is an oligodendroglial protein that decelerates cell differentiation through deacetylating alpha-tubulin. *J Neurosci* **27**, 2606-2616 (2007).

Harting, K. & Knoll, B. SIRT2-mediated protein deacetylation: An emerging key regulator in brain physiology and pathology. *Eur J Cell Biol* **89**, 262-269.

Taylor, D. M. *et al.* A brain-permeable small molecule reduces neuronal cholesterol by inhibiting activity of sirtuin 2 deacetylase. *ACS Chem Biol* **6**, 540-546.

Luthi-Carter, R. *et al.* SIRT2 inhibition achieves neuroprotection by decreasing sterol biosynthesis. *Proc Natl Acad Sci U S A* **107**, 7927-7932.

Beirowski, B. *et al.* Sir-two-homolog 2 (Sirt2) modulates peripheral myelination through polarity protein Par-3/atypical protein kinase C (aPKC) signaling. *Proc Natl Acad Sci U S A*.

Kim, S. H., Lu, H. F. & Alano, C. C. Neuronal Sirt3 protects against excitotoxic injury in mouse cortical neuron culture. *PLoS One* **6**, e14731.

Someya, S. *et al.* Sirt3 mediates reduction of oxidative damage and prevention of age-related hearing loss under caloric restriction. *Cell* **143**, 802-812.

Qiu, X., Brown, K., Hirschey, M. D., Verdin, E. & Chen, D. Calorie restriction reduces oxidative stress by SIRT3-mediated SOD2 activation. *Cell Metab* **12**, 662-667.

Bell, E. L. & Guarente, L. The SirT3 Divining Rod Points to Oxidative Stress. *Mol Cell* **42**, 561-568.

Rose, G. *et al.* Variability of the SIRT3 gene, human silent information regulator Sir2 homologue, and survivorship in the elderly. *Exp Gerontol* **38**, 1065-1070 (2003).

Halaschek-Wiener, J. *et al.* Genetic variation in healthy oldest-old. *PLoS One* **4**, e6641 (2009).

Hirschey, M. D. *et al.* SIRT3 regulates mitochondrial fatty-acid oxidation by reversible enzyme deacetylation. *Nature* **464**, 121-125.

Hafner, A. V. *et al.* Regulation of the mPTP by SIRT3-mediated deacetylation of CypD at lysine 166 suppresses age-related cardiac hypertrophy. *Aging (Albany NY)* **2**, 914-923.

Haigis, M. C. *et al.* SIRT4 inhibits glutamate dehydrogenase and opposes the effects of calorie restriction in pancreatic beta cells. *Cell* **126**, 941-954 (2006).

Nasrin, N. *et al.* SIRT4 regulates fatty acid oxidation and mitochondrial gene expression in liver and muscle cells. *J Biol Chem* **285**, 31995-32002.

Glorioso, C., Oh, S., Douillard, G. G. & Sibille, E. Brain molecular aging, promotion of neurological disease and modulation by Sirtuin5 longevity gene polymorphism. *Neurobiol Dis* **41**, 279-290.

Nakagawa, T., Lomb, D. J., Haigis, M. C. & Guarente, L. SIRT5 Deacetylates carbamoyl phosphate synthetase 1 and regulates the urea cycle. *Cell* **137**, 560-570 (2009).

Ogura, M. *et al.* Overexpression of SIRT5 confirms its involvement in deacetylation and activation of carbamoyl phosphate synthetase 1. *Biochem Biophys Res Commun* **393**, 73-78.

Schwer, B. *et al.* Neural sirtuin 6 (Sirt6) ablation attenuates somatic growth and causes obesity. *Proc Natl Acad Sci U S A* **107**, 21790-21794.

Mao, Z. *et al.* SIRT6 promotes DNA repair under stress by activating PARP1. *Science* **332**, 1443-1446.

Michishita, E. *et al.* SIRT6 is a histone H3 lysine 9 deacetylase that modulates telomeric chromatin. *Nature* **452**, 492-496 (2008).

Kawahara, T. L. *et al.* Dynamic chromatin localization of sirt6 shapes stress- and aging-related transcriptional networks. *PLoS Genet* **7**, e1002153.

Minagawa, S. *et al.* Accelerated epithelial cell senescence in IPF and the inhibitory role of SIRT6 in TGF-beta-induced senescence of human bronchial epithelial cells. *Am J Physiol Lung Cell Mol Physiol* **300**, L391-401.

Kawahara, T. L. *et al.* SIRT6 links histone H3 lysine 9 deacetylation to NF-kappaB-dependent gene expression and organismal life span. *Cell* **136**, 62-74 (2009).

Mostoslavsky, R. *et al.* Genomic instability and aging-like phenotype in the absence of mammalian SIRT6. *Cell* **124**, 315-329 (2006).

Vakhrusheva, O., Braeuer, D., Liu, Z., Braun, T. & Bober, E. Sirt7-dependent inhibition of cell growth and proliferation might be instrumental to mediate tissue integrity during aging. *J Physiol Pharmacol* **59 Suppl 9**, 201-212 (2008).

Ford, E. *et al.* Mammalian Sir2 homolog SIRT7 is an activator of RNA polymerase I transcription. *Genes Dev* **20**, 1075-1080 (2006).

Vakhrusheva, O. *et al.* Sirt7 increases stress resistance of cardiomyocytes and prevents apoptosis and inflammatory cardiomyopathy in mice. *Circ Res* **102**, 703-710 (2008).

Kaeberlein, M., McVey, M. & Guarente, L. The SIR2/3/4 complex and SIR2 alone promote longevity in *Saccharomyces cerevisiae* by two different mechanisms. *Genes Dev* **13**, 2570-2580 (1999).

Rogina, B. & Helfand, S. L. Sir2 mediates longevity in the fly through a pathway related to calorie restriction. *Proc Natl Acad Sci U S A* **101**, 15998-16003 (2004).

Tissenbaum, H. A. & Guarente, L. Increased dosage of a sir-2 gene extends lifespan in *Caenorhabditis elegans*. *Nature* **410**, 227-230 (2001).

Burnett, C. *et al.* Absence of effects of Sir2 overexpression on lifespan in *C. elegans* and *Drosophila*. *Nature* **477**, 482-485 (2011).

Crujeiras, A. B., Parra, D., Goyenechea, E. & Martinez, J. A. Sirtuin gene expression in human mononuclear cells is modulated by caloric restriction. *Eur J Clin Invest* **38**, 672-678 (2008).

Fontana, L., Meyer, T. E., Klein, S. & Holloszy, J. O. Long-term calorie restriction is highly effective in reducing the risk for atherosclerosis in humans. *Proc Natl Acad Sci U S A* **101**, 6659-6663 (2004).

Holloszy, J. O. & Fontana, L. Caloric restriction in humans. *Exp Gerontol* **42**, 709-712 (2007).

Omodei, D. & Fontana, L. Calorie restriction and prevention of age-associated chronic disease. *FEBS Lett* **585**, 1537-1542 (2011).

Fontana, L., Partridge, L. & Longo, V. D. Extending healthy life span--from yeast to humans. *Science* **328**, 321-326 (2010).

Lin, S. J., Ford, E., Haigis, M., Liszt, G. & Guarente, L. Calorie restriction extends yeast life span by lowering the level of NADH. *Genes Dev* **18**, 12-16 (2004).

Partridge, L., Piper, M. D. & Mair, W. Dietary restriction in Drosophila. *Mech Ageing Dev* **126**, 938-950 (2005).

Qin, W. *et al.* Calorie restriction attenuates Alzheimer's disease type brain amyloidosis in Squirrel monkeys (*Saimiri sciureus*). *J Alzheimers Dis* **10**, 417-422 (2006).

Witte, A. V., Fobker, M., Gellner, R., Knecht, S. & Floel, A. Caloric restriction improves memory in elderly humans. *Proc Natl Acad Sci U S A* **106**, 1255-1260 (2009).

Merry, B. J. Oxidative stress and mitochondrial function with aging--the effects of calorie restriction. *Aging Cell* **3**, 7-12 (2004).

Morgan, T. E., Wong, A. M. & Finch, C. E. Anti-inflammatory mechanisms of dietary restriction in slowing aging processes. *Interdiscip Top Gerontol* **35**, 83-97 (2007).

Patel, N. V. *et al.* Caloric restriction attenuates Abeta-deposition in Alzheimer transgenic models. *Neurobiol Aging* **26**, 995-1000 (2005).

Heilbronn, L. K. *et al.* Effect of 6-month calorie restriction on biomarkers of longevity, metabolic adaptation, and oxidative stress in overweight individuals: a randomized controlled trial. *JAMA* **295**, 1539-1548 (2006).

Lin, S. J. *et al.* Calorie restriction extends *Saccharomyces cerevisiae* lifespan by increasing respiration. *Nature* **418**, 344-348 (2002).

Mattson, M. P. Dietary factors, hormesis and health. *Ageing Res Rev* **7**, 43-48 (2008).

Schulz, T. J. *et al.* Glucose restriction extends *Caenorhabditis elegans* life span by inducing mitochondrial respiration and increasing oxidative stress. *Cell Metab* **6**, 280-293 (2007).

Li, X. & Kazgan, N. Mammalian sirtuins and energy metabolism. *Int J Biol Sci* **7**, 575-587 (2011).

Bordone, L. *et al.* SIRT1 transgenic mice show phenotypes resembling calorie restriction. *Aging Cell* **6**, 759-767 (2007).

Qin, W. *et al.* Regulation of forkhead transcription factor FoxO3a contributes to calorie restriction-induced prevention of Alzheimer's disease-type amyloid neuropathology and spatial memory deterioration. *Ann N Y Acad Sci* **1147**, 335-347 (2008).

Kojro, E. & Fahrenholz, F. The non-amyloidogenic pathway: structure and function of alpha-secretases. *Subcell Biochem* **38**, 105-127 (2005).

Donmez, G., Wang, D., Cohen, D. E. & Guarente, L. SIRT1 suppresses beta-amyloid production by activating the alpha-secretase gene ADAM10. *Cell* **142**, 320-332 (2010).

Thornton, E., Vink, R., Blumbergs, P. C. & Van Den Heuvel, C. Soluble amyloid precursor protein alpha reduces neuronal injury and improves functional outcome following diffuse traumatic brain injury in rats. *Brain Res* **1094**, 38-46 (2006).

Rardin, M. J. *et al.* Label-free quantitative proteomics of the lysine acetylome in mitochondria identifies substrates of SIRT3 in metabolic pathways. *Proc Natl Acad Sci U S A* **110**, 6601-6606 (2013).

Ahuja, N. *et al.* Regulation of insulin secretion by SIRT4, a mitochondrial ADP-ribosyltransferase. *J Biol Chem* **282**, 33583-33592 (2007).

Nasrin, N. *et al.* SIRT4 regulates fatty acid oxidation and mitochondrial gene expression in liver and muscle cells. *J Biol Chem* **285**, 31995-32002 (2010).

Nishida, Y. *et al.* SIRT5 Regulates both Cytosolic and Mitochondrial Protein Malonylation with Glycolysis as a Major Target. *Mol Cell* **59**, 321-332 (2015).

Cheng, A. *et al.* Mitochondrial SIRT3 Mediates Adaptive Responses of Neurons to Exercise and Metabolic and Excitatory Challenges. *Cell Metab* **23**, 128-142 (2016).

Someya, S. *et al.* Sirt3 mediates reduction of oxidative damage and prevention of age-related hearing loss under caloric restriction. *Cell* **143**, 802-812 (2010).

Liu, C. *et al.* Resveratrol improves neuron protection and functional recovery in rat model of spinal cord injury. *Brain Res* **1374**, 100-109 (2011).

Moriya, J. *et al.* Resveratrol improves hippocampal atrophy in chronic fatigue mice by enhancing neurogenesis and inhibiting apoptosis of granular cells. *Biol Pharm Bull* **34**, 354-359 (2011).

Narita, K., Hisamoto, M., Okuda, T. & Takeda, S. Differential neuroprotective activity of two different grape seed extracts. *PLoS One* **6**, e14575 (2011).

Baur, J. A. & Sinclair, D. A. Therapeutic potential of resveratrol: the in vivo evidence. *Nat Rev Drug Discov* **5**, 493-506 (2006).

Borra, M. T., Smith, B. C. & Denu, J. M. Mechanism of human SIRT1 activation by resveratrol. *J Biol Chem* **280**, 17187-17195 (2005).

Brown, V. A. *et al.* Repeat dose study of the cancer chemopreventive agent resveratrol in healthy volunteers: safety, pharmacokinetics, and effect on the insulin-like growth factor axis. *Cancer Res* **70**, 9003-9011 (2010).

Chandrashekara, K. T. & Shakarad, M. N. Aloe vera or resveratrol supplementation in larval diet delays adult aging in the fruit fly, *Drosophila melanogaster*. *J Gerontol A Biol Sci Med Sci* **66**, 965-971 (2011).

Dave, M. *et al.* The antioxidant resveratrol protects against chondrocyte apoptosis via effects on mitochondrial polarization and ATP production. *Arthritis Rheum* **58**, 2786-2797 (2008).

Lagouge, M. *et al.* Resveratrol improves mitochondrial function and protects against metabolic disease by activating SIRT1 and PGC-1 α . *Cell* **127**, 1109-1122 (2006).

Valenzano, D. R. *et al.* Resveratrol prolongs lifespan and retards the onset of age-related markers in a short-lived vertebrate. *Current biology : CB* **16**, 296-300 (2006).

Wood, J. G. *et al.* Sirtuin activators mimic caloric restriction and delay ageing in metazoans. *Nature* **430**, 686-689 (2004).

Kaeberlein, M. *et al.* Substrate-specific activation of sirtuins by resveratrol. *J Biol Chem* **280**, 17038-17045 (2005).

Miller, R. A. *et al.* Rapamycin, but not resveratrol or simvastatin, extends life span of genetically heterogeneous mice. *J Gerontol A Biol Sci Med Sci* **66**, 191-201 (2011).

Pearson, K. J. *et al.* Resveratrol delays age-related deterioration and mimics transcriptional aspects of dietary restriction without extending life span. *Cell Metab* **8**, 157-168 (2008).

Truelsen, T., Thudium, D. & Gronbaek, M. Amount and type of alcohol and risk of dementia: the Copenhagen City Heart Study. *Neurology* **59**, 1313-1319 (2002).

Mukhopadhyay, P. *et al.* Restoration of altered microRNA expression in the ischemic heart with resveratrol. *PLoS One* **5**, e15705 (2010).

Wang, H. *et al.* Resveratrol in cardiovascular disease: what is known from current research? *Heart Fail Rev* **17**, 437-448 (2012).

Chung, S. *et al.* Regulation of SIRT1 in cellular functions: role of polyphenols. *Arch Biochem Biophys* **501**, 79-90 (2010).

Pacholec, M. *et al.* SRT1720, SRT2183, SRT1460, and resveratrol are not direct activators of SIRT1. *J Biol Chem* **285**, 8340-8351 (2010).

Gertz, M. *et al.* A molecular mechanism for direct sirtuin activation by resveratrol. *PLoS One* **7**, e49761 (2012).

Guarente, L. Mitochondria--a nexus for aging, calorie restriction, and sirtuins? *Cell* **132**, 171-176 (2008).

Mukherjee, S., Lekli, I., Gurusamy, N., Bertelli, A. A. & Das, D. K. Expression of the longevity proteins by both red and white wines and their cardioprotective components, resveratrol, tyrosol, and hydroxytyrosol. *Free Radic Biol Med* **46**, 573-578 (2009).

Schirmer, H. *et al.* Modulatory effect of resveratrol on SIRT1, SIRT3, SIRT4, PGC1alpha and NAMPT gene expression profiles in wild-type adult zebrafish liver. *Mol Biol Rep* **39**, 3281-3289 (2012).

Rayalam, S., Yang, J. Y., Ambati, S., Della-Fera, M. A. & Baile, C. A. Resveratrol induces apoptosis and inhibits adipogenesis in 3T3-L1 adipocytes. *Phytother Res* **22**, 1367-1371 (2008).

Quideau, S. Plant "polyphenolic" small molecules can induce a calorie restriction-mimetic life-span extension by activating sirtuins: will "polyphenols" someday be used as chemotherapeutic drugs in Western medicine? *Chembiochem* **5**, 427-430 (2004).

Nerurkar, P. V. *et al.* Momordica charantia (bitter melon) attenuates high-fat diet-associated oxidative stress and neuroinflammation. *J Neuroinflammation* **8**, 64 (2011).

Arai, S. Studies on functional foods in Japan--state of the art. *Biosci Biotechnol Biochem* **60**, 9-15 (1996).

Li, Q. *et al.* Long-term green tea catechin administration prevents spatial learning and memory impairment in senescence-accelerated mouse prone-8 mice by decreasing Abeta1-42 oligomers and upregulating synaptic plasticity-related proteins in the hippocampus. *Neuroscience* **163**, 741-749 (2009).

Saul, N., Pietsch, K., Menzel, R., Sturzenbaum, S. R. & Steinberg, C. E. Catechin induced longevity in *C. elegans*: from key regulator genes to disposable soma. *Mech Ageing Dev* **130**, 477-486 (2009).

Mrak, R. E. & Griffin, W. S. Potential inflammatory biomarkers in Alzheimer's disease. *J Alzheimers Dis* **8**, 369-375 (2005).

Johnston, H., Boutin, H. & Allan, S. M. Assessing the contribution of inflammation in models of Alzheimer's disease. *Biochem Soc Trans* **39**, 886-890 (2011).

Santangelo, C. *et al.* Polyphenols, intracellular signalling and inflammation. *Ann Ist Super Sanita* **43**, 394-405 (2007).

Ahmed, S. *et al.* Green tea polyphenol epigallocatechin-3-gallate inhibits the IL-1 beta-induced activity and expression of cyclooxygenase-2 and nitric oxide synthase-2 in human chondrocytes. *Free Radic Biol Med* **33**, 1097-1105 (2002).

Bhardwaj, A. *et al.* Resveratrol inhibits proliferation, induces apoptosis, and overcomes chemoresistance through down-regulation of STAT3 and nuclear factor-kappaB-regulated antiapoptotic and cell survival gene products in human multiple myeloma cells. *Blood* **109**, 2293-2302 (2007).

Capiralla, H. *et al.* Resveratrol mitigates lipopolysaccharide- and Abeta-mediated microglial inflammation by inhibiting the TLR4/NF-kappaB/STAT signaling cascade. *J Neurochem* **120**, 461-472 (2012).

Khan, N., Afaq, F., Saleem, M., Ahmad, N. & Mukhtar, H. Targeting multiple signaling pathways by green tea polyphenol (-)-epigallocatechin-3-gallate. *Cancer Res* **66**, 2500-2505 (2006).

Xie, B., Shi, H., Chen, Q. & Ho, C. T. Antioxidant properties of fractions and polyphenol constituents from green, oolong and black teas. *Proceedings of the National Science Council, Republic of China. Part B, Life sciences* **17**, 77-84 (1993).

Rojanathammanee, L., Puig, K. L. & Combs, C. K. Pomegranate polyphenols and extract inhibit nuclear factor of activated T-cell activity and microglial activation in vitro and in a transgenic mouse model of Alzheimer disease. *J Nutr* **143**, 597-605 (2013).

Bastianetto, S., Krantic, S., Chabot, J. G. & Quirion, R. Possible involvement of programmed cell death pathways in the neuroprotective action of polyphenols. *Curr Alzheimer Res* **8**, 445-451 (2011).

Parihar, M. S. & Brewer, G. J. Mitochondrial failure in Alzheimer disease. *Am J Physiol Cell Physiol* **292**, C8-23 (2007).

Casley, C. S., Canevari, L., Land, J. M., Clark, J. B. & Sharpe, M. A. Beta-amyloid inhibits integrated mitochondrial respiration and key enzyme activities. *Journal of neurochemistry* **80**, 91-100 (2002).

Carrasco-Pozo, C., Mizgier, M. L., Speisky, H. & Gotteland, M. Differential protective effects of quercetin, resveratrol, rutin and epigallocatechin gallate against mitochondrial dysfunction induced by indomethacin in Caco-2 cells. *Chem Biol Interact* **195**, 199-205 (2012).

Carrasco-Pozo, C., Gotteland, M. & Speisky, H. Apple peel polyphenol extract protects against indomethacin-induced damage in Caco-2 cells by preventing mitochondrial complex I inhibition. *J Agric Food Chem* **59**, 11501-11508 (2011).

Long, J., Gao, H., Sun, L., Liu, J. & Zhao-Wilson, X. Grape extract protects mitochondria from oxidative damage and improves locomotor dysfunction and extends lifespan in a Drosophila Parkinson's disease model. *Rejuvenation Res* **12**, 321-331 (2009).

Dragicevic, N. *et al.* Green tea epigallocatechin-3-gallate (EGCG) and other flavonoids reduce Alzheimer's amyloid-induced mitochondrial dysfunction. *Journal of Alzheimer's disease : JAD* **26**, 507-521 (2011).

Panickar, K. S. & Anderson, R. A. Effect of polyphenols on oxidative stress and mitochondrial dysfunction in neuronal death and brain edema in cerebral ischemia. *Int J Mol Sci* **12**, 8181-8207 (2011).

Herbig, U., Jobling, W. A., Chen, B. P., Chen, D. J. & Sedivy, J. M. Telomere shortening triggers senescence of human cells through a pathway involving ATM, p53, and p21(CIP1), but not p16(INK4a). *Mol Cell* **14**, 501-513 (2004).

Cawthon, R. M., Smith, K. R., O'Brien, E., Sivatchenko, A. & Kerber, R. A. Association between telomere length in blood and mortality in people aged 60 years or older. *Lancet* **361**, 393-395 (2003).

Panosian, L. A. *et al.* Telomere shortening in T cells correlates with Alzheimer's disease status. *Neurobiol Aging* **24**, 77-84 (2003).

Takubo, K. *et al.* Changes of telomere length with aging. *Geriatr Gerontol Int* **10 Suppl 1**, S197-206 (2010).

Guan, J. Z. *et al.* A percentage analysis of the telomere length in Parkinson's disease patients. *J Gerontol A Biol Sci Med Sci* **63**, 467-473 (2008).

Kang, H. T., Lee, H. I. & Hwang, E. S. Nicotinamide extends replicative lifespan of human cells. *Aging Cell* **5**, 423-436 (2006).

Richards, J. B. *et al.* Homocysteine levels and leukocyte telomere length. *Atherosclerosis* **200**, 271-277 (2008).

Richards, J. B. *et al.* Higher serum vitamin D concentrations are associated with longer leukocyte telomere length in women. *Am J Clin Nutr* **86**, 1420-1425 (2007).

Xu, Q. *et al.* Multivitamin use and telomere length in women. *Am J Clin Nutr* **89**, 1857-1863 (2009).

Ornish, D. *et al.* Increased telomerase activity and comprehensive lifestyle changes: a pilot study. *Lancet Oncol* **9**, 1048-1057 (2008).

Uchiumi, F. *et al.* The effect of resveratrol on the Werner syndrome RecQ helicase gene and telomerase activity. *Curr Aging Sci* **4**, 1-7 (2011).

Chan, R., Woo, J., Suen, E., Leung, J. & Tang, N. Chinese tea consumption is associated with longer telomere length in elderly Chinese men. *Br J Nutr* **103**, 107-113 (2010).

- De Bacquer, D., Clays, E., Delanghe, J. & De Backer, G. Epidemiological evidence for an association between habitual tea consumption and markers of chronic inflammation. *Atherosclerosis* **189**, 428-435 (2006).
- Mirabello, L. *et al.* The association between leukocyte telomere length and cigarette smoking, dietary and physical variables, and risk of prostate cancer. *Aging Cell* **8**, 405-413 (2009).
- Sheng, R., Gu, Z. L. & Xie, M. L. Epigallocatechin gallate, the major component of polyphenols in green tea, inhibits telomere attrition mediated cardiomyocyte apoptosis in cardiac hypertrophy. *Int J Cardiol* (2011).
- Wang, P., Zhang, Z., Sun, Y., Liu, X. & Tong, T. The two isomers of HDTIC compounds from Astragali Radix slow down telomere shortening rate via attenuating oxidative stress and increasing DNA repair ability in human fetal lung diploid fibroblast cells. *DNA Cell Biol* **29**, 33-39 (2010).
- Bernardes de Jesus, B. *et al.* The telomerase activator TA-65 elongates short telomeres and increases health span of adult/old mice without increasing cancer incidence. *Aging Cell* **10**, 604-621 (2011).
- Palacios, J. A. *et al.* SIRT1 contributes to telomere maintenance and augments global homologous recombination. *J Cell Biol* **191**, 1299-1313 (2010).
- Narala, S. R. *et al.* SIRT1 acts as a nutrient-sensitive growth suppressor and its loss is associated with increased AMPK and telomerase activity. *Mol Biol Cell* **19**, 1210-1219 (2008).
- Barger, J. L., Kayo, T., Pugh, T. D., Prolla, T. A. & Weindruch, R. Short-term consumption of a resveratrol-containing nutraceutical mixture mimics gene expression of long-term caloric restriction in mouse heart. *Exp Gerontol* **43**, 859-866 (2008).
- Parachikova, A., Green, K. N., Hendrix, C. & LaFerla, F. M. Formulation of a medical food cocktail for Alzheimer's disease: beneficial effects on cognition and neuropathology in a mouse model of the disease. *PLoS One* **5**, e14015 (2010).
- Scheepens, A., Tan, K. & Paxton, J. W. Improving the oral bioavailability of beneficial polyphenols through designed synergies. *Genes Nutr* **5**, 75-87 (2010).
- Souto, E. B., Severino, P., Basso, R. & Santana, M. H. Encapsulation of antioxidants in gastrointestinal-resistant nanoparticulate carriers. *Methods Mol Biol* **1028**, 37-46 (2013).
- Doggui, S., Dao, L. & Ramassamy, C. Potential of drug-loaded nanoparticles for Alzheimer's disease: diagnosis, prevention and treatment. *Therapeutic delivery* **3**, 1025-1027 (2012).
- Sahni, J. K. *et al.* Neurotherapeutic applications of nanoparticles in Alzheimer's disease. *J Control Release* **152**, 208-231 (2011).
- Smith, A. *et al.* Nanolipidic particles improve the bioavailability and alpha-secretase inducing ability of epigallocatechin-3-gallate (EGCG) for the treatment of Alzheimer's disease. *Int J Pharm* **389**, 207-212 (2010).
- Smith, A. J., Kavuru, P., Wojtas, L., Zaworotko, M. J. & Shytle, R. D. Cocrystals of quercetin with improved solubility and oral bioavailability. *Molecular pharmaceuticals* **8**, 1867-1876 (2011).
- Haigis, M. C. & Sinclair, D. A. Mammalian sirtuins: biological insights and disease relevance. *Annu Rev Pathol* **5**, 253-295 (2010).
- Haigis, M. C. & Sinclair, D. A. Mammalian sirtuins: biological insights and disease relevance. *Annu Rev Pathol* **5**, 253-295.
- Gueguen, C., Palmier, B., Plotkine, M., Marchand-Leroux, C. & Besson, V. C. Neurological and histological consequences induced by in vivo cerebral oxidative stress: evidence for beneficial effects of SRT1720, a sirtuin 1 activator, and sirtuin 1-mediated neuroprotective effects of poly(ADP-ribose) polymerase inhibition. *PLoS One* **9**, e87367 (2014).
- Alcendor, R. R. *et al.* Sirt1 regulates aging and resistance to oxidative stress in the heart. *Circ Res* **100**, 1512-1521 (2007).

Lattanzio, F. *et al.* Human apolipoprotein E4 modulates the expression of Pin1, Sirtuin 1, and Presenilin 1 in brain regions of targeted replacement apoE mice. *Neuroscience* **256**, 360-369 (2014).

Wang, H. F., Li, Q., Feng, R. L. & Wen, T. Q. Transcription levels of sirtuin family in neural stem cells and brain tissues of adult mice. *Cellular and molecular biology Suppl.* **58**, OL1737-1743 (2012).

Kumar, R. *et al.* Sirtuin1: a promising serum protein marker for early detection of Alzheimer's disease. *PLoS One* **8**, e61560 (2013).

Kumar, R. *et al.* Identification of serum sirtuins as novel noninvasive protein markers for frailty. *Aging Cell* **13**, 975-980 (2014).

Ren, Y. *et al.* Effect of breed on the expression of Sirtuins (Sirt1-7) and antioxidant capacity in porcine brain. *Animal : an international journal of animal bioscience* **7**, 1994-1998 (2013).

Graff, J. *et al.* A dietary regimen of caloric restriction or pharmacological activation of SIRT1 to delay the onset of neurodegeneration. *J Neurosci* **33**, 8951-8960 (2013).

Pais, T. F. *et al.* The NAD-dependent deacetylase sirtuin 2 is a suppressor of microglial activation and brain inflammation. *EMBO J* **32**, 2603-2616 (2013).

Komlos, D. *et al.* Glutamate dehydrogenase 1 and SIRT4 regulate glial development. *Glia* **61**, 394-408 (2013).

Shih, J., Mason, A., Liu, L., Higashimori, H. & Donmez, G. Loss of SIRT4 decreases GLT-1-dependent glutamate uptake and increases sensitivity to kainic acid. *J Neurochem* (2014).

Glorioso, C., Oh, S., Douillard, G. G. & Sibille, E. Brain molecular aging, promotion of neurological disease and modulation by sirtuin 5 longevity gene polymorphism. *Neurobiol Dis* **41**, 279-290 (2011).

Favero, G., Rezzani, R. & Rodella, L. F. Sirtuin 6 nuclear localization at cortical brain level of young diabetic mice: An immunohistochemical study. *Acta histochemica* (2013).

Schwer, B. *et al.* Neural sirtuin 6 (Sirt6) ablation attenuates somatic growth and causes obesity. *Proc Natl Acad Sci U S A* **107**, 21790-21794 (2010).

Liszt, G., Ford, E., Kurtev, M. & Guarente, L. Mouse Sir2 homolog SIRT6 is a nuclear ADP-ribosyltransferase. *J Biol Chem* **280**, 21313-21320 (2005).

Toiber, D. *et al.* SIRT6 recruits SNF2H to DNA break sites, preventing genomic instability through chromatin remodeling. *Mol Cell* **51**, 454-468 (2013).

Zhong, L. & Mostoslavsky, R. SIRT6: a master epigenetic gatekeeper of glucose metabolism. *Transcription* **1**, 17-21 (2010).

Korner, S. *et al.* Differential sirtuin expression patterns in amyotrophic lateral sclerosis (ALS) postmortem tissue: neuroprotective or neurotoxic properties of sirtuins in ALS? *Neurodegenerative diseases* **11**, 141-152 (2013).

Hoppner, S., Schanzer, W. & Thevis, M. Mass spectrometric studies on the in vitro generated metabolites of SIRT1 activating drugs for doping control purposes. *Journal of mass spectrometry : JMS* **48**, 830-843 (2013).

Gatlin, C. L., Kleemann, G. R., Hays, L. G., Link, A. J. & Yates, J. R., 3rd. Protein identification at the low femtomole level from silver-stained gels using a new fritless electrospray interface for liquid chromatography-microspray and nanospray mass spectrometry. *Anal Biochem* **263**, 93-101 (1998).

Hou, X. *et al.* Cellular responses during morphological transformation in *Azospirillum brasilense* and its flcA knockout mutant. *PLoS One* **9**, e114435 (2014).

Coumans, J. V., Poljak, A., Raftery, M. J., Backhouse, D. & Pereg-Gerk, L. Analysis of cotton (*Gossypium hirsutum*) root proteomes during a compatible interaction with the black root rot fungus *Thielaviopsis basicola*. *Proteomics* **9**, 335-349 (2009).

Guillemin, G. J. *et al.* Characterization of the Kynurenine Pathway in Human Neurons. *J Neurosci* **27**, 12884-12892 (2007).

Guillemin, G. J. *et al.* Kynurenine pathway metabolism in human astrocytes: a paradox for neuronal protection. *J Neurochem* **78**, 1-13 (2001).

Simpson, R. *Proteins and Proteomics: A Laboratory Manual*. (Cold Spring Harbor Laboratory Press, 2002).

Muenchhoff, J. *et al.* Plasma protein profiling of mild cognitive impairment and Alzheimer's disease across two independent cohorts. *J Alzheimers Dis* **43**, 1355-1373 (2015).

Sheipouri, D. *et al.* Characterisation of the kynurenine pathway in skin-derived fibroblasts and keratinocytes. *Journal of cellular biochemistry* **116**, 903-922 (2015).

Wu, W. *et al.* Expression of tryptophan 2,3-dioxygenase and production of kynurenine pathway metabolites in triple transgenic mice and human Alzheimer's disease brain. *PLoS one* **8**, e59749 (2013).

Liebler, D. C. & Zimmerman, L. J. Targeted quantitation of proteins by mass spectrometry. *Biochemistry* **52**, 3797-3806 (2013).

Doerr, A. Mass spectrometry-based targeted proteomics. *Nature methods* **10**, 23 (2013).

Ji, S., Doucette, J. R. & Nazarali, A. J. Sirt2 is a novel in vivo downstream target of Nkx2.2 and enhances oligodendroglial cell differentiation. *Journal of molecular cell biology* **3**, 351-359 (2011).

Oh, C. L., E.; Lee YS.; Shin, DH. SIRT2 Protein Expression in Normal and Aged Rat Brain. *J Korean Geriatr Soc* **16**, 27-33 (2012).

Pandithage, R. *et al.* The regulation of SIRT2 function by cyclin-dependent kinases affects cell motility. *J Cell Biol* **180**, 915-929 (2008).

Luthi-Carter, R. *et al.* SIRT2 inhibition achieves neuroprotection by decreasing sterol biosynthesis. *Proc Natl Acad Sci U S A* **107**, 7927-7932 (2010).

Maxwell, M. M. *et al.* The Sirtuin 2 microtubule deacetylase is an abundant neuronal protein that accumulates in the aging CNS. *Hum Mol Genet* **20**, 3986-3996 (2011).

Jeong, H. *et al.* Sirt1 mediates neuroprotection from mutant huntingtin by activation of the TORC1 and CREB transcriptional pathway. *Nature medicine* **18**, 159-165 (2012).

Khan, R. S., Dine, K., Das Sarma, J. & Shindler, K. S. SIRT1 activating compounds reduce oxidative stress mediated neuronal loss in viral induced CNS demyelinating disease. *Acta neuropathologica communications* **2**, 3 (2014).

Satoh, A. *et al.* Sirt1 extends life span and delays aging in mice through the regulation of Nk2 homeobox 1 in the DMH and LH. *Cell Metab* **18**, 416-430 (2013).

Lu, C. T. *et al.* The potential of SIRT6 and SIRT7 as circulating markers for head and neck squamous cell carcinoma. *Anticancer research* **34**, 7137-7143 (2014).

Lee, N. *et al.* Comparative interactomes of SIRT6 and SIRT7: Implication of functional links to aging. *Proteomics* **14**, 1610-1622 (2014).

Iwahara, T., Bonasio, R., Narendra, V. & Reinberg, D. SIRT3 functions in the nucleus in the control of stress-related gene expression. *Molecular and cellular biology* **32**, 5022-5034 (2012).

Li, F. *et al.* NADP(+)-IDH Mutations Promote Hypersuccinylation that Impairs Mitochondria Respiration and Induces Apoptosis Resistance. *Mol Cell* **60**, 661-675 (2015).

Braidy, N. *et al.* Differential expression of sirtuins in the aging rat brain. *Frontiers in cellular neuroscience* **9**, 167 (2015).

Luna, B. *et al.* Proteomic and Mitochondrial Genomic Analyses of Pediatric Brain Tumors. *Molecular neurobiology* (2014).

Herskovits, A. Z. & Guarente, L. SIRT1 in neurodevelopment and brain senescence. *Neuron* **81**, 471-483 (2014).

Harting, K. & Knoll, B. SIRT2-mediated protein deacetylation: An emerging key regulator in brain physiology and pathology. *Eur J Cell Biol* **89**, 262-269 (2010).

Zhang, F. *et al.* Protective effects and mechanisms of sirtuins in the nervous system. *Prog Neurobiol* **95**, 373-395 (2011).

Donmez, G. & Outeiro, T. F. SIRT1 and SIRT2: emerging targets in neurodegeneration. *EMBO molecular medicine* **5**, 344-352 (2013).

Villalba, J. M. & Alcain, F. J. Sirtuin activators and inhibitors. *Biofactors* **38**, 349-359 (2012).

Zhu, Y. *et al.* Exploring the electrostatic repulsion model in the role of Sirt3 in directing MnSOD acetylation status and enzymatic activity. *Free Radic Biol Med* **53**, 828-833 (2012).

Wong, D. W., Soga, T. & Parhar, I. S. Aging and chronic administration of serotonin-selective reuptake inhibitor citalopram upregulate Sirt4 gene expression in the preoptic area of male mice. *Frontiers in genetics* **6**, 281 (2015).

Sibille, E. *et al.* Lack of serotonin1B receptor expression leads to age-related motor dysfunction, early onset of brain molecular aging and reduced longevity. *Molecular psychiatry* **12**, 1042-1056, 1975 (2007).

Zhong, L. *et al.* The histone deacetylase Sirt6 regulates glucose homeostasis via Hif1alpha. *Cell* **140**, 280-293 (2010).

Kawahara, T. L. *et al.* Dynamic chromatin localization of Sirt6 shapes stress- and aging-related transcriptional networks. *PLoS Genet* **7**, e1002153 (2011).

Li, L. *et al.* SIRT7 is a histone desuccinylase that functionally links to chromatin compaction and genome stability. *Nature communications* **7**, 12235 (2016).

Braid, N., Jayasena, T., Poljak, A. & Sachdev, P. S. Sirtuins in cognitive ageing and Alzheimer's disease. *Current opinion in psychiatry* **25**, 226-230 (2012).

Porquet, D. *et al.* Dietary resveratrol prevents Alzheimer's markers and increases life span in SAMP8. *Age* (2012).

Corpas, R. *et al.* SIRT1 Overexpression in Mouse Hippocampus Induces Cognitive Enhancement Through Proteostatic and Neurotrophic Mechanisms. *Molecular neurobiology* (2016).

Jayasena, T. *et al.* Application of Targeted Mass Spectrometry for the Quantification of Sirtuins in the Central Nervous System. *Scientific reports* **6**, 35391 (2016).

Simpson, R. J. Staining proteins in gels with coomassie blue. *CSH protocols* **2007**, pdb prot4719 (2007).

Huffaker, T. C., Thomas, J. H. & Botstein, D. Diverse effects of beta-tubulin mutations on microtubule formation and function. *J Cell Biol* **106**, 1997-2010 (1988).

dos Remedios, C. G. *et al.* Actin binding proteins: regulation of cytoskeletal microfilaments. *Physiological reviews* **83**, 433-473 (2003).

Molden, R. C., Bhanu, N. V., LeRoy, G., Arnaudo, A. M. & Garcia, B. A. Multi-faceted quantitative proteomics analysis of histone H2B isoforms and their modifications. *Epigenetics & chromatin* **8**, 15 (2015).

Walther, E. U. *et al.* Genomic sequences of aldolase C (Zebrafish II) direct lacZ expression exclusively in non-neuronal cells of transgenic mice. *Proc Natl Acad Sci U S A* **95**, 2615-2620 (1998).

Deber, C. M. & Reynolds, S. J. Central nervous system myelin: structure, function, and pathology. *Clinical biochemistry* **24**, 113-134 (1991).

Rosen, D. R. *et al.* Mutations in Cu/Zn superoxide dismutase gene are associated with familial amyotrophic lateral sclerosis. *Nature* **362**, 59-62 (1993).

Huang, S., Litt, M. & Felsenfeld, G. Methylation of histone H4 by arginine methyltransferase PRMT1 is essential in vivo for many subsequent histone modifications. *Genes Dev* **19**, 1885-1893 (2005).

Minarik, P., Tomaskova, N., Kollarova, M. & Antalík, M. Malate dehydrogenases--structure and function. *General physiology and biophysics* **21**, 257-265 (2002).

Hara, M. R. *et al.* S-nitrosylated GAPDH initiates apoptotic cell death by nuclear translocation following Siah1 binding. *Nature cell biology* **7**, 665-674 (2005).

- Devenish, R. J., Prescott, M., Roucou, X. & Nagley, P. Insights into ATP synthase assembly and function through the molecular genetic manipulation of subunits of the yeast mitochondrial enzyme complex. *Biochim Biophys Acta* **1458**, 428-442 (2000).
- Pickart, C. M. & Eddins, M. J. Ubiquitin: structures, functions, mechanisms. *Biochim Biophys Acta* **1695**, 55-72 (2004).
- Jarvis, R. M., Hughes, S. M. & Ledgerwood, E. C. Peroxiredoxin 1 functions as a signal peroxidase to receive, transduce, and transmit peroxide signals in mammalian cells. *Free Radic Biol Med* **53**, 1522-1530 (2012).
- Vizin, T. & Kos, J. Gamma-enolase: a well-known tumour marker, with a less-known role in cancer. *Radiology and oncology* **49**, 217-226 (2015).
- Neckers, L. & Ivy, S. P. Heat shock protein 90. *Current opinion in oncology* **15**, 419-424 (2003).
- Ibsen, K. H. Interrelationships and functions of the pyruvate kinase isozymes and their variant forms: a review. *Cancer Res* **37**, 341-353 (1977).
- Strange, R. C., Spiteri, M. A., Ramachandran, S. & Fryer, A. A. Glutathione-S-transferase family of enzymes. *Mutat Res* **482**, 21-26 (2001).
- Weir, H. J., Lane, J. D. & Balthasar, N. SIRT3: A Central Regulator of Mitochondrial Adaptation in Health and Disease. *Genes & cancer* **4**, 118-124 (2013).
- Lutz, M. I., Milenkovic, I., Regelsberger, G. & Kovacs, G. G. Distinct patterns of sirtuin expression during progression of Alzheimer's disease. *Neuromolecular medicine* **16**, 405-414 (2014).
- Yang, W. *et al.* Mitochondrial Sirt3 Expression is Decreased in APP/PS1 Double Transgenic Mouse Model of Alzheimer's Disease. *Neurochem Res* **40**, 1576-1582 (2015).
- Kim, S. H., Lu, H. F. & Alano, C. C. Neuronal Sirt3 protects against excitotoxic injury in mouse cortical neuron culture. *PLoS One* **6**, e14731 (2011).
- Agarwal, B. & Baur, J. A. Resveratrol and life extension. *Ann N Y Acad Sci* **1215**, 138-143 (2011).
- Liu, G. *et al.* Loss of NAD-Dependent Protein Deacetylase Sirtuin-2 Alters Mitochondrial Protein Acetylation and Dysregulates Mitophagy. *Antioxid Redox Signal* (2016).
- Law, I. K. *et al.* Identification and characterization of proteins interacting with SIRT1 and SIRT3: implications in the anti-aging and metabolic effects of sirtuins. *Proteomics* **9**, 2444-2456 (2009).
- Morales, I., Guzman-Martinez, L., Cerda-Troncoso, C., Farias, G. A. & Maccioni, R. B. Neuroinflammation in the pathogenesis of Alzheimer's disease. A rational framework for the search of novel therapeutic approaches. *Frontiers in cellular neuroscience* **8**, 112 (2014).
- Rojo, L. E., Fernandez, J. A., Maccioni, A. A., Jimenez, J. M. & Maccioni, R. B. Neuroinflammation: implications for the pathogenesis and molecular diagnosis of Alzheimer's disease. *Arch Med Res* **39**, 1-16 (2008).
- Brewer, G. J. & Ashford, J. W. Human serum stimulates Alzheimer markers in cultured hippocampal neurons. *J Neurosci Res* **33**, 355-369 (1992).
- Bradford, H. F. *et al.* Antibodies in serum of patients with Alzheimer's disease cause immunolysis of cholinergic nerve terminals from the rat cerebral cortex. *Can J Neurol Sci* **16**, 528-534 (1989).
- Hirayama, M., Lisak, R. P. & Silberberg, D. H. Serum-mediated oligodendrocyte cytotoxicity in multiple sclerosis patients and controls. *Neurology* **36**, 276-278 (1986).
- Ruijs TC, O. A., Antel JP. Serum cytotoxicity to human and rat oligodendrocytes in culture. *Brain Research* **517**, 99-104 (1990).
- Bradbury, K., Aparicio, S. R., Sumner, D. W. & Bird, C. C. Role of complement in demyelination in vitro by multiple sclerosis serum and other neurological disease sera. *J Neurol Sci* **65**, 293-305 (1984).

Ulrich, J. & Lardi, H. Multiple sclerosis: demyelination and myelination inhibition of organotypic tissue cultures of the spinal cord by sera of patients with multiple sclerosis and other neurological diseases. *J Neurol* **218**, 7-16 (1978).

Kumar, A. *et al.* Human serum from patients with septic shock activates transcription factors STAT1, IRF1, and NF-kappaB and induces apoptosis in human cardiac myocytes. *J Biol Chem* **280**, 42619-42626 (2005).

McKhann, G. *et al.* Clinical diagnosis of Alzheimer's disease: report of the NINCDS-ADRDA Work Group under the auspices of Department of Health and Human Services Task Force on Alzheimer's Disease. *Neurology* **34**, 939-944 (1984).

Sachdev, P. S. *et al.* The Sydney Memory and Ageing Study (MAS): methodology and baseline medical and neuropsychiatric characteristics of an elderly epidemiological non-demented cohort of Australians aged 70-90 years. *Int Psychogeriatr* **22**, 1248-1264 (2010).

Petersen, R. C. Mild cognitive impairment as a diagnostic entity. *J Intern Med* **256**, 183-194 (2004).

Atanassov, C. L. *et al.* Effect of ammonia on endocytosis and cytokine production by immortalized human microglia and astroglia cells. *Neurochem Int* **27**, 417-424 (1995).

Peudenier, S., Hery, C., Montagnier, L. & Tardieu, M. Human microglial cells: characterization in cerebral tissue and in primary culture, and study of their susceptibility to HIV-1 infection. *Ann Neurol* **29**, 152-161 (1991).

de Gannes, F. M., Merle, M., Canioni, P. & Voisin, P. J. Metabolic and cellular characterization of immortalized human microglial cells under heat stress. *Neurochem Int* **33**, 61-73 (1998).

Kemp, A. S., Vernon, J., Muller-Eberhard, H. J. & Bau, D. C. Complement C8 deficiency with recurrent meningococemia: examination of meningococcal opsonization. *Aust Paediatr J* **21**, 169-171 (1985).

Carmichael, J., DeGraff, W. G., Gazdar, A. F., Minna, J. D. & Mitchell, J. B. Evaluation of a tetrazolium-based semiautomated colorimetric assay: assessment of chemosensitivity testing. *Cancer Res* **47**, 936-942 (1987).

Kawada, K. *et al.* Comparison of chemosensitivity tests: clonogenic assay versus MTT assay. *Acta medica Okayama* **56**, 129-134 (2002).

Bernofsky, C. & Swan, M. An improved cycling assay for nicotinamide adenine dinucleotide. *Anal Biochem* **53**, 452-458 (1973).

Mitchell, D. B. & Acosta, D. Evaluation of the cytotoxicity of tricyclic antidepressants in primary cultures of rat hepatocytes. *Journal of toxicology and environmental health* **7**, 83-92 (1981).

Bhattacharya, R. & Tulsawani, R. In vitro and in vivo evaluation of various carbonyl compounds against cyanide toxicity with particular reference to alpha-ketoglutaric acid. *Drug and chemical toxicology* **31**, 149-161 (2008).

Zhang, X. *et al.* Cytotoxicity evaluation of three pairs of hexabromocyclododecane (HBCD) enantiomers on Hep G2 cell. *Toxicol In Vitro* **22**, 1520-1527 (2008).

Schuh, R. A. *et al.* Adaptation of microplate-based respirometry for hippocampal slices and analysis of respiratory capacity. *J Neurosci Res* **89**, 1979-1988 (2011).

Braidy, N. *et al.* Alpha-synuclein transmission and mitochondrial toxicity in primary human foetal enteric neurons in vitro. *Neurotoxicity research* **25**, 170-182 (2014).

Braidy, N. *et al.* Uptake and mitochondrial dysfunction of alpha-synuclein in human astrocytes, cortical neurons and fibroblasts. *Translational neurodegeneration* **2**, 20 (2013).

Pesta, D. & Gnaiger, E. High-resolution respirometry: OXPHOS protocols for human cells and permeabilized fibers from small biopsies of human muscle. *Methods Mol Biol* **810**, 25-58 (2012).

Searle, B. C. Scaffold: a bioinformatic tool for validating MS/MS-based proteomic studies. *Proteomics* **10**, 1265-1269 (2010).

Keller, A., Nesvizhskii, A. I., Kolker, E. & Aebersold, R. Empirical statistical model to estimate the accuracy of peptide identifications made by MS/MS and database search. *Anal Chem* **74**, 5383-5392 (2002).

Ishihama, Y. *et al.* Exponentially modified protein abundance index (emPAI) for estimation of absolute protein amount in proteomics by the number of sequenced peptides per protein. *Mol Cell Proteomics* **4**, 1265-1272 (2005).

Lim, Y. A. *et al.* Abeta and human amylin share a common toxicity pathway via mitochondrial dysfunction. *Proteomics* **10**, 1621-1633 (2010).

Song, F. *et al.* Plasma protein profiling of Mild Cognitive Impairment and Alzheimer's disease using iTRAQ quantitative proteomics. *Proteome science* **12**, 5 (2014).

Triglia, R. P. & Linscott, W. D. Titers of nine complement components, conglutinin and C3b-inactivator in adult and fetal bovine sera. *Mol Immunol* **17**, 741-748 (1980).

Rainard, P. Complement factor B and the alternative pathway of complement activation in bovine milk. *J Dairy Res* **69**, 1-12 (2002).

Defazio, G. *et al.* Parkinsonian serum carries complement-dependent toxicity for rat mesencephalic dopaminergic neurons in culture. *Brain Res* **633**, 206-212 (1994).

Agoropoulou, C., Wing, M. G. & Wood, A. CD59 expression and complement susceptibility of human neuronal cell line (NTERA2). *Neuroreport* **7**, 997-1004 (1996).

Starr, J. M., Farrall, A. J., Armitage, P., McGurn, B. & Wardlaw, J. Blood-brain barrier permeability in Alzheimer's disease: a case-control MRI study. *Psychiatry Res* **171**, 232-241 (2009).

Fonseca, M. I. *et al.* Treatment with a C5aR antagonist decreases pathology and enhances behavioral performance in murine models of Alzheimer's disease. *J Immunol* **183**, 1375-1383 (2009).

Shen, Y., Li, R., McGeer, E. G. & McGeer, P. L. Neuronal expression of mRNAs for complement proteins of the classical pathway in Alzheimer brain. *Brain Res* **769**, 391-395 (1997).

Rogers, J. *et al.* Complement activation by beta-amyloid in Alzheimer disease. *Proc Natl Acad Sci U S A* **89**, 10016-10020 (1992).

Singhrao, S. K., Neal, J. W., Rushmere, N. K., Morgan, B. P. & Gasque, P. Spontaneous classical pathway activation and deficiency of membrane regulators render human neurons susceptible to complement lysis. *Am J Pathol* **157**, 905-918 (2000).

Walker, D. G., Yasuhara, O., Patston, P. A., McGeer, E. G. & McGeer, P. L. Complement C1 inhibitor is produced by brain tissue and is cleaved in Alzheimer disease. *Brain Res* **675**, 75-82 (1995).

Yang, L. B., Li, R., Meri, S., Rogers, J. & Shen, Y. Deficiency of complement defense protein CD59 may contribute to neurodegeneration in Alzheimer's disease. *J Neurosci* **20**, 7505-7509 (2000).

McGeer, P. L. *et al.* Detection of the membrane inhibitor of reactive lysis (CD59) in diseased neurons of Alzheimer brain. *Brain Res* **544**, 315-319 (1991).

Haga, S., Ikeda, K., Sato, M. & Ishii, T. Synthetic Alzheimer amyloid beta/A4 peptides enhance production of complement C3 component by cultured microglial cells. *Brain Res* **601**, 88-94 (1993).

Shen, Y. *et al.* Complement activation by neurofibrillary tangles in Alzheimer's disease. *Neurosci Lett* **305**, 165-168 (2001).

Thambisetty, M. *et al.* Proteome-based identification of plasma proteins associated with hippocampal metabolism in early Alzheimer's disease. *J Neurol* **255**, 1712-1720 (2008).

Hye, A. *et al.* Proteome-based plasma biomarkers for Alzheimer's disease. *Brain* **129**, 3042-3050 (2006).

Akuffo, E. L. *et al.* The discovery and early validation of novel plasma biomarkers in mild-to-moderate Alzheimer's disease patients responding to treatment with rosiglitazone. *Biomarkers* **13**, 618-636 (2008).

Yasojima, K., Schwab, C., McGeer, E. G. & McGeer, P. L. Up-regulated production and activation of the complement system in Alzheimer's disease brain. *Am J Pathol* **154**, 927-936 (1999).

Tanskanen, M. *et al.* Cerebral amyloid angiopathy in a 95+ cohort: complement activation and apolipoprotein E (ApoE) genotype. *Neuropathol Appl Neurobiol* **31**, 589-599 (2005).

Kiddle, S. J. *et al.* Candidate blood proteome markers of Alzheimer's disease onset and progression: a systematic review and replication study. *J Alzheimers Dis* **38**, 515-531 (2014).

Thambisetty, M. *et al.* Plasma biomarkers of brain atrophy in Alzheimer's disease. *PLoS One* **6**, e28527 (2011).

Bennett, S. *et al.* Plasma levels of complement 4a protein are increased in Alzheimer's disease. *Alzheimer Dis Assoc Disord* **26**, 329-334 (2012).

Guntert, A. *et al.* Plasma gelsolin is decreased and correlates with rate of decline in Alzheimer's disease. *J Alzheimers Dis* **21**, 585-596 (2010).

Zhang, R. *et al.* Mining biomarkers in human sera using proteomic tools. *Proteomics* **4**, 244-256 (2004).

Lee, J. W. *et al.* Fibrinogen gamma-A chain precursor in CSF: a candidate biomarker for Alzheimer's disease. *BMC Neurol* **7**, 14 (2007).

van Oijen, M., Witteman, J. C., Hofman, A., Koudstaal, P. J. & Breteler, M. M. Fibrinogen is associated with an increased risk of Alzheimer disease and vascular dementia. *Stroke* **36**, 2637-2641 (2005).

Jung, S. M. *et al.* Both plasma retinol-binding protein and haptoglobin precursor allele 1 in CSF: candidate biomarkers for the progression of normal to mild cognitive impairment to Alzheimer's disease. *Neurosci Lett* **436**, 153-157 (2008).

Johnson, G. *et al.* Cerebrospinal fluid protein variations in common to Alzheimer's disease and schizophrenia. *Appl Theor Electrophor* **3**, 47-53 (1992).

Castano, E. M., Roher, A. E., Esh, C. L., Kokjohn, T. A. & Beach, T. Comparative proteomics of cerebrospinal fluid in neuropathologically-confirmed Alzheimer's disease and non-demented elderly subjects. *Neurol Res* **28**, 155-163 (2006).

Yu, H. L., Chertkow, H. M., Bergman, H. & Schipper, H. M. Aberrant profiles of native and oxidized glycoproteins in Alzheimer plasma. *Proteomics* **3**, 2240-2248 (2003).

Arai, T., Miklossy, J., Klegeris, A., Guo, J. P. & McGeer, P. L. Thrombin and prothrombin are expressed by neurons and glial cells and accumulate in neurofibrillary tangles in Alzheimer disease brain. *J Neuropathol Exp Neurol* **65**, 19-25 (2006).

Grammas, P., Samany, P. G. & Thirumangalakudi, L. Thrombin and inflammatory proteins are elevated in Alzheimer's disease microvessels: implications for disease pathogenesis. *J Alzheimers Dis* **9**, 51-58 (2006).

Akiyama, H., Ikeda, K., Kondo, H. & McGeer, P. L. Thrombin accumulation in brains of patients with Alzheimer's disease. *Neurosci Lett* **146**, 152-154 (1992).

Puchades, M. *et al.* Proteomic studies of potential cerebrospinal fluid protein markers for Alzheimer's disease. *Brain Res Mol Brain Res* **118**, 140-146 (2003).

Davidsson, P. *et al.* Proteome analysis of cerebrospinal fluid proteins in Alzheimer patients. *Neuroreport* **13**, 611-615 (2002).

Trouw, L. A. *et al.* C4b-binding protein in Alzheimer's disease: binding to Abeta1-42 and to dead cells. *Mol Immunol* **45**, 3649-3660 (2008).

Howard, J. & Pilkington, G. J. Antibodies to fibronectin bind to plaques and other structures in Alzheimer's disease and control brain. *Neurosci Lett* **118**, 71-76 (1990).

- Moreno-Flores, M. T., Martin-Aparicio, E., Salinero, O. & Wandosell, F. Fibronectin modulation by A beta amyloid peptide (25-35) in cultured astrocytes of newborn rat cortex. *Neurosci Lett* **314**, 87-91 (2001).
- Paul, J., Strickland, S. & Melchor, J. P. Fibrin deposition accelerates neurovascular damage and neuroinflammation in mouse models of Alzheimer's disease. *J Exp Med* **204**, 1999-2008 (2007).
- Vlassenko, A. G. *et al.* Spatial correlation between brain aerobic glycolysis and amyloid-beta (Abeta) deposition. *Proc Natl Acad Sci U S A* **107**, 17763-17767 (2010).
- Powers, W. J., Rosenbaum, J. L., Dence, C. S., Markham, J. & Videen, T. O. Cerebral glucose transport and metabolism in preterm human infants. *Journal of cerebral blood flow and metabolism : official journal of the International Society of Cerebral Blood Flow and Metabolism* **18**, 632-638 (1998).
- Wirth, M. *et al.* Associations between Alzheimer disease biomarkers, neurodegeneration, and cognition in cognitively normal older people. *JAMA neurology* **70**, 1512-1519 (2013).
- Ossenkopp, R. *et al.* Is Verbal Episodic Memory in Elderly with Amyloid Deposits Preserved Through Altered Neuronal Function? *Cerebral cortex* (2013).
- Liang, W. S. *et al.* Alzheimer's disease is associated with reduced expression of energy metabolism genes in posterior cingulate neurons. *Proc Natl Acad Sci U S A* **105**, 4441-4446 (2008).
- Bigl, M., Bruckner, M. K., Arendt, T., Bigl, V. & Eschrich, K. Activities of key glycolytic enzymes in the brains of patients with Alzheimer's disease. *Journal of neural transmission* **106**, 499-511 (1999).
- Blalock, E. M. *et al.* Incipient Alzheimer's disease: microarray correlation analyses reveal major transcriptional and tumor suppressor responses. *Proc Natl Acad Sci U S A* **101**, 2173-2178 (2004).
- Velliquette, R. A., O'Connor, T. & Vassar, R. Energy inhibition elevates beta-secretase levels and activity and is potentially amyloidogenic in APP transgenic mice: possible early events in Alzheimer's disease pathogenesis. *J Neurosci* **25**, 10874-10883 (2005).
- Newington, J. T. *et al.* Overexpression of pyruvate dehydrogenase kinase 1 and lactate dehydrogenase A in nerve cells confers resistance to amyloid beta and other toxins by decreasing mitochondrial respiration and reactive oxygen species production. *J Biol Chem* **287**, 37245-37258 (2012).
- Korolainen, M. A. *et al.* Oxidative modification of proteins in the frontal cortex of Alzheimer's disease brain. *Neurobiol Aging* **27**, 42-53 (2006).
- Di Domenico, F. *et al.* Redox proteomics analysis of HNE-modified proteins in Down syndrome brain: clues for understanding the development of Alzheimer disease. *Free Radic Biol Med* **71**, 270-280 (2014).
- Mocali, A. *et al.* Altered proteolysis in fibroblasts of Alzheimer patients with predictive implications for subjects at risk of disease. *Int J Alzheimers Dis* **2014**, 520152 (2014).
- Krako, N. *et al.* Characterization of mitochondrial dysfunction in the 7PA2 cell model of Alzheimer's disease. *J Alzheimers Dis* **37**, 747-758 (2013).
- Newington, J. T., Harris, R. A. & Cumming, R. C. Reevaluating Metabolism in Alzheimer's Disease from the Perspective of the Astrocyte-Neuron Lactate Shuttle Model. *Journal of Neurodegenerative Diseases* **2013**, 13 (2013).
- Bouras, C., Hof, P. R., Giannakopoulos, P., Michel, J. P. & Morrison, J. H. Regional distribution of neurofibrillary tangles and senile plaques in the cerebral cortex of elderly patients: a quantitative evaluation of a one-year autopsy population from a geriatric hospital. *Cerebral cortex* **4**, 138-150 (1994).
- Price, J. L. & Morris, J. C. Tangles and plaques in nondemented aging and "preclinical" Alzheimer's disease. *Ann Neurol* **45**, 358-368 (1999).

Andreu, C. I., Woehlbier, U., Torres, M. & Hetz, C. Protein disulfide isomerases in neurodegeneration: from disease mechanisms to biomedical applications. *FEBS Lett* **586**, 2826-2834 (2012).

Voloboueva, L. A., Emery, J. F., Sun, X. & Giffard, R. G. Inflammatory response of microglial BV-2 cells includes a glycolytic shift and is modulated by mitochondrial glucose-regulated protein 75/mortalin. *FEBS Lett* **587**, 756-762 (2013).

Harrison, P. J. *et al.* Heat shock protein (hsx70) mRNA expression in human brain: effects of neurodegenerative disease and agonal state. *Neuropathology and applied neurobiology* **19**, 10-21 (1993).

Hamos, J. E. *et al.* Expression of heat shock proteins in Alzheimer's disease. *Neurology* **41**, 345-350 (1991).

Perri, E., Parakh, S. & Atkin, J. Protein Disulphide Isomerases: emerging roles of PDI and ERp57 in the nervous system and as therapeutic targets for ALS. *Expert opinion on therapeutic targets*, 1-13 (2016).

Parakh, S. & Atkin, J. D. Novel roles for protein disulphide isomerase in disease states: a double edged sword? *Frontiers in cell and developmental biology* **3**, 30 (2015).

Hoffstrom, B. G. *et al.* Inhibitors of protein disulfide isomerase suppress apoptosis induced by misfolded proteins. *Nature chemical biology* **6**, 900-906 (2010).

Tsukita, S., Yonemura, S. & Tsukita, S. ERM proteins: head-to-tail regulation of actin-plasma membrane interaction. *Trends in biochemical sciences* **22**, 53-58 (1997).

Solinet, S. *et al.* The actin-binding ERM protein Moesin binds to and stabilizes microtubules at the cell cortex. *J Cell Biol* **202**, 251-260 (2013).

Liu, T. F. *et al.* Fueling the flame: bioenergy couples metabolism and inflammation. *Journal of leukocyte biology* **92**, 499-507 (2012).

Gut, P. & Verdin, E. The nexus of chromatin regulation and intermediary metabolism. *Nature* **502**, 489-498 (2013).

Barnum, S. R. Complement biosynthesis in the central nervous system. *Crit Rev Oral Biol Med* **6**, 132-146 (1995).

Maffioletti, E., Tardito, D., Gennarelli, M. & Bocchio-Chiavetto, L. Micro spies from the brain to the periphery: new clues from studies on microRNAs in neuropsychiatric disorders. *Frontiers in cellular neuroscience* **8**, 75 (2014).

Lau, P., Sala Frigerio, C. & De Strooper, B. Variance in the identification of microRNAs deregulated in Alzheimer's disease and possible role of lincRNAs in the pathology: The need of larger datasets. *Ageing Res Rev* (2014).

Francioso, A. *et al.* beta-sheet interfering molecules acting against beta-amyloid aggregation and fibrillogenesis. *Bioorg Med Chem* **23**, 1671-1683 (2015).

Barthel, H., Seibyl, J. & Sabri, O. The role of positron emission tomography imaging in understanding Alzheimer's disease. *Expert review of neurotherapeutics* **15**, 395-406 (2015).

Vassar, R. BACE1 inhibitor drugs in clinical trials for Alzheimer's disease. *Alzheimer's research & therapy* **6**, 89 (2014).

Wilkins, H. M. & Swerdlow, R. H. Amyloid precursor protein processing and bioenergetics. *Brain research bulletin* (2016).

Sakono, M. & Zako, T. Amyloid oligomers: formation and toxicity of Abeta oligomers. *FEBS J* **277**, 1348-1358 (2010).

Nguyen, K. V. The human beta-amyloid precursor protein: biomolecular and epigenetic aspects. *Biomolecular concepts* **6**, 11-32 (2015).

Kim, H. J. *et al.* Selective neuronal degeneration induced by soluble oligomeric amyloid beta protein. *FASEB J* **17**, 118-120 (2003).

Ferreira, S. T., Vieira, M. N. & De Felice, F. G. Soluble protein oligomers as emerging toxins in Alzheimer's and other amyloid diseases. *IUBMB life* **59**, 332-345 (2007).

Jin, M. & Selkoe, D. J. Systematic analysis of time-dependent neural effects of soluble amyloid beta oligomers in culture and in vivo: Prevention by scyllo-inositol. *Neurobiol Dis* **82**, 152-163 (2015).

Pagani, L. & Eckert, A. Amyloid-Beta interaction with mitochondria. *Int J Alzheimers Dis* **2011**, 925050 (2011).

Wang, X., Su, B., Perry, G., Smith, M. A. & Zhu, X. Insights into amyloid-beta-induced mitochondrial dysfunction in Alzheimer disease. *Free Radic Biol Med* **43**, 1569-1573 (2007).

Muirhead, K. E., Borger, E., Aitken, L., Conway, S. J. & Gunn-Moore, F. J. The consequences of mitochondrial amyloid beta-peptide in Alzheimer's disease. *The Biochemical journal* **426**, 255-270 (2010).

Pandey, K. B. & Rizvi, S. I. Plant polyphenols as dietary antioxidants in human health and disease. *Oxidative medicine and cellular longevity* **2**, 270-278 (2009).

Jayasena, T. *et al.* The role of polyphenols in the modulation of sirtuins and other pathways involved in Alzheimer's disease. *Ageing Res Rev* **12**, 867-883 (2013).

Ehrnhoefer, D. E. *et al.* EGCG redirects amyloidogenic polypeptides into unstructured, off-pathway oligomers. *Nature structural & molecular biology* **15**, 558-566 (2008).

Doig, A. J. & Derreumaux, P. Inhibition of protein aggregation and amyloid formation by small molecules. *Current opinion in structural biology* **30**, 50-56 (2015).

Thapa, A., Jett, S. D. & Chi, E. Y. Curcumin Attenuates Amyloid-beta Aggregate Toxicity and Modulates Amyloid-beta Aggregation Pathway. *ACS chemical neuroscience* **7**, 56-68 (2016).

Reddy, P. H. *et al.* Protective effects of a natural product, curcumin, against amyloid beta induced mitochondrial and synaptic toxicities in Alzheimer's disease. *Journal of investigative medicine : the official publication of the American Federation for Clinical Research* (2016).

Yang, F. *et al.* Curcumin inhibits formation of amyloid beta oligomers and fibrils, binds plaques, and reduces amyloid in vivo. *J Biol Chem* **280**, 5892-5901 (2005).

Albani, D. *et al.* The SIRT1 activator resveratrol protects SK-N-BE cells from oxidative stress and against toxicity caused by alpha-synuclein or amyloid-beta (1-42) peptide. *J Neurochem* **110**, 1445-1456 (2009).

Regitz, C., Fitzenberger, E., Mahn, F. L., Dussling, L. M. & Wenzel, U. Resveratrol reduces amyloid-beta (A β (1-42))-induced paralysis through targeting proteostasis in an Alzheimer model of *Caenorhabditis elegans*. *European journal of nutrition* **55**, 741-747 (2016).

Wang, S. H., Liu, F. F., Dong, X. Y. & Sun, Y. Thermodynamic analysis of the molecular interactions between amyloid beta-peptide 42 and (-)-epigallocatechin-3-gallate. *The journal of physical chemistry. B* **114**, 11576-11583 (2010).

Vauzour, D., Rodriguez-Mateos, A., Corona, G., Oruna-Concha, M. J. & Spencer, J. P. Polyphenols and human health: prevention of disease and mechanisms of action. *Nutrients* **2**, 1106-1131 (2010).

Williams, R. J. & Spencer, J. P. Flavonoids, cognition, and dementia: actions, mechanisms, and potential therapeutic utility for Alzheimer disease. *Free Radic Biol Med* **52**, 35-45 (2012).

Lamport, D. J. *et al.* The effect of flavanol-rich cocoa on cerebral perfusion in healthy older adults during conscious resting state: a placebo controlled, crossover, acute trial. *Psychopharmacology* **232**, 3227-3234 (2015).

Valls-Pedret, C. *et al.* Polyphenol-rich foods in the Mediterranean diet are associated with better cognitive function in elderly subjects at high cardiovascular risk. *J Alzheimers Dis* **29**, 773-782 (2012).

Nurk, E. *et al.* Intake of flavonoid-rich wine, tea, and chocolate by elderly men and women is associated with better cognitive test performance. *J Nutr* **139**, 120-127 (2009).

Haigis, M. C. & Guarente, L. P. Mammalian sirtuins--emerging roles in physiology, aging, and calorie restriction. *Genes Dev* **20**, 2913-2921 (2006).

Stefani, M. & Rigacci, S. Beneficial properties of natural phenols: highlight on protection against pathological conditions associated with amyloid aggregation. *Biofactors* **40**, 482-493 (2014).

Lahey-Beitia, J., Berrocal, R., Rao, K. S. & Durant, A. A. Polyphenols as therapeutic molecules in Alzheimer's disease through modulating amyloid pathways. *Molecular neurobiology* **51**, 466-479 (2015).

Chan, S. *et al.* Metal chelation, radical scavenging and inhibition of A β (4)(2) fibrillation by food constituents in relation to Alzheimer's disease. *Food chemistry* **199**, 185-194 (2016).

Irwin, J. A., Wong, H. E. & Kwon, I. Different fates of Alzheimer's disease amyloid-beta fibrils remodeled by biocompatible small molecules. *Biomacromolecules* **14**, 264-274 (2013).

Haque, A. M. *et al.* Long-term administration of green tea catechins improves spatial cognition learning ability in rats. *J Nutr* **136**, 1043-1047 (2006).

Ringman, J. M., Frautschy, S. A., Cole, G. M., Masterman, D. L. & Cummings, J. L. A potential role of the curry spice curcumin in Alzheimer's disease. *Curr Alzheimer Res* **2**, 131-136 (2005).

Ono, K., Hasegawa, K., Naiki, H. & Yamada, M. Curcumin has potent anti-amyloidogenic effects for Alzheimer's beta-amyloid fibrils in vitro. *J Neurosci Res* **75**, 742-750 (2004).

Garcia-Alloza, M., Borrelli, L. A., Rozkalne, A., Hyman, B. T. & Bacskai, B. J. Curcumin labels amyloid pathology in vivo, disrupts existing plaques, and partially restores distorted neurites in an Alzheimer mouse model. *J Neurochem* **102**, 1095-1104 (2007).

Marambaud, P., Zhao, H. & Davies, P. Resveratrol promotes clearance of Alzheimer's disease amyloid-beta peptides. *J Biol Chem* **280**, 37377-37382 (2005).

Turner, R. S. *et al.* A randomized, double-blind, placebo-controlled trial of resveratrol for Alzheimer disease. *Neurology* **85**, 1383-1391 (2015).

Lekli, I., Ray, D. & Das, D. K. Longevity nutrients resveratrol, wines and grapes. *Genes Nutr* **5**, 55-60 (2010).

Mosmann, T. Rapid colorimetric assay for cellular growth and survival: application to proliferation and cytotoxicity assays. *Journal of immunological methods* **65**, 55-63 (1983).

Quideau, S., Deffieux, D., Douat-Casassus, C. & Pouysegu, L. Plant polyphenols: chemical properties, biological activities, and synthesis. *Angewandte Chemie* **50**, 586-621 (2011).

Kennard, M. L., Feldman, H., Yamada, T. & Jefferies, W. A. Serum levels of the iron binding protein p97 are elevated in Alzheimer's disease. *Nature medicine* **2**, 1230-1235 (1996).

Bilgic, B., Pfefferbaum, A., Rohlfing, T., Sullivan, E. V. & Adalsteinsson, E. MRI estimates of brain iron concentration in normal aging using quantitative susceptibility mapping. *Neuroimage* **59**, 2625-2635 (2012).

Smith, D. G., Cappai, R. & Barnham, K. J. The redox chemistry of the Alzheimer's disease amyloid beta peptide. *Biochim Biophys Acta* **1768**, 1976-1990 (2007).

Cuajungco, M. P., Faget, K. Y., Huang, X., Tanzi, R. E. & Bush, A. I. Metal chelation as a potential therapy for Alzheimer's disease. *Ann N Y Acad Sci* **920**, 292-304 (2000).

Cheng, X. R. *et al.* Surface plasmon resonance imaging of amyloid-beta aggregation kinetics in the presence of epigallocatechin gallate and metals. *Analytical chemistry* **85**, 2049-2055 (2013).

Camilleri, A. *et al.* Mitochondrial membrane permeabilisation by amyloid aggregates and protection by polyphenols. *Biochim Biophys Acta* **1828**, 2532-2543 (2013).

Santos, A. C. *et al.* Effect of naturally occurring flavonoids on lipid peroxidation and membrane permeability transition in mitochondria. *Free Radical Biology and Medicine* **24**, 1455-1461 (1998).

Van Acker, S. A. *et al.* Structural aspects of antioxidant activity of flavonoids. *Free Radical Biology and Medicine* **20**, 331-342 (1996).

Deviene, K. F. *et al.* Antioxidant activity of isocoumarins isolated from *Paepalanthus bromelioides* on mitochondria. *Phytochemistry* **68**, 1075-1080 (2007).

Dorta, D. J. *et al.* Antioxidant activity of flavonoids in isolated mitochondria. *Phytotherapy Research* **22**, 1213-1218 (2008).

Morel, I., Lescoat, G., Cillard, P. & Cillard, J. Role of flavonoids and iron chelation in antioxidant action. *Methods in enzymology (USA)* (1994).

Cao, G., Sofic, E. & Prior, R. L. Antioxidant and prooxidant behavior of flavonoids: structure-activity relationships. *Free Radical Biology and Medicine* **22**, 749-760 (1997).

Molino, S. *et al.* Polyphenols in dementia: From molecular basis to clinical trials. *Life Sci* **161**, 69-77 (2016).

Mecocci, P. & Polidori, M. C. Antioxidant clinical trials in mild cognitive impairment and Alzheimer's disease. *Biochim Biophys Acta* **1822**, 631-638 (2012).

Vassallo, N. & Scerri, C. Mediterranean diet and dementia of the Alzheimer type. *Curr Aging Sci* **6**, 150-162 (2013).

Cao, L. *et al.* Dietary Patterns and Risk of Dementia: a Systematic Review and Meta-Analysis of Cohort Studies. *Molecular neurobiology* **53**, 6144-6154 (2016).

Burton-Freeman, B. M., Sandhu, A. K. & Edirisinghe, I. Red Raspberries and Their Bioactive Polyphenols: Cardiometabolic and Neuronal Health Links. *Advances in nutrition* **7**, 44-65 (2016).

Pandey, K. B. & Rizvi, S. I. Markers of oxidative stress in erythrocytes and plasma during aging in humans. *Oxidative medicine and cellular longevity* **3**, 2-12 (2010).

Kim, T. S. *et al.* Decreased plasma antioxidants in patients with Alzheimer's disease. *Int J Geriatr Psychiatry* **21**, 344-348 (2006).

Montine, T. J. *et al.* Lipid peroxidation in aging brain and Alzheimer's disease. *Free Radic Biol Med* **33**, 620-626 (2002).

Hohsfield, L. A. & Humpel, C. Intravenous infusion of monocytes isolated from 2-week-old mice enhances clearance of Beta-amyloid plaques in an Alzheimer mouse model. *PLoS One* **10**, e0121930 (2015).

Castellano, J. M., Kirby, E. D. & Wyss-Coray, T. Blood-Borne Revitalization of the Aged Brain. *JAMA neurology* **72**, 1191-1194 (2015).

Obregon, D. F. *et al.* ADAM10 activation is required for green tea (-)-epigallocatechin-3-gallate-induced alpha-secretase cleavage of amyloid precursor protein. *J Biol Chem* **281**, 16419-16427 (2006).

Feldman, J. L. *et al.* Kinetic and Structural Basis for Acyl-Group Selectivity and NAD(+) Dependence in Sirtuin-Catalyzed Deacylation. *Biochemistry* **54**, 3037-3050 (2015).

Appendix

Publications:

Jayasena T, Poljak A, Smythe G, Braidy N, Münch G, Sachdev P (2013). The role of polyphenols in the modulation of sirtuins and other pathways involved in Alzheimer's disease. Ageing Research Reviews 12(4):867-883

Jayasena T, Poljak A, Braidy N, Zhong L, Rowlands B, Muenchhoff J, Grant R, Smythe G, Teo C, Raftery M, Sachdev P (2016). Application of Targeted Mass Spectrometry for the Quantification of Sirtuins in the Central Nervous System. Scientific Reports 2016 Oct 20;6:35391.

Jayasena T, Poljak A, Braidy N, Smythe G, Raftery M, Hill M, Brodaty H, Trollor J, Kochan N, Sachdev P (2015). Upregulation of glycolytic enzymes, mitochondrial dysfunction and increased cytotoxicity in glial cells treated with Alzheimer's disease plasma. PLoS One 10(3):e0116092.

The role of polyphenols in the modulation of sirtuins and other pathways involved in Alzheimer's disease



Neuropsychiatric Institute, The Prince of Wales Hospital, Sydney, Australia

© 2013 Elsevier B.V. All rights reserved.

1568-1637/\$ – see front matter © 2013 Elsevier B.V. All rights reserved.
<http://dx.doi.org/10.1016/j.arr.2013.06.003>

to oxidative damage due to its high oxygen consumption, relatively low antioxidant levels, high content of redox-active metals (copper and iron), and limited regenerative capacity, and thus free radicals have been hypothesised to play an important role in the brain age-ing process (Honda et al., 2004; Reiter, 1995; Romano et al., 2010; Smith et al., 1996).

Ageing is also the main risk factor in the development of Alzheimer's disease (AD), with the vast majority of cases developing after the age of sixty-five. Thus, oxidative damage is also thought to be an important factor in the pathogenesis of this disease and indeed seems to be one of the earliest events (Jomova et al., 2010; Nunomura et al., 2001; Smith et al., 1996). Markers of free-radical damage such as increased protein and DNA oxidation, enhanced lipid peroxidation, advanced glycation end products, carbonyls, dityrosine, malondialdehyde, and peroxynitrite damage have all been reported to occur in AD (Aksenov et al., 2001; Greilberger et al., 2008; Hensley et al., 1998; Lovell and Markesbery, 2007; Montine et al., 2002; Munch et al., 1997; Sasaki et al., 1998; Smith et al., 1997b). Furthermore, decreased levels of plasma antioxidants have been seen in AD patients (Kim et al., 2006).

A hallmark of AD is the presence in the brain of extracellular amyloid plaques, mainly containing aggregated amyloid (A β) peptides. These A β plaques are another source of oxidative stress in AD as they sequester divalent metals such as copper and iron, which have the potential to catalyse free radical formation (Atwood et al., 2003). Copper and iron in abnormally high concentrations and markers representing oxidative stress have been found in amyloid plaques, and are elevated in the neocortex of the AD brain (Jomova et al., 2010; Lovell et al., 1998; Maynard et al., 2005; Roberts et al., 2012; Smith et al., 2000). Iron has been shown to facilitate the aggregation and deposition of A β and also induce aggregation of the major constituent of neurofibrillary tangles, hyperphosphorylated tau (Mantyh et al., 1993; Yamamoto et al., 2002). Amyloid plaques are sites of chronic inflammation in the AD brain, and this represents another source of oxidative stress due to the release of superoxide and nitric oxide (Butterfield, 2002; Reynolds et al., 2007; Wang et al., 2004).

Polyphenols may hold potential therapeutic benefits in age-related disorders due to their potent free-radical scavenging and antioxidant effects (Salah et al., 1995). Polyphenols are secondary plant metabolites that are involved in plant defence against pathogens and ultraviolet damage (Manach et al., 2004). They are found in many fruits, herbs and vegetables and thus serve as important dietary micronutrients. Chemically, polyphenols include a wide variety of biomolecules which contain several hydroxyl groups on one or more aromatic rings. They can be divided into various groups according to chemical structure – including flavonoids, stilbenes and lignans (D'Archivio et al., 2007; Tsao, 2010). Natural phenolics are compounds which contain hydroxyl groups on only a single aromatic ring and therefore are smaller in size than polyphenols. They include phenolic acids and phenolic alcohols (see Table 1 for further details).

Recently, the potential role of polyphenols in ageing and neurodegeneration has widened with discoveries that they can modulate various important pathways in the pathogenesis of AD by reducing amyloid aggregation and inflammation and modulating a class of proteins called sirtuins which are involved in longevity and cell survival. This review aims to highlight some of these new effects of polyphenols with a focus on how polyphenols may influence amyloid aggregation and the sirtuin family of proteins.

2. Modulation of oxidative stress by polyphenols

Polyphenols are well known as antioxidants and direct scavengers of free radicals (Lodovici et al., 2001; Robak and Gryglewski,

1988; Salah et al., 1995). In addition, polyphenols can act as metal chelators (Brown et al., 1998; Hider et al., 2001; Moridani et al., 2003), which adds to the antioxidant effects of these compounds through inhibition of transition metal-catalysed free radical formation (Jomova et al., 2010). Chelation of transition metals such as Fe²⁺ can directly reduce the rate of the Fenton reaction thus preventing oxidation caused by highly reactive hydroxyl radicals (Cheng and Breen, 2000; Lopes et al., 1999). Epigallocatechin gallate (EGCG), a green tea polyphenol, for example has also been shown to be a potent chelator of transition metals such as copper and iron (Mandel et al., 2008a), and inhibits over 90% of iron-mediated DNA damage caused by Fe²⁺ and H₂O₂ (Mandel et al., 2011). It has also been found that polyphenols are involved in the regeneration of essential vitamins (Mandel et al., 2008c; Pedrielli and Skibsted, 2002). Polyphenols can induce antioxidant enzymes such as glutathione peroxidase, catalase, superoxide dismutase, as well as hydrogen peroxide and superoxide anions, and inhibit the expression of enzymes such as xanthine oxidase, which is involved in the generation of free radicals (Alvarez-Suarez et al., 2011; Frei and Higdon, 2003; Lee et al., 2006; Luceri et al., 2002; Luczaj et al., 2004; Mandel et al., 2008b, 2011; Moskaug et al., 2005; Sanbongi et al., 1997). These multiple antioxidant effects prevent oxidative damage to important cellular components and have led to investigation of polyphenols as therapeutic agents for the treatment of AD, to combat the increase in oxidative stress seen in this disease.

3. Effects of polyphenols on amyloid and tau aggregation

The A β deposited in AD is derived from the larger amyloid pre-cursor protein (APP). Surface APP can be endocytosed, and then undergo various forms of processing, one of which results in the formation of A β peptides (Selkoe, 1998). These peptides have the ability to aggregate and generate the amyloid that is found in the AD brain. The toxic potential of the A β peptide depends on its conformational state and peptide length, with A β (1–42) being more toxic than A β (1–40) and A β (1–42) oligomers are thought to be the most toxic form (Walsh and Selkoe, 2007). Metal ions such as copper, iron and zinc also influence the aggregation state of A β peptides (Mantyh et al., 1993).

Several studies have suggested that polyphenols may have anti-amyloidogenic effects. A number of polyphenols including tannic acid, quercetin, kaempferol, curcumin, catechin and epicatechin were shown to dose-dependently inhibit the formation of A β fibrils as well as their elongation (Ono et al., 2003, 2004). In addition, polyphenols can bind directly to A β or mature aggregates and impair their stability, as all the compounds tested destabilised pre-formed A β fibrils (Ono et al., 2003). EGCG significantly inhibits A β aggregation and has the ability to remodel large A β fibrils into smaller aggregates which display no toxic effects (Bieschke et al., 2010) (see Fig. 1). Fish oil has been shown to have a synergistic effect in combination with EGCG with co-treatment leading to a reduction in A β plaque formation and levels of A β (1–40) and A β (1–42) in AD transgenic Tg2576 mice (Giunta et al., 2010).

Tannic acid was shown to reduce A β deposits as well as A β species including oligomers in the transgenic AD mouse brain (Mori et al., 2012; Ono et al., 2003). Tannic acid decreased cleavage of the -carboxyl-terminal APP fragment, lowered APP- production, and attenuated neuroinflammation (Mori et al., 2012). It is thought to work by inhibiting amyloidogenic APP metabolism as a result of reducing -site APP cleaving enzyme 1 expression and lowering -secretase activity (Mori et al., 2012). EGCG was also shown to down-regulate APP levels and cerebral amyloidosis in Alzheimer transgenic mice (Rezai-Zadeh et al., 2005).

Curcumin, found in the spice turmeric, has been shown to prevent brain lipid peroxidation in rats and increase glutathione

Table 1
Classification and dietary sources of polyphenols and phenolics.

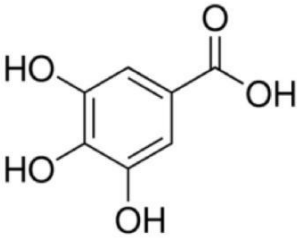
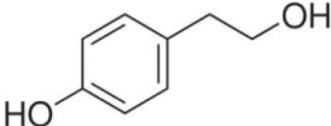
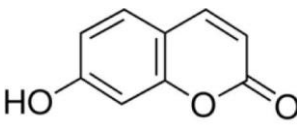
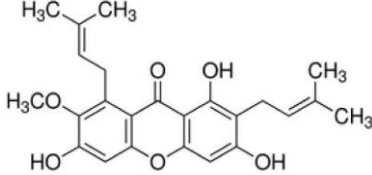
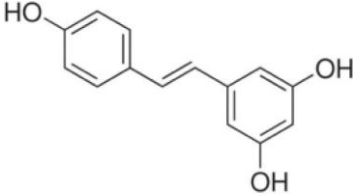
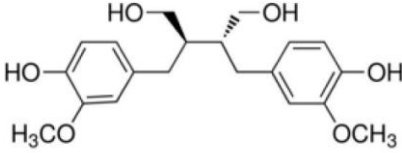
Polyphenol class	Examples	Structure	Plant source
Phenolic acids	Gallic acid Caffeic acid Ferulic acid Curcumin (derivative of ferulic acid)	 <p>(Gallic Acid)</p>	Clove 7.8 g/kg (Shan et al., 2005), Chestnut 4.8 g/kg (Do Carmo Barbosa Mendes De Vasconcelos et al., 2007), Red wine 7.8–70.8 mg/L (Burns et al., 2000), Blackberries 80–270 mg/kg (Manach et al., 2004)
Phenolic alcohols	Tyrosol Oleuropein	 <p>(Tyrosol)</p>	Black olives 144 mg/kg, olive oil 5.3 mg/kg (Perez-Jimenez et al., 2010)
Coumarins	Umbelliferone Aesculetin Scopoletin	 <p>(Umbelliferone)</p>	Wine 0.05 mg/L (Alonso et al., 2004)
Xanthenes	Mangostin Mangiferin	 <p>(α-mangostin)</p>	Mangosteen 0.91–55.1 g/kg (Walker, 2007); Mango 31.7 mg/kg (Sulaiman and Ooi, 2012)
Stilbenes	Resveratrol Piceatannol	 <p>(Resveratrol)</p>	Red wine 1.9–27.8 mg/L (Vitrac et al., 2005), Cranberry 19.2 mg/kg (Ehala et al., 2005), Peanut 11.2 mg/kg (Chukwumah et al., 2007)
Lignans	Secoisolariciresinol Matairesinol Lariciresinol	 <p>(Secoisolariciresinol)</p>	Linseed 3.7 g/kg, Flax seed 3.35 g/kg (Penalvo et al., 2005)

Table 1 (Continued)

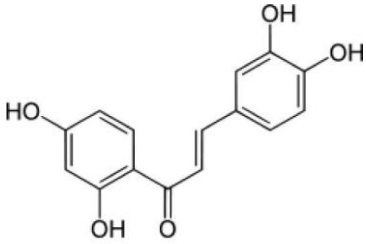
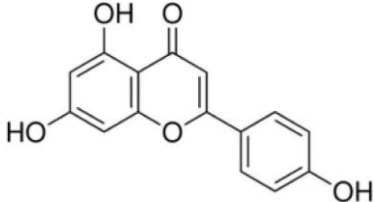
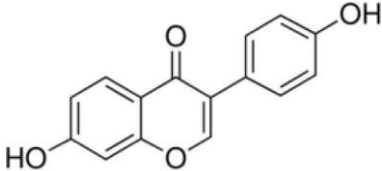
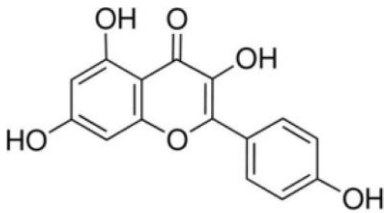
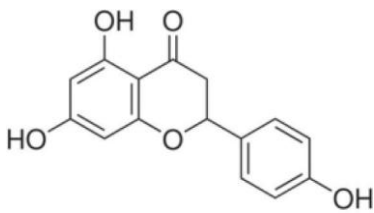
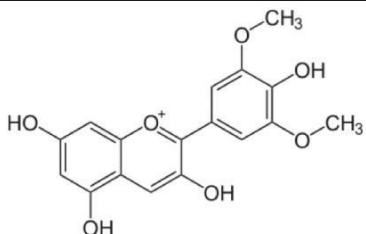
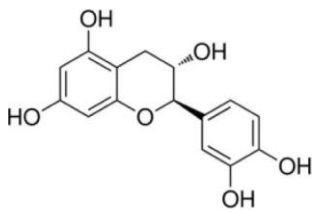
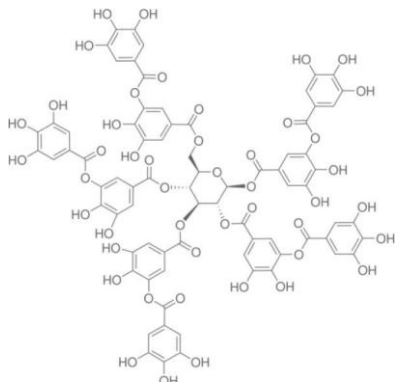
Polyphenol class	Examples	Structure	Plant source
Chalcones	Butein Cardamonin Phloridzin		Apple 6.4–91.1 mg/kg (Vrhovsek et al., 2004)
		(Butein)	
Flavones	Apigenin Luteolin Diosmetin		Parsley 0.24–1.85 g/kg, Celery 20–140 mg/kg, Capsicum 5–10 mg/kg (Justesen et al., 1998 ; Manach et al., 2004)
		(Apigenin)	
Isoflavones	Daidzein Genistein Glycitein		Soybeans 0.2–0.9 g/kg, Miso 0.25–0.9 g/kg, Tofu 0.08–0.7 g/kg, Tempeh 0.43–0.53 g/kg (Manach et al., 2004)
		(Daidzein)	
Flavonols	Kaempferol Quercetin Myricetin Fisetin		Kale 0.3–0.6 g/kg, Onion 0.35–1.2 g/kg, Ginseng 4.3–6.6 g/kg (Justesen et al., 1998 ; Manach et al., 2004)
		(Kaempferol)	
Flavanones	Naringenin Hesperidin		Grapefruit juice 100–650 mg/L, lemon juice 50–300 mg/kg (Justesen et al., 1998 ; Manach et al., 2004)
		(Naringenin)	

Table 1 (Continued)

Polyphenol class	Examples	Structure	Plant source
Anthocyanidins	Malvidin Cyanidin Pelargonidin		Cherry 0.35–4.5 g/kg, Rhubarb 2.0 g/kg, Strawberry 0.15–0.75 g/kg (Manach et al., 2004)
		(Malvidin)	
Flavanols (monomer)	Catechin Epicatechin Gallocatechin Epigallocatechin gallate		Beans 350–550 mg/kg, Apricot 100–250 mg/kg, Green tea 100–800 mg/L, Chocolate 460–610 mg/kg, Red wine 203–805 mg/L (Arts et al., 2000a,b; Manach et al., 2004; Pellegrini et al., 2000)
		(Catechin)	
Flavanols (polymer)	Tannic acid Proanthocyanidins		Cinnamon 81 mg/kg, chocolate 16 mg/kg, grape seed 35 mg/kg (Gu et al., 2004)
		(Tannic acid)	

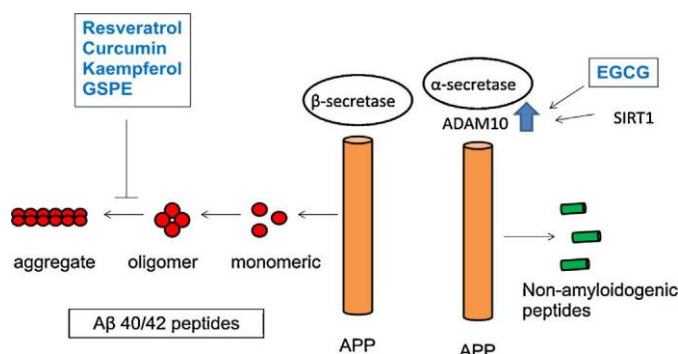


Fig. 1. Influence of SIRT1 and polyphenols on amyloid precursor protein (APP) processing and amyloid formation. SIRT1 and the green tea polyphenol (–)-epigallocatechin-3-gallate (EGCG) activate ADAM10 and thus enhance α-secretase APP processing leading to the generation of non-amyloidogenic peptides (Donmez et al., 2010; Obregon et al., 2006). Resveratrol is able to selectively remodel toxic amyloid aggregates into non-toxic species (Ladiwala et al., 2010). Polyphenols such as curcumin, kaempferol and grape seed extract polyphenols (GSEPE) also have the ability to reduce A levels in the brain (Ono et al., 2003).

levels and the activity of other detoxifying enzymes (Jena et al., 2012; Khurana et al., 2012). Curcumin has also been shown to protect cells against A β -induced oxidative insult (Huang et al., 2012). When administered to AD transgenic mice, curcumin was found to prevent protein oxidation and inflammation and reduce the formation of soluble and insoluble A β by up to 50% (Lim et al., 2001).

Luteolin, a citrus polyphenol was found to reduce A β peptide production in cultured neurons and decreased amyloidogenic α-secretase APP processing (Rezai-Zadeh et al., 2009). In the AD mouse model Tg2576 mice, luteolin along with a structurally similar compound, diosmin, were both shown to reduce soluble A β levels (Rezai-Zadeh et al., 2009).

In a recent study anthocyanin-enriched fractions of bilberry and blackberry extracts were found to modulate APP processing and significantly alter A β 40 and A β 42 levels. Both compounds also alleviated spatial working memory deficits in a mouse model of AD (Vepsäläinen et al., 2013). Cinnamon extract was also found to reduce A β aggregation and plaque formation as well as improve cognitive behaviour in AD transgenic mice (Frydman-Marom et al., 2011).

Abnormal folding of the microtubule-associated protein tau leads to aggregation of tau into neurofibrillary tangles, another major pathological hallmark of AD. It has been shown that

polyphenols derived from grape seed extract reduce tau pathology in mouse models of AD (Ksiezak-Reding et al., 2012; Santa-Maria et al., 2012; Wang et al., 2010a). These polyphenols also enhanced disaggregation of neurofibrillary filaments, and improved structural stability (Ksiezak-Reding et al., 2012; Wang et al., 2010a). EGCG has also been shown to modulate tau pathology in a mouse model of Alzheimer's disease (Rezai-Zadeh et al., 2008). Tannic acid has recently been shown to dose-dependently inhibit tau aggregation and polymerisation through formation of a hairpin binding motif (Yao et al., 2013).

4. Role of sirtuins in AD and longevity

Sirtuins are a class of proteins that possess deacetylase or mono-ribosyltransferase activity and play critical roles in cell survival in response to oxidative stress and caloric restriction (CR) regimes (Horio et al., 2011; Yamamoto et al., 2007). In mammals, seven sirtuins (SIRT1–7) have been identified. All mammalian sirtuins contain a conserved NAD-binding and catalytic domain, but differ in their N and C-terminal domains (Horio et al., 2011). They have different specific substrates including histones, transcriptional regulators and enzymes (Yamamoto et al., 2007). They also have various biological functions, are localised in specific cell compartments, and play various roles in health and disease including ageing and neurodegeneration (Yamamoto et al., 2007) (see Table 2).

Sirtuins can affect ROS production and increase resistance to its damaging effects. Oxidative stress has been shown to decrease SIRT1 expression in the rat hippocampus and cortex (Wu et al., 2006). SIRT1 overexpression prevents oxidative stress-induced apoptosis and increases resistance to oxidative stress through regulation of the FOXO family of forkhead transcription factors (Brunet et al., 2004). The only cytoplasmic sirtuin protein SIRT2, has been shown to increase in response to oxidative stress but promotes cell death through FOXO proteins (Wang et al., 2007). SIRT3, a mitochondrial protein, reduces oxidative stress through activation of superoxidase dismutase activity (Qiu et al., 2010). Recent work has shown that SIRT3 mRNA expression is elevated in response to increased mitochondrial ROS production in primary mouse hippocampal cells and the SIRT3 over-expression increases neuronal lifespan (Weir et al., 2012). In AD transgenic mice SIRT3 expression was shown to mirror the pattern of A deposition (Weir et al., 2012). This study also showed a significant increase in SIRT3 expression in the AD temporal cortex of human post-mortem brain tissue (Weir et al., 2012). SIRT6, like the founding member of the sirtuin family SIRT1, is a nuclear protein which is involved in oxidative-stress induced DNA repair through its activation of the PARP-1 DNA repair enzyme (Mao et al., 2011) (for a summary see Table 2 and Fig. 2).

Interest in sirtuins increased greatly after the discovery that the sirtuin gene, Sir2 (SIRT1 being the equivalent in mammals) extends yeast lifespan up to 30% (Kaeberlein et al., 1999). A similar effect was found in nematodes and flies and it was thought the effect may occur through a pathway related to caloric restriction (Rogina and Helfand, 2004; Tissenbaum and Guarente, 2001). Recent work however suggests that the effects on longevity may not be as strong as were observed in the early studies as controlling for genetic background removed any effects on longevity (Burnett et al., 2011). The sirtuin system is strongly influenced by caloric restriction (CR), which refers to a reduction in calorie intake without malnutrition (Crujeiras et al., 2008). CR has been shown to have a wide range of benefits in humans (Fontana et al., 2004; Holloszy and Fontana, 2007; Omodei and Fontana, 2011) and life span extension in many species from yeast, fruit flies, nematodes, rodents to primates (Fontana et al., 2010; Lin et al., 2004; Partridge et al., 2005; Qin et al., 2006a). Furthermore, CR for 3 months was found

to improve memory functions in the elderly (Witte et al., 2009). CR is also known to modulate neuroinflammation and oxidative stress in various animal models (Merry, 2004; Morgan et al., 2007; Patel et al., 2005).

The mechanism by which CR increases life span is still unclear. Some theories include reduced cellular divisions, reduced metabolic rate, reduced production of ROS and hormesis (Heilbronn et al., 2006; Lin et al., 2002; Mattson, 2008; Schulz et al., 2007). Hormesis is used to describe the beneficial actions resulting from the response of an organism to a low-intensity biological stressor (Mattson, 2008). The hormesis theory of CR proposes that diet imposes a low-intensity biological stress on the organism, which causes a defence response that helps protect it against the causes of ageing (Mattson, 2008). Therefore, it is highly likely that CR places the organism in a defensive state, and enables it to survive adversity, leading to improved health and life span.

Evidence suggests that some of the beneficial effects of CR occur through its influence on sirtuins. The functions of mitochondrial sirtuins suggest that they control activity of several metabolic enzymes and play a crucial role in metabolic adaptation to dietary conditions, such as CR and fasting (Li and Kazgan, 2011) (see Table 2). It has also been reported that CR does not extend lifespan in SIRT1-deficient mice, suggesting that CR works via activation of SIRT1 (Bordone et al., 2007; Qin et al., 2006a). Conversely, transgenic mice overexpressing SIRT1 display a number of phenotypic features, such as increased metabolic activity, glucose tolerance, and reduced body weight and cholesterol levels (Bordone et al., 2007). The ability of SIRT1 to mimic the anti-ageing effects of CR is most likely linked to its regulation of various proteins and genes involved in oxidative stress, inflammation, amyloidogenesis and synaptic plasticity (see Table 2 and Fig. 2).

CR prevents A neuropathology in animal models of AD and modulation of SIRT1 expression or activity may be a mechanism by which CR influences AD-type neuropathology (Qin et al., 2006a,b, 2008). In one study 30% CR resulted in significantly lower levels of A (1–40) and A (1–42) in the temporal cortex of Squirrel monkeys relative to control fed monkeys. The cortical A levels were inversely correlated with SIRT1 protein concentrations in the same brain region, and there was also a selective elevation of β -secretase activity (Qin et al., 2006a). As mentioned previously, the cleavage of the membrane-bound APP leads to a range of protein fragments that have a role in AD pathogenesis (Kojro and Fahrenholz, 2005). Cleavage of APP by β -secretase leads to the formation of APPs $_{\beta}$, and together with γ -secretase leads to the generation of the A peptides (1–40) and (1–42). The latter is thought to be the main toxic component in AD (Kojro and Fahrenholz, 2005). If APP is processed by γ -secretase, then the formation of these pathogenic peptides is prevented, and instead a fragment APPs $_{\gamma}$ that is associated with a neuroprotective effect is generated (Donmez et al., 2010; Thornton et al., 2006). SIRT1 is able to modulate APP processing by activating the expression of the γ -secretase gene ADAM10, thereby reducing brain levels of A (1–42) as well as A (1–40) (Donmez et al., 2010) (see Fig. 1). Moreover, deacetylation of the retinoic acid receptor (RAR) by SIRT1 can induce transcription of the ADAM10 gene and suppress the production of the neurotoxic A (1–42) peptide (Donmez et al., 2010). There is however, no published literature to date on the effects of CR or sirtuin activation in AD using human clinical trials.

5. Polyphenols, sirtuins and ageing

The most studied polyphenol which shows effects on the sirtuin family of proteins is resveratrol which is found in its highest levels in grape seed and skin as well as in red wine. It has been discovered that apart from its free radical scavenging and antioxidant

Table 2

Role of the sirtuin family in calorie restriction, ageing and neurodegeneration.

Name	Location	Involvement in calorie restriction, ageing and neurodegeneration
SIRT1	Nucleus	<p>Suppresses amyloid production by promoting γ-secretase cleavage of APP and Induces the Notch pathway, involved in repair of neuronal damage in the brain (Donmez et al., 2010).</p> <p>Ameliorates learning impairment and neurodegeneration in mouse models (Kim et al., 2007).</p> <p>Regulates proteins and genes involved in antioxidant response (FOXO3), apoptosis (p53) and anti-inflammatory response (NF B) (Brunet et al., 2004; Chen et al., 2005; Langley et al., 2002; Yeung et al., 2004).</p> <p>Modulates memory formation and synaptic plasticity. Activation of SIRT1 in brain enhances, and its deletion impairs, memory function and synaptic plasticity in mice (Michan et al., 2010).</p> <p>Protects neurons against metabolic imbalance (Ramadori et al., 2011).</p> <p>Reduction in SIRT1 is associated with accumulation of Aβ and tau (Julien et al., 2009; Qin et al., 2006b).</p> <p>Promotes feeding behaviour during dietary limited conditions including calorie restriction or fasting (Cohen et al., 2009).</p> <p>Mouse knock-outs show impaired cognitive abilities, decreased dendritic branching, length and complexity, lower levels of oxidised proteins and lipids in the brain, lower growth hormone levels, and shortened lifespan (Akieda-Asai et al., 2010; Li et al., 2008a; Michan et al., 2010).</p>
SIRT2	Cytoplasm	<p>Enhances apoptosis and atrophy, SIRT2 inhibition is neuroprotective (Hasegawa et al., 2010; Liu et al., 2012; Outeiro et al., 2007; Spires-Jones et al., 2012).</p> <p>A tubulin deacetylase which regulates cell division and differentiation and accumulates with age (Maxwell et al., 2011).</p> <p>Impairs neurite outgrowth and oligodendrocyte differentiation and promotes axonal degeneration (Harting and Knoll, 2010; Li et al., 2007; Suzuki and Koike, 2007a).</p> <p>Small molecule inhibitor of SIRT2 showed neuroprotection via cholesterol-reducing properties in a Huntington's disease model (Luthi-Carter et al., 2010; Taylor et al., 2011).</p> <p>Upregulates in response to calorie restriction and oxidative stress, and promotes cell death under severe stress conditions via interaction with FOXO3a (Wang et al., 2007).</p> <p>Involved in myelin formation (Beirowski et al., 2011).</p>
SIRT3	Mitochondria	<p>Over-expressed in response to oxidative stress and significantly elevated in human AD post mortem brain tissue (Weir et al., 2012).</p> <p>Protects against excitotoxic injury in neurons (Kim et al., 2011).</p> <p>Plays a role in CR-mediated reduction in oxidative stress and decreases reactive oxygen species by increasing activity of superoxide dismutase (Bell and Guarente, 2011; Qiu et al., 2010; Someya et al., 2010).</p> <p>Variability of the SIRT3 gene may have a role in human longevity (Halaschek-Wiener et al., 2009; Rose et al., 2003).</p> <p>SIRT3 upregulates fatty acid oxidation and lowers ATP levels during fasting (Hirschey et al., 2010).</p> <p>Involved in the maintenance of mitochondrial function by preventing premature opening of the mitochondrial permeability transition pore (Hafner et al., 2010).</p>
SIRT4	Mitochondria	<p>Downregulates glutamate dehydrogenase activity, and controls insulin secretion in response to calorie restriction (Haigis et al., 2006).</p>
SIRT5	Mitochondria	<p>Negatively regulates fatty acid oxidation in combination with SIRT1 (Nasrin et al., 2010).</p> <p>SIRT5 promoter polymorphism is associated with a higher brain molecular ageing (Glorioso et al., 2011).</p> <p>Involved in regulation of the urea cycle during fasting and calorie restriction (Nakagawa et al., 2009; Nakamura et al., 2012; Ogura et al., 2010).</p>
SIRT6	Nucleus	<p>Involved in DNA double strand break repair following oxidative stress by inducing PARP1 activity (Lombard et al., 2008; Mao et al., 2011, 2012).</p> <p>SIRT6 associates with telomeric chromatin and depletion of SIRT6 results in premature cellular senescence and telomere dysfunction (Kawahara et al., 2011; Michishita et al., 2009).</p> <p>Prevention of transforming growth factor-β-induced cell senescence in human epithelial cells (Minagawa et al., 2011).</p> <p>Neuronal SIRT6 is involved in regulation of somatic growth and obesity prevention in mice (Schwer et al., 2010).</p> <p>SIRT6 genes suppress NF-kappaB signalling and thus can delay the ageing process and extend lifespan (Kawahara et al., 2009).</p> <p>SIRT6-knockout mice exhibit genomic instability, ageing-like phenotypes and die from hypoglycaemia by 4–5 weeks. Stem cells that are deficient in SIRT6 show genomic instability (Mostoslavsky et al., 2006).</p>
SIRT7	Nucleus	<p>SIRT7 overexpression in fibroblasts inhibits cell growth and proliferation and promotes cell cycle arrest (Vakhrusheva et al., 2008a).</p> <p>SIRT7 deficient mice exhibit heart hypertrophy, inflammatory cardiomyopathy and a reduced lifespan (Vakhrusheva et al., 2008b).</p> <p>Positive regulator of RNA polymerase I transcription (Ford et al., 2006).</p>

properties, resveratrol has many of the same benefits as calorie restriction. Resveratrol is associated with neuroprotective effects (Liu et al., 2011; Moriya et al., 2011; Narita et al., 2011), and other beneficial effects including maintenance of mitochondrial integrity, reduction of insulin-like growth factor-1 expression, activation of SIRT1, and increased longevity in some animals models (Baur and Sinclair, 2006; Borra et al., 2005; Brown et al., 2010; Chandrasekara and Shkarad, 2011; Dave et al., 2008; Howitz et al., 2003; Lagouge et al., 2006; Valenzano et al., 2006; Wood et al., 2004), though life span effects are controversial (Kaeberlein et al., 2005; Miller et al., 2011; Pearson et al., 2008). Epidemiological evidence suggests red wine, which is rich in resveratrol, reduces the risk of dementia (Truelsen et al., 2002).

Resveratrol has also been shown to improve outcomes after ischaemic episodes in the heart and brain of mice by a SIRT1-mediated process (Mukhopadhyay et al., 2010; Wang et al., 2012). Resveratrol strongly stimulates SIRT1 deacetylase activity in a dose-dependent manner by increasing its binding affinity to both

the acetylated substrate and NAD⁺ (Chung et al., 2010). Whether resveratrol is a direct or indirect activator of SIRT1 remains controversial (Gertz et al., 2012; Pacholec et al., 2010). Resveratrol and CR have also been shown to modulate mitochondrial sirtuins (Gertz et al., 2012; Guarente, 2008; Qiu et al., 2010; Someya et al., 2010). Resveratrol-fed rats showed increased expression of SIRT3 and SIRT4 in the heart compared to control-fed mice (Mukherjee et al., 2009), however the opposite effect was seen in the liver of a zebrafish model (Schirmer et al., 2012). Resveratrol also increased expression of SIRT3 in adipocytes (Rayalam et al., 2008). Resveratrol mediated changes to sirtuin expression in the brain have yet to be intensively studied. Investigation of polyphenolic sirtuin-activating compounds are thought to hold promise for enhancing longevity (Howitz et al., 2003; Quideau, 2004).

A variety of polyphenols (or foods rich in polyphenolic compounds) have been investigated for their effects on AD and longevity (see Table 3). Interestingly, many of these compounds influence sirtuins through direct or indirect pathways. For example,

Table 3

Influence of polyphenols on sirtuins and pathways involved in ageing and AD.

Polyphenol and source	Effect on sirtuins	Influence in AD	Influence in ageing
Resveratrol (grapes, red wine, peanuts)	Increased SIRT1, SIRT2, SIRT3, SIRT4 and SIRT7 (Lagouge et al., 2006; Mukherjee et al., 2009; Schirmer et al., 2012; Suzuki and Koike, 2007b; Yu et al., 2009); Normalised SIRT1 and SIRT3 ethanol-induced elevation in rat liver tissue (Oliva et al., 2008); Inhibits human SIRT3 and stimulates SIRT5 (Gertz et al., 2012);	Selectively remodels toxic amyloid aggregates (Ladiwala et al., 2010); Reduces A β plaques and toxicity in animal models (Karuppagounder et al., 2009; Porquet et al., 2012)	Increases longevity in a variety of organisms from yeast to mammals (Agarwal and Baur, 2011; Barger et al., 2008b; Chandrashekar and Shakarad, 2011; Fernandez and Fraga, 2011; Mouchiroud et al., 2010; Porquet et al., 2012; Wood et al., 2004)
Quercetin (tea, onions, apples)	Increased SIRT1 (Davis et al., 2009)	Reduces A β -mediated cytotoxicity and oxidative stress (Ansari et al., 2009; Belinha et al., 2007; Heo and Lee, 2004); decreases neuronal α -secretase activity (Shimmyo et al., 2008)	Extends life span in worms and yeast (Howitz et al., 2003; Pietsch et al., 2009)
Butein (Chinese lacquer tree)	Increased SIRT1 (Chung et al., 2010; Howitz et al., 2003)	Neuroprotective and anti-inflammatory effects (Cho et al., 2012); protects cells against oxidative stress through influence on antioxidant enzyme expression (Yang et al., 2011)	Lengthens life span in yeast (Howitz et al., 2003)
Fisetin (strawberries, blueberries, cucumber)	Increased SIRT1 (Howitz et al., 2003)	Regulates levels of glutathione and mitochondrial function during oxidative stress (Maher, 2009); inhibits A β fibril formation (Akaishi et al., 2008)	Extends life span in yeast, worms and flies (Howitz et al., 2003; Kampkotter et al., 2007; Wood et al., 2004)
Kaempferol (tea, leek, tomato)	Increased SIRT3 (Marfe et al., 2009)	Inhibit A β formation and toxicity as well as reversed A β -induced impaired performance in mice (Kim et al., 2010; Ono et al., 2003; Roth et al., 1999)	Extends life span in worms (Kampkotter et al., 2007)
Catechins (chocolate, bitter melon, green tea)	Increased SIRT1 and SIRT3 in mice (Nerurkar et al., 2011) and increased Sir2 activity in yeast	Attenuates oxidative stress and neuroinflammation (Nerurkar et al., 2011); Neuroprotective and metal chelating properties (Mandel et al., 2008a); Inhibits formation of fibrillar A β (Mandel et al., 2008b,c); modulates tau and enhances cognition (Rezai-Zadeh et al., 2008); modulates APP cleavage (Rezai-Zadeh et al., 2005)	Increases lifespan in worms, flies and mice (Kumari et al., 1997; Li et al., 2008b; Zhang et al., 2009) and delays memory regression in animal models of ageing (Li et al., 2009a; Unno et al., 2007)
Curcumin (turmeric)	Not known	Reduces A β levels through influence on APP in AD mice (Zhang et al., 2010) and enhances memory in AD rat model (Ahmed et al., 2010)	Extends life span in flies and mice (Kitani et al., 2007; Lee et al., 2010)
Phloridzin (apple)	Increased Sir1 activity in yeast (Xiang et al., 2011)	Upregulates superoxide dismutase and catalase genes (Xiang et al., 2011)	Extend lifespan of flies (Peng et al., 2011)
Procyanidins (apple, cocoa)	No extension of lifespan in worms lacking Sir2.1 (Sunagawa et al., 2011)	Increased resistance to oxidative stress in yeast and worms; improved cognition in elderly human subjects and aged rats (Bisson et al., 2008; Desideri et al., 2012; Xu et al., 2011)	Increase lifespan of worms, flies and rats (Peng et al., 2011; Sunagawa et al., 2011)
Proanthocyanidins (persimmon, cinnamon, grape, blueberry, blackcurrant)	Increased SIRT1 expression (Yokozawa et al., 2011)	Suppress brain oxidative stress (Asha Devi et al., 2011); inhibit formation of advanced glycation end products (Peng et al., 2010); inhibits tau aggregation (Peterson et al., 2009); improves learning and memory in mice (Yokozawa et al., 2011); modulates APP processing as well as spatial working memory deficits in a mouse model of AD (Vepsäläinen et al., 2013)	Increase lifespan in worms and mice (Wilson et al., 2006; Yokozawa et al., 2009)
Astragaloside (astragalus root)	Not known	Prevents amyloid induced memory and neuronal loss in AD mouse model (Li et al., 2009b; Tohda et al., 2006)	Reduced DNA damage after oxidative stress and increased telomere length in mice fibroblasts (Lei et al., 2003; Wang et al., 2010b)
Naringin (centella asiatica, citrus fruits)	Normalised ethanol-induced increase in SIRT1 in rat liver tissue (Oliva et al., 2008)	Cognitive enhancing effects (Kumar et al., 2010; Veerendra Kumar and Gupta, 2003); reduces brain A β levels and is protective against A β -induced neurotoxicity (Dhanasekaran et al., 2009).	Not known
Xanthones (mango, mangosteen)	Not known	Improved learning ability and memory retention in mice and prevented cell damage (Biradar et al., 2012); Inhibits A β aggregation and A β -induced cytotoxicity (Moongkarndi et al., 2010; Wang et al., 2012); Prevents free radical induced oxidative damage in rat brain tissue (Marquez-Valadez et al., 2009)	Inhibits telomerase activity in cancer cells (Wu et al., 2004)
Apigenin (celery)	Not known	Reversed cognitive deficits in aged mice (Patil et al., 2003); Reduce levels of A β by inhibiting α -secretase activity (Shimmyo et al., 2008)	Not known
Isoflavones (soy)	Increased expression of SIRT1 (Rasbach and Schnellmann, 2008)	Protects against A β induced toxicity and inhibits aggregation (Gutierrez-Zepeda et al., 2005; Ma et al., 2009; Yang et al., 2010)	Enhanced cognitive performance in senescence-accelerated mice (Yang et al., 2010)

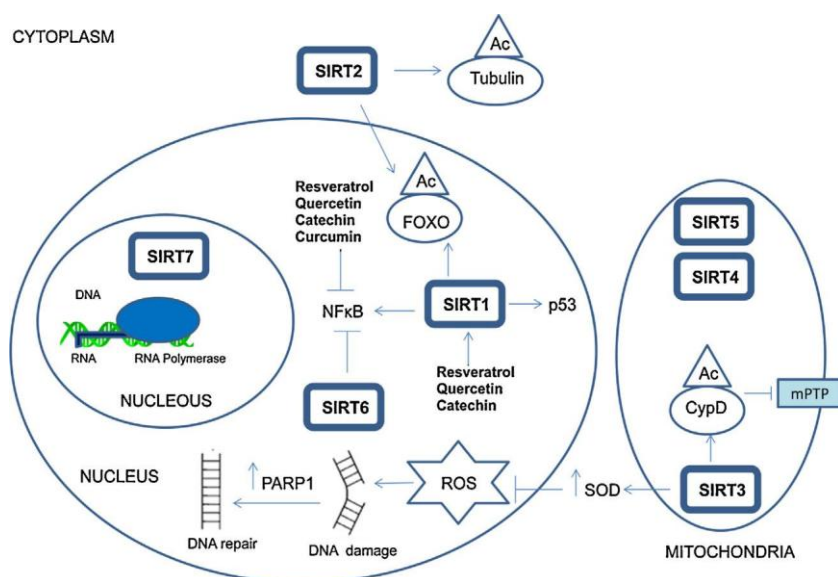


Fig. 2. Potential roles and mechanisms of action of SIRT1-7 and the influence of polyphenols. SIRT1 induces a neuroprotective effect through its interaction with FOXO proteins, p53 and NF B (Brunet et al., 2004; Chen et al., 2005; Langley et al., 2002). SIRT1 is also directly activated by resveratrol. SIRT2 is involved in regulation of the cell cycle as well as neurite outgrowth and axonal degeneration, possibly through its ability to deacetylate tubulin (Maxwell et al., 2011; Wang et al., 2007). SIRT2 is upregulated in response to calorie restriction and oxidative stress, and promotes cell death under severe stress conditions via interaction with FOXO3a (Wang et al., 2007). SIRT3 reduces oxidative stress by increasing superoxide dismutase activity (Qiu et al., 2010). It also deacetylates cyclophilin D (which regulates opening of the mPTP) and thus prevents age-related increase in mitochondrial swelling due to increased opening of the mPTP (Hafner et al., 2010). Very little is known about the other two mitochondrial sirtuins, SIRT4 and SIRT5. SIRT6 is involved in DNA repair following oxidative stress through activation of the DNA repair enzyme PARP-1 (Mao et al., 2011). SIRT7 is thought to be involved in RNA transcription as it activates RNA polymerase 1 transcription (Ford et al., 2006). Resveratrol has been found to activate SIRT1, SIRT2, SIRT3, SIRT4 and SIRT7 protein and/or gene expression in cells and animal models (Lagouge et al., 2006; Mukherjee et al., 2009; Schirmer et al., 2012; Suzuki and Koike, 2007b; Vakhrusheva et al., 2008b; Yu et al., 2009). SIRT1 has also been found to be activated by other polyphenols including quercetin, catechins and kaempferol (Chung et al., 2010; Davis et al., 2009; Marfe et al., 2009; Nerurkar et al., 2011). The anti-inflammatory activity of phenolic compounds has been demonstrated in a number of in vitro and in vivo studies. Polyphenols including catechins, resveratrol and curcumin can reduce inflammation through down-regulation of NF B function (Capiralla et al., 2012; Choi et al., 2009).

in a recent study, the functional food, bitter melon was found to attenuate oxidative stress and neuroinflammation in mice on a high fat diet (Nerurkar et al., 2011). Functional foods are foods or food components which beyond providing basic nutritional needs, also have physiological/pharmacological benefits or reduce the risk of chronic diseases (Arai, 1996). Bitter melon was also found to regulate sirtuin protein and mRNA expression. A high fat diet significantly reduced SIRT1 mRNA expression by 20%, and brain SIRT1 protein levels were reduced by 25% in C57BL/6 female mice (Nerurkar et al., 2011). Feeding of bitter melon normalised both. Interestingly, bitter melon not only normalised SIRT3 levels but also up-regulated SIRT3 mRNA by 20% (Nerurkar et al., 2011). Bitter melon also attenuated oxidative stress and neuroinflammation marker levels caused by the high fat diet. The bitter melon extract contains a variety of polyphenols including gallic acid, genisteic acid, chlorogenic acid and epicatechin, but the most abundant polyphenol isolated was catechin (Nerurkar et al., 2011). Catechins are also most abundant in tea, cocoa and berries and daily consumption of catechin increases life span and delays memory regression in animal models of ageing (Li et al., 2009a; Saul et al., 2009).

Another traditional food *Centella asiatica* has been reported to have a variety of beneficial effects on A β -mediated toxicity, and to promote longevity (Dhanasekaran et al., 2009). It contains numerous polyphenols including quercetin, kaempferol, catechin, rutin and naringin, some of which are potent antioxidants and have demonstrated effects on sirtuins (Table 3). Therefore *C. asiatica* may have the ability to modulate the effects of oxidative stress in the brain directly, and through regulation of sirtuin activity since several of its polyphenols influence the activity and expression of sirtuins. Most of the work to date has focused on SIRT1 as it is the mammalian homolog of yeast Sir2, which was the first organism in which sirtuin functions were studied. SIRT1 was also the first sirtuin which was shown to be activated by a polyphenol, namely

resveratrol. Future investigation into the interaction between sirtuins (especially SIRT2-7) and polyphenols may help determine which polyphenols are specific to which sirtuins and which if any have a general effect on the whole group of proteins.

6. Protective effects of polyphenols against inflammation

Excessive inflammation is considered a critical factor in the pathogenesis of AD. The AD brain has an increased expression of pro-inflammatory cytokines such as interleukin-1 and tumour necrosis factor and evidence of microglial activation (Mrak and Griffin, 2005). Several inflammatory genes are associated with an increased risk of AD, and epidemiological studies on AD patients using non-steroidal anti-inflammatory drugs suggest some benefits (Johnston et al., 2011). Inflammation is also another source of oxidative stress as superoxide and nitric oxide are released.

The anti-inflammatory activity of phenolic compounds has been demonstrated in a number of in vitro and in vivo studies (Santangelo et al., 2007). Polyphenols may affect inflammation not only as antioxidants, but also as modulators of inflammatory redox signalling pathways. Polyphenols can work as modifiers of signal transduction pathways to elicit their beneficial effects (Santangelo et al., 2007). These compounds express anti-inflammatory activity by modulating the expression of pro-inflammatory genes such as cyclooxygenase, lipoxygenase, nitric oxide synthases and several important cytokines, mainly acting through nuclear factor-kappaB and mitogen-activated protein kinase signalling (Ahmed et al., 2002; Bhardwaj et al., 2007; Capiralla et al., 2012; Khan et al., 2006; Santangelo et al., 2007; Xie et al., 1993).

In a transgenic mouse model of AD, treatment with pomegranate extract was found to reduce microgliosis and A β deposition. Significant behavioural improvements were also seen and correlated with decreased tumour necrosis factor

concentration and lower nuclear factor of activated T-cell activity in the pomegranate-fed mice. Pomegranate polyphenols punicalagin and ellagic acid were also shown to decrease A β -induced tumour necrosis factor in cultured mouse microglia (Rojanathammanee et al., 2013).

Polyphenols may also modulate programmed cell death pathways. Resveratrol, EGCG and luteolin have been shown to significantly inhibit the activation of caspase-3 and are able to modulate mitogen-activated protein kinases known to play an important role in neuronal apoptosis (Bastianetto et al., 2011).

7. Protective effects of polyphenols on mitochondrial dysfunction

Changes to the mitochondria seem to be another pathological characteristic of AD. The AD brain shows a reduction in a number of mitochondrial enzyme activities including dehydrogenase enzymes such as pyruvate dehydrogenase, and cyclooxygenase enzymes (Parihar and Brewer, 2007). The cause is unknown, although oxidative stress is thought to play a role. Furthermore the number of intact, normal appearing mitochondria has been shown to decline in the AD brain, particularly in hippocampal neurons (Parihar and Brewer, 2007). Elevation of intracellular A levels may also potentially alter mitochondrial function and lead to increased reactive oxygen species generation (Casley et al., 2002).

Polyphenols have also been proposed to protect mitochondrial function, as has been shown for quercetin, rutin and resveratrol (Carrasco-Pozo et al., 2012). Apple peel polyphenols have similar protective effects by preventing mitochondrial complex I inhibition (Carrasco-Pozo et al., 2011). Grape seed extract has been shown to protect the enzyme activities of the mitochondrial respiratory electron transport chain (complexes I and II) and pyruvate dehydrogenase against oxidative stress (Long et al., 2009). EGCG and luteolin have been found to restore amyloid-induced mitochondrial dysfunction by reducing reactive oxygen species production and normalising mitochondrial membrane potential and cellular ATP levels (Dragicevic et al., 2011). Moreover, polyphenols have also been reported to exert their anti-apoptotic action by inhibiting apoptosis-inducing factor release from mitochondria, thus providing a new mechanism of action for polyphenols (Panickar and Anderson, 2011).

8. Involvement of polyphenols in telomere maintenance

The role of a number of polyphenols in the maintenance of telomere length has been investigated (see Table 3). Telomeres are specialised nucleoprotein structures that protect the ends of eukaryotic chromosomes from unscheduled DNA repair reactions and degradation. Due to the intrinsic inability of the DNA replication machinery to copy the end of linear molecules, and the endogenous DNA end-degrading activity, telomeres become progressively shorter after every cell division cycle. When a critical number of replications are reached, the cells enter senescence (Herbig et al., 2004) or the end of their replicative ability (Hayflick limit).

In humans, several studies have described an inverse correlation between telomere length and age or age-related disease (Cawthon et al., 2003; Panossian et al., 2003; Takubo et al., 2010). Telomere length shortens with normal ageing, life stress, inflammation and chronic diseases (Herbig et al., 2004) and telomere dysfunction is linked to the pathogenesis of age-related diseases including AD (Guan et al., 2008; Panossian et al., 2003). Various nutrients such as nicotinamide and vitamins A, D, C and E are positively associated with telomere length (Kang et al., 2006; Richards et al., 2007, 2008; Xu et al., 2009) via mechanisms that reflect their

role in cellular functions, including DNA repair and chromosome maintenance, DNA methylation, inflammation, oxidative stress modulation and activity of the enzyme telomerase which repairs chromosome ends by adding telomeric repeat subunits. Healthy lifestyles and diets are positively correlated with telomere length. Changes in diet and lifestyle can modulate telomerase activity in peripheral blood mononuclear cells, although it is not yet clear if this translates to changes in telomere length (Ornish et al., 2008).

Resveratrol has been shown to induce telomere maintenance factor WRN helicase (Uchiumi et al., 2011). Another study showed that habitual tea drinkers have longer telomeres in peripheral blood cells than those who drink tea less often (Chan et al., 2010). This may possibly be due to the anti-inflammatory effect of tea polyphenols (De Bacquer et al., 2006). Similarly, the dietary administration of grape seed polyphenols to mice resulted in a trend for longer telomeres compared with controls (Thomas et al., 2009). It is clear that diet and lifestyle can together play a pivotal role in influencing inflammation, oxidative stress and psychological stress, all of which cause telomere attrition. A healthy lifestyle with a diet rich in fruits and vegetables combined with exercise and lower body mass index is indeed associated with longer telomeres (Mirabello et al., 2009). EGCG, quercetin and carvediol were shown to prevent telomere shortening and oxidative stress markers in rat cardiomyocytes after cardiac hypertrophy (Sheng et al., 2011). Two isomers, 4-Hydroxy-5-hydroxymethyl-[1,3]dioxolan-2,6-spirane-5,6,7,8-tetrahydro-indolizine-3-carbaldehyde (HDTIC-1 and HDTIC-2) extracted from *Astragalus membranaceus* root have been shown to extend lifespan of human foetal lung fibroblasts (Wang et al., 2010b). Cells pre-treated with these compounds show a significant reduction in DNA damage after exposure to oxidative stress. The authors hypothesised that the *Astragalus* root extract related delay in replicative senescence was due to the combined effects of: (1) reduction in telomere shortening rate, (2) reduced DNA damage and (3) improvement in DNA repair (Wang et al., 2010b). A small-molecule activator of telomerase known as TA-65 has been purified from the root of the *Astragalus*, and is capable of increasing average telomere length and decreasing the percentage of critically short telomeres, and attenuating DNA damage in mouse fibroblasts (Bernardes de Jesus et al., 2011).

More recently, SIRT1 was reported to be a positive regulator of telomere length in vivo and to attenuate age related telomere shortening, an effect dependent on telomerase activity (Palacios et al., 2010). By contrast, another study found that SIRT1 inhibition was associated with increased telomerase activity in human cells (Narala et al., 2008). These findings link SIRT1 to telomere biology and global DNA repair. Furthermore this effect does not appear to be specific to SIRT1 alone. SIRT6 is associated with telomeric chromatin, and depletion of SIRT6 has been shown to result in pre-mature cellular senescence and telomere dysfunction (Michishita et al., 2008).

9. Therapeutic potential

As the human population continues to age, interventions that improve the quality of life and delay the onset of age-related diseases are highly desirable. Polyphenols are candidates for such interventions through their diverse biochemical roles including free radical scavenging, protein homeostasis, metal chelation, telomere maintenance and stimulation of sirtuins. Their potent effects in combination with little or no known toxicity may give them a therapeutic advantage. In the past, clinical trials using vitamins and antioxidants have frequently had equivocal outcomes in the treatment of AD. One explanation for the failure of single drugs or natural compounds in AD is that this disorder has multiple aetiologies, involving various pathological and molecular

events occurring in parallel or sequentially. This has led to the assumption that a single drug targeting two or more active neuroprotective moieties or a combination of compounds, targeting multiple pathological aspects of the disease, may offer a superior therapeutic benefit over a drug targeting one pathway alone. For example, a treatment regime using a mixture of polyphenols which together exhibit antioxidant, metal chelating, anti-amyloidogenic and sirtuin activation properties may prove to be superior. Initial studies using polyphenol combination therapy or “cocktails” have shown some promising preliminary results (Barger et al., 2008a; Parachikova et al., 2010).

Another important issue is the bioavailability of such compounds. Most polyphenols have poor bioavailability following oral ingestion (Scheepens et al., 2010). Those found in food take the form of glycosides, esters or polymers which cannot be absorbed directly and therefore must be hydrolysed by microflora or enzymes of the small intestine (Manach et al., 2004). A further confounder for the central nervous system is that polyphenols cannot pass easily through the blood brain barrier. There are however, various strategies currently under investigation to improve bioactivity. It has been found that some polyphenols can specifically modify metabolic and transport processes that govern bioavailability (Scheepens et al., 2010). Therefore, specific synergistic combinations and interactions could be designed to improve entry into the brain. Another promising method is the use of nanoparticle carriers coupled to polyphenols (Souto et al., 2013). Brain permeable nanoparticles may be used to enhance entry of poorly absorbed phenolic compounds into the brain (Bonda et al., 2012; Dogguit et al., 2012; Sahni et al., 2011). Creation and administration of EGCG nanolipidic complexes were found to double the oral bioavailability of EGCG in male Sprague-Dawley rats and also improve the EGCG's ability to enhance -secretase activity in vitro (Smith et al., 2010). Cocrystallisation is another technique which could increase solubility and thus bioavailability of polyphenols. This procedure used with quercetin has shown promising results with cocrystals of quercetin showing significant increases in solubility and oral bioavailability (Smith et al., 2011).

10. Conclusion

The emerging view that polyphenols may exert a variety of modulatory actions which influence the pathogenesis of AD has brought attention to functions beyond their usual antioxidant activities. A clearer understanding of the mechanisms of action of polyphenols, as modulators of cell signalling, their role in amyloid and tau disaggregation, telomere and mitochondria maintenance and modulation of sirtuins, and the influence of their metabolism on these properties, are pivotal for the evaluation of these potent biomolecules as inhibitors of neurodegeneration, and in developing effective treatment regimes for AD. This appears to be a promising area for future work.

Acknowledgements

This work was supported by a National Health & Medical Research Council of Australia Capacity Building Grant (ID No. 568940) and Program Grant (ID No. 568969) and a UNSW Faculty of Medicine Research Grant. NB is the recipient of an Alzheimer's Australia Viertel Foundation Postdoctoral Research Fellowship at the University of New South Wales. TJ is a recipient of the University of New South Wales Postgraduate Award (UPA). The authors thank the Rebecca Cooper Medical Research Foundation for their ongoing financial support.

References

- Agarwal, B., Baur, J.A., 2011. Resveratrol and life extension. *Annals of the New York Academy of Sciences* 1215, 138–143.
- Ahmed, S., Rahman, A., Hasnain, A., Lalonde, M., Goldberg, V.M., Haqqi, T.M., 2002. Green tea polyphenol epigallocatechin-3-gallate inhibits the IL-1 beta-induced activity and expression of cyclooxygenase-2 and nitric oxide synthase-2 in human chondrocytes. *Free Radical Biology and Medicine* 33, 1097–1105.
- Ahmed, T., Enam, S.A., Gilani, A.H., 2010. Curcuminoids enhance memory in an amyloid-infused rat model of Alzheimer's disease. *Neuroscience* 169, 1296–1306.
- Akaishi, T., Morimoto, T., Shibao, M., Watanabe, S., Sakai-Kato, K., Utsunomiya-Tate, N., Abe, K., 2008. Structural requirements for the flavonoid fisetin in inhibiting fibril formation of amyloid beta protein. *Neuroscience Letters* 444, 280–285.
- Akieda-Asai, S., Zaima, N., Ikegami, K., Kahyo, T., Yao, I., Hatanaka, T., Iemura, S., Sugiyama, R., Yokozeki, T., Eishi, Y., Koike, M., Ikeda, K., Chiba, T., Yamaza, H., Shimokawa, I., Song, S.Y., Matsuno, A., Mizutani, A., Sawabe, M., Chao, M.V., Tanaka, M., Kanaho, Y., Natsume, T., Sugimura, H., Date, Y., McBurney, M.W., Guarente, L., Setou, M., 2010. SIRT1 Regulates Thyroid-Stimulating Hormone Release by Enhancing PIP5Kgamma Activity through Deacetylation of Specific Lysine Residues in Mammals. *PLoS One* 5, e11755.
- Aksenov, M.Y., Aksenova, M.V., Butterfield, D.A., Geddes, J.W., Markesbery, W.R., 2001. Protein oxidation in the brain in Alzheimer's disease. *Neuroscience* 103, 373–383.
- Alonso, Á.M., Castro, R., Rodríguez, M.C., Guillén, D.A., Barroso, C.G., 2004. Study of the antioxidant power of brandies and vinegars derived from Sherry wines and correlation with their content in polyphenols. *Food Research International* 37, 715–721.
- Alvarez-Suarez, J.M., Dekanski, D., Ristic, S., Radonjic, N.V., Petronijevic, N.D., Giampieri, F., Astolfi, P., Gonzalez-Paramas, A.M., Santos-Buelga, C., Tulipani, S., Quiles, J.L., Mezzetti, B., Battino, M., 2011. Strawberry polyphenols attenuate ethanol-induced gastric lesions in rats by activation of antioxidant enzymes and attenuation of MDA increase. *PLoS One* 6, e25878.
- Ansari, M.A., Abdul, H.M., Joshi, G., Opii, W.O., Butterfield, D.A., 2009. Protective effect of quercetin in primary neurons against Abeta(1-42): relevance to Alzheimer's disease. *Journal of Nutritional Biochemistry* 20, 269–275.
- Arai, S., 1996. Studies on functional foods in Japan—state of the art. *Bioscience, Biotechnology, and Biochemistry* 60, 9–15.
- Arts, I.C., van de Putte, B., Hollman, P.C., 2000a. Catechin contents of foods commonly consumed in The Netherlands. 1. Fruits, vegetables, staple foods, and processed foods. *Journal of Agricultural and Food Chemistry* 48, 1746–1751.
- Arts, I.C., van De Putte, B., Hollman, P.C., 2000b. Catechin contents of foods commonly consumed in The Netherlands. 2. Tea, wine, fruit juices, and chocolate milk. *Journal of Agricultural and Food Chemistry* 48, 1752–1757.
- Asha Devi, S., Sagar Chandrasekar, B.K., Manjula, K.R., Ishii, N., 2011. Grape seed proanthocyanidin lowers brain oxidative stress in adult and middle-aged rats. *Experimental Gerontology* 46, 958–964.
- Atwood, C.S., Obrenovich, M.E., Liu, T., Chan, H., Perry, G., Smith, M.A., Martins, R.N., 2003. Amyloid-beta: a chameleon walking in two worlds: a review of the trophic and toxic properties of amyloid-beta. *Brain Research* 973, 1–16.
- Barger, J.L., Kaye, T., Pugh, T.D., Prolla, T.A., Weindruch, R., 2008a. Short-term consumption of a resveratrol-containing nutraceutical mixture mimics gene expression of long-term caloric restriction in mouse heart. *Experimental Gerontology* 43, 859–866.
- Barger, J.L., Kaye, T., Vann, J.M., Arias, E.B., Wang, J., Hacker, T.A., Wang, Y., Raedestorff, D., Morrow, J.D., Leeuwenburgh, C., Allison, D.B., Saupe, K.W., Cartee, G.D., Weindruch, R., Prolla, T.A., 2008b. A low dose of dietary resveratrol partially mimics caloric restriction and retards aging parameters in mice. *PLoS One* 3, e2264.
- Barnham, K.J., Masters, C.L., Bush, A.I., 2004. Neurodegenerative diseases and oxidative stress. *Nature Reviews Drug Discovery* 3, 205–214.
- Bastianetto, S., Krantic, S., Chabot, J.G., Quirion, R., 2011. Possible involvement of programmed cell death pathways in the neuroprotective action of polyphenols. *Current Alzheimer Research* 8, 445–451.
- Baur, J.A., Sinclair, D.A., 2006. Therapeutic potential of resveratrol: the in vivo evidence. *Nature Reviews Drug Discovery* 5, 493–506.
- Beirowski, B., Gustin, J., Armour, S.M., Yamamoto, H., Viader, A., North, B.J., Michan, S., Baloh, R.H., Golden, J.P., Schmidt, R.E., Sinclair, D.A., Auwerx, J., Milbrandt, J., 2011. Sir-two-homolog 2 (Sirt2) modulates peripheral myelination through polarity protein Par-3/atypical protein kinase C (aPKC) signaling. *Proceedings of the National Academy of Sciences of the United States of America* 108, E952–E961.
- Belinha, I., Amorim, M.A., Rodrigues, P., de Freitas, V., Moradas-Ferreira, P., Mateus, N., Costa, V., 2007. Quercetin increases oxidative stress resistance and longevity in *Saccharomyces cerevisiae*. *Journal of Agricultural and Food Chemistry* 55, 2446–2451.
- Bell, E.L., Guarente, L., 2011. The SirT3 divining rod points to oxidative stress. *Molecular Cell* 42, 561–568.
- Bernardes de Jesus, B., Schmeberger, K., Vera, E., Tejera, A., Harley, C.B., Blasco, M.A., 2011. The telomerase activator TA-65 elongates short telomeres and increases health span of adult/old mice without increasing cancer incidence. *Aging Cell* 10, 604–621.
- Bhardwaj, A., Sethi, G., Vadhan-Raj, S., Bueso-Ramos, C., Takada, Y., Gaur, U., Nair, A.S., Shishodia, S., Aggarwal, B.B., 2007. Resveratrol inhibits proliferation, induces apoptosis, and overcomes chemoresistance through down-regulation of STAT3

- and nuclear factor-kappaB-regulated antiapoptotic and cell survival gene products in human multiple myeloma cells. *Blood* 109, 2293–2302.
- Bieschke, J., Russ, J., Friedrich, R.P., Ehrnhoefer, D.E., Wobst, H., Neugebauer, K., Wanker, E.E., 2010. EGCG remodels mature alpha-synuclein and amyloid-beta fibrils and reduces cellular toxicity. *Proceedings of the National Academy of Sciences of the United States of America* 107, 7710–7715.
- Biradar, S.M., Joshi, H., Chheda, T.K., 2012. Neuropharmacological effect of Mangiferin on brain cholinesterase and brain biogenic amines in the management of Alzheimer's disease. *European Journal of Pharmacology* 683, 140–147.
- Bisson, J.F., Nejd, A., Rozan, P., Hidalgo, S., Lalonde, R., Messaoudi, M., 2008. Effects of long-term administration of a cocoa polyphenolic extract (Acticoa powder) on cognitive performances in aged rats. *British Journal of Nutrition* 100, 94–101.
- Bonda, D.J., Liu, G., Men, P., Perry, G., Smith, M.A., Zhu, X., 2012. Nanoparticle delivery of transition-metal chelators to the brain: Oxidative stress will never see it coming! *CNS & Neurological Disorders: Drug Targets* 11, 81–85.
- Bordone, L., Cohen, D., Robinson, A., Motta, M.C., van Veen, E., Czopik, A., Steele, A.D., Crowe, H., Marmor, S., Luo, J., Gu, W., Guarente, L., 2007. SIRT1 transgenic mice show phenotypes resembling calorie restriction. *Aging Cell* 6, 759–767.
- Borra, M.T., Smith, B.C., Denu, J.M., 2005. Mechanism of human SIRT1 activation by resveratrol. *Journal of Biological Chemistry* 280, 17187–17195.
- Brown, J.E., Khodr, H., Hider, R.C., Rice-Evans, C.A., 1998. Structural dependence of flavonoid interactions with Cu²⁺ ions: implications for their antioxidant properties. *The Biochemical Journal* 330 (Pt 3), 1173–1178.
- Brown, V.A., Patel, K.R., Viskaduraki, M., Crowell, J.A., Perloff, M., Booth, T.D., Vasilinin, G., Sen, A., Schinas, A.M., Piccirilli, G., Brown, K., Steward, W.P., Gescher, A.J., Brenner, D.E., 2010. Repeat dose study of the cancer chemopreventive agent resveratrol in healthy volunteers: safety, pharmacokinetics, and effect on the insulin-like growth factor axis. *Cancer Research* 70, 9003–9011.
- Brunet, A., Sweeney, L.B., Sturgill, J.F., Chua, K.F., Greer, P.L., Lin, Y., Tran, H., Ross, S.E., Mostoslavsky, R., Cohen, H.Y., Hu, L.S., Cheng, H.L., Jedrychowski, M.P., Gygi, S.P., Sinclair, D.A., Alt, F.W., Greenberg, M.E., 2004. Stress-dependent regulation of FOXO transcription factors by the SIRT1 deacetylase. *Science* 303, 2011–2015.
- Buettner, G.R., Jurkiewicz, B.A., 1996. Catalytic metals, ascorbate and free radicals: combinations to avoid. *Radiation research* 145, 532–541.
- Burnett, C., Valentini, S., Cabreiro, F., Goss, M., Somogyvari, M., Piper, M.D., Hod-dinott, M., Sutphin, G.L., Leko, V., McElwee, J.J., Vazquez-Manrique, R.P., Orfila, A.M., Ackerman, D., Au, C., Vinti, G., Riesen, M., Howard, K., Neri, C., Bedalov, A., Kaeblerlein, M., Soti, C., Partridge, L., Gems, D., 2011. Absence of effects of Sir2 overexpression on lifespan in *C. elegans* and *Drosophila*. *Nature* 477, 482–485.
- Burns, J., Gardner, P.T., O'Neil, J., Crawford, S., Morecroft, I., McPhail, D.B., Lister, C., Matthews, D., MacLean, M.R., Lean, M.E., Duthie, G.G., Crozier, A., 2000. Relationship among antioxidant activity, vasodilation capacity, and phenolic content of red wines. *Journal of Agricultural and Food Chemistry* 48, 220–230.
- Butterfield, D.A., 2002. Amyloid beta-peptide (1–42)-induced oxidative stress and neurotoxicity: implications for neurodegeneration in Alzheimer's disease brain. A review. *Free Radical Research* 36, 1307–1313.
- Capiralla, H., Vingtdex, V., Zhao, H., Sankowski, R., Al-Abed, Y., Davies, P., Marambaud, P., 2012. Resveratrol mitigates lipopolysaccharide- and Abeta-mediated microglial inflammation by inhibiting the TLR4/NF-kappaB/STAT signaling cascade. *Journal of Neurochemistry* 120, 461–472.
- Carrasco-Pozo, C., Gotteland, M., Speisky, H., 2011. Apple peel polyphenol extract protects against indomethacin-induced damage in Caco-2 cells by preventing mitochondrial complex I inhibition. *Journal of Agricultural and Food Chemistry* 59, 11501–11508.
- Carrasco-Pozo, C., Mizgier, M.L., Speisky, H., Gotteland, M., 2012. Differential protective effects of quercetin, resveratrol, rutin and epigallocatechin gallate against mitochondrial dysfunction induced by indomethacin in Caco-2 cells. *Chemico-Biological Interactions* 195, 199–205.
- Casley, C.S., Canevari, L., Land, J.M., Clark, J.B., Sharpe, M.A., 2002. Beta-amyloid inhibits integrated mitochondrial respiration and key enzyme activities. *Journal of neurochemistry* 80, 91–100.
- Cawthon, R.M., Smith, K.R., O'Brien, E., Sivatchenko, A., Kerber, R.A., 2003. Association between telomere length in blood and mortality in people aged 60 years or older. *Lancet* 361, 393–395.
- Chan, R., Woo, J., Suen, E., Leung, J., Tang, N., 2010. Chinese tea consumption is associated with longer telomere length in elderly Chinese men. *British Journal of Nutrition* 103, 107–113.
- Chandrasekara, K.T., Shakarad, M.N., 2011. Aloe vera or resveratrol supplementation in larval diet delays adult aging in the fruit fly, *Drosophila melanogaster*. *Journals of Gerontology, Series A: Biological Sciences and Medical Sciences* 66, 965–971.
- Chen, J., Zhou, Y., Mueller-Stainer, S., Chen, L.F., Kwon, H., Yi, S., Mucke, L., Gan, L., 2005. SIRT1 protects against microglia-dependent amyloid-beta toxicity through inhibiting NF-kappaB signaling. *Journal of Biological Chemistry* 280, 40364–40374.
- Cheng, I.F., Breen, K., 2000. On the ability of four flavonoids, baiclein, luteolin, naringenin, and quercetin, to suppress the Fenton reaction of the iron-ATP complex. *Biomaterials: An International Journal on the Role of Metal Ions in Biology, Biochemistry, and Medicine* 13, 77–83.
- Cho, N., Choi, J.H., Yang, H., Jeong, E.J., Lee, K.Y., Kim, Y.C., Sung, S.H., 2012. Neuroprotective and anti-inflammatory effects of flavonoids isolated from *Rhus verniciflua* in neuronal HT22 and microglial BV2 cell lines. *Food and chemical toxicology: an international journal published for the British Industrial Biological Research Association* 50, 1940–1945.
- Choi, K.C., Jung, M.G., Lee, Y.H., Yoon, J.C., Kwon, S.H., Kang, H.B., Kim, M.J., Cha, J.H., Kim, Y.J., Jun, W.J., Lee, J.M., Yoon, H.G., 2009. Epigallocatechin-3-gallate, a histone acetyltransferase inhibitor, inhibits EBV-induced B lymphocyte transformation via suppression of RelA acetylation. *Cancer Research* 69, 583–592.
- Chukwumah, Y., Walker, L., Vogler, B., Verghese, M., 2007. Changes in the phyto-chemical composition and profile of raw, boiled, and roasted peanuts. *Journal of Agricultural and Food Chemistry* 55, 9266–9273.
- Chung, S., Yao, H., Caito, S., Hwang, J.W., Arunachalam, G., Rahman, I., 2010. Regulation of SIRT1 in cellular functions: role of polyphenols. *Archives of Biochemistry and Biophysics* 501, 79–90.
- Cohen, D.E., Supinski, A.M., Bonkowski, M.S., Donmez, G., Guarente, L.P., 2009. Neuronal SIRT1 regulates endocrine and behavioral responses to calorie restriction. *Genes and Development* 23, 2812–2817.
- Crujeiras, A.B., Parra, D., Goyenechea, E., Martinez, J.A., 2008. Sirtuin gene expression in human mononuclear cells is modulated by caloric restriction. *European Journal of Clinical Investigation* 38, 672–678.
- D'Archivio, M., Filesi, C., Di Benedetto, R., Gargiulo, R., Giovannini, C., Masella, R., 2007. Polyphenols, dietary sources and bioavailability. *Annali dell'Istituto Superiore di Sanita* 43, 348–361.
- Dave, M., Attur, M., Palmer, G., Al-Mussawir, H.E., Kennish, L., Patel, J., Abramson, S.B., 2008. The antioxidant resveratrol protects against chondrocyte apoptosis via effects on mitochondrial polarization and ATP production. *Arthritis and Rheumatism* 58, 2786–2797.
- Davis, J.M., Murphy, E.A., Carmichael, M.D., 2009a. Effects of the dietary flavonoid quercetin upon performance and health. *Current sports medicine reports* 8, 206–213.
- Davis, J.M., Murphy, E.A., Carmichael, M.D., Davis, B., 2009b. Quercetin increases brain and muscle mitochondrial biogenesis and exercise tolerance. *American Journal of Physiology. Regulatory, Integrative and Comparative Physiology* 296, R1071–R1077.
- De Bacquer, D., Clays, E., Delanghe, J., De Backer, G., 2006. Epidemiological evidence for an association between habitual tea consumption and markers of chronic inflammation. *Atherosclerosis* 189, 428–435.
- Desideri, G., Kwik-Uribe, C., Grassi, D., Necozione, S., Ghiadoni, L., Mastroiaco, D., Raffaele, A., Ferri, L., Bocale, R., Lechiara, M.C., Marini, C., Ferri, C., 2012. Benefits in cognitive function, blood pressure, and insulin resistance through cocoa flavanol consumption in elderly subjects with mild cognitive impairment: the Cocoa, Cognition, and Aging (CoCoA) study. *Hypertension* 60, 794–801.
- Dhanasekaran, M., Holcomb, L.A., Hitt, A.R., Tharakan, B., Porter, J.W., Young, K.A., Manyam, B.V., 2009. Centella asiatica extract selectively decreases amyloid beta levels in hippocampus of Alzheimer's disease animal model. *Phytotherapy Research* 23, 14–19.
- Do Carmo Barbosa Mendes De Vasconcelos, M., Bennett, R.N., Rosa, E.A., Ferreira Cardoso, J.V., 2007. Primary and secondary metabolite composition of kernels from three cultivars of Portuguese chestnut (*Castanea sativa* Mill.) at different stages of industrial transformation. *Journal of Agricultural and Food Chemistry* 55, 3508–3516.
- Doggui, S., Dao, L., Ramassamy, C., 2012. Potential of drug-loaded nanoparticles for Alzheimer's disease: diagnosis, prevention and treatment. *Therapeutic delivery* 3, 1025–1027.
- Donmez, G., Wang, D., Cohen, D.E., Guarente, L., 2010. SIRT1 suppresses beta-amyloid production by activating the alpha-secretase gene ADAM10. *Cell* 142, 320–332.
- Dragicevic, N., Smith, A., Lin, X., Yuan, F., Copes, N., Delic, V., Tan, J., Cao, C., Shytle, R.D., Bradshaw, P.C., 2011. Green tea epigallocatechin-3-gallate (EGCG) and other flavonoids reduce Alzheimer's amyloid-induced mitochondrial dysfunction. *Journal of Alzheimer's disease: JAD* 26, 507–521.
- Ehala, S., Vaht, M., Kaljurand, M., 2005. Characterization of phenolic profiles of Northern European berries by capillary electrophoresis and determination of their antioxidant activity. *Journal of Agricultural and Food Chemistry* 53, 6484–6490.
- Fernandez, A.F., Fraga, M.F., 2011. The effects of the dietary polyphenol resveratrol on human healthy aging and lifespan. *Epigenetics* 6, 870–874.
- Fontana, L., Meyer, T.E., Klein, S., Holloszy, J.O., 2004. Long-term calorie restriction is highly effective in reducing the risk for atherosclerosis in humans. *Proceedings of the National Academy of Sciences of the United States of America* 101, 6659–6663.
- Fontana, L., Partridge, L., Longo, V.D., 2010. Extending healthy life span—from yeast to humans. *Science* 328, 321–326.
- Ford, E., Voit, R., Liszt, G., Magin, C., Grummt, I., Guarente, L., 2006. Mammalian Sir2 homolog SIRT7 is an activator of RNA polymerase I transcription. *Genes and Development* 20, 1075–1080.
- Frei, B., Higdon, J.V., 2003. Antioxidant activity of tea polyphenols in vivo: evidence from animal studies. *Journal of Nutrition* 133, 3275S–3284S.
- Frydman-Marom, A., Levin, A., Farfara, D., Benromano, T., Scherzer-Attali, R., Peled, S., Vassar, R., Segal, D., Gazit, E., Frenkel, D., Ovadia, M., 2011. Orally administered cinnamon extract reduces beta-amyloid oligomerization and corrects cognitive impairment in Alzheimer's disease animal models. *PLoS One* 6, e16564.
- Gertz, M., Nguyen, G.T., Fischer, F., Suenkel, B., Schlicker, C., Franzel, B., Tomaschewski, J., Aladini, F., Becker, C., Wolters, D., Steegborn, C., 2012. A molecular mechanism for direct sirtuin activation by resveratrol. *PLoS One* 7, e49761.
- Giunta, B., Hou, H., Zhu, Y., Salemi, J., Ruscin, A., Shytle, R.D., Tan, J., 2010. Fish oil enhances anti-amyloidogenic properties of green tea EGCG in Tg2576 mice. *Neuroscience Letters* 471, 134–138.
- Glorioso, C., Oh, S., Douillard, G.G., Sibille, E., 2011. Brain molecular aging, promotion of neurological disease and modulation by sirtuin 5 longevity gene polymorphism. *Neurobiology of Disease* 41, 279–290.
- Greilberger, J., Koidl, C., Greilberger, M., Lamprecht, M., Schroecksnadel, K., Leblhuber, F., Fuchs, D., Oertl, K., 2008. Malondialdehyde, carbonyl proteins and

- albumin-disulphide as useful oxidative markers in mild cognitive impairment and Alzheimer's disease. *Free Radical Research* 42, 633–638.
- Gu, L., Kelm, M.A., Hammerstone, J.F., Beecher, G., Holden, J., Haytowitz, D., Gebhardt, S., Prior, R.L., 2004. Concentrations of proanthocyanidins in common foods and estimations of normal consumption. *Journal of Nutrition* 134, 613–617.
- Guan, J.Z., Maeda, T., Sugano, M., Oyama, J., Higuchi, Y., Suzuki, T., Makino, N., 2008. A percentage analysis of the telomere length in Parkinson's disease patients. *Journals of Gerontology Series A: Biological Sciences and Medical Sciences* 63, 467–473.
- Guarente, L., 2008. Mitochondria—a nexus for aging, calorie restriction, and sirtuins? *Cell* 132, 171–176.
- Gutierrez-Zepeda, A., Santell, R., Wu, Z., Brown, M., Wu, Y., Khan, I., Link, C.D., Zhao, B., Luo, Y., 2005. Soy isoflavone genistein protects against beta amyloid-induced toxicity and oxidative stress in transgenic *Caenorhabditis elegans*. *BMC Neuro-science* 6, 54.
- Hafner, A.V., Dai, J., Gomes, A.P., Xiao, C.Y., Palmeira, C.M., Rosenzweig, A., Sinclair, D.A., 2010. Regulation of the mPTP by SIRT3-mediated deacetylation of CypD at lysine 166 suppresses age-related cardiac hypertrophy. *Aging (Albany NY)* 2, 914–923.
- Haigis, M.C., Mostoslavsky, R., Haigis, K.M., Fahie, K., Christodoulou, D.C., Murphy, A.J., Valenzuela, D.M., Yancopoulos, G.D., Karow, M., Blander, G., Wolberger, C., Prolla, T.A., Weindruch, R., Alt, F.W., Guarente, L., 2006. SIRT4 inhibits glutamate dehydrogenase and opposes the effects of calorie restriction in pancreatic beta cells. *Cell* 126, 941–954.
- Halaschek-Wiener, J., Amirabasi-Beik, M., Monfared, N., Pieczyk, M., Sailer, C., Kol-lar, A., Thomas, R., Agalaridis, G., Yamada, S., Oliveira, L., Collins, J.A., Meneilly, G., Marra, M.A., Madden, K.M., Le, N.D., Connors, J.M., Brooks-Wilson, A.R., 2009. Genetic variation in healthy oldest-old. *PLoS One* 4, e6641.
- Harman, D., 1956. Aging: a theory based on free radical and radiation chemistry. *Journal of Gerontology* 11, 298–300.
- Harting, K., Knoll, B., 2010. SIRT2-mediated protein deacetylation: An emerging key regulator in brain physiology and pathology. *European Journal of Cell Biology* 89, 262–269.
- Hasegawa, T., Baba, T., Kobayashi, M., Konno, M., Sugeno, N., Kikuchi, A., Itoyama, Y., Takeda, A., 2010. Role of TPPP/p25 on alpha-synuclein-mediated oligodendroglial degeneration and the protective effect of SIRT2 inhibition in a cellular model of multiple system atrophy. *Neurochemistry International* 57, 857–866.
- Heilbronn, L.K., de Jonge, L., Frisard, M.I., DeLany, J.P., Larson-Meyer, D.E., Rood, J., Nguyen, T., Martin, C.K., Volaufova, J., Most, M.M., Greenway, F.L., Smith, S.R., Deutsch, W.A., Williamson, D.A., Ravussin, E., Pennington, C.T., 2006. Effect of 6-month calorie restriction on biomarkers of longevity, metabolic adaptation, and oxidative stress in overweight individuals: a randomized controlled trial. *JAMA* 295, 1539–1548.
- Hensley, K., Maidt, M.L., Yu, Z., Sang, H., Markesbery, W.R., Floyd, R.A., 1998. Electrochemical analysis of protein nitrotyrosine and dityrosine in the Alzheimer brain indicates region-specific accumulation. *Journal of Neuroscience* 18, 8126–8132.
- Heo, H.J., Lee, C.Y., 2004. Protective effects of quercetin and vitamin C against oxidative stress-induced neurodegeneration. *Journal of Agricultural and Food Chemistry* 52, 7514–7517.
- Herbig, U., Jobling, W.A., Chen, B.P., Chen, D.J., Sedivy, J.M., 2004. Telomere shortening triggers senescence of human cells through a pathway involving ATM, p53, and p21(CIP1), but not p16(INK4a). *Molecular Cell* 14, 501–513.
- Hider, R.C., Liu, Z.D., Khodr, H.H., 2001. Metal chelation of polyphenols. *Methods in Enzymology* 335, 190–203.
- Hirschey, M.D., Shimazu, T., Goetzman, E., Jing, E., Schwer, B., Lombard, D.B., Grueter, C.A., Harris, C., Biddinger, S., Ilkayeva, O.R., Stevens, R.D., Li, Y., Saha, A.K., Ruderman, N.B., Bain, J.R., Newgard, C.B., Farese Jr., R.V., Alt, F.W., Kahn, C.R., Verdin, E., 2010. SIRT3 regulates mitochondrial fatty-acid oxidation by reversible enzyme deacetylation. *Nature* 464, 121–125.
- Holloszy, J.O., Fontana, L., 2007. Caloric restriction in humans. *Experimental Gerontology* 42, 709–712.
- Honda, K., Casadesus, G., Petersen, R.B., Perry, G., Smith, M.A., 2004. Oxidative stress and redox-active iron in Alzheimer's disease. *Annals of the New York Academy of Sciences* 1012, 179–182.
- Horio, Y., Hayashi, T., Kuno, A., Kunimoto, R., 2011. Cellular and molecular effects of sirtuins in health and disease. *Clinical Science (London)* 121, 191–203.
- Howitz, K.T., Bitterman, K.J., Cohen, H.Y., Lamming, D.W., Lavu, S., Wood, J.G., Zipkin, R.E., Chung, P., Kisielewski, A., Zhang, L.L., Scherer, B., Sinclair, D.A., 2003. Small molecule activators of sirtuins extend *Saccharomyces cerevisiae* lifespan. *Nature* 425, 191–196.
- Huang, H.C., Chang, P., Dai, X.L., Jiang, Z.F., 2012. Protective effects of curcumin on amyloid-beta-induced neuronal oxidative damage. *Neurochemical Research* 37, 1584–1597.
- Jena, S., Dandapat, J., Chainy, G.B., 2012. Curcumin differentially regulates the expression of superoxide dismutase in cerebral cortex and cerebellum of L: -thyroxine (T4)-induced hyperthyroid rat brain. *Neurological Sciences*.
- Johnston, H., Boutin, H., Allan, S.M., 2011. Assessing the contribution of inflammation in models of Alzheimer's disease. *Biochemical Society Transactions* 39, 886–890.
- Jomova, K., Vondrakova, D., Lawson, M., Valko, M., 2010. Metals, oxidative stress and neurodegenerative disorders. *Molecular and Cellular Biochemistry* 345, 91–104.
- Julien, C., Tremblay, C., Emond, V., Lebbadi, M., Salem Jr., N., Bennett, D.A., Calon, F., 2009. Sirtuin 1 reduction parallels the accumulation of tau in Alzheimer disease. *Journal of Neuropathology & Experimental Neurology* 68, 48–58.
- Justesen, U., Knuthsen, P., Leth, T., 1998. Quantitative analysis of flavonols, flavones, and flavanones in fruits, vegetables and beverages by high-performance liquid chromatography with photo-diode array and mass spectrometric detection. *Journal of Chromatography A* 799, 101–110.
- Kaeberlein, M., McVey, M., Guarente, L., 1999. The SIR2/3/4 complex and SIR2 alone promote longevity in *Saccharomyces cerevisiae* by two different mechanisms. *Genes and Development* 13, 2570–2580.
- Kaeberlein, M., McDonagh, T., Heltweg, B., Hixon, J., Westman, E.A., Caldwell, S.D., Napper, A., Curtis, R., DiStefano, P.S., Fields, S., Bedalov, A., Kennedy, B.K., 2005. Substrate-specific activation of sirtuins by resveratrol. *Journal of Biological Chemistry* 280, 17038–17045.
- Kampkotter, A., Gombitang Nkwonkam, C., Zurawski, R.F., Timpel, C., Chovolou, Y., Watjen, W., Kahl, R., 2007. Effects of the flavonoids kaempferol and fisetin on thermotolerance, oxidative stress and FoxO transcription factor DAF-16 in the model organism *Caenorhabditis elegans*. *Archives of toxicology* 81, 849–858.
- Kang, H.T., Lee, H.I., Hwang, E.S., 2006. Nicotinamide extends replicative lifespan of human cells. *Aging Cell* 5, 423–436.
- Karuppagounder, S.S., Pinto, J.T., Xu, H., Chen, H.L., Beal, M.F., Gibson, G.E., 2009. Dietary supplementation with resveratrol reduces plaque pathology in a transgenic model of Alzheimer's disease. *Neurochemistry International* 54, 111–118.
- Kawahara, T.L., Michishita, E., Adler, A.S., Damian, M., Berber, E., Lin, M., McCord, R.A., Ongaigui, K.C., Boxer, L.D., Chang, H.Y., Chua, K.F., 2009. SIRT6 links histone H3 lysine 9 deacetylation to NF-kappaB-dependent gene expression and organismal life span. *Cell* 136, 62–74.
- Kawahara, T.L., Rapicavoli, N.A., Wu, A.R., Qu, K., Quake, S.R., Chang, H.Y., 2011. Dynamic chromatin localization of Sirt6 shapes stress- and aging-related transcriptional networks. *PLoS Genet* 7, e1002153.
- Khan, N., Afaq, F., Saleem, M., Ahmad, N., Mukhtar, H., 2006. Targeting multiple signaling pathways by green tea polyphenol (-)-epigallocatechin-3-gallate. *Can-cer Research* 66, 2500–2505.
- Khurana, S., Jain, S., Mediratta, P.K., Banerjee, B.D., Sharma, K.K., 2012. Protective role of curcumin on colchicine-induced cognitive dysfunction and oxidative stress in rats. *Human and Experimental Toxicology* 31, 686–697.
- Kim, T.S., Pae, C.U., Yoon, S.J., Jang, W.Y., Lee, N.J., Kim, J.J., Lee, S.J., Lee, C., Paik, I.H., Lee, C.U., 2006. Decreased plasma antioxidants in patients with Alzheimer's disease. *International Journal of Geriatric Psychiatry* 21, 344–348.
- Kim, D., Nguyen, M.D., Dobbin, M.M., Fischer, A., Sananbenesi, F., Rodgers, J.T., Delalle, I., Baur, J.A., Sui, G., Armour, S.M., Puigserver, P., Sinclair, D.A., Tsai, L.H., 2007. SIRT1 deacetylase protects against neurodegeneration in models for Alzheimer's disease and amyotrophic lateral sclerosis. *EMBO Journal* 26, 3169–3179.
- Kim, J.K., Choi, S.J., Cho, H.Y., Hwang, H.J., Kim, Y.J., Lim, S.T., Kim, C.J., Kim, H.K., Peterson, S., Shin, D.H., 2010. Protective effects of kaempferol (3,4',5,7-tetrahydroxyflavone) against amyloid beta peptide (Aβeta)-induced neurotoxicity in ICR mice. *Bioscience, Biotechnology, and Biochemistry* 74, 397–401.
- Kim, S.H., Lu, H.F., Alano, C.C., 2011. Neuronal Sirt3 protects against excitotoxic injury in mouse cortical neuron culture. *PLoS One* 6, e14731.
- Kitani, K., Osawa, T., Yokozawa, T., 2007. The effects of tetrahydrocurcumin and green tea polyphenol on the survival of male C57BL/6 mice. *Biogerontology* 8, 567–573.
- Kojro, E., Fahrenholz, F., 2005. The non-amyloidogenic pathway: structure and function of alpha-secretases. *Sub-Cellular Biochemistry* 38, 105–127.
- Ksiezak-Reding, H., Ho, L., Santa-Maria, I., Diaz-Ruiz, C., Wang, J., Pasinetti, G.M., 2012. Ultrastructural alterations of Alzheimer's disease paired helical filaments by grape seed-derived polyphenols. *Neurobiology of Aging* 33, 1427–1439.
- Kumar, A., Prakash, A., Dogra, S., 2010. Naringin alleviates cognitive impairment, mitochondrial dysfunction and oxidative stress induced by D-galactose in mice. *Food and chemical toxicology: an international journal published for the British Industrial Biological Research Association.*, 626–632.
- Kumari, M.V., Yoneda, T., Hiramatsu, M., 1997. Effect of beta CATECHIN on the life span of senescence accelerated mice (SAM-P8 strain). *Biochemistry and molecular biology international* 41, 1005–1011.
- Ladiwala, A.R., Lin, J.C., Bale, S.S., Marcelino-Cruz, A.M., Bhattacharya, M., Dordick, J.S., Tessier, P.M., 2010. Resveratrol selectively remodels soluble oligomers and fibrils of amyloid Aβeta into off-pathway conformers. *Journal of Biological Chemistry* 285, 24228–24237.
- Lagouge, M., Argmann, C., Gerhart-Hines, Z., Meziane, H., Lerin, C., Daussin, F., Mes-sadeq, N., Milne, J., Lambert, P., Elliott, P., Geny, B., Laakso, M., Puigserver, P., Auwerx, J., 2006. Resveratrol improves mitochondrial function and protects against metabolic disease by activating SIRT1 and PGC-1α. *Cell* 127, 1109–1122.
- Langley, E., Pearson, M., Faretta, M., Bauer, U.M., Frye, R.A., Minucci, S., Pelicci, P.G., Kouzarides, T., 2002. Human SIR2 deacetylates p53 and antagonizes PML/p53-induced cellular senescence. *EMBO Journal* 21, 2383–2396.
- Lee, K.W., Kundu, J.K., Kim, S.O., Chun, K.S., Lee, H.J., Surh, Y.J., 2006. Cocoa polyphenols inhibit phorbol ester-induced superoxide anion formation in cultured HL-60 cells and expression of cyclooxygenase-2 and activation of NF-kappaB and MAPKs in mouse skin in vivo. *Journal of Nutrition* 136, 1150–1155.
- Lee, K.S., Lee, B.S., Semnani, S., Avanesian, A., Um, C.Y., Jeon, H.J., Seong, K.M., Yu, K., Min, K.J., Jafari, M., 2010. Curcumin extends life span, improves health span, and modulates the expression of age-associated aging genes in *Drosophila melanogaster*. *Rejuvenation Research* 13, 561–570.
- Lei, H., Wang, B., Li, W.P., Yang, Y., Zhou, A.W., Chen, M.Z., 2003. Anti-aging effect of astragalosides and its mechanism of action. *Acta Pharmacologica Sinica* 24, 230–234.
- Li, X., Kazgan, N., 2011. Mammalian sirtuins and energy metabolism. *International Journal of Biological Sciences* 7, 575–587.

- Li, W., Zhang, B., Tang, J., Cao, Q., Wu, Y., Wu, C., Guo, J., Ling, E.A., Liang, F., 2007. Sirtuin 2, a mammalian homolog of yeast silent information regulator-2 longevity regulator, is an oligodendroglial protein that decelerates cell differentiation through deacetylating alpha-tubulin. *Journal of Neuroscience* 27, 2606–2616.
- Li, Y., Xu, W., McBurney, M.W., Longo, V.D., 2008a. Sirt1 inhibition reduces IGF-1/IRS-2/Ras/ERK1/2 signaling and protects neurons. *Cell Metab* 8, 38–48.
- Li, Y.M., Chan, H.Y., Yao, X.Q., Huang, Y., Chen, Z.Y., 2008b. Green tea catechins and broccoli reduce fat-induced mortality in *Drosophila melanogaster*. *Journal of Nutritional Biochemistry* 19, 376–383.
- Li, Q., Zhao, H.F., Zhang, Z.F., Liu, Z.G., Pei, X.R., Wang, J.B., Li, Y., 2009a. Long-term green tea catechin administration prevents spatial learning and memory impairment in senescence-accelerated mouse prone-8 mice by decreasing Abeta1-42 oligomers and upregulating synaptic plasticity-related proteins in the hippocampus. *Neuroscience* 163, 741–749.
- Li, W., Yin, Y., Gong, H., Wu, G., Zhu, F., 2009b. [Protective effects of AST and ASI on memory impairment and its mechanism in senescent rats treated by GC]. *Zhongguo Zhong Yao Za Zhi* 34, 199–203.
- Lim, G.P., Chu, T., Yang, F., Beech, W., Frautschi, S.A., Cole, G.M., 2001. The curry spice curcumin reduces oxidative damage and amyloid pathology in an Alzheimer transgenic mouse. *Journal of Neuroscience* 21, 8370–8377.
- Lin, S.J., Kaeblerlein, M., Andalis, A.A., Sturtz, L.A., Defossez, P.A., Culotta, V.C., Fink, G.R., Guarente, L., 2002. Calorie restriction extends *Saccharomyces cerevisiae* lifespan by increasing respiration. *Nature* 418, 344–348.
- Lin, S.J., Ford, E., Haigis, M., Liszt, G., Guarente, L., 2004. Calorie restriction extends yeast life span by lowering the level of NADH. *Genes and Development* 18, 12–16.
- Liu, C., Shi, Z., Fan, L., Zhang, C., Wang, K., Wang, B., 2011. Resveratrol improves neuron protection and functional recovery in rat model of spinal cord injury. *Brain Research* 1374, 100–109.
- Liu, L., Arun, A., Ellis, L., Peritore, C., Dommez, G., 2012. Sirtuin 2 (SIRT2) enhances 1-methyl-4-phenyl-1,2,3,6-tetrahydropyridine (MPTP)-induced nigrostriatal damage via deacetylating forkhead box O3a (Foxo3a) and activating Bim protein. *Journal of Biological Chemistry* 287, 32307–32311.
- Lodovici, M., Guglielmi, F., Casalini, C., Meoni, M., Cheynier, V., Dolara, P., 2001. Antioxidant and radical scavenging properties in vitro of polyphenolic extracts from red wine. *European Journal of Nutrition* 40, 74–77.
- Lombard, D.B., Schwer, B., Alt, F.W., Mostoslavsky, R., 2008. SIRT6 in DNA repair, metabolism and ageing. *Journal of Internal Medicine* 263, 128–141.
- Long, J., Gao, H., Sun, L., Liu, J., Zhao-Wilson, X., 2009. Grape extract protects mitochondria from oxidative damage and improves locomotor dysfunction and extends lifespan in a *Drosophila* Parkinson's disease model. *Rejuvenation Research* 12, 321–331.
- Lopes, G.K., Schulman, H.M., Hermes-Lima, M., 1999. Polyphenol tannic acid inhibits hydroxyl radical formation from Fenton reaction by complexing ferrous ions. *Biochimica et Biophysica Acta* 1472, 142–152.
- Lovell, M.A., Markesbery, W.R., 2007. Oxidative DNA damage in mild cognitive impairment and late-stage Alzheimer's disease. *Nucleic Acids Research* 35, 7497–7504.
- Lovell, M.A., Robertson, J.D., Teesdale, W.J., Campbell, J.L., Markesbery, W.R., 1998. Copper, iron and zinc in Alzheimer's disease senile plaques. *Journal of the Neurological Sciences* 158, 47–52.
- Luceri, C., Caderni, G., Sanna, A., Dolara, P., 2002. Red wine and black tea polyphenols modulate the expression of cyclooxygenase-2, inducible nitric oxide synthase and glutathione-related enzymes in azoxymethane-induced f344 rat colon tumors. *Journal of Nutrition* 132, 1376–1379.
- Luczaj, W., Waszkiewicz, E., Skrzydlewska, E., Roszkowska-Jakimiec, W., 2004. Green tea protection against age-dependent ethanol-induced oxidative stress. *Journal of Toxicology and Environmental Health, Part A* 67, 595–606.
- Luthi-Carter, R., Taylor, D.M., Pallos, J., Lambert, E., Amore, A., Parker, A., Moffitt, H., Smith, D.L., Runne, H., Gokke, O., Kuhn, A., Xiang, Z., Maxwell, M.M., Reeves, S.A., Bates, G.P., Neri, C., Thompson, L.M., Marsh, J.L., Kazantsev, A.G., 2010. SIRT2 inhibition achieves neuroprotection by decreasing sterol biosynthesis. *Proceedings of the National Academy of Sciences of the United States of America* 107, 7927–7932.
- Ma, W.W., Xiang, L., Yu, H.L., Yuan, L.H., Guo, A.M., Xiao, Y.X., Li, L., Xiao, R., 2009. Neuroprotection of soyabean isoflavone co-administration with folic acid against beta-amyloid 1-40-induced neurotoxicity in rats. *British Journal of Nutrition* 102, 502–505.
- Maier, P., 2009. Modulation of multiple pathways involved in the maintenance of neuronal function during aging by fisetin. *Genes Nutr* 4, 297–307.
- Manach, C., Scalbert, A., Morand, C., Remesy, C., Jimenez, L., 2004. Polyphenols: food sources and bioavailability. *American Journal of Clinical Nutrition* 79, 727–747.
- Mandel, S.A., Amit, T., Kalfon, L., Reznichenko, L., Weinreb, O., Youdim, M.B., 2008a. Cell signaling pathways and iron chelation in the neurorestorative activity of green tea polyphenols: special reference to epigallocatechin gallate (EGCG). *Journal of Alzheimer's Disease* 15, 211–222.
- Mandel, S.A., Amit, T., Kalfon, L., Reznichenko, L., Youdim, M.B., 2008b. Targeting multiple neurodegenerative diseases etiologies with multimodal-acting green tea catechins. *Journal of Nutrition* 138, 1578S–1583S.
- Mandel, S.A., Amit, T., Weinreb, O., Reznichenko, L., Youdim, M.B., 2008c. Simultaneous manipulation of multiple brain targets by green tea catechins: a potential neuroprotective strategy for Alzheimer and Parkinson diseases. *CNS Neuro-science & Therapeutics* 14, 352–365.
- Mandel, S.A., Amit, T., Weinreb, O., Youdim, M.B., 2011. Understanding the broad-spectrum neuroprotective action profile of green tea polyphenols in aging and neurodegenerative diseases. *Journal of Alzheimer's Disease* 25, 187–208.
- Mantyh, P.W., Ghilardi, J.R., Rogers, S., DeMaster, E., Allen, C.J., Stimson, E.R., Maggio, J.E., 1993. Aluminum, iron, and zinc ions promote aggregation of physiologically concentrations of beta-amyloid peptide. *Journal of Neurochemistry* 61, 1171–1174.
- Mao, Z., Hine, C., Tian, X., Van Meter, M., Au, M., Vaidya, A., Seluanov, A., Gorbunova, V., 2011. SIRT6 promotes DNA repair under stress by activating PARP1. *Science* 332, 1443–1446.
- Mao, Z., Tian, X., Van Meter, M., Ke, Z., Gorbunova, V., Seluanov, A., 2012. Sirtuin 6 (SIRT6) rescues the decline of homologous recombination repair during replicative senescence. *Proceedings of the National Academy of Sciences of the United States of America* 109, 11800–11805.
- Marfe, G., Tafani, M., Indelicato, M., Sinibaldi-Salimei, P., Reali, V., Pucci, B., Fini, M., Russo, M.A., 2009. Kaempferol induces apoptosis in two different cell lines via Akt inactivation, Bax and SIRT3 activation, and mitochondrial dysfunction. *Journal of Cellular Biochemistry* 106, 643–650.
- Marquez-Valadez, B., Lugo-Huitron, R., Valdivia-Cerda, V., Miranda-Ramirez, L.R., Perez-De La Cruz, V., Gonzalez-Cuautencos, O., Rivero-Cruz, I., Mata, R., San-tamaria, A., Pedraza-Chaverri, J., 2009. The natural xanthone alpha-mangostin reduces oxidative damage in rat brain tissue. *Nutritional Neuroscience* 12, 35–42.
- Mattson, M.P., 2008. Dietary factors, hormesis and health. *Ageing Research Reviews* 7, 43–48.
- Maxwell, M.M., Tomkinson, E.M., Nobles, J., Wizenman, J.W., Amore, A.M., Quinti, L., Chopra, V., Hersch, S.M., Kazantsev, A.G., 2011. The Sirtuin 2 microtubule deacetylase is an abundant neuronal protein that accumulates in the aging CNS. *Human Molecular Genetics* 20, 3986–3996.
- Maynard, C.J., Bush, A.I., Masters, C.L., Cappai, R., Li, Q.X., 2005. Metals and amyloid-beta in Alzheimer's disease. *International Journal of Experimental Pathology* 86, 147–159.
- Merry, B.J., 2004. Oxidative stress and mitochondrial function with aging—the effects of calorie restriction. *Aging Cell* 3, 7–12.
- Michan, S., Li, Y., Chou, M.M., Parrella, E., Ge, H., Long, J.M., Allard, J.S., Lewis, K., Miller, M., Xu, W., Mervis, R.F., Chen, J., Guerin, K.I., Smith, L.E., McBurney, M.W., Sinclair, D.A., Baudry, M., de Cabo, R., Longo, V.D., 2010. SIRT1 is essential for normal cognitive function and synaptic plasticity. *Journal of Neuroscience* 30, 9695–9707.
- Michishita, E., McCord, R.A., Berber, E., Kioi, M., Padilla-Nash, H., Damian, M., Che-ung, P., Kusumoto, R., Kawahara, T.L., Barrett, J.C., Chang, H.Y., Bohr, V.A., Ried, T., Gozani, O., Chua, K.F., 2008. SIRT6 is a histone H3 lysine 9 deacetylase that modulates telomeric chromatin. *Nature* 452, 492–496.
- Michishita, E., McCord, R.A., Boxer, L.D., Barber, M.F., Hong, T., Gozani, O., Chua, K.F., 2009. Cell cycle-dependent deacetylation of telomeric histone H3 lysine K56 by human SIRT6. *Cell Cycle* 8, 2664–2666.
- Miller, R.A., Harrison, D.E., Astle, C.M., Baur, J.A., Boyd, A.R., de Cabo, R., Fernandez, E., Flurkey, K., Javors, M.A., Nelson, J.F., Orihuela, C.J., Pletcher, S., Sharp, Z.D., Sinclair, D., Starnes, J.W., Wilkinson, J.E., Nadon, N.L., Strong, R., 2011. Rapamycin, but not resveratrol or simvastatin, extends life span of genetically heterogeneous mice. *Journals of Gerontology Series A: Biological Sciences and Medical Sciences* 66, 191–201.
- Minagawa, S., Araya, J., Numata, T., Nojiri, S., Hara, H., Yumino, Y., Kawaishi, M., Odaka, M., Morikawa, T., Nishimura, S.L., Nakayama, K., Kuwano, K., 2011. Accelerated epithelial cell senescence in IPF and the inhibitory role of SIRT6 in TGF-beta-induced senescence of human bronchial epithelial cells. *American Journal of Physiology Lung Cellular and Molecular Physiology* 300, L391–L401.
- Mirabello, L., Huang, W.Y., Wong, J.Y., Chatterjee, N., Reding, D., Crawford, E.D., De Vivo, I., Hayes, R.B., Savage, S.A., 2009. The association between leukocyte telomere length and cigarette smoking, dietary and physical variables, and risk of prostate cancer. *Aging Cell* 8, 405–413.
- Montine, T.J., Neely, M.D., Quinn, J.F., Beal, M.F., Markesbery, W.R., Roberts, L.J., Morrow, J.D., 2002. Lipid peroxidation in aging brain and Alzheimer's disease. *Free Radical Biology and Medicine* 33, 620–626.
- Moongkarndi, P., Srisawat, C., Saetun, P., Jantaravinid, J., Peerapittayamongkol, C., Soisampankul, R., Junnu, S., Sinchaikul, S., Chen, S.T., Charoensilp, P., Thong-boonkerd, V., Neungton, N., 2010. Protective effect of mangosteen extract against beta-amyloid-induced cytotoxicity, oxidative stress and altered proteome in SK-N-SH cells. *Journal of Proteome Research* 9, 2076–2086.
- Morgan, T.E., Wong, A.M., Finch, C.E., 2007. Anti-inflammatory mechanisms of dietary restriction in slowing aging processes. *Interdisciplinary Topics in Gerontology* 35, 83–97.
- Mori, T., Rezaei-Zadeh, K., Koyama, N., Arendash, G.W., Yamaguchi, H., Kakuda, N., Horikoshi-Sakuraba, Y., Tan, J., Town, T., 2012. Tannic acid is a natural beta-secretase inhibitor that prevents cognitive impairment and mitigates Alzheimer-like pathology in transgenic mice. *Journal of Biological Chemistry* 287, 6912–6927.
- Moridani, M.Y., Pourahmad, J., Bui, H., Siraki, A., O'Brien, P.J., 2003. Dietary flavonoid iron complexes as cytoprotective superoxide radical scavengers. *Free Radical Biology and Medicine* 34, 243–253.
- Moriya, J., Chen, R., Yamakawa, J., Sasaki, K., Ishigaki, Y., Takahashi, T., 2011. Resveratrol improves hippocampal atrophy in chronic fatigue mice by enhancing neurogenesis and inhibiting apoptosis of granular cells. *Biological and Pharmacological Bulletin* 34, 354–359.
- Moskang, J.O., Carlsen, H., Myhrstad, M.C., Blomhoff, R., 2005. Polyphenols and glutathione synthesis regulation. *American Journal of Clinical Nutrition* 81, 277S–283S.

- Mostoslavsky, R., Chua, K.F., Lombard, D.B., Pang, W.W., Fischer, M.R., Gellon, L., Liu, P., Mostoslavsky, G., Franco, S., Murphy, M.M., Mills, K.D., Patel, P., Hsu, J.T., Hong, A.L., Ford, E., Cheng, H.L., Kennedy, C., Nunez, N., Bronson, R., Frendewey, D., Auerbach, W., Valenzuela, D., Karow, M., Hottiger, M.O., Hursting, S., Barrett, J.C., Guarente, L., Mulligan, R., Dipple, B., Yancopoulos, G.D., Alt, F.W., 2006. Genomic instability and aging-like phenotype in the absence of mammalian SIRT6. *Cell* 124, 315–329.
- Mouchiroud, L., Molin, L., Dalliere, N., Solari, F., 2010. Life span extension by resveratrol, rapamycin, and metformin: The promise of dietary restriction mimetics for an healthy aging. *Biofactors* 36, 377–382.
- Mrak, R.E., Griffin, W.S., 2005. Potential inflammatory biomarkers in Alzheimer's disease. *Journal of Alzheimer's Disease* 8, 369–375.
- Mukherjee, S., Lekli, I., Gurusamy, N., Bertelli, A.A., Das, D.K., 2009. Expression of the longevity proteins by both red and white wines and their cardioprotective components, resveratrol, tyrosol, and hydroxytyrosol. *Free Radical Biology and Medicine* 46, 573–578.
- Mukhopadhyay, P., Mukherjee, S., Ahsan, K., Bagchi, A., Pacher, P., Das, D.K., 2010. Restoration of altered microRNA expression in the ischemic heart with resveratrol. *PLoS One* 5, e15705.
- Munch, G., Keis, R., Wessels, A., Riederer, P., Bahner, U., Heidland, A., Niwa, T., Lemke, H.D., Schinzel, R., 1997. Determination of advanced glycation end products in serum by fluorescence spectroscopy and competitive ELISA. *European Journal of Clinical Chemistry and Clinical Biochemistry: Journal of the Forum of European Clinical Chemistry Societies* 35, 669–677.
- Nakagawa, T., Lomb, D.J., Haigis, M.C., Guarente, L., 2009. SIRT5 deacetylates carbamoyl phosphate synthetase 1 and regulates the urea cycle. *Cell* 137, 560–570.
- Nakamura, Y., Ogura, M., Ogura, K., Tanaka, D., Inagaki, N., 2012. SIRT5 deacetylates and activates urate oxidase in liver mitochondria of mice. *FEBS Letters* 586, 4076–4081.
- Narala, S.R., Allsopp, R.C., Wells, T.B., Zhang, G., Prasad, P., Coussens, M.J., Rossi, D.J., Weissman, I.L., Vaziri, H., 2008. SIRT1 acts as a nutrient-sensitive growth suppressor and its loss is associated with increased AMPK and telomerase activity. *Molecular Biology of the Cell* 19, 1210–1219.
- Narita, K., Hisamoto, M., Okuda, T., Takeda, S., 2011. Differential neuroprotective activity of two different grape seed extracts. *PLoS One* 6, e14575.
- Nasrin, N., Wu, X., Fortier, E., Feng, Y., Bare, O.C., Chen, S., Ren, X., Wu, Z., Streeper, R.S., Bordone, L., 2010. SIRT4 regulates fatty acid oxidation and mitochondrial gene expression in liver and muscle cells. *Journal of Biological Chemistry* 285, 31995–32002.
- Nerurkar, P.V., Johns, L.M., Buesa, L.M., Kipyakwai, G., Volper, E., Sato, R., Shah, P., Feher, D., Williams, P.G., Nerurkar, V.R., 2011. Momordica charantia (bitter melon) attenuates high-fat diet-associated oxidative stress and neuroinflammation. *Journal of Neuroinflammation* 8, 64.
- Nunomura, A., Perry, G., Aliev, G., Hirai, K., Takeda, A., Balraj, E.K., Jones, P.K., Ghan-bari, H., Wataya, T., Shimohama, S., Chiba, S., Atwood, C.S., Petersen, R.B., Smith, M.A., 2001. Oxidative damage is the earliest event in Alzheimer disease. *Journal of Neuropathology and Experimental Neurology* 60, 759–767.
- Obregon, D.F., Rezaei-Zadeh, K., Bai, Y., Sun, N., Hou, H., Ehrhart, J., Zeng, J., Mori, T., Arendash, G.W., Shytle, D., Town, T., Tan, J., 2006. ADAM10 activation is required for green tea (-)-epigallocatechin-3-gallate-induced alpha-secretase cleavage of amyloid precursor protein. *Journal of Biological Chemistry* 281, 16419–16427.
- Ogura, M., Nakamura, Y., Tanaka, D., Zhuang, X., Fujita, Y., Obara, A., Hamasaki, A., Hosokawa, M., Inagaki, N., 2010. Overexpression of SIRT5 confirms its involvement in deacetylation and activation of carbamoyl phosphate synthetase 1. *Biochemical and Biophysical Research Communications* 393, 73–78.
- Oliva, J., French, B.A., Li, J., Bardag-Gorce, F., Fu, P., French, S.W., 2008. Sirt1 is involved in energy metabolism: the role of chronic ethanol feeding and resveratrol. *Experimental and Molecular Pathology* 85, 155–159.
- Omodei, D., Fontana, L., 2011. Calorie restriction and prevention of age-associated chronic disease. *FEBS Letters* 585, 1537–1542.
- Ono, K., Yoshiike, Y., Takashima, A., Hasegawa, K., Naiki, H., Yamada, M., 2003. Potent anti-amyloidogenic and fibrildestabilizing effects of polyphenols in vitro: implications for the prevention and therapeutics of Alzheimer's disease. *Journal of Neurochemistry* 87, 172–181.
- Ono, K., Hasegawa, K., Naiki, H., Yamada, M., 2004. Anti-amyloidogenic activity of tannic acid and its activity to destabilize Alzheimer's beta-amyloid fibrils in vitro. *Biochimica et Biophysica Acta* 1690, 193–202.
- Ornish, D., Lin, J., Daubenmier, J., Weidner, G., Epel, E., Kemp, C., Magbanua, M.J., Marlin, R., Yglecias, L., Carroll, P.R., Blackburn, E.H., 2008. Increased telomerase activity and comprehensive lifestyle changes: a pilot study. *Lancet Oncology* 9, 1048–1057.
- Outeiro, T.F., Kontopoulos, E., Altmann, S.M., Kufareva, I., Strathearn, K.E., Amore, A.M., Volk, C.B., Maxwell, M.M., Rochet, J.C., McLean, P.J., Young, A.B., Abagyan, R., Feany, M.B., Hyman, B.T., Kazantsev, A.G., 2007. Sirtuin 2 inhibitors rescue alpha-synuclein-mediated toxicity in models of Parkinson's disease. *Science* 317, 516–519.
- Pacholec, M., Bleasdale, J.E., Chrnyk, B., Cunningham, D., Flynn, D., Garofalo, R.S., Griffith, D., Griffor, M., Loulakis, P., Pabst, B., Qiu, X., Stockman, B., Thanabal, V., Varghese, A., Ward, J., Withka, J., Ahn, K., 2010. SIRT1720, SIRT2183, SIRT1460, and resveratrol are not direct activators of SIRT1. *Journal of Biological Chemistry* 285, 8340–8351.
- Palacios, J.A., Herranz, D., De Bonis, M.L., Velasco, S., Serrano, M., Blasco, M.A., 2010. SIRT1 contributes to telomere maintenance and augments global homologous recombination. *Journal of Cell Biology* 191, 1299–1313.
- Panickar, K.S., Anderson, R.A., 2011. Effect of polyphenols on oxidative stress and mitochondrial dysfunction in neuronal death and brain edema in cerebral ischemia. *International Journal of Molecular Sciences* 12, 8181–8207.
- Panosian, L.A., Porter, V.R., Valenzuela, H.F., Zhu, X., Reback, E., Masterman, D., Cummings, J.L., Effros, R.B., 2003. Telomere shortening in T cells correlates with Alzheimer's disease status. *Neurobiology of Aging* 24, 77–84.
- Parachikova, A., Green, K.N., Hendrix, C., LaFerla, F.M., 2010. Formulation of a medical food cocktail for Alzheimer's disease: beneficial effects on cognition and neuropathology in a mouse model of the disease. *PLoS One* 5, e14015.
- Parihar, M.S., Brewer, G.J., 2007. Mitochondrial failure in Alzheimer disease. *American Journal of Physiology: Cell Physiology* 292, C8–C23.
- Partridge, L., Piper, M.D., Mair, W., 2005. Dietary restriction in Drosophila. Mechanisms of Ageing and Development 126, 938–950.
- Patel, N.V., Gordon, M.N., Connor, K.E., Good, R.A., Engelman, R.W., Mason, J., Morgan, D.G., Morgan, T.E., Finch, C.E., 2005. Caloric restriction attenuates Abeta-deposition in Alzheimer transgenic models. *Neurobiology of Aging* 26, 995–1000.
- Patil, C.S., Singh, V.P., Satyanarayan, P.S., Jain, N.K., Singh, A., Kulkarni, S.K., 2003. Protective effect of flavonoids against aging- and lipopolysaccharide-induced cognitive impairment in mice. *Pharmacology* 69, 59–67.
- Pearson, K.J., Baur, J.A., Lewis, K.N., Peshkin, L., Price, N.L., Labinskyy, N., Swindell, W.R., Kamara, D., Minor, R.K., Perez, E., Jamieson, H.A., Zhang, Y., Dunn, S.R., Sharma, K., Pleshko, N., Woollett, L.A., Csiszar, A., Ikeno, Y., Le Couteur, D., Elliott, P.J., Becker, K.G., Navas, P., Ingram, D.K., Wolf, N.S., Ungvari, Z., Sinclair, D.A., de Cabo, R., 2008. Resveratrol delays age-related deterioration and mimics transcriptional aspects of dietary restriction without extending life span. *Cell Metabolism* 8, 157–168.
- Pedrielli, P., Skibsted, L.H., 2002. Antioxidant synergy and regeneration effect of quercetin, (-)-epicatechin, and (+)-catechin on alpha-tocopherol in homogeneous solutions of peroxidizing methyl linoleate. *Journal of Agricultural and Food Chemistry* 50, 7138–7144.
- Pellegrini, N., Simonetti, P., Gardana, C., Brenna, O., Brighenti, F., Pietta, P., 2000. Polyphenol content and total antioxidant activity of vint novelli (young red wines). *Journal of Agricultural and Food Chemistry* 48, 732–735.
- Penalvo, J.L., Haajanen, K.M., Botting, N., Adlercreutz, H., 2005. Quantification of lignans in food using isotope dilution gas chromatography/mass spectrometry. *Journal of Agricultural and Food Chemistry* 53, 9342–9347.
- Peng, X., Ma, J., Chao, J., Sun, Z., Chang, R.C., Tse, I., Li, E.T., Chen, F., Wang, M., 2010. Beneficial effects of cinnamon proanthocyanidins on the formation of specific advanced glycation endproducts and methylglyoxal-induced impairment on glucose consumption. *Journal of Agricultural and Food Chemistry* 58, 6692–6696.
- Peng, C., Chan, H.Y., Huang, Y., Yu, H., Chen, Z.Y., 2011. Apple polyphenols extend the mean lifespan of Drosophila melanogaster. *Journal of Agricultural and Food Chemistry* 59, 2097–2106.
- Perez-Jimenez, J., Neveu, V., Vos, F., Scalbert, A., 2010. Systematic analysis of the content of 502 polyphenols in 452 foods and beverages: an application of the phenol-explorer database. *Journal of Agricultural and Food Chemistry* 58, 4959–4969.
- Peterson, D.W., George, R.C., Scaramozzino, F., LaPointe, N.E., Anderson, R.A., Graves, D.J., Lew, J., 2009. Cinnamon extract inhibits tau aggregation associated with Alzheimer's disease in vitro. *Journal of Alzheimer's Disease* 17, 585–597.
- Pietsch, K., Saul, N., Menzel, R., Sturzenbaum, S.R., Steinberg, C.E., 2009. Quercetin mediated lifespan extension in Caenorhabditis elegans is modulated by age-1, daf-2, sek-1 and unc-43. *Biogerontology* 10, 565–578.
- Porquet, D., Casadesus, G., Bayod, S., Vicente, A., Canudas, A.M., Vilaplana, J., Pelegri, C., Sanfeliu, C., Camins, A., Pallas, M., Del Valle, J., 2012. Dietary resveratrol prevents Alzheimer's markers and increases life span in SAMP8. *Age*.
- Qin, W., Chachich, M., Lane, M., Roth, G., Bryant, M., de Cabo, R., Ottinger, M.A., Mattison, J., Ingram, D., Gandy, S., Pasinetti, G.M., 2006a. Calorie restriction attenuates Alzheimer's disease type brain amyloidosis in Squirrel monkeys (Saimiri sciureus). *Journal of Alzheimer's Disease* 10, 417–422.
- Qin, W., Yang, T., Ho, L., Zhao, Z., Wang, J., Chen, L., Zhao, W., Thiagarajan, M., MacGrogan, D., Rodgers, J.T., Puigserver, P., Sadoshima, J., Deng, H., Pedrini, S., Gandy, S., Sauve, A.A., Pasinetti, G.M., 2006b. Neuronal SIRT1 activation as a novel mechanism underlying the prevention of Alzheimer disease amyloid neuropathology by calorie restriction. *Journal of Biological Chemistry* 281, 21745–21754.
- Qin, W., Zhao, W., Ho, L., Wang, J., Walsh, K., Gandy, S., Pasinetti, G.M., 2008. Regulation of forkhead transcription factor FoxO3a contributes to calorie restriction-induced prevention of Alzheimer's disease-type amyloid neuropathology and spatial memory deterioration. *Annals of the New York Academy of Sciences* 1147, 335–347.
- Qiu, X., Brown, K., Hirschey, M.D., Verdin, E., Chen, D., 2010. Calorie restriction reduces oxidative stress by SIRT3-mediated SOD2 activation. *Cell Metabolism* 12, 662–667.
- Quideau, S., 2004. Plant "polyphenolic" small molecules can induce a calorie restriction-mimetic life-span extension by activating sirtuins: will "polyphenols" someday be used as chemotherapeutic drugs in Western medicine? *Chembiochem* 5, 427–430.
- Ramadori, G., Fujikawa, T., Anderson, J., Berglund, E.D., Frazao, R., Michan, S., Vianna, C.R., Sinclair, D.A., Elias, C.F., Coppari, R., 2011. SIRT1 deacetylase in SF1 neurons protects against metabolic imbalance. *Cell Metabolism* 14, 301–312.
- Rasbach, K.A., Schnellmann, R.G., 2008. Isoflavones promote mitochondrial biogenesis. *Journal of Pharmacology and Experimental Therapeutics* 325, 536–543.

- Rayalam, S., Yang, J.Y., Ambati, S., Della-Fera, M.A., Baile, C.A., 2008. Resveratrol induces apoptosis and inhibits adipogenesis in 3T3-L1 adipocytes. *Phytotherapy Research* 22, 1367–1371.
- Reiter, R.J., 1995. Oxidative processes and antioxidative defense mechanisms in the aging brain. *FASEB Journal* 9, 526–533.
- Reynolds, A., Laurie, C., Mosley, R.L., Gendelman, H.E., 2007. Oxidative stress and the pathogenesis of neurodegenerative disorders. *International Review of Neurobiology* 82, 297–325.
- Rezaei-Zadeh, K., Shytle, D., Sun, N., Mori, T., Hou, H., Jeanniton, D., Ehrhart, J., Townsend, K., Zeng, J., Morgan, D., Hardy, J., Town, T., Tan, J., 2005. Green tea epigallocatechin-3-gallate (EGCG) modulates amyloid precursor protein cleavage and reduces cerebral amyloidosis in Alzheimer transgenic mice. *Journal of Neuroscience* 25, 8807–8814.
- Rezaei-Zadeh, K., Arendash, G.W., Hou, H., Fernandez, F., Jensen, M., Runfeldt, M., Shytle, R.D., Tan, J., 2008. Green tea epigallocatechin-3-gallate (EGCG) reduces beta-amyloid mediated cognitive impairment and modulates tau pathology in Alzheimer transgenic mice. *Brain Research* 1214, 177–187.
- Rezaei-Zadeh, K., Douglas Shytle, R., Bai, Y., Tian, J., Hou, H., Mori, T., Zeng, J., Obregon, D., Town, T., Tan, J., 2009. Flavonoid-mediated presenilin-1 phosphorylation reduces Alzheimer's disease beta-amyloid production. *Journal of Cellular and Molecular Medicine* 13, 574–588.
- Richards, J.B., Valdes, A.M., Gardner, J.P., Paximadas, D., Kimura, M., Nessa, A., Lu, X., Surdulescu, G.L., Swaminathan, R., Spector, T.D., Aviv, A., 2007. Higher serum vitamin D concentrations are associated with longer leukocyte telomere length in women. *American Journal of Clinical Nutrition* 86, 1420–1425.
- Richards, J.B., Valdes, A.M., Gardner, J.P., Kato, B.S., Siva, A., Kimura, M., Lu, X., Brown, M.J., Aviv, A., Spector, T.D., 2008. Homocysteine levels and leukocyte telomere length. *Atherosclerosis* 200, 271–277.
- Robak, J., Gryglewski, R.J., 1988. Flavonoids are scavengers of superoxide anions. *Biochemical Pharmacology* 37, 837–841.
- Roberts, B.R., Ryan, T.M., Bush, A.L., Masters, C.L., Duce, J.A., 2012. The role of metallobiology and amyloid-beta peptides in Alzheimer's disease. *Journal of Neurochemistry* 120 (Suppl. 1), 149–166.
- Rogina, B., Helfand, S.L., 2004. Sir2 mediates longevity in the fly through a pathway related to calorie restriction. *Proceedings of the National Academy of Sciences of the United States of America* 101, 15998–16003.
- Rojanathamane, L., Puig, K.L., Combs, C.K., 2013. Pomegranate polyphenols and extract inhibit nuclear factor of activated T-cell activity and microglial activation in vitro and in a transgenic mouse model of Alzheimer disease. *Journal of Nutrition* 143, 597–605.
- Romano, A.D., Serviddio, G., de Mattheis, A., Bellanti, F., Vendemiale, G., 2010. Oxidative stress and aging. *Journal of Nephrology* 23 (Suppl. 15), S29–S36.
- Rose, G., Dato, S., Altomare, K., Bellizzi, D., Garasto, S., Greco, V., Passarino, G., Feraco, E., Mari, V., Barbi, C., BonaFe, M., Franceschi, C., Tan, Q., Boiko, S., Yashin, A.I., De Benedictis, G., 2003. Variability of the SIRT3 gene, human silent information regulator Sir2 homologue, and survivorship in the elderly. *Experimental Gerontology* 38, 1065–1070.
- Roth, A., Schaffner, W., Hertel, C., 1999. Phytoestrogen kaempferol (3,4',5,7-tetrahydroxyflavone) protects PC12 and T47D cells from beta-amyloid-induced toxicity. *Journal of Neuroscience Research* 57, 399–404.
- Sahni, J.K., Doggui, S., Ali, J., Baboota, S., Dao, L., Ramassamy, C., 2011. Neurotherapeutic applications of nanoparticles in Alzheimer's disease. *Journal of Controlled Release* 152, 208–231.
- Salah, N., Miller, N.J., Panganga, G., Tijburg, L., Bolwell, G.P., Rice-Evans, C., 1995. Polyphenolic flavanols as scavengers of aqueous phase radicals and as chain-breaking antioxidants. *Archives of Biochemistry and Biophysics* 322, 339–346.
- Sanbongi, C., Suzuki, N., Sakane, T., 1997. Polyphenols in chocolate, which have antioxidant activity, modulate immune functions in humans in vitro. *Cellular Immunology* 177, 129–136.
- Santa-Maria, I., Diaz-Ruiz, C., Ksiezak-Reding, H., Chen, A., Ho, L., Wang, J., Pasinetti, G.M., 2012. GSPE interferes with tau aggregation in vivo: implication for treating tauopathy. *Neurobiology of Aging* 33, 2072–2081.
- Santangelo, C., Vari, R., Scazzocchio, B., Di Benedetto, R., Fiesi, C., Masella, R., 2007. Polyphenols, intracellular signalling and inflammation. *Annali dell'Istituto Superiore di Sanita* 43, 394–405.
- Sasaki, N., Fukatsu, R., Tsuzuki, K., Hayashi, Y., Yoshida, T., Fujii, N., Koike, T., Wakayama, I., Yanagihara, R., Garruto, R., Amano, N., Makita, Z., 1998. Advanced glycation end products in Alzheimer's disease and other neurodegenerative diseases. *American Journal of Pathology* 153, 1149–1155.
- Saul, N., Pietsch, K., Menzel, R., Sturzenbaum, S.R., Steinberg, C.E., 2009. Catechin induced longevity in *C. elegans*: from key regulator genes to disposable soma. *Mechanisms of Ageing and Development* 130, 477–486.
- Scheepens, A., Tan, K., Paxton, J.W., 2010. Improving the oral bioavailability of beneficial polyphenols through designed synergies. *Genes & Nutrition* 5, 75–87.
- Schirmer, H., Pereira, T.C., Rico, E.P., Rosemberg, D.B., Bonan, C.D., Bogo, M.R., Souto, A.A., 2012. Modulatory effect of resveratrol on SIRT1, SIRT3, SIRT4, PGC1alpha and NAMPT gene expression profiles in wild-type adult zebrafish liver. *Molecular Biology Reports* 39, 3281–3289.
- Schulz, T.J., Zarse, K., Voigt, A., Urban, N., Birringer, M., Ristow, M., 2007. Glucose restriction extends *Caenorhabditis elegans* life span by inducing mitochondrial respiration and increasing oxidative stress. *Cell Metabolism* 6, 280–293.
- Schwer, B., Schumacher, B., Lombard, D.B., Xiao, C., Kurtev, M.V., Gao, J., Schneider, J.I., Chai, H., Bronson, R.T., Tsai, L.H., Deng, C.X., Alt, F.W., 2010. Neural sirtuin 6 (Sirt6) ablation attenuates somatic growth and causes obesity. *Proceedings of the National Academy of Sciences of the United States of America* 107, 21790–21794.
- Selkoe, D.J., 1998. The cell biology of beta-amyloid precursor protein and presenilin in Alzheimer's disease. *Trends in Cell Biology* 8, 447–453.
- Shan, B., Cai, Y.Z., Sun, M., Corke, H., 2005. Antioxidant capacity of 26 spice extracts and characterization of their phenolic constituents. *Journal of Agricultural and Food Chemistry* 53, 7749–7759.
- Sheng, R., Gu, Z.L., Xie, M.L., 2011. Epigallocatechin gallate, the major component of polyphenols in green tea, inhibits telomere attrition mediated cardiomyocyte apoptosis in cardiac hypertrophy. *International Journal of Cardiology*.
- Shimmyo, Y., Kihara, T., Akaike, A., Niidome, T., Sugimoto, H., 2008. Flavonols and flavones as BACE-1 inhibitors: structure-activity relationship in cell-free, cell-based and in silico studies reveal novel pharmacophore features. *Biochimica et Biophysica Acta* 1780, 819–825.
- Smith, M.A., Perry, G., Richey, P.L., Sayre, L.M., Anderson, V.E., Beal, M.F., Kowall, N., 1996. Oxidative damage in Alzheimer's. *Nature* 382, 120–121.
- Smith, M.A., Harris, P.L., Sayre, L.M., Perry, G., 1997a. Iron accumulation in Alzheimer disease is a source of redox-generated free radicals. *Proceedings of the National Academy of Sciences of the United States of America* 94, 9866–9868.
- Smith, M.A., Richey Harris, P.L., Sayre, L.M., Beckman, J.S., Perry, G., 1997b. Widespread peroxynitrite-mediated damage in Alzheimer's disease. *Journal of Neuroscience* 17, 2653–2657.
- Smith, M.A., Rottkamp, C.A., Nunomura, A., Raina, A.K., Perry, G., 2000. Oxidative stress in Alzheimer's disease. *Biochimica et Biophysica Acta* 1502, 139–144.
- Smith, A., Giunta, B., Bickford, P.C., Fountain, M., Tan, J., Shytle, R.D., 2010. Nanolipidic particles improve the bioavailability and alpha-secretase inducing ability of epigallocatechin-3-gallate (EGCG) for the treatment of Alzheimer's disease. *International Journal of Pharmaceutics* 389, 207–212.
- Smith, A.J., Kavuru, P., Wojtas, L., Zaworotko, M.J., Shytle, R.D., 2011. Cocrystals of quercetin with improved solubility and oral bioavailability. *Molecular Pharmaceutics* 8, 1867–1876.
- Someya, S., Yu, W., Hallows, W.C., Xu, J., Vann, J.M., Leeuwenburgh, C., Tanokura, M., Denu, J.M., Prolla, T.A., 2010. Sirt3 mediates reduction of oxidative damage and prevention of age-related hearing loss under caloric restriction. *Cell* 143, 802–812.
- Souto, E.B., Severino, P., Basso, R., Santana, M.H., 2013. Encapsulation of antioxidants in gastrointestinal-resistant nanoparticulate carriers. *Methods in Molecular Biology* 1028, 37–46.
- Spies-Jones, T.L., Fox, L.M., Rozkalne, A., Pitstick, R., Carlson, G.A., Kazantsev, A.G., 2012. Inhibition of Sirtuin 2 with Sulfolobenzoic Acid Derivative AK1 is Non-Toxic and Potentially Neuroprotective in a Mouse Model of Frontotemporal Dementia. *Frontiers in Pharmacology* 3, 42.
- Sulaiman, S.F., Ooi, K.L., 2012. Polyphenolic and Vitamin C Contents and Antioxidant Activities of Aqueous Extracts from Mature-Green and Ripe Fruit Fleshes of *Mangifera* sp. *Journal of Agricultural and Food Chemistry* 60, 11832–11838.
- Sunagawa, T., Shimizu, T., Kanda, T., Tagashira, M., Sami, M., Shirasawa, T., 2011. Pro-cyanidins from apples (*Malus pumila* Mill.) extend the lifespan of *Caenorhabditis elegans*. *Planta Medica* 77, 122–127.
- Suzuki, K., Koike, T., 2007a. Mammalian Sir2-related protein (SIRT) 2-mediated modulation of resistance to axonal degeneration in slow Wallerian degeneration mice: a crucial role of tubulin deacetylation. *Neuroscience* 147, 599–612.
- Suzuki, K., Koike, T., 2007b. Resveratrol abolishes resistance to axonal degeneration in slow Wallerian degeneration (WldS) mice: activation of SIRT2, an NAD-dependent tubulin deacetylase. *Biochemical and Biophysical Research Communications* 359, 665–671.
- Takubo, K., Aida, J., Izumiya-Shimomura, N., Ishikawa, N., Sawabe, M., Kurabayashi, R., Shirahishi, H., Arai, T., Nakamura, K., 2010. Changes of telomere length with aging. *Geriatrics & Gerontology International* 10 (Suppl. 1), S197–S206.
- Taylor, D.M., Balabadra, U., Xiang, Z., Woodman, B., Meade, S., Amore, A., Maxwell, M.M., Reeves, S., Bates, G.P., Luthi-Carter, R., Lowden, P.A., Kazantsev, A.G., 2011. A brain-permeable small molecule reduces neuronal cholesterol by inhibiting activity of sirtuin 2 deacetylase. *ACS Chemical Biology* 6, 540–546.
- Thomas, P., Wang, Y.J., Zhong, J.H., Kosaraju, S., O'Callaghan, N.J., Zhou, X.F., Fenech, M., 2009. Grape seed polyphenols and curcumin reduce genomic instability events in a transgenic mouse model for Alzheimer's disease. *Mutation Research* 661, 25–34.
- Thornton, E., Vink, R., Blumbergs, P.C., Van Den Heuvel, C., 2006. Soluble amyloid precursor protein alpha reduces neuronal injury and improves functional outcome following diffuse traumatic brain injury in rats. *Brain Research* 1094, 38–46.
- Tissenbaum, H.A., Guarente, L., 2001. Increased dosage of a sir-2 gene extends life-span in *Caenorhabditis elegans*. *Nature* 410, 227–230.
- Tohda, C., Tamura, T., Matsuyama, S., Komatsu, K., 2006. Promotion of axonal maturation and prevention of memory loss in mice by extracts of *Astragalus mongolicus*. *British Journal of Pharmacology* 149, 532–541.
- Truelsen, T., Thudium, D., Gronbaek, M., 2002. Amount and type of alcohol and risk of dementia: the Copenhagen City Heart Study. *Neurology* 59, 1313–1319.
- Tsao, R., 2010. Chemistry and biochemistry of dietary polyphenols. *Nutrients* 2, 1231–1246.
- Uchiyama, F., Watanabe, T., Hasegawa, S., Hoshi, T., Higami, Y., Tanuma, S., 2011. The effect of resveratrol on the Werner syndrome RecQ helicase gene and telomerase activity. *Current Aging Science* 4, 1–7.
- Unno, K., Takabayashi, F., Yoshida, H., Choba, D., Fukutomi, R., Kikunaga, N., Kishido, T., Oku, N., Hoshino, M., 2007. Daily consumption of green tea catechin delays memory regression in aged mice. *Biogerontology* 8, 89–95.
- Vakhrusheva, O., Brauer, D., Liu, Z., Braun, T., Bober, E., 2008a. Sirt7-dependent inhibition of cell growth and proliferation might be instrumental to mediate

- tissue integrity during aging. *Journal of Physiology and Pharmacology* 59 (Suppl. 9), 201–212.
- Vakhrusheva, O., Smolka, C., Gajawada, P., Kostin, S., Boettger, T., Kubin, T., Braun, T., Bober, E., 2008b. Sirt7 increases stress resistance of cardiomyocytes and prevents apoptosis and inflammatory cardiomyopathy in mice. *Circulation Research* 102, 703–710.
- Valenzano, D.R., Terzibasi, E., Genade, T., Cattaneo, A., Domenici, L., Cellarino, A., 2006. Resveratrol prolongs lifespan and retards the onset of age-related markers in a short-lived vertebrate. *Current Biology*: CB 16, 296–300.
- Veerendra Kumar, M.H., Gupta, Y.K., 2003. Effect of Centella asiatica on cognition and oxidative stress in an intracerebroventricular streptozotocin model of Alzheimer's disease in rats. *Clinical and Experimental Pharmacology and Physiology* 30, 336–342.
- Vepsäläinen, S., Koivisto, H., Pekkarinen, E., Mäkinen, P., Dobson, G., McDougall, G.J., Stewart, D., Haapasalo, A., Karjalainen, R.O., Tanila, H., Hiltunen, M., 2013. Anthocyanin-enriched bilberry and blackcurrant extracts modulate amyloid precursor protein processing and alleviate behavioral abnormalities in the APP/PS1 mouse model of Alzheimer's disease. *Journal of Nutrition Biochemistry* 24, 360–370.
- Vitrac, X., Bornet, A., Vanderlinde, R., Valls, J., Richard, T., Delaunay, J.C., Merillon, J.M., Teissedre, P.L., 2005. Determination of stilbenes (delta-viniferin, trans-astringin, trans-piceid, cis- and trans-resveratrol, epsilon-viniferin) in Brazilian wines. *Journal of Agricultural and Food Chemistry* 53, 5664–5669.
- Vrhovsek, U., Rigo, A., Tonon, D., Mattivi, F., 2004. Quantitation of polyphenols in different apple varieties. *Journal of Agricultural and Food Chemistry* 52, 6532–6538.
- Walker, E.B., 2007. HPLC analysis of selected xanthenes in mangosteen fruit. *Journal of Separation Science* 30, 1229–1234.
- Walsh, D.M., Selkoe, D.J., 2007. A beta oligomers - a decade of discovery. *Journal of Neurochemistry* 101, 1172–1184.
- Wang, Q., Rowan, M.J., Anwyl, R., 2004. Beta-amyloid-mediated inhibition of NMDA receptor-dependent long-term potentiation induction involves activation of microglia and stimulation of inducible nitric oxide synthase and superoxide. *Journal of Neuroscience* 24, 6049–6056.
- Wang, F., Nguyen, M., Qin, F.X., Tong, Q., 2007. SIRT2 deacetylates FOXO3a in response to oxidative stress and caloric restriction. *Aging Cell* 6, 505–514.
- Wang, J., Santa-Maria, I., Ho, L., Ksiazek-Reding, H., Ono, K., Teplow, D.B., Pasinetti, G.M., 2010a. Grape derived polyphenols attenuate tau neuropathology in a mouse model of Alzheimer's disease. *Journal of Alzheimer's Disease* 22, 653–661.
- Wang, P., Zhang, Z., Sun, Y., Liu, X., Tong, T., 2010b. The two isomers of HDTIC compounds from Astragali Radix slow down telomere shortening rate via attenuating oxidative stress and increasing DNA repair ability in human fetal lung diploid fibroblast cells. *DNA and Cell Biology* 29, 33–39.
- Wang, H., Yang, Y.J., Qian, H.Y., Zhang, Q., Xu, H., Li, J.J., 2012. Resveratrol in cardiovascular disease: what is known from current research? *Heart Failure Reviews* 17, 437–448.
- Weir, H.J., Murray, T.K., Kehoe, P.G., Love, S., Verdin, E.M., O'Neill, M.J., Lane, J.D., Balthasar, N., 2012. CNS SIRT3 expression is altered by reactive oxygen species and in Alzheimer's disease. *PLoS One* 7, e48225.
- Wilson, M.A., Shukitt-Hale, B., Kalt, W., Ingram, D.K., Joseph, J.A., Wolkow, C.A., 2006. Blueberry polyphenols increase lifespan and thermotolerance in *Caenorhabditis elegans*. *Aging Cell* 5, 59–68.
- Witte, A.V., Fobker, M., Gellner, R., Knecht, S., Floel, A., 2009. Caloric restriction improves memory in elderly humans. *Proceedings of the National Academy of Sciences of the United States of America* 106, 1255–1260.
- Wood, J.G., Rogina, B., Lavu, S., Howitz, K., Helfand, S.L., Tatar, M., Sinclair, D., 2004. Sirtuin activators mimic caloric restriction and delay ageing in metazoans. *Nature* 430, 686–689.
- Wu, Z.Q., Guo, Q.L., You, Q.D., Zhao, L., Gu, H.Y., 2004. Gambogic acid inhibits proliferation of human lung carcinoma SPC-A1 cells in vivo and in vitro and represses telomerase activity and telomerase reverse transcriptase mRNA expression in the cells. *Biological and Pharmaceutical Bulletin* 27, 1769–1774.
- Wu, A., Ying, Z., Gomez-Pinilla, F., 2006. Oxidative stress modulates Sir2alpha in rat hippocampus and cerebral cortex. *European Journal of Neuroscience* 23, 2573–2580.
- Xiang, L., Sun, K., Lu, J., Weng, Y., Taoka, A., Sakagami, Y., Qi, J., 2011. Anti-aging effects of phloridzin, an apple polyphenol, on yeast via the SOD and Sir2 genes. *Bioscience, Biotechnology, and Biochemistry* 75, 854–858.
- Xie, B., Shi, H., Chen, Q., Ho, C.T., 1993. Antioxidant properties of fractions and polyphenol constituents from green, oolong and black teas. *Proceedings of the National Science Council, Republic of China. Part B, Life sciences* 17, 77–84.
- Xu, Q., Parks, C.G., DeRoo, L.A., Cawthon, R.M., Sandler, D.P., Chen, H., 2009. Multivitamin use and telomere length in women. *American Journal of Clinical Nutrition* 89, 1857–1863.
- Xu, J., Rong, S., Xie, B., Sun, Z., Deng, Q., Bao, W., Wang, D., Yao, P., Huang, F., Liu, L., 2011. Changes in the nitric oxide system contribute to effect of procyanidins extracted from the lotus seedpod ameliorating memory impairment in cognitively impaired aged rats. *Rejuvenation Research* 14, 33–43.
- Yamamoto, A., Shin, R.W., Hasegawa, K., Naiki, H., Sato, H., Yoshimasu, F., Kita-moto, T., 2002. Iron (III) induces aggregation of hyperphosphorylated tau and its reduction to iron (II) reverses the aggregation: implications in the formation of neurofibrillary tangles of Alzheimer's disease. *Journal of Neurochemistry* 82, 1137–1147.
- Yamamoto, H., Schoonjans, K., Auwerx, J., 2007. Sirtuin functions in health and disease. *Molecular Endocrinology* 21, 1745–1755.
- Yang, H., Jin, G.-F., Ren, D.-D., Luo, S.-J., Zhou, T.-H., 2010. Neuro-protective Mechanism of Isoflavones on Senescence-accelerated Mice. *Chinese Journal of Natural Medicines* 8, 280–284.
- Yang, Y.C., Lii, C.K., Lin, A.H., Yeh, Y.W., Yao, H.T., Li, C.C., Liu, K.L., Chen, H.W., 2011. Induction of glutathione synthesis and heme oxygenase 1 by the flavonoids butein and phloretin is mediated through the ERK/Nrf2 pathway and protects against oxidative stress. *Free Radical Biology and Medicine* 51, 2073–2081.
- Yao, J., Gao, X., Sun, W., Yao, T., Shi, S., Ji, L., 2013. Molecular hairpin: a possible model for inhibition of tau aggregation by tannic acid. *Biochemistry* 52, 1893–1902.
- Yeung, F., Hoberg, J.E., Ramsey, C.S., Keller, M.D., Jones, D.R., Frye, R.A., Mayo, M.W., 2004. Modulation of NF-kappaB-dependent transcription and cell survival by the SIRT1 deacetylase. *EMBO Journal* 23, 2369–2380.
- Yokozawa, T., Lee, Y.A., Zhao, Q., Matsumoto, K., Cho, E.J., 2009. Persimmon oligomeric proanthocyanidins extend life span of senescence-accelerated mice. *Journal of Medicinal Food* 12, 1199–1205.
- Yokozawa, T., Lee, Y.A., Cho, E.J., Matsumoto, K., Park, C.H., Shibahara, N., 2011. Anti-aging effects of oligomeric proanthocyanidins isolated from persimmon fruits. *Drug Discoveries & Therapeutics* 5, 109–118.
- Yu, W., Fu, Y.C., Zhou, X.H., Chen, C.J., Wang, X., Lin, R.B., Wang, W., 2009. Effects of resveratrol on H₂O₂-induced apoptosis and expression of SIRT1 in H9c2 cells. *Journal of Cellular Biochemistry* 107, 741–747.
- Zhang, L., Jie, G., Zhang, J., Zhao, B., 2009. Significant longevity-extending effects of EGCG on *Caenorhabditis elegans* under stress. *Free Radical Biology and Medicine* 46, 414–421.
- Zhang, C., Browne, A., Child, D., Tanzi, R.E., 2010. Curcumin decreases amyloid-beta peptide levels by attenuating the maturation of amyloid-beta precursor protein. *Journal of Biological Chemistry* 285, 28472–28480.

SCIENTIFIC REPORTS

OPEN

Application of Targeted Mass Spectrometry for the Quantification of Sirtuins in the Central Nervous System

received: 02 February 2016
accepted: 28 September 2016
Published: 20 October 2016

T. Jayasena¹, A. Poljak^{1,2,3}, N. Braidy¹, L. Zhong², B. Rowlands³, J. Muenchhoff¹, R. Grant^{3,4}, G. Smythe³, C. Teo⁵, M. Raftery² & P. Sachdev^{1,6}

Sirtuin proteins have a variety of intracellular targets, thereby regulating multiple biological pathways including neurodegeneration. However, relatively little is currently known about the role or expression of the 7 mammalian sirtuins in the central nervous system. Western blotting, PCR and ELISA are the main techniques currently used to measure sirtuin levels. To achieve sufficient sensitivity and selectivity in a multiplex-format, a targeted mass spectrometric assay was developed and validated for the quantification of all seven mammalian sirtuins (SIRT1-7). Quantification of all peptides was by multiple reaction monitoring (MRM) using three mass transitions per protein-specific peptide, two specific peptides for each sirtuin and a stable isotope labelled internal standard. The assay was applied to a variety of samples including cultured brain cells, mammalian brain tissue, CSF and plasma. All sirtuin peptides were detected in the human brain, with SIRT2 being the most abundant. Sirtuins were also detected in human CSF and plasma, and guinea pig and mouse tissues. In conclusion, we have successfully applied MRM mass spectrometry for the detection and quantification of sirtuin proteins in the central nervous system, paving the way for more quantitative and functional studies.

Sirtuins are a class of proteins that possess histone deacetylase or mono-ribosyltransferase activity and play critical roles in cell survival in response to oxidative stress and caloric restriction (CR) regimes¹. In mammals, seven sirtuins (SIRT1-7) have been identified. All mammalian sirtuins contain a conserved NAD-binding and catalytic domain, but differ in their N and C-terminal domains. They have different specific substrates including histones, transcriptional regulators and enzymes. They localise to cell compartments which regulate cellular structure, metabolism and gene expression, including the cytoskeleton (SIRT2), mitochondria (SIRT3, SIRT4 and SIRT5) and nucleus/nucleolus (SIRT1, SIRT6 and SIRT7), and play important roles in health and disease¹. SIRT1 is the best characterized and has the broadest substrate specificity. Sirtuins have emerged as critical modulators of metabolic adaptive responses, and their activities have been linked to ageing and multiple diseases, from metabolic abnormalities to neurodegeneration.

Sirtuins can affect reactive oxygen species (ROS) production and promote resistance to their damaging effects. Oxidative stress has been shown to decrease SIRT1 expression in the hippocampus and cortex, possibly by direct degradation by ROS². SIRT1 overexpression prevents oxidative stress-induced apoptosis and increases resistance to oxidative stress through regulation of the FOXO family of forkhead transcription factors³. The cytoplasmic sirtuin protein SIRT2, has been shown to increase in response to oxidative stress but promotes cell death through FOXO proteins⁴. SIRT3, a mitochondrial protein, reduces oxidative stress through activation of superoxide dismutase⁵. SIRT6 and SIRT7, like the founding member of the sirtuin family SIRT1, are nuclear proteins involved in oxidative-stress induced DNA repair through activation of the PARP-1 DNA repair enzyme.

¹Centre for Healthy Brain Ageing (CHeBA), School of Psychiatry, University of New South Wales, Sydney, Australia. ²Bioanalytical Mass Spectrometry Facility, Mark Wainwright Analytical Centre, University of New South Wales, Sydney, Australia. ³School of Medical Sciences, University of New South Wales, Sydney, Australia. ⁴Sydney Medical School, University of Sydney, Sydney, Australia. ⁵Minimally Invasive Cancer Centre, Prince of Wales Hospital, Sydney, Australia. ⁶Neuropsychiatric Institute, the Prince of Wales Hospital, Sydney, Australia. Correspondence and requests for materials should be addressed to P.S. (email: p.sachdev@unsw.edu.au)

Name	Areas detected in CNS	Function in CNS	Techniques used
SIRT1	Human hippocampus and cortex ⁶ . Has also been detected in human serum at approx 8.16 ng/μl ⁸ . Mouse neural stem cells and adult mouse brain ⁷ . Porcine brain ²¹ .	Modulates memory formation and synaptic plasticity. Reduces with age in mice. Metabolic sensor.	TR-qPCR ⁶ , immunohistochemistry ⁴¹ , western blotting, surface plasmon resonance and ELISA ⁸ .
SIRT2	Mouse neural stem cells and adult mouse brain ⁷ . Porcine brain ²¹ . Human serum ⁹ .	Inhibitor of microglia-mediated inflammation and neurotoxicity ¹⁸ . Impairs neurite outgrowth and oligodendrocyte differentiation. Involved in myelin formation.	Mouse knockouts ¹⁸ , western blotting.
SIRT3	Cortex, Hippocampus and Cerebellum ¹⁰ . Mouse neural stem cells and adult mouse brain ⁷ . Porcine brain ²¹ . Rat brain. Human serum ⁹ .	Responses to oxidative stress and involved in maintenance of mitochondrial function.	Western blotting and qPCR ¹⁰ .
SIRT4	Mouse neural stem cells and adult mouse brain ⁷ . Porcine brain ²¹ . Rat cortical cells and brain tissue ⁴² .	Regulation of glial development ⁴² ; involved in glutamate transport and protective role against excitotoxicity ⁴³ .	qPCR, western blotting and immunofluorescence ^{21,42} .
SIRT5	Mouse neural stem cells and adult mouse brain ⁷ . Porcine brain ²¹ .	SIRT5 gene polymorphism may promote molecular brain aging and be a risk factor for mitochondrial dysfunction-related diseases ⁴⁴ .	qPCR ²¹ .
SIRT6	Mainly localised in the nucleus in the cortical layers ⁴⁵ . Mouse neural stem cells and adult mouse brain ^{7,40,41} . Rat brain. Porcine brain ²¹ .	Regulator of somatic growth by modulating neural chromatin and gene activity ⁴⁰ . Modulated DNA repair in the brain ⁴⁶ . Suppresses proinflammatory gene expression.	Brain specific mouse knockout models and primary brain cell models ^{40,46,47} ; immunohistochemistry ⁴³ ; western blotting, immunofluorescence ⁴⁷ .
SIRT7	Mouse neural stem cells and adult mouse brain ⁷ . Porcine brain ²¹ .	Positive regulator of RNA polymerase I transcription.	Mouse knockout ⁴⁶ .

Table 1. Expression of sirtuins in the CNS and current methods used for analysis.

SIRT1 is expressed in the adult brain, in the cortex, hippocampus, cerebellum, and hypothalamus, and in lower levels in the white matter⁶. Among the brain cell types, SIRT1 is predominantly expressed in neurons and viewed as a nuclear protein⁶. The mRNAs for all seven sirtuins have been identified in mouse brain tissue and also neural stem cells⁷. SIRT1, SIRT2 and SIRT3 have also been detected in human serum, and levels were shown to decline with age and were linked to frailty^{8,9}. SIRT3 is elevated at both the mRNA and protein levels in Alzheimer's disease (AD) *post mortem* brain tissue compared to controls¹⁰.

The most common techniques currently utilised for detecting a change in sirtuin levels at the mRNA or pro-teins level are PCR and western blotting, respectively (see Table 1). Other studies have used methods such as immunohistochemistry, surface plasmon resonance and ELISA assays (see Table 1). The majority of these methods are only semi-quantitative with moderate sensitivity, use antibodies which may not have sufficient specificity or detect expression at the mRNA level which may not reflect protein expression. Furthermore, there is no current assay which detects multiple sirtuins simultaneously.

Quantitative expression analysis of mammalian sirtuin proteins (especially SIRT2-7), across cell and tissue types is limited in the current literature. Previous studies have shown an increase in SIRT3 in AD *post-mortem* brain tissue using western blotting for protein expression and multiplex qPCR to assay SIRT3 mRNA levels¹⁰. Both SIRT3 protein and mRNA were shown to be significantly elevated in the AD group¹⁰. Another recent paper detected SIRT1 in human serum samples using western blotting, surface plasmon resonance and ELISA to measure SIRT1 protein levels⁸. SIRT1 declines with age and is more dramatically reduced in MCI and AD patients compared to age matched controls, suggesting that SIRT1 may warrant further investigation as a potential plasma biomarker for AD⁸. SIRT1 and SIRT3 levels in serum were found to be significantly lower in frail subjects as compared to the non-frail⁹. Another study reported a decrease in SIRT1 and SIRT2 mRNA levels using quantitative real time PCR in the primary motor cortex of human *post-mortem* amyotrophic lateral sclerosis brain tissue¹¹.

Mass spectrometry has been used to successfully assay metabolites of SIRT1 activator drugs in plasma and urine¹², but to date has not been used to quantify protein levels directly. Mass spectrometry has a great advantage over the conventionally used antibody based methods, such as western blotting, in that it offers greater specificity, linearity, reproducibility and typical limits of quantification down to the low fmol range. It also removes some of the antibody specificity issues that are associated with methods such as western blotting and ELISA, as peptides unique to each protein are measured. Targeted MRM based mass spectrometry may provide a more specific and sensitive method to detect and quantify sirtuin expression at the protein level, providing a tool for comprehensive sirtuin protein expression analysis. The aim of this study was to develop a targeted mass spectrometry method using multiple reaction monitoring (MRM) to quantify the seven human sirtuins at the protein level and to apply the assay to CNS biological samples.

Results

Peptide standards. Standard curves for sirtuin peptides are shown in Fig. 1. The LOD and LOQ were determined when the signal to noise ratio of the transition with the highest intensity was approximately 3:1 and 10:1 respectively. All peptides had good linearity in the 1–200 fmol/μl range and intra- and inter-assay variance was <10% and less than < 14% respectively. Representative chromatograms for each of the 14 peptides are shown in Supplementary Figure S1.

Sirtuin peptide standard curves spiked with buffer only (0.1% formic acid and no gel bit), blank gel bits and gel bits containing Hu6 depleted plasma had very similar regression equations and slopes, indicating modest matrix effects (Supplementary Figure S2). Sirtuin recoveries (from the gel spike experiment, Supplementary Figure S8), relative to sirtuin run in buffer only achieved 61–96% recovery and 58–131% recovery for the 5 μg and 2 μg sirtuin levels respectively (Supplementary Table S1).

Quantification of sirtuin expression in cells and tissues. In all the human primary brain cell types and human brain cell lines SIRT1, 2, 3, 6 and 7 were detected and quantified (Fig. 2). All seven sirtuins were detected

in human control brain tissue, with SIRT2 highly expressed (Fig. 3, Panel A). Detergent fractionation into subcellular groups improved identification of mitochondrial sirtuins (SIRT3–5) (Fig. 3, Panel B).

We were also able to quantify some sirtuins in guinea pig and mouse tissue due to their common sequences with human sirtuin peptides. SIRT1–3 levels in the guinea pig (Fig. 4, Panel A) and SIRT 1 and 3 levels in mouse organs (Fig. 4, Panel B) were quantified. Furthermore the method could be adapted for all sirtuins from other species with purchase of the appropriate synthetic peptides and their heavy internal standards. Supplementary Table S2 shows the level of homology (or identity) of human SIRT1–7 peptide sequences with mouse and guinea pig. All samples were fractionation on a 1D-SDS-PAGE to reduce sample complexity and improve detection sensitivity. A workflow of the sample preparation procedure can be found in Supplementary Figure S3.

Another important issue is the existence of splice variants or isoforms of the sirtuin proteins. Supplementary Table S3 lists the sequences of all sirtuin isoforms and the location of the two MRM peptides within each sequence. The majority of sirtuin isoforms contain both peptides, and all contain at least one of the two peptide sequences used for quantification in this study.

Validation of MRM method with established protocols. Human brain cells and tissue samples were compared with established protocols for sirtuin detection such as immunohistochemical staining, PCR and western blotting. Immunohistochemical staining showed that all seven sirtuins are expressed in astrocytes (Fig. 5, panel A, rows 1–4) and control human frontal lobe brain tissue (Fig. 5, panel A, row 5). PCR identified SIRT1 and SIRT2 mRNA in control human frontal, occipital and hippocampus brain tissue (Fig. 5, panel B). Western blotting confirmed the identification of SIRT1, 2 and 3 in control human frontal lobe brain tissue (Fig. 5, panel C and Supplementary Figure S4).

Quantification of sirtuins in CSF and immunodepleted plasma. SIRT1 was quantified in the CSF of five control patients and in control plasma immunodepleted of the six most abundant proteins. SIRT1 was the only sirtuin detected and was found to range from 4.30 ± 0.19 to 5.09 ± 0.53 fmol/ μ g total protein in CSF and 8.68 ± 0.35 fmol/ μ g total protein in plasma. Individual data can be found in Supplementary Figure S5. SIRT2–7 in CSF and immunodepleted plasma were found to be below the detection limits of the assay. All samples were fractionated by 1D-SDS-PAGE to reduce sample complexity and a workflow of the sample preparation procedure can be found in Supplementary Figure S3.

Discussion

The rapid expansion of instruments and software in the field of targeted protein quantification by MRM is expected to have vast applications in quantitative protein biochemistry^{13,14}. Most of the currently used protocols to measure sirtuin changes in the CNS have utilised methods such as ELISA, surface Plasmon resonance, western blotting and fluorescent staining. Mass spectrometry provides a platform that overcomes some of the limitations of antibody based approaches for protein quantification, in particular providing a level of specificity not available with the other approaches. Isotopically labelled peptide standards allow for quantification of protein levels and also provide the ability to monitor stability of analytes throughout the sample processing steps. This greatly simplifies the development of assays compared with standard immunological formats such as ELISA where well-characterised antibodies are needed. Furthermore MRM facilitates multiplexed analysis, identifying several proteins in a single run, thereby maximising information obtained per sample, minimising assay time while at the same time conserving precious samples. It measures several transitions per quantified protein, thus generating several independent measurements, and with the use of heavy peptide standards allows for generation of standard curves and accurate quantification. This approach has advantages over methods such as western blotting and staining techniques which are semi-quantitative at best and lack the level of structural specificity achieved by mass spectrometry. Our MRM approach is also complementary to PCR which targets mRNA levels only.

Perhaps the major limitation to mass spectrometry based protein quantification is throughput and cost. Immunological assays can be performed in 96 well plate formats and plate readers allow measurement of an entire plate in a single run. Mass spectrometry requires each sample to be run individually with longer run times. However one of the main advantages of mass spectrometry is its ability to specifically and accurately distinguish different isoforms or modified forms of proteins, even in complex samples. The sensitivity of mass spectrometry is very high but limitations to sensitivity of quantitative assays are often caused by the dynamic range of the proteins in the sample. Future developments in mass spectrometer analysers and detectors may help address this limitation. Even so, it is probable that improved sample purification/fractionation procedures will continue to be a vital element of the most challenging and complex proteomics problems, and to achieve the required sensitivity for robust quantification. For example in this study all samples were fractionation on a 1D-SDS-PAGE gel and gel bands excised and tryptic digested prior to MRM analysis to reduce sample complexity. A workflow of the sample preparation procedure can be found in Supplementary Figure S3.

MRM mass spectrometry was successfully utilised in this study to quantify seven mammalian sirtuins in human brain cells, tissues and fluid. Furthermore the method can be used to measure sirtuin expression in animal tissues, such as mouse and guinea pig, in cases where peptide sequences are identical to the human standards. In line with previous data, our results affirm that there is significant divergence in abundance amongst members of the sirtuin family of proteins in the brain. We report SIRT1 and SIRT2 to be the most abundant sirtuins in cultured brain cells with SIRT1 highest in neurons and SIRT2 highest in oligodendrocytes, validating previous studies showing SIRT2 to be highly expressed in oligodendrocytes¹⁵. Our study and others have also found SIRT2 expressed in neurons and glial cells^{16,17}. Further validation with higher sample numbers and across a wider range of cell lines may help elucidate differences between cell types for the lower abundant sirtuins.

We found SIRT2 to be the most abundant sirtuin in the adult human frontal lobe and cortex and cerebellum homogenates from the guinea pig. SIRT2 is known to co-localise with microtubules and functions as a

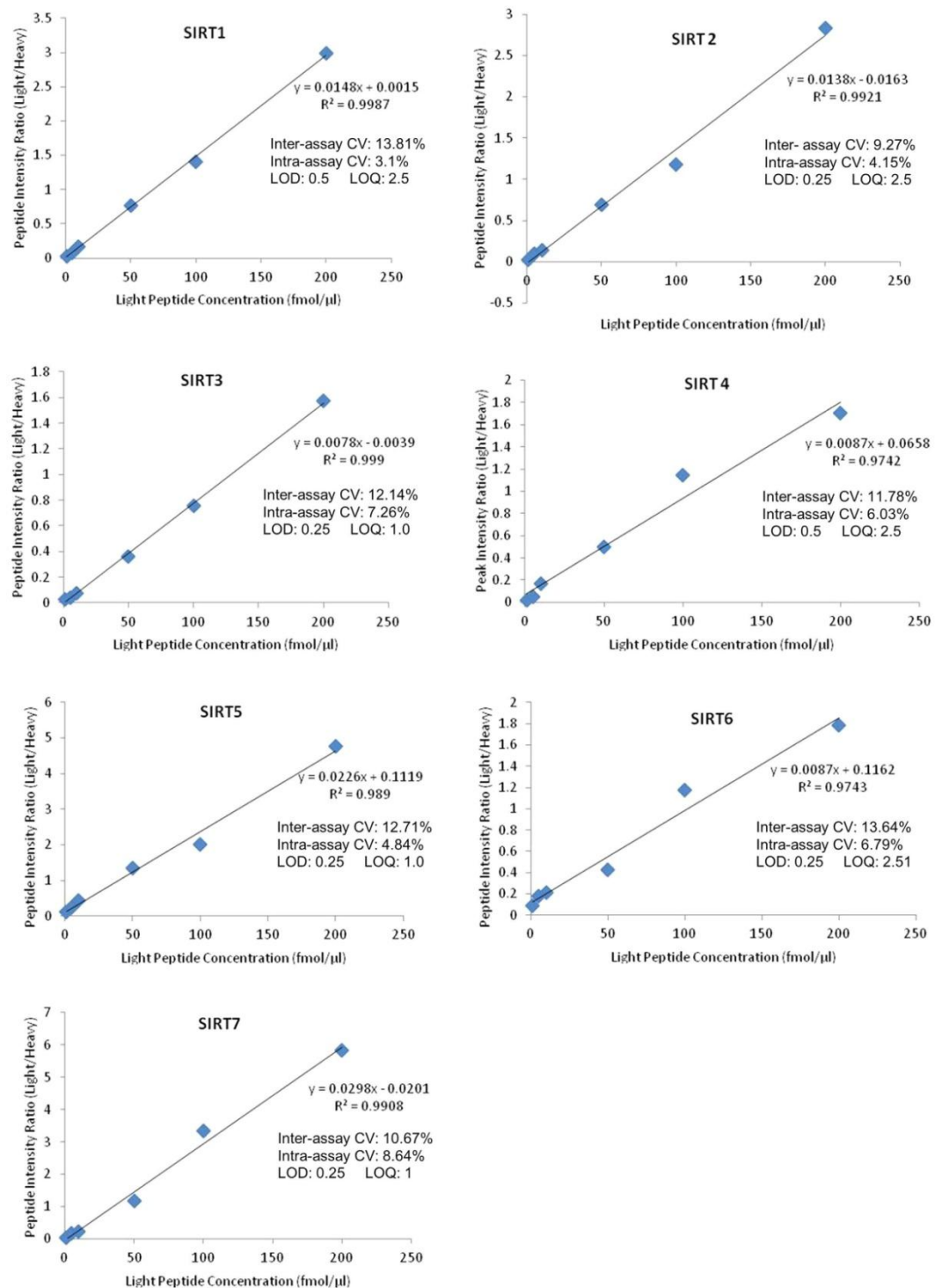


Figure 1. Sirtuin peptide standard curves, variance and limits of detection and quantification. Sirtuin peptide standard curves (average of the peak area ratios for the two peptides, in triplicate for each sirtuin, with heavy peptide spike of 100 fmol/ μ l). Both inter- and intra-assay variance were calculated for three replicates and the LOD and LOQ are shown in fmol/ μ l. CVs calculated using peptide peak area ratios (light/heavy) at the 100 fmol/ μ l peptide concentration level. Individual chromatograms for each of the 14 peptides can be found in Supplementary Figure S1.

tubulin-deacetylase. It is a suppressor of microglial activation and brain inflammation, with reduced levels of SIRT2 leading to increased production of free radicals and neurotoxicity, while its overexpression inhibits brain inflammation¹⁸. In other studies, however, it has been shown to increase in cells with oxidative stress and promote death cell⁴. In addition, SIRT2 inhibition has been shown to protect against Parkinson's disease and Huntington's

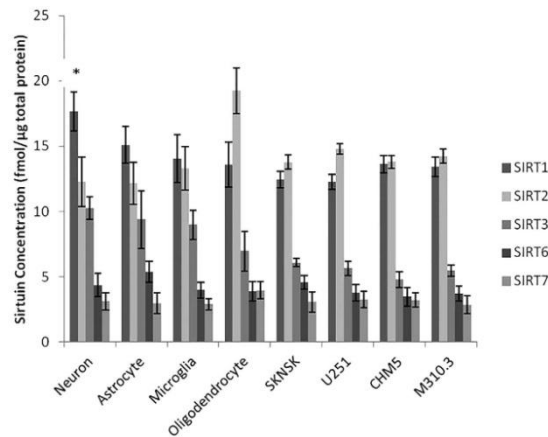


Figure 2. Sirtuin expression in primary cultured brain cells and cell lines. In primary neurons SIRT1 was found to be the most abundant sirtuin ($*p < 0.05$) compared to other neuronal sirtuins ($n = 3$). SIRT2 was found to be abundant in primary oligodendrocytes ($*p < 0.05$) compared to other cell types ($n = 3$). SIRT1 and SIRT2 were the most abundant in all the cell cultures. SIRT4 and SIRT5 were below the detection limits and only small amounts of SIRT6 and SIRT7 were detected.

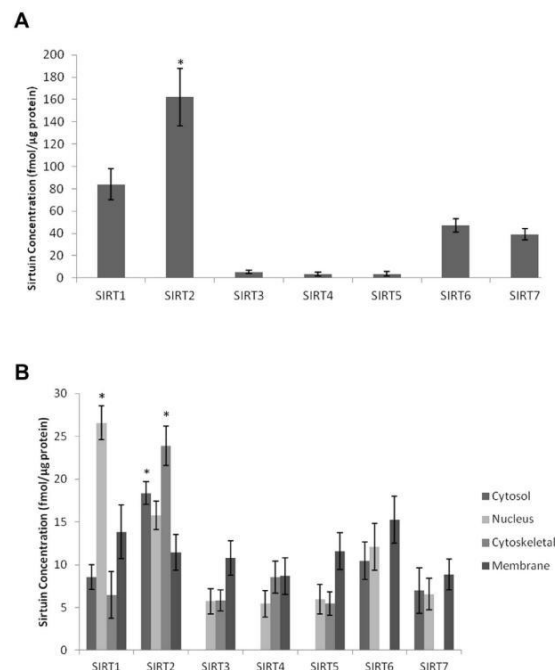


Figure 3. Sirtuin expression in human frontal lobe brain tissue. Sirtuin expression in unfractionated (Panel A) and fractionated (Panel B) human frontal lobe brain tissue. All seven sirtuins were detected in unfractionated human frontal lobe brain tissue with SIRT2 the most abundant ($*p < 0.05$) compared to all other sirtuins (Panel A). The mitochondrial sirtuins (SIRT3-5) were found to be close to the LOQ, but their signals improved following fractionation of the tissue into cytosolic, nuclear, cytoskeletal and membrane fractions (Panel B). Fractionation showed SIRT1 and SIRT2 expressed in all fractions, whereas SIRT3-5 were below the LOD in the cytosol and SIRT6 and SIRT7 were below the LOD in the cytoskeletal fraction. SIRT1 was most abundant in the nucleus and SIRT2 in the cytoskeletal fraction ($*p < 0.05$, Panel B). In the cytosol, SIRT2 was the most abundant sirtuin ($*p < 0.05$), and all sirtuins were captured in the membrane fraction.

disease^{19,20}. Previously published results have shown SIRT2 to be abundant in the brain and serum^{9,11,21,22} and our study provides further evidence for this and shows that it is also abundant in the guinea pig brain.

SIRT1 was the second-most abundant sirtuin in the brain and the only sirtuin detected in the CSF and plasma using our method. SIRT1 is a neuroprotective factor in a variety of models of neurodegenerative diseases, including Huntington's disease, Multiple Sclerosis and AD^{23,24}. It increases following exposure to cellular stressors, including energy/nutrient depletion and has been linked to increased lifespan in animal models²⁵. We were only

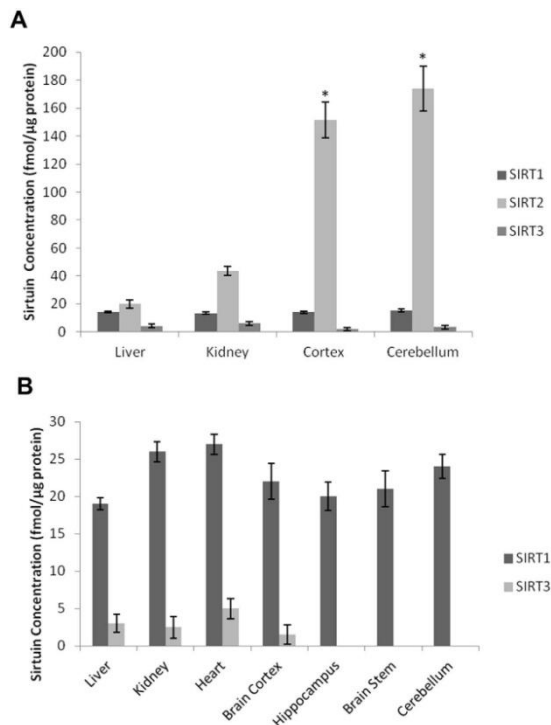


Figure 4. SIRT1-3 protein expression in animal organs. SIRT1-3 protein expression in guinea pig (Panel A) and mouse organs (Panel B). SIRT2 was found to be the most abundant sirtuin in guinea pig, with higher levels expressed in the brain (* $p < 0.01$, $n = 2$) compared to liver and kidney. SIRT2 in mouse was not quantified due to peptide sequence difference with the human peptide standards.

able to detect SIRT1 in both CSF and plasma while Kumar *et al.* have recently identified SIRT1, SIRT2 and SIRT3 in human serum using surface plasmon resonance⁹. The use of more sensitive mass spectrometry instrumentation, and/or fractionation or enrichment of plasma proteins, may improve sensitivity for the other sirtuins in plasma.

The mitochondrial sirtuins SIRT3–5 were found at lower levels in human brain but detection was improved after detergent fractionation. Further fractionation of samples or purification/enrichment of mitochondria may facilitate improved mitochondrial sirtuin quantification. Our data also show that SIRT6 and SIRT7 are the third and fourth most abundant members of the sirtuins family in the adult human frontal lobe. Both SIRT6 and SIRT7 have been associated with the maintenance of DNA stability and promotion of DNA repair following exposure to cellular stressors^{26,27}.

We also confirm that mammalian sirtuins are localised to several subcellular compartments. While SIRT1, SIRT6 and SIRT7 are predominantly found in nuclear fractions, they are also detected in cytosol, cytoskeleton and membrane fractions, albeit at much lower levels. Similarly, although SIRT2 is the only human sirtuin primarily localised in the cytoplasm, it may also be found at lower levels in the nucleus and cellular membrane. Our data confirm that SIRT1 and SIRT2 may interact with both the nuclear and cytoplasmic subcellular compartments. Similarly, while the mitochondrial sirtuins (SIRT3–5) were previously reported to be exclusively localised to the mitochondria, other studies have reported the localisation of several variants in the nucleus as well as the cytoplasm, in line with our study²⁸. SIRT5 has recently been found to have both desuccinylase and de-malonylase activities in both the mitochondria and cytosol^{29,30}. The expression patterns of sirtuins in brain cells remains controversial and it is unclear whether certain sirtuins are specific to cell types. Our MRM study indicates that the majority of sirtuins (SIRT1, 2, 6 and 7) are present across all the main brain cell types.

For validation, analyses of the samples by immunohistochemical staining confirmed that all seven sirtuins are found in human primary astrocytes (Fig. 5, panel A row 1–5). PCR detected SIRT1 and SIRT2 mRNA in frontal, occipital and hippocampal brain tissue (Fig. 5, panel B). Western blotting identified protein levels in frontal lobe brain tissue with SIRT2 showing the strongest bands (Fig. 5, panel C and supplementary Figure S4), in good agreement with the results from our MRM assay (Fig. 3).

Various studies have demonstrated that abnormal changes to sirtuin proteins occur during disease states as well as ageing. SIRT2 accumulates with age in the mouse brain and spinal cord²². Other recent studies have shown that SIRT1 decreases with age in the rat brain³¹ and SIRT2 is upregulated in brain tumours³². Hence, there is great value in developing robust quantitative assays such as MRM mass spectrometry to accurately quantify these proteins in control vs disease states. Another important aspect of sirtuin biology is that their deacetylase activity is nicotinamide and NAD^+ dependent, establishing a direct link between their function and energy metabolism. To improve sensitivity, we found our fractionation method of running the samples on SDS PAGE and excising gel bands corresponding to the molecular weights of the intact sirtuin proteins to improve detection sensitivity.

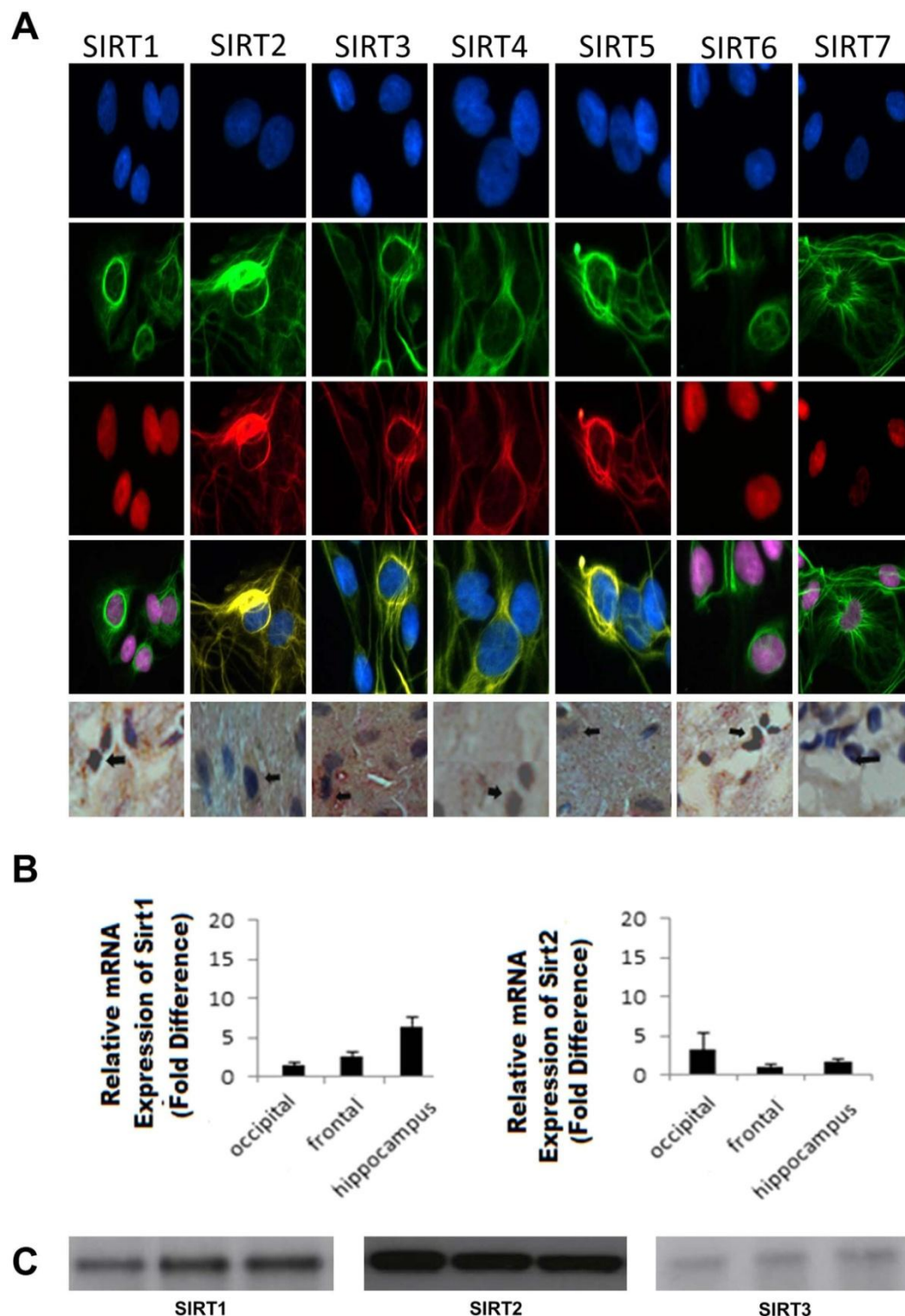


Figure 5. Sirtuin expression in human brain cells and tissue using immunohistochemical staining of astrocytes (Panel A row 1–4) and human frontal lobe brain tissue (Panel A, row 5), PCR of SIRT1 and SIRT2 mRNA in occipital, frontal and hippocampal human control brain (Panel B) and cropped images of western blotting of SIRT1–3 protein expression in human control frontal lobe brain tissue ($n=3$) at molecular weights of approx 40 kDa, 50 kDa and 30 kDa respectively (Panel C). Full length blots are presented in Supplementary Figure S4.

The use of more sensitive mass spectrometers with high resolution MRM capability may improve detection of low abundant sirtuins and/or allow removal of the gel fractionation step. This would allow for sample lysates to be digested and analysed directly and decrease sample processing time. Using hybrid mass spectrometers capable

of high resolution and accurate mass measurements such as the quadrupole-orbitrap may overcome these issues and yield better sensitivity for high-complexity samples. This will help future validation of levels in large cohorts which may be useful for the identification of sirtuins as potential biomarkers.

Collectively, our results add further insights to the limited data which currently exist regarding the expression of sirtuins in the human CNS. This technique provides a powerful tool and helps improve upon the limitations of current protocols. While mass spectrometry based assays for protein quantification may still have some barriers to overcome before they can be used in a clinical setting due to low throughput and expense compared to methods such as ELISA, they have great value in investigating lower abundance proteins such as sirtuins in complex samples such as the brain with great sensitivity and specificity. Furthermore the current approach could be extended to develop isotope specific sirtuin assays, or extended to other species by use of appropriate synthetic peptide standards. MRM mass spectrometry can also be utilised for the quantification of sirtuin related metabolites and thus targeted mass spectrometry methodologies have the potential to not only validate and complement currently established methods for investigation of sirtuin protein expression changes but can also help build a larger view of sirtuin biology in the normal brain and in disease conditions by linking sirtuin protein expression with metabolism.

Methods

Selection of target sirtuin peptides. Recombinant protein standards were purchased for seven human sirtuins (Cayman Chemical, USA), and 5 µg of each was run by 1D SDS-PAGE gel and colloidal coomassie stained. Sirtuin bands were excised, trypsin digested overnight followed by LC-MS/MS analysis on a QToF Ultima API hybrid tandem mass spectrometer (Micromass, UK) as previously described^{33–35} and a detailed method is provided in Supplementary Protocols. The two peptides with the highest signal intensity for each sirtuin were cross-referenced with Skyline software (MacCoss Lab Software, USA). Peptide sequences were checked to ensure no overlap with other sirtuins. Sirtuin standards were run using MRM LC-MS/MS on a 4000 Q TRAQ (SCIEX, USA) mass spectrometer to ensure good signals were detected for all 14 peptides selected for the final list (two unique peptides for each sirtuin). See Supplementary Tables S2 and S4 and supplementary protocols for peptide sequences and light and heavy product ions for all 14 peptides. The full list of transitions and corresponding collision energies and MRM method details are provided in Supplementary Table S5.

Targeted mass spectrometry. MRM analyses were performed on a 4000 Q TRAP hybrid triple quadrupole linear ion trap mass spectrometer (SCIEX, USA) interfaced with a nanospray ion source, operating in positive ion mode and controlled by Analyst 1.5 software. Peptides were concentrated and desalted onto a micro C18 precolumn (500 µm × 2 mm, Michrom Bioresources, USA) with H₂O:CH₃CN (98:2, 0.05% TFA) at 15 µl/min. After a 4 min wash, the pre-column was automatically switched (10 port valve, Valco, USA) into line with a nano column (as described in the previous section). Peptides were eluted using a linear gradient of H₂O:CH₃CN (98:2, 0.1% formic acid) to H₂O:CH₃CN (36:64, 0.1% formic acid) at ~300 nl/min over 30 minutes. Samples were analysed with an ion spray voltage of 2.4 kV, curtain gas flow of 12 and nebulizing gas flow of 5 L/min. Quadrupoles were operated in the low resolution mode, and the dwell time was 50 ms. For validation runs, the MRM experiment triggered MS/MS spectrum acquisition. MS/MS spectra were acquired in the trap mode (enhanced product ion) with dynamic fill time, Q1 was operated using low resolution. Each sirtuin protein (SIRT1–7, 2 peptides per protein) were run with 12 transition ions per run, per protein and with a 50 ms dwell time. See Supplementary Table S5 for a full list of transitions for each peptide and corresponding collision energies (estimated using Skyline software).

Sirtuin Peptide Standards. Multiple point calibration was used where a series of standard ‘light’ peptides with known concentrations together with fixed amounts of stable isotope-labelled ‘heavy’ peptides (100 fmol/µl) were used to generate calibration curves (Fig. 1). The curves were expressed as ratios of light/heavy peak area (y-axis) versus concentration of light peptide (x-axis) for each of the 14 peptides selected. A commercially available stable isotope-labelled peptide standard (AQUA peptide, Sigma, USA) was used for absolute quantification of proteins. This heavy surrogate of each of the peptide standards is added at a constant level to all samples and standards and is used for correction of sample losses during workup and normalisation across runs, allowing accurate quantification of the target protein in samples. Peptides labelled with a stable isotope (¹³C and ¹⁵N) are chemically identical to their native counterparts and have identical chromatographic behaviour but can be distinguished from the calibration standards based on a small specific mass difference.

Preparation of Cell Cultures, Tissues, CSF and Plasma. *Cells.* Adult human primary micro-glia, astrocytes, neurons and oligodendrocytes were cultured from resected normal adult brain tissue following removal of brain tumour with informed consent at the Minimally Invasive Cancer Centre, Prince of Wales Hospital, Sydney, Australia. Astrocytes were prepared from the mixed brain cell cultures using a protocol previously described by Guillemain *et al.*³⁶. Cell culture procedures are described in detail in Supplementary Protocols. All cells and cell lines were lysed using RIPA buffer followed by probe sonication and cell debris removed by centrifugation at 10,000RPM for 5 min. Total protein concentration was assayed in the supernatant using the Pierce BCA protein assay kit (Life Technologies, Australia), and three 10 µg replicates were run by 1D SDS-PAGE followed by colloidal coomassie staining.

Human Tissues. 20 µg of protein from five individual control post mortem brain tissue samples were extracted as described for cells in the previous section, and run on a 1D SDS-PAGE gel and coomassie stained. Detailed patient information including age, sex and post-mortem tissue collection times can be found in Supplementary

Table S6. For the fractionated samples, 200 mg of frontal lobe brain tissue from five control subjects were pooled and differential detergent fractionation performed to obtain cytosol, nucleus, cytoskeletal and membrane protein fractions³⁷. Each fraction (20 µg) was run on a 1D SDS-PAGE gel and coomassie stained.

Animals. Female guinea pigs (Dunkin–Hartley) and C57BL6 mice were housed in temperature-controlled rooms (21–22 °C; 49–55% humidity) with 12 h light-dark cycle (lights on 7:00–19:00). Food and water was available *ad libitum*. Wild type mice and guinea pig organs were lysed (RIPA buffer) by probe sonication. Proteins (20 µg/lane) were run by 1D SDS-PAGE and coomassie stained. Protein concentrations were determined using the Pierce BCA protein assay kit (Life Technologies, Australia).

CSF and plasma. CSF samples were collected by standard lumbar puncture from five patients assessed as clinically well after investigation for suspected meningitis (Supplementary Figure S5), returning normal results for routine CSF pathology markers (white cell count, protein, glucose and bacterial sterility). Aliquots (50 µl) from each patient were obtained for our study. Control human plasma from a healthy individual was immunodepleted of the six most abundant plasma proteins using an Hu6 column (Agilent, USA) according to manufacturer's instructions³⁸. For immunodepletion using the Multiple Affinity Removal System Hu6 column and buffer kit (Agilent, Santa Clara, CA, USA). 24 µl EDTA plasma was diluted into 120 µl Buffer A. 100 µl of this diluted EDTA plasma was injected onto the Hu6 column connected to a HP 1090 HPLC system (Agilent, Santa Clara, CA, USA) and the low abundance protein fraction was collected following manufacturer's instructions. The low abundance protein fractions from six injections were pooled, buffer exchanged and concentrated into 45 mM NaHCO₃ using Amicon 3 kDa centrifugal devices (Millipore, Billerica, MA, USA). CSF protein (5 µg) and depleted plasma protein (20 µg) as determined by a BCA protein assay were run on a 1D SDS-PAGE gel and colloidal coomassie stained.

For all samples, the band corresponding to the molecular weight for each sirtuin was excised (see Supplementary Figure S6), de-stained and trypsin digested overnight with heavy sirtuin peptides added as internal standards to all samples prior to digestion (the internal standard was added at a constant level to all samples and standards, and was at about the midrange of the standard curve). The tryptic peptides were dried under vacuum (Savant Speedvac, Thermo Scientific, USA), reconstituted in 0.1% formic acid (5 µl), injected into the mass spectrometer (1 µl) and analysed using MRM. Peak area ratios (light/heavy) were calculated for each endogenous peptide (light) relative to the spiked isotope- labelled (heavy) peptide using Skyline MRM analysis software. Protein concentrations were determined using calibration curves. All samples were fractionated by 1D-SDS-PAGE to reduce sample complexity. A workflow of the sample preparation procedure can be found in Supplementary Figure S3.

To test for matrix effects relevant to the in-gel processed sirtuins, Hu6 depleted plasma was run by SDS-PAGE (see Supplementary Figure S7) and sirtuin peptide standard curves prepared by spiking with excised gel bits taken from the expected migration position of the intact sirtuin. Additional matrices tested included buffer only (0.1% formic acid, no gel bit), a blank gel bit, and the spiked standard curves are shown in Supplementary Figure S2.

To determine recoveries of sirtuin proteins, commercial intact sirtuin standards were run by SDS PAGE (5 µg per lane). Hu6 high abundance depleted plasma spiked with 2 µg and 5 µg of the sirtuin standard for SIRT1, 2, 3, 5 and 6 were also run on the same gel (Supplementary Figure S8). Sirtuin 5 µg spike recoveries were calculated in the LAP spike relative to the sirtuin 5 µg standard protein in buffer only samples. The sirtuin 2 µg spike recoveries were calculated in the LAP spike relative to values extrapolated from the results of the sirtuin 5 µg standard protein in buffer only samples (Supplementary Table S1).

Sirtuin mRNA Expression in Human Brain Tissue using PCR. For the gene expression studies RNA was extracted from human brain cells using RNeasy mini kits (Qiagen, Germany). The cDNA was prepared using SuperScript III First-Strand Synthesis System and random hexamers (Invitrogen Corporation, USA) as previously described³⁹. Detailed protocol and primer sequences are described in Supplementary Protocols and Supplementary Table S7 respectively.

Sirtuin Expression in Human Brain Cells and Tissue using immunohistochemical staining.

Post mortem brain tissue from a male patient aged 63 years was obtained from the Sydney Brain Bank. Immunohistochemical staining was performed as previously published⁴⁰ and was performed using anti-human sirtuin (1:250) primary antibodies (raised in rabbit). The full protocol description can be found in Supplementary Protocols.

Sirtuin Protein Expression in human control brain tissue using western blotting.

Protein from three individual control post mortem frontal brain tissue samples were extracted as described in the previous section, and run on a 1D SDS-PAGE gel (20 µg protein per lane), and western blotted with antibodies for SIRT1, SIRT2 and SIRT3 (details provided in Supplementary Protocols and list of antibodies used in Supplementary Table S8).

Statistics. Sirtuin concentrations are presented as means ± SEM using peak area ratios of light and heavy peptides obtained from Skyline MRM Proteomics software v3.1 (MacCoss Lab, USA). Sirtuins were quantified based on an average of data from both peptides used for each sirtuin where possible. Statistical comparisons were performed using two-tailed student t-tests assuming equal variance. Differences between groups were considered statistically significant at the p < 0.05 level.

Ethics. All human and animal brain tissue samples were obtained and experiments conducted in accordance with the guidelines of the National Health and Medical Research Council of Australia and were approved by the University of New South Wales Human Research Ethics Committee (human brain tissue reference number HC12563) and the University of New South Wales Animal Care Ethics Committee (guinea pig tissue reference number 14/40B and mice 13/39B). Adult human primary microglia, astrocytes, neurons and oligodendrocytes were cultured from resected normal adult brain tissue following removal of brain tumour with informed consent at the Minimally Invasive Cancer Centre, Prince of Wales Hospital, Sydney, Australia (reference number X12-0314 and HREC/12/RPAH/481). All control CSF samples were obtained with ethics approval from the Sydney Adventist Hospital, Sydney Australia, with informed consent obtained from all subjects (reference number SAHHREC #13-02).

References

- Haigis, M. C. & Sinclair, D. A. Mammalian sirtuins: biological insights and disease relevance. *Annu Rev Pathol* **5**, 253–295 (2010).
- Gueguen, C., Palmier, B., Plotkine, M., Marchand-Leroux, C. & Bessson, V. C. Neurological and histological consequences induced by *in vivo* cerebral oxidative stress: evidence for beneficial effects of SIRT1720, a sirtuin 1 activator, and sirtuin 1-mediated neuroprotective effects of poly(ADP-ribose) polymerase inhibition. *PLoS One* **9**, e87367 (2014).
- Alcendor, R. R. *et al.* Sirt1 regulates aging and resistance to oxidative stress in the heart. *Circ Res* **100**, 1512–1521 (2007).
- Wang, F., Nguyen, M., Qin, F. X. & Tong, Q. SIRT2 deacetylates FOXO3a in response to oxidative stress and caloric restriction. *Aging Cell* **6**, 505–514 (2007).
- Qiu, X., Brown, K., Hirschey, M. D., Verdin, E. & Chen, D. Calorie restriction reduces oxidative stress by SIRT3-mediated SOD2 activation. *Cell Metab* **12**, 662–667 (2010).
- Lattanzio, F. *et al.* Human apolipoprotein E4 modulates the expression of Pin1, Sirtuin 1, and Presenilin 1 in brain regions of targeted replacement apoE mice. *Neuroscience* **256**, 360–369 (2014).
- Wang, H. F., Li, Q., Feng, R. L. & Wen, T. Q. Transcription levels of sirtuin family in neural stem cells and brain tissues of adult mice. *Cellular and molecular biology Suppl.* **58**, OL1737–OL1743 (2012).
- Kumar, R. *et al.* Sirtuin1: a promising serum protein marker for early detection of Alzheimer's disease. *PLoS One* **8**, e61560 (2013).
- Kumar, R. *et al.* Identification of serum sirtuins as novel noninvasive protein markers for frailty. *Aging Cell* **13**, 975–980 (2014).
- Weir, H. J. *et al.* CNS SIRT3 expression is altered by reactive oxygen species and in Alzheimer's disease. *PLoS One* **7**, e48225 (2012).
- Korner, S. *et al.* Differential sirtuin expression patterns in amyotrophic lateral sclerosis (ALS) postmortem tissue: neuroprotective or neurotoxic properties of sirtuins in ALS? *Neuro-degenerative diseases* **11**, 141–152 (2013).
- Hoppner, S., Schanzer, W. & Thevis, M. Mass spectrometric studies on the *in vitro* generated metabolites of SIRT1 activating drugs for doping control purposes. *Journal of mass spectrometry: JMS* **48**, 830–843 (2013).
- Liebler, D. C. & Zimmerman, L. J. Targeted quantitation of proteins by mass spectrometry. *Biochemistry* **52**, 3797–3806 (2013).
- Doerr, A. Mass spectrometry-based targeted proteomics. *Nature methods* **10**, 23 (2013).
- Ji, S., Doucette, J. R. & Nazarali, A. J. Sirt2 is a novel *in vivo* downstream target of Nkx2.2 and enhances oligodendroglial cell differentiation. *Journal of molecular cell biology* **3**, 351–359 (2011).
- Oh, C. L. E., Lee, Y. S. & Shin, D. H. SIRT2 Protein Expression in Normal and Aged Rat Brain. *J Korean Geriatr Soc* **16**, 27–33 (2012).
- Pandithage, R. *et al.* The regulation of SIRT2 function by cyclin-dependent kinases affects cell motility. *J Cell Biol* **180**, 915–929 (2008).
- Pais, T. F. *et al.* The NAD-dependent deacetylase sirtuin 2 is a suppressor of microglial activation and brain inflammation. *EMBO J* **32**, 2603–2616 (2013).
- Outeiro, T. F. *et al.* Sirtuin 2 inhibitors rescue alpha-synuclein-mediated toxicity in models of Parkinson's disease. *Science* **317**, 516–519 (2007).
- Luthi-Carter, R. *et al.* SIRT2 inhibition achieves neuroprotection by decreasing sterol biosynthesis. *Proc Natl Acad Sci USA* **107**, 7927–7932 (2010).
- Ren, Y. *et al.* Effect of breed on the expression of Sirtuins (Sirt1–7) and antioxidant capacity in porcine brain. *Animal: an international journal of animal bioscience* **7**, 1994–1998 (2013).
- Maxwell, M. M. *et al.* The Sirtuin 2 microtubule deacetylase is an abundant neuronal protein that accumulates in the aging CNS. *Hum Mol Genet* **20**, 3986–3996 (2011).
- Jeong, H. *et al.* Sirt1 mediates neuroprotection from mutant huntingtin by activation of the TORC1 and CREB transcriptional pathway. *Nature medicine* **18**, 159–165 (2012).
- Khan, R. S., Dine, K., Das Sarma, J. & Shindler, K. S. SIRT1 activating compounds reduce oxidative stress mediated neuronal loss in viral induced CNS demyelinating disease. *Acta neuropathologica communications* **2**, 3 (2014).
- Satoh, A. *et al.* Sirt1 extends life span and delays aging in mice through the regulation of Nk2 homeobox 1 in the DMH and LH. *Cell Metab* **18**, 416–430 (2013).
- Lu, C. T. *et al.* The potential of SIRT6 and SIRT7 as circulating markers for head and neck squamous cell carcinoma. *Anticancer research* **34**, 7137–7143 (2014).
- Lee, N. *et al.* Comparative interactomes of SIRT6 and SIRT7: Implication of functional links to aging. *Proteomics* **14**, 1610–1622 (2014).
- Iwahara, T., Bonasio, R., Narendra, V. & Reinberg, D. SIRT3 functions in the nucleus in the control of stress-related gene expression. *Molecular and cellular biology* **32**, 5022–5034 (2012).
- Nishida, Y. *et al.* SIRT5 Regulates both Cytosolic and Mitochondrial Protein Malonylation with Glycolysis as a Major Target. *Mol Cell* **59**, 321–332 (2015).
- Li, F. *et al.* NADP(+)-IDH Mutations Promote Hypersuccinylation that Impairs Mitochondria Respiration and Induces Apoptosis Resistance. *Mol Cell* **60**, 661–675 (2015).
- Braidy, N. *et al.* Differential expression of sirtuins in the aging rat brain. *Frontiers in cellular neuroscience* **9**, 167 (2015).
- Luna, B. *et al.* Proteomic and Mitochondrial Genomic Analyses of Pediatric Brain Tumors. *Molecular neurobiology* **52**(3), 1341–63 (2015).
- Gatlin, C. L., Kleemann, G. R., Hays, L. G., Link, A. J. & Yates, J. R. 3rd Protein identification at the low femtomole level from silver-stained gels using a new fritless electrospray interface for liquid chromatography-microspray and nanospray mass spectrometry. *Anal Biochem* **263**, 93–101 (1998).
- Hou, X. *et al.* Cellular responses during morphological transformation in *Azospirillum brasilense* and Its flcA knockout mutant. *PLoS One* **9**, e114435 (2014).
- Coumans, J. V., Poljak, A., Raftery, M. J., Backhouse, D. & Pereg-Gerk, L. Analysis of cotton (*Gossypium hirsutum*) root proteomes during a compatible interaction with the black root rot fungus *Thielaviopsis basicola*. *Proteomics* **9**, 335–349 (2009).
- Guillemin, G. J. *et al.* Kynurenine pathway metabolism in human astrocytes: a paradox for neuronal protection. *J Neurochem* **78**, 1–13 (2001).
- Simpson, R. *Proteins and Proteomics: A Laboratory Manual*. (Cold Spring Harbor Laboratory Press, 2002).

- Muenchhoff, J. *et al.* Plasma protein profiling of mild cognitive impairment and Alzheimer's disease across two independent cohorts. *J Alzheimers Dis* **43**, 1355–1373 (2015).
- Sheipouri, D. *et al.* Characterisation of the kynurenine pathway in skin-derived fibroblasts and keratinocytes. *Journal of cellular biochemistry* **116**, 903–922 (2015).
- Wu, W. *et al.* Expression of tryptophan 2,3-dioxygenase and production of kynurenine pathway metabolites in triple transgenic mice and human Alzheimer's disease brain. *PLoS one* **8**, e59749 (2013).
- Graff, J. *et al.* A dietary regimen of caloric restriction or pharmacological activation of SIRT1 to delay the onset of neurodegeneration. *J Neurosci* **33**, 8951–8960 (2013).
- Komlos, D. *et al.* Glutamate dehydrogenase 1 and SIRT4 regulate glial development. *Glia* **61**, 394–408 (2013).
- Shih, J., Mason, A., Liu, L., Higashimori, H. & Donmez, G. Loss of SIRT4 decreases GLT-1-dependent glutamate uptake and increases sensitivity to kainic acid. *J Neurochem* (2014).
- Glorioso, C., Oh, S., Douillard, G. G. & Sibille, E. Brain molecular aging, promotion of neurological disease and modulation by sirtuin 5 longevity gene polymorphism. *Neurobiol Dis* **41**, 279–290 (2011).
- Favero, G., Rezzani, R. & Rodella, L. F. Sirtuin 6 nuclear localization at cortical brain level of young diabetic mice: An immunohistochemical study. *Acta histochemica* (2013).
- Schwer, B. *et al.* Neural sirtuin 6 (Sirt6) ablation attenuates somatic growth and causes obesity. *Proc Natl Acad Sci USA* **107**, 21790–21794 (2010).
- Liszt, G., Ford, E., Kurtev, M. & Guarente, L. Mouse Sir2 homolog SIRT6 is a nuclear ADP-ribosyltransferase. *J Biol Chem* **280**, 21313–21320 (2005).
- Toiber, D. *et al.* SIRT6 recruits SNF2H to DNA break sites, preventing genomic instability through chromatin remodeling. *Mol Cell* **51**, 454–468 (2013).
- Zhong, L. & Mostoslavsky, R. SIRT6: a master epigenetic gatekeeper of glucose metabolism. *Transcription* **1**, 17–21 (2010).

Acknowledgements

This work was facilitated by the Australian National Health and Medical Research Council Program Grant (NHMRC) 350833, Capacity Building Grant 568940, The Australian Research Council Discovery Project Grant DP120102078 and the Rebecca L. Cooper Medical Research Foundation, the UNSW Faculty of Medicine Research Grant to Dr Nady Braidy and the Alzheimer's Australia Viertel Foundation. The financial support of these organizations is gratefully acknowledged. Dr Nady Braidy is also the recipient of an NHMRC Postdoctoral Research Fellowship at the University of New South Wales. Tharusha Jayasena is a recipient of the University of New South Wales Postgraduate Award (UPA). The mass spectrometry work was carried out in the Bioanalytical Mass Spectrometry Facility at the University of New South Wales, and subsidised access to this facility is gratefully acknowledged. The authors thank Dr Sophia Dean for her assistance with revising and formatting the manuscript.

Author Contributions

P.S., A.P., T.J. and G.S. conceived and planned the project. T.J. performed experimental work (MRM assay development and validation, cell culture, protein extraction, 1D SDS/PAGE) and wrote the main manuscript text. A.P., L.Z. and M.R. assisted with mass spectrometry instrumentation setup, maintenance and optimisation. N.B. performed all experimental work for and prepared Figure 5, Panel A and B. B.R. was involved in animal care of the guinea pig and mice used. J.M. performed Hu6 depletion of high abundance plasma proteins. R.G. was involved in collection of CSF samples. C.T. surgically removed brain tumors and provided samples. All authors reviewed the manuscript.

Additional Information

Supplementary information accompanies this paper at <http://www.nature.com/srep>

Competing financial interests: The authors declare no competing financial interests.

How to cite this article: Jayasena, T. *et al.* Application of Targeted Mass Spectrometry for the Quantification of Sirtuins in the Central Nervous System. *Sci. Rep.* **6**, 35391; doi: 10.1038/srep35391 (2016).



This work is licensed under a Creative Commons Attribution 4.0 International License. The images or other third party material in this article are included in the article's Creative Commons license, unless indicated otherwise in the credit line; if the material is not included under the Creative Commons license, users will need to obtain permission from the license holder to reproduce the material. To view a copy of this license, visit <http://creativecommons.org/licenses/by/4.0/>

© The Author(s) 2016

SUPPLEMENTARY INFORMATION

Application of Targeted Mass Spectrometry for the Quantification of Sirtuins in the Central Nervous System

T. Jayasena^a, A. Poljak^{a,b,c}, N. Braidy^a, L. Zhong^b, B. Rowlands^c, J. Muenchhoff^a, R. Grant^{c,f}, G. Smythe^c, C. Teo^d, M. Raftery^b, and P. Sachdev^{a,e,*}

^aCentre for Healthy Brain Ageing (CHeBA), School of Psychiatry, University of New South Wales, Sydney, Australia

^bBioanalytical Mass Spectrometry Facility, Mark Wainwright Analytical Centre, University of New South Wales, Sydney, Australia

^cSchool of Medical Sciences, University of New South Wales, Sydney, Australia

^dMinimally Invasive Cancer Centre, Prince of Wales Hospital, Sydney, Australia

^eNeuropsychiatric Institute, the Prince of Wales Hospital, Sydney, Australia

^fSydney Medical School, University of Sydney, Sydney, Australia

* Corresponding Author: Prof. P. Sachdev, Neuropsychiatric Institute, the Prince of Wales Hospital, Randwick NSW 2031, Australia. Tel: +61-2-93823763, Fax: +61-2-93823774 E-mail: p.sachdev@unsw.edu.au

SUPPLEMENTARY PROTOCOLS

a) Selection of Peptides

Digested peptides were separated by nano-LC using a Cap-LC autosampler system (Waters, USA). Samples (5 µl) were concentrated and desalted onto a micro C18 precolumn (500 µm x 2 mm, Michrom Bioresources, Auburn, CA) with H₂O:CH₃CN (98:2, 0.05% HFBA) at 15 µl/min. After a 4 min wash, the pre-column was automatically switched (Valco 10 port valve, Houston, TX) into line with a fritless nano column (75 µm x ~12 cm) containing Magic C18 (~10cm, 200Å, Michrom). Peptides were eluted using a linear gradient of H₂O:CH₃CN (98:2, 0.1% formic acid) to H₂O:CH₃CN (55:45, 0.1% formic acid) at ~300 nl/min over 30 min. The precolumn was connected via a fused silica capillary (10 cm, 25 µ) to a low volume tee (Upchurch Scientific) where high voltage (2400 V) was applied and the column tip positioned ~1 cm from the Z-spray inlet of an QToF Ultima API hybrid tandem mass spectrometer (Micromass, UK). Positive ions were generated by electrospray and the QToF operated in data dependent acquisition mode (DDA). A ToF MS survey scan was acquired (m/z 350-1700, 1 s) and the two largest multiply charged ions (counts > 20) were sequentially selected by Q1 for MS-MS analysis. Argon was used as collision gas and an optimum collision energy chosen (based on charge state and mass). Tandem mass spectra were accumulated for up to 2 s (m/z 50-2000). Peak lists were submitted to the database search program Mascot (Matrix Science, UK) to confirm identification of sirtuin peptides.

b) Sirtuin standards and calibration curves

Isotopically labelled internal standards are excellent tools to normalise the variability in sample handling, injection volume and the performance of the mass spectrometer. Synthetic light and heavy peptides were purchased from GL Biochem (China) and Sigma-Aldrich (USA) respectively. Calibration curves in the range of 1-200 fmol/µl (three replicates using three transitions) were prepared. Heavy peptide (100 fmol/µl) was added to all standards and peptide ratios (light/heavy) were obtained using Skyline MRM analysis software. Average inter- and intra- assay %CV values (n=3) were calculated for each of the seven sirtuins. The linear range, limit of detection (LOD) and limit of quantification (LOQ) were determined. A signal-to-noise ratio of >3:1 and >10:1 was used to define LOD and LOQ respectively.

Cell Culture

Cells were cultured in medium RPMI 1640 supplemented with 10% foetal bovine serum, 1% 1-glutamax, 1% antibacterial/antifungal, and 0.5% glucose. Cells were maintained at 37°C in a

humidified atmosphere containing 95% air/5% CO₂. Cells were seeded into 24-well tissue culture plates to a density of 1×10^5 cells 24 hours prior to experimentation. Neurons were prepared from the same mixed brain cell cultures as previously described (Guillemin et al., 2007). Briefly, cells were plated in 24-well culture plates coated with Matrigel (1/20 in Neurobasal) and maintained in Neurobasal medium supplemented with 1% B-27 supplement, 1% Glutamax, 1% antibiotic/antifungal, 0.5% HEPES buffer, and 0.5% glucose. Microglia were prepared from the mixed brain cell cultures using a published protocol (Guillemin et al., 2001). Briefly, the original mixed brain cell culture was shaken at 220 rpm for 2 h, floating cells were centrifuged, transferred to Permanox chamber slides (NUNC) at a density of 5×10^5 cells/ml and grown in DMEM supplemented with 10% fetal calf serum (FCS), 1% L-glutamax, 0.5% glucose, IL-3 (300 IU/ml), macrophage colony-stimulating factor (M-CSF) (50 IU/ml), and 1% antibiotic/antifungal. Oligodendrocytes were prepared from the mixed brain cell cultures using a published protocol (Guillemin et al., 2001). Briefly, cells were seeded and grown in flasks coated with poly-L-lysine to confluence at 34°C, the permissive temperature, in DMEM/F12 supplemented with 10% FBS, 1% antibiotic/antifungal, 1% of G418 (Invitrogen, Melbourne, Australia) and then shifted to 39°C, the non-permissive temperature that leads to the 'differentiated' state for 72 hours. Cells were cultured in medium RPMI supplemented with 1% myelin binding protein, 1% L-glutamax, and 1% antibacterial/antifungal. CNS cell lines of neurons (SKNSH), astrocytes (U251), oligodendrocytes (M310) and microglia (CHM5) were cultured in medium RPMI supplemented with 10% foetal bovine serum, 1% L-glutamax, 1% antibacterial/antifungal, and 0.5% glucose. All cells were maintained at 37°C in a humidified atmosphere containing 95% air/5% CO₂. Cells were seeded into 24-well tissue culture plates (3 wells per cell type) to a density of 1×10^5 cells 24 hours prior to experimentation. Wells were pooled prior to cell lysis and probe sonication and all measurements were performed in triplicate.

PCR

Briefly, for each reaction 2 µl of diluted cDNA, 10 µL of SYBR green master mix, 0.15 µL of 10 µM forward and reverse primers and 7.7 µl of nuclease-free water was used making a total volume of 20 µl. Q-PCR was carried out using the Mx3500P Real-Time PCR system (Stratagene, Australia). The primer sequences are shown in Supplementary Table S7. The relative expression levels of sirtuin transcripts were calculated using a mathematical model based on the individual Q-PCR primer efficiencies and the quantified values were normalized against the housekeeping gene 18S. From

these values, fold-differences in the levels of transcripts between individual cell cultures were calculated according to the formula $2^{-\Delta\Delta Ct}$

Immunohistochemical Staining

Formalin fixed blocks from the hippocampal region were embedded in paraffin and cut into 5 μ m sections on superfrost plus slides. For sirtuin staining, sections were deparaffinised in xylene for 20 min and rehydrated through graded alcohol treatment. Antigen retrieval was performed through the use of Target Retrieval solution pH 6 (DAKO, Denmark) and autoclaving at 121°C for 20 min. Endogenous peroxidase was blocked using 3% w/v hydrogen peroxide for 5 min and endogenous biotin was blocked as described previously. After incubation with 10% horse serum for 30 min to block non-specific binding, sections were incubated with anti-human sirtuin (1:250) primary antibodies (raised in rabbit), for 2 hours at ambient temperature. After three rinses, sections were incubated with secondary antibodies–biotinylated goat-anti rabbit or mouse (Vector Laboratories, USA, 1:200) for 30 min at ambient temperature followed by 30 min treatment with avidin-biotin-complex (ABC) elite (Vector). Labelling was visualized with liquid DAB and sections were counterstained and mounted. Negative controls for non-specific staining included replacement of the primary antibody by normal rabbit or mouse IgG.

Western Blotting

The gel was electroblotted (20V, 110mA, 90mins) onto a nitrocellulose membrane in transfer buffer of 50mM tris, 40mM glycine, 1.3mM SDS, 20% methanol, pH 9.2. After transfer of proteins, the membrane was incubated in 10% skim milk powder solution containing primary sirtuin antibody. SIRT1, SIRT2 and SIRT3 rabbit polyclonal antibodies were used (1:1000 dilution, Abcam, UK), followed by a secondary antibody (1:100,000 dilution of anti-mouse IgG, Pierce, USA). See Supplementary Table S8 for full antibody details and dilutions. Chemiluminescence blots were developed using 1:1 solution of Super Signal West Femto luminol and peroxide buffer (Pierce, USA) according to manufacturer's instructions.

References

- Guillemin, G.J. *et al* Characterization of the kynurenine pathway in human neurons. *J Neurosci* **27**, 12884-92 (2007).
- Guillemin, G. J. *et al*. Kynurenine pathway metabolism in human astrocytes: a paradox for neuronal protection. *J Neurochem* **78**, 1-13 (2001).

Supplementary Table S1. Sirtuin recovery using the full protocol (sirtuins run by SDS/PAGE) with spiking into matrices consisting of either buffer only (5µg sirtuin) or low abundance plasma (LAP) proteins with either 5µg or 2µg sirtuin spiked. Sirtuin 5µg spike recoveries were calculated in the LAP spike relative to sirtuin 5µg standard protein in buffer only samples. Sirtuin 2µg spike recoveries were calculated in the LAP spike relative to values extrapolated from the results of the sirtuin 5µg standard protein in buffer only samples. The peak ratios and percentage recovery values is from three transitions used for each of the two sirtuin peptides per sirtuin protein and were obtained from one gel lane per sirtuin protein. The gel on which these samples were run is shown in Figure S8.

	Avg Peak Intensity Ratio (Light/Heavy)	Avg Peak Intensity Ratio (Light/Heavy)	% Recovery	%Recovery
	DINTIEDAVK	TSVAGTVR	DINTIEDAVK	TSVAGTVR
SIRT1 Std 5µg	0.0106	0.0196		
SIRT1 Std 2µg (extrapolated)	0.0042	0.0078		
SIRT1 Std 5µg + 20µg LAP	0.0080	0.0178	76.10	90.79
SIRT1 Std 2µg + 20µg LAP	0.0046	0.0101	108.50	128.83
	LLDELTLEGVAR	IFSEVTPK	LLDELTLEGVAR	IFSEVTPK
SIRT2 Std 5µg	0.0656	0.0514		
SIRT2 Std 2µg (extrapolated)	0.0262	0.0206		
SIRT2 Std 5µg + 20µg LAP	0.0523	0.0496	79.70	96.34
SIRT2 Std 2µg + 20µg LAP	0.0245	0.0219	93.51	106.31
	LYTQNIDGLER	VSGIPASK	LYTQNIDGLER	VSGIPASK
SIRT3 Std 5µg	0.1015	0.0085		
SIRT3 Std 2µg (extrapolated)	0.0406	0.0034		
SIRT3 Std 5µg + 20µg LAP	0.0620	0.0067	61.08	78.80
SIRT3 Std 2µg + 20µg LAP	0.0236	0.0035	58.13	102.9
	VVVITQNIDELHR	NLLEIHGSLFK	VVVITQNIDELHR	NLLEIHGSLFK
SIRT5 Std 5µg	0.0224	0.0271		
SIRT5 Std 2µg (extrapolated)	0.00896	0.01084		
SIRT5 Std 5µg + 20µg LAP	0.01812	0.0198	80.89	73.33
SIRT5 Std 2µg + 20µg LAP	0.0093	0.0104	103.80	95.94

	FLVSQNV DGLHVR	LVIVNLQPTK	FLVSQNV DGLHVR	LVIVNLQPTK
SIRT6 Std 5µg	0.0789	0.0837		
SIRT6 Std 2µg (extrapolated)	0.0316	0.0335		
SIRT6 Std 5µg + 20µg LAP	0.0571	0.0743	72.37	88.76
SIRT6 Std 2µg + 20µg LAP	0.0326	0.0459	103.16	131.14

Supplementary Table S2. Human sirtuin peptide homology with guinea pig and mouse. Sequence variations from the human are highlighted in red.

Sirtuin	Human Peptide	Homology in Guinea Pig and Mice
SIRT1	DINTIEDAVK	Identical sequence found in both Guinea Pig and Mouse
	TSVAGTVR	In Mice: TSVAE T VR In GP: TSVAE T VR
SIRT2	LLDELTLEGVAR	Identical sequence found in Guinea Pig In Mice: LLDELTLEGV T R
	IFSEVTPK	In mice: IFSE A TP R In GP: L FS D VTPK
SIRT3	LYTQNIDGLER	Identical sequence found in both Guinea Pig and Mouse
	VSGIPASK	In mice: A SGIPASK In GP: A SGIPASK
SIRT4	RPIQHGDFVR	In mice: RPIQH I DFVR In GP: RPIQH S DFVR
	FILTAWEK	In mice: FILT A RE Q In GP: F LT A Q D K
SIRT5	VVVITQNIDELHR	Identical sequence found in Mouse In GP: V A VITQNIDELH L R
	NLLEIHGSLFK	In mice: NLLEIHGT L FK In GP: NL V EIHGT I FK
SIRT6	FLVSQNVDGLHVR	Identical sequence found in both Guinea Pig and Mouse
	LVIVNLQPTK	Identical sequence found in both Guinea Pig and Mouse
SIRT7	LLAESADLVTELQGR	In mice: LLAES E DLVTELQGR In GP: LLAES E DLVTELQGR
	DTIVHFGER	Identical sequence found in both Guinea Pig and Mouse

Supplementary Table S3. Sequences of all 7 human sirtuins and their isoforms (obtained from UniProt). The peptides used for MRM quantification experiments are highlighted in red and in larger font size. All sirtuin isoforms contain at least one of the peptides used for quantification, and both peptides are represented in the majority of isoforms.

SIRT1 Isoform 1	<p>>sp Q96EB6 SIR1_HUMAN NAD-dependent protein deacetylase sirtuin-1 OS=Homo sapiens GN=SIRT1 PE=1 SV=2 MADEAALALQPGGSPAAGADREAASSPAGEPLRKRPRRDGPGLERSPGEPGGAAPER EVPAAARGCPGAAAAALWREAEEAAAAGGEQEAQATAAAGEGDNGPGLQGSPREP PLADNLYDEDDDDDEGEEEEAAAAAIGYRDNLLFGDEIITNGFHSCESDEEDRASHASS DWTPRPRIGPYTFVQQHLMIGTDPRTILKDLLPETIPPELDDMTLWQIVINILSEPPKRR KRKDINTIEDAVKLLQECKKIIVLTGAGVSVSCGIPDFRSRDGIYARLAVDFPDLDPDQA MFDIEYFRKDPRPFFKFAKEIYPGQFQPSLCHKFIALSDKEGKLLRNYTQNIDTLEQVAGIQ RIIQCHGSFATASCLICKYKVDCEAVRGDIFNQVVP RCP RCPADEPLAIMKPEIVFFGENL PEQFHRA MKYDKDEV DLLVIGSS LKVRPVALIPSSIPHEVPQILINREPLPHLHFDV LELGD CDVIINELCHRLGGEYAKLCCNPVKLSEITEKPPRTQKELAYLSELPTPLHVSEDSSSPERT SPPDSSVIVTLLDQAAKSNDLDVSESKGCMEEKQEVQTSRNVESIAEQMENPDLKNV GSSTGEKNERTSVAGTVRKCWPNRVAKEQISRRLDGNQYLFLPPNRYIFHGAEVYSDS EDDV LSSSSCGSNSDSGTCQSPSLEEPMEDESEIEEFYNGLEDEPDVPERAGGAGFGTDG DDQEAINEAISVKQEV TDMNYP SNKS</p>
SIRT1 Isoform 2	<p>>sp Q96EB6-2 SIR1_HUMAN Isoform 2 of NAD-dependent protein deacetylase sirtuin-1 OS=Homo sapiens GN=SIRT1 MADEAALALQPGGSPAAGADREAASSPAGEPLRKRPRRDGPGLERSPGEPGGAAPER EVPAAARGCPGAAAAALWREAEEAAAAGGEQEAQATAAAGEGDNGPGLQGSPREP PLADNLYDEDDDDDEGEEEEAAAAAIGYRDNLLFGDEIITNGFHSCESDEEDRASHASS DWTPRPRIGPYTFVQQHLMIGTDPRTILKDLLPETIPPELDDMTLWQIVINILSEPPKRR KRKDINTIEDAVKLLQECKKIIVLTGAGVSVSCGIPDFRSRDGIYARLAVDFPDLDPDQA MFDIEYFRKDPRPFFKFAKEIYPGQFQPSLCHKFIALSDKEGKLLRNYTQNIDTLEQVAGIQ RIIQCHGSFATASCLICKYKVDCEAVRGDIFNQVVP RCP RCPADEPLAIMKPEIVFFGENL PEQFHRA MKYDKDEV DLLVIGSS LKVRPVALIPSNQYLFLPPNRYIFHGAEVYSDSEDDV LSSSSCGSNSDSGTCQSPSLEEPMEDESEIEEFYNGLEDEPDVPERAGGAGFGTDGDDQ EAINEAISVKQEV TDMNYP SNKS</p>
SIRT2 Isoform 1	<p>>sp Q8IXJ6 SIR2_HUMAN NAD-dependent protein deacetylase sirtuin-2 OS=Homo sapiens GN=SIRT2 PE=1 SV=2 MAEPDPSHPLETQAGKVQEAQDSDSDSEGGAAGGEADMDFLRNLF SQ TSLG SQKER LDEL TLEGVARYMQSERCRRVICLVGAGISTSAGIPDFRSPSTGLYDNLEKYHLPYPE AIFEISYFKKHPEPFFALAKELYPGQFKPTICHYFMRL LKDKG LLLRCYTQNIDTLER IAGLE QEDLVEAHGTFYTS HCVSASCRHEYPLSWMKEKIFSEVTPKCEDCQSLVKPDIVFFGES LPARFFSCMQSDFLKVDLLVMGTS LQVQPFASLISKAPLSTPRLLINKEKAGQSDPFLG MIMGLGGGMDFD SKKAYRDVAWLGECDQGCLALAE LLGWKKELEDLVRREHASIDAQ SGAGVPNPSTSASPKKSPPPAKDEARTTEREKPQ</p>

SIRT2 Isoform 2	>sp Q8IXJ6-2 SIR2_HUMAN Isoform 2 of NAD-dependent protein deacetylase sirtuin-2 OS=Homo sapiens GN=SIRT2 MDFLRNLFSQTLGLSQQKER LLDELTEGVAR YMQSERCRRVICLVGAGISTSAGIPDF RSPSTGLYDNLEKYHLPYPEAIFEISYFKKHPEPFFALAKELYPGQFKPTICHYFMRLKDKG LLRCYTQNIDTLERAGLEQEDLVEAHGTFYTSCHVSASCRHEYPLSWMKEK IFSEVTPK K CEDCQSLVKPDIVFFGESLPARFFSCMQSDFLKVDLLVMGTSLQVQPFASLISKAPLST PRLLINKEKAGQSDPFLGMIMGLGGGMDFDSSKAYRDVAWLGECDQGCLALAEELLGW KKELEDLVRREHASIDAQSGAGVNPSTASPKKSPPPAKDEARTTEREKPQ
SIRT2 Isoform 3	>sp Q8IXJ6-3 SIR2_HUMAN Isoform 3 of NAD-dependent protein deacetylase sirtuin-2 OS=Homo sapiens GN=SIRT2 MPLAECPSRCCLSSFRSVDLRLNLFSTGLSQQKER LLDELTEGVAR YMQSERCRR VICLVGAGISTSAGIPDFRSPSTGLYDNLEKYHLPYPEAIFEISYFKKHPEPFFALAKELYPGQ FKPTICHYFMRLKDKGLLRCYTQNIDTLERAGLEQEDLVEAHGTFYTSCHVSASCRHE YPLSWMKEK IFSEVTPK CEDCQSLVKPDIVFFGESLPARFFSCMQSDFLKVDLLVMGT SLQVQPFASLISKAPLSTPRLLINKEKAGQSDPFLGMIMGLGGGMDFDSSKAYRDVAWL GECDQGCLALAEELLGWKKELEDLVRREHASIDAQSGAGVNPSTASPKKSPPPAKDEA RTTEREKPQ
SIRT2 Isoform 4	>sp Q8IXJ6-4 SIR2_HUMAN Isoform 4 of NAD-dependent protein deacetylase sirtuin-2 OS=Homo sapiens GN=SIRT2 MAEPDPSHPLETQAGKVQEAQDSDSDSEGGAGGEADMDFLRLNLFSTGLSQQKER LLDELTEGVAR YMQSERCRRVICLVGAGISTSAGIPDFRSPSTGLYDNLEKYHLPYPE AIFEISYFKKHPEPFFALAKELYPGQFKPTICHYFMRLKDKGLLRCYTQNIDTLERAGLE QEDLVEAHGTFYTSCHVSASCRHEYPLSWMKEK IFSEVTPK CEDCQSLVKPDIVFFGES LPARFFSCMQSDFLKVDLLVMGTSLQGRGLAG
SIRT2 Isoform 5	>sp Q8IXJ6-5 SIR2_HUMAN Isoform 5 of NAD-dependent protein deacetylase sirtuin-2 OS=Homo sapiens GN=SIRT2 MAEPDRRRVICLVGAGISTSAGIPDFRSPSTGLYDNLEKYHLPYPEAIFEISYFKKHPEPFFA LAKELYPGQFKPTICHYFMRLKDKGLLRCYTQNIDTLERAGLEQEDLVEAHGTFYTSCH VSASCRHEYPLSWMKEK IFSEVTPK CEDCQSLVKPDIVFFGESLPARFFSCMQSDFLKV DLLVMGTSLQVQPFASLISKAPLSTPRLLINKEKAGQSDPFLGMIMGLGGGMDFDSSK AYRDVAWLGECDQGCLALAEELLGWKKELEDLVRREHASIDAQSGAGVNPSTASPKK SPPPAKDEARTTEREKPQ
SIRT3 Isoform 1	>sp Q9NTG7 SIR3_HUMAN NAD-dependent protein deacetylase sirtuin-3, mitochondrial OS=Homo sapiens GN=SIRT3 PE=1 SV=2 MAFWGWRAAAALRLWGRVVERVEAGGGVGPFQACGCRLVLGGRDDVSAGLRGSHG ARGEP LDPARPLQRPPEVPRAFRRQPRAAAPSFFFSSIKGGRRSISFSVGASSVVGSGSSDKG KLSLQDVAELIRARACQRVVVMVGAGISTPSGIPDFRSPGSGLYSNLQQYDLPYPEAIFEL PFFFHNPKPFFTLAKELYPGNYKPNVTHYFLRLLHDKGLLLR LYTQNIDGLERVSGIPA SK LVEAHGTFASATCTVCQRPFGEDIRADVMADRVPRCPVCTGVVKPDIVFFGEPLPQ RFLHVVDFPMADLLILGTSLEVEPFASLTEAVRSSVPRLINRDLVGPLAWHPRSRDVA

	QLGDVVHGVESLVELLGWTEEMRDLVQRETGKLDGPKD
SIRT3 Isoform 2	>sp Q9NTG7-2 SIR3_HUMAN Isoform 2 of NAD-dependent protein deacetylase sirtuin-3, mitochondrial OS=Homo sapiens GN=SIRT3 MVGAGISTPSGIPDFRSPGSLYSNLQQYDLPYEAFELPFFFHNPKEFTLAKELYPGNY KPNVTHYFLRLLHDKGLLLR LYTQNI DGLERVSGIPASK LVEAHGTFASATCTVCQR PFPGEDIRADVMADRVPRCPVCTGVVKPDIVFFGEPLPQRFLHVVDFPMADLLLILGTS LEVEPFASLTEAVRSSVPRLINRDLVGPLAWHPRSRDVAQLGDVVHGVESLVELLGWT EEMRDLVQRETGKLDGPKD
SIRT4	>sp Q9Y6E7 SIR4_HUMAN NAD-dependent protein lipoamidase sirtuin-4, mitochondrial OS=Homo sapiens GN=SIRT4 PE=1 SV=1 MKMSFALTFRSAKGRWIANPSQPCSKASIGLFPASPPLDPEKVKELQRFITLSKRLLVM TGAGISTESGIPDYRSEKVGLYARTDR RPIQHGD FVR SAPIRQRYWARNFVGWPQFS SHQPNPAHWALSTWEKLGKLYWLVTQNV DALHTKAGSRRLTELHGCM DRVLC LDCGE QTPRGVLQERFQVLNPTWSAEAHGLAPDGDVFLSEEQVRSFQVPTCVQC GGHLKPDV VFFGDTVNPDKVDFVHKRVKEADSLLVGSSLQVYSGYR FILTAWEK KLPIAILNIGPTR SDDLACLKLN SRCGELLPLIDPC
SIRT5 Isoform 1	>sp Q9NXA8 SIR5_HUMAN NAD-dependent protein deacetylase sirtuin-5, mitochondrial OS=Homo sapiens GN=SIRT5 PE=1 SV=2 MRPLQIVPSRLISQLYCGLKPPASTRNQICLKMARPSSSMADFRKFFAKAKHIVIISGAGV SAESGVPTFRGAGGYWRKWQAQDLATPLAFAHNPSRVWEFYHYRREVMGSKEPNAG HRAIAECETRLGKQGRR VVITQNI DELHR KAGTK NLLEIHGSLFK TRCTSCGVVA ENYKSPICPALSGKGAPEPGTQDASIPVEKLPRCEEAGCGGLLRPHV VWFGENLDPAILE EVDRELAHCDLCLVVGTS SVVYPAAMFAPQVAARGVPVAEFNTETTPATNRF RFHFQG PCGTTLPEALACHENETVS
SIRT5 Isoform 2	>sp Q9NXA8-2 SIR5_HUMAN Isoform 2 of NAD-dependent protein deacetylase sirtuin-5, mitochondrial OS=Homo sapiens GN=SIRT5 MRPLQIVPSRLISQLYCGLKPPASTRNQICLKMARPSSSMADFRKFFAKAKHIVIISGAGV SAESGVPTFRGAGGYWRKWQAQDLATPLAFAHNPSRVWEFYHYRREVMGSKEPNAG HRAIAECETRLGKQGRR VVITQNI DELHR KAGTK NLLEIHGSLFK TRCTSCGVVA ENYKSPICPALSGKGAPEPGTQDASIPVEKLPRCEEAGCGGLLRPHV VWFGENLDPAILE EVDRELAHCDLCLVVGTS SVVYPAAMFAPQVAARGVPVAEFNTETTPATNRF SHLISISS LIIKN
SIRT5 Isoform 3	>sp Q9NXA8-3 SIR5_HUMAN Isoform 3 of NAD-dependent protein deacetylase sirtuin-5, mitochondrial OS=Homo sapiens GN=SIRT5 MRPLQIVPSRLISQLYCGLKPPASTRNQICLKMARPSSSMADFRKFFAKAKHIVIISGAGV SAESGVPTFRGAGGYWRKWQAQDLATPLAFAHNPSRVWEFYHYRREVMGSKEPNAG HRAIAECETRLGKQGRR VVITQNI DELHR KAGTK NLLEIHGSLFK TRCTSCGVVA ENYKSPICPALSGKGCEEAGCGGLLRPHV VWFGENLDPAILEEVDRELAHCDLCLVVGTS SVVYPAAMFAPQVAARGVPVAEFNTETTPATNRF RFHFQGPCGTTLPEALACHENETV S
SIRT5 Isoform 4	>sp Q9NXA8-4 SIR5_HUMAN Isoform 4 of NAD-dependent protein deacetylase

	<p>sirtuin-5, mitochondrial OS=Homo sapiens GN=SIRT5</p> <p>MGSKEPNAGHRAIAECETRLGKQGRVVVITQNIDELHRKAGTKNLLEIHGSLFKT</p> <p>RCTSCGVVAENYKSPICPALSGKGAPEPGTQDASIPVEKLPRCEEAGCGLLRPHVWVF</p> <p>GENLDPAILLEEVDRELAHCDLCLVVGTSVVYPAAMFAPQVAARGVPVAEFNTETTPAT</p> <p>NRFRHFQGPCGTTLPEALACHENETVS</p>
SIRT6 Isoform 1	<p>>sp Q8N6T7 SIR6_HUMAN NAD-dependent protein deacetylase sirtuin-6</p> <p>OS=Homo sapiens GN=SIRT6 PE=1 SV=2</p> <p>MSVNYAAGLSPYADKGKCGLPEIFDPPEELERKVVWELARLVWQSSSVVFHTGAGISTAS</p> <p>GIPDFRGPHGVWTMEERGLAPKFDTTFESARPTQTHMALVQLERVGLLRFLVSQNV</p> <p>DGLHVRSGFPRDKLAELHGNMFVEECAKCKTQYVRDVTVGTMGLKATGRLCTVAKA</p> <p>RGLRACRGELRDTILDWEDSLPDRDLALADEASRNADLSITLGTSLQIRPSGNLPLATKRR</p> <p>GGRLVIVNLQPTKHDRHADLRIHGYVDEVMTRLMKHLGLEIPAWDGPRVLERALPPL</p> <p>PRPPTPKLEPKESPTRINGSIPAGPKQEPCAQHNGSEPASPKRERPTSPAPHRPPKRVKA</p> <p>KAVPS</p>
SIRT6 Isoform 2	<p>>sp Q8N6T7-2 SIR6_HUMAN Isoform 2 of NAD-dependent protein</p> <p>deacetylase sirtuin-6 OS=Homo sapiens GN=SIRT6</p> <p>MSVNYAAGLSPYADKGKCGLPEIFDPPEELERKVVWELARLVWQSSSVVFHTGAGISTAS</p> <p>GIPDFRGPHGVWTMEERGLAPKFDTTFESARPTQTHMALVQLERVGLLRFLVSQNV</p> <p>DGLHVRSGFPRDKLAELHGNMFVEECAKCKTQYVRDVTVGTMGLKATGRLCTVAKA</p> <p>RGLRACRNADLSITLGTSLQIRPSGNLPLATKRRGGRLVIVNLQPTKHDRHADLRIHGY</p> <p>VDEVMTRLMKHLGLEIPAWDGPRVLERALPPLPRPPTPKLEPKESPTRINGSIPAGPKQ</p> <p>EPCAQHNGSEPASPKRERPTSPAPHRPPKRVKAKAVPS</p>
SIRT7 Isoform 1	<p>>sp Q9NRC8 SIR7_HUMAN NAD-dependent protein deacetylase sirtuin-7</p> <p>OS=Homo sapiens GN=SIRT7 PE=1 SV=1</p> <p>MAAGGLSRSEKAAERVRLREEQQRERLRQVSRIIRKAAAERSAEEGRLLAESADLV</p> <p>TELQGRSRRREGLKRRQEEVCDDPEELRGKVRELASAVRNAKYLVVYTGAGISTAASIP</p> <p>DYRGPNGVWTLQKGRSVSAADLSEAEP TLTHMSITRLHEQKL VQHVVSNCDGLHLR</p> <p>SGLPRTAISELHGNMYIEVCTSCVPNREYVRVFDVTERTALHRHQTGRTCHKCGTQLRD</p> <p>TIVHFGERGTLGQPLNWEAATEAASRADTILCGSSLVKKYPRLWCMTKPPSRRPKL</p> <p>YIVNLQWTPKDDWAALKLHGKDDVMRLMAELGLEIPAYSRWQDPIFSLATPLRAGE</p> <p>EGSHSRKSLCRSREEAPPGDRGAPLSSAPILGGWFGRGCTKRTKRKKVT</p>
SIRT7 Isoform 2	<p>>sp Q9NRC8-2 SIR7_HUMAN Isoform 2 of NAD-dependent protein</p> <p>deacetylase sirtuin-7 OS=Homo sapiens GN=SIRT7</p> <p>MAAGGLSRSEKAAERVRLREEQQRERLRQVSRIIRKAAAERSAEEGRLLAESADLV</p> <p>TELQGRSRRREGLKRRQEEVCDDPEELRGKVRELASAVRNAKYLVVYTGAGISTAASIP</p> <p>DYRGPNGVWTLQKGRSVSAADLSEAEP TLTHMSITRLHEQKL VRLGGWYTCQGPGR</p> <p>APWCPVGN</p>
SIRT7 Isoform 3	<p>>sp Q9NRC8-3 SIR7_HUMAN Isoform 3 of NAD-dependent protein</p> <p>deacetylase sirtuin-7 OS=Homo sapiens GN=SIRT7</p> <p>MPGPRRRSPSACPQVSRIIRKAAAERSAEEGRLLAESADLVTELQGRSRRREGLKRR</p>

QEEVCDDPEELRGKVRELASAVRNAKYLVVYTGAGISTAASIPDYRGPNGVWTLQKGR
SVSAADLSEAEP TLTHMSITRLHEQKLQHVVSQNC DGLHRSGLPRTAISELHGNMYIE
VCTSCVPNREYVRVFDVTERTALHRHQTGRTCHKCGTQLRDTIVHFGERTLGQPLNW
EAATEAASRADTILCLGSSLKVLKKYPRLWCMTKPPSRRPKLYIVNLQWTPKDDWAALKL
HGKCDDVMRLLMAELGLEIPAYSRVL

Supplementary Table S4. List of 14 unique sirtuin peptides selected for sirtuin protein quantification. Arg and Lys amino acids highlighted in bold used in ‘heavy’ peptides, labelled with a stable isotope (^{13}C and ^{15}N). Precursor charge state for all peptides was 2⁺.

Sirtuin	Peptide	Light Precursor Ion <i>m/z</i>	Heavy Precursor Ion <i>m/z</i>
SIRT1	DINTIEDAVK	559.2904	563.2975
	TSVAGTVR	395.7245	400.7286
SIRT2	LLDEELTLEGVAR	664.8746	669.8788
	IFSEVTPK	460.758	464.7651
SIRT3	LYTQNIDGLER	661.341	666.3451
	VSGIPASK	379.724	383.7311
SIRT4	RPIQHGDFVR	612.8334	617.8376
	FILTAWEK	504.2817	508.2888
SIRT5	VVVITQNIDELHR	512.6229	515.9589
	NLLEIHGSLFK	635.8613	639.8613
SIRT6	FLVSQNVDGLHVR	742.4044	747.4086
	LVIVNLQPTK	562.8555	566.8626
SIRT7	LLAESADLVTELQGR	807.9385	812.9426
	DTIVHFGER	537.2724	542.2765

Supplementary Table S5. List of product and transition ions with collision energies used for all 14 selected sirtuin peptides. Each sirtuin protein (SIRT1-7, with 2 peptides per protein) was run with 12 transition ions per run, per protein and with a 50ms dwell time. Precursor charge state for all peptides was 2⁺.

Precursor Ion <i>m/z</i>	Transition Ion	Peptide	Declustering Potential	Collision Energy
559.2904	889.4625	SIRT1.DINTIEDAVK.y8.light	71.9	27.6
559.2904	775.4196	SIRT1.DINTIEDAVK.y7.light	71.9	27.6
559.2904	674.3719	SIRT1.DINTIEDAVK.y6.light	71.9	27.6
563.2975	897.4767	SIRT1.DINTIEDAVK.y8.heavy	71.9	27.6
563.2975	783.4338	SIRT1.DINTIEDAVK.y7.heavy	71.9	27.6
563.2975	682.3861	SIRT1.DINTIEDAVK.y6.heavy	71.9	27.6
395.7245	602.362	SIRT1.TSVAGTVR.y6.light	60	18.3
395.7245	503.2936	SIRT1.TSVAGTVR.y5.light	60	18.3
395.7245	432.2565	SIRT1.TSVAGTVR.y4.light	60	18.3
400.7286	612.3703	SIRT1.TSVAGTVR.y6.heavy	60	18.3
400.7286	513.3019	SIRT1.TSVAGTVR.y5.heavy	60	18.3
400.7286	442.2648	SIRT1.TSVAGTVR.y4.heavy	60	18.3
664.8746	858.5043	SIRT2.LLDELTLEGVAR.y8.light	79.6	33.6
664.8746	745.4203	SIRT2.LLDELTLEGVAR.y7.light	79.6	33.6
664.8746	644.3726	SIRT2.LLDELTLEGVAR.y6.light	79.6	33.6
669.8788	868.5126	SIRT2.LLDELTLEGVAR.y8.heavy	79.6	33.6
669.8788	755.4285	SIRT2.LLDELTLEGVAR.y7.heavy	79.6	33.6
669.8788	654.3809	SIRT2.LLDELTLEGVAR.y6.heavy	79.6	33.6
460.758	807.4247	SIRT2.IFSEVTPK.y7.light	64.7	22
460.758	660.3563	SIRT2.IFSEVTPK.y6.light	64.7	22
460.758	573.3243	SIRT2.IFSEVTPK.y5.light	64.7	22
464.7651	815.4389	SIRT2.IFSEVTPK.y7.heavy	64.7	22
464.7651	668.3705	SIRT2.IFSEVTPK.y6.heavy	64.7	22
464.7651	581.3385	SIRT2.IFSEVTPK.y5.heavy	64.7	22
661.341	944.4796	SIRT3.LYTQNIDGLER.y8.light	79.3	33.4
661.341	816.421	SIRT3.LYTQNIDGLER.y7.light	79.3	33.4
661.341	702.3781	SIRT3.LYTQNIDGLER.y6.light	79.3	33.4
666.3451	954.4879	SIRT3.LYTQNIDGLER.y8.heavy	79.3	33.4
666.3451	826.4293	SIRT3.LYTQNIDGLER.y7.heavy	79.3	33.4
666.3451	712.3863	SIRT3.LYTQNIDGLER.y6.heavy	79.3	33.4
379.724	659.3723	SIRT3.VSGIPASK.y7.light	58.8	17.4
379.724	572.3402	SIRT3.VSGIPASK.y6.light	58.8	17.4
379.724	515.3188	SIRT3.VSGIPASK.y5.light	58.8	17.4
383.7311	667.3865	SIRT3.VSGIPASK.y7.heavy	58.8	17.4

383.7311	580.3544	SIRT3.VSGIPASK.y6.heavy	58.8	17.4
383.7311	523.333	SIRT3.VSGIPASK.y5.heavy	58.8	17.4
612.8334	1068.559	SIRT4.RPIQHGDFVR.y9.light	75.8	30.7
612.8334	971.5057	SIRT4.RPIQHGDFVR.y8.light	75.8	30.7
612.8334	858.4217	SIRT4.RPIQHGDFVR.y7.light	75.8	30.7
617.8376	1078.567	SIRT4.RPIQHGDFVR.y9.heavy	75.8	30.7
617.8376	981.514	SIRT4.RPIQHGDFVR.y8.heavy	75.8	30.7
617.8376	868.4299	SIRT4.RPIQHGDFVR.y7.heavy	75.8	30.7
504.2817	747.4036	SIRT4.FILTAWEK.y6.light	67.9	24.5
504.2817	634.3195	SIRT4.FILTAWEK.y5.light	67.9	24.5
504.2817	533.2718	SIRT4.FILTAWEK.y4.light	67.9	24.5
508.2888	755.4178	SIRT4.FILTAWEK.y6.heavy	67.9	24.5
508.2888	642.3337	SIRT4.FILTAWEK.y5.heavy	67.9	24.5
508.2888	541.286	SIRT4.FILTAWEK.y4.heavy	67.9	24.5
512.6229	896.4585	SIRT5.VVVITQNIDELHR.y7.light	68.5	23
512.6229	782.4155	SIRT5.VVVITQNIDELHR.y6.light	68.5	23
512.6229	669.3315	SIRT5.VVVITQNIDELHR.y5.light	68.5	23
515.9589	906.4667	SIRT5.VVVITQNIDELHR.y7.heavy	68.5	23
515.9589	792.4238	SIRT5.VVVITQNIDELHR.y6.heavy	68.5	23
515.9589	679.3397	SIRT5.VVVITQNIDELHR.y5.heavy	68.5	23
635.8613	930.5043	SIRT5.NLLEIHGSLFK.y8.light	77.5	32
635.8613	801.4618	SIRT5.NLLEIHGSLFK.y7.light	77.5	32
635.8613	688.3777	SIRT5.NLLEIHGSLFK.y6.light	77.5	32
639.8684	938.5185	SIRT5.NLLEIHGSLFK.y8.heavy	77.5	32
639.8684	809.4759	SIRT5.NLLEIHGSLFK.y7.heavy	77.5	32
639.8684	696.3919	SIRT5.NLLEIHGSLFK.y6.heavy	77.5	32
742.4044	1124.581	SIRT6.FLVSQNV DGLHVR.y10.light	85.2	38.1
742.4044	909.4901	SIRT6.FLVSQNV DGLHVR.y8.light	85.2	38.1
742.4044	696.3787	SIRT6.FLVSQNV DGLHVR.y6.light	85.2	38.1
747.4086	1134.589	SIRT6.FLVSQNV DGLHVR.y10.heavy	85.2	38.1
747.4086	919.4984	SIRT6.FLVSQNV DGLHVR.y8.heavy	85.2	38.1
747.4086	706.387	SIRT6.FLVSQNV DGLHVR.y6.heavy	85.2	38.1
562.8555	912.5513	SIRT6.LVIVNLQPTK.y8.light	72.1	27.8
562.8555	799.4672	SIRT6.LVIVNLQPTK.y7.light	72.1	27.8
562.8555	700.3988	SIRT6.LVIVNLQPTK.y6.light	72.1	27.8
566.8626	920.5655	SIRT6.LVIVNLQPTK.y8.heavy	72.1	27.8
566.8626	807.4814	SIRT6.LVIVNLQPTK.y7.heavy	72.1	27.8
566.8626	708.413	SIRT6.LVIVNLQPTK.y6.heavy	72.1	27.8
807.9385	915.5258	SIRT7.LLAESADLVTELQGR.y8.light	90	41.8
807.9385	802.4417	SIRT7.LLAESADLVTELQGR.y7.light	90	41.8
807.9385	703.3733	SIRT7.LLAESADLVTELQGR.y6.light	90	41.8

812.9426	925.5341	SIRT7.LLAESADLVTELQGR.y8.heavy	90	41.8
812.9426	812.45	SIRT7.LLAESADLVTELQGR.y7.heavy	90	41.8
812.9426	713.3816	SIRT7.LLAESADLVTELQGR.y6.heavy	90	41.8
537.2724	958.5105	SIRT7.DTIVHFGGER.y8.light	70.3	26.4
537.2724	857.4628	SIRT7.DTIVHFGGER.y7.light	70.3	26.4
537.2724	744.3787	SIRT7.DTIVHFGGER.y6.light	70.3	26.4
542.2765	968.5188	SIRT7.DTIVHFGGER.y8.heavy	70.3	26.4
542.2765	867.4711	SIRT7.DTIVHFGGER.y7.heavy	70.3	26.4
542.2765	754.387	SIRT7.DTIVHFGGER.y6.heavy	70.3	26.4

Supplementary Table S6. Human frontal lobe brain tissue sample and subject details.

Patient	Sex	Age at death	Post mortem tissue collection time
1	Male	72	24h
2	Female	71	24h
3	Male	72	24h
4	Male	71	29h
5	Male	54	24h

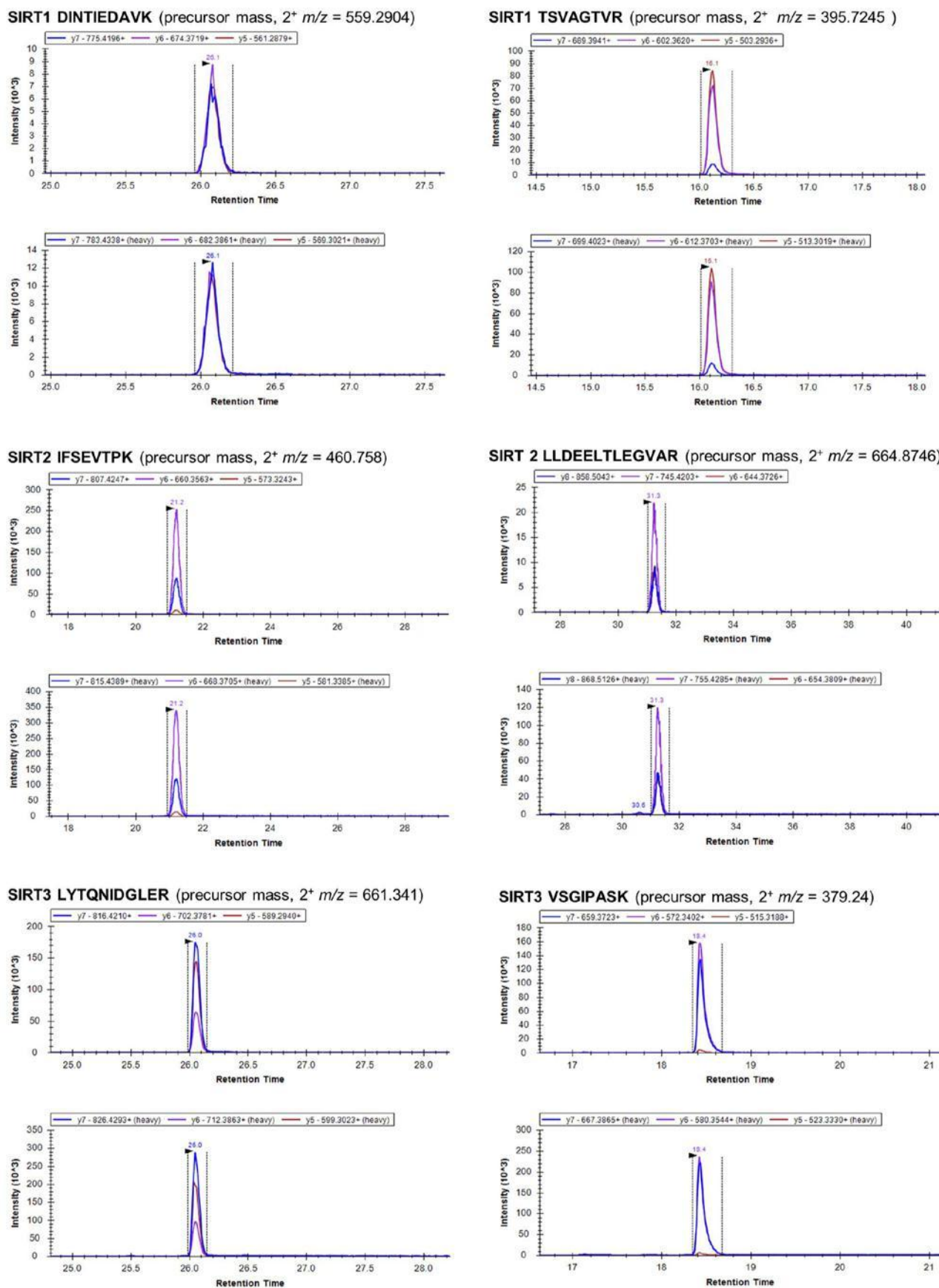
Supplementary Table S7. Real-time primer sequences used for PCR analysis.

Primer name	Oligo name	Sequence (5'→3')
SIRT1-Forw	NM_012238-Forw	CAC-CAG-AAA-GAA-CTT-CAC-CAC-CAG
SIRT1-Rev	NM_012238-Rev	ACC-ATC-AAG-CCG-CCT-ACT-AAT-CTG
SIRT2-Forw	AJ505014-Forw	AGG-GAC-AAG-GAG-CAG-GGT-TC
SIRT2-Rev	AJ505014-Rev	GAA-GAG-AGA-CAG-CGG-CAG-GAC
SIRT3-Forw	NM_12239-Forw	GAG-GTT-CTT-GCT-GCA-TGT-GGT-TG
SIRT3-Rev	NM_12239-Rev	AGT-TTC-CCG-CTG-CAC-AAG-GTC
SIRT4-Forw	NM_012240-Forw	TTG-TGC-CAG-CAA-GTC-CTC-CTC
SIRT4-Rev	NM_012240-Rev	GTC-TCT-TGG-AAA-GGG-TGA-TGA-AGC
SIRT5-Forw	NM_12241-Forw	TCC-AGC-GTC-CAC-ACG-AAA-CC
SIRT5-Rev	NM_12241-Rev	AAC-ACC-AGC-TCC-TGA-GAT-GAT-GAC
SIRT6-Forw	NM_016539-Forw	GCT-GGA-GCC-CAA-GGA-GGA-ATC
SIRT6-Rev	NM_016539-Rev	AGT-AAC-AAA-GTG-AGA-CCA-CGA-GAG
SIRT7-Forw	NM_016538-Forw	GAG-CCA-ACC-CTC-ACC-CAC-ATG
SIRT7-Rev	NM_016538-Rev	ACG-CAG-GAG-GTA-CAG-ACT-TCA-ATG
GAPDH-Forw	NM_017008-Forw	TGG-AGT-CTA-CTG-GCG-TCT-T
GAPDH –Rev	NM_017008-Rev	TGT-CAT-ATT-TCT-CGT-GGT-TCA

Supplementary Table S8. Antibodies and dilutions used for western blotting.

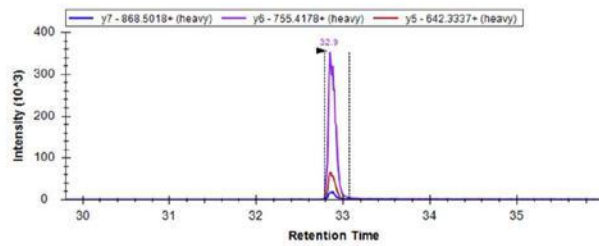
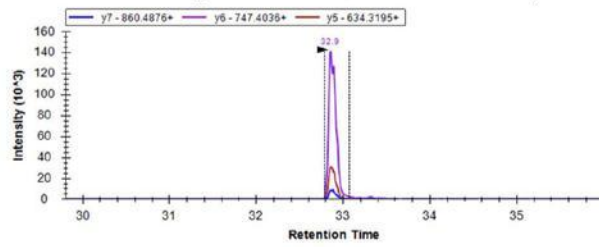
Antibody	Dilution	Manufacturer
Rabbit Polyclonal SIRT1	1:1000	Abcam (Cambridge, UK)
Rabbit Polyclonal SIRT2	1:1000	Abcam (Cambridge, UK)
Rabbit Polyclonal SIRT3	1:1000	Abcam (Cambridge, UK)

Supplementary Figure S1. Representative chromatograms for all 14 sirtuin peptides used in the MRM method, showing transition ions, retention times and signal intensities. The vertical dotted lines either side of the peak clusters indicate the boundaries for peak area integration.

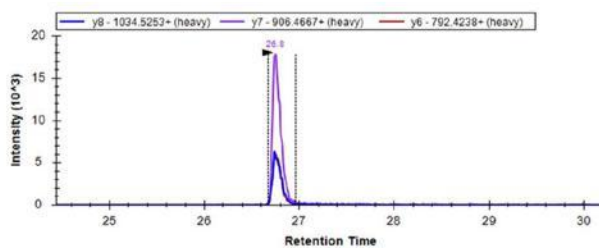
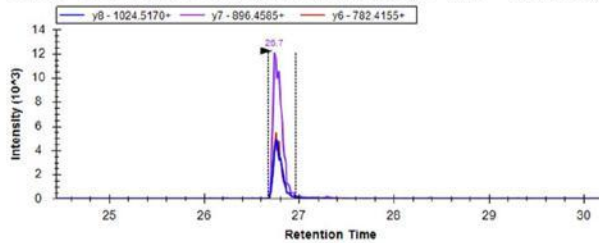


Supplementary Figure S1 continued.

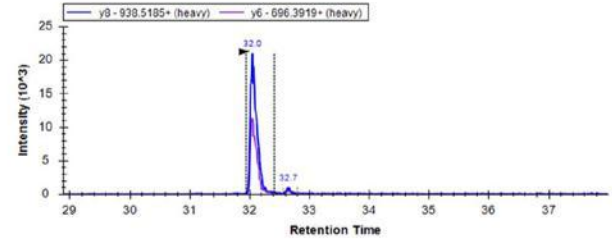
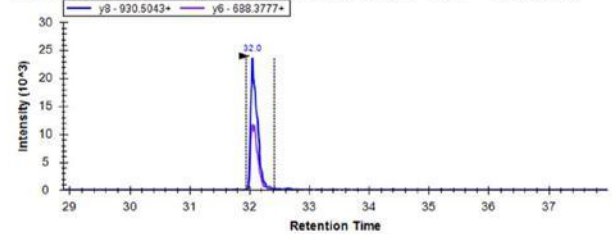
SIRT4 FILTAWEK (precursor mass, 2^+ m/z = 612.8334)



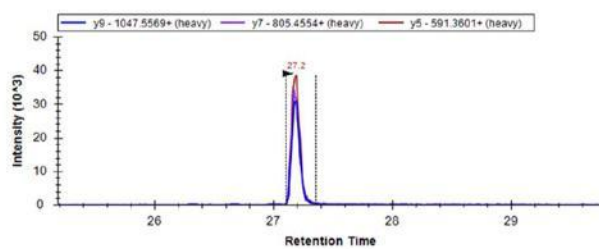
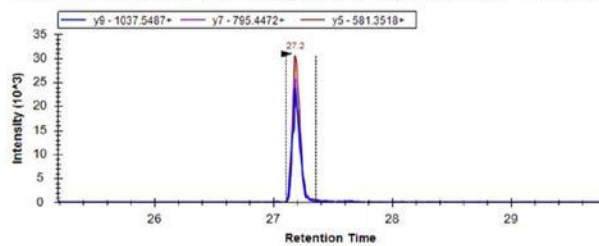
SIRT5 VVITQNIDELHR (precursor mass, 2^+ m/z = 512.6229)



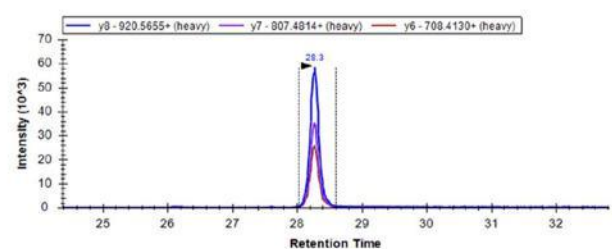
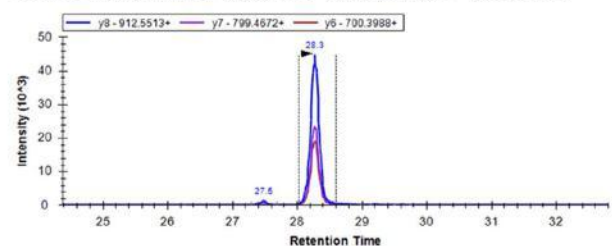
SIRT5 NLEIHGSLFK (precursor mass, 2^+ m/z = 635.8613)



SIRT6 FLVSQNVDDLHVR (precursor mass, 2^+ m/z = 742.4044)

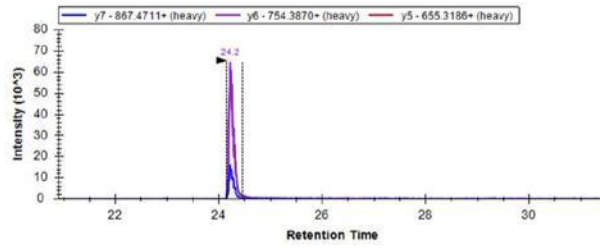
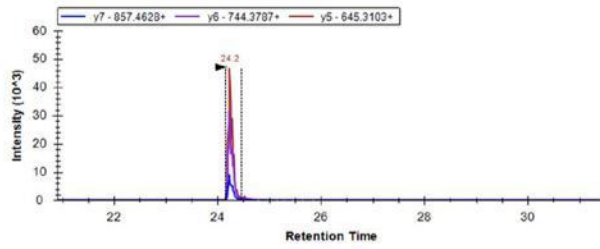


SIRT6 LVIVNLQPTK (precursor mass, 2^+ m/z = 562.8555)

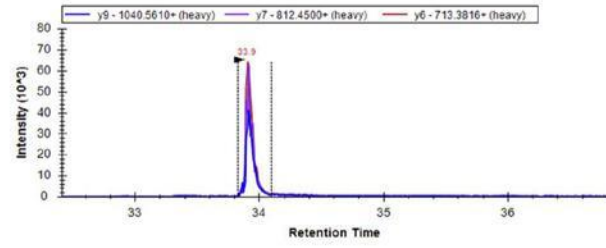
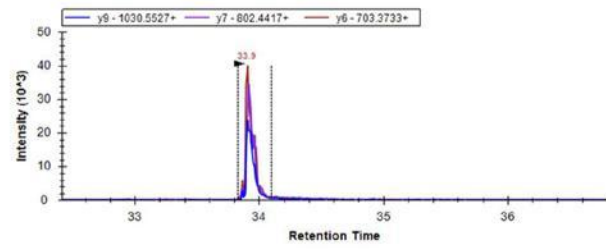


Supplementary Figure S1 continued.

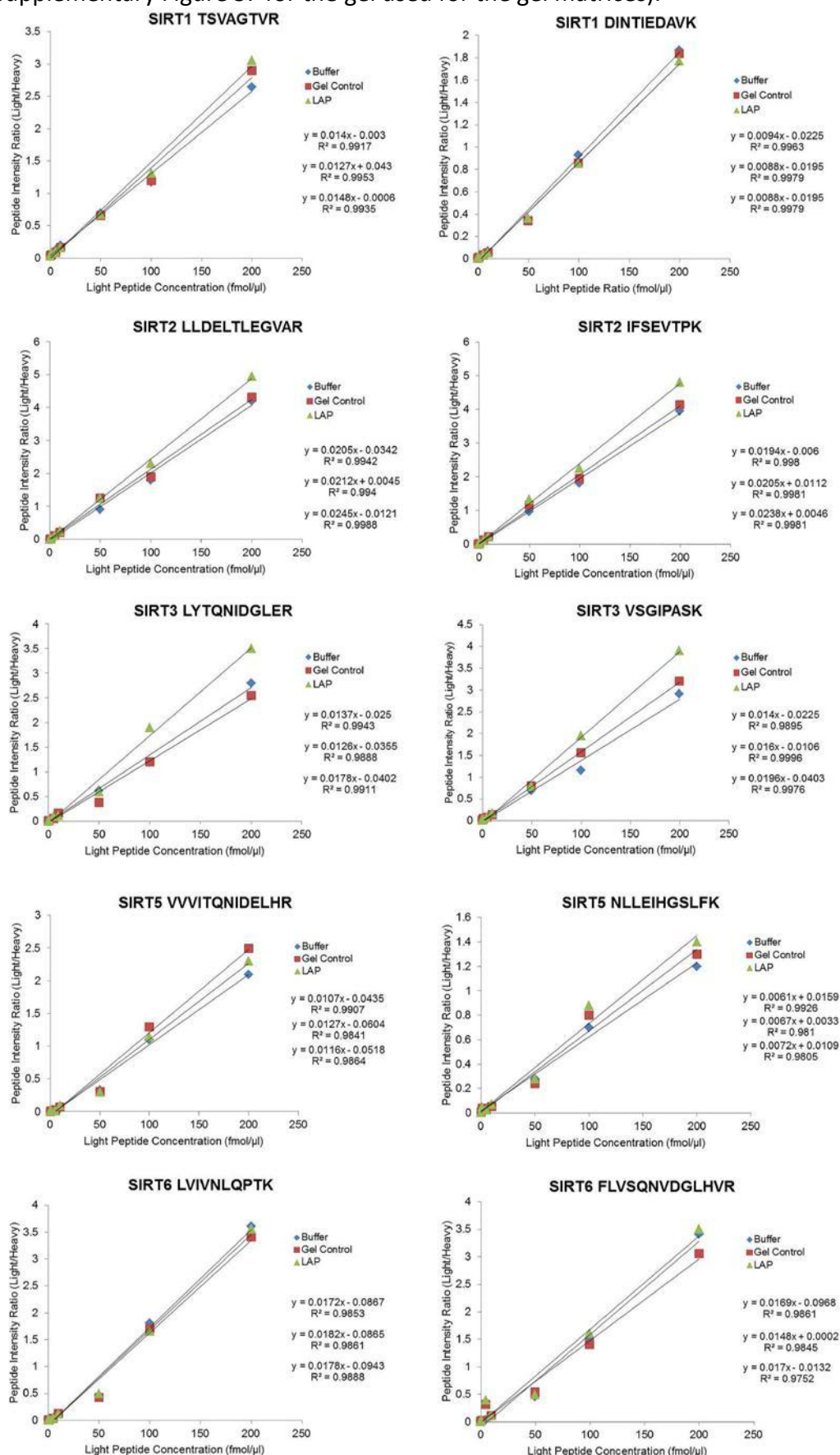
SIRT7 DTIVHFGER (precursor mass, $2^+ m/z = 537.2724$)



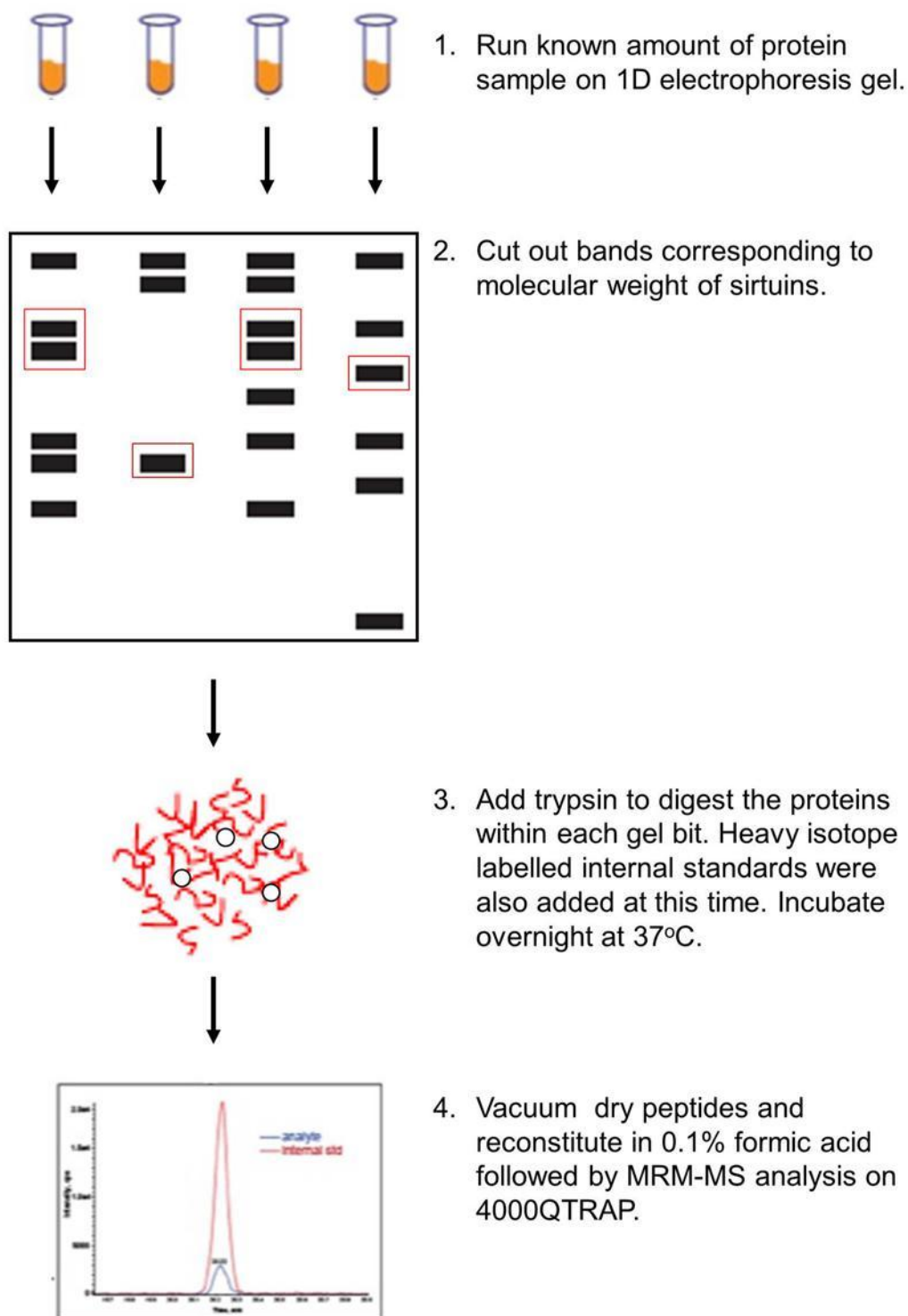
SIRT7 LLAESADLVTELQGR (precursor mass, $2^+ m/z = 807.9385$)



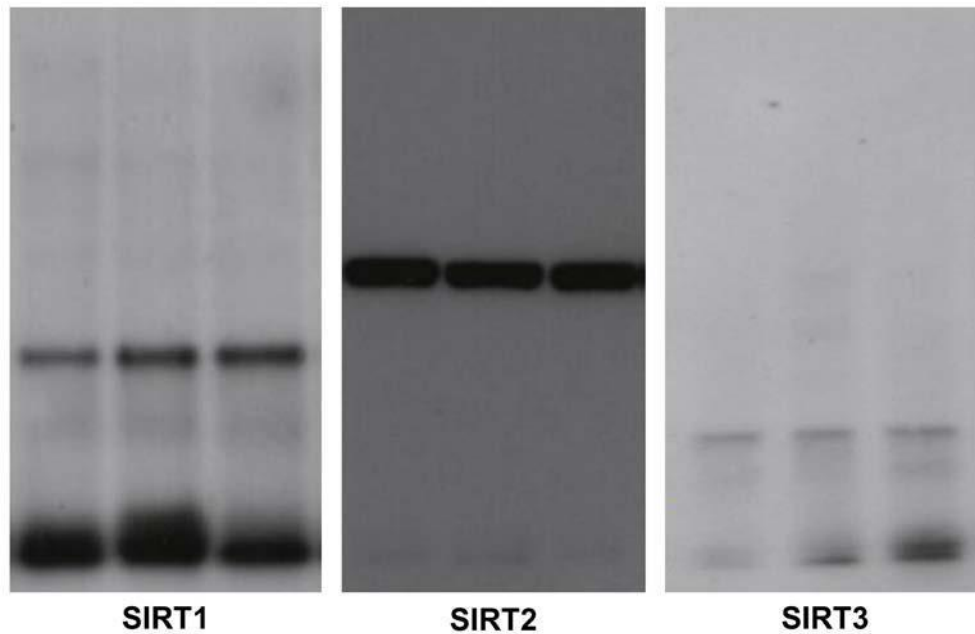
Supplementary Figure S2. Sirtuin peptide standard curves prepared in several matrices, including buffer only, a blank gel control, a gel containing low abundance plasma proteins (see Supplementary Figure S7 for the gel used for the gel matrices).



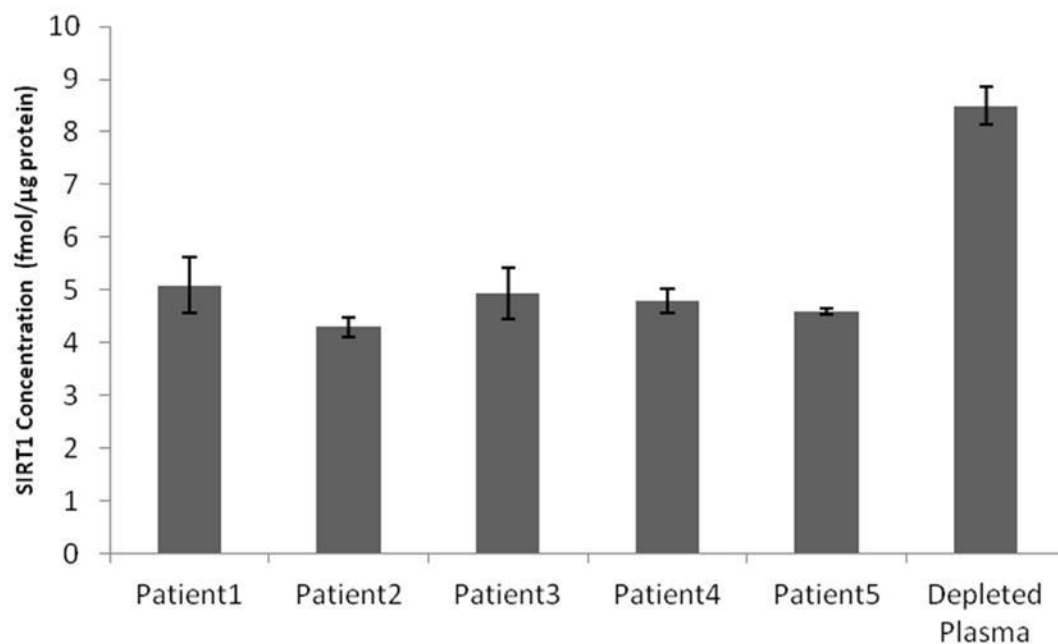
Supplementary Figure S3. Sample fractionation and MRM workflow.



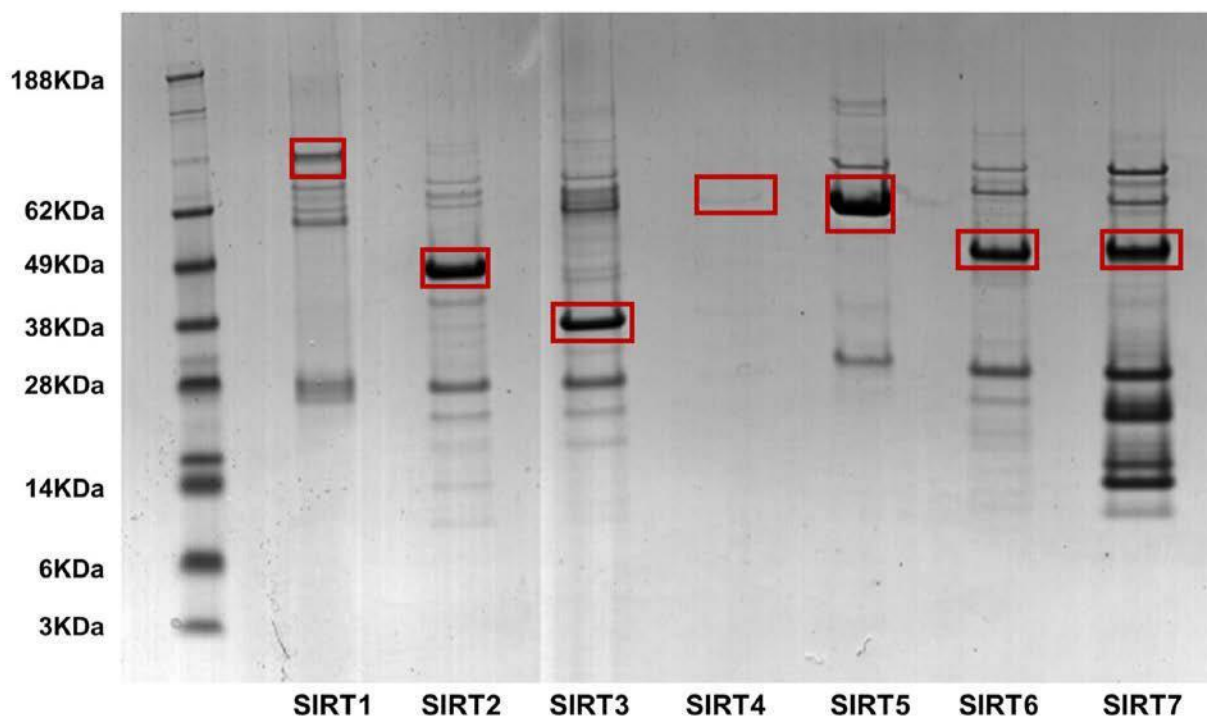
Supplementary Figure S4. Full length western blots of SIRT1-3 protein expression in human control frontal lobe brain tissue (n=3 individuals) at molecular weights of approx 40kDa, 50kDa and 30kDa respectively. All blots were run under the same experimental protocols with 1:1000 dilution of primary antibodies. The exposure times shown are 3hrs, 30sec and overnight for SIRT1, SIRT2 and SIRT3 respectively.



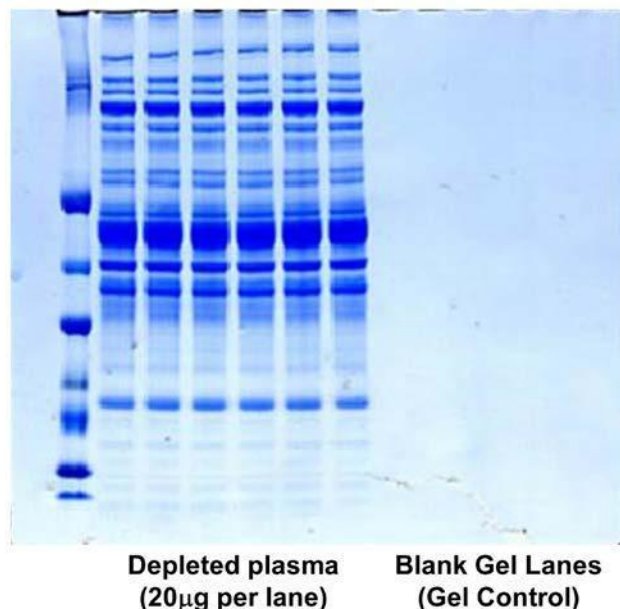
Supplementary Figure S5. SIRT1 levels in CSF and depleted plasma. SIRT1 levels in CSF (n=5) samples and a plasma sample depleted of the six most abundant plasma proteins (high abundance protein removal was achieved using an Agilent Hu6 affinity column).



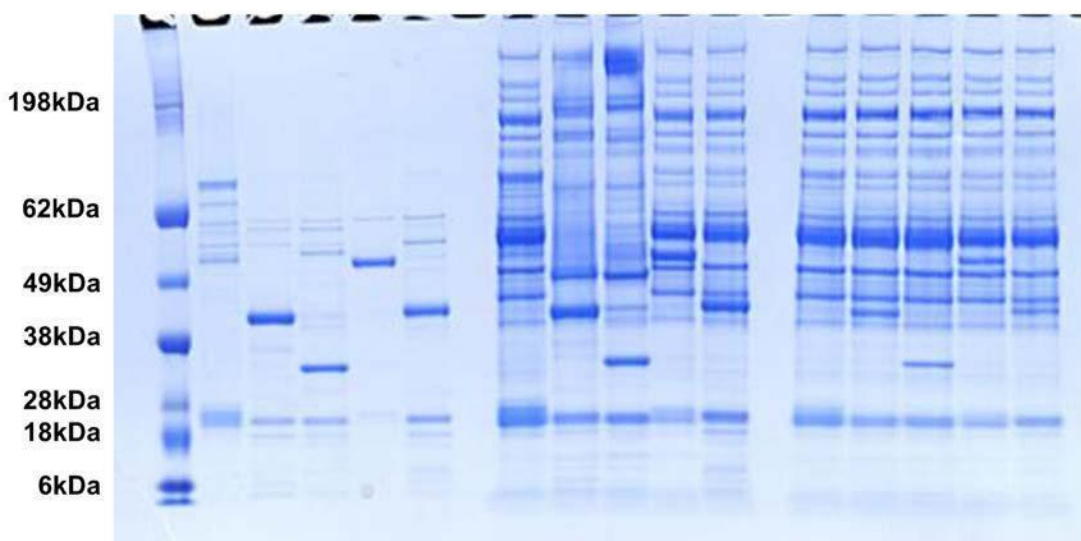
Supplementary Figure S6. Representative colloidal coomassie stained SDS PAGE gel of recombinant sirtuin protein standards highlighted in red boxes with the bands cut corresponding to the molecular weight of each full length sirtuin. Note the presence of host cell contaminants in most of the preparations, especially SIRT7, and the particularly low yield of SIRT4. These preparations were adequate to validate good signal intensity for each of the two peptides per sirtuin used for MRM quantification. SIRT1, 2, 3, 5 and 6 were also used to estimate recoveries using the full protocol (see Supplementary Figure S7 and Supplementary Table S1), in buffer only vs LAP spiked samples.



Supplementary Figure S7. A typical colloidal coomassie stained SDS/PAGE gel used to assess matrix effects on standard curves. Bands were cut from positions at which intact sirtuin proteins would typically be expected, and used to test matrix effects on the synthetic peptide standards. In addition to this, intact commercial recombinant sirtuin preparations were spiked into depleted plasma and run by SDS/PAGE (see Supplementary Figure S8).



Supplementary Figure S8. Colloidal oomassie stained SDS/PAGE gel used for sirtuin recovery experiments. Lane 1: prestained molecular weight markers; Lanes 2-6: commercial SIRT1, 2, 3, 5 and 6 recombinant sirtuin protein standards (5ug per lane. This amount was based on the manufacturer's indicated quantification of vial contents.); Lanes 8-12: 20ug Depleted plasma spiked with 5ug of sirtuin standards 1, 2, 3, 5 and 6; Lanes 14-18: Depleted plasma spiked with 2ug of sirtuin standards 1, 2, 3, 5 and 6. Sirtuins 4 and 7 were not used for this experiment as the SIRT4 yield was very low, and SIRT7 was particularly impure (see Supplementary Figure S6).



RESEARCH ARTICLE

Upregulation of Glycolytic Enzymes, Mitochondrial Dysfunction and Increased Cytotoxicity in Glial Cells Treated with Alzheimer's Disease Plasma

Tharusha Jayasena^{1,2}, Anne Poljak^{1,2,4*}, Nady Braidy², George Smythe^{1,4}, Mark Raftery¹, Mark Hill⁴, Henry Brodaty^{2,5}, Julian Trollor^{2,3}, Nicole Kochan^{2,3}, Perminder Sachdev^{2,3}

1 Bioanalytical Mass Spectrometry Facility, MW Analytical Centre, University of New South Wales, Sydney, Australia, 2 Centre for Healthy Brain Ageing, School of Psychiatry, University of New South Wales, Sydney, Australia, 3 Neuropsychiatric Institute, the Prince of Wales Hospital, Sydney, Australia, 4 School of Medical Sciences, University of New South Wales, Sydney, Australia, 5 Dementia Collaborative Research Centre, University of New South Wales, Sydney, Australia

* a.poljak@unsw.edu.au



OPEN ACCESS

Citation: Jayasena T, Poljak A, Braidy N, Smythe G, Raftery M, Hill M, et al. (2015) Upregulation of Glycolytic Enzymes, Mitochondrial Dysfunction and Increased Cytotoxicity in Glial Cells Treated with Alzheimer's Disease Plasma. PLoS ONE 10(3): e0116092. doi:10.1371/journal.pone.0116092

Academic Editor: Wenhui Hu, Temple University School of Medicine, UNITED STATES

Received: August 20, 2014

Accepted: December 4, 2014

Published: March 18, 2015

Copyright: © 2015 Jayasena et al. This is an open access article distributed under the terms of the [Creative Commons Attribution License](http://creativecommons.org/licenses/by/4.0/), which permits unrestricted use, distribution, and reproduction in any medium, provided the original author and source are credited.

Data Availability Statement: All relevant data are within the paper and its Supporting Information files.

Funding: This work was facilitated by the generous financial support of the Rebecca L Cooper Medical Research

Foundation (<http://www.cooperfoundation.org.au>) and The University of New South Wales, Equity and Diversity Unit.

This study is supported by the NHMRC Program Grants (ID 350833 and ID 568969) awarded to Professors Sachdev and Brodaty and Dr Trollor. None of the authors have any conflicts of interests with regard to this work. Mass spectrometry analyses were carried out at the

Abstract

Alzheimer's disease (AD) is a neurodegenerative disorder associated with increased oxidative stress and neuroinflammation. Markers of increased protein, lipid and nucleic acid oxidation and reduced activities of antioxidant enzymes have been reported in AD plasma. Amyloid plaques in the AD brain elicit a range of reactive inflammatory responses including complement activation and acute phase reactions, which may also be reflected in plasma. Previous studies have shown that human AD plasma may be cytotoxic to cultured cells. We investigated the effect of pooled plasma (n = 20 each) from healthy controls, individuals with amnesic mild cognitive impairment (aMCI) and Alzheimer's disease (AD) on cultured microglial cells. AD plasma was found to significantly decrease cell viability and increase glycolytic flux in microglia compared to plasma from healthy controls. This effect was prevented by the heat inactivation of complement. Proteomic methods and isobaric tags (iTRAQ) found the expression level of complement and other acute phase proteins to be altered in MCI and AD plasma and an upregulation of key enzymes involved in the glycolysis pathway in cells exposed to AD plasma. Altered expression levels of acute phase reactants in AD plasma may alter the energy metabolism of glia.

Introduction

Alzheimer's disease (AD) is a neurodegenerative disorder that results in the progressive and irreversible loss of cholinergic neurons in specific areas of the brain [1]. Amnesic Mild Cognitive Impairment (aMCI) is considered to be a pre-dementia stage of AD [2], with a proportion of aMCI cases progressing to AD with time. AD is characterised by an abnormal accumulation of amyloid β (A β) and tau proteins, increased oxidative stress and redox metals in the brain all of

Bioanalytical Mass Spectrometry Facility, UNSW, and was supported in part by grants from the Australian Government Systemic Infrastructure Initiative and Major National Research Facilities Program and by the UNSW Capital Grants Scheme (<http://www.bmsf.unsw.edu.au/aboutus/funding.htm>). The funders had

no role in study design, data collection and analysis, decision to publish, or preparation of the manuscript.

Competing Interests: The authors have declared that no competing interests exist.

which are associated with an immunological response [3]. A β primarily accumulates extracellularly and eventually leads to the formation of amyloid plaques, the main pathological hall-mark of AD. The accumulation of A β appears also appears to occur in synaptic mitochondria leading to impaired respiration and increased oxidative stress [4].

Damage to the blood-brain barrier is thought to occur in AD, and this may increase movement of proteins between the brain and the vasculature [5]. It is therefore possible that AD and its precursor, MCI, may be associated with the presence of specific biomarkers detectable in plasma and recent work has successfully used a panel of plasma biomarkers to predict disease severity and progression from MCI to dementia [6]. There are a number of proposed plasma biomarkers for AD, some of which reflect increased protein, lipid and nucleic acid oxidation and reduced activities of antioxidant enzymes in the AD brain [7–13]. AD has been reported to be associated with reduced plasma levels of vitamin A, C and E [9]. Isoprostanes, which arise from free-radical-mediated peroxidation of polyunsaturated fatty acids, are elevated in the AD brain, CSF and plasma [11]. 4-hydroxynonenal, another product of lipid peroxidation, is also increased in AD plasma [8].

A variety of inflammatory markers are increased with the onset of AD pathology, including cytokines and chemokines, coagulation factors and acute-phase reactive proteins as well as reactive astrocytes and activated microglial cells, the main cells involved in the neuroinflammation process [3,14]. Previous studies have shown that upregulation of the acute phase protein clusterin in plasma, is associated with prevalence, rate of progression, brain atrophy and disease severity in AD patients [15,16]. Other studies however have found no difference and suggest against the idea that acute phase protein changes in the CNS can be detected in plasma [17,18]. Alternatively, AD may be associated with a more widespread immune dysregulation, detectable in plasma.

Previous studies investigating the effects of human AD plasma on cells in culture have found differential effects on protein expression and cell biology. One study aimed to determine if exposure to serum from AD patients would affect markers for AD brain lesions [19], and found that 24 hour exposure to AD serum increased four molecular markers characteristic of AD senile plaques and neurofibrillary tangles (NFTs) in rat hippocampal neurons [19]. These markers were Alz-50, beta-amyloid, MAP2 and ubiquitin [19]. This stimulation of AD markers by human serum suggests that the genesis of both neuronal plaques and tangles may arise from exposure of susceptible neurons to toxic serum factors and/or failure to detoxify these factors. Another study found that antibodies in serum of patients with AD caused immunolysis of cholinergic nerve terminals from the rat cerebral cortex, supporting the hypothesis that autoimmune mechanisms may operate in the pathogenesis of AD [20].

Other studies have shown that serum of multiple sclerosis patients causes demyelination in rat CNS explant cultures and also induces cytotoxicity in rat oligodendrocytes in culture [21,22]. Demyelination was present not only in multiple sclerosis sera but was also found in sera from patients with other neurological diseases and complement was shown to be a factor involved in the effect [23,24]. In yet another study, human serum from patients with septic shock was shown to induce apoptosis in human cardiac myocytes [25]. This work demonstrated the utility of examining effects of disease plasma on cell culture systems, to facilitate the study of both disease markers and disease mechanisms.

Since previous studies indicate that AD plasma may contain oxidative stress markers as well as cytotoxic factors, we investigated the effect of the addition of pooled control, MCI and AD plasma from 20 individuals each on a microglial cell line. Cell viability, proliferation and mitochondrial function were investigated following 48 hour treatment with non heat-inactivated plasma and plasma in which complement proteins had been deactivated. We also tested the effect of commercially purchased complement factors alone and in combination on cultured glia. We then undertook proteomic analysis of the plasma from each group and iTRAQ quantitative

proteomic analysis of cell extracts exposed to plasma from each group to investigate possible plasma protein alterations unique to MCI or AD, to detect any protein aberrations within the cells treated with the plasma and to correlate these findings to cell viability and mitochondrial function assays measured *in vitro*.

Materials and Methods

Subjects

Age matched healthy control ($n = 20$), amnesic mild cognitive impairment (aMCI, $n = 20$), and probable AD ($n = 20$) plasmas were pooled and used in both the cell culture and plasma proteomics experiments. AD patients were recruited from the Memory Clinic of the Department of Old Age Psychiatry of the Prince of Wales Hospital and participants in a clinical drug trial of donepezil (Aricept). All met the NINCDS-ADRDA criteria [26] for probable AD. The aMCI subjects were recruited from the Memory and Ageing Study, a longitudinal study of community dwelling individuals aged 70–90 [27]. The diagnosis of aMCI was determined using the Petersen Criteria as follows [28]: (i) subjective complaint of memory impairment, (ii) objective impairment in memory (performance >1.5 SD below normal for age on a standardised memory test) (iii) essentially preserved general cognitive function (MMSE ≥ 24) (iv) intact functional activities as indicated by instrumental activities of daily living; and (v) not meeting DSM-IV criteria for dementia. Healthy control subjects had a normal performance for age on a range of neuropsychological tests and intact functional activities. Ethics committee approval was obtained from the University of New South Wales (UNSW) and the South Eastern Sydney Illawarra Area Health Service (SESAHS) ethics committees and written informed consent was obtained from all participants.

Cell Culture

CHME-5 cells are a human microglial cell line obtained from embryonic fetal human microglia through transformation with SV-40 virus [29,30] and were a generous gift from Prof Gilles Guillemin (Macquarie University, Sydney, Australia). These cells express antigens present on adult human microglia, secrete pro-inflammatory cytokines upon activation, exhibit properties of primary human microglia and have been successfully used as a model of microglial activation by others [29,31]. Cells were maintained in RPMI1640 cell culture medium, supplemented with 10% heat inactivated foetal bovine serum, 2 mM L-glutamine, and 1% penicillin/streptomycin, at 37°C in a humidified atmosphere containing 95% air/5% CO₂. Before experimentation, cells were seeded into 24 or 96 well culture plates to a density of approximately 1×10^4 or 2×10^3 cells respectively. Cells were left overnight and then supplemented with up to 20% (by volume) heat-inactivated and non heat-inactivated control, MCI or AD plasma for 48 hours. For the cell viability and iTRAQ proteomic analyses cells were washed to remove all plasma, and lysed in RIPA buffer (Thermo Fisher Scientific, IL, USA) followed by sonication. For the complement factor experiments cells were seeded into plates and treated with 1, 5 or 10 µg of each complement factor or the complement standard (in a total volume of 200 µL cell culture media) and then incubated for 48 hours. These concentrations are within the physiological range of these proteins in plasma [32].

MTT Cell Proliferation Assay

In actively proliferating cells, an increase in 3-[4,5-dimethylthiazol-2-yl]-2,5-diphenyl tetrazolium bromide (MTT) conversion in cells relative to controls represents an increase in cellular

proliferative activity. Conversely, in cells that are undergoing apoptosis, MTT conversion, and thus biological activity, decreases. Cell proliferation was analysed using established protocols [33,34].

NAD(H) Assay

Damaged cells show mitochondrial dysfunction, which results in decreased cellular nicotinamide adenine dinucleotide (NAD) levels. Intracellular NAD(H) concentration was quantified using the thiazolyl blue microcycling assay established by Bernofsky and Swan and adapted here for the 24 well plate format [35].

Lactate Dehydrogenase (LDH) Leakage

Cytoplasmic enzyme leakage has been shown to be a useful tool for measuring early cellular damage or impairment [12], and has also been used as a sign of cytotoxicity [36,37]. LDH is re-released from cells due to loss of membrane integrity. Therefore LDH was measured in the cell culture medium as well as in cell homogenates as another measure of cell viability.

XF24 Microplate-Based Respirometry as a measure of mitochondrial function

To determine the effect of human control, MCI and AD plasma on oxygen consumption rates (OCRs; an indicator of mitochondrial respiration) and extracellular acidification rates (ECARs; a measure of glycolytic flux) in the microglial cell line, the Seahorse XF24, extracellular flux analyzer (Seahorse Bioscience, North Billerica, MA, USA) was employed and assays performed as previously described [38–40]. The basal control ratio (BCR) and the uncoupling ratio (UCR) were determined as previously described [41]. Essentially, the BCR is a measure of how close the basal level of respiration is to the maximum level of respiration. The closer this ratio is to 1, the greater the mitochondrial malfunction. The UCR is a measurement of mitochondrial functional integrity and measures the ratio of uncoupled to physiologically normal respiration levels. The greater the maximum level of respiration, the greater the mitochondrial functional integrity.

Fractionation of Plasma

Control, MCI and AD plasma from 20 subjects was pooled and fractionated by two methods. To fractionate it into its protein and metabolite fractions, a PD10 column separation method was used. The PD10 column was washed with MilliQ water before the addition of 500 μ L of plasma. The flow-through was collected as 750 μ L fractions topping the column with MilliQ water. In total 20 fractions were collected and the absorbances read at 280nm. For the proteomics analysis, fractionation into low and high abundant protein fractions was undertaken using an MARS-Hu6 column (Agilent Technologies, CA, USA) according to the manufacturer's instructions. The MARS-Hu6 column depletes the top 6 contaminating proteins (albumin, IgG, IgA, transferrin, haptoglobin and antitrypsin) from plasma. This eliminates the masking effect of highly abundant proteins so lower-abundant proteins can be more easily detected. The low abundance fraction produced was used for the proteomic analysis experiments.

Proteomics of MCI and AD plasma

A one dimensional SDS 4–12% NuPAGE (Thermo Fisher Scientific Inc, MA, USA) gel was run using the low abundance fraction from each of the three groups. The gel was colloidal coomassie-stained [42], and the lanes uniformly cut into 7–8 bits using a gridcutter and mount from

The Gel Company, CA, USA. The gel bits were trypsin digested and then analysed using mass spectrometry as outlined in detail in [S1 Methods](#).

Peak lists were generated by MassLynx (version 4.0 SP1, Micromass) using the Mass Measure program and submitted to the database search program Mascot (version 2.2, Matrix Science, London, England). Search parameters were: Precursor and product ion tolerances ± 0.25 and 0.2 Da respectively; Met(O) and Cys-carboxyamidomethyl were specified as variable modification, enzyme specificity was trypsin, one missed cleavage was possible on the NCBI database.

Scaffold Q+ (version 4.3.4), Proteome Software, Portland, OR, USA) was used to identify any altered proteins between the groups. The Scaffold programme uses mass spectrometric data to identify protein changes in biological samples by collating Mascot data and using the ProteinProphet algorithm [43]. We compared the normalised total spectral count values from Scaffold [44] with the emPAI values from Mascot [45], which uses a different algorithm for spectral counting.

iTRAQ Proteomics of Cell Lysates Treated with Human Control, MCI and AD Plasma

Two biological replicates of cells treated with 10% (by volume) non-heat inactivated fetal bovine serum, human control, MCI or AD plasma were washed to remove all plasma/serum and then lysed using RIPA buffer and probe sonicated. Total protein concentrations were determined using the Bicinchoninic acid (BCA) protein assay kit (Pierce, IL, USA). The total protein (120 μ g) from each sample was reduced with 2 μ l of 5mM tris-(2-carboxyethyl) phosphine (TCEP) for 60 min at 60°C followed by alkylation with 200 mM iodoacetamide (1 μ L) for 10 min at room temperature. To remove any buffer components incompatible with mass spectrometry a buffer exchange was performed with 50 mM NaHCO₃ using Microcon centrifugal filter devices with a 3,000 Da nominal molecular weight limit membrane (Millipore, MA, USA) to give a final protein concentration of 1 μ g/ μ l.

For tryptic digestion 100 μ g total protein from each sample was incubated overnight at 37°C with 4 μ g of trypsin. Samples were labelled using the 8-plex iTRAQ kit (Applied Biosystems, CA, USA). Each iTRAQ reporter label was mixed with a biological replicate of cell lysate sample, pH adjusted to basic (ca pH = 9) with 2 μ l of 50 mM of Na₂CO₃ and incubated for 2 hours. The reporter masses for the samples were labelled as follows: fetal bovine serum; 113 and 117, human control plasma; 114 and 118, human MCI plasma; 115 and 119, human AD plasma; 116 and 121. Sample clean-up was performed using a strong cation exchange cartridge (Applied Biosystems, CA, USA) and a syringe pump at a flow rate of 9.5 ml/hr, and using the manufacturer's protocol.

Sample was then passed through a C18 Peptide Macrotrap (Michrom Bioresources, CA, USA). The flow-through from the C18 step was passed through an Oasis cartridge (Waters, MA, USA) to maximise peptide recovery and the two eluants pooled and dried under vacuum, resuspended in 0.2% heptafluorobutyric acid and then analysed using mass spectrometry as outlined in detail in [S1 Methods](#).

Protein identification and quantification was performed using the MS/MS data (WIFF files) and the Paragon algorithm as implemented in Protein Pilot v4.0 software (Applied Biosystems, CA, USA) using the NCBI database. Only proteins identified with a ProteinPilot unused score of 1.3 (greater than 95% confidence in sequence identity) were accepted as previously described [46,47]. The unused score is a ProteinPilot generated value for the level of confidence in protein sequence identification. As an approximate guide, ProteinPilot unused scores give the following percentage levels of confidence; score 1.3 (95% confidence), score 2 (99% confidence), score 3 (99.9% confidence) [46]. The only fixed modification used was

Table 1. Cell viability as measured by MTT absorbance (abs) at 570nm, LDH release and intracellular NAD levels of microglial cells after 48 hour incubation in pooled, non heat inactivated and heat inactivated MCI and AD plasma.

		Non Heat Inactivated Plasma									Heat Inactivated Plasma					
		Control MTT abs	Control NAD (ng)	Control LDH Activity (U/L)	MCI MTT abs	MCI NAD (ng)	MCI LDH Activity (U/L)	AD MTT abs	AD NAD (ng)	AD LDH Activity (U/L)	Control MTT abs	Control NAD (ng)	MCI MTT abs	MCI NAD (ng)	AD MTT abs	AD NAD (ng)
5% plasma	Mean	0.21	10.71		0.23	10.84		0.14	10.3							
	SEM	0.05	3.84		0.05	1.26		0.03*	1.82							
10% plasma	Mean	0.13	3.61	Media 3.35 Lysate 11.4	0.09	2.35	Media 2.7 Lysate 13.06	0.04	0.89	Media 6.09 Lysate 7.76	0.13		0.11		0.11	
	SEM	0.03	1.25	Media 0.36 Lysate 1.19	0.02	0.85	Media 0.3 Lysate 1.22	0.01**	1.3*	Media 1.05* Lysate 1.0	0.03		0.04		0.02	
20% plasma	Mean	0.06	0.79		0.06	0.56		0.03	0			14.02		12.3		12.1
	SEM	0.01	0.14		0.004	0.07		0.004**	0**			1.15		0.60		0.65

p 0.05 vs Control,

p 0.01 vs Control

Cell viability was determined by measurement of cell proliferation, intracellular NAD levels and LDH activity in cell culture media and cell lysate homogenates. n = 9 (nine replicates) for cell proliferation measurements, n = 6 (six replicates) for NAD concentration and LDH activity. Plasma used for the measurements were obtained from the pooled plasma of 20 patients from each of the three groups (Control, MCI and AD) investigated. Three concentration levels of plasma were tested: 5%, 10% and 20% plasma as a percentage of total media volume.

doi:10.1371/journal.pone.0116092.t001

iodoacetamide alkylation of cysteine residues. Mass tolerances were set to 50ppm for the precursor and 0.2 Da for the fragment ions. Autobias correction was applied to correct for any systematic bias in total protein concentration during sample pooling. Both biological replicates for the three human plasma types (control, MCI and AD) were compared to the fetal bovine serum control (iTRAQ reporter 117) and data exported to Microsoft Excel software (Microsoft, WA, USA).

Protein interactions between dysregulated proteins were determined using the web-based bioinformatics tool STRING v9.1 (<http://string-db.org>). STRING has a database that collates information on protein-protein interactions and associations. It scores and weights connections and provides predicted interaction network maps from literature mining searches. The 27 proteins which were significantly deregulated in glia treated with AD plasma, but not deregulated in either control or MCI plasma treated glia were analysed in STRING v9.1. MCL clustering was used with the 2 clusters option picked and with the confidence view selected to display the strength of evidence for protein associations and analysis of enrichment was also performed.

Statistics

All cell viability values are presented as means \pm SEM. Statistical comparisons were performed using two-tailed student t-tests assuming equal variance. Differences between treatment groups were considered statistically significant at the $p < 0.05$ level. Scaffold values are represented as normalised total spectral counts and p-values for significantly altered proteins were obtained using the ProteinProphet algorithm of the Scaffold Q+ software (Proteome Software, OR, USA). All iTRAQ values are presented as ratios of cells treated with human plasma to cells treated with fetal bovine serum control. Ratios and p-values for significantly altered proteins were obtained through the Paragon algorithm of the Protein Pilot v4.0 software (Applied Bio-systems, CA, USA).

Results

Cell Proliferation

Cells treated with non heat-inactivated pooled control and AD plasma for 48 hours showed a significant decrease in cell proliferation in cells treated with AD plasma compared to controls (Table 1). The addition of MCI plasma to the cells also caused a similar drop in cell proliferation, though not reaching statistical significance (Table 1). Mild heat treatment at 56°C for 30 minutes is an established approach for inactivating complement proteins [48,49]. Such heat treatment prevented the effects of MCI and AD plasma on cell proliferation (Table 1).

To determine whether the effect on cell proliferation was exclusively due to the protein component or to both the protein and low molecular weight components of plasma we separated proteins and metabolites. Plasma was fractionated using a PD10 column into its protein and metabolite portions to determine which portion of the plasma was causing the cytotoxic effect (Fig. 1). Addition of these two fractions to the cells showed that it was exclusively the protein portion which was initiating the reduction in cell proliferation (Fig. 1). Protein fractions of both MCI and AD plasma were found to significantly reduce cell proliferation (Fig. 1). The metabolite fraction of the plasma had no significant effect on microglial proliferation (Fig. 1).

Treatment of the cells with complement factors C1q, C1 inhibitor, C4, C5 and C9 effected a downward trend in cell proliferation with increasing concentration, but did not reach significance (Table 2). In combination, the factors were found to reduce cell proliferation at the highest concentration tested. The human complement standard which contains the factors C1q,

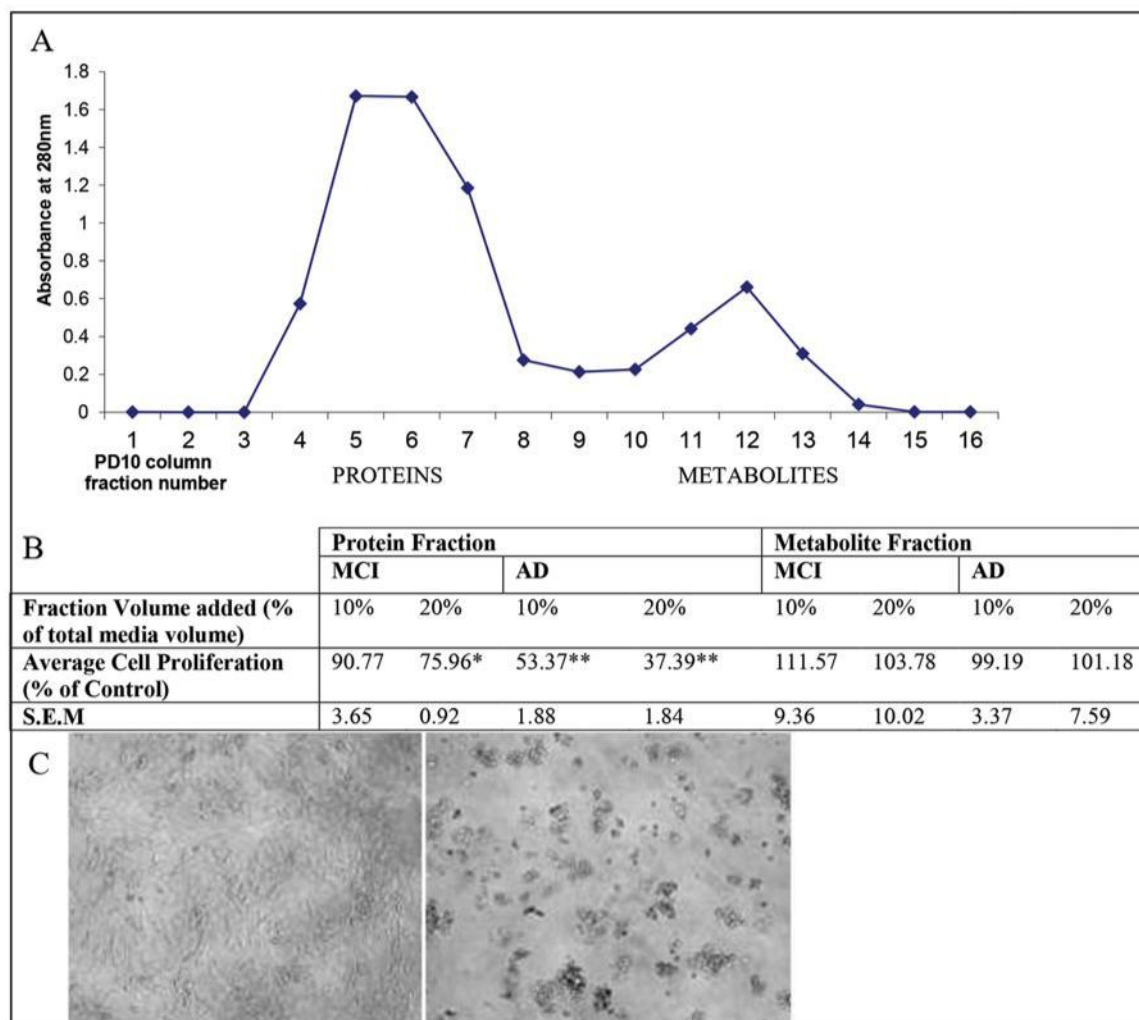


Fig 1. Fractionation of non heat inactivated control plasma into protein and metabolite fractions and the effects of plasma treatment on cell proliferation. Panel A: Fractionation of non heat inactivated control plasma into protein and metabolite fractions using PD10 column Panel B: Effect of these fractions on cell proliferation. Three replicates were performed. Plasma used for the measurements were obtained from the pooled plasma of 20 patients from each of the three groups (Control, MCI and AD). * $p < 0.01$ vs Control, ** $p < 0.001$ vs Control. Panel C: Images of microglia after 48 hour incubation with non heat inactivated 20% control plasma (left) and 20% AD plasma (right), showing increased toxicity and reduced cell proliferation in the AD plasma treated cells.

doi:10.1371/journal.pone.0116092.g001

C2, C3, C4, C5, C6, C7, C8, C9 and factor B was found to be the most potent at preventing cell proliferation (Table 2).

NAD levels and LDH Leakage

Incubation with non heat inactivated plasma caused a significant drop in cell viability as reflected in lower NAD levels, for cells treated with both MCI and AD plasma, compared to controls (Table 1). This result was again prevented by plasma heat inactivation (Table 1). The addition of human complement standard containing C1q, C2, C3, C4, C5, C6, C7, C8, C9 and factor B was found to significantly reduce NAD levels in the microglia (Table 2).

A significant increase in LDH leakage into the cell culture medium was seen in cells incubated with non heat inactivated AD plasma (Table 1). A concurrent decrease was seen in the amount of intracellular LDH in these same cells (Table 1).

Table 2. Cell viability of microglial cells after 48 hour incubation with human complement components (C1q, C1 inhibitor, C4, C5 and C9), both individually and in combination with each other; and a human complement standard containing complement components C1q, C2, C3, C4, C5, C6, C7, C8, C9 and factor B.

	Cell Proliferation (abs at 570nm)	Complement C1q	Complement C1 inhibitor	Complement C4	Complement C5	Complement C9	C1q + C4	C5 + C9	C1q, C1inhib, C4, C5 + C9	Complement Standard	Complement Standard NAD concentration (ng)
Control (0µg/µl)	Average	0.317	0.609	0.454	0.375	0.324	0.384	0.356	0.378	0.511	0.114
	SEM	0.019	0.07	0.025	0.031	0.014	0.025	0.018	0.013	0.004	0.003
0.005µg/µl	Average	0.3	0.593	0.458	0.382	0.333	0.377	0.371	0.377	0.426	0.104
	SEM	0.042	0.02	0.019	0.028	0.0098	0.019	0.025	0.019	0.031	0.010
0.025µg/µl	Average	0.31	0.571	0.461	0.364	0.336	0.366	0.359	0.331*	0.210**	0.094
	SEM	0.018	0.03	0.02	0.025	0.0096	0.025	0.021	0.015	0.036	0.063
0.05µg/µl	Average	0.267	0.49	0.435	0.355	0.344	0.289*	0.265*	0.292*	0.129**	0.063*
	SEM	0.0075	0.05	0.019	0.03	0.021	0.027	0.013	0.024	0.018	0.0024

Cell viability was determined by MTT assay of cell proliferation and intracellular NAD levels (for complement standard samples). Replicates included n = 6 for cell proliferation measurements and, n = 3 for NAD concentrations.

p 0.05 vs Control,
p 0.01 vs Control

doi:10.1371/journal.pone.0116092.t002

Biological Effects of Exposure to Alzheimer's Disease Plasma in Glia

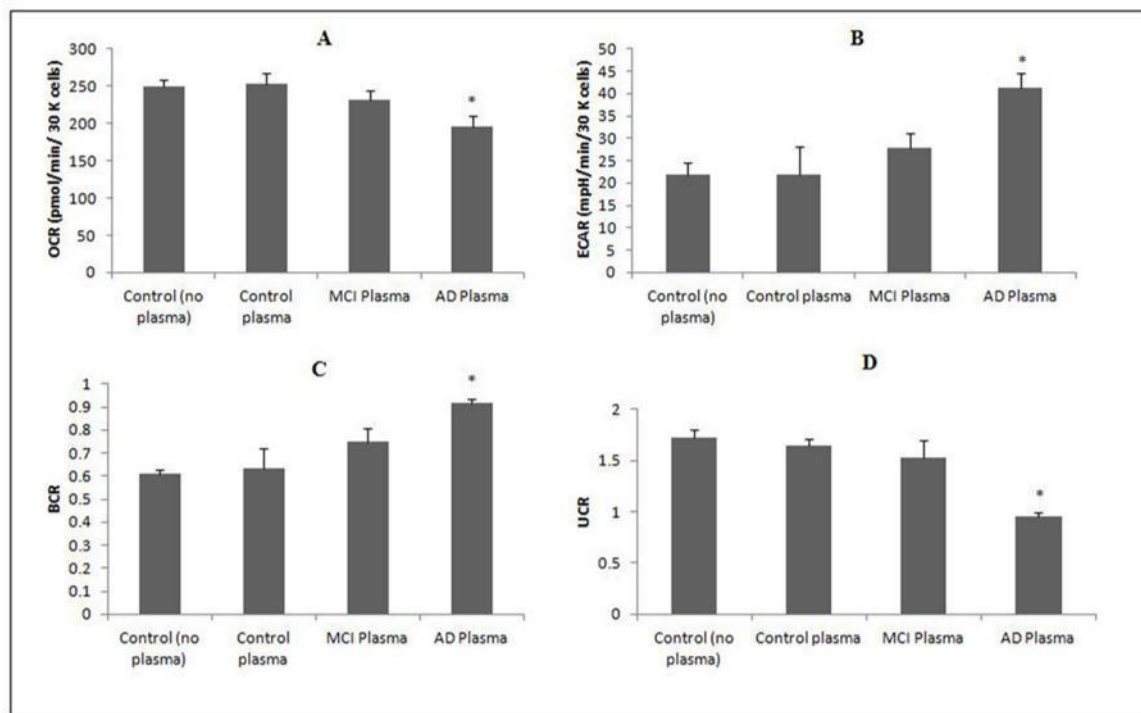


Fig 2. Effects of human plasma on cellular bioenergetics in a microglial cell line. (A) Effect of human plasma on oxygen consumption rates (OCR) in a microglial cell line for 48 hours. * $p < 0.05$ compared to non-treated cells (control); ($n = 4$ for each treatment group). (B) Effect of human plasma on extracellular acidification rates (ECAR) in a microglial cell line for 48 hours. * $p < 0.05$ compared to non-treated cells (control); ($n = 4$ for each treatment group). (C) Effect of human plasma on the basal control ratio (BCR) in a microglial cell line for 48 hours. * $p < 0.05$ compared to non-treated cells (control); ($n = 4$ for each treatment group). (D) Effect of human plasma on the uncoupling ratio (UCR) in a microglial cell line for 48 hours. * $p < 0.05$ compared to non-treated cells (control); ($n = 4$ for each treatment group).

doi:10.1371/journal.pone.0116092.g002

Mitochondrial Function and Cellular Bioenergetics

To determine whether mitochondrial bioenergetic mechanisms are associated with AD pathogenesis, we assessed mitochondrial function in glial cells treated with human plasma using the Seahorse XF24 (Seahorse Bioscience, MA, USA). We observed a significant decrease in OCRs and an increase in ECAR for cells treated with AD plasma and MCI plasma effected similar trends though did not achieve statistical significance (Fig. 2). We also observed a significant in-crease in the BCR and a decline in the UCR in microglial cells after 48 hour incubation with AD plasma (Fig. 2), consistent with impaired mitochondrial function and increased shift towards glycolysis.

Plasma fractionation and 1D gel electrophoresis

Fractionation using the MARS-Hu6 column provided a baseline separation of low and high abundant proteins (Fig. 3). These fractions were run on a 1D SDS NuPage gel and proteins were shown to be effectively separated with a substantial depletion of high abundant proteins, revealing many lower abundant protein bands in the low abundant fraction (Fig. 3).

Proteomics of MCI and AD plasma

Following proteomic analysis of pooled control, MCI and AD plasma, normalised total spectral counts using Scaffold software and emPAI values from Mascot showed complement component 2, fibronectin and fibrinogen to be significantly increased in the AD groups compared to

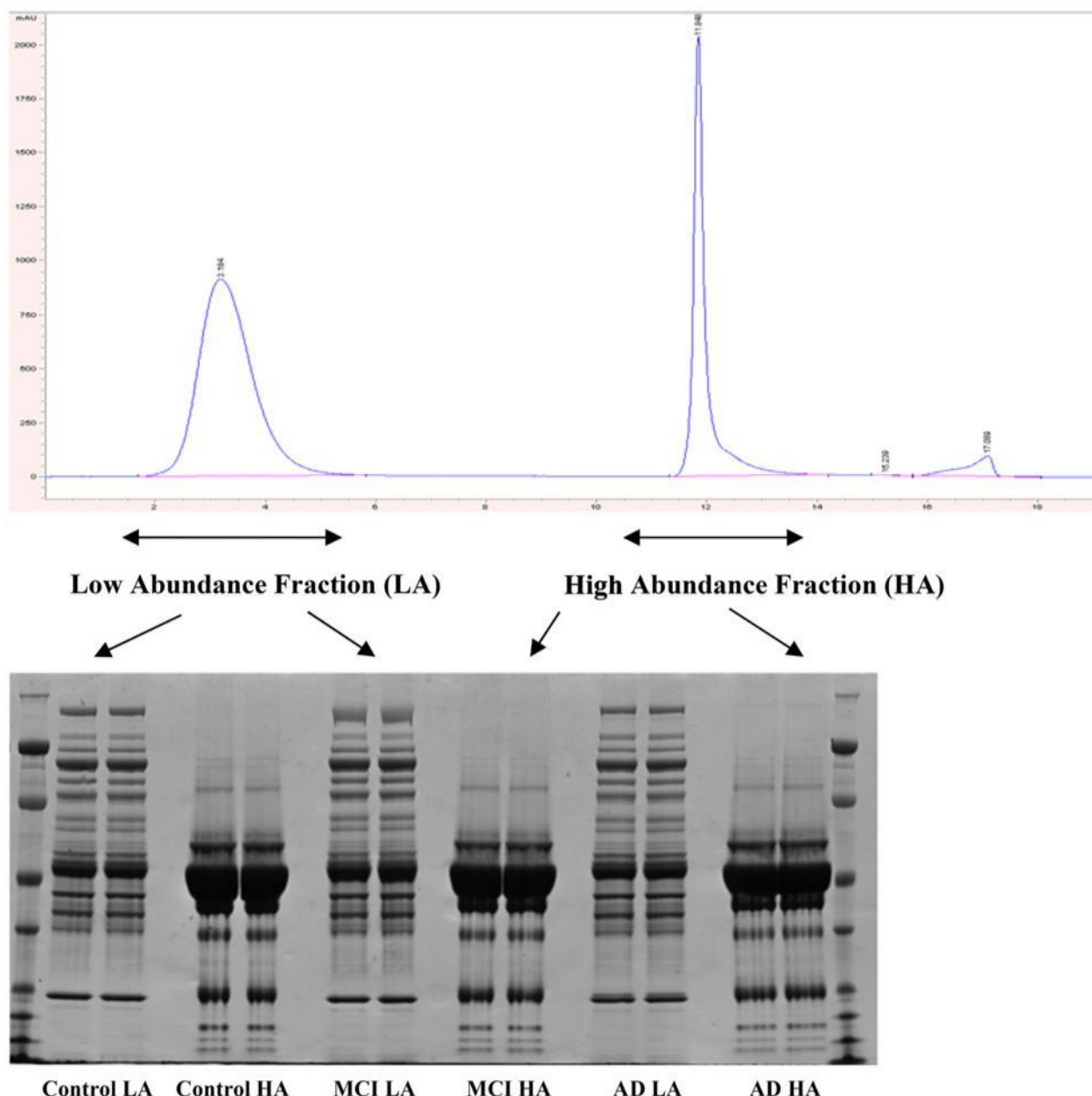


Fig 3. Chromatogram of fractionation using Hu6 column and 1D SDS/PAGE of these fractions. Low abundant proteins are eluted first (first peak on chromatogram) and high abundant proteins are eluted after (second peak). Gel shows significant depletion of high abundant proteins in the low abundant fractions. Loading was 50 µg/lane. First and last lanes contained molecular weight markers. Each fraction was run in duplicate.

doi:10.1371/journal.pone.0116092.g003

the control group (Table 3). Thrombin was decreased in the MCI and AD patients compared to controls (Table 3). A full list of proteins identified and normalised spectral counts in human control, MCI and AD plasma can be found in S1 Table and the peptide false discovery rate analysis can be found in S1 Fig.

Table 3. Average normalised spectral counts (obtained from Scaffold) and emPAI values (obtained from Mascot) of significantly deregulated proteins identified in pooled plasma samples between the Control, MCI and AD groups.

		Complement component 2 (gi 14550407)			Complement component 1 inhibitor (gi 114642584)			Complement component 4 binding protein (gi 4502503)			Fibronectin (gi 109658664)			Thrombin (gi 119588383)			Fibrinogen (gi 70906435)			Alpha-1B-glycoprotein (gi 46577680)		
		C	MCI	AD	C	MCI	AD	C	MCI	AD	C	MCI	AD	C	MCI	AD	C	MCI	AD	C	MCI	AD
Normalised Spectral Count	Average	0	0.82	2.77	9.98	7.45	11.30	4.18	3.38	4.51	18.9	15.1	32.2	10.34	5.57	6.29	39.78	35.93	43.19	6.08	8.32	7.64
	S.E.M	0	0.50	0.29	1.0	0.46	2.10	0.51	0.46	0.83	0.18	2.55	2.29	1.18	0.50	0.88	5.58	2.42	7.25	0.49	0.70	1.01
	p-value		0.015#	0.000074**		p = 0.06 vs AD						0.0025##	0.0012**		0.098*	0.033*					0.040*	
emPAI value	Average	0.08	0.06	0.145	0.74	0.62	0.95	0.35	0.18	0.26	0.39	0.30	0.64	0.83	0.46	0.48	5.40	4.74	7.87	0.78	0.86	0.75
	S.E.M	0.010	0.020	0.014	0.090	0.06	0.13	0.027	0.037	0.029	0.068	0.065	0.033	0.068	0.055	0.033	0.48	0.62	0.71	0.10	0.032	0.029
	p-value		0.014#	0.025*		p = 0.06 vs AD			0.013*			0.0071##	0.0018**		0.0057*	0.0034*		0.016#	0.036*		0.050#	

Values are averages from 4 replicates. Plasma used was obtained from the pooled plasma of 20 patients from each of the three groups (Control, MCI and AD) with depletion of high abundance proteins.

p 0.05 vs Control
p 0.01 vs Control
p 0.05 vs AD
p 0.01 vs AD

doi:10.1371/journal.pone.0116092.t003

iTRAQ proteomic analysis of cell lysates treated with Control, MCI and AD plasma

Differential protein expression in glial cells treated with fetal bovine serum (control) or human plasma from control, MCI and AD subjects were analysed with two biological replicates performed using an 8-plex iTRAQ experimental design. In total, 791 proteins were identified with 95% or greater confidence in correct protein sequence identification and 750 proteins with a false discovery rate of 5% (see [S2 Table](#) for full summary of identified proteins and [S3 Table](#) for full false discovery rate analysis). Forty-one proteins were found altered between the MCI and AD groups of cellular lysates ([Table 4](#)). The highest numbers of dysregulated proteins were found in the cells treated with AD plasma ([Table 4](#), 27 proteins highlighted in bold). Interestingly a significant number of proteins involved in the glycolysis cycle were shown to be upregulated in this group, namely glyceraldehyde-3-phosphate dehydrogenase, phosphoglycerate kinase, enolase, aldolase and pyruvate kinase. These enzymes catalyse five of the ten enzyme reactions of the pathway and their functions are shown in [Fig. 4](#). Transketolase was also shown to be significantly elevated in both the AD plasma treated cell sample replicates. This enzyme is part of the pentose phosphate pathway and connects this pathway to glycolysis. Analysis of protein interactions of the 27 dysregulated glial proteins treated with AD plasma using the on-line STRING v9.1 tool confirmed a significant enrichment of proteins involved in glucose metabolism ([Fig. 5](#) and [Table 5](#)).

Discussion

A variety of studies have looked at the effects of plasma on cell cultures in different diseases. For example, Brewer et al found 24 hr exposure of human serum from AD patients to rat hippocampal neurons increased four molecular markers characteristic of Alzheimer senile plaques and neurofibrillary tangles [19]. Another study has shown that Parkinsonian serum has complement-dependent toxicity to rat dopaminergic neurons [50]. A study using a differentiated neuronal cell line investigated the susceptibility of neuronal cells to human complement. It was found that human serum caused lysis of the neurons by complement, as tested by cell viability. The effect was lost when cells were treated with complement-depleted serum by heat inactivation [51].

Our cell culture results also showed that the loss of cell viability and reduction in cell proliferation caused by AD plasma can be prevented by inhibiting the activity of plasma complement proteins. Alterations in peripheral proteins may reflect changes in the brain, especially since damage to the blood-brain-barrier (BBB) resulting in increased permeability has been reported in MCI and AD [52,53]. This suggests that complement may have the capacity to play a role in the cell loss seen in AD. Complement factors may work synergistically to cause loss in cell viability. We observed reduced cell viability when cells were exposed to the complement standard mixture, as compared to addition of single complement factors ([Table 2](#)). However in all cases we observed a downward trend in cell viability as complement concentration levels increased regardless of the number of complement proteins present. The data achieved statistical significance with exposure to as few as two complement factors ([Table 2](#)), indicating that the full spectrum of complement proteins are not necessary for cytotoxicity. Indeed it has been found that treatment of a transgenic mouse model with an agonist to a single complement receptor, C5aR, decreased pathology and improved behavioural performance [54].

There is significant evidence for the involvement of inflammation in the pathogenesis of Alzheimer's disease. In the AD brain, damaged neurons and highly insoluble A β peptide deposits and NFTs provide stimuli for inflammation [3,14]. Various neuroinflammatory mediators including complement activators and inhibitors, chemokines, cytokines, radical oxygen species and inflammatory enzymes have been shown to be altered in AD [3,14]. Another

Table 4. Dysregulated proteins in glial cells treated with human control, MCI and AD plasma compared to FBS (non human serum control) following iTRAQ analysis.

Protein Function	Accession #	Name	Replicate 1		Replicate 2		Replicate 1		Replicate 2		Replicate 1		Replicate 2	
			Ctrl:FBS	PVal	Ctrl:FBS	PVal	MCI:FBS	PVal	MCI:FBS	PVal	AD:FBS	PVal	AD:FBS	PVal
Glycolysis	gi 7669492	glyceraldehyde-3-phosphate dehydrogenase	0.97	0.524	1.02	0.603	0.98	0.676	0.98	0.655	1.27	3.4E-5*	1.32	1.0E-4*
	gi 4505763	phosphoglycerate kinase 1	1.07	0.175	1.05	0.322	1.05	0.279	1.06	0.207	1.2	7.0E-5*	1.31	1.1E-4*
	gi 4503571	alpha-enolase isoform 1	0.93	0.12	0.98	0.753	0.99	0.719	0.98	0.553	1.19	2.7E-4*	1.22	1.0E-4*
	gi 342187211	fructose-bisphosphate aldolase A	0.99	0.829	1	0.989	1.02	0.836	1	0.991	1.2	0.004*	1.22	0.001*
	gi 33286418	pyruvate kinase isozymes M1/M2	0.98	0.746	1.02	0.726	1.01	0.869	1.03	0.6	1.22	0.008*	1.22	0.002*
	gi 4507521	transketolase isoform 1	0.98	0.686	1.01	0.881	1.04	0.323	0.99	0.749	1.13	0.022*	1.16	0.002*
Chaperone	gi 20070125	protein disulfide-isomerase precursor	0.98	0.566	0.96	0.352	0.93	0.057	1.01	0.821	0.93	0.026*	0.98	0.478
	gi 153792590	heat shock protein HSP 90-alpha	1.03	0.679	1.05	0.601	1.06	0.512	1.06	0.473	1.3	0.036*	1.2	0.059
	gi 66933005	calnexin precursor	1	0.942	0.98	0.7	0.94	0.315	0.93	0.149	0.92	0.266	0.88	0.010*
	gi 5031973	protein disulfide-isomerase A6 precursor	0.97	0.429	0.98	0.662	0.94	0.134	1	0.952	0.96	0.546	0.91	0.019*
	gi 21361657	protein disulfide-isomerase A3 precursor	0.96	0.427	0.98	0.653	0.9	0.013*	1	0.871	0.92	0.117	0.89	0.06
	gi 16507237	78 kDa glucose-regulated protein precursor	0.99	0.806	0.97	0.729	0.92	0.038*	0.98	0.643	0.91	0.101	0.91	0.108
Cytoskeletal	gi 4505257	moesin	1.08	0.265	1.14	0.243	1.12	0.106	1.03	0.721	1.22	0.021*	1.2	0.028*
	gi 21614499	ezrin	1.06	0.498	0.95	0.718	1.05	0.555	1.13	0.446	1.31	0.033*	0.9	0.712
	gi 38176300	nestin	0.99	0.773	1	0.984	0.97	0.518	1.04	0.354	0.94	0.173	0.85	0.004*
	gi 44680105	caldesmon isoform 1	0.91	0.154	0.97	0.773	0.9	0.174	0.94	0.478	0.87	0.085	0.86	0.027*
	gi 19920317	cytoskeleton-associated protein 4	0.85	0.049*	0.77	0.012*	0.92	0.229	0.79	0.032*	0.74	1.0E-4*	0.77	0.019*
	gi 62414289	vimentin	0.97	0.23	1	0.965	0.9	2.4E-4*	0.99	0.778	0.97	0.261	0.96	0.277

(Continued)

Table 4. (Continued)

Protein Function	Accession #	Name	Replicate 1		Replicate 2		Replicate 1		Replicate 2		Replicate 1		Replicate 2	
			Ctrl:FBS	PVal	Ctrl:FBS	PVal	MCI:FBS	PVal	MCI:FBS	PVal	AD:FBS	PVal	AD:FBS	PVal
Proteolysis	gi 4506713	ubiquitin-40S ribosomal protein S27a	0.98	0.738	0.82	0.159	1.06	0.286	1.04	0.594	0.84	0.066	0.77	0.022*
	gi 66346681	plasminogen activator inhibitor 1	1.04	0.587	0.99	0.922	1	0.999	0.93	0.476	0.97	0.612	0.79	0.023*
	gi 54792069	small ubiquitin-related modifier 2	1.15	0.291	1.02	0.948	1.46	0.083	1.41	0.052	1.23	0.26	1.29	0.043*
	gi 109637759	calpastatin isoform f	0.86	0.228	0.75	0.138	0.81	0.24	0.88	0.46	0.82	0.206	0.74	0.045*
Translation	gi 4503471	elongation factor 1- α 1	0.97	0.493	1.02	0.76	0.93	0.225	0.97	0.563	1.13	0.024*	1.24	0.014*
	gi 17158044	40S ribosomal protein S6	0.95	0.62	0.54	0.063	0.83	0.091	0.7	0.172	0.74	0.041*	0.72	0.178
	gi 15431288	60S ribosomal protein L10a	1.14	0.206	1.31	0.037*	1.19	0.098	1.27	0.048*	1.41	0.079	1.06	0.732
	gi 214010226	40S ribosomal protein S24 isoform d	0.68	0.062	0.66	0.015*	0.75	0.011*	0.66	0.085	0.6	0.063	0.64	0.022*
	gi 124494254	proliferation-associated protein 2G4	0.97	0.897	0.99	0.974	1.36	0.040*	1.22	0.194	1.24	0.276	1.15	0.146
Transcription	gi 4885379	histone H1.4	0.86	0.158	0.78	0.053	0.79	0.063	0.96	0.61	0.58	0.006*	0.79	0.349
	gi 4885377	histone H1.3	1.04	0.538	1.21	0.386	0.94	0.438	1.18	0.369	0.75	0.012*	0.96	0.613
	gi 4885381	histone H1.5	0.83	0.011*	0.77	0.057	0.79	0.006*	0.9	0.164	0.65	3.4E-4*	0.85	0.205
	gi 4885375	histone H1.2	0.87	0.059	0.73	0.002*	0.74	0.002*	0.95	0.468	0.54	0.001*	0.76	0.102
Immune response	gi 4502101	annexin A1	1	0.999	0.99	0.848	0.93	0.161	1.02	0.794	0.87	0.023*	0.83	0.042*
	gi 50845388	annexin A2 isoform 1	1.04	0.339	1.1	0.021*	0.89	8.0E-4*	0.99	0.647	0.95	0.192	0.93	0.1
	gi 48255891	glucosidase 2 subunit beta	1.04	0.679	1.13	0.292	1.14	0.081	1.16	0.012*	1.01	0.914	1.05	0.584
Antioxidant	gi 32189392	peroxiredoxin-2 isoform a	1.34	0.096	1.2	0.268	1.28	0.15	1.16	0.454	1.19	0.026*	1.28	0.146
	gi 4505591	peroxiredoxin-1	1.01	0.871	0.95	0.379	1.01	0.871	0.96	0.479	1.07	0.223	1.17	0.021*
Cell Growth Regulation	gi 4503057	alpha-crystallin B chain	1.04	0.429	1.02	0.718	1.04	0.45	0.99	0.931	1.24	0.002*	1.26	0.043*
	gi 19743823	integrin beta-1 isoform 1A precursor	1.32	0.102	1.05	0.81	1.14	0.259	1.52	0.038*	1.35	0.069	1.08	0.829
Fatty Acid Metabolism	gi 4557585	fatty acid-binding protein, brain	0.85	0.22	0.84	0.176	0.8	0.228	0.87	0.353	0.9	0.247	0.83	0.049*
	gi 4758504	3-hydroxyacyl-CoA dehydrogenase	1.17	0.445	1.09	0.795	1.33	0.097	1.57	0.015*	1.18	0.49	1.14	0.381

(Continued)

Table 4. (Continued)

Protein Function	Accession #	Name	Replicate 1		Replicate 2		Replicate 1		Replicate 2		Replicate 1		Replicate 2	
			Ctrl:FBS	PVal	Ctrl:FBS	PVal	MCI:FBS	PVal	MCI:FBS	PVal	AD:FBS	PVal	AD:FBS	PVal
Energy Metabolism	gi 19923437	GTP:AMP phosphotransferase	1.4	0.083	1.27	0.371	1.46	0.047*	1.14	0.44	1.43	0.052	1.43	0.149

Cells were incubated with plasma in two 24 well plates, 3 wells for each of the plasma types were pooled from each plate to obtain two biological replicates for the 8-plex iTRAQ experiment. iTRAQ reporter ratios and p-values for altered proteins are shown for both replicates. Proteins found to be dysregulated in MCI and AD treated cells are shown in table. Proteins dysregulated only in cells treated with AD plasma are highlighted in bold. Full list of identified proteins can be found in [S2 Table](#).

* p = 0.05 vs Fetal Bovine Serum Control

doi:10.1371/journal.pone.0116092.t004

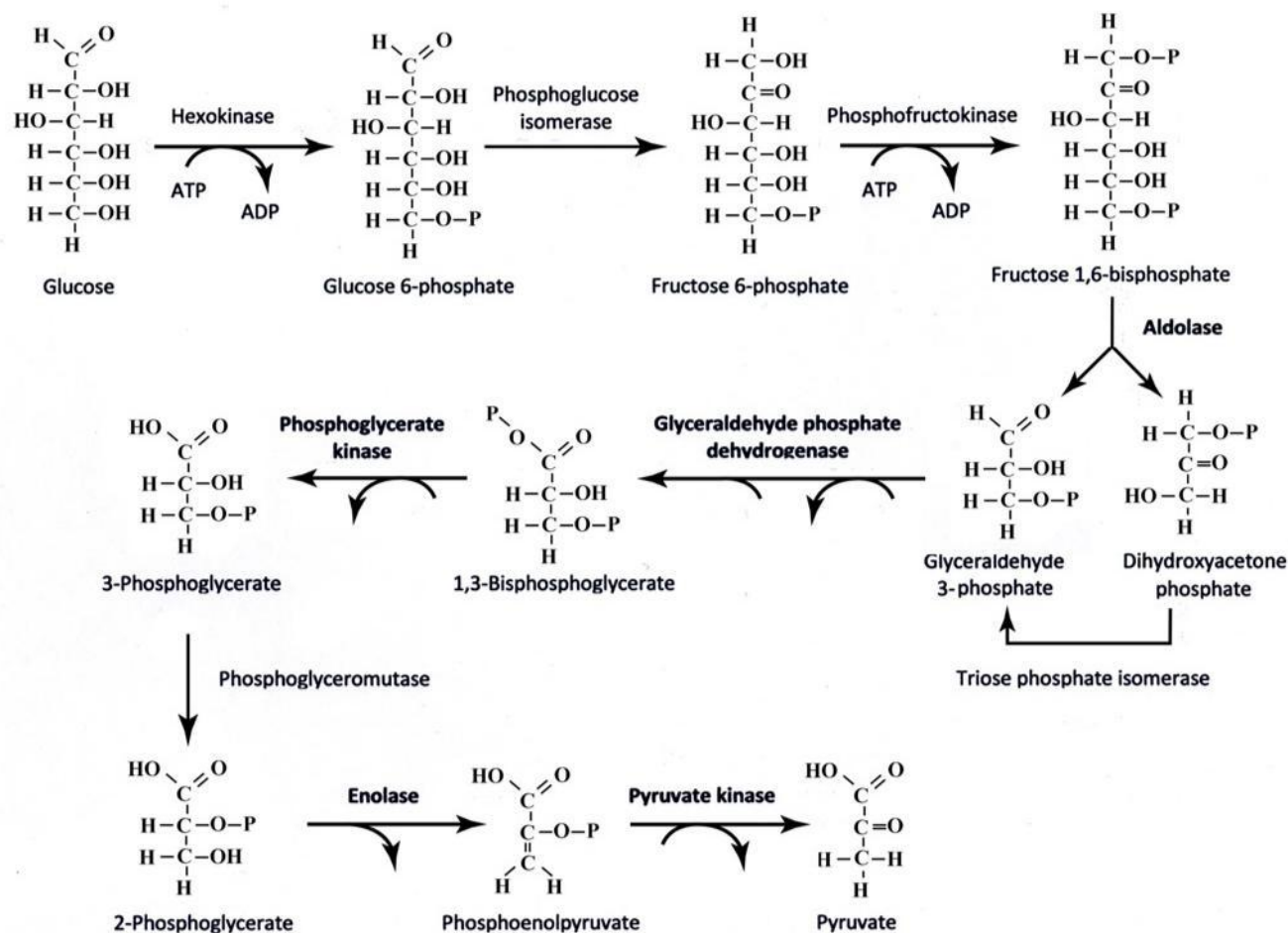


Fig 4. Glycolysis Pathway highlighting enzymes which were shown to be upregulated in cells treated with AD plasma.

doi:10.1371/journal.pone.0116092.g004

prominent feature of AD neuropathology is the association of activated proteins of the classical complement pathway with the lesions. The full-range of classical pathway complement pro-teins from C1q to C5b-9, known as the membrane attack complex, has been found highly local-ised with A β deposits in neuritic plaques [55,56]. It is also present in dystrophic neurites in AD. The fact that complement activation has progressed until the final membrane attack com-plex stage and the observation that complement regulators have also been found in association with the AD lesions indicates a disturbance in the regulatory mechanisms controlling comple-ment activation in this disease [57–60].

A β itself can induce complement-mediated toxicity against neurons in culture, suggesting that A β -induced complement activation may contribute to the neuropathogenesis of AD [56,61]. Hyperphosphorylated tau protein, the main component of NFTs, is also a potent stimulator of the complement cascade. Purified NFTs have been shown to activate the complement system in plasma, resulting in a significant increase in levels of membrane attack complexes [62]. Tau and A β are both able to increase inflammatory responses and cytokine production. Since the comple-ment system is strongly activated in AD, it could possibly participate either in the exacerbation or amelioration of the pathology. Because A β deposits and extracellular NFTs are present during early preclinical until terminal stages of AD, their ability to activate complement provides a mechanism for initiating and sustaining chronic, low-level inflammatory responses that may

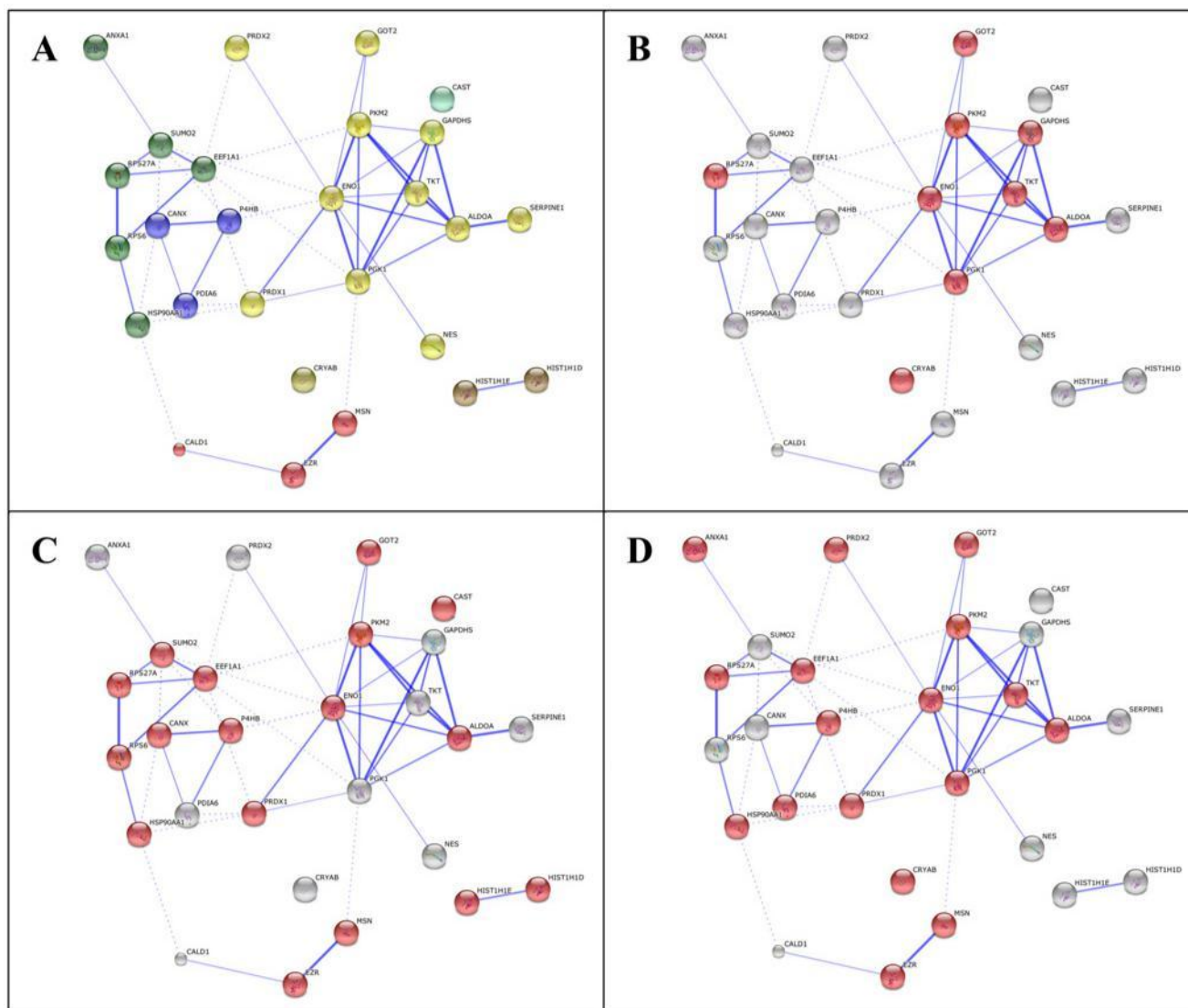


Fig 5. The 27 proteins which were significantly deregulated in glia treated with AD plasma, but not deregulated in either control or MCI plasma treated glia (shown in Table 4) were analysed in STRING v9.1. MCL clustering was used with the 2 clusters option picked and with the confidence view selected to display the strength of evidence for protein associations (panel A). Analysis of enrichment was also performed and the most significantly enriched biological process was glucose metabolic process (FDR p-value = 1.759×10^{-8} , with the 9 proteins involved in this process shown in panel B). Other distinct biological processes which were also significantly enriched included response to hydrogen peroxide (FDR p-value = 3.559×10^{-2} with 4 proteins involved; ANXA1, PRDX1, PRDX2, CRYAB) and membrane to membrane docking (FDR p-value = 4.299×10^{-2} with 2 proteins involved; MSN, EZR). Several molecular functions were also enriched, the most significant being RNA binding (FDR p-value = 5.340×10^{-9} with 17 proteins involved shown in panel C). Another distinct and significantly enriched molecular function is thioredoxin peroxidase activity (FDR p-value = 9.220×10^{-3} with 4 proteins involved; PRDX1, PRDX2). Several cellular components were also enriched, the most significant of these being extracellular vesicle/exosome (FDR p-value = 5.019×10^{-9} with 17 proteins involved as shown in panel D). Multiple other significantly enriched cellular components were also observed, and all enriched protein groups are shown in Table 5.

doi:10.1371/journal.pone.0116092.g005

accumulate over the disease course. This supports the idea that the complement system cascade intervention might be a useful pharmacological approach to treat early stages of AD.

Proteomic analysis of MCI and AD plasma in this study revealed a number of proteins which were significantly altered between the three groups. The majority of these proteins were acute phase reactants, including proteins which were related to the complement system (Table 3). This supports the results from other published studies using mainly proteomic techniques which have

Table 5. STRING v9.1 analysis of the 27 proteins deregulated only in glia exposed to AD plasma (shown in Table 4), for enrichment in gene ontology biological processes. Glucose metabolism was found to be the most significant biological process, and is also highlighted in the STRING network map (Fig. 5).

Molecular Function Enrichment GO_ID	Term	Number of Proteins	p-value	p-value FDR	p-value Bonferroni
GO:0003723	RNA Binding	17	1.94E-12	5.34E-09	7.51E-09
GO:0044822	Poly(A) RNA Binding	16	2.75E-12	5.34E-09	1.07E-08
GO:0008379	Thioredoxin peroxidase activity	2	8.88E-06	9.22E-03	3.45E-02
GO:0003676	Nucleic acid binding	16	9.50E-06	9.22E-03	3.69E-02
GO:0051920	Peroxisome oxidoreductase activity	2	2.95E-05	2.29E-02	1.15E-01
Biological Process Enrichment GO_ID	Term	Number of Proteins	p-value	p-value FDR	p-value Bonferroni
GO:0006006	Glucose metabolic process	9	1.42E-12	1.76E-08	1.76E-08
GO:0019318	Hexose metabolic process	9	7.28E-12	4.51E-08	9.02E-08
GO:0005996	Monosaccharide metabolic process	9	3.63E-11	1.50E-07	4.49E-07
GO:0046364	Monosaccharide biosynthetic process	6	2.23E-10	6.89E-07	2.75E-06
GO:0016051	Carbohydrate biosynthetic process	7	7.56E-10	1.87E-06	9.35E-06
GO:0006094	Gluconeogenesis	5	5.43E-09	1.12E-05	6.73E-05
GO:0019319	Hexose biosynthetic process	5	9.29E-09	1.64E-05	1.15E-04
GO:0042542	Response to hydrogen peroxide	4	2.30E-05	3.56E-02	2.85E-01
GO:0022614	Membrane to membrane docking	2	3.13E-05	4.30E-02	3.87E-01
GO:0016584	Nucleosome positioning	2	6.56E-05	8.12E-02	8.12E-01
Cellular Component Enrichment GO_ID	Term	Number of Proteins	p-value	p-value FDR	p-value Bonferroni
GO:0070062	Extracellular vesicular exosome	17	1.04E-11	5.02E-09	1.51E-08
GO:0044421	Extracellular region part	18	1.23E-09	4.44E-07	1.77E-06
GO:0005576	Extracellular region	18	1.08E-07	3.06E-05	1.57E-04
GO:0031988	Membrane-bounded vesicle	15	1.27E-07	3.06E-05	1.84E-04
GO:0031982	Vesicle	15	1.83E-07	3.77E-05	2.64E-04
GO:0043233	Organelle lumen	16	2.50E-07	4.32E-05	3.62E-04
GO:0042470	Melanosome	5	2.98E-07	4.32E-05	4.32E-04
GO:0005829	Cytosol	15	1.22E-06	1.47E-04	1.77E-03
GO:0070013	Intracellular organelle lumen	13	5.33E-05	5.93E-03	7.71E-02

GO:0031254	Cell trailing edge	2	7.00E-05	6.76E-03	1.01E-01
GO:0001931	Uropod	2	7.00E-05	6.76E-03	1.01E-01
GO:0030016	Myofibril	4	1.41E-04	1.28E-02	2.05E-01
GO:0016323	Basolateral plasma membrane	4	1.51E-04	1.29E-02	2.19E-01
GO:0043292	Contractile fiber	4	1.66E-04	1.33E-02	2.40E-01
GO:0060205	Cytoplasmic membrane-bound vesicle lumen	3	2.64E-04	1.91E-02	3.82E-01
GO:0031983	Vesicle lumen	3	2.64E-04	1.91E-02	3.82E-01
GO:0031528	Microvillus membrane	2	2.98E-04	2.05E-02	4.31E-01
GO:0016023	Cytoplasmic membrane-bounded vesicle	7	3.68E-04	2.42E-02	5.32E-01
GO:0005719	Nuclear euchromatin	2	5.70E-04	3.43E-02	8.24E-01
GO:0000791	Euchromatin	2	7.98E-04	4.62E-02	1.00E+00

doi:10.1371/journal.pone.0116092.t005

shown changes in complement protein levels and other acute phase proteins in AD plasma [5,47,63,64]. A summary of proteins found altered in such studies is provided in Table 6 and some of the proteins found in our study overlap with those found by other groups using larger cohorts of patients. One study has also shown a correlation between brain hippocampal volume changes and plasma levels of acute phase proteins, including complement [63].

Interestingly one of the complement proteins that was reduced in the AD plasma, complement 4 binding protein (C4BP) is a complement inhibitor which is detected in A β plaques and on apoptotic cells in the AD brain [65]. *In vitro*, C4BP binds apoptotic and necrotic but not viable brain cells. It also binds to A β (1–42) peptide directly and limits the extent of complement activation by A β [65]. C4BP levels in CSF of dementia patients and controls were low compared to levels in plasma and correlated with CSF levels of other inflammation-related factors [65]. Therefore it possibly protects against excessive complement activation in AD brains.

Fibronectin is present in plaques of AD brains and may modify biosynthesis of APP in microglia [66]. Addition of A β to cultured astrocytes has been shown to induce a marked increase in the production of fibronectin [67]. This suggests that *in vivo* fibronectin accumulation in senile plaques may be the result, at least in part, of the response of reactive astrocytes to the presence of A β . Fibrinogen is associated with an increased risk of AD and vascular dementia [68]. Our study found fibronectin and fibrinogen to be significantly increased in the AD group compared to controls (Table 3).

Furthermore, we have also shown that treatment with AD plasma can affect cellular bioenergetics in a microglial cell line, by increasing glycolysis to compensate for declining oxygen consumption and mitochondrial respiration (Fig. 2). The reduction in cerebral glucose metabolism, as measured by FDG-PET, is a common diagnostic tool for AD. Positron emission tomography (PET) imaging has identified a strong correlation between the spatial distribution of increased glycolysis, and A β plaques in the AD brain [69]. It is estimated that aerobic glycolysis accounts for up to 90% of glucose consumed [70]. By contrast, a recent neuroimaging study which

Table 6. Summary of previous studies showing changes in acute phase proteins in Alzheimer's disease.

Name	Site of effect	Function	Modification	Reference
Alpha-2-macroglobulin	plasma	Inhibitor of coagulation; inhibitor of fibrinolysis	Increased in MCI and AD	[5,47]
Complement C3	plasma	Most abundant protein of the complement system, enhances response	Increased in AD	[101–104]
Complement C4	plasma	Protein involved in the complement system and undergoes cleavage	Increased in AD	[5,105]
C4b-binding protein	plasma	Inhibits C4 and binds necrotic cells	Decreased in MCI and AD	[47]
Complement C5	plasma	Fifth component of the complement pathway	Increased in MCI	[47]
Complement C9	mRNA and protein levels, vascular amyloid deposits	Involved in MAC formation	Increased in AD brain areas, increased deposition in vascular plaques	[101,102,106]
Complement factor H	plasma	Regulation of alternative pathway of the complement system, ensuring no damage to host tissue	Increased in AD	[5,107]
Fibrinogen	plasma	Involved in blood clotting	Decreased in AD	[47,104,108,109]
Haptoglobin	Plasma, CSF	Binds free haemoglobin thereby reducing its oxidative activity	Increased in AD plasma, decreased in CSF of MCI and AD patients. Other studies show increase in CSF of AD	[110,111]
Hemopexin	plasma and CSF	Binds heme, preserves iron levels in the body	Increased in AD	[105,112,113]
Thrombin	Brain tissue, amyloid plaques, neurofibrillary tangles	Coagulation protein that converts fibrinogen into fibrin, also catalyses other coagulation related reactions	Increased in AD	[114–116]
Transthyretin	Plasma, CSF	Carrier of the thyroid hormone thyroxine	Decreased in AD	[47,112,117,118]

doi:10.1371/journal.pone.0116092.t006

correlated multimodal neuronal parameters including glucose metabolism and hippocampal volume with A β deposition in cognitively normal older individuals, did not find any association between the multimodal neurodegenerative biomarkers [71]. However, diminished neuronal integrity and cognitive function correlated with an increased A β burden in brain regions that are most affected by AD pathology [71]. Increased glycolysis was associated with better verbal episodic memory in individuals with elevated amyloid levels in another study [72]. The increased shift towards glycolysis may occur in regions of the brain most vulnerable to insult, or may occur in response to A β accumulation during ageing. Loss of this protective mechanism may increase the vulnerability of certain brain regions to A β -induced neurotoxicity.

Quantitative iTRAQ analysis of glial cells treated with human AD plasma showed the high-est number of dysregulated proteins (Table 4). The most significantly enriched biological process was glucose metabolism (Fig. 5 and Table 5), and a significant number of upregulated glycolytic proteins were found (highlighted in bold in Fig. 4), which is in agreement with the ECAR effect we found in cellular biogenetics using mitochondrial function assays (Fig. 2). Increased expression of glyceraldehyde-3-phosphate dehydrogenase, phosphoglycerate kinase, enolase, aldolase and pyruvate kinase may increase glycolytic flux leading to the accumulation of pyruvate and thus stimulating anaerobic metabolism to lactic acid. We found an increased level of LDH activity in the cell culture media and an increase in extracellular acidification, as indicated by the increase in ECAR in the microglial cells exposed to human AD plasma (Fig. 2). These findings suggest a role for mitochondrial bioenergetic deficits in AD pathogenesis. Our study is consistent with previous PET metabolic analyses in individuals with AD, MCI, or incipient to late AD [73]. Our findings are also consistent with microarray analyses and activity assays of ageing, incipient AD, and AD human samples and rodent models which indicate that genes and the catalytic activity of several glycolytic enzymes are altered in AD or MCI patients [74,75]. Similarly, increased amyloid production and nerve cell atrophy have been shown to induce mitochondrial dysfunction [76]. Overexpression of pyruvate dehydrogenase kinase and lactate dehydrogenase in neurons has been shown to provide resistance to A β toxicity and reduces mitochondrial respiration and oxidative stress [77]. Previous proteomic studies have also revealed that enzymes involved in energy metabolism show altered oxidative modification in the AD brain [78]. A recent study has also shown a number of proteins significantly oxidised in the Down syndrome brain with and without AD pathology [79]. A significant number of proteins involved in energy metabolism were identified including some of the glycolysis enzymes which we found altered in our study.

We also report an increase in the protein expression of the enzyme transketolase in microglial cells in response to human AD plasma. Transketolase is a thiamine-dependent enzyme which catalyses the first reaction in the pentose phosphate pathway. Transketolase alterations have been previously identified in (i) several probable AD patients regardless of age-of-onset and severity of disease; (ii) all early-onset AD patients and APOE ϵ 4/4 carriers; and (iii) nearly half of asymptomatic AD relatives [80]. Increased transketolase activity has also been correlated with increased levels of BACE1, the key rate-limiting enzyme for the production of the A β peptide [80].

Increased oxidative stress, mitochondrial dysfunction and alterations to energy metabolism have all been implicated as early events in the pathogenesis of AD. Cellular models for AD have been shown to display functional impairment of the mitochondrial respiratory chain, and a decrease in oxygen respiration and ATP production [81]. All functional measures highlight biogenetic impairment of the AD cells with a correlation to the accumulation of amyloid peptides [81].

Factors which induce the upregulation of glycolysis in glial cells treated with AD plasma remain unclear. Apart from the acute phase proteins found altered in our study, small molecules in plasma may also play a role in the upregulation of glycolytic enzymes. A recent study of metabolomic profiling of plasma from an AD mouse model found significant changes to several metabolites involved in energy metabolism, linking neuroinflammation with metabolic disturbance in AD [82]. Since oxidative stress is thought to be an important factor in the pathogenesis of AD, the effects of this may also be detected in the circulation in levels of markers such as isoprostanes. Isoprostanes have been shown to be elevated in the AD brain and CSF [83], however recent evidence suggests this may not be reflected in plasma [84], consequently additional work is warranted. Aerobic glycolysis has also been correlated spatially with amyloid deposition in AD brains [69]. It has also been shown that elevated levels of the enzymes pyruvate dehydrogenase kinase and lactate dehydrogenase provide resistance to amyloid and other neurotoxins [77]. The ability of the brain to maintain expression of these enzymes involved in

mitochondrial energy metabolism may explain why some individuals could show high levels of amyloid deposition without neurodegeneration [77,85–87]. In our study, the indicators of increased glycolysis in microglia may be a compensatory action caused by the loss of cell viability and mitochondrial function following exposure to AD plasma. Altered activities of key glyco-lytic enzymes have also been found in hippocampal, frontal and temporal cortex of AD brains and thought to possibly be related to the astrogliosis that occurs in AD [74].

Chaperone proteins are thought to be involved in the pathogenesis of several neurodegenerative and amyloidogenic diseases [88,89]. A number of chaperone proteins such as protein disulfide isomerases were found to be downregulated in cells treated with MCI and AD plasma. Protein disulfide isomerases can inhibit the aggregation of misfolded proteins and are also involved in modulating apoptosis and endoplasmic reticulum redox balance [90]. It has been shown that the proinflammatory activation of microglia suppresses mitochondrial function and increases glycolysis and overexpression of mitochondrial chaperone mortalin can attenuate this effect [91]. Heat shock proteins are chaperone proteins which have a important impact on the proteotoxic effects of tau and A β accumulation. Immunohistochemical studies and expression analyses in AD brain tissue have shown that expression levels of a number of heat shock proteins are upregulated and it has been hypothesised that this effect may be due to a hybridisation of activated glia and dysregulated/stressed neurons [92,93]. Dysregulated chaperone proteins in the cells in our study may reflect a homeostatic attempt to clear toxic plasma proteins and protect mitochondrial function.

Cytoskeletal proteins are another group of altered proteins identified in our iTRAQ proteomics data (Table 4). Nestin expression is seen during pathological situations and is a marker of cell proliferation and is reduced in the cells treated with AD plasma, supporting our MTT data (Table 1 and Fig. 1). Ezrin and moesin are involved in crosslinking actin filaments with plasma membranes and stabilising microtubules respectively [94,95] and both were found to be upregulated in cells treated with AD plasma. The antioxidant proteins peroxiredoxins were also found to be elevated in cells exposed to AD plasma which may also be another indication of a compensatory mechanism to attempt to attenuate the toxic effects of AD plasma.

In conclusion, this study shows that plasma expression levels of acute phase proteins are altered in AD and MCI, supporting a role for increased inflammatory activity in this disease which is detectable in the plasma. Cells exposed to AD plasma show an upregulation of glycolysis possibly as a compensatory mechanism in response to compromised mitochondrial function. Together our observations lend support to an emerging body of evidence that inflammation and metabolism are closely linked processes, which are regulated by transcriptional and protein translation events [96,97]. In the CNS, complement proteins are synthesised by a variety of cells including neurons, microglia, astrocytes, oligodendrocytes and endothelial cells [98]. Since disruptions in the blood-brain-barrier have been reported in AD there is a possible source of increased complement levels in the AD brain from plasma. It is however likely that there may be other thermolabile factors in disease plasma which facilitate the cytotoxic and glycolytic effects in microglia, one example may be micro RNAs as they are emerging as important factors in neurogenesis, synaptic plasticity and AD [99,100]. Other yet to be characterised substances may also make a significant contribution. This study shows that the use of biological assays in combination with proteomic analysis may help uncover possible mechanisms of disease and may be complementary techniques to validate cellular changes and effects in a range of biological samples.

Supporting Information

S1 Fig. Scaffold peptide false discovery analysis. Peptide FDR analysis using Scaffold v4 with peptide ROC curve.
(PDF)

S1 Methods. Detailed mass spectrometry protocols. Detailed mass spectrometry protocols for proteomics of depleted control, MCI and AD plasma and iTRAQ proteomic analysis of microglial cell lysates treated with control, MCI and AD plasma.
(PDF)

S1 Table. Protein summary of human control, MCI and AD plasma. Name and accession of proteins identified in human control, MCI and AD plasma and normalised spectral counts for replicates from Scaffold v4 software.
(PDF)

S2 Table. Proteomic of glial cells treated with human plasma. Protein summary of identified proteins with unused score 1.3 in glial cells treated with control, MCI and AD plasma, showing unused score, percentage coverage, accession number, name, number of peptides, iTRAQ ratios and p-values for both biological replicates. Significantly upregulated proteins are highlighted in red and downregulated proteins in blue.
(PDF)

S3 Table. False discovery rate analysis summary for iTRAQ. FDR analysis summary at the protein, peptide and spectral levels for iTRAQ experiment from Protein Pilot v4.
(PDF)

Acknowledgments

The authors thank Prof Gilles Guillemain (Motor neuron and other degenerative diseases re-search group, ASAM, Macquarie University, Sydney, Australia) for his kind donation of the microglia cells and Jason Nunes from Proteome Software for his help with the statistical analysis of the proteomics data. We are grateful to the staff of the Memory and Ageing Study for clinical data collection and South Eastern Area Laboratory Services for blood collection. None of the authors have any conflicts of interests with regard to this work. Mass spectrometry analyses were carried out at the Bioanalytical Mass Spectrometry Facility, UNSW, Australia.

Author Contributions

Conceived and designed the experiments: TJ AP NB GS MH PS. Performed the experiments: TJ NB. Analyzed the data: TJ AP NB. Contributed reagents/materials/analysis tools: AP MR HB JT NK PS. Wrote the paper: TJ AP NB GS PS. Design of study and diagnoses: HB JT NK PS. Editing/Feedback on Manuscript: AP NB GS MR MH HB JT NK PS.

References

- Shen Y, Meri S (2003) Yin and Yang: complement activation and regulation in Alzheimer's disease. *Prog Neurobiol* 70: 463–472. PMID: [14568360](#)
- Mosconi L, Brys M, Glodzik-Sobanska L, De Santi S, Rusinek H, et al. (2007) Early detection of Alzheimer's disease using neuroimaging. *Exp Gerontol* 42: 129–138. PMID: [16839732](#)
- Morales I, Guzman-Martinez L, Cerda-Troncoso C, Farias GA, Maccioni RB (2014) Neuroinflammation in the pathogenesis of Alzheimer's disease. A rational framework for the search of novel therapeutic approaches. *Front Cell Neurosci* 8: 112. doi: [10.3389/fncel.2014.00112](#) PMID: [24795567](#)
- Du H, Guo L, Yan SS (2012) Synaptic mitochondrial pathology in Alzheimer's disease. *Antioxid Redox Signal* 16: 1467–1475. doi: [10.1089/ars.2011.4277](#) PMID: [21942330](#)
- Hye A, Lynham S, Thambisetty M, Causevic M, Campbell J, et al. (2006) Proteome-based plasma bio-markers for Alzheimer's disease. *Brain* 129: 3042–3050. PMID: [17071923](#)
- Hye A, Riddoch-Contreras J, Baird AL, Ashton NJ, Bazenet C, et al. (2014) Plasma proteins predict conversion to dementia from prodromal disease. *Alzheimers Dement*.

- Butterfield DA, Castegna A, Lauderback CM, Drake J (2002) Evidence that amyloid beta-peptide-induced lipid peroxidation and its sequelae in Alzheimer's disease brain contribute to neuronal death. *Neurobiol Aging* 23: 655–664. PMID: [12392766](#)
- McGrath LT, McGleenon BM, Brennan S, McColl D, Mc IS, et al. (2001) Increased oxidative stress in Alzheimer's disease as assessed with 4-hydroxynonenal but not malondialdehyde. *QJM* 94: 485–490. PMID: [11528012](#)
- Zaman Z, Roche S, Fielden P, Frost PG, Niriella DC, et al. (1992) Plasma concentrations of vitamins A and E and carotenoids in Alzheimer's disease. *Age Ageing* 21: 91–94. PMID: [1575097](#)
- Pratico D, Clark CM, Liun F, Rokach J, Lee VY, et al. (2002) Increase of brain oxidative stress in mild cognitive impairment: a possible predictor of Alzheimer disease. *Arch Neurol* 59: 972–976. PMID: [12056933](#)
- Pratico D, Clark CM, Lee VM, Trojanowski JQ, Rokach J, et al. (2000) Increased 8,12-iso-iPF2alpha-VI in Alzheimer's disease: correlation of a noninvasive index of lipid peroxidation with disease severity. *Ann Neurol* 48: 809–812. PMID: [11079549](#)
- Mitchell DB, Acosta D (1981) Evaluation of the cytotoxicity of tricyclic antidepressants in primary cultures of rat hepatocytes. *J Toxicol Environ Health* 7: 83–92. PMID: [7265300](#)
- Cocciolo A, Di Domenico F, Coccia R, Fiorini A, Cai J, et al. (2012) Decreased expression and increased oxidation of plasma haptoglobin in Alzheimer disease: Insights from redox proteomics. *Free Radic Biol Med* 53: 1868–1876. doi: [10.1016/j.freeradbiomed.2012.08.596](#) PMID: [23000119](#)
- Rojo LE, Fernandez JA, Maccioni AA, Jimenez JM, Maccioni RB (2008) Neuroinflammation: implications for the pathogenesis and molecular diagnosis of Alzheimer's disease. *Arch Med Res* 39: 1–16. PMID: [18067990](#)
- Thambisetty M, Simmons A, Velayudhan L, Hye A, Campbell J, et al. (2010) Association of plasma clusterin concentration with severity, pathology, and progression in Alzheimer disease. *Arch Gen Psychiatry* 67: 739–748. doi: [10.1001/archgenpsychiatry.2010.78](#) PMID: [20603455](#)
- Schrijvers EM, Koudstaal PJ, Hofman A, Breteler MM (2011) Plasma clusterin and the risk of Alzheimer disease. *JAMA* 305: 1322–1326. doi: [10.1001/jama.2011.381](#) PMID: [21467285](#)
- Asuni AA, Gray B, Bailey J, Skipp P, Perry VH, et al. (2014) Analysis of the hippocampal proteome in ME7 prion disease reveals a predominant astrocytic signature and highlights the brain-restricted production of clusterin in chronic neurodegeneration. *J Biol Chem* 289: 4532–4545. doi: [10.1074/jbc.M113.502690](#) PMID: [24366862](#)
- Silajdzic E, Minthon L, Bjorkqvist M, Hansson O (2012) No diagnostic value of plasma clusterin in Alzheimer's disease. *PLoS One* 7: e50237. doi: [10.1371/journal.pone.0050237](#) PMID: [23209684](#)
- Brewer GJ, Ashford JW (1992) Human serum stimulates Alzheimer markers in cultured hippocampal neurons. *J Neurosci Res* 33: 355–369. PMID: [1335088](#)
- Bradford HF, Foley P, Docherty M, Fillit H, Luine VN, et al. (1989) Antibodies in serum of patients with Alzheimer's disease cause immunolysis of cholinergic nerve terminals from the rat cerebral cortex. *Can J Neurol Sci* 16: 528–534. PMID: [2804815](#)
- Hirayama M, Lisak RP, Silberberg DH (1986) Serum-mediated oligodendrocyte cytotoxicity in multiple sclerosis patients and controls. *Neurology* 36: 276–278. PMID: [3945400](#)
- Ruijs TCOA, Antel JP (1990) Serum cytotoxicity to human and rat oligodendrocytes in culture. *Brain Research* 517: 99–104. PMID: [2376011](#)
- Bradbury K, Aparicio SR, Sumner DW, Bird CC (1984) Role of complement in demyelination in vitro by multiple sclerosis serum and other neurological disease sera. *J Neurol Sci* 65: 293–305. PMID: [6491691](#)
- Ulrich J, Lardi H (1978) Multiple sclerosis: demyelination and myelination inhibition of organotypic tissue cultures of the spinal cord by sera of patients with multiple sclerosis and other neurological diseases. *J Neurol* 218: 7–16. PMID: [77321](#)
- Kumar A, Michael P, Brabant D, Parissenti AM, Ramana CV, et al. (2005) Human serum from patients with septic shock activates transcription factors STAT1, IRF1, and NF-kappaB and induces apoptosis in human cardiac myocytes. *J Biol Chem* 280: 42619–42626. PMID: [16223733](#)
- McKhann G, Drachman D, Folstein M, Katzman R, Price D, et al. (1984) Clinical diagnosis of Alzheimer's disease: report of the NINCDS-ADRDA Work Group under the auspices of Department of Health and Human Services Task Force on Alzheimer's Disease. *Neurology* 34: 939–944. PMID: [6610841](#)
- Sachdev PS, Brodaty H, Reppermund S, Kochan NA, Trollor JN, et al. (2010) The Sydney Memory and Ageing Study (MAS): methodology and baseline medical and neuropsychiatric characteristics of an elderly epidemiological non-demented cohort of Australians aged 70–90 years. *Int Psychogeriatr* 22: 1248–1264. doi: [10.1017/S1041610210001067](#) PMID: [20637138](#)

- Petersen RC (2004) Mild cognitive impairment as a diagnostic entity. *J Intern Med* 256: 183–194. PMID: [15324362](#)
- Atanassov CL, Muller CD, Dumont S, Rebel G, Poindron P, et al. (1995) Effect of ammonia on endo-cytosis and cytokine production by immortalized human microglia and astroglia cells. *Neurochem Int* 27: 417–424. PMID: [8845742](#)
- Peudener S, Hery C, Montagnier L, Tardieu M (1991) Human microglial cells: characterization in ce-rebral tissue and in primary culture, and study of their susceptibility to HIV-1 infection. *Ann Neurol* 29: 152–161. PMID: [1707249](#)
- de Gannes FM, Merle M, Canioni P, Voisin PJ (1998) Metabolic and cellular characterization of immortalized human microglial cells under heat stress. *Neurochem Int* 33: 61–73. PMID: [9694044](#)
- Kemp AS, Vernon J, Muller-Eberhard HJ, Bau DC (1985) Complement C8 deficiency with recurrent meningococemia: examination of meningococcal opsonization. *Aust Paediatr J* 21: 169–171. PMID: [4062713](#)
- Carmichael J, DeGraff WG, Gazdar AF, Minna JD, Mitchell JB (1987) Evaluation of a tetrazolium-based semiautomated colorimetric assay: assessment of chemosensitivity testing. *Cancer Res* 47: 936–942. PMID: [3802100](#)
- Kawada K, Yonei T, Ueoka H, Kiura K, Tabata M, et al. (2002) Comparison of chemosensitivity tests: clonogenic assay versus MTT assay. *Acta Med Okayama* 56: 129–134. PMID: [12108583](#)
- Bernofsky C, Swan M (1973) An improved cycling assay for nicotinamide adenine dinucleotide. *Anal Biochem* 53: 452–458. PMID: [4351948](#)
- Bhattacharya R, Tulsawani R (2008) In vitro and in vivo evaluation of various carbonyl compounds against cyanide toxicity with particular reference to alpha-ketoglutaric acid. *Drug Chem Toxicol* 31: 149–161. PMID: [18161514](#)
- Zhang X, Yang F, Xu C, Liu W, Wen S, et al. (2008) Cytotoxicity evaluation of three pairs of hexabro-mocyclododecane (HBCD) enantiomers on Hep G2 cell. *Toxicol In Vitro* 22: 1520–1527. doi: [10.1016/j.tiv.2008.05.006](#) PMID: [18644697](#)
- Schuh RA, Clerc P, Hwang H, Mehrabian Z, Bittman K, et al. (2011) Adaptation of microplate-based respirometry for hippocampal slices and analysis of respiratory capacity. *J Neurosci Res* 89: 1979–1988. doi: [10.1002/jnr.22650](#) PMID: [21520220](#)
- Braidy N, Gai WP, Xu YH, Sachdev P, Guillemin GJ, et al. (2014) Alpha-synuclein transmission and mitochondrial toxicity in primary human foetal enteric neurons in vitro. *Neurotox Res* 25: 170–182. doi: [10.1007/s12640-013-9420-5](#) PMID: [24026637](#)
- Braidy N, Gai WP, Xu YH, Sachdev P, Guillemin GJ, et al. (2013) Uptake and mitochondrial dysfunction of alpha-synuclein in human astrocytes, cortical neurons and fibroblasts. *Transl Neurodegener* 2: 20. doi: [10.1186/2047-9158-2-20](#) PMID: [24093918](#)
- Pesta D, Gnaiger E (2012) High-resolution respirometry: OXPHOS protocols for human cells and per-meabilized fibers from small biopsies of human muscle. *Methods Mol Biol* 810: 25–58. doi: [10.1007/978-1-61779-382-0_3](#) PMID: [22057559](#)
- Simpson RJ (2007) Staining proteins in gels with coomassie blue. *CSH Protoc* 2007: doi: [10.1101/pdb.prot4719](#) PMID: [21357065](#)
- Searle BC (2010) Scaffold: a bioinformatic tool for validating MS/MS-based proteomic studies. *Proteo-mics* 10: 1265–1269. doi: [10.1002/pmic.200900437](#) PMID: [20077414](#)
- Keller A, Nesvizhskii AI, Kolker E, Aebersold R (2002) Empirical statistical model to estimate the accuracy of peptide identifications made by MS/MS and database search. *Anal Chem* 74: 5383–5392. PMID: [12403597](#)
- Ishihama Y, Oda Y, Tabata T, Sato T, Nagasu T, et al. (2005) Exponentially modified protein abundance index (emPAI) for estimation of absolute protein amount in proteomics by the number of sequenced peptides per protein. *Mol Cell Proteomics* 4: 1265–1272. PMID: [15958392](#)
- Lim YA, Rhein V, Baysang G, Meier F, Poljak A, et al. (2010) Abeta and human amylin share a common toxicity pathway via mitochondrial dysfunction. *Proteomics* 10: 1621–1633. doi: [10.1002/pmic.200900651](#) PMID: [20186753](#)
- Song F, Poljak A, Kochan NA, Raftery M, Brodaty H, et al. (2014) Plasma protein profiling of Mild Cognitive Impairment and Alzheimer's disease using iTRAQ quantitative proteomics. *Proteome Sci* 12: 5. doi: [10.1186/1477-5956-12-5](#) PMID: [24433274](#)
- Triglia RP, Linscott WD (1980) Titers of nine complement components, conglutinin and C3b-inactivator in adult and fetal bovine sera. *Mol Immunol* 17: 741–748. PMID: [7432351](#)
- Rainard P (2002) Complement factor B and the alternative pathway of complement activation in bovine milk. *J Dairy Res* 69: 1–12. PMID: [12047100](#)

- Defazio G, Dal Toso R, Benvegnu D, Minozzi MC, Cananzi AR, et al. (1994) Parkinsonian serum carries complement-dependent toxicity for rat mesencephalic dopaminergic neurons in culture. *Brain Res* 633: 206–212. PMID: [7907931](#)
- Agoropoulou C, Wing MG, Wood A (1996) CD59 expression and complement susceptibility of human neuronal cell line (NTERA2). *Neuroreport* 7: 997–1004. PMID: [8804039](#)
- Starr JM, Farrall AJ, Armitage P, McGurn B, Wardlaw J (2009) Blood-brain barrier permeability in Alzheimer's disease: a case-control MRI study. *Psychiatry Res* 171: 232–241. doi: [10.1016/j.psychres.2008.04.003](#) PMID: [19211227](#)
- Zipser BD, Johanson CE, Gonzalez L, Berzin TM, Tavares R, et al. (2007) Microvascular injury and blood-brain barrier leakage in Alzheimer's disease. *Neurobiol Aging* 28: 977–986. PMID: [16782234](#)
- Fonseca MI, Ager RR, Chu SH, Yazan O, Sanderson SD, et al. (2009) Treatment with a C5aR antagonist decreases pathology and enhances behavioral performance in murine models of Alzheimer's disease. *J Immunol* 183: 1375–1383. doi: [10.4049/jimmunol.0901005](#) PMID: [19561098](#)
- Shen Y, Li R, McGeer EG, McGeer PL (1997) Neuronal expression of mRNAs for complement proteins of the classical pathway in Alzheimer brain. *Brain Res* 769: 391–395. PMID: [9374212](#)
- Rogers J, Cooper NR, Webster S, Schultz J, McGeer PL, et al. (1992) Complement activation by beta-amyloid in Alzheimer disease. *Proc Natl Acad Sci U S A* 89: 10016–10020. PMID: [1438191](#)
- Singh Rao SK, Neal JW, Rushmere NK, Morgan BP, Gasque P (2000) Spontaneous classical pathway activation and deficiency of membrane regulators render human neurons susceptible to complement lysis. *Am J Pathol* 157: 905–918. PMID: [10980130](#)
- Walker DG, Yasuhara O, Patston PA, McGeer EG, McGeer PL (1995) Complement C1 inhibitor is produced by brain tissue and is cleaved in Alzheimer disease. *Brain Res* 675: 75–82. PMID: [7796155](#)
- Yang LB, Li R, Meri S, Rogers J, Shen Y (2000) Deficiency of complement defense protein CD59 may contribute to neurodegeneration in Alzheimer's disease. *J Neurosci* 20: 7505–7509. PMID: [11027207](#)
- McGeer PL, Walker DG, Akiyama H, Kawamata T, Guan AL, et al. (1991) Detection of the membrane inhibitor of reactive lysis (CD59) in diseased neurons of Alzheimer brain. *Brain Res* 544: 315–319. PMID: [1710165](#)
- Haga S, Ikeda K, Sato M, Ishii T (1993) Synthetic Alzheimer amyloid beta/A4 peptides enhance production of complement C3 component by cultured microglial cells. *Brain Res* 601: 88–94. PMID: [8431789](#)
- Shen Y, Lue L, Yang L, Roher A, Kuo Y, et al. (2001) Complement activation by neurofibrillary tangles in Alzheimer's disease. *Neurosci Lett* 305: 165–168. PMID: [11403931](#)
- Thambisetty M, Hye A, Foy C, Daly E, Glover A, et al. (2008) Proteome-based identification of plasma proteins associated with hippocampal metabolism in early Alzheimer's disease. *J Neurol* 255: 1712–1720. doi: [10.1007/s00415-008-0006-8](#) PMID: [19156487](#)
- Akuffo EL, Davis JB, Fox SM, Gloger IS, Hosford D, et al. (2008) The discovery and early validation of novel plasma biomarkers in mild-to-moderate Alzheimer's disease patients responding to treatment with rosiglitazone. *Biomarkers* 13: 618–636. doi: [10.1080/13547500802445199](#) PMID: [18830857](#)
- Trouw LA, Nielsen HM, Minthon L, Londos E, Landberg G, et al. (2008) C4b-binding protein in Alzheimer's disease: binding to Aβ1–42 and to dead cells. *Mol Immunol* 45: 3649–3660. doi: [10.1016/j.molimm.2008.04.025](#) PMID: [18556068](#)
- Howard J, Pilkington GJ (1990) Antibodies to fibronectin bind to plaques and other structures in Alzheimer's disease and control brain. *Neurosci Lett* 118: 71–76. PMID: [2259470](#)
- Moreno-Flores MT, Martin-Aparicio E, Salinero O, Wandosell F (2001) Fibronectin modulation by Aβ peptide (25–35) in cultured astrocytes of newborn rat cortex. *Neurosci Lett* 314: 87–91. PMID: [11698153](#)
- Paul J, Strickland S, Melchor JP (2007) Fibrin deposition accelerates neurovascular damage and neuroinflammation in mouse models of Alzheimer's disease. *J Exp Med* 204: 1999–2008. PMID: [17664291](#)
- Vlasko AG, Vaishnavi SN, Couture L, Sacco D, Shannon BJ, et al. (2010) Spatial correlation between brain aerobic glycolysis and amyloid-beta (Aβ) deposition. *Proc Natl Acad Sci U S A* 107: 17763–17767. doi: [10.1073/pnas.1010461107](#) PMID: [20837517](#)
- Powers WJ, Rosenbaum JL, Dence CS, Markham J, Videen TO (1998) Cerebral glucose transport and metabolism in preterm human infants. *J Cereb Blood Flow Metab* 18: 632–638. PMID: [9626187](#)
- Wirth M, Villeneuve S, Haase CM, Madison CM, Oh H, et al. (2013) Associations between Alzheimer disease biomarkers, neurodegeneration, and cognition in cognitively normal older people. *JAMA Neurol* 70: 1512–1519. doi: [10.1001/jamaneurol.2013.4013](#) PMID: [24166579](#)

- Ossenkoppele R, Madison C, Oh H, Wirth M, van Berckel BN, et al. (2013) Is Verbal Episodic Memory in Elderly with Amyloid Deposits Preserved Through Altered Neuronal Function? *Cereb Cortex*.
- Liang WS, Reiman EM, Valla J, Dunckley T, Beach TG, et al. (2008) Alzheimer's disease is associated with reduced expression of energy metabolism genes in posterior cingulate neurons. *Proc Natl Acad Sci U S A* 105: 4441–4446. doi: [10.1073/pnas.0709259105](https://doi.org/10.1073/pnas.0709259105) PMID: [18332434](https://pubmed.ncbi.nlm.nih.gov/18332434/)
- Bigl M, Bruckner MK, Arendt T, Bigl V, Eschrich K (1999) Activities of key glycolytic enzymes in the brains of patients with Alzheimer's disease. *J Neural Transm* 106: 499–511. PMID: [10443553](https://pubmed.ncbi.nlm.nih.gov/10443553/)
- Blalock EM, Geddes JW, Chen KC, Porter NM, Markesbery WR, et al. (2004) Incipient Alzheimer's disease: microarray correlation analyses reveal major transcriptional and tumor suppressor re-sponses. *Proc Natl Acad Sci U S A* 101: 2173–2178. PMID: [14769913](https://pubmed.ncbi.nlm.nih.gov/14769913/)
- Velliquette RA, O'Connor T, Vassar R (2005) Energy inhibition elevates beta-secretase levels and activity and is potentially amyloidogenic in APP transgenic mice: possible early events in Alzheimer's disease pathogenesis. *J Neurosci* 25: 10874–10883. PMID: [16306400](https://pubmed.ncbi.nlm.nih.gov/16306400/)
- Newington JT, Rappon T, Albers S, Wong DY, Rylett RJ, et al. (2012) Overexpression of pyruvate dehydrogenase kinase 1 and lactate dehydrogenase A in nerve cells confers resistance to amyloid beta and other toxins by decreasing mitochondrial respiration and reactive oxygen species production. *J Biol Chem* 287: 37245–37258. doi: [10.1074/jbc.M112.366195](https://doi.org/10.1074/jbc.M112.366195) PMID: [22948140](https://pubmed.ncbi.nlm.nih.gov/22948140/)
- Korolainen MA, Goldsteins G, Nyman TA, Alafuzoff I, Koistinaho J, et al. (2006) Oxidative modification of proteins in the frontal cortex of Alzheimer's disease brain. *Neurobiol Aging* 27: 42–53. PMID: [16298240](https://pubmed.ncbi.nlm.nih.gov/16298240/)
- Di Domenico F, Pupo G, Tramutola A, Giorgi A, Schinina ME, et al. (2014) Redox proteomics analysis of HNE-modified proteins in Down syndrome brain: clues for understanding the development of Alzheimer disease. *Free Radic Biol Med* 71: 270–280. doi: [10.1016/j.freeradbiomed.2014.03.027](https://doi.org/10.1016/j.freeradbiomed.2014.03.027) PMID: [24675226](https://pubmed.ncbi.nlm.nih.gov/24675226/)
- Mocali A, Della Malva N, Abete C, Mitidieri Costanza VA, Bavazzano A, et al. (2014) Altered proteolysis in fibroblasts of Alzheimer patients with predictive implications for subjects at risk of disease. *Int J Alzheimers Dis* 2014: 520152. doi: [10.1155/2014/520152](https://doi.org/10.1155/2014/520152) PMID: [24949214](https://pubmed.ncbi.nlm.nih.gov/24949214/)
- Krako N, Magnifico MC, Arese M, Meli G, Forte E, et al. (2013) Characterization of mitochondrial dysfunction in the 7PA2 cell model of Alzheimer's disease. *J Alzheimers Dis* 37: 747–758. doi: [10.3233/JAD-130728](https://doi.org/10.3233/JAD-130728) PMID: [23948918](https://pubmed.ncbi.nlm.nih.gov/23948918/)
- Kim E, Jung YS, Kim H, Kim JS, Park M, et al. (2014) Metabolomic signatures in peripheral blood associated with Alzheimer's disease amyloid-beta-induced neuroinflammation. *J Alzheimers Dis* 42: 421–433. doi: [10.3233/JAD-132165](https://doi.org/10.3233/JAD-132165) PMID: [24898638](https://pubmed.ncbi.nlm.nih.gov/24898638/)
- Pratico D (2010) The neurobiology of isoprostanes and Alzheimer's disease. *Biochim Biophys Acta* 1801: 930–933. doi: [10.1016/j.bbalip.2010.01.009](https://doi.org/10.1016/j.bbalip.2010.01.009) PMID: [20116452](https://pubmed.ncbi.nlm.nih.gov/20116452/)
- Mufson EJ, Leurgans S (2010) Inability of plasma and urine F2A-isoprostane levels to differentiate mild cognitive impairment from Alzheimer's disease. *Neurodegener Dis* 7: 139–142. doi: [10.1159/000289224](https://doi.org/10.1159/000289224) PMID: [20197693](https://pubmed.ncbi.nlm.nih.gov/20197693/)
- Newington JT, Harris RA, Cumming RC (2013) Reevaluating Metabolism in Alzheimer's Disease from the Perspective of the Astrocyte-Neuron Lactate Shuttle Model. *Journal of Neurodegenerative Diseases* 2013: 13.
- Bouras C, Hof PR, Giannakopoulos P, Michel JP, Morrison JH (1994) Regional distribution of neurofibrillary tangles and senile plaques in the cerebral cortex of elderly patients: a quantitative evaluation of a one-year autopsy population from a geriatric hospital. *Cereb Cortex* 4: 138–150. PMID: [8038565](https://pubmed.ncbi.nlm.nih.gov/8038565/)
- Price JL, Morris JC (1999) Tangles and plaques in nondemented aging and "preclinical" Alzheimer's disease. *Ann Neurol* 45: 358–368. PMID: [10072051](https://pubmed.ncbi.nlm.nih.gov/10072051/)
- Gestwicki JE, Garza D (2012) Protein quality control in neurodegenerative disease. *Prog Mol Biol Transl Sci* 107: 327–353. doi: [10.1016/B978-0-12-385883-2.00003-5](https://doi.org/10.1016/B978-0-12-385883-2.00003-5) PMID: [22482455](https://pubmed.ncbi.nlm.nih.gov/22482455/)
- Asuni AA, Pankiewicz JE, Sadowski MJ (2013) Differential molecular chaperone response associated with various mouse adapted scrapie strains. *Neurosci Lett* 538: 26–31. doi: [10.1016/j.neulet.2013.01.027](https://doi.org/10.1016/j.neulet.2013.01.027) PMID: [23370284](https://pubmed.ncbi.nlm.nih.gov/23370284/)
- Andreu CI, Woehlbier U, Torres M, Hetz C (2012) Protein disulfide isomerases in neurodegeneration: from disease mechanisms to biomedical applications. *FEBS Lett* 586: 2826–2834. doi: [10.1016/j.febslet.2012.07.023](https://doi.org/10.1016/j.febslet.2012.07.023) PMID: [22828277](https://pubmed.ncbi.nlm.nih.gov/22828277/)
- Voloboueva LA, Emery JF, Sun X, Giffard RG (2013) Inflammatory response of microglial BV-2 cells includes a glycolytic shift and is modulated by mitochondrial glucose-regulated protein 75/mortalin. *FEBS Lett* 587: 756–762. doi: [10.1016/j.febslet.2013.01.067](https://doi.org/10.1016/j.febslet.2013.01.067) PMID: [23395614](https://pubmed.ncbi.nlm.nih.gov/23395614/)

- Harrison PJ, Procter AW, Exworthy T, Roberts GW, Najlerahim A, et al. (1993) Heat shock protein (hsx70) mRNA expression in human brain: effects of neurodegenerative disease and agonal state. *Neuropathol Appl Neurobiol* 19: 10–21. PMID: [8386339](#)
- Hamos JE, Oblas B, Pulaski-Salo D, Welch WJ, Bole DG, et al. (1991) Expression of heat shock pro-teins in Alzheimer's disease. *Neurology* 41: 345–350. PMID: [2005999](#)
- Tsukita S, Yonemura S, Tsukita S (1997) ERM proteins: head-to-tail regulation of actin-plasma mem-brane interaction. *Trends Biochem Sci* 22: 53–58. PMID: [9048483](#)
- Solinet S, Mahmud K, Stewman SF, Ben El Kadhi K, Decelle B, et al. (2013) The actin-binding ERM protein Moesin binds to and stabilizes microtubules at the cell cortex. *J Cell Biol* 202: 251–260. doi: [10.1083/jcb.201304052](#) PMID: [23857773](#)
- Liu TF, Brown CM, El Gazzar M, McPhail L, Millet P, et al. (2012) Fueling the flame: bioenergy couples metabolism and inflammation. *J Leukoc Biol* 92: 499–507. doi: [10.1189/jlb.0212078](#) PMID: [22571857](#)
- Gut P, Verdin E (2013) The nexus of chromatin regulation and intermediary metabolism. *Nature* 502: 489–498. doi: [10.1038/nature12752](#) PMID: [24153302](#)
- Barnum SR (1995) Complement biosynthesis in the central nervous system. *Crit Rev Oral Biol Med* 6: 132–146. PMID: [7548620](#)
- Maffioletti E, Tardito D, Gennarelli M, Bocchio-Chiavetto L (2014) Micro spies from the brain to the pe-riphery: new clues from studies on microRNAs in neuropsychiatric disorders. *Front Cell Neurosci* 8: 75. doi: [10.3389/fncel.2014.00075](#) PMID: [24653674](#)
- Lau P, Sala Frigerio C, De Strooper B (2014) Variance in the identification of microRNAs deregulated in Alzheimer's disease and possible role of lincRNAs in the pathology: The need of larger datasets. *Ageing Res Rev*.
- Yasojima K, Schwab C, McGeer EG, McGeer PL (1999) Up-regulated production and activation of the complement system in Alzheimer's disease brain. *Am J Pathol* 154: 927–936. PMID: [10079271](#)
- Tanskanen M, Lindsberg PJ, Tienari PJ, Polvikoski T, Sulkava R, et al. (2005) Cerebral amyloid angiopathy in a 95+ cohort: complement activation and apolipoprotein E (ApoE) genotype. *Neuro-pathol Appl Neurobiol* 31: 589–599. PMID: [16281907](#)
- Kiddle SJ, Sattlecker M, Proitsi P, Simmons A, Westman E, et al. (2014) Candidate blood proteome markers of Alzheimer's disease onset and progression: a systematic review and replication study. *J Alzheimers Dis* 38: 515–531. doi: [10.3233/JAD-130380](#) PMID: [24121966](#)
- Thambisetty M, Simmons A, Hye A, Campbell J, Westman E, et al. (2011) Plasma biomarkers of brain atrophy in Alzheimer's disease. *PLoS One* 6: e28527. doi: [10.1371/journal.pone.0028527](#) PMID: [22205954](#)
- Bennett S, Grant M, Creese AJ, Mangialasche F, Cecchetti R, et al. (2012) Plasma levels of comple-ment 4a protein are increased in Alzheimer's disease. *Alzheimer Dis Assoc Disord* 26: 329–334. doi: [10.1097/WAD.0b013e318239dcbd](#) PMID: [22052466](#)
- Guntert A, Campbell J, Saleem M, O'Brien DP, Thompson AJ, et al. (2010) Plasma gelsolin is de-created and correlates with rate of decline in Alzheimer's disease. *J Alzheimers Dis* 21: 585–596. doi: [10.3233/JAD-2010-100279](#) PMID: [20571216](#)
- Zhang R, Barker L, Pinchev D, Marshall J, Rasamoeliso M, et al. (2004) Mining biomarkers in human sera using proteomic tools. *Proteomics* 4: 244–256. PMID: [14730686](#)
- Lee JW, Namkoong H, Kim HK, Kim S, Hwang DW, et al. (2007) Fibrinogen gamma-A chain precursor in CSF: a candidate biomarker for Alzheimer's disease. *BMC Neurol* 7: 14. PMID: [17565664](#)
- van Oijen M, Witteman JC, Hofman A, Koudstaal PJ, Breteler MM (2005) Fibrinogen is associated with an increased risk of Alzheimer disease and vascular dementia. *Stroke* 36: 2637–2641. PMID: [16269641](#)
- Jung SM, Lee K, Lee JW, Namkoong H, Kim HK, et al. (2008) Both plasma retinol-binding protein and haptoglobin precursor allele 1 in CSF: candidate biomarkers for the progression of normal to mild cog-nitive impairment to Alzheimer's disease. *Neurosci Lett* 436: 153–157. doi: [10.1016/j.neulet.2008.03.010](#) PMID: [18378077](#)
- Johnson G, Brane D, Block W, van Kammen DP, Gurklis J, et al. (1992) Cerebrospinal fluid protein variations in common to Alzheimer's disease and schizophrenia. *Appl Theor Electrophor* 3: 47–53. PMID: [1282367](#)
- Castano EM, Roher AE, Esh CL, Kokjohn TA, Beach T (2006) Comparative proteomics of cerebrospi-nal fluid in neuropathologically-confirmed Alzheimer's disease and non-demented elderly subjects. *Neurol Res* 28: 155–163. PMID: [16551433](#)
- Yu HL, Chertkow HM, Bergman H, Schipper HM (2003) Aberrant profiles of native and oxidized glyco-proteins in Alzheimer plasma. *Proteomics* 3: 2240–2248. PMID: [14595822](#)

- Arai T, Miklossy J, Klegeris A, Guo JP, McGeer PL (2006) Thrombin and prothrombin are expressed by neurons and glial cells and accumulate in neurofibrillary tangles in Alzheimer disease brain. *J Neuropathol Exp Neurol* 65: 19–25. PMID: [16410745](#)
- Grammas P, Samany PG, Thirumangalakudi L (2006) Thrombin and inflammatory proteins are elevated in Alzheimer's disease microvessels: implications for disease pathogenesis. *J Alzheimers Dis* 9: 51–58. PMID: [16627934](#)
- Akiyama H, Ikeda K, Kondo H, McGeer PL (1992) Thrombin accumulation in brains of patients with Alzheimer's disease. *Neurosci Lett* 146: 152–154. PMID: [1491781](#)
- Puchades M, Hansson SF, Nilsson CL, Andreasen N, Blennow K, et al. (2003) Proteomic studies of potential cerebrospinal fluid protein markers for Alzheimer's disease. *Brain Res Mol Brain Res* 118: 140–146. PMID: [14559363](#)
- Davidsson P, Westman-Brinkmalm A, Nilsson CL, Lindbjör M, Paulson L, et al. (2002) Proteome analysis of cerebrospinal fluid proteins in Alzheimer patients. *Neuroreport* 13: 611–615. PMID: [11973456](#)

Scaffold False Discovery Rate Analysis

Scaffold Version: Scaffold_4.3.4

Protein Grouping Strategy: Experiment-wide grouping with binary peptide-protein weights

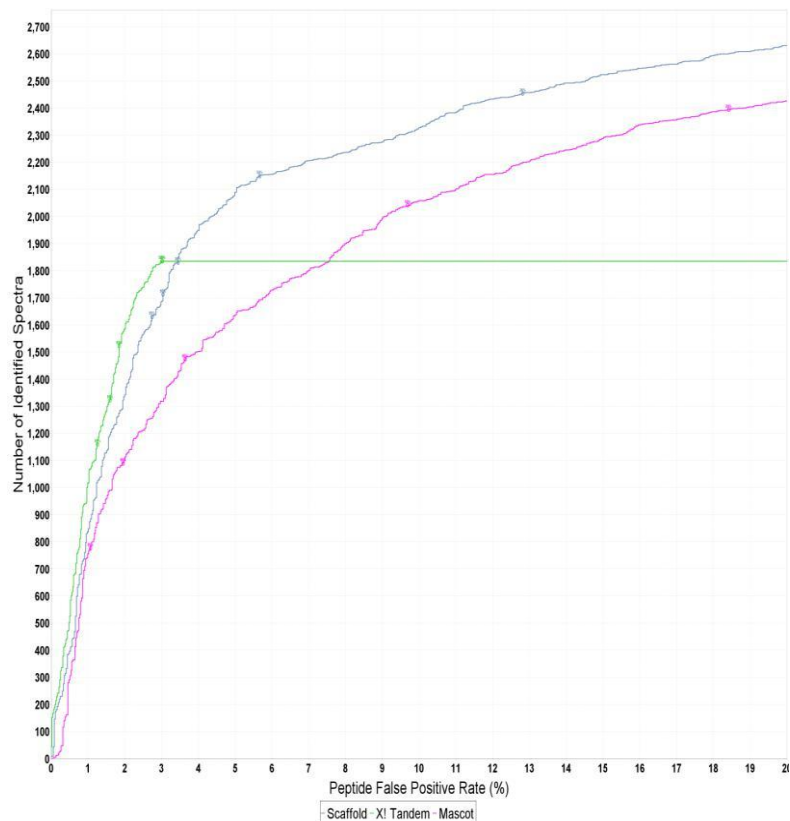
Peptide Thresholds: 95.0% minimum

Protein Thresholds: 99.0% minimum and 2 peptides minimum

107 Proteins identified at 99.0% minimum

Peptide FDR: 5.2% (Prophet)

Figure S1 - Scaffold Peptide ROC Plot



Supplementary Methods S1

Detailed Mass Spectrometry Protocol for Proteomic Analysis of Human Control, MCI and AD Plasma

Digested peptides were separated by nano-LC using a Cap-LC autosampler system (Waters, Milford MA). Samples (5 μ l) were concentrated and desalted onto a micro C18 precolumn (500 μ m x 2 mm, Michrom Bioresources, Auburn, CA) with H₂O:CH₃CN (98:2, 0.05 % HFBA) at 15 μ l/min. After a 4 min wash the precolumn was automatically switched (Valco 10 port valve, Houston, TX) into line with a fritless nano column (75 μ m x ~12 cm) containing Magic C18 (~10cm, 200Å, Michrom) manufactured according to Gatlin [35]. Peptides were eluted using a linear gradient of H₂O:CH₃CN (98:2, 0.1 % formic acid) to H₂O:CH₃CN (55:45, 0.1 % formic acid) at ~300 nl/min over 30 min. The precolumn was connected via a fused silica capillary (10 cm, 25 μ) to a low volume tee (Upchurch Scientific) where HV (2400 V) was applied and the column tip positioned ~ 1 cm from the Z-spray inlet of a QToF Ultima API hybrid tandem mass spectrometer (Micromass, Manchester, UK). Positive ions were generated by electrospray and the QToF operated in data dependent acquisition mode (DDA). A ToF MS survey scan was acquired (m/z 350-1700, 1 s) and the 2 largest multiply charged ions (counts > 20) were sequentially selected by Q1 for MS-MS analysis. Argon was used as collision gas and an optimum collision energy chosen (based on charge state and mass). Tandem mass spectra were accumulated for up to 2 s (m/z 50-2000).

Detailed Mass Spectrometry Protocol for iTRAQ Proteomic Analysis of Cell Lysates Treated with Human Control, MCI and AD Plasma

Chromatography was performed using an LC Packings capillary HPLC system (Dionex, Amsterdam, Netherlands), comprised of an Ultimate pump system, Switchos valve unit and Famos autosampler. Samples (iTRAQ labelled peptide mixtures) were captured onto a C18 pre-column cartridge (500 μ m x 2 mm, Michrom Bioresources, Auburn, CA). After a 10 min wash to remove any residual buffers or salts, the pre-column was automatically switched into line with a capillary column (75 μ m x ~12 cm) containing C18 reverse phase packing material (ReproSil-Pur 120 C18-AQ, 1.9 μ M, Dr Maisch, Ammerbuch-Entringen, Germany). Peptides were eluted using a 240 min linear gradient of H₂O:CH₃CN (98:2, 0.1 % formic acid) to H₂O:CH₃CN (20:80, 0.1 % formic acid) at ~300 nl/min. The precolumn was connected via a fused silica capillary (10 cm, 25 μ) to a low

volume tee (Upchurch Scientific, WA, USA) where high voltage (2300 V) was applied and the column tip positioned ~ 1 cm from the spray inlet of a TripleTOF 5600 hybrid tandem mass spectrometer (ABSciex, CA, USA). Positive ions were generated by electrospray and the instrument operated in information dependent acquisition (IDA) mode. A TOF MS survey scan was acquired (m/z 350-1700, 0.75 s) and the three largest multiply charged ions (counts > 20, charge state ≥ 2 and ≤ 4) were sequentially selected by Q1 for MS-MS analysis. Nitrogen was used as collision gas and an optimum collision energy automatically chosen (based on charge state and mass). Tandem mass spectra were accumulated for up to 2.5 s (m/z 65-2000).

Table S1 - Normalised Total Spectra Counts for Control, MCI and AD plasma using Scaffold v4.3.4 (significantly altered proteins in bold)

#	Identified Proteins (107)	Accession Number	AD plasma replicates				MCI Plasma replicates				Control plasma replicates			
			AD1	AD2	AD3	AD4	MCI1	MCI2	MCI3	MCI4	C1	C2	C3	C4
1	Alpha-2-macroglobulin precursor gi 112911 (+2)		100.27	99.586	119.25	107.24	131.22	99.621	116.67	104.21	149.75	162.1	122.29	98.57
2	apolipoprotein B precursor [Ho gi 105990532 (+1)		93.535	112.74	89.439	89.941	131.95	124.53	90.063	73.558	74.876	93.006	57.683	95.39
3	Chain A, Human Serum Albumin gi 122920512 (+4)		86.052	115.24	83.051	65.726	137.05	132.62	75.735	67.428	81.562	90.349	73.834	71.543
4	complement component 3 prec gi 115298678		94.283	84.554	112.86	103.78	110.08	104.6	112.58	112.38	116.33	102.31	124.6	111.29
5	keratin 1 [Homo sapiens], gi 39 gi 11935049		53.876	57.622	83.051	53.619	35.721	39.226	96.204	149.16	52.815	47.832	101.52	71.543
6	fibrinogen, alpha polypeptide is gi 11761629 (+2)		39.659	30.69	40.461	32.863	32.076	29.886	47.078	34.736	31.421	30.559	41.532	41.336
7	proapolipoprotein gi 178775		41.155	35.701	27.684	34.593	46.657	39.848	28.656	28.606	63.511	53.146	23.073	31.797
8	hCG2001591 [Homo sapiens] gi 119623974 (+2)		41.155	35.074	29.813	39.782	39.367	43.584	30.703	32.692	36.77	39.195	29.995	42.926
9	Chain A, Trypsin In Complex Wit gi 110590762 (+3)		23.945	17.537	10.648	17.296	29.889	29.264	12.281	6.1298	40.112	35.209	16.151	22.258
10	fibrinogen, beta chain prepropr gi 70906435		36.666	30.69	63.885	41.511	34.263	31.754	34.797	42.909	32.758	27.902	50.761	47.695
11	keratin 10 (epidermolytic hyper gi 119581085 (+2)		26.938	40.711	53.238	13.837	18.225	15.566	47.078	63.342	28.079	20.594	64.605	28.617
12	similar to Keratin, type I cytoske gi 114667176		19.455	21.295	27.684	20.756	13.851	17.434	32.75	67.428	20.725	21.923	34.61	12.719
13	fibrinogen gamma chain, isoform gi 119625320 (+4)		29.183	23.174	12.777	13.837	28.431	25.528	20.469	12.26	28.079	30.559	18.459	25.437
14	keratin 2 [Homo sapiens], gi 64 gi 47132620		29.183	27.558	63.885	19.026	19.683	21.169	55.266	55.169	31.421	24.58	46.146	27.027
15	ceruloplasmin (ferroxidase), isoform gi 119599289 (+3)		23.945	21.921	17.036	13.837	23.328	20.547	18.422	12.26	16.713	17.937	13.844	17.488
16	Fibronectin 1 [Homo sapiens], g gi 109658664 (+11)		32.924	38.206	29.813	27.674	19.683	18.056	14.328	8.1731	18.719	19.266	18.459	19.078
17	Complement factor H precursor gi 158517847 (+3)		20.204	13.779	23.425	22.485	19.683	7.4716	22.516	20.433	14.039	18.601	23.073	19.078
18	inter-alpha (globulin) inhibitor H gi 119606782 (+3)		19.455	22.548	8.518	15.567	9.4771	10.585	12.281	8.1731	11.365	15.944	11.537	12.719
19	hemopexin [Homo sapiens], gi gi 11321561 (+6)		11.224	12.527	10.648	5.1889	15.309	14.943	14.328	8.1731	16.045	16.608	11.537	9.539
20	inter-alpha (globulin) inhibitor H gi 119585668 (+3)		20.952	10.648	17.036	13.837	14.58	11.83	14.328	10.216	13.371	12.622	9.2293	20.668
21	Chain A, Crystal Structure Of Th gi 28373620 (+1)		14.217	11.9	8.518	10.378	11.664	13.075	8.1875	12.26	15.376	13.951	9.2293	15.898
22	inter-alpha (globulin) inhibitor H gi 119585664 (+1)		13.469	20.042	12.777	10.378	10.206	12.453	16.375	16.346	7.3539	11.294	16.151	11.129
23	Chain A, Tertiary Structures Of T gi 2098257 (+3)		15.714	12.527	17.036	15.567	17.496	13.698	10.234	10.216	16.713	15.28	18.459	17.488
24	Complement factor B [Homo sa gi 13278732 (+2)		11.224	8.7686	4.259	5.1889	6.5611	9.9621	2.0469	4.0866	10.028	11.294	4.6146	6.3594
25	Chain I, 2.5a Crystal Structure O gi 52695711 (+1)		12.721	11.274	8.518	12.107	13.122	11.207	6.1407	6.1298	10.028	7.972	6.922	17.488
26	apolipoprotein A-IV precursor [gi 178757 (+2)		11.224	9.3949	2.1295	1.7296	10.206	8.7168	4.0938	4.0866	9.3595	8.6363	2.3073	4.7695
27	gelsolin isoform 32 gi 114626427 (+2)		11.972	7.5159	4.259	10.378	10.206	9.9621	8.1875	10.216	8.691	9.9649	4.6146	6.3594

28 Chain A, Crystal Structure Of Cle gi 443345	6.7345	5.6369	12.777	19.026	5.1031	6.8489	14.328	10.216	4.0112	6.6433	16.151	12.719
29 complement component 1 inhi gi 114642584 (+8)	9.7276	7.5159	10.648	17.296	8.0191	7.4716	6.1407	8.1731	8.0225	9.9649	9.2293	12.719
30 Complement component 5 [Ho gi 109731812 (+2)	5.9862	6.2633	4.259	8.6482	5.1031	5.6037	4.0938	6.1298	8.0225	8.6363	2.3073	11.129
31 Alpha-1B-glycoprotein precursor gi 46577680 (+1)	6.7345	6.2633	10.648	6.9185	8.0191	6.8489	10.234	8.1731	6.6854	6.6433	4.6146	6.3594
32 plasminogen gi 387026 (+1)	6.7345	8.7686	2.1295	0	4.3741	8.7168	4.0938	0	5.3483	8.6363	6.922	1.5898
33 Kininogen 1 [Homo sapiens] gi 37748641 (+2)	8.9794	6.2633	6.3885	12.107	9.4771	4.981	2.0469	6.1298	4.6798	5.979	11.537	6.3594
34 apolipoprotein E mutant E3K gi 364011 (+1)	6.7345	5.6369	10.648	5.1889	4.3741	5.6037	8.1875	6.1298	4.0112	5.3146	9.2293	9.539
35 alpha-1-microglobulin/bikunin p gi 4502067 (+1)	6.7345	6.8896	4.259	5.1889	5.8321	6.2263	4.0938	2.0433	5.3483	4.6503	6.922	3.1797
36 coagulation factor II (thrombin) gi 119588383 (+4)	4.4897	5.6369	6.3885	8.6482	5.8321	6.2263	4.0938	6.1298	8.691	9.3006	13.844	9.539
37 Angiotensinogen (serpin peptid gi 15079348 (+10)	9.7276	8.1422	10.648	8.6482	8.0191	7.4716	10.234	8.1731	8.0225	8.6363	4.6146	7.9492
38 alpha-1-acid glycoprotein 1 prec gi 1197209 (+2)	6.7345	6.2633	4.259	3.4593	7.2901	5.6037	4.0938	4.0866	2.0056	5.979	2.3073	6.3594
39 Alpha-2-HS-glycoprotein precu gi 112910 (+2)	6.7345	3.758	6.3885	6.9185	8.0191	4.3584	8.1875	2.0433	6.6854	5.3146	11.537	11.129
40 haptoglobin, isoform CRA_a [Ho gi 119579598	9.7276	2.5053	2.1295	3.4593	6.5611	7.4716	4.0938	2.0433	3.3427	1.993	2.3073	1.5898
41 apolipoprotein H precursor [Ho gi 153266841 (+2)	5.238	4.3843	0	1.7296	2.916	4.3584	2.0469	0	2.6742	5.3146	0	4.7695
42 apolipoprotein J precursor gi 178855 (+6)	4.4897	1.879	2.1295	1.7296	3.645	2.4905	4.0938	4.0866	2.6742	1.993	0	7.9492
43 Chain A, The Structure Of Penta gi 576259	4.4897	5.0106	4.259	3.4593	3.645	3.1132	6.1407	4.0866	4.0112	5.979	2.3073	3.1797
44 apolipoprotein D, apoD [human gi 619383	2.9931	2.5053	4.259	3.4593	2.916	1.8679	4.0938	2.0433	2.6742	2.6573	4.6146	0
45 retinol binding protein 4, plasm gi 119570453 (+6)	2.9931	2.5053	2.1295	1.7296	1.458	3.7358	0	0	2.6742	2.6573	2.3073	1.5898
46 paraoxonase 1 [Homo sapiens], gi 19923106	4.4897	2.5053	4.259	1.7296	5.1031	2.4905	4.0938	4.0866	4.0112	3.3216	4.6146	1.5898
47 Vitronectin [Homo sapiens], gi gi 13477169 (+2)	2.9931	3.1316	6.3885	3.4593	3.645	4.3584	4.0938	6.1298	3.3427	4.6503	6.922	3.1797
48 complement component 4 bind gi 4502503	3.7414	3.1316	4.259	6.9185	3.645	3.7358	4.0938	2.0433	4.6798	2.6573	4.6146	4.7695
49 histidine-rich glycoprotein precu gi 4504489	4.4897	6.8896	0	1.7296	1.458	1.8679	4.0938	4.0866	2.0056	1.993	6.922	3.1797
50 Keratin, type I microfibrillar 48 k gi 125090	0	0	0	17.296	0	6.2263	0	0	0.6685	3.986	0	0
51 similar to afamin gi 114594313 (+1)	2.9931	3.758	2.1295	0	1.458	3.1132	2.0469	4.0866	1.3371	1.993	4.6146	3.1797
52 complement component 6, isof gi 119576417 (+4)	4.4897	3.1316	0	6.9185	2.916	1.8679	4.0938	0	2.6742	2.6573	4.6146	1.5898
53 unnamed protein product [Hom gi 158261613 (+1)	4.4897	3.1316	2.1295	1.7296	3.645	3.7358	2.0469	2.0433	3.3427	2.6573	0	7.9492
54 type II intermediate-filament pr gi 246276	0	0	0	19.026	0	4.981	0	0	0	0	0	0
55 complement component 7, isof gi 119576411 (+4)	3.7414	4.3843	2.1295	3.4593	1.458	3.7358	4.0938	2.0433	2.6742	3.3216	0	1.5898
56 heparin cofactor II isoform 1 [Pa gi 114685230 (+5)	1.4966	1.2527	2.1295	0	1.458	0.6226	0	2.0433	0.6685	1.3287	2.3073	4.7695
57 complement component 9, isof gi 119576390 (+3)	5.238	3.758	2.1295	3.4593	4.3741	3.7358	4.0938	2.0433	2.6742	2.6573	4.6146	6.3594
58 complement component 1, q su gi 150036344 (+5)	2.9931	1.879	2.1295	1.7296	2.916	1.8679	2.0469	2.0433	2.0056	2.6573	0	3.1797
59 serine (or cysteine) proteinase i gi 114665618 (+6)	2.2448	1.879	2.1295	3.4593	1.458	1.8679	4.0938	2.0433	2.0056	0.6643	6.922	7.9492
60 unnamed protein product [Hom gi 16553735 (+2)	2.2448	1.2527	4.259	3.4593	1.458	1.8679	4.0938	2.0433	1.3371	2.6573	4.6146	4.7695

61	inter-alpha (globulin) inhibitor H gi 119585666 (+5)	1.4966	1.2527	2.1295	1.7296	2.187	1.8679	2.0469	0	1.3371	1.3287	2.3073	3.1797
62	Complement component 8, gam gi 109731764 (+4)	2.2448	1.2527	2.1295	1.7296	1.458	1.2453	4.0938	2.0433	2.6742	1.3287	0	3.1797
63	unnamed protein product [Hom gi 1335054	2.2448	0.6263	0	0	1.458	1.2453	8.1875	6.1298	2.0056	1.993	2.3073	3.1797
64	serum amyloid A4, constitutive gi 10835095 (+3)	2.9931	1.2527	2.1295	0	0	1.8679	0	2.0433	0.6685	0.6643	0	1.5898
65	keratin 5 [Homo sapiens], gi 14 gi 119395754 (+1)	0	10.021	4.259	0	0	0	6.1407	6.1298	5.3483	0	2.3073	6.3594
66	hCG2040284 [Homo sapiens] gi 119598461 (+2)	2.2448	2.5053	0	0	1.458	2.4905	0	0	2.0056	1.3287	0	0
67	alpha-1-acid glycoprotein 2 prec gi 29170378 (+2)	1.4966	1.879	4.259	1.7296	3.645	3.7358	2.0469	0	2.0056	3.986	0	1.5898
68	Complement C1r subcomponen gi 115204 (+6)	2.2448	2.5053	0	1.7296	0.729	1.8679	0	2.0433	1.3371	2.6573	0	1.5898
69	Chain A, Human Apolipoprotein gi 157831482	0	0	0	5.1889	0	0	2.0469	0	0	0	2.3073	0
70	alpha S1 casein gi 159793187 (+6)	0	0	4.259	0	0	0	6.1407	8.1731	0	0	6.922	0
71	similar to Ficolin (collagen/fibrin gi 114555009 (+4)	1.4966	1.879	2.1295	1.7296	1.458	1.2453	2.0469	0	1.3371	1.3287	2.3073	1.5898
72	C-type lectin domain family 3, m gi 156627579 (+2)	0.7483	1.879	0	1.7296	0.729	1.2453	2.0469	0	2.0056	1.3287	2.3073	3.1797
73	protein S (alpha) gi 114588068 (+5)	0	0.6263	0	0	0	1.2453	4.0938	0	0.6685	1.3287	0	1.5898
74	Kallikrein B, plasma (Fletcher fa gi 109659056 (+4)	0	3.1316	0	0	0	1.2453	0	0	2.0056	3.3216	0	0
75	hair type II keratin intermediate gi 1308	0	0	0	20.756	0	8.0942	0	0	0	2.6573	0	0
76	alpha-2-glycoprotein 1, zinc gi 114614917 (+6)	2.2448	1.2527	0	0	1.458	0.6226	0	2.0433	0.6685	0.6643	0	1.5898
77	hypothetical protein LOC50742 gi 134085840	0	0	0	17.296	0	7.4716	0	0	0	0.6643	0	0
78	alpha-2-plasmin inhibitor [Hom gi 115583663 (+5)	0	1.2527	0	0	1.458	0.6226	0	0	1.3371	0.6643	2.3073	0
79	apolipoprotein M [Homo sapien gi 22091452 (+1)	0.7483	0.6263	0	0	0	1.8679	0	0	0.6685	0	0	0
80	Rubber elongation factor protei gi 132270	0.7483	0	0	1.7296	0	0	4.0938	2.0433	0	1.3287	2.3073	1.5898
81	complement factor B isoform 1 gi 109070536	7.4828	6.8896	2.1295	3.4593	0	6.8489	0	0	6.6854	6.6433	0	0
82	coagulation factor XII (Hageman gi 119605410 (+6)	1.4966	0.6263	0	1.7296	0	0	0	0	0	0	0	1.5898
83	hypothetical protein LOC53959 gi 149642659	0	0	0	17.296	0	7.4716	0	0	0	0	0	0
84	Chain A, Thyroxine-Binding Glob gi 114793604 (+5)	0.7483	1.2527	0	0	0.729	1.2453	0	0	0.6685	0.6643	0	0
85	complement component 2 prec gi 14550407 (+4)	2.9931	2.5053	2.1295	3.4593	0	1.2453	0	2.0433	0	0	0	0
86	keratin 6A [Homo sapiens] gi 114644568 (+5)	6.7345	11.274	0	0	0	0	0	6.1298	8.0225	0	0	4.7695
87	pregnancy-zone protein isoform gi 114643429 (+4)	0	0	0	10.378	14.58	12.453	14.328	12.26	18.051	17.273	0	9.539
88	hypothetical protein isoform 2 gi 114654573 (+4)	1.4966	1.2527	0	0	2.187	1.8679	0	0	0.6685	0	0	1.5898
89	Chain A, Structural Changes Of T gi 1065033 (+143)	0.7483	0.6263	2.1295	0	0.729	1.2453	0	0	0.6685	0.6643	2.3073	0
90	hemoglobin alpha-1 globin chai gi 13650074 (+22)	0.7483	0.6263	0	1.7296	0	1.2453	2.0469	0	0	0	0	3.1797
91	lumican isoform 1 gi 114646184 (+4)	0.7483	1.879	0	0	0	0	0	0	0	0	2.3073	0
92	unnamed protein product [Hom gi 158257796 (+3)	0	2.5053	0	0	0	0	0	0	1.3371	2.6573	0	0
93	complement component 8, beta gi 119627047 (+4)	1.4966	1.2527	0	1.7296	0.729	0	2.0469	0	0	0	0	1.5898

94	similar to Fibrinogen beta chain	gi 119908847	2.9931	3.1316	0	0	0	3.1132	0	0	3.3427	1.993	6.922	0
95	similar to apolipoprotein F	gi 114644115 (+3)	0.7483	0	0	0	0	1.2453	2.0469	0	0	0.6643	0	1.5898
96	lipoprotein CIII	gi 224917	0	0.6263	4.259	3.4593	0	0	0	0	0	0	4.6146	0
97	Human Vitamin D Binding Prote	gi 18655424 (+1)	13.469	11.9	8.518	10.378	0	13.075	0	12.26	14.039	0	0	15.898
98	complement component 8, alph	gi 114556800 (+5)	0.7483	1.2527	0	1.7296	0	0.6226	0	0	0.6685	0	0	0
99	attractin, isoform CRA_b [Homo	gi 119630936 (+6)	0	0	0	0	0	0	2.0469	2.0433	0	1.3287	2.3073	0
100	keratin associated protein 13.1	gi 41350563	0	0	0	6.9185	0	0.6226	0	0	0	0	0	0
101	hair keratin A1	gi 115495167	0	0	0	13.837	0	6.8489	0	0	0	0	0	0
102	fibulin 1 isoform 3	gi 109094533 (+5)	0.7483	0.6263	0	0	0	0.6226	0	0	1.3371	0	0	0
103	similar to fibrinogen, gamma ch	gi 73977992 (+2)	0	8.1422	0	6.9185	0	0	0	0	0	0	0	12.719
104	hypothetical protein	gi 119922176 (+2)	0	0	0	6.9185	0	0.6226	0	0	0	0	0	0
105	Chain A, Apo-Human Serum Tra	gi 110590597 (+6)	0	1.879	0	0	0	0	0	0	0	0	0	0
106	Chain A, Yeast Alcohol Dehydro	gi 112491285 (+4)	0	1.2527	0	0	0	0	0	0	0	0	0	0
107	Keratin-associated protein 11-1	gi 52783049	0	0	0	5.1889	0	0	0	0	0	0	0	0

Charge state deconvolution and deisotoping were not performed. All MS/MS samples were analysed using Mascot (Matrix Science, London, UK). Mascot was set up to search the NCBI nr database (33055681 entries). Mascot was searched with a fragment ion mass tolerance of 0.20Da and a parent tolerance of 0.25Da. Oxidation of methionine and iodoacetamide derivative of cysteine were specified as variable modifications.

Scaffold was used to validate MS/MS based peptide and protein identifications. Peptide identifications were accepted if they could be established at greater than 95.0% probability by the Peptide Prophet algorithm. Protein identifications were accepted if they could be established at greater than 99.0% probability and contained at least 2 identified peptides. Protein probabilities were assigned by the Protein Prophet algorithm.

Table S2 - Protein Summary for iTRAQ Experiment with microglia treated with human control, MCI and AD plasma from Protein Pilot v4.0

114: Microglia treated with Control Plasma replicate 1; **115:** Microglia treated with MCI plasma replicate 1; **116:** Microglia treated with AD plasma replicate 1 **117:** Microglia treated with Fetal Bovine Serum
118: Microglia treated with Control plasma replicate 2; **119:** Microglia treated with MCI plasma replicate 2; **121:** Microglia treated with AD plasma replicate 2

Upregulated proteins are shown in red and downregulated proteins are shown in blue

Unused	%Cov (95)	Accession	Name	Peptides (95%)	114:117	PVal 114:117	115:117	PVal 115:117	116:117	PVal 116:117	118:117	PVal 118:117	119:117	PVal 119:117	121:117	PVal 121:117
	72.54	gi 7669492	glyceraldehyde-3-phosphate dehydrogenase isoform 1 [Homo sapiens]	62	0.97414	0.52389	0.9826	0.676093	1.273859	3.43E-05	1.02487	0.60275	0.976086	0.65477	1.31801	0.0001
64.83	76.27	gi 4503571	alpha-enolase isoform 1 [Homo sapiens]	62	0.9323	0.11964	0.98826	0.719005	1.192321	0.00027	0.98271	0.75327	0.97853	0.55307	1.22469	0.000105
	55.88	gi 4505763	phosphoglycerate kinase 1 [Homo sapiens]	27	1.07208	0.17501	1.0474	0.279231	1.203913	7.01E-05	1.04557	0.32215	1.062029	0.20679	1.30616	0.000111
	61.48	gi 342187211	fructose-bisphosphate aldolase A isoform 2 [Homo sapiens]	27	0.98961	0.82864	1.01971	0.836449	1.204599	0.00446	1.00107	0.9894	1.000761	0.99085	1.2183	0.001405
77.64	69.11	gi 33286418	pyruvate kinase isozymes M1/M2 isoform a [Homo sapiens]	49	0.97698	0.74623	1.00909	0.869057	1.22076	0.00752	1.02407	0.72615	1.027908	0.59976	1.2245	0.001615
49.96	46.39	gi 4507521	transketolase isoform 1 [Homo sapiens]	34	0.9812	0.68558	1.04368	0.323134	1.130957	0.02218	1.01055	0.88087	0.987174	0.74884	1.15666	0.001681
74.49	23.07	gi 38176300	nestin [Homo sapiens]	42	0.98677	0.77329	0.96911	0.518102	0.943442	0.17346	0.99888	0.98412	1.036204	0.35449	0.85376	0.004498

37.03	38.85	gi 66933005	calnexin precursor [Homo sapiens] elongation factor 1-	22	0.99713	0.94162	0.94451	0.31514	0.924302	0.26575	0.9798	0.70005	0.932549	0.14875	0.87883	0.010136
	72.51	gi 4503471	alpha 1 [Homo sapiens] cytoskeleton-	54	0.96687	0.49315	0.93464	0.225032	1.131237	0.0241	1.02401	0.75967	0.967436	0.56314	1.24135	0.014366
	29.73	gi 19920317	associated protein 4 [Homo sapiens] protein disulfide-	17	0.84689	0.04873	0.92014	0.229067	0.736276	0.0001	0.76848	0.01158	0.78562	0.03204	0.76711	0.018819
30.5	47.73	gi 5031973	isomerase A6 precursor [Homo sapiens]	22	0.9654	0.42869	0.944	0.133813	0.957242	0.54622	0.97927	0.66221	1.002759	0.95171	0.90975	0.019165
20.99	59.3	gi 4505591	peroxiredoxin-1 [Homo sapiens]	15	1.01122	0.8714	1.00843	0.871252	1.071734	0.22303	0.95462	0.37925	0.963405	0.47862	1.1723	0.021238
	13.15	gi 214010226	40S ribosomal protein S24 isoform d [Homo sapiens]	4	0.67916	0.06245	0.75061	0.010725	0.60023	0.06339	0.66105	0.01456	0.664317	0.08515	0.63548	0.021809
18.45	46.15	gi 4506713	ubiquitin-40S ribosomal protein S27a precursor [Homo sapiens]	11	0.98274	0.73773	1.05902	0.285887	0.836245	0.0664	0.82362	0.15854	1.037765	0.59399	0.77292	0.022464
	19.9	gi 66346681	plasminogen activator inhibitor 1 RNA- binding protein isoform 2 [Homo sapiens]	7	1.04273	0.58745	1.00011	0.999016	0.966927	0.6123	0.98868	0.92202	0.927851	0.47639	0.78652	0.023336
21.89	15.51	gi 44680105	caldesmon isoform 1 [Homo sapiens]	11	0.90827	0.1536	0.89843	0.174139	0.874096	0.0854	0.97455	0.77315	0.936821	0.47815	0.85601	0.026671
41.45	38.13	gi 4505257	moesin [Homo sapiens]	23	1.07974	0.26539	1.11677	0.105786	1.224702	0.02088	1.13547	0.24289	1.029872	0.72063	1.20124	0.028037
38.53	62.14	gi 4502101	annexin A1 [Homo sapiens]	23	1.00008	0.99855	0.92705	0.161224	0.872665	0.02261	0.98702	0.84843	1.015028	0.79418	0.8338	0.042088
17.57	59.43	gi 4503057	alpha-crystallin B chain [Homo sapiens]	12	1.03866	0.42864	1.04427	0.449927	1.237261	0.00212	1.02433	0.71835	0.994397	0.93124	1.26081	0.042824
2.32	12.63	gi 54792069	small ubiquitin- related modifier 2 isoform a precursor [Homo sapiens]	2	1.14799	0.29051	1.45937	0.083382	1.231096	0.26043	1.01658	0.94786	1.407796	0.05217	1.28827	0.043238

9.54	13.73	gi 109637759	calpastatin isoform f [Homo sapiens]	7	0.86253	0.228	0.80906	0.239705	0.817004	0.20571	0.74525	0.1378	0.884395	0.46022	0.74361	0.045267
	22.73	gi 4557585	fatty acid-binding protein, brain [Homo sapiens]	4	0.85065	0.21974	0.79912	0.227698	0.90105	0.24714	0.84292	0.17597	0.873763	0.35343	0.83176	0.049333
	24.27	gi 4503143	cathepsin D preproprotein [Homo sapiens]	10	0.95791	0.58116	1.0536	0.628932	1.106723	0.5541	1.06446	0.69411	0.9615	0.74084	1.16945	0.058726
50.95	32.2	gi 153792590	heat shock protein HSP 90-alpha isoform 1 [Homo sapiens]	33	1.03008	0.67865	1.06218	0.512408	1.299528	0.03574	1.04757	0.60122	1.055205	0.4726	1.20463	0.058983
45.71	56.44	gi 21361657	protein disulfide- isomerase A3 precursor [Homo sapiens]	37	0.9619	0.42744	0.89756	0.012721	0.924691	0.11729	0.98181	0.65258	0.995083	0.87086	0.89188	0.059792
14.84	80	gi 5032057	protein S100-A11 [Homo sapiens]	16	1.04077	0.52822	0.94971	0.423999	0.863005	0.05467	1.04763	0.46558	0.98643	0.82636	0.86681	0.060101
15.61	63.49	gi 31543380	protein DJ-1 [Homo sapiens]	8	0.87038	0.05065	1.0421	0.587302	1.041927	0.75125	0.95154	0.45415	0.994383	0.95366	1.16939	0.069841
	57.3	gi 66392203	NME1-NME2 protein [Homo sapiens]	11	1.05003	0.63669	1.05967	0.740323	1.119333	0.36696	1.10984	0.37772	1.046986	0.7303	1.22055	0.086404
	38.67	gi 20149594	heat shock protein HSP 90-beta [Homo sapiens]	33	0.94769	0.31531	1.04297	0.30697	1.114919	0.12151	1.03159	0.49331	1.024515	0.70189	1.12563	0.088957
11.8	13.04	gi 56699409	RNA-binding motif protein, X chromosome isoform 1 [Homo sapiens]	6	0.92096	0.49133	0.87494	0.158879	0.877598	0.12292	1.0088	0.9293	0.966318	0.74655	0.87719	0.094431
	48.24	gi 5803225	14-3-3 protein epsilon [Homo sapiens]	16	1.02601	0.76029	0.91136	0.328953	1.11497	0.15435	0.96656	0.78874	0.960346	0.44181	1.14985	0.097089
52.59	69.47	gi 50845388	annexin A2 isoform 1 [Homo sapiens]	52	1.03601	0.33861	0.89261	0.000799	0.952177	0.19231	1.09683	0.02102	0.986273	0.64679	0.93349	0.100108
7.85	53.99	gi 4885375	histone H1.2 [Homo sapiens]	16	0.87375	0.05937	0.7433	0.00219	0.542623	0.00103	0.73003	0.00159	0.947048	0.46755	0.75976	0.101682

24.44	gi 4506661	60S ribosomal protein L7a [Homo sapiens]	6	1.12561	0.37809	1.10248	0.529482	1.115835	0.16495	1.03566	0.61818	1.010542	0.93949	1.25406	0.104774	
65.26	54.13	gi 16507237	78 kDa glucose-regulated protein precursor [Homo sapiens]	42	0.99068	0.80644	0.91924	0.037995	0.914667	0.10089	0.97414	0.72851	0.975383	0.64284	0.90792	0.107537
65.68	gi 21735621	malate dehydrogenase, mitochondrial precursor [Homo sapiens]	21	0.98306	0.72628	0.96187	0.550987	1.082983	0.19161	0.99879	0.98249	1.003288	0.95569	1.09901	0.108722	
6.298	gi 4504763	integrin alpha-V isoform 1 precursor [Homo sapiens]	6	1.10731	0.34169	1.50407	0.12905	0.922235	0.67208	1.35084	0.4102	1.65825	0.06426	1.25584	0.110681	
3.27	3.004	gi 38327625	citrate synthase, mitochondrial precursor [Homo sapiens]	2	0.90179	0.42891	1.04244	0.800114	0.948916	0.85177	1.10885	0.48796	0.896501	0.31286	1.30983	0.112072
1.04	gi 4505541	general vesicular transport factor p115 [Homo sapiens]	1	1.03	0.9444	1.16908	0.359291	1.468988	0.16016	1.34375	0.59047	1.403052	0.25749	1.86084	0.114754	
11.64	4.447	gi 223029410	talin-1 [Homo sapiens]	7	0.7748	0.08765	1.01838	0.916424	0.810045	0.62668	0.53988	0.04862	0.830302	0.16782	0.80491	0.115327
15.01	30.56	gi 24431933	reticulon-4 isoform B [Homo sapiens]	9	1.03261	0.79202	0.92584	0.443218	0.86613	0.3369	0.98962	0.93193	0.999494	0.99403	0.75832	0.118577
40.45	gi 4502389	barrier-to-autointegration factor [Homo sapiens]	3	1.01481	0.90604	0.79065	0.497285	0.785352	0.47056	0.77148	0.48763	1.065285	0.63782	0.60144	0.122476	
21.8	gi 15431297	60S ribosomal protein L13 isoform 1 [Homo sapiens]	6	1.00852	0.94051	1.04466	0.512794	0.999406	0.99678	0.99211	0.96695	1.008986	0.93835	0.85176	0.122519	
6	11.89	gi 169404009	translocon-associated protein subunit alpha precursor [Homo sapiens]	3	0.95232	0.61818	0.87112	0.397806	0.856702	0.23079	1.06776	0.59316	0.959057	0.73145	0.80544	0.122538

4.09	37.5	gi 51036603	guanine nucleotide-binding protein G(I)/G(S)/G(O) subunit gamma-12 precursor [Homo sapiens] peptidyl-prolyl cis-trans isomerase A [Homo sapiens]	3	0.82618	0.40915	0.66391	0.07069	0.823514	0.43842	0.91099	0.71981	0.765134	0.40552	0.64208	0.124749
60.61		gi 10863927	profilin-1 [Homo sapiens]	21	0.98345	0.72502	1.04141	0.522254	1.157293	0.14108	1.04379	0.67672	1.040531	0.7547	1.13552	0.125378
14.61	62.86	gi 4826898	trifunctional enzyme subunit alpha, mitochondrial precursor [Homo sapiens]	11	0.93252	0.25277	0.9354	0.272724	1.1113	0.10339	0.95098	0.4023	0.930043	0.40442	1.13055	0.127681
18.74		gi 20127408	HLA class I histocompatibility antigen, A-1 alpha chain precursor [Homo sapiens]	9	0.93017	0.43003	0.88367	0.537465	0.804996	0.40295	1.0888	0.67464	0.886635	0.51654	0.85087	0.130116
20		gi 24797067	protein transport Sec61 subunit alpha isoform 1 [Homo sapiens]	8	0.88901	0.29354	0.94676	0.494894	0.929581	0.37731	0.97793	0.82815	0.935571	0.41568	0.85741	0.130658
6.37	14.08	gi 7019415	putative pre-mRNA-splicing factor ATP-dependent RNA helicase DHX15 [Homo sapiens]	5	0.79339	0.19075	0.97595	0.796917	0.744264	0.37933	0.62065	0.1723	0.702107	0.27466	0.70581	0.136075
6.289		gi 68509926	probable ATP-dependent RNA helicase DDX17 isoform 1 [Homo sapiens]	5	0.62423	0.18212	0.47583	0.334467	1.130629	0.43257	0.77012	0.46447	0.811996	0.64092	0.49002	0.13646
4.664		gi 38201710		3	0.79915	0.61738	0.91094	0.620215	0.750311	0.21345	0.80939	0.28139	0.780581	0.24321	0.63829	0.138851

5.383	gi 4757732	apoptosis-inducing factor 1, mitochondrial isoform 1 precursor [Homo sapiens]	2	1.38271	0.07172	1.19782	0.407886	1.088847	0.41412	1.28989	0.41554	1.162864	0.38478	1.34436	0.140307
24.62	gi 238776833	THO complex subunit 4 [Homo sapiens]	6	0.83702	0.04946	0.94848	0.403375	0.86749	0.31273	0.87675	0.42273	0.897684	0.40794	0.88435	0.14495
43.94	gi 32189392	peroxiredoxin-2 isoform a [Homo sapiens]	10	1.34013	0.09637	1.27568	0.14954	1.190778	0.02567	1.19692	0.26779	1.15698	0.45387	1.28334	0.145991
2.03	gi 124494254	proliferation-associated protein 2G4 [Homo sapiens]	1	0.96538	0.89731	1.35889	0.039772	1.239406	0.2757	0.98931	0.97425	1.219182	0.19368	1.14722	0.146018
14.1	gi 19923437	GTP:AMP phosphotransferase, mitochondrial isoform a [Homo sapiens]	3	1.39625	0.08317	1.46051	0.046626	1.432712	0.05166	1.27401	0.37104	1.138681	0.44	1.42747	0.148779
20.35 55.61	gi 21361091	ubiquitin carboxyl-terminal hydrolase isozyme L1 [Homo sapiens]	12	0.94536	0.55362	1.07884	0.312914	1.099702	0.14413	0.92686	0.5639	0.969563	0.73363	1.14064	0.149277
11.48	gi 14141159	heterogeneous nuclear ribonucleoprotein H3 isoform b [Homo sapiens]	5	0.8342	0.1545	0.96127	0.711873	0.817383	0.18652	0.86804	0.22181	0.778232	0.09066	0.71379	0.153676
51.55	gi 5729877	heat shock cognate 71 kDa protein isoform 1 [Homo sapiens]	39	1.02418	0.63104	0.9707	0.403987	1.061664	0.19288	0.9861	0.86555	0.965753	0.41121	1.06446	0.153957
23.65	gi 4557032	L-lactate dehydrogenase B chain [Homo sapiens]	6	0.93851	0.60795	1.08169	0.304175	1.185435	0.06437	0.88422	0.54126	1.059711	0.73119	1.12483	0.154941

			non-histone														
5.92	32	gi 48255933	chromosomal protein HMG-14 [Homo sapiens]	3	0.91603	0.6829	0.98843	0.959112	0.811181	0.18646	0.82704	0.40778	0.919272	0.33885	0.87101	0.160101	
13	45.56	gi 4507651	tropomyosin alpha-4 chain isoform 2 [Homo sapiens]	13	0.9197	0.35893	0.94139	0.238868	0.978656	0.86419	0.77351	0.09697	0.898614	0.18298	0.88635	0.160554	
2.03	11.8	gi 15451856	caveolin-1 isoform alpha [Homo sapiens]	1	0.99581	0.97294	0.88967	0.446766	0.866877	0.38527	0.89103	0.45106	0.978481	0.86208	0.68415	0.162168	
7.77	28.87	gi 4506761	protein S100-A10 [Homo sapiens]	6	1.05949	0.39457	0.98038	0.763376	0.915157	0.21142	0.9942	0.92867	1.068271	0.33669	0.83821	0.162865	
	34.94	gi 94721252	vesicle-associated membrane protein-associated protein A isoform 2 [Homo sapiens]	8	1.227	0.01851	0.97704	0.71228	1.185619	0.34812	1.26298	0.03566	1.170574	0.09287	1.22005	0.164682	
8.4	33.14	gi 4507669	translationally-controlled tumor protein [Homo sapiens]	6	1.08576	0.52472	1.09398	0.508183	1.116665	0.46569	1.13494	0.37263	1.084082	0.68352	1.23937	0.170834	
	10.25	gi 25188179	voltage-dependent anion-selective channel protein 3 isoform 1 [Homo sapiens]	3	1.02508	0.91757	1.16013	0.376609	1.484604	0.36729	1.26373	0.25659	0.81173	0.69302	1.54434	0.177514	
	10.84	gi 17158044	40S ribosomal protein S6 [Homo sapiens]	2	0.95076	0.6196	0.82852	0.091434	0.738315	0.04109	0.53979	0.06305	0.69574	0.1722	0.71755	0.1779	
	4.09	gi 33350932	cytoplasmic dynein 1 heavy chain 1 [Homo sapiens]	13	1.57248	0.29762	1.57923	0.217808	1.282865	0.35371	1.80211	0.13401	1.017224	0.96817	1.5064	0.181445	
	7.064	gi 50592988	cytochrome b-c1 complex subunit 2, mitochondrial precursor [Homo sapiens]	2	0.81533	0.4452	0.69962	0.31094	0.740066	0.414	0.68865	0.20942	0.423321	0.20012	0.70978	0.181631	

			T-complex protein 1 subunit epsilon [Homo sapiens]	6	0.88391	0.83878	1.03728	0.930669	1.416377	0.6002	1.44063	0.48371	1.130974	0.78207	0.69751	0.182052
25.85	24.2	gi 19923142	importin subunit beta-1 [Homo sapiens]	17	1.05472	0.72744	1.03584	0.67655	1.133016	0.19697	1.16673	0.15872	0.998602	0.98495	1.13234	0.185815
6.49	17.1	gi 38372925	basigin isoform 2 [Homo sapiens]	4	1.01305	0.85925	1.00488	0.960318	0.988465	0.91265	0.947	0.49923	1.10776	0.58434	0.89814	0.189596
	14.29	gi 78214522	60S ribosomal protein L38 [Homo sapiens]	1	0.96672	0.84305	0.91545	0.719896	0.828098	0.3865	0.66688	0.42456	1.096426	0.88091	0.40804	0.191292
3.66	11.28	gi 5729875	membrane-associated progesterone receptor component 1 [Homo sapiens]	3	1.29932	0.22776	1.19393	0.255245	0.922448	0.82759	1.2013	0.35792	1.273844	0.11659	1.30413	0.191907
1.96	2.809	gi 5803023	vesicular integral-membrane protein VIP36 precursor [Homo sapiens]	1	1.25437	0.44629	0.9238	0.572269	1.003053	0.9813	1.24652	0.57488	0.725378	0.19242	0.72577	0.192623
19.62	28.1	gi 5032093	neutral amino acid transporter B(0) isoform 1 [Homo sapiens]	14	0.99773	0.98539	0.97139	0.597192	0.993195	0.94792	1.06033	0.30024	1.012247	0.93042	0.90298	0.192785
	12.15	gi 7657581	calcium-binding mitochondrial carrier protein Aralar2 isoform 2 [Homo sapiens]	5	1.24309	0.38294	1.04897	0.552228	1.137596	0.35039	1.21757	0.22643	1.018496	0.82502	0.77457	0.197527
	34.01	gi 194248072	heat shock 70 kDa protein 1A/1B [Homo sapiens]	20	1.00579	0.94158	1.09057	0.121139	1.049526	0.65628	1.07026	0.41274	0.957757	0.53605	1.1032	0.200776
	27.06	gi 11321585	guanine nucleotide-binding protein subunit beta-1 [Homo sapiens]	7	0.73007	0.19568	0.64127	0.141431	0.681516	0.19847	0.71464	0.34485	1.037866	0.77339	0.74014	0.204888

11.47	43.36	gi 4885381	histone H1.5 [Homo sapiens]	15	0.83443	0.01052	0.79034	0.005847	0.651536	0.00034	0.77306	0.05702	0.897578	0.16378	0.84588	0.205013
	14.2	gi 156523968	poly [ADP-ribose]	10	1.21558	0.14288	1.17066	0.120212	1.051162	0.47741	1.0265	0.87789	1.061355	0.76352	1.172	0.207123
3.04	3.187	gi 77404397	staphylococcal nuclease domain-containing protein 1 [Homo sapiens]	3	1.17405	0.49812	1.22773	0.468987	1.488215	0.12081	1.08531	0.69621	1.110144	0.54598	1.36789	0.210295
	5.495	gi 4503583	epoxide hydrolase 1 precursor [Homo sapiens]	2	0.84869	0.29741	0.72711	0.197375	1.081442	0.45904	0.87687	0.24494	0.884422	0.60119	0.86167	0.213117
	24.41	gi 9845502	40S ribosomal protein SA [Homo sapiens]	6	1.03724	0.74771	1.08735	0.352101	1.152088	0.1949	1.2666	0.02453	0.950464	0.75669	1.16312	0.215801
	24.35	gi 4506631	60S ribosomal protein L30 [Homo sapiens]	2	1.14158	0.69687	1.10043	0.803557	1.054163	0.80851	1.05796	0.56652	1.038772	0.81646	1.12587	0.218553
8.3	22.18	gi 11559923	eukaryotic translation initiation factor 4H isoform 1 [Homo sapiens]	5	1.12264	0.68798	1.25954	0.340565	1.042103	0.8514	1.01228	0.88499	1.066275	0.614	1.09901	0.225424
13.87	gi 40068518	6-phosphogluconate dehydrogenase, decarboxylating [Homo sapiens]	5	0.81545	0.14339	0.94935	0.623335	1.02256	0.78535	0.79003	0.11995	0.8653	0.35679	0.77777	0.227224	
2.113.371	gi 24797106	FAS-associated factor 2 [Homo sapiens]	1	1.06334	0.65017	1.45771	0.417112	1.365147	0.33565	1.01105	0.94592	1.360478	0.20061	1.30254	0.231693	
	9.594	gi 5453549	peroxiredoxin-4 precursor [Homo sapiens]	3	1.09696	0.59119	1.16346	0.599874	1.087432	0.78277	1.19647	0.61772	1.284313	0.55549	1.31451	0.235158
3.24	7.754	gi 23397429	eukaryotic translation initiation factor 3 subunit M [Homo sapiens]	2	0.89871	0.47538	1.31111	0.222737	1.013742	0.93117	0.81456	0.2861	1.138485	0.56671	1.28961	0.236077

			cleavage and polyadenylation specificity factor subunit 6 [Homo sapiens]	1	0.90214	0.50643	1.11391	0.867037	1.458042	0.54873	1.06447	0.65983	1.296901	0.68157	1.30871	0.236755
			sodium/potassium-transporting ATPase subunit alpha-1 isoform c [Homo sapiens]	18	1.02552	0.80461	1.00024	0.998588	0.844812	0.12679	0.91605	0.50142	0.914821	0.38021	0.91843	0.239598
			chloride intracellular channel protein 1 [Homo sapiens]	6	0.90088	0.30114	0.95147	0.772095	1.09574	0.46797	0.96541	0.77434	0.984818	0.91828	0.88861	0.24316
4.53	6.239	gi 107708703	glucose-6-phosphate 1-dehydrogenase isoform a [Homo sapiens]	2	1.20426	0.33865	1.43066	0.189014	1.624618	0.2636	1.55257	0.22793	1.448891	0.23758	1.30435	0.249744
6.35	24.44	gi 7657532	protein S100-A6 [Homo sapiens]	3	0.98566	0.85809	1.09844	0.296211	1.059034	0.49517	1.03444	0.67966	1.031681	0.7023	1.1115	0.250352
21.3	42.45	gi 5803227	14-3-3 protein theta [Homo sapiens] PREDICTED: POTE ankyrin domain	17	0.97905	0.87629	1.0435	0.605723	0.966232	0.87085	0.92408	0.61253	1.178148	0.16	1.1743	0.251827
2	8.744	gi 88953571	family member I isoform 2 [Homo sapiens]	34	0.86459	0.70652	0.90932	0.524006	0.832067	0.32213	0.85508	0.3682	0.725671	0.19692	0.78485	0.253517
32.32	35.84	gi 5031877	lamin-B1 isoform 1 [Homo sapiens] 3-ketoacyl-CoA	18	0.94349	0.56293	0.90136	0.275431	0.918949	0.44907	0.93501	0.4858	0.893712	0.32872	0.89476	0.254337
5.39	11.56	gi 4501853	thiolase, peroxisomal isoform a [Homo sapiens]	3	2.16834	0.1858	1.18441	0.641874	1.62163	0.13731	1.42343	0.17432	1.2076	0.45654	1.25897	0.259562
	9.246	gi 7661920	eukaryotic initiation factor 4A-III [Homo sapiens]	2	1.29956	0.34769	1.01607	0.902547	1.212463	0.31844	1.27806	0.42026	0.783348	0.76584	0.79002	0.262826
50.42	31.55	gi 55956788	nucleolin [Homo sapiens]	29	1.05759	0.23708	1.02976	0.572142	0.98183	0.74371	1.09084	0.15784	1.007521	0.87671	1.05735	0.263211

2.95	3.655	gi 308818200	di-hydropyrimidinase-related protein 3 isoform 1 [Homo sapiens]	2	1.34309	0.06857	1.2031	0.161372	0.967412	0.85001	1.52203	0.03584	1.210626	0.5645	1.23319	0.263459
	32.08	gi 23308577	phosphoglycerate dehydrogenase [Homo sapiens]	17	1.06596	0.47514	0.97881	0.832898	1.203403	0.08204	1.02448	0.76084	1.029579	0.60888	1.15234	0.267369
25.86	13.07	gi 4758012	clathrin heavy chain 1 [Homo sapiens]	16	0.99052	0.92065	0.94667	0.522496	1.13722	0.24734	0.88892	0.13223	0.916398	0.48145	1.09911	0.268588
	30.23	gi 4502985	cytochrome c oxidase subunit 6B1 [Homo sapiens]	2	0.90839	0.35899	0.88557	0.684512	0.735976	0.10006	0.76604	0.22395	0.772901	0.17148	0.81212	0.274825
	8.225	gi 153945728	microtubule-associated protein 1B [Homo sapiens]	17	0.94326	0.58955	0.9836	0.825151	0.952414	0.62219	0.87584	0.26177	0.900398	0.23709	0.88394	0.275407
	84.33	gi 62414289	vimentin [Homo sapiens]	111	0.96853	0.22969	0.8979	0.00024	0.966613	0.26142	0.99839	0.96544	0.992586	0.77803	0.96001	0.276668
	84.33	gi 62414289	vimentin [Homo sapiens]	111	0.96853	0.22969	0.8979	0.00024	0.966613	0.26142	0.99839	0.96544	0.992586	0.77803	0.96001	0.276668
	27.31	gi 5453555	GTP-binding nuclear protein Ran [Homo sapiens]	5	0.98859	0.87907	1.14585	0.42636	1.194501	0.25584	1.03131	0.69113	0.94485	0.71941	1.14543	0.276881
6.52	14.19	gi 4507171	SPARC precursor [Homo sapiens]	3	0.9158	0.47886	1.02166	0.864754	0.936253	0.51281	0.94402	0.83367	0.974326	0.78471	0.73391	0.27843
32.05	53.69	gi 32189394	ATP synthase subunit beta, mitochondrial precursor [Homo sapiens]	26	1.06947	0.33782	1.02526	0.810252	1.085629	0.19352	1.06683	0.36414	1.062145	0.36963	1.05613	0.282311
	32.7	gi 4502551	calumenin isoform a precursor [Homo sapiens]	11	1.0541	0.35248	0.92044	0.374923	1.046819	0.65407	1.02137	0.84663	1.013005	0.8751	0.90294	0.28484
30.99	46.28	gi 4757900	calreticulin precursor [Homo sapiens]	22	0.97558	0.48559	0.9151	0.110982	0.924536	0.15201	1.02055	0.6353	1.000256	0.99424	0.94295	0.285087

			60S ribosomal protein L24 [Homo sapiens]	2	0.88742	0.57195	0.87413	0.254582	0.97148	0.78669	0.90032	0.34225	0.858709	0.57737	0.81159	0.285288
4.33	12.64	gi 19557691	surfeit locus protein 4 [Homo sapiens]	3	1.07383	0.75128	0.79406	0.111418	0.815363	0.65159	1.00065	0.99896	0.826807	0.64556	0.68096	0.286924
14.4	25.05	gi 34147630	mitochondrial elongation factor Tu, precursor [Homo sapiens]	8	1.24054	0.2593	1.00401	0.978324	1.262414	0.32398	1.23422	0.17278	1.179966	0.2319	1.20203	0.287698
	20	gi 262118227	cytochrome c oxidase subunit 7A2, mitochondrial precursor [Homo sapiens]	2	1.1199	0.72902	0.90201	0.486512	0.756671	0.2722	1.38307	0.18831	0.946541	0.67701	1.2207	0.292914
32.21		gi 5901912	calmodulin [Homo sapiens]	4	0.97733	0.85572	1.0233	0.851035	1.04108	0.74264	0.91374	0.49865	1.008276	0.91537	0.83326	0.292997
5.497		gi 157694492	myb-binding protein 1A isoform 2 [Homo sapiens]	5	1.00363	0.98643	0.9421	0.906806	0.905539	0.52855	1.10364	0.52725	0.925595	0.78667	0.80372	0.296452
4.38	38.46	gi 4504253	histone H2A.X [Homo sapiens]	55	1.02226	0.91213	0.96013	0.770314	0.821872	0.25679	1.0363	0.92006	0.957424	0.76937	0.90772	0.304709
17.58		gi 4506003	serine/threonine- protein phosphatase PP1-alpha catalytic subunit isoform 1 [Homo sapiens]	6	1.48714	0.13004	1.10011	0.713846	1.277277	0.52397	1.33377	0.25545	1.172138	0.4535	1.28387	0.30728
11.93	21.53	gi 42794771	thioredoxin domain- containing protein 5 isoform 1 precursor [Homo sapiens]	7	1.14981	0.0688	1.00059	0.996582	1.070191	0.40696	0.96876	0.79451	0.947137	0.80295	1.09618	0.309544
2.19	4.61	gi 4504619	insulin-like growth factor-binding protein 7 isoform 1 precursor [Homo sapiens]	1	0.84172	0.29423	0.98065	0.834212	1.054621	0.66737	1.60677	0.49731	1.126455	0.67446	0.83734	0.310771

			ornithine aminotransferase, mitochondrial isoform 1 [Homo sapiens] endoplasmic reticulum resident protein 29 isoform 1 precursor [Homo sapiens] NAD(P)H dehydrogenase [quinone] 1 isoform a [Homo sapiens] phosphatidylethanolamine-binding protein 1 preproprotein [Homo sapiens] 60S ribosomal protein L15 isoform 1 [Homo sapiens] 40S ribosomal protein S5 [Homo sapiens] actin, alpha skeletal muscle [Homo sapiens] heat shock protein beta-1 [Homo sapiens] prostaglandin E synthase 3 [Homo sapiens] ATP-dependent RNA helicase A [Homo sapiens]												
7.745	gi 4557809		6	1.24849	0.12014	1.16548	0.620637	1.100635	0.88714	0.97603	0.91645	1.240592	0.14432	1.12319	0.31102
16.48	gi 5803013		4	0.84553	0.25641	1.10238	0.275949	1.055268	0.87182	0.88294	0.27119	0.94896	0.7498	1.17577	0.31394
6.07 16.79	gi 4505415		5	1.36635	0.37502	1.01123	0.930016	1.33663	0.34932	1.45685	0.29703	1.027479	0.83314	1.57378	0.314236
2.22	7.487	gi 4505621	1	0.96277	0.8957	1.09319	0.533952	0.903624	0.4929	1.02145	0.91865	1.219476	0.35161	1.19588	0.321973
4.412	gi 358356404		1	0.87189	0.36029	0.93705	0.674173	1.013222	0.93016	1.11807	0.32778	1.005237	0.93799	0.93831	0.322112
31.86	gi 13904870		7	0.9506	0.72658	1.0316	0.603441	0.924649	0.46719	0.99064	0.95691	1.001791	0.98677	1.091	0.322428
48.28	gi 4501881		84	0.70402	0.19171	0.88213	0.452415	0.895226	0.49113	0.9076	0.68294	0.910421	0.74174	0.83025	0.335221
61.46	gi 4504517		14	1.03033	0.75301	1.09164	0.398213	1.129264	0.45398	1.07204	0.36605	1.008009	0.93325	1.14863	0.335319
3 15.63	gi 23308579		2	1.09274	0.60681	1.33151	0.112159	1.200575	0.47968	1.17833	0.45949	1.215746	0.48534	1.12312	0.341192
23.31	gi 100913206		25	1.01038	0.85557	0.98092	0.810188	1.026626	0.71249	0.99051	0.9034	0.908446	0.21786	0.93231	0.343017

6	15.03	gi 5453597	F-actin-capping protein subunit alpha-1 [Homo sapiens]	3	1.08743	0.8451	1.19702	0.574836	1.148574	0.63926	0.8406	0.67537	1.190998	0.50429	1.17969	0.344035
	8.013	gi 7705855	estradiol 17-beta-dehydrogenase 12 [Homo sapiens]	2	1.35665	0.14963	1.58221	0.299346	1.327157	0.60819	0.82147	0.54246	2.201652	0.16227	1.17915	0.348877
32.68	55.25	gi 4885379	histone H1.4 [Homo sapiens]	18	0.86188	0.15805	0.79458	0.062715	0.581451	0.00631	0.783	0.05277	0.955935	0.61036	0.78812	0.349009
	32.02	gi 4503529	eukaryotic initiation factor 4A-I isoform 1 [Homo sapiens]	13	1.04269	0.74889	1.03994	0.678853	1.271338	0.05202	1.0321	0.8665	0.954919	0.82177	1.16915	0.351373
	14.38	gi 4506691	40S ribosomal protein S16 [Homo sapiens]	2	0.97562	0.80498	1.08435	0.534558	0.91199	0.46498	0.90795	0.25085	1.061548	0.63913	1.08996	0.352086
5.35	21.47	gi 89903012	cell division control protein 42 homolog isoform 1 [Homo sapiens]	4	0.84946	0.37036	0.96503	0.661392	0.873435	0.40147	0.85893	0.56613	0.93952	0.65745	0.8919	0.363234
4.28	8.456	gi 4826659	F-actin-capping protein subunit beta isoform 1 [Homo sapiens]	2	0.67802	0.35754	0.69959	0.172607	0.851274	0.65389	0.86143	0.37487	0.66671	0.15342	0.85952	0.369847
16.25	8.025	gi 7669550	vinculin isoform meta-VCL [Homo sapiens]	7	0.88768	0.17609	0.86082	0.075983	0.892825	0.45546	0.90485	0.43053	0.975215	0.86887	0.89204	0.37485
	23.14	gi 35493916	dolichyl-diphosphooligosaccharide--protein glycosyltransferase subunit 2 isoform 1 precursor [Homo sapiens]	16	0.97184	0.85688	0.82452	0.080194	0.845658	0.09154	0.94712	0.71073	0.862415	0.34484	0.82828	0.378348
14	22.43	gi 4758112	spliceosome RNA helicase DDX39B [Homo sapiens]	11	0.76734	0.20451	1.11319	0.323403	0.756887	0.24072	1.25882	0.36395	0.926787	0.45626	0.75424	0.37859
11.59	15.71	gi 7549809	plastin-3 isoform 1 [Homo sapiens]	9	1.12989	0.64507	0.90527	0.733379	1.317888	0.17397	0.86056	0.69041	0.96376	0.83803	1.20141	0.379589

9	0.85201	0.64513	0.93269	0.807974	1.291011	0.53085	1.19777	0.7306	1.030423	0.92072	1.31892	0.380861
5	1.16862	0.44494	1.33119	0.096689	1.177838	0.49	1.0947	0.79475	1.573738	0.01477	1.13974	0.381154
2	0.97294	0.92271	1.26859	0.287512	1.130249	0.50102	1.09105	0.81061	0.985191	0.90638	1.15704	0.386139
2	0.80818	0.51448	0.95702	0.88235	0.88861	0.73781	0.93516	0.86581	0.90713	0.71945	0.74119	0.387206
2	0.96152	0.7616	0.50291	0.169483	0.979637	0.92474	1.28961	0.57091	0.61504	0.12877	0.86852	0.391631
6	0.859	0.1927	0.99136	0.910421	1.174134	0.18032	1.15622	0.23457	0.965199	0.70957	1.10427	0.395095
3	1.23708	0.47402	0.95535	0.724579	1.41888	0.35286	0.98525	0.96622	1.213987	0.63144	1.1551	0.397981
1	0.7038	0.17472	0.74995	0.303498	0.81862	0.29299	1.06878	0.74451	0.721986	0.50264	0.74921	0.401414
6	1.12182	0.58683	1.07692	0.62046	1.139729	0.42901	1.17579	0.43977	1.065154	0.63398	1.10216	0.401429

25.7	38.78	gi 4506243	polypyrimidine tract-binding protein 1 isoform a [Homo sapiens]	18	1.06292	0.50756	1.06923	0.515736	1.03194	0.7921	1.05954	0.60728	1.071681	0.34712	1.09726	0.405096
9.37	13.6	gi 4503249	protein DEK isoform 1 [Homo sapiens]	6	0.90486	0.7789	0.82548	0.362847	0.887533	0.5517	0.78952	0.49732	0.937237	0.82238	0.72629	0.405633
14.64	25.24	gi 213511508	B-cell receptor-associated protein 31 isoform a [Homo sapiens]	10	0.9788	0.86518	0.94279	0.594634	0.912101	0.48864	1.007	0.95315	1.037329	0.68442	0.92084	0.409043
7.42	23.37	gi 219555707	eukaryotic translation initiation factor 5A-1 isoform A [Homo sapiens]	12	0.93983	0.54649	0.9442	0.764423	0.988686	0.90673	0.86285	0.22899	0.906192	0.37119	0.80789	0.411159
1.55	4.286	gi 151101292	thioredoxin-related transmembrane protein 1 precursor [Homo sapiens]	1	1.06382	0.75255	0.97657	0.857522	0.819195	0.30702	0.88399	0.46597	0.94309	0.88688	0.87165	0.412176
2.73	1.905	gi 65506891	4F2 cell-surface antigen heavy chain isoform c [Homo sapiens]	1	0.98317	0.93864	0.84624	0.244296	1.115642	0.53319	0.93078	0.55737	1.007492	0.96461	1.15408	0.413802
	12.29	gi 4504897	importin subunit alpha-2 [Homo sapiens]	4	1.62496	0.16839	1.58207	0.135682	1.24339	0.36447	1.51981	0.50696	1.039731	0.89515	1.5101	0.415434
68.18		gi 226529917	triosephosphate isomerase isoform 2 [Homo sapiens]	18	0.89284	0.09459	0.9824	0.725009	1.039563	0.50875	0.86402	0.04131	0.996977	0.94683	1.0504	0.4184
45.92		gi 10835063	nucleophosmin isoform 1 [Homo sapiens]	27	1.05093	0.20853	0.98486	0.687201	0.932746	0.16808	1.0139	0.77562	0.993499	0.88674	0.96765	0.418435
52.68		gi 4506667	60S acidic ribosomal protein P0 [Homo sapiens]	10	1.07767	0.28966	0.92404	0.551593	0.973779	0.83745	1.06728	0.4878	1.123923	0.35376	1.08972	0.4209
9.86	54.29	gi 11128019	cytochrome c [Homo sapiens]	7	1.02581	0.90995	1.1736	0.485643	1.168768	0.23072	1.206	0.51323	1.136284	0.41989	1.14466	0.422321

1.67	3.499	gi 5803181	stress-induced-phosphoprotein 1 [Homo sapiens]	1	0.71762	0.41633	0.77017	0.230487	0.873029	0.40131	0.75715	0.48774	0.672277	0.46885	1.13446	0.423418
6.23	5.735	gi 147777000	mannosyl-oligosaccharide glucosidase isoform 1 [Homo sapiens]	4	1.08059	0.53739	1.14425	0.238759	1.1575	0.39612	1.20626	0.22942	1.027046	0.82377	1.22927	0.424115
2.06	1.744	gi 13375618	delta(24)-sterol reductase precursor [Homo sapiens]	1	0.96975	0.95351	1.02975	0.912942	0.726643	0.58232	1.01279	0.96941	0.809533	0.46642	0.69083	0.428542
4.59	33.59	gi 6912616	histone H2A.V isoform 1 [Homo sapiens]	9	0.95702	0.75379	0.85738	0.31234	0.799618	0.39941	0.95914	0.85394	0.973601	0.77491	0.91318	0.430038
12.27	17.53	gi 47132620	keratin, type II cytoskeletal 2 epidermal [Homo sapiens]	10	0.94036	0.69134	1.17098	0.215737	0.949491	0.52853	1.22133	0.14278	1.251278	0.05142	1.10158	0.431077
29.14	48.39	gi 24119203	tropomyosin alpha-3 chain isoform 2 [Homo sapiens]	17	1.09868	0.52294	1.13547	0.264856	1.02411	0.77098	1.07533	0.58977	1.025008	0.85158	1.10599	0.4331
4.54	1.504	gi 7305053	myoferlin isoform a [Homo sapiens]	3	1.03642	0.91549	1.07562	0.753873	0.677725	0.15841	1.17281	0.35344	0.804299	0.27121	0.80158	0.434082
5.17	11.54	gi 71772415	40S ribosomal protein S15a [Homo sapiens]	2	1.08261	0.30057	0.86993	0.526937	1.005628	0.96992	1.06918	0.64765	0.895366	0.53786	0.9438	0.435165
19.01	71.69	gi 5031635	cofilin-1 [Homo sapiens]	13	0.98335	0.79485	1.06505	0.609521	1.073792	0.50449	0.94654	0.66373	1.006219	0.93333	1.08085	0.437716
4.87	17.72	gi 5031741	dnaJ homolog subfamily A member 2 [Homo sapiens]	4	1.02126	0.95399	0.95642	0.65181	0.777159	0.21533	1.08462	0.83024	1.354666	0.12297	1.18166	0.440861
3.65	23.53	gi 20357529	guanine nucleotide-binding protein G(I)/G(S)/G(T) subunit beta-2 [Homo sapiens]	5	1.12035	0.48505	1.20046	0.396539	1.116905	0.28669	0.87631	0.53161	1.27117	0.30243	1.06684	0.441087
3.09	9.509	gi 38201714	ELAV-like protein 1 [Homo sapiens]	3	1.41868	0.19346	1.17549	0.435049	1.144978	0.407	1.38872	0.18715	1.15082	0.57414	1.18829	0.441784

	30.82	gi 148833484	poly(rC)-binding protein 2 isoform c [Homo sapiens]	10	0.8692	0.5888	0.79919	0.127357	1.023241	0.9611	0.89854	0.74636	0.88669	0.61133	0.80637	0.442107
60.22	77.33	gi 4501887	actin, cytoplasmic 2 [Homo sapiens]	122	1.04669	0.76057	0.9772	0.835104	1.156228	0.46372	1.12886	0.57932	0.952823	0.68722	1.13584	0.443001
64.06	45.78	gi 27436946	lamin isoform A [Homo sapiens]	33	1.00508	0.89186	0.97829	0.718695	0.922786	0.10936	0.99433	0.90623	0.986285	0.69962	0.95111	0.446249
	20.35	gi 4502847	cold-inducible RNA-binding protein [Homo sapiens]	4	0.77481	0.23807	0.96341	0.8403	0.974154	0.9343	0.84858	0.47177	0.883339	0.43224	0.88827	0.446678
2.34	40	gi 15617199	histone H2A type 3 [Homo sapiens]	42	1.09822	0.74304	0.87151	0.415005	0.765686	0.38284	1.16096	0.38969	1.043543	0.75415	0.88391	0.448851
1.81	6.704	gi 7706495	dnaJ homolog subfamily B member 11 precursor [Homo sapiens]	2	0.93474	0.87702	0.53691	0.101191	0.806413	0.2753	0.5963	0.38777	0.827227	0.3501	0.79794	0.450096
	25.6	gi 4506707	40S ribosomal protein S25 [Homo sapiens]	4	1.05992	0.71046	0.99801	0.984935	0.891834	0.22233	1.00881	0.92385	1.001775	0.9825	0.93387	0.453378
	31.16	gi 195972866	keratin, type I cytoskeletal 10 [Homo sapiens]	18	0.99279	0.96579	1.17686	0.25241	1.082097	0.65185	1.1831	0.40404	1.176889	0.26041	1.15457	0.453813
1.82	8.824	gi 72534660	serine/arginine-rich splicing factor 7 isoform 1 [Homo sapiens]	2	1.01438	0.96006	1.32191	0.462731	1.03348	0.93519	0.9051	0.57763	1.129918	0.43756	1.25841	0.454052
	3.239	gi 21361282	serine/arginine-rich splicing factor 4 [Homo sapiens]	2	0.86496	0.58839	0.9941	0.985146	0.989135	0.93152	0.69451	0.50631	0.947242	0.68143	0.83973	0.454583
	24.34	gi 11968182	40S ribosomal protein S18 [Homo sapiens]	4	0.9108	0.17598	0.9615	0.565209	0.836623	0.29264	0.96303	0.84958	1.048824	0.83849	0.92731	0.46041
9.36	13.58	gi 62750354	matrin-3 isoform a [Homo sapiens]	11	1.04516	0.83428	1.19344	0.652837	1.008595	0.97584	0.94902	0.77475	1.150566	0.455	1.23023	0.463137
	9.359	gi 71773106	AP-2 complex subunit beta isoform a [Homo sapiens]	6	1.03159	0.80628	0.90953	0.514151	0.860359	0.37066	0.88525	0.43526	0.974676	0.93431	0.80142	0.464299

5.49	20.15	gi 51599151	calpain small subunit 1 [Homo sapiens]	3	1.0993	0.90564	1.2801	0.713734	1.693094	0.48935	1.52327	0.58126	0.975995	0.97003	1.2446	0.464515
6.79	1.756	gi 91208426	pre-mRNA-processing-splicing factor 8 [Homo sapiens]	4	0.74541	0.52013	0.93731	0.762332	0.802356	0.39367	0.788	0.63705	0.875564	0.80852	0.82589	0.46519
8.029		gi 13904866	60S ribosomal protein L28 isoform 2 [Homo sapiens]	1	1.1852	0.61711	1.19004	0.350877	1.095949	0.54876	1.1129	0.49895	1.056091	0.72529	1.26634	0.469429
22.18		gi 4506663	60S ribosomal protein L8 [Homo sapiens]	3	1.34108	0.1674	1.18917	0.596438	0.934418	0.82729	1.33352	0.31409	1.327422	0.05463	1.3069	0.473156
59.02	46.15	gi 4503483	elongation factor 2 [Homo sapiens]	39	0.94928	0.36084	1.04053	0.380718	1.053971	0.35544	0.9786	0.75631	0.929768	0.18854	1.04154	0.473738
4.45	4.67	gi 197276600	microtubule-associated protein 4 isoform 4 [Homo sapiens]	4	1.27162	0.35766	1.30783	0.138875	0.971935	0.77141	1.24298	0.34491	1.142233	0.44348	1.17	0.47386
62.4		gi 20070125	protein disulfide-isomerase precursor [Homo sapiens]	36	0.9796	0.56599	0.92769	0.057465	0.928316	0.02639	0.96119	0.35188	1.007923	0.82127	0.97761	0.477783
8.82	44.44	gi 5031749	non-histone chromosomal protein HMG-17 [Homo sapiens]	7	1.02829	0.76222	0.94558	0.568522	0.847099	0.15126	0.96638	0.60275	0.990646	0.88526	0.95379	0.477923
8.82	44.44	gi 5031749	non-histone chromosomal protein HMG-17 [Homo sapiens]	7	1.02829	0.76222	0.94558	0.568522	0.847099	0.15126	0.96638	0.60275	0.990646	0.88526	0.95379	0.477923
9.854		gi 48762932	T-complex protein 1 subunit theta [Homo sapiens]	4	0.92715	0.48706	0.96602	0.82075	0.929325	0.69985	0.87594	0.5857	1.082928	0.61024	0.86331	0.478863
2.383		gi 54112121	splicing factor 3B subunit 3 [Homo sapiens]	3	0.81032	0.48085	0.98602	0.920135	1.05857	0.67167	0.5949	0.49536	1.079662	0.84245	0.89031	0.48195

7.161	gi 4758756	nucleosome assembly protein 1-like 1 [Homo sapiens]	2	1.062	0.82004	1.2756	0.571647	1.408068	0.46674	1.48367	0.24859	1.196134	0.33178	1.30001	0.484108
62.57	gi 5453740	myosin regulatory light chain 12A [Homo sapiens]	12	1.03618	0.53408	1.07574	0.396769	1.10096	0.25569	1.06196	0.4021	1.059293	0.3758	0.9605	0.484747
11.87	gi 373251164	glutaminase kidney isoform, mitochondrial isoform 2 [Homo sapiens]	6	0.74804	0.21256	0.77018	0.315563	0.807316	0.31161	0.7773	0.4977	0.717889	0.29766	0.84106	0.487298
2.85	1.876 gi 41393608	reticulon-3 isoform b [Homo sapiens] pyruvate dehydrogenase E1	2	0.80302	0.36014	0.86762	0.389095	0.664497	0.27998	0.77081	0.7731	0.900955	0.48418	0.7174	0.493207
2.9	8.914 gi 156564403	component subunit beta, mitochondrial isoform 1 precursor [Homo sapiens]	2	1.45512	0.16682	1.33691	0.487042	1.523417	0.43403	1.45412	0.24868	1.41206	0.69537	1.298	0.49854
51.12	71.17 gi 29788785	tubulin beta chain [Homo sapiens]	51	0.90405	0.36942	0.91409	0.416252	1.033772	0.7416	0.9256	0.47261	0.917076	0.43044	1.07465	0.499031
8.385	gi 17402900	far upstream element- binding protein 1 [Homo sapiens]	6	1.03031	0.66506	1.10446	0.493208	0.912083	0.35392	1.08702	0.37794	1.001769	0.9928	1.14004	0.499632
14.91	gi 5453832	hypoxia up-regulated protein 1 precursor [Homo sapiens]	10	1.03014	0.81577	0.97909	0.8833	0.952214	0.64282	0.98593	0.92964	0.952431	0.60746	0.87514	0.500821
5.32 5.253	gi 66933016	inosine-5'- monophosphate dehydrogenase 2 [Homo sapiens]	4	1.03226	0.89524	1.09494	0.50848	1.268973	0.42403	1.3762	0.15979	1.245079	0.48519	1.19792	0.502222

2.63	5.122	gi 4504957	lysosome-associated membrane glycoprotein 2 isoform A precursor [Homo sapiens]	2	0.54855	0.55156	1.08974	0.849683	0.484158	0.57545	0.37086	0.39568	0.6991	0.54638	0.51917	0.506245
4.23	31.03	gi 4826848	NADH dehydrogenase [ubiquinone] 1 alpha subcomplex subunit 5 [Homo sapiens]	2	1.46828	0.41391	1.14203	0.815197	0.917116	0.54645	1.22387	0.73155	1.096227	0.88499	1.28746	0.506837
6.17	6.658	gi 4503131	catenin beta-1 [Homo sapiens]	3	0.41141	0.15644	0.66533	0.51162	0.503723	0.46341	0.41106	0.25461	0.599967	0.48447	0.41318	0.507001
63.94	40.4	gi 12025678	alpha-actinin-4 [Homo sapiens] heterogeneous nuclear	36	0.97761	0.81249	1.05219	0.64193	1.086704	0.45213	1.05716	0.61573	0.980235	0.82704	1.07302	0.511242
	15.43	gi 332801090	ribonucleoprotein D- like isoform b [Homo sapiens]	6	1.00871	0.91679	1.05032	0.446338	0.913776	0.26441	0.98511	0.90239	1.054689	0.41219	0.89372	0.512474
	44.33	gi 4507677	endoplasmic reticulum precursor [Homo sapiens]	42	0.9961	0.93353	0.94848	0.248495	0.968327	0.51543	0.9863	0.81623	0.976286	0.57443	0.96779	0.512923
	4.478	gi 5803149	transmembrane emp24 domain- containing protein 2 precursor [Homo sapiens]	1	1.41839	0.40694	1.2308	0.287656	1.26119	0.2614	1.52491	0.1496	1.161351	0.65161	1.39668	0.513323
2.0362.25		gi 5174735	tubulin beta-4B chain [Homo sapiens]	42	0.85065	0.43007	0.9246	0.575418	0.790037	0.41365	0.90389	0.49652	1.074749	0.66239	1.09878	0.518424
11.66	16.6	gi 19923653	PC4 and SFRS1- interacting protein isoform 2 [Homo sapiens]	8	1.17679	0.73143	1.56402	0.358592	0.968929	0.9434	1.46777	0.32185	1.363601	0.25718	1.28947	0.522585

5.85	10.4	gi 60279268	65 kDa splicing factor U2AF subunit isoform b [Homo sapiens]	4	1.2201	0.66253	1.02211	0.952784	1.130686	0.83639	0.93141	0.83825	1.173532	0.5247	1.13973	0.52352
			lysosome-associated membrane glycoprotein 1 precursor [Homo sapiens]	3	0.92406	0.43426	1.07253	0.481096	0.862072	0.21099	0.78483	0.09717	0.937752	0.51208	0.78737	0.525828
17.81	20.36	gi 4758138	probable ATP-dependent RNA helicase DDX5 [Homo sapiens] high mobility group	9	1.02008	0.93999	1.03103	0.885579	1.087795	0.60812	0.90254	0.59855	0.900662	0.697	0.85903	0.527072
2.84	15.89	gi 22208971	protein HMG-I/HMG-Y isoform a [Homo sapiens] minor	2	1.16637	0.22879	1.11889	0.314787	0.942611	0.76233	0.96675	0.72794	1.098282	0.38348	1.06576	0.530562
2.52	2.347	gi 30581111	histocompatibility antigen H13 isoform 3 [Homo sapiens]	1	0.96889	0.88579	1.0853	0.672652	0.932619	0.85235	0.80742	0.27991	0.966258	0.79095	0.57797	0.530633
			heterogeneous nuclear ribonucleoprotein R isoform 2 [Homo sapiens]	12	1.1786	0.36141	1.03955	0.91766	1.411819	0.05493	1.20407	0.33353	1.512006	0.06272	1.34337	0.531745
3.639		gi 21361361	acetolactate synthase-like protein [Homo sapiens]	2	0.96311	0.95496	1.11329	0.773986	1.2958	0.74466	1.02802	0.94228	0.89748	0.78731	1.2972	0.533523
4.592		gi 4506609	60S ribosomal protein L19 [Homo sapiens]	1	1.28745	0.58224	1.12827	0.259487	1.136556	0.75982	1.21129	0.29878	1.386144	0.3114	1.23701	0.533725
24.42	42.35	gi 5453539	multifunctional protein ADE2 isoform 2 [Homo sapiens]	14	1.00356	0.9713	1.00013	0.998729	1.148299	0.30568	1.09789	0.39572	0.967332	0.82108	1.06801	0.541305

33.86	6.371	gi 126032350	DNA-dependent protein kinase catalytic subunit isoform 2 [Homo sapiens] catechol O-	22	1.20563	0.32156	1.04779	0.533682	1.107957	0.44994	1.05744	0.66483	1.165061	0.4342	1.10473	0.543078
6.03	17.34	gi 4502969	methyltransferase isoform MB-COMT [Homo sapiens]	4	0.93424	0.61858	0.80864	0.279603	0.927369	0.90939	1.13765	0.41947	0.713404	0.1827	0.77919	0.546947
7.11	29.53	gi 5031851	stathmin isoform a [Homo sapiens] keratin, type II	5	1.00604	0.96349	1.00856	0.924299	1.159543	0.4121	0.99103	0.96627	0.904638	0.20568	1.16846	0.547923
26.6	25.31	gi 119395750	cytoskeletal 1 [Homo sapiens] proliferating cell nuclear antigen [Homo sapiens] interleukin enhancer-	19	0.9346	0.43611	0.95497	0.621952	1.108099	0.40979	1.19886	0.10667	1.200578	0.05109	1.04931	0.549805
1.66	10.73	gi 4505641	binding factor 3 isoform a [Homo sapiens] alpha-actinin-1	3	0.95874	0.74344	0.76238	0.351143	0.672644	0.18698	0.43342	0.07491	0.500235	0.27736	0.56731	0.556316
17.5	14.43	gi 24234750	isoform b [Homo sapiens]	10	1.2214	0.42885	1.08192	0.713069	1.193625	0.35476	1.21833	0.49341	0.91235	0.70867	1.04385	0.557202
17.62	37.67	gi 4501891	RNA-binding protein FUS isoform 1 [Homo sapiens] splicing factor 1	33	1.14984	0.38813	1.13194	0.32002	1.205048	0.21244	1.01236	0.92856	1.162788	0.20884	1.08371	0.560889
2.12	7.034	gi 4826734	isoform 4 [Homo sapiens] histone-binding protein KBDP /	4	0.94968	0.70164	0.86002	0.376919	0.888291	0.45267	0.98973	0.93593	0.969715	0.81381	0.92116	0.568145
4.09	5.954	gi 295842307	isoform 1 [Homo sapiens]	3	0.94439	0.91318	1.24603	0.673259	0.931656	0.89132	1.241	0.722	1.023873	0.94625	1.28342	0.570229
5.48	6.397	gi 311078508	kinectin isoform a [Homo sapiens]	3	1.10172	0.52866	0.99141	0.969002	0.914266	0.62674	0.9097	0.7392	1.184806	0.19987	0.89257	0.571518
9.97	6.485	gi 33620775		8	1.05966	0.69111	1.19364	0.149146	1.159778	0.26147	0.79517	0.22887	0.90011	0.62253	0.90417	0.572624

1.025	gi 32967311	ephrin type-A receptor 2 precursor [Homo sapiens]	1	0.9746	0.94795	1.05692	0.85878	1.210665	0.32138	1.1077	0.56043	1.387491	0.37876	1.08739	0.574518	
40.89	35.24	gi 6005942	transitional endoplasmic reticulum ATPase [Homo sapiens]	25	0.97357	0.71935	0.95857	0.555716	1.12462	0.17086	1.01768	0.8572	0.946802	0.38291	0.95645	0.575353
21.4	gi 78000183	60S ribosomal protein L14 [Homo sapiens]	5	1.04335	0.72706	0.99861	0.994141	0.968287	0.89286	1.18263	0.33665	0.920667	0.68297	0.89227	0.575757	
1.903	gi 4504747	integrin alpha-3 isoform a precursor [Homo sapiens]	2	1.226	0.2114	0.8335	0.417073	0.827589	0.60291	1.01131	0.98103	1.119362	0.30086	1.06507	0.578152	
10.41	gi 91199540	dihydrolipoyl dehydrogenase, mitochondrial precursor [Homo sapiens]	4	1.1821	0.51111	1.02828	0.834679	1.282727	0.58737	1.05334	0.70556	1.129976	0.66848	1.19902	0.58019	
2.25	3.558	gi 25777612	26S proteasome non- ATPase regulatory subunit 3 [Homo sapiens]	2	0.8381	0.48744	1.10067	0.583873	1.099142	0.73254	0.63133	0.3464	0.970719	0.81572	0.63441	0.581959
11.11	11.62	gi 48255891	glucosidase 2 subunit beta isoform 2 precursor [Homo sapiens]	6	1.03946	0.67934	1.13566	0.081367	1.012411	0.9142	1.13026	0.29235	1.162264	0.01179	1.05193	0.584009
18.97	17.57	gi 4503841	X-ray repair cross- complementing protein 6 [Homo sapiens]	11	0.97292	0.81085	1.00878	0.880034	0.998476	0.98044	0.92188	0.2548	1.058863	0.64942	0.9691	0.58695
20.54	gi 4506455	reticulocalbin-1 precursor [Homo sapiens]	4	0.9615	0.61475	1.05458	0.619085	0.942759	0.64057	1.04202	0.67339	0.937237	0.68695	0.92712	0.58783	
11.48	49.46	gi 7661678	Rap-1b isoform 1 precursor [Homo sapiens]	9	1.04781	0.8059	0.91308	0.460369	1.104292	0.36436	1.11936	0.62485	0.863622	0.22512	1.13417	0.589483

18.53	gi 57863257	T-complex protein 1 subunit alpha isoform a [Homo sapiens]	6	0.99365	0.97173	1.10198	0.768095	0.820472	0.46263	0.92611	0.65421	1.094258	0.72633	1.15002	0.592124	
4	19.33	gi 4506697	40S ribosomal protein S20 isoform 2 [Homo sapiens] delta(3,5)-Delta(2,4)-dienoyl-CoA isomerase, mitochondrial precursor [Homo sapiens]	2	1.16724	0.3705	1.38228	0.267105	1.193196	0.66439	1.42943	0.38635	1.142585	0.66025	1.2463	0.592284
5.183	gi 70995211	40S ribosomal protein S14 [Homo sapiens] peptidyl-prolyl cis-trans isomerase B precursor [Homo sapiens]	1	1.02368	0.95347	1.20449	0.732047	0.8886	0.71644	0.98045	0.87509	1.373089	0.27118	1.07641	0.594433	
15.23	gi 68160922	far upstream element-binding protein 2 [Homo sapiens]	2	0.89167	0.72053	1.24591	0.353475	1.058112	0.75346	1.02913	0.93338	1.107532	0.68517	1.16347	0.601089	
23.39	50	gi 4758950	OCIA domain-containing protein 2 isoform 1 [Homo sapiens]	15	0.96317	0.36944	0.91885	0.055881	0.933665	0.26808	0.99647	0.94972	0.960674	0.37431	0.96843	0.603144
9.423	gi 154355000	histone H1.3 [Homo sapiens] 40S ribosomal protein S19 [Homo sapiens] ras-related protein	8	1.08689	0.50836	1.05982	0.68563	0.932229	0.61558	1.1761	0.473	1.185571	0.19675	1.09494	0.609018	
3.71	14.94	gi 62244044	containing protein 2 isoform 1 [Homo sapiens]	2	1.06593	0.75131	1.07831	0.465847	0.860725	0.46251	0.71107	0.43904	0.881257	0.32917	0.84963	0.609097
6.07	43.44	gi 4885377	histone H1.3 [Homo sapiens] 40S ribosomal protein S19 [Homo sapiens] ras-related protein	14	1.04454	0.53785	0.93529	0.437735	0.754462	0.01216	1.21122	0.38623	1.178831	0.3691	0.96051	0.612951
19.31	gi 4506695	40S ribosomal protein S19 [Homo sapiens] ras-related protein	3	1.18345	0.60921	1.09019	0.861537	0.929737	0.8499	1.1507	0.69475	1.276557	0.41324	1.20276	0.61489	
22.49	gi 354721184	Rab-5C isoform b [Homo sapiens]	5	0.9894	0.89493	1.06862	0.461529	1.002682	0.98651	0.96801	0.8683	0.969061	0.76529	1.08543	0.617855	
19.23	gi 4506743	40S ribosomal protein S8 [Homo sapiens]	7	1.17932	0.49985	1.18919	0.299259	1.224889	0.46026	1.20005	0.31305	1.077038	0.79546	1.1569	0.618747	

25.41	gi 40254924	leucine-rich repeat-containing protein 59 [Homo sapiens]	7	1.17331	0.02623	1.05979	0.327971	0.949168	0.65078	1.1888	0.01927	1.124964	0.16462	1.04358	0.620272	
46.54	43.1	gi 4758304	isomerase A4 precursor [Homo sapiens]	29	0.94767	0.13639	0.94301	0.132998	0.926221	0.06328	0.91517	0.09507	0.961057	0.40127	1.02263	0.620681
183.84	45.56	gi 12667788	myosin-9 [Homo sapiens]	131	0.98833	0.75974	0.97703	0.492793	1.006742	0.82829	0.98619	0.77237	0.960691	0.2	1.01558	0.622695
10.97	gi 61743954	neuroblast differentiation-associated protein AHNAK isoform 1 [Homo sapiens]	12	0.96465	0.7331	1.01859	0.841517	0.948976	0.63379	0.99368	0.95963	1.066503	0.5159	0.95444	0.625648	
4.3	8.462	gi 42734430	polymerase I and transcript release factor [Homo sapiens]	3	0.95085	0.86297	0.89311	0.699758	0.803026	0.67284	0.87765	0.59893	0.805946	0.69619	0.89028	0.628441
17.87	gi 34147513	Rab-7a [Homo sapiens]	5	0.95351	0.73379	0.76061	0.213252	0.854884	0.35362	0.81528	0.41645	1.001302	0.98901	0.94089	0.631549	
17.26	gi 228008400	heterogeneous nuclear ribonucleoprotein Q isoform 6 [Homo sapiens]	14	1.21817	0.42309	1.24361	0.309094	1.08515	0.76039	1.27522	0.33853	1.195927	0.2873	1.09644	0.632009	
35.05	gi 4506741	40S ribosomal protein S7 [Homo sapiens]	6	1.00409	0.9778	0.96526	0.812921	0.909794	0.66104	0.9513	0.54511	0.966876	0.7708	0.92787	0.634911	
60.5	gi 4757826	beta-2-microglobulin precursor [Homo sapiens]	6	1.26003	0.50144	0.8665	0.306054	1.14102	0.77709	1.42354	0.55364	0.945291	0.79075	0.8252	0.638802	
9.813	gi 223890243	60S ribosomal protein L10 isoform a [Homo sapiens]	2	1.14824	0.20993	1.03798	0.754032	1.268798	0.08304	1.15213	0.28899	1.087423	0.68281	1.04897	0.641001	

16.25	45.18	gi 153070260	myristoylated alanine-rich C-kinase substrate [Homo sapiens]	9	0.983	0.80578	0.9737	0.694966	0.988063	0.84891	0.99415	0.92598	0.997562	0.96911	1.03013	0.641041
34.42	55.7	gi 156071459	ADP/ATP translocase 2 [Homo sapiens]	29	1.03376	0.68358	0.9262	0.376592	0.988751	0.95299	0.97673	0.78837	0.96945	0.77703	0.9515	0.641079
2.17	0.4867	gi 54607053	translational activator GCN1 [Homo sapiens]	1	1.28676	0.24123	1.07193	0.906543	0.741843	0.68752	0.71728	0.66122	1.331493	0.53099	0.83414	0.644476
2.39	5.917	gi 4502981	cytochrome c oxidase subunit 4 isoform 1, mitochondrial precursor [Homo sapiens]	1	0.86484	0.25424	0.99029	0.964486	1.020714	0.83282	0.8429	0.23318	1.026772	0.81804	1.0846	0.645195
1.43	0.9151	gi 29826341	calmodulin-binding transcription activator 2 isoform 1 [Homo sapiens]	2	1.02264	0.97348	1.1667	0.370435	1.013866	0.97412	1.00199	0.99841	0.997553	0.99617	0.82669	0.646072
18	89.63	gi 4504981	galectin-1 [Homo sapiens]	13	0.94609	0.56748	1.06686	0.337019	0.998775	0.99189	0.98275	0.86625	0.982519	0.85361	0.96945	0.646657
30.18	31.63	gi 34932414	non-POU domain-containing octamer-binding protein isoform 1 [Homo sapiens]	18	1.02179	0.71872	0.95014	0.56712	0.987357	0.85793	1.00228	0.97442	0.979062	0.76057	0.95323	0.661185
20.86	21.51	gi 18201905	glucose-6-phosphate isomerase isoform 2 [Homo sapiens]	14	0.8891	0.11886	0.99188	0.914596	1.007987	0.93038	0.92749	0.67746	1.005971	0.94939	1.03989	0.662333
1.69	10.67	gi 4758040	cytochrome c oxidase subunit 6C proprotein [Homo sapiens]	2	0.85609	0.37626	1.19072	0.565045	0.999303	0.99786	1.33632	0.67643	1.130728	0.64572	1.06285	0.662841
6.13	6.647	gi 87196351	ATP-dependent RNA helicase DDX3X isoform 1 [Homo sapiens]	3	1.18019	0.51813	1.21877	0.602725	0.919683	0.75389	0.73428	0.20041	1.18035	0.41588	1.05972	0.665489

58.07	gi 14043072	heterogeneous nuclear ribonucleoproteins A2/B1 isoform B1 [Homo sapiens] 40S ribosomal	24	0.99729	0.99214	0.89746	0.632954	0.951845	0.82147	1.04794	0.90827	0.952007	0.78644	0.91491	0.666499
15.36	gi 15055539	protein S2 [Homo sapiens] 60S ribosomal	4	0.98191	0.94926	1.00864	0.979743	0.878588	0.57863	1.02254	0.91929	0.956993	0.88491	1.1123	0.670417
11.41	gi 4506649	protein L3 isoform a [Homo sapiens] NAD(P) transhydrogenase,	3	0.86881	0.71238	0.92019	0.286429	0.938384	0.8218	0.99791	0.9954	0.829736	0.47181	0.90558	0.673162
3.95 2.855	gi 122939155	mitochondrial [Homo sapiens] tropomyosin alpha-1	3	1.00797	0.94948	1.13779	0.597416	1.143784	0.49699	0.8888	0.4475	0.881076	0.48103	1.13072	0.673925
29.93	gi 63252900	chain isoform 4 [Homo sapiens] splicing factor, proline- and	10	1.08825	0.37639	1.04674	0.732007	1.130557	0.28152	1.16461	0.14713	0.981288	0.89392	1.04555	0.674296
22.02 20.65	gi 4826998	glutamine-rich [Homo sapiens] cytochrome c oxidase	19	0.97461	0.91414	1.03224	0.88877	0.887348	0.62919	0.97859	0.93981	1.022428	0.92594	0.90595	0.674537
17.62	gi 251831110	subunit II [Homo sapiens] 60S ribosomal	3	0.80403	0.69103	0.86297	0.299261	0.722846	0.28015	0.6475	0.10402	0.866816	0.66375	0.91801	0.675132
19.68	gi 4506607	protein L18 isoform 1 [Homo sapiens] 10 kDa heat shock	3	0.96035	0.7603	0.87805	0.465616	0.962498	0.839	0.88382	0.53872	1.032148	0.81521	0.89035	0.675519
74.51	gi 4504523	protein, mitochondrial [Homo sapiens] 60S ribosomal	8	0.99268	0.88544	0.97341	0.600927	0.974775	0.61892	0.97012	0.56798	0.974523	0.6162	1.02344	0.675919
19.44	gi 67189747	protein L6 [Homo sapiens] 60S ribosomal	5	1.02062	0.76923	0.84308	0.303084	1.054461	0.51107	1.04638	0.62651	0.978707	0.85244	0.95504	0.677122
29.17	gi 67944630	protein L9 [Homo sapiens]	5	1.15467	0.38103	1.15642	0.137453	1.229212	0.2788	0.96642	0.85104	1.288677	0.12373	0.93631	0.677782

2.18	2.71	gi 19923193	hsc70-interacting protein [Homo sapiens]	1	0.95037	0.83989	0.96798	0.821141	0.800799	0.76442	1.21002	0.30454	0.833078	0.31592	0.84992	0.678324
13.2	29.47	gi 55956921	heterogeneous nuclear ribonucleoprotein A/B isoform b [Homo sapiens]	9	1.0958	0.21875	0.95419	0.514181	0.998728	0.98187	1.06164	0.42607	1.077823	0.36657	1.03855	0.682577
4.49	15.75	gi 217330646	activated RNA polymerase II transcriptional coactivator p15 [Homo sapiens]	2	1.00545	0.95064	0.93514	0.513028	0.866581	0.5256	0.9196	0.27018	0.941666	0.70261	0.93123	0.689454
7.02	12.25	gi 10835067	lupus La protein [Homo sapiens]	4	0.89702	0.81509	1.02335	0.970048	0.912524	0.7839	0.7299	0.73114	0.740666	0.69847	0.84575	0.690483
4.6	48.99	gi 156071462	ADP/ATP translocase 3 [Homo sapiens]	27	1.12804	0.72644	1.12233	0.745559	1.261938	0.52519	1.17129	0.68662	1.088808	0.69381	1.11963	0.691645
4.14	16.17	gi 39725636	transmembrane emp24 domain-containing protein 9 precursor [Homo sapiens]	3	1.09319	0.53296	1.04374	0.761259	1.333761	0.26105	0.73663	0.19907	0.970606	0.87339	1.08416	0.691946
4.38	12.82	gi 16117789	60S ribosomal protein L34 [Homo sapiens]	2	0.87852	0.5603	0.88838	0.470693	0.772053	0.45763	0.59708	0.13049	0.960721	0.77356	0.75407	0.692607
28.84	30.2	gi 50345984	ATP synthase subunit alpha, mitochondrial isoform a precursor [Homo sapiens]	21	0.95209	0.43118	0.97584	0.817633	0.944751	0.56027	0.99797	0.98171	0.942627	0.43909	1.03342	0.693136
20.15	55.88	gi 4504297	histone H3.1 [Homo sapiens]	20	1.11344	0.49506	0.89675	0.505913	0.998635	0.99393	1.19646	0.59173	0.925642	0.59705	0.94698	0.696575
19.47	39.46	gi 221307584	prohibitin-2 isoform 1 [Homo sapiens]	14	1.03343	0.73666	0.93609	0.6425	0.962379	0.72427	0.95351	0.83651	0.943864	0.59801	1.0389	0.697615
18.66	33.42	gi 93141020	core histone macro-H2A.1 isoform 2 [Homo sapiens]	12	1.03657	0.80111	0.98151	0.885185	1.032144	0.80074	0.93467	0.77516	1.039574	0.78897	0.94747	0.698714

17.45	gi 47132595	phosphate carrier protein, mitochondrial isoform b precursor [Homo sapiens] cytochrome c oxidase subunit 5B,	5	1.06729	0.32103	0.95402	0.461468	1.101687	0.16278	0.99838	0.98638	1.049733	0.44725	1.04113	0.699173
27.91	gi 17017988	mitochondrial precursor [Homo sapiens] CD44 antigen	4	1.01292	0.91838	1.27302	0.344714	0.87403	0.55306	0.53226	0.34154	1.014991	0.92652	0.92066	0.701532
11.59	gi 48255935	isoform 1 precursor [Homo sapiens]	9	0.99745	0.96815	1.05606	0.470139	0.974859	0.77069	1.02163	0.80288	0.952887	0.7142	0.95638	0.702046
6.26	41.78	gi 83376130 elongation factor 1-beta [Homo sapiens]	5	1.06939	0.52176	0.99888	0.998173	1.26491	0.11474	1.26122	0.61166	1.299958	0.42094	1.17718	0.702982
24.64	16.54	gi 23510340 ubiquitin-like modifier-activating enzyme 1 [Homo sapiens]	17	0.86945	0.13185	0.89243	0.154395	1.047217	0.59847	0.8588	0.06201	0.98632	0.84641	1.03481	0.70466
2.08	13.04	gi 5453559 ATP synthase subunit d, mitochondrial isoform a [Homo sapiens]	1	1.54649	0.1424	1.23522	0.663545	1.086338	0.55674	1.28814	0.2495	1.425763	0.40471	1.21003	0.705296
12.34	2.626	gi 41322916 plectin isoform 1 [Homo sapiens] heterogeneous nuclear	10	0.95217	0.8024	1.34488	0.401625	1.034696	0.93365	1.19649	0.63772	1.423922	0.15327	1.12662	0.707928
32.53	gi 14043070	ribonucleoprotein A1 isoform b [Homo sapiens]	23	1.05591	0.75886	0.96459	0.690319	1.149365	0.41417	1.20924	0.58318	1.019104	0.89852	1.07093	0.708404
4.16	12.32	gi 6912634 60S ribosomal protein L13a isoform 1 [Homo sapiens]	3	0.95479	0.81055	0.87337	0.259546	1.140071	0.34559	0.89491	0.55672	1.120049	0.45983	0.95566	0.711813
10.8	26.28	gi 21614499 ezrin [Homo sapiens]	15	1.06182	0.49832	1.05333	0.555483	1.307711	0.03294	0.94707	0.71822	1.133167	0.4463	0.89818	0.712349

—

		dolichyl- diphosphooligosacch													
21.58	gi 4506675	aride--protein glycosyltransferase subunit 1 precursor [Homo sapiens]	12	1.05826	0.57928	0.982	0.858546	0.991824	0.94215	1.03226	0.81042	0.962578	0.72136	1.03882	0.713397
14.9	gi 19743875	fumarate hydratase, mitochondrial [Homo sapiens]	5	1.23102	0.54474	0.98192	0.924664	1.139205	0.30063	0.85337	0.73457	1.058899	0.90011	1.1213	0.713871
15.3	gi 52630342	HLA class I histocompatibility antigen, Cw-1 alpha chain precursor [Homo sapiens]	6	0.97171	0.88809	1.02558	0.936087	1.027002	0.79844	0.88162	0.32984	0.853302	0.58819	0.90592	0.715453
65.58	gi 380837121	vesicle-trafficking protein SEC22b precursor [Homo sapiens]	20	1.10024	0.05719	1.03229	0.495044	1.038818	0.5283	1.06556	0.32572	0.996953	0.97062	1.03531	0.723297
5.752	gi 394025723	very long-chain specific acyl-CoA dehydrogenase, mitochondrial	3	0.74699	0.59182	0.76043	0.55318	0.988837	0.95255	0.65897	0.26758	0.911972	0.79251	0.72594	0.725427
22.11	gi 42476281	isoform 3 [Homo sapiens] voltage- dependent anion-selective channel protein 2 isoform 2 [Homo sapiens]	7	0.98794	0.90701	0.94137	0.558142	0.967298	0.81086	1.19774	0.20741	0.999744	0.998	0.97538	0.726116
7.612	gi 21536286	creatine kinase B-type [Homo sapiens]	2	0.93056	0.85493	0.75114	0.745502	0.851942	0.75556	0.70757	0.23455	0.726465	0.72965	0.86017	0.728049
22.58	gi 15431288	60S ribosomal protein L10a [Homo sapiens]	5	1.13923	0.20613	1.19379	0.097845	1.405531	0.07869	1.30502	0.03712	1.272751	0.04776	1.06428	0.731592

6.093	gi 4885281	glutamate dehydrogenase 1, mitochondrial precursor [Homo sapiens] 40S ribosomal	3	1.03466	0.82658	1.31687	0.384031	0.988878	0.95217	1.03104	0.84229	0.9713	0.90753	1.04757	0.734971
39.92	gi 378548190	protein S3 isoform 1 [Homo sapiens] ADP-ribosylation	10	1.05379	0.67765	0.90108	0.325676	0.998495	0.98928	0.95251	0.73441	1.080897	0.54587	1.05154	0.736446
28.89	gi 4502205	factor 4 [Homo sapiens] heterogeneous nuclear	5	1.12509	0.85061	0.88053	0.643544	1.213056	0.76438	0.7777	0.57084	0.860941	0.67797	0.83245	0.740092
11.04	gi 52632383	ribonucleoprotein L isoform a [Homo sapiens] RPS10-NUDT3	6	1.1947	0.19772	1.03175	0.790467	1.158331	0.37641	1.06595	0.63342	0.987748	0.89712	1.04132	0.742688
10.65	gi 321117084	protein [Homo sapiens] 60S ribosomal	3	1.01139	0.94355	1.0143	0.970992	0.922407	0.5861	1.00405	0.96666	1.059227	0.64926	0.96851	0.743459
50.71	gi 4506605	protein L23 [Homo sapiens] cytochrome c oxidase subunit 5A,	5	0.87865	0.74322	0.95354	0.771566	0.815871	0.53752	1.04347	0.881	0.760368	0.11783	0.92817	0.750798
18.67	gi 190885499	mitochondrial precursor [Homo sapiens] high mobility group	3	1.04812	0.65287	1.12766	0.567805	0.993509	0.97116	0.77747	0.09934	1.026415	0.78893	1.04016	0.752238
27.27	gi 194688135	protein B2 [Homo sapiens] transmembrane emp24 domain-	7	1.06464	0.85993	1.01726	0.972515	1.015592	0.97689	1.02219	0.96616	0.999257	0.99421	0.91965	0.760339
21.92	gi 98986464	containing protein 10 precursor [Homo sapiens] DNA topoisomerase	6	0.88786	0.72101	0.78503	0.248243	0.818962	0.61315	0.91388	0.79432	0.896156	0.53912	0.92621	0.763469
4.637	gi 19913406	2-alpha [Homo sapiens]	7	1.19997	0.81665	1.39591	0.184234	1.329365	0.30032	1.49119	0.45954	1.127594	0.8554	1.14999	0.764389

			heterogeneous													
19.02	gi 5803036	nuclear	ribonucleoprotein A0	5	1.05968	0.83796	0.97227	0.854566	1.114078	0.49743	1.07709	0.79112	1.012741	0.96513	1.05259	0.765253
19.03	48.66	gi 4758638	[Homo sapiens] peroxiredoxin-6	9	0.96744	0.76701	1.1843	0.204936	1.193197	0.07085	0.98306	0.94703	1.00903	0.97102	1.07972	0.767286
10.43	gi 4502285	[Homo sapiens] sarcoplasmic/endoplasmic reticulum	calcium ATPase 2 isoform a [Homo sapiens]	7	1.10151	0.66208	1.04782	0.815902	1.335057	0.31594	1.0606	0.84338	1.01103	0.93739	1.06943	0.767545
10.29	26.43	gi 73760405	thymopoietin isoform beta [Homo sapiens]	7	1.05181	0.61144	1.12399	0.350742	0.91077	0.54197	0.84554	0.35827	0.975897	0.80234	0.96391	0.768285
73.91	gi 4506671	60S acidic ribosomal protein P2 [Homo sapiens]		7	1.08556	0.34581	1.0435	0.605096	1.058493	0.49566	1.11581	0.23312	1.056699	0.50924	1.0239	0.768286
5.06	12.77	gi 163644321	cytochrome b-c1 complex subunit Rieske, mitochondrial [Homo sapiens]	3	0.75455	0.71922	0.57239	0.407115	0.771567	0.45298	0.86607	0.39779	0.948623	0.69406	0.84441	0.772512
4.75	14.44	gi 311771647	actin-related protein 2/3 complex subunit 4 isoform c [Homo sapiens]	2	1.08265	0.87616	0.96313	0.925078	1.106502	0.78565	0.72989	0.67988	0.828008	0.34231	1.1508	0.773513
65.79	gi 41399285	protein, mitochondrial [Homo sapiens]	60 kDa heat shock	57	1.00869	0.83404	1.0126	0.787426	1.000185	0.99618	0.99905	0.9821	0.998881	0.96892	1.00977	0.773751
36.93	gi 14110414	heterogeneous nuclear	ribonucleoprotein D0 isoform c [Homo sapiens]	11	0.99292	0.95083	0.93943	0.765849	0.999996	1	0.90384	0.55038	0.911699	0.637	0.96899	0.774905
31.82	gi 14277700	40S ribosomal	protein S12 [Homo sapiens]	5	1.01814	0.89192	0.83278	0.636779	1.036141	0.79088	1.09946	0.53195	0.947092	0.70597	1.03925	0.774943

43.03	gi 4506597	60S ribosomal protein L12 [Homo sapiens]	5	1.12104	0.41768	0.99867	0.991624	1.142792	0.27762	1.15111	0.36571	1.168818	0.22156	0.97404	0.775656
2.14	1.183	gi 69354671	1	0.97085	0.91323	1.37039	0.194106	1.471155	0.16004	0.99946	0.99909	1.19076	0.84283	0.88838	0.777605
15.77	gi 38455427	1 isoform a [Homo sapiens]	9	1.00106	0.99697	0.9324	0.78378	0.94696	0.89777	0.73934	0.19109	0.953969	0.86496	0.88244	0.781297
3.55	3.568	gi 25777600	2	0.5996	0.2571	0.72519	0.44323	0.696634	0.17297	0.78612	0.64533	0.951232	0.78597	0.90594	0.783538
37.56	gi 4758988	26S proteasome non-ATPase regulatory subunit 1 isoform 1 [Homo sapiens]	6	0.99181	0.96521	0.92253	0.748232	0.935789	0.76268	0.90523	0.4775	0.908909	0.59598	0.95635	0.786256
16.67	gi 7706244	2 precursors [Homo sapiens]	2	0.67103	0.589	1.19653	0.60623	1.002143	0.99217	0.80534	0.65969	0.637288	0.47229	0.87021	0.787415
2.13	1.915	gi 338827685	2	0.71448	0.18213	1.31353	0.221365	1.383797	0.18813	0.99862	0.9911	0.962428	0.76468	0.92112	0.789026
10.09	gi 20070197	AP-2 complex subunit alpha-2 isoform 1 [Homo sapiens]	4	1.04981	0.70743	0.9536	0.607867	1.072354	0.48364	1.0482	0.65371	1.145003	0.10928	0.95791	0.795514
5.68	1.27	gi 114155142	3	0.95437	0.71923	1.55827	0.139745	1.144505	0.69242	1.20935	0.80201	1.199909	0.83418	1.21081	0.797233
5.361	gi 42544159	105 kDa [Homo sapiens]	5	1.03791	0.83751	0.71001	0.495345	0.921183	0.61123	0.87039	0.52533	0.997984	0.98476	0.95339	0.800479

			complement	sapiens]
			component 1 Q	
			subcomponent-	
31.56	gi 4502491		binding protein,	
			mitochondrial	
			precursor [Homo	
			sapiens] delta-1-	
			pyrroline-5-	
5.75	7.296	gi 21361368	carboxylate synthase	
			isoform 1 [Homo	
			sapiens]	
			40S ribosomal	
18.54	gi 4506685		protein S13 [Homo	
			sapiens]	
30.7	gi 4502923	calponin	-3 [Homo	
			sapiens]	
8.48	9.269	gi 29029559	exportin-2 isoform 1	
			[Homo sapiens]	
8.48	9.269	gi 29029559	exportin-2 isoform 1	
			[Homo sapiens]	
14.77	50.49	gi 77539758	histone H4 [Homo	
			sapiens]	
			60S ribosomal	
4.48	43.75	gi 4506613	protein L22	
			proprotein [Homo	
			sapiens]	
51.1	gi 4505773	prohibitin	[Homo	
			sapiens]	
			elongation factor 1-	
18.99	gi 4503481	gamma	[Homo	
			sapiens]	
			chloride intracellular	
18.97	gi 7330335	channel protein 4		
			[Homo sapiens]	
			chromobox protein	
30.6	gi 20544151	homolog 3	[Homo	

9	1.00508	0.9556	1.08064	0.456452	3	1.08761	0.76023	1.14249	0.606873	0.916121	0.50274	1.29959	0.53768	0.975734	0.92692	1.07487	0.821474
	1.010557	0.92983	1.20337	0.33467													
	1.019807	0.90324	0.91517	0.802382													
3	0.9781	0.9669	0.85497	0.50659	0.897332	0.73533	0.78013	0.6573	0.641257	0.47964	1.06857	0.80268					
3	0.99031	0.93996	0.84468	0.333348	1.051426	0.71728	0.7756	0.29608	0.912275	0.4263	0.97195	0.802778					
15	1.02544	0.70414	1.05062	0.341917	0.941943	0.35536	0.95816	0.58435	1.044902	0.49742	1.01242	0.806483					
5	1.09982	0.8148	0.8955	0.765058	1.387637	0.56142	0.88907	0.77044	0.874732	0.85614	1.12938	0.809937					
5	1.09982	0.8148	0.8955	0.765058	1.387637	0.56142	0.88907	0.77044	0.874732	0.85614	1.12938	0.809937					
28	1.11512	0.252	0.94207	0.44027	1.094707	0.25106	1.24563	0.0212	0.995098	0.94742	1.09363	0.814591					
5	0.92582	0.39406	0.88941	0.431866	0.985671	0.87993	1.04055	0.82157	0.807588	0.15141	1.03663	0.815932					
12	0.96556	0.73689	1.04412	0.592809	1.132968	0.46259	1.04172	0.8169	1.082056	0.61104	0.97867	0.817195					
6	1.03165	0.89414	0.94509	0.835196	1.099946	0.45211	0.90037	0.57359	1.077196	0.62388	1.04039	0.819465					
4	1.02164	0.91147	1.13859	0.422729	1.466823	0.16472	1.11304	0.48267	1.016055	0.92994	0.97107	0.819961					

8.04	9.255	gi 5730027	KH domain-containing, RNA-binding, signal transduction-associated protein 1 [Homo sapiens]	5	1.06558	0.65957	0.93595	0.427594	0.998715	0.99478	0.95233	0.74678	0.92066	0.80624	0.96775	0.822087
3.383	gi 19743823	isoform 1A precursor [Homo sapiens]	3	1.32055	0.10167	1.13929	0.259019	1.350968	0.06939	1.04784	0.8101	1.521222	0.03788	1.08382	0.82873	
172.41	48.02	gi 160420317	filamin-A isoform 2 [Homo sapiens]	119	0.97842	0.41197	0.99518	0.85802	0.967653	0.27161	0.98363	0.61147	0.984986	0.55125	0.99244	0.828854
20.61	gi 16579885	60S ribosomal protein L4 [Homo sapiens]	7	1.07615	0.33021	1.01311	0.924931	1.084191	0.48575	1.04919	0.72858	0.997751	0.98856	0.9789	0.833723	
32.11	gi 4504041	guanine nucleotide-binding protein G(i) subunit alpha-2 isoform 1 [Homo sapiens]	9	1.13704	0.56315	0.96894	0.813532	1.020694	0.96158	0.93776	0.64576	1.055722	0.81975	1.02806	0.8344	
16.02	gi 5802974	thioredoxin-dependent peroxide reductase, mitochondrial isoform a precursor [Homo sapiens]	4	0.96798	0.81028	0.95634	0.515702	1.033963	0.62264	1.22076	0.55074	0.991637	0.90516	1.02995	0.835193	
9.494	gi 4506681	40S ribosomal protein S11 [Homo sapiens]	2	0.99409	0.97465	1.13149	0.545044	1.047803	0.88522	1.08859	0.77372	0.982615	0.92298	1.06109	0.835841	
8.42	9.772	gi 154354966	mitochondrial inner membrane protein isoform 3 [Homo sapiens]	5	1.0206	0.93464	1.03532	0.871746	0.988825	0.96777	0.9628	0.86904	1.0296	0.89968	0.96498	0.837598
4.45	61.11	gi 28173554	histone H2B type 3-B [Homo sapiens]	43	1.02072	0.90655	0.96056	0.861582	1.037087	0.84719	1.18373	0.44769	0.948548	0.65963	1.0357	0.838179
18.29	gi 4506901	serine/arginine-rich splicing factor 3 [Homo sapiens]	3	0.9852	0.96279	1.1985	0.438019	1.078372	0.69505	1.06264	0.90255	0.984337	0.93061	0.92951	0.838933	

18.42	gi 4507793	ubiquitin-conjugating enzyme E2 N [Homo sapiens]	1	1.16792	0.65472	1.21634	0.809184	1.932162	0.44384	1.52095	0.40788	0.920573	0.83344	1.21791	0.840396	
1.927.042	gi 5174449	histone H1x [Homo sapiens]	1	0.85343	0.28064	0.85981	0.345885	0.741735	0.07861	0.83554	0.26722	0.963425	0.82536	1.04754	0.841578	
38.34	gi 10835049	transforming protein RhoA precursor [Homo sapiens]	8	0.99703	0.98135	0.79242	0.729798	0.851819	0.80345	1.07826	0.72817	0.687668	0.33072	0.822	0.841902	
3.96	3.659	gi 166795299	solute carrier family 2, facilitated glucose transporter member 1 [Homo sapiens]	2	1.04935	0.91109	0.94918	0.915556	0.754969	0.25409	1.11376	0.68062	1.154167	0.39811	1.02541	0.847455
20.38	gi 5803137	putative RNA-binding protein 3 [Homo sapiens]	1	1.08481	0.88279	0.85746	0.624625	0.849487	0.80461	1.20187	0.86022	0.779833	0.50567	0.93073	0.84798	
2.204	gi 7661936	scaffold attachment factor B2 [Homo sapiens]	2	1.01899	0.91967	1.04755	0.836359	1.058761	0.80586	0.94253	0.81642	1.236486	0.51996	0.95485	0.848025	
16.74	gi 73486658	aspartate aminotransferase, mitochondrial precursor [Homo sapiens]	5	0.96036	0.87103	0.97537	0.860831	1.070459	0.6887	1.07102	0.52078	1.011362	0.91313	1.03523	0.849832	
6.79	29.52	gi 50592994	thioredoxin isoform 1 [Homo sapiens]	4	0.87285	0.42193	1.06975	0.476514	1.075307	0.44631	0.97736	0.91538	0.937442	0.49301	0.9463	0.854211
23.82	61.48	gi 4507879	voltage-dependent anion-selective channel protein 1 [Homo sapiens]	14	0.97731	0.69263	0.92668	0.34112	0.913339	0.34029	0.97341	0.74774	0.978336	0.79238	1.0166	0.858966
3.32	12.62	gi 4758018	calponin-2 isoform a [Homo sapiens]	3	1.19158	0.71105	1.19474	0.741549	0.728561	0.79122	1.01345	0.96606	0.868569	0.78228	1.14008	0.860278
26.37	gi 299523086	mesencephalic astrocyte-derived neurotrophic factor precursor [Homo sapiens]	5	1.11545	0.57209	1.11679	0.585957	1.029277	0.91557	1.01628	0.94928	1.076269	0.66921	1.04584	0.860548	

			heterogeneous													
20.63	gi 34740329	nuclear	ribonucleoprotein A3	10	1.10445	0.17571	0.9032	0.316306	1.145317	0.40173	1.07986	0.8933	1.122994	0.34016	1.02019	0.860986
			[Homo sapiens] 3-hydroxyacyl-CoA dehydratase 3 [Homo sapiens]	4	0.84957	0.44745	0.8334	0.161112	1.038632	0.8902	0.95966	0.90221	1.045877	0.88382	0.9249	0.862774
			heterogeneous nuclear													
24.93	gi 14141152		ribonucleoprotein M isoform a [Homo sapiens]	17	1.08628	0.35293	1.03725	0.695026	1.026806	0.73823	0.99633	0.96725	1.016342	0.83824	0.98941	0.873553
3.23	12.07	gi 170763500	protein SET isoform 1 [Homo sapiens]	4	1.0848	0.69043	1.03571	0.725061	1.088743	0.67097	0.98089	0.84488	1.116083	0.53368	0.97681	0.873979
12.24	64.24	gi 88999583	myosin light polypeptide 6 isoform 2 [Homo sapiens]	15	0.94267	0.343	0.9248	0.245371	0.932394	0.26936	0.99883	0.9843	0.985798	0.8209	0.9908	0.876608
			vacuolar ATPase assembly integral													
2.04	11.88	gi 63025214	membrane protein VMA21 [Homo sapiens]	1	0.90619	0.51417	0.99561	0.972821	1.057661	0.75898	1.18775	0.61068	1.014332	0.97255	0.96105	0.878343
7.9	9.387	gi 29789090	protein RCC2 [Homo sapiens]	4	1.11316	0.66394	1.06546	0.807756	1.060682	0.8303	0.96863	0.86843	1.225477	0.32522	1.03343	0.879579
			heterogeneous nuclear													
27.24	41.98	gi 117190254	ribonucleoproteins C1/C2 isoform b [Homo sapiens]	17	1.02698	0.67678	0.92177	0.182329	0.974944	0.74372	1.04255	0.69517	0.976558	0.74628	0.99	0.88068
			transferrin receptor													
18.26	15.39	gi 189458819	protein 1 [Homo sapiens]	11	1.11446	0.42576	0.99792	0.991522	1.124781	0.5508	1.14668	0.4871	0.988161	0.94215	0.94789	0.881912
			T-complex protein 1													
8.03	10.46	gi 63162572	subunit gamma isoform a [Homo sapiens]	4	0.82695	0.56059	0.81169	0.577272	1.153473	0.80554	0.82045	0.75663	1.050539	0.85656	0.93205	0.890922

5.536	gi 11056044	inorganic pyrophosphatase [Homo sapiens]	1	1.04929	0.9395	0.99655	0.995222	1.184591	0.80537	1.15813	0.82207	1.036608	0.79363	1.15318	0.891584	
0.6877	gi 56676335	telomere-associated protein RIF1 isoform 1 [Homo sapiens]	1	1.08279	0.66024	0.87066	0.777724	0.618766	0.34994	0.55636	0.52788	0.984399	0.9835	0.92906	0.892763	
16.95	gi 315221152	60S ribosomal protein L11 isoform 2 [Homo sapiens]	4	1.06126	0.56421	0.99761	0.975118	1.065146	0.43782	0.95199	0.536	1.085682	0.32948	0.98499	0.89321	
27.44	gi 4504425	high mobility group protein B1 [Homo sapiens]	8	1.025	0.85145	0.92685	0.563656	0.927637	0.65527	1.01212	0.93795	0.957028	0.6268	0.97689	0.893937	
13.77	28.61	gi 24308201	adipocyte plasma membrane-associated protein [Homo sapiens]	10	0.83601	0.21067	1.06307	0.479644	0.886176	0.51837	0.86221	0.20778	0.968326	0.63722	1.03196	0.894531
26.57	gi 4506701	40S ribosomal protein S23 [Homo sapiens]	3	0.87112	0.40648	0.72728	0.199117	0.817343	0.42284	0.7103	0.30555	1.074612	0.66576	1.01694	0.896721	
45.19	gi 4506693	40S ribosomal protein S17 [Homo sapiens]	6	0.99431	0.97242	0.97255	0.722537	1.038886	0.75248	1.03874	0.67553	1.034698	0.66409	0.98707	0.899802	
20.93	gi 5453603	T-complex protein 1 subunit beta isoform 1 [Homo sapiens]	6	1.09951	0.79704	1.08657	0.641929	1.428159	0.05029	1.03563	0.83282	0.912354	0.81703	1.02791	0.899862	
46.15	gi 21464101	14-3-3 protein gamma [Homo sapiens]	15	1.02568	0.83239	1.03997	0.769753	0.969569	0.85613	0.90003	0.52358	0.991797	0.94948	0.96655	0.900023	
16.61	9.229	gi 256222411	filamin-B isoform 1 [Homo sapiens]	20	0.98336	0.8992	1.02555	0.853117	1.118949	0.54084	0.99812	0.9923	0.991695	0.90764	0.97554	0.900285
4.3	11.45	gi 388240801	lamin-B2 [Homo sapiens]	7	0.87942	0.71958	1.10445	0.77971	0.78914	0.61079	0.91952	0.83412	0.95001	0.85965	0.94256	0.901109
2.058	gi 39753957	torsin-1A-interacting protein 1 isoform 2 [Homo sapiens]	1	0.83348	0.33185	0.96138	0.867541	1.103016	0.62859	0.87927	0.53707	1.083103	0.74121	1.05113	0.903757	

22.16	gi 14141193	40S ribosomal protein S9 [Homo sapiens]	5	0.99992	0.99954	0.92862	0.763386	0.945508	0.76024	0.95503	0.83905	1.075762	0.60233	1.01905	0.904019	
8.11	27.47	gi 34098946	nuclease-sensitive element-binding protein 1 [Homo sapiens]	5	1.07413	0.56558	1.14988	0.476996	1.06747	0.59239	1.0434	0.82634	1.220969	0.45264	1.0157	0.90823
2.15	8.894	gi 42822874	ribonuclease inhibitor [Homo sapiens]	2	0.80302	0.27929	0.90655	0.700213	1.344467	0.6081	1.12269	0.45072	1.136887	0.41847	0.98588	0.909263
2.452	gi 225543215	antigen KI-67 isoform 2 [Homo sapiens]	4	1.03006	0.8092	0.87668	0.728422	1.203502	0.26766	1.24771	0.44123	1.27859	0.18565	1.03634	0.910268	
3.52	50.74	gi 4885385	histone H3.3 [Homo sapiens]	11	0.96893	0.81563	0.94274	0.67602	1.054957	0.7012	0.9351	0.87652	1.046815	0.7414	1.02837	0.910912
22.4	gi 4506457	reticulocalbin-2 precursor [Homo sapiens]	5	1.38471	0.39167	1.2916	0.445955	1.296941	0.47927	1.43781	0.41555	1.536593	0.26422	1.06997	0.911035	
2.682	gi 50659095	nucleolar RNA helicase 2 isoform 1 [Homo sapiens]	2	1.01952	0.95996	1.38491	0.187652	1.017043	0.89225	1.16703	0.36259	0.984875	0.91557	0.97993	0.915927	
3.63	9.016	gi 5031777	isocitrate dehydrogenase [NAD] subunit alpha, mitochondrial precursor [Homo sapiens]	2	1.16688	0.3754	1.19345	0.716846	1.497555	0.3531	1.59903	0.20131	1.23718	0.57148	1.03029	0.917579
25	gi 15431301	60S ribosomal protein L7 [Homo sapiens]	7	0.92425	0.48551	1.03374	0.876283	0.95133	0.5483	0.99818	0.99234	1.082148	0.57258	1.0118	0.917983	
24	gi 256222019	ras-related protein Rab-10 [Homo sapiens]	5	0.94102	0.6384	0.90518	0.403307	0.902896	0.68559	0.80889	0.38432	0.987171	0.95238	0.95457	0.918074	

3.12	2.979	gi 22749415	aride--dolichyl- diphosphooligosacch protein	1	1.06993	0.62139	1.02313	0.947688	0.891197	0.48906	1.44778	0.43354	1.22369	0.29182	0.94878	0.91885
			glycosyltransferase subunit STT3A [Homo sapiens] NADH dehydrogenase [ubiquinone] iron-													
5.682		gi 4758788	sulfur protein 3, mitochondrial precursor [Homo sapiens] electron transfer flavoprotein subunit	1	1.09954	0.75239	1.00194	0.98818	1.04381	0.83939	1.10044	0.84765	1.189316	0.20548	1.01421	0.919937
21.92		gi 4503607	alpha, mitochondrial isoform a [Homo sapiens]	7	0.745	0.58946	1.25831	0.663793	0.924426	0.79947	0.83736	0.64983	0.555631	0.57613	0.93131	0.921689
7.143		gi 4759160	small nuclear ribonucleoprotein Sm D3 [Homo sapiens]	1	0.90276	0.57568	0.9279	0.468609	0.88426	0.48308	0.81171	0.52085	0.831009	0.17558	0.98806	0.923847
23.08		gi 4758302	enhancer of rudimentary homolog [Homo sapiens]	3	1.03392	0.80889	1.12985	0.460855	1.232816	0.30435	1.13608	0.57846	0.945932	0.6978	1.02672	0.926136
2.46	3.648	gi 5031703	ras GTPase-activating protein-binding protein 1 [Homo sapiens]	1	0.92013	0.57087	0.85965	0.452881	0.880045	0.48158	0.95338	0.81138	0.917742	0.69749	0.95912	0.926288
4.52	7.756	gi 56549640	septin-2 [Homo sapiens]	3	0.99332	0.99483	1.23575	0.823806	1.353351	0.76378	1.72484	0.58133	1.284647	0.70863	0.93565	0.926332
1.68	5.263	gi 4758356	flap endonuclease 1 [Homo sapiens] 40S ribosomal	1	1.15011	0.39223	1.10884	0.675855	1.067793	0.6274	1.00338	0.98366	0.94599	0.67436	1.01114	0.929123
11.37	23.19	gi 4506725	protein S4, X isoform X isoform [Homo sapiens]	5	0.97449	0.7355	0.92138	0.507416	0.964998	0.73662	1.12599	0.23149	0.953784	0.56743	1.00613	0.930998

6.34	23.31	gi 7305503	stomatin-like protein 2 [Homo sapiens]	5	1.17661	0.76853	1.01792	0.956275	0.970179	0.89195	1.06593	0.66163	0.877609	0.82736	1.03079	0.931181
10.33	10.26	gi 55770844	catenin alpha-1 [Homo sapiens] 14-3-3 protein	6	1.03773	0.77724	1.42203	0.622809	1.56616	0.3328	1.23645	0.37736	0.997016	0.98129	1.04962	0.932653
46.12		gi 4507953	zeta/delta [Homo sapiens] tubulin beta-3 chain	15	0.89929	0.60586	0.98527	0.856421	1.099533	0.64591	0.782	0.35808	0.893897	0.20654	1.01769	0.935496
42.89		gi 50592996	isoform 1 [Homo sapiens] catenin delta-1	29	0.78939	0.25372	1.16165	0.795319	0.842534	0.33496	0.84947	0.34915	0.973308	0.83089	1.03767	0.937168
5.112		gi 332688210	isoform 1AC [Homo sapiens]	4	1.02514	0.97096	0.55873	0.469676	1.062146	0.89209	1.20211	0.85366	0.898966	0.87101	0.97397	0.939865
6.9858.88		gi 4507729	tubulin beta-2A chain [Homo sapiens]	41	0.948	0.76834	0.9999	0.99978	0.903984	0.61965	0.88799	0.79613	0.752115	0.29768	0.96998	0.940554
16.43	40.26	gi 24234747	interleukin enhancer-binding factor 2 isoform 1 [Homo sapiens]	13	1.0511	0.7347	0.91691	0.632643	0.969474	0.89625	0.95433	0.83549	0.978358	0.87143	0.98794	0.942942
25.2		gi 4505753	phosphoglycerate mutase 1 [Homo sapiens] hexokinase-1 isoform	8	0.96526	0.90588	1.29984	0.237936	0.99391	0.9809	1.07441	0.81875	0.812698	0.54835	1.02478	0.944817
5.972		gi 15991831	HKI-ta/tb [Homo sapiens] 60S ribosomal	4	1.10822	0.50056	1.13319	0.676442	1.011951	0.97474	1.03129	0.9428	0.989503	0.97605	0.98934	0.947689
14.19		gi 4506625	protein L27a [Homo sapiens]	2	0.99323	0.96296	1.09852	0.728854	0.889413	0.73997	1.01465	0.96828	0.90663	0.53302	1.02292	0.950836
5.31	19.58	gi 4757908	calcyphosin isoform a [Homo sapiens]	4	0.7789	0.18217	1.03856	0.851888	0.898004	0.30411	0.85694	0.39045	0.957459	0.62455	0.98766	0.952912
3.08	4.58	gi 11386147	proactivator polypeptide isoform a preproprotein [Homo sapiens]	2	0.7416	0.68952	1.1469	0.767531	0.803347	0.76691	0.88676	0.90596	1.279128	0.79946	1.05125	0.953217

36.71	60.31	gi 4502107	annexin A5 [Homo sapiens] ras-related protein	28	1.02188	0.71923	1.04762	0.283796	1.041221	0.53751	1.02478	0.79402	1.003106	0.9381	1.00371	0.960815
11.11		gi 4758984	Rab-11A isoform 1 [Homo sapiens]	2	1.05913	0.823	0.92678	0.757553	1.219468	0.2448	1.02015	0.94044	0.980833	0.91924	1.01765	0.961985
9.559		gi 127139033	NADPH--cytochrome P450 reductase [Homo sapiens]	5	1.46665	0.26812	1.35078	0.78343	1.750845	0.28485	1.50179	0.58197	1.396446	0.19557	1.01903	0.963064
9.428		gi 304555583	elongation factor 1-delta isoform 1 [Homo sapiens]	4	1.05626	0.86542	1.13667	0.76818	1.069415	0.889	1.01608	0.96552	1.236347	0.55616	1.01694	0.964416
19.2	40	gi 4504245	histone H2A type 1-C [Homo sapiens] neutral alpha-	42	1.03017	0.86464	0.91872	0.699991	0.933817	0.74092	1.19479	0.32328	0.974854	0.83978	0.99492	0.967249
25.54	15.89	gi 38202257	glucosidase AB isoform 2 precursor [Homo sapiens] heterogeneous	14	1.04371	0.617	1.12201	0.3039	1.067465	0.42923	1.09288	0.44729	1.079871	0.33047	1.00402	0.967442
32.07		gi 5031753	nuclear ribonucleoprotein H [Homo sapiens] leucine-rich PPR motif-containing	18	0.97527	0.83475	0.82622	0.394135	1.084716	0.50783	0.92009	0.68814	0.934815	0.65578	0.99293	0.972627
17		gi 31621305	protein, mitochondrial precursor [Homo sapiens] leucine-rich PPR motif-containing	16	1.03366	0.87957	0.98367	0.912034	1.06177	0.80072	1.01847	0.89318	1.135167	0.43715	0.99557	0.974808
17		gi 31621305	protein, mitochondrial precursor [Homo sapiens] -2 [Homo sapiens]	16	1.03366	0.87957	0.98367	0.912034	1.06177	0.80072	1.01847	0.89318	1.135167	0.43715	0.99557	0.974808
80.9		gi 4507357	transgelin-2 [Homo sapiens]	44	0.94206	0.15285	0.98498	0.707045	0.982281	0.65704	0.95133	0.34752	0.973675	0.50977	0.99881	0.976356
33.33		gi 4506715	40S ribosomal protein S28 [Homo sapiens]	2	1.06887	0.59919	1.27592	0.261705	1.038603	0.6719	1.2457	0.32914	1.089153	0.60128	1.00461	0.986721

[illegible]

11.28	gi 28178832	isocitrate dehydrogenase [NADP], mitochondrial precursor [Homo sapiens]	5	1.30054	0.97425	1.043614	0.95524	1.064548	1.35882
12.65	gi 285002233	glycerol-3-phosphate dehydrogenase, mitochondrial precursor [Homo sapiens]	8	0.63612	0.43177	0.605118	0.60499	0.806922	0.5378
9.02	44.56 gi 28395033	rho-related GTP-binding protein RhoC precursor [Homo sapiens]	6	1.92031	0.99363	1.700983	1.06466	1.078723	1.42801
8.89	4.503 gi 38201623	eukaryotic translation initiation factor 4 gamma 1 isoform 5 [Homo sapiens]	9	0.66325	1.16796	0.670461	0.73769	1.420639	0.48499
6.069	gi 4507943	exportin -1 [Homo sapiens]	4						
8	79.82 gi 4506669	60S acidic ribosomal protein P1 isoform 1 [Homo sapiens]	7	1.06983	0.97872	1.0065	1.03349	0.986462	0.95046
8.063	gi 45387945	extended synaptotagmin-2 [Homo sapiens]	4						
7.63	13.58 gi 4507353	TATA-binding protein-associated factor 2N isoform 2 [Homo sapiens]	5						
7.35	56.82 gi 11056061	thymosin beta-4 [Homo sapiens]	5	0.92823	1.03146	1.020059	0.8738	0.987755	1.09835

7.22	4.92	gi 4503509	eukaryotic translation initiation factor 3 subunit A [Homo sapiens]	5	2.39279	4.4105	2.463701	3.54179	2.01806	2.10314
7.069		gi 385298680	116 kDa U5 small nuclear ribonucleoprotein component isoform c [Homo sapiens]	6						
6.54	3.137	gi 40217847	U5 small nuclear ribonucleoprotein 200 kDa helicase [Homo sapiens]	6	1.14194	1.62901	0.86916	0.90805	1.30212	0.33775
4.864		gi 21361370	glycogen phosphorylase, brain form [Homo sapiens]	4	0.74647	0.88615	0.815465	0.71197	0.782035	1.25844
3.298		gi 54112117	splicing factor 3B subunit 1 isoform 1 [Homo sapiens]	3						
6.23	5.349	gi 71773329	annexin A6 isoform 1 [Homo sapiens]	3	4.50272	3.54499	4.594796	3.09253	3.811192	5.69826
5.579		gi 109148542	alanine--tRNA ligase, cytoplasmic [Homo sapiens]	3	0.82244	0.9845	0.950517	0.84237	0.686344	1.03448
20.49		gi 7706322	UPF0568 protein C14orf166 [Homo sapiens]	5						
25.17		gi 194097323	enoyl-CoA hydratase, mitochondrial [Homo sapiens]	7	2.03732	1.74468	2.134784	1.98122	1.267649	3.15589
28.65		gi 222352151	poly(rC)-binding protein 1 [Homo sapiens]	8	0.92485	0.81808	1.163378	1.00833	0.545206	1.00614
30.2		gi 50593002	U2 small nuclear ribonucleoprotein A' [Homo sapiens]	6	1.12271	0.91509	1.310521	1.0248	1.543845	1.43563

9.605	gi 4502643	T-complex protein 1 subunit zeta isoform a [Homo sapiens]	4	0.66609	0.49984	1.35727	1.1912	0.776804	0.82225
4.986.839	gi 45827806	atlastin-3 [Homo sapiens]	3						
6.071	gi 38327039	heat shock 70 kDa protein 4 [Homo sapiens]	3						
4.75 27.57	gi 6912238	peroxiredoxin-5, mitochondrial isoform a precursor [Homo sapiens]	5	0.7021	1.18907	1.478837	0.4313	1.39936	1.21253
7.559	gi 4758786	NADH dehydrogenase [ubiquinone] iron-sulfur protein 2, mitochondrial isoform 1 precursor [Homo sapiens]	2						
4.63 6.966	gi 18677735	protein PRRC1 [Homo sapiens]	3						
14.94	gi 23110942	proteasome subunit alpha type-5 isoform 1 [Homo sapiens]	3						
4.46 12.4	gi 269914128	OCIA domain-containing protein 1 isoform 4 [Homo sapiens]	2	1.21801	1.37961	1.346004	1.48184	1.117946	1.18723
4.44 10.44	gi 4502049	aldose reductase [Homo sapiens]	4	1.47454	1.36634	1.409654	0.99615	0.923845	1.00292
9.053	gi 5453595	adenylyl cyclase-associated protein 1 [Homo sapiens]	4	1.57866	1.2196	2.380994	1.61705	1.994657	2.52747
4.4 5.615	gi 4506341	ATP-binding cassette sub-family D member 3 isoform a [Homo sapiens]	3	0.32324	0.75219	1.198383	1.30105	1.203778	1.54799

		FACT complex							
3.725	gi 6005757	subunit SPT16	2						
		[Homo sapiens]							
		phosphatidylinositol-							
		binding clathrin							
6.442	gi 56788366	assembly protein	3	0.84523	0.80269	1.0253	0.9725	0.986006	0.97061
		isoform 1 [Homo							
		sapiens]							
		dihydropyrimidinase-							
4.32	6.795	gi 308818195	2						
		related protein 2							
		isoform 1 [Homo							
		sapiens]							
		procollagen-lysine,2-							
		oxoglutarate 5-							
6.369	gi 4505891	dioxygenase 3	5						
		precursor							
		[Homo sapiens]							
		tenascin precursor							
4.17	1.681	gi 153946395	2						
		[Homo sapiens]							
		alpha-aminoadipic							
		semialdehyde							
5.479	gi 319655561	dehydrogenase	3						
		isoform 2 [Homo							
		sapiens]							
		vacuolar protein							
4.14	3.894	gi 17999541	3						
		sorting-associated							
		protein 35 [Homo							
		sapiens] glycine--							
		tRNA ligase							
6.225	gi 116805340	precursor [Homo	2	0.80401	0.7306	0.752112	0.67938	0.6988	0.817
		sapiens]							
		non-specific lipid-							
4.12	5.368	gi 302344762	2						
		transfer protein							
		isoform 6							
		proprotein							
		[Homo sapiens]							

2.758	gi 148536855	coatomer subunit alpha isoform 1 [Homo sapiens] actin- related protein 2	3	0.84495	1.14378	0.879331	1.20518	0.78377	0.92041	
12.28	gi 53692187	isoform a [Homo sapiens]	3							
6.528	gi 5803187	transaldolase [Homo sapiens]	3							
6.742	gi 6598323	rab GDP dissociation inhibitor beta isoform 1 [Homo sapiens]	2	1.31164	1.35366	1.719467	1.22879	1.907645	1.82516	
4.11	17.34	gi 5454090	protein translocon-associated subunit delta isoform 2 precursor [Homo sapiens]	2	1.09614	1.01594	1.240244	1.2115	1.02137	1.06552
4.1	2.276	gi 21361794	NEDD8-associated cullin-associated protein 1 [Homo sapiens] ATP-citrate synthase	3						
2.816	gi 38569421	isoform 1 [Homo sapiens]	2	1.47681	1.78721	2.177375	1.43963	1.056422	1.85165	
12.5	gi 19923315	serine hydroxymethyltransfe rase, mitochondrial isoform 1 precursor [Homo sapiens]	5	2.17269	1.45205	1.733907	1.84592	1.6707	1.17943	
3.904	gi 109134349	coatomer subunit gamma-2 [Homo sapiens]	2							
7.196	gi 195539395	26S protease regulatory subunit 10B [Homo sapiens]	2	0.78017	0.46331	1.391888	1.14351	0.599761	1.27963	

14.64	gi 30410792	proteasome activator complex subunit 2 [Homo sapiens]	3	1.35076	1.30523	0.949045	1.36713	1.264915	0.92517
8.119	gi 166795301	prenylcysteine oxidase 1 precursor [Homo sapiens]	3	1.05175	0.98525	1.0761	0.91641	0.986455	0.77613
4.02	4.662 gi 8922712	septin-11 [Homo sapiens]	2						
5.568	gi 37537716	eukaryotic translation initiation factor 5 [Homo sapiens]	3						
4.01	29.13 gi 17933772	protein S100-A16 [Homo sapiens]	2	0.91551	0.57837	1.177884	1.32834	1.245144	1.04009
4	64.97 gi 393715091	tubulin alpha-1A chain isoform 1 [Homo sapiens]	61	0.86763	1.09195	1.091364	0.95509	0.999499	1.17204
4	17.76 gi 151108473	mitochondrial fission 1 protein [Homo sapiens]	2						
4	41.07 gi 7705501	transmembrane protein 14C [Homo sapiens]	2						
27.97	gi 21956645	myotrophin [Homo sapiens]	3						
3.85	4.626 gi 25777602	26S proteasome non-ATPase regulatory subunit 2 [Homo sapiens]	3						
1.638	gi 110611220	ribosome-binding protein 1 [Homo sapiens]	2						
3.68	4.777 gi 4758648	kinesin-1 heavy chain [Homo sapiens]	4						
19.44	gi 4759212	tubulin-specific chaperone A [Homo sapiens]	4	0.72985	0.79919	0.8261	0.89374	0.765348	0.87837

6.383	gi 4501993	alkyldihydroxyaceton ephosphate synthase, precursor [Homo sapiens]	3	1.3973	1.20706	1.229661	1.30968	0.870439	0.9839
6.713	gi 9951915	adenosylhomocystein ase isoform 1 [Homo sapiens]	3	0.91699	1.54572	0.960423	0.51959	1.187545	1.25412
3.47	11.58 gi 397138571	PREDICTED: putative trypsin-6 isoform 2 [Homo sapiens]	6	0.6452	0.71299	0.688758	0.84167	0.871762	0.4976
5.369	gi 4503971	rab GDP dissociation inhibitor alpha [Homo sapiens]	2						
3.41	3.436 gi 56676330	heterochromatin protein 1-binding protein 3 [Homo sapiens]	3	0.93177	1.38266	0.985569	0.63015	1.159698	0.87353
16.67	gi 28933465	syntaxin -12 [Homo sapiens]	3	0.65228	1.28782	1.08027	0.56742	0.870332	1.17819
8.754	gi 14591909	60S ribosomal protein L5 [Homo sapiens]	2	0.96889	1.29402	0.971669	1.24532	1.17296	0.77783
3.212	gi 45827771	enhancer of mRNA- decapping protein 4 [Homo sapiens]	2						
6.25	gi 38150007	small nuclear ribonucleoprotein- associated proteins B and B' isoform B' [Homo sapiens] DNA damage-binding	2	0.94294	0.69364	0.869764	0.63095	0.803134	0.49355
1.404	gi 148529014	protein 1 [Homo sapiens]	2						

10.32	gi 4503139	cathepsin B preproprotein [Homo sapiens]	2	0.70471	0.80279	0.654314	0.69681	0.634219	0.7471	
11.01	gi 346644849	DNA-(apurinic or apyrimidinic site) lyase [Homo sapiens]	3	1.2326	1.04638	1.573288	1.95319	1.46752	1.26419	
3.15	13.95	gi 7705696	thioredoxin domain- containing protein 12 precursor [Homo sapiens]	2						
3.06	9.44	gi 6005721	erlin-2 isoform 1 [Homo sapiens] calpain-2 catalytic	3	1.05746	1.13755	0.971272	1.06971	0.825092	1.21269
3.714	gi 157389005	subunit isoform 1 [Homo sapiens]	2							
2.93	20.61	gi 5802966	destrin isoform a [Homo sapiens]	3	0.86667	1.08644	1.071251	0.54751	0.656449	0.63406
2.93	6.395	gi 217272851	prolyl 4-hydroxylase subunit alpha-1 isoform 3 precursor [Homo sapiens]	2	1.05682	0.51686	1.175281	1.00522	0.697477	1.48189
0.8478	gi 194595509	spectrin alpha chain, brain isoform 1 [Homo sapiens]	2							
9.562	gi 5454088	acidic leucine- rich nuclear phosphoprotein 32 family member B [Homo sapiens]	2							
2.81	18.62	gi 7657257	mitochondrial import receptor subunit TOM20 homolog [Homo sapiens]	2	1.12647	0.96503	0.830369	1.03807	0.875227	0.89786
2.71	9.603	gi 386781571	radixin isoform 1 [Homo sapiens]	6	0.81532	1.25499	1.601472	0.54108	0.565041	1.1877

9.375	gi 42761474	CD59 glycoprotein preproprotein [Homo sapiens]	1	0.86805	0.97073	0.997505	1.10319	0.866608	0.84686
2.65	1.65	gi 9257257	WD repeat-containing protein 1 isoform 1 [Homo sapiens]	1					
2.64	7.125	gi 365192532	myosin-10 isoform 1 [Homo sapiens]	15	0.66064	0.65413	1.10042	0.93428	0.603853
5.534	gi 219283152	apoptosis inhibitor 5 isoform a [Homo sapiens]	4	0.85311	1.16414	1.634897	1.38697	1.133337	1.00298
2.61	7.116	gi 30410796	proteasome activator complex subunit 3 isoform 2 [Homo sapiens]	3	0.63085	0.92394	0.72022	0.36527	0.9777
12.16	gi 4507231	single-stranded DNA-binding protein, mitochondrial precursor [Homo sapiens]	3	1.58337	1.341	1.461128	1.51503	1.563343	1.89598
7.182	gi 7657441	28 kDa heat- and acid-stable phosphoprotein [Homo sapiens]	1	0.85503	0.87906	0.343909	0.40988	0.740731	1.13019
2.58	10.82	gi 13569879	acidic leucine-rich nuclear phosphoprotein 32 family member E isoform 1 [Homo sapiens]	3					
2.51	1.262	gi 283436220	ATPase family AAA domain-containing protein 3A isoform 1 [Homo sapiens]	1	0.57696	0.62027	0.424078	0.20236	0.411318
2.492.839	gi 4885409	vigilin isoform a [Homo sapiens]	2						

2.45	5.919	gi 12056465	rRNA 2'-O-methyltransferase fibrillarin [Homo sapiens]	2	0.84699	1.04848	0.77802	0.72476	0.814099	1.04849
2.43	7.67	gi 512285701	malate dehydrogenase, cytoplasmic isoform 1 [Homo sapiens]	2	0.88475	0.75548	0.903711	0.51043	0.991972	0.72992
2.42	16.39	gi 21040371	ATP-dependent RNA helicase DDX39A [Homo sapiens]	5						
2.42	9.394	gi 19923181	PDZ and LIM domain protein 4 isoform 1 [Homo sapiens]	3	0.74782	1.03132	1.006054	0.97864	1.449987	1.22062
2.4	32.52	gi 4507949	14-3-3 protein beta/alpha [Homo sapiens]	14	1.25318	1.06152	1.807213	1.40418	0.817041	1.31435
2.38	1.307	gi 11225260	DNA topoisomerase 1 [Homo sapiens]	1	0.66957	0.99773	1.318882	0.92511	1.109218	1.38873
2.36	5.966	gi 7657649	tropomodulin-3 [Homo sapiens]	1	0.54916	0.58171	0.468889	0.03686	0.571124	0.66021
2.35	14.81	gi 4505357	NADH dehydrogenase [ubiquinone] 1 alpha subcomplex subunit 4 [Homo sapiens]	1	1.14039	0.96507	1.457507	0.9558	1.061194	1.20029
2.34	1.223	gi 124494238	unconventional myosin-Ic isoform a [Homo sapiens]	1	0.62802	0.55643	0.50495	0.18695	0.410643	0.63169
2.33	1.135	gi 30581135	structural maintenance of chromosomes protein 1A [Homo sapiens]	2						

		heterogeneous nuclear							
2.57	gi 21536326	ribonucleoprotein U-like protein 1 isoform a [Homo sapiens]	1	0.27416	0.26981	0.297418	0.21473	0.517851	0.40407
4.837	gi 38202214	protein transport protein Sec23A [Homo sapiens]	2						
1.844	gi 10190742	ubiquitin carboxyl-terminal hydrolase 29 [Homo sapiens]	1						
2.3	12.24	gi 66737374 protein S100-A13 [Homo sapiens]	1	1.52857	0.65298	0.87031	1.73263	1.020324	1.2015
2.29	10.38	gi 373432684 ubiquitin-conjugating enzyme E2 L3 isoform 4 [Homo sapiens]	3						
2.29	6.407	gi 4759034 eukaryotic peptide chain release factor subunit 1 [Homo sapiens]	2	0.79436	0.80778	0.666296	0.44907	0.246555	0.56426
2.28	4.723	gi 316983160 NADH-ubiquinone oxidoreductase 75 kDa subunit, mitochondrial isoform 5 [Homo sapiens]	2						
23.2	gi 4502203	factor 3 [Homo sapiens] ADP-ribosylation	4	1.20672	1.21644	1.051839	1.28095	0.886377	1.39553
1.534	gi 33356174	pinin [Homo sapiens]	1	0.85067	0.83291	1.13135	0.86094	1.075418	0.5121
2.26	4.172	gi 33469968 DNA replication licensing factor MCM7 isoform 1 [Homo sapiens]	2	0.66264	0.98625	1.075919	0.92704	0.936778	0.82464

2.25	1.436	gi 296317244	extended synaptotagmin-1	2						
			isoform 1 [Homo sapiens]							
			40S ribosomal							
13.1		gi 4506687	protein S15 [Homo sapiens]	2	0.72722	0.74515	0.691769	0.38782	0.804124	0.74194
			ATP synthase subunit O, mitochondrial							
2.25	7.981	gi 4502303	precursor [Homo sapiens]	2	1.18023	1.17369	0.871478	0.88042	0.799421	0.82527
			eukaryotic translation initiation factor 6							
2.25	10.62	gi 31563374	isoform c [Homo sapiens]	1						
			coatamer subunit							
1.957		gi 11863154	delta isoform 1 [Homo sapiens]	1						
			nodal modulator 2							
1.579		gi 51944971	isoform 1 precursor [Homo sapiens]	1						
			SWI/SNF complex subunit SMARCC2							
2.24	1.062	gi 21237808	isoform b [Homo sapiens]	1						
			ras-related protein							
4.889		gi 7661922	Rab-21 [Homo sapiens]	1	1.2084	0.76928	1.115088	0.71112	0.929048	0.73102
			nuclear pore membrane							
0.9009		gi 27477134	glycoprotein 210 precursor [Homo sapiens]	1						
2.231.794		gi 24797086	importin-5 [Homo sapiens]	1	1.02307	1.20567	1.213528	1.21964	0.937203	0.83983

2.22	1.463	gi 61742777	leucyl-cystinyl aminopeptidase	1						
			isoform 1 [Homo sapiens]							
			glutamine--tRNA							
2.968		gi 4826960	ligase [Homo sapiens]	2						
			procollagen							
2.21	1.286	gi 31377697	galactosyltransferase 1 precursor [Homo sapiens]	1	0.89469	0.93139	1.864245	1.28507	2.11273	1.20325
			DNA repair protein							
1.372		gi 19924129	RAD50 [Homo sapiens]	1						
			methionine--tRNA							
2.111		gi 14043022	ligase, cytoplasmic [Homo sapiens]	1						
			60S ribosomal							
5.882		gi 4506623	protein L27 [Homo sapiens]	1	1.10035	0.91496	0.965733	1.13191	0.864173	1.03142
			LETM1 and EF-hand domain-containing							
2.17	1.894	gi 6912482	protein 1, mitochondrial precursor [Homo sapiens]	1	0.71105	0.92143	1.40973	1.03453	0.92632	0.9231
			beta-hexosaminidase							
2.17	1.799	gi 4504373	subunit beta preproprotein [Homo sapiens]	1						
			nuclear pore complex							
2.16	0.8333	gi 21264365	protein Nup98- Nup96	1						
			isoform 1 [Homo sapiens]							

0.65	gi 52630326	chromodomain-helicase-DNA-binding protein 3 isoform 1 [Homo sapiens]	1							
2.16	7.489	gi 38505222	protein disulfide-isomerase TMX3 precursor [Homo sapiens]	3	0.79121	0.71153	0.996528	0.97663	0.65292	0.96825
2.16	6.297	gi 4504511	dnaJ homolog subfamily A member 1 [Homo sapiens]	1	0.7664	1.08557	0.631588	0.45396	0.520625	0.50215
2.15	0.742	gi 21040326	protein SON isoform F [Homo sapiens]	2	0.50701	0.5684	0.514403	1.07732	0.679063	1.01611
2.15	1.086	gi 112382237	synemin isoform A [Homo sapiens]	1						
0.8696	gi 22202611	carboxypeptidase D isoform 1 precursor [Homo sapiens]	1	0.98697	0.81086	1.696009	1.31237	1.248185	1.63565	
1.732	gi 17149828	NatA auxiliary subunit [Homo sapiens]	1							
0.7216	gi 254939537	unconventional myosin-XIX isoform 2 [Homo sapiens]	1							
2.15	1.514	gi 333033787	nascent polypeptide-associated complex subunit alpha isoform a [Homo sapiens]	1	1.09531	0.98972	1.223688	0.95587	1.039843	0.96309

			39S ribosomal							
2.15	17.17	gi 27436901	protein L12, mitochondrial [Homo sapiens]	2	1.43183	1.09845	1.298743	1.5196	0.923348	0.5195
2.15	3.024	gi 5730023	ruvB-like 2 [Homo sapiens]	1						
2.15	3.024	gi 5730023	ruvB-like 2 [Homo sapiens]	1						
5.155		gi 4505119	methyl-CpG-binding domain protein 3 [Homo sapiens]	1						
2.14	16.38	gi 7524346	adenylate kinase 2, mitochondrial isoform b [Homo sapiens]	4	1.3076	1.68282	1.177596	1.40287	1.297324	1.02061
2.12	4.242	gi 30089972	peroxisomal acyl- coenzyme A oxidase 1 isoform a [Homo sapiens]	3	0.68112	0.64966	1.304939	0.76658	0.415005	1.11262
2.12	0.7937	gi 62241042	bifunctional glutamate/proline-- tRNA ligase [Homo sapiens]	1						
3.109		gi 37594471	3-hydroxyisobutyryl- CoA hydrolase, mitochondrial isoform 1 precursor [Homo sapiens]	1	1.03883	1.04724	0.897887	0.7685	0.744229	0.95015
0.8649		gi 7662180	centrosomal protein of 104 kDa [Homo sapiens]	1	0.93559	0.78752	0.838642	0.90171	0.888156	0.80893
2.12	8.264	gi 4826964	UV excision repair protein RAD23 homolog A isoform 1 [Homo sapiens]	1						

			glutamate-rich WD							
2.12	3.587	gi 237820620	repeat-containing protein 1 [Homo sapiens]	1						
2.11	5.419	gi 5453629	dynactin subunit 2 isoform 1 [Homo sapiens]	2	1.03997	0.76595	1.000128	0.98143	0.874996	1.13523
2.11	6.579	gi 7706497	UMP-CMP kinase isoform a [Homo sapiens]	2	0.84369	0.62042	1.25376	1.12914	1.027527	0.9796
2.11	12.78	gi 5901926	cleavage and polyadenylation specificity factor subunit 5 [Homo sapiens]	1	1.40339	1.13078	2.007566	1.89092	1.45933	1.30963
2.1	2.178	gi 4506103	interferon-induced, double-stranded RNA-activated protein kinase isoform a [Homo sapiens]	1						
2.1	16.81	gi 5902102	small nuclear ribonucleoprotein Sm D1 [Homo sapiens]	1	1.06963	1.11104	1.238307	1.14907	0.987501	1.01882
2.09	10.23	gi 153791352	POTE ankyrin domain family member F [Homo sapiens]	45						
2.09	1.441	gi 27477136	zinc finger CCCH-type antiviral protein 1 isoform 1 [Homo sapiens]	1						
2.09	5.329	gi 45827712	protein quaking isoform HQK-7B [Homo sapiens]	2						

2.08	7.322	gi 5031631	lysosome membrane protein 2 isoform 1	2						
			precursor [Homo sapiens] tricarboxylate transport protein,							
	7.717	gi 21389315	mitochondrial isoform a precursor [Homo sapiens] nucleobindin-2	1						
	2.143	gi 4826870	precursor [Homo sapiens]	1						
2.08	6.186	gi 223555917	protein LYRIC [Homo sapiens]	1						
2.08	4.658	gi 14719402	ribosome biogenesis regulatory protein	1	1.01198	0.95753	0.794942	1.12435	1.176603	0.75437
			homolog [Homo sapiens]							
2.08	3.464	gi 255958289	perilipin-3 isoform 2 [Homo sapiens]	1						
2.08	10.11	gi 4506203	proteasome subunit beta type-7	2						
			proprotein [Homo sapiens] heterogeneous							
15.66		gi 4826760	nuclear ribonucleoprotein F [Homo sapiens]	10						
2.07	63.64	gi 10863895	thymosin beta-10 [Homo sapiens]	4	0.95092	1.06945	1.129401	0.97323	1.04227	1.02178
2.07	1.448	gi 133925811	transportin-1 isoform 1 [Homo sapiens]	1						
			nucleobindin-1							
2.82		gi 20070228	precursor [Homo sapiens]	1						

2.07	3.761	gi 42542379	serine/arginine repetitive matrix	2						
			protein 1 [Homo sapiens]							
			transcription factor							
10.68		gi 83641885	BTF3 isoform A	2	0.84445	0.94586	0.965018	1.10656	0.886324	1.11327
			[Homo sapiens]							
			exosome complex							
5.515		gi 17402904	component MTR3	1	0.73338	0.7553	0.937293	1.04302	0.94509	1.08138
			[Homo sapiens]							
2.06	3.664	gi 117938759	protein ALEX XLas	2	0.79719	1.3224	0.93709	1.06557	1.270463	1.04841
			[Homo sapiens]							
			treacle protein							
0.7087		gi 57164975	isoform b [Homo sapiens]	1	0.78893	0.91721	0.515189	0.61893	0.519783	0.68702
			membrane-associated progesterone receptor							
2.06	10.12	gi 291621647	component 2 [Homo sapiens]	2	1.41716	1.55355	1.276417	1.66223	1.337127	1.38874
			NADH-cytochrome b5 reductase 3							
2.06	3.593	gi 284448551	isoform 3 [Homo sapiens]	1	0.67991	0.59962	1.002967	0.87319	0.970829	0.83486
			phenylalanine--tRNA							
2.06	2.756	gi 4758340	ligase alpha subunit	1						
			[Homo sapiens]							
			6-							
2.06	1.923	gi 48762920	phosphofructokinase, liver type [Homo sapiens]	1						
			V-type proton							
2.06	2.917	gi 19913424	ATPase catalytic subunit A [Homo sapiens]	1						

6.557	gi 13376840	WD repeat-containing protein 61 [Homo sapiens]	1	1.08326	0.77932	0.993702	1.19976	0.904646	0.81726
4.157	gi 109452587	protein FAM98B	1	0.92196	1.00054	1.440914	1.02121	1.427297	0.86005
2.06	20.33	gi 212276121	2						
1.351	gi 217416374	malignant T-cell-amplified sequence 1 isoform 2 [Homo sapiens]	1						
1.351	gi 217416374	coiled-coil domain-containing protein 164 [Homo sapiens]	1						
2.05	2.848	gi 83700233	1						
2.116	gi 123173757	eukaryotic translation initiation factor 3 subunit C [Homo sapiens]	1						
2.116	gi 123173757	ribonucleoprotein PTB-binding 1 [Homo sapiens]	1						
1.729	gi 21361659	importin -9 [Homo sapiens]	1						
7.317	gi 371872778	transmembrane and coiled-coil domain-containing protein 1 isoform b [Homo sapiens]	1	1.24359	1.33452	1.106128	0.63591	1.539528	0.99547
2.05	5.414	gi 13027602	1						
2.146	gi 148596949	DDRGK domain-containing protein 1 precursor [Homo sapiens]	1	0.95672	0.96839	0.740136	1.56721	0.678062	0.57317
8.072	gi 209969700	nucleolar and coiled-coiled-coil domain-containing protein 124 [Homo sapiens]	2						

2.05	3.07	gi 4506753	ruvB-like 1 [Homo sapiens] proteasome subunit	1						
	8.974	gi 4506181	alpha type-2 [Homo sapiens]	2	1.01666	1.14002	0.840779	0.73922	0.93359	0.91044
2.05	6	gi 83921614	cytochrome b5 type B [Homo sapiens] ubiquitin carboxyl-terminal hydrolase 7	1	1.75772	4.65792	2.081941	1.80761	1.731172	1.11116
	1.815	gi 150378533	26S protease regulatory subunit 7	1						
2.04	3.695	gi 4506209	isoform 1 [Homo sapiens] inhibitor of nuclear factor kappa-B kinase-interacting protein	1	0.55722	1.89039	2.196407	2.30166	1.325583	1.15757
	6	gi 42491362	isoform 2 [Homo sapiens] stromal interaction molecule 1 precursor	1	1.33451	0.97453	0.847668	1.18622	1.052938	0.72269
	2.044	gi 21070997	acyl-coenzyme A thioesterase 9, mitochondrial	1						
	3.795	gi 81295407	isoform a precursor [Homo sapiens] histone deacetylase complex subunit	1						
2.04	9.302	gi 215490089	SAP18 [Homo sapiens] secretory carrier-associated membrane protein 3 isoform 2	1						
2.04	4.984	gi 16445421	[Homo sapiens]	1						

2.04	16.13	gi 13775198	SH3 domain-binding glutamic acid-rich- like protein 3 [Homo sapiens]	1	1.17325	1.93406	1.533712	0.74937	2.796483	1.02523
2.04	5.556	gi 4885413	histidine triad nucleotide-binding protein 1 [Homo sapiens]	1	1.08696	1.08068	1.320304	1.09545	0.955904	1.13904
2.03	0.8224	gi 12083581	1- phosphatidylinositol 4,5-bisphosphate phosphodiesterase beta-1 isoform a [Homo sapiens]	1						
2.03	6.912	gi 24308295	grpE protein homolog 1, mitochondrial precursor [Homo sapiens]	2						
2.493		gi 47458820	signal transducer and activator of transcription 3 isoform 3 [Homo sapiens]	1						
2.03	2.513	gi 33457336	interferon regulatory factor 2-binding protein- like [Homo sapiens]	1	0.85583	0.76036	1.050461	0.80003	0.814673	0.70424
1.183		gi 112789528	cohesin subunit SA-2 isoform a [Homo sapiens]	1	0.43056	0.45479	0.738483	0.83165	0.690343	0.78841
2.03	2.108	gi 156416003	succinate dehydrogenase [ubiquinone] flavoprotein subunit, mitochondrial [Homo sapiens]	1	1.91777	2.26216	2.547209	1.10328	2.323811	1.762

2.03	1.116	gi 375298678	tripartite motif-containing protein 46 isoform 3 [Homo sapiens] actin-related protein	1						
7.303	gi 5031597	2/3	complex subunit 3 [Homo sapiens]	1	1.13189	1.17068	1.715736	1.03642	0.949944	1.34422
2.03	4.286	gi 156631005	26S proteasome non-ATPase regulatory subunit 8 [Homo sapiens]	1						
1.783	gi 20127450	type	protein kinase C beta isoform 2 [Homo sapiens]	1						
2.03	4.306	gi 5729991	26S protease regulatory subunit 6B isoform 1 [Homo sapiens]	1						
4.375	gi 46593007		cytochrome b-c1 complex subunit 1, mitochondrial precursor [Homo sapiens]	2						
2.03	5.389	gi 156416000	ubiquitin-fold modifier-conjugating enzyme 1 [Homo sapiens]	1	1.02711	0.9376	1.189223	1.25373	0.952967	1.2758
2.243	gi 164519136		endothelin-converting enzyme 1 isoform 3 [Homo sapiens]	1	0.46947	1.08796	0.734908	0.60167	0.984969	0.70464
2.919	gi 27262628		nuclear autoantigenic sperm protein isoform 2 [Homo sapiens]	1	1.17216	1.29347	1.231107	1.42517	0.964626	1.11173

6.757	gi 8922331	protein mago nashi homolog 2 [Homo sapiens] cAMP-specific 3',5'-cyclic	1	0.96856	0.79949	0.987411	0.42568	0.737719	0.60271
1.11	gi 82799484	phosphodiesterase 4B isoform 3 [Homo sapiens]	1						
6.667	gi 23065552	glutathione S-transferase Mu 3 [Homo sapiens]	1						
2.02	3.957 gi 42476108	neuronal membrane glycoprotein M6-a isoform 1 [Homo sapiens]	1	0.96611	0.86918	0.528097	0.77639	0.964402	0.7135
7.282	gi 4502419	flavin reductase (NADPH) [Homo sapiens]	1	0.82492	0.76531	0.45059	0.59814	0.256164	0.86739
2.02	7.627 gi 4759158	small nuclear ribonucleoprotein Sm D2 isoform 1 [Homo sapiens]	1	0.81977	0.97189	0.852765	1.01776	0.888338	1.01979
2.02	10.87 gi 118402586	lactoylglutathione lyase [Homo sapiens]	1						
12.95	gi 31543397	phosphoglycerate kinase 2 [Homo sapiens]	6						
4.326	gi 40538799	ubiquitin-4 [Homo sapiens]	2	1.18846	1.60339	0.711944	1.67087	1.463316	1.57243
2.414	gi 262359914	excitatory amino acid transporter 1 isoform 2 [Homo sapiens]	2	1.73275	2.19773	1.971571	2.32741	1.602276	1.20143
3.667	gi 5031599	actin-related protein 2/3 complex subunit 2 [Homo sapiens]	1	2.27054	1.63589	2.338493	1.29921	0.955917	0.99613

2.01	4.645	gi 4506387	protein RAD23	2								
			UV excision repair homolog B isoform 1 [Homo sapiens]									
			mitochondrial import inner membrane									
2.193		gi 48526509	translocase subunit TIM50 [Homo sapiens]	1								
2.01	7.339	gi 10801345	eukaryotic translation initiation factor 3	2								
			subunit K [Homo sapiens]									
2.01	5.859	gi 21361565	ATP synthase subunit b, mitochondrial	1								
			precursor [Homo sapiens]									
9.434		gi 4506629	60S ribosomal protein L29 [Homo sapiens]	1	1.17387	1.89628	1.432563	1.65658	1.126862	1.46405		
11.5		gi 5032133	eukaryotic translation initiation factor 1 [Homo sapiens]	1								
2	21.54	gi 4507951	14-3-3 protein eta [Homo sapiens] paraspeckle	10								
2	5.545	gi 109240550	component 1 [Homo sapiens]	3	0.87887	1.04839	0.999175	0.77477	0.444983	0.87935		
2	9.79	gi 5453599	F-actin-capping protein subunit alpha- 2 [Homo sapiens]	2	1.68511	1.74422	1.030252	0.81911	1.008209	0.92859		
2	11.84	gi 8923557	protein C20orf11 [Homo sapiens]	2								

2	6.806	gi 4504001	gap junction alpha-1 protein [Homo sapiens]	2						
2	1.751	gi 16306548	serine--tRNA ligase, cytoplasmic [Homo sapiens]	1						
2	4.595	gi 40806190	TMEM189-UBE2V1 fusion protein [Homo sapiens]	2	1.07323	0.77767	0.860442	0.77759	0.910226	1.2448
2	2.063	gi 32307144	procollagen-lysine,2-oxoglutarate 5-dioxygenase 1 precursor [Homo sapiens]	2						
2	4.665	gi 31377663	armadillo repeat-containing protein 10 isoform a [Homo sapiens]	1						
2	8.78	gi 22538465	proteasome subunit beta type-3 [Homo sapiens]	2						
2	3.169	gi 116256489	septin-9 isoform c [Homo sapiens]	1						
2	3.409	gi 24430151	26S protease regulatory subunit 4 [Homo sapiens]	2						
2	2.318	gi 14589889	cadherin-2 preproprotein [Homo sapiens]	1						
2	8.553	gi 4505893	proteolipid protein 2 [Homo sapiens]	1	1.02496	0.98235	1.004735	1.11342	0.972551	1.01897
2	16.76	gi 13376717	optic atrophy 3 protein isoform b [Homo sapiens]	1						
2	2.195	gi 112789562	gamma-interferon-inducible protein 16 isoform 2 [Homo sapiens]	1	1.037	0.5475	0.795671	0.88866	0.763422	0.71412

2	4.583	gi 149193321	G-rich sequence factor 1 isoform 1 [Homo sapiens]	1						
2	3.788	gi 58761500	obg-like ATPase 1 isoform 1 [Homo sapiens]	2						
2	10.14	gi 7705636	vesicle transport protein GOT1B [Homo sapiens]	1	6.49616	2.27653	4.414598	4.37636	2.95415	3.01594
2	5.234	gi 4506491	replication factor C subunit 4 [Homo sapiens]	1						
2	9.418	gi 5174723	mitochondrial import receptor subunit TOM40 homolog [Homo sapiens]	2						
2	3.65	gi 21264355	SWI/SNF-related matrix-associated actin-dependent regulator of chromatin subfamily E member 1 [Homo sapiens]	1						
2	11.96	gi 4507129	small nuclear ribonucleoprotein E [Homo sapiens]	3	0.9772	0.90978	1.049372	1.20251	1.077493	0.90789
2	7.246	gi 70608174	tumor protein D52 isoform 2 [Homo sapiens]	1						
2	12.82	gi 13491174	MARCKS-related protein [Homo sapiens]	2	1.18191	1.19468	1.390571	1.32367	1.278538	1.18775
2	9.028	gi 260763955	NADH dehydrogenase [ubiquinone] 1 alpha subcomplex subunit 13 [Homo sapiens]	1						

2	4.016	gi 222080062	NADH dehydrogenase [ubiquinone] flavoprotein 2, mitochondrial precursor [Homo sapiens]	1						
2	6.771	gi 93277094	protein FAM210B [Homo sapiens] cleavage and polyadenylation specificity factor subunit 7 isoform 1 [Homo sapiens] peptidyl-prolyl cis-	1	1.49494	1.14174	2.094259	3.25341	2.226591	2.03697
2	4.864	gi 217035102	trans isomerase FKBP2 precursor [Homo sapiens] small nuclear ribonucleoprotein G [Homo sapiens]	1						
2	10.56	gi 206725530	PRA1 family protein 2 [Homo sapiens] translocon-associated protein subunit gamma [Homo sapiens]	1	1.1698	1.31058	1.179651	1.26741	1.467394	1.16345
2	15.79	gi 4507133	mitochondrial import inner membrane translocase subunit Tim13 [Homo sapiens]	1	1.20281	1.13479	1.173929	1.2955	0.868648	0.98349
2	6.18	gi 6005794	PRA1 family protein 3 [Homo sapiens]	1		0.96158	2.671536	0.63546	1.864812	1.05061
2	7.568	gi 6005884	CD70 antigen [Homo sapiens]	1						
2	14.74	gi 11024700		4						
2	10.11	gi 5453704		1	2.88799					
2	7.254	gi 4507605		1						

			sodium-coupled							
2	3.175	gi 5870893	neutral amino acid transporter 3 [Homo sapiens]	1	0.79604	1.03163	0.501218	0.83569	0.968156	0.28512
2	3.686	gi 25470886	DAZ-associated protein 1 isoform b [Homo sapiens]	1						
2	5.24	gi 282165814	transmembrane emp24 domain-containing protein 5 isoform 1 precursor [Homo sapiens]	1						
2	8.553	gi 4758714	microsomal glutathione S-transferase 3 [Homo sapiens]	2	1.07214	0.77882	1.157946	0.94076	1.049032	1.0345
2	15.23	gi 5453678	epididymal secretory protein E1 precursor [Homo sapiens]	1						
2	4.58	gi 18379349	synaptic vesicle membrane protein VAT-1 homolog [Homo sapiens]	2						
2	10.78	gi 46276863	parathymosin [Homo sapiens]	1	0.75017	1.47755	1.608629	1.14413	1.249661	1.06365
2	20.2	gi 14211889	protein dpy-30 homolog [Homo sapiens]	1	1.06193	0.74713	0.785391	1.0061	0.706888	0.70462
2	8.791	gi 7657176	protein canopy homolog 2 isoform 1 precursor [Homo sapiens]	1						
2	14.53	gi 7657609	signal peptidase complex catalytic subunit SEC11A [Homo sapiens]	1						

			peptidyl-prolyl cis-							
2	4.911	gi 4503727	trans isomerase FKBP3 [Homo sapiens]	1	0.6618	0.88653	0.711606	0.64077	0.791742	0.88282
2	5.425	gi 5032069	splicing factor 3B subunit 4 [Homo sapiens]	1						
2	4.032	gi 221316575	lymphocyte function- associated antigen 3 isoform 2 [Homo sapiens]	1	1.10848	0.95693	1.071785	0.83056	0.940833	0.95787
2	8.475	gi 341915584	PREDICTED: prothymosin alpha- like [Homo sapiens]	1	1.05324	1.3211	1.186233	1.03384	1.033843	1.26186
2.64		gi 259155315	mitochondrial 2- oxoglutarate/malate carrier protein isoform 2 [Homo sapiens]	1	1.82798	2.05946	1.756294	1.94721	1.415	1.33975
1.93	11.86	gi 5729850	binding guanine nucleotide- protein G(k) subunit alpha [Homo sapiens]	3	0.56981	0.66885	0.601442	0.40964	0.354968	0.60163
6.077		gi 4502227	ADP- ribosylation factor-like protein 1 [Homo sapiens]	1						
1.85	7.519	gi 4503659	ubiquitin-like protein fubi and ribosomal protein S30 precursor [Homo sapiens]	1	1.93251	0.52726	0.873157	1.16378	0.939255	1.03131
1.83	1.74	gi 52485606	formin-like protein 2 [Homo sapiens]	2						
3.93		gi 4505585	platelet-activating factor acetylhydrolase IB subunit beta isoform a [Homo sapiens]	1						

			CD97 antigen							
1.8	2.545	gi 68508955	isoform 3 preproprotein [Homo sapiens]	1						
1.79	3.438	RRRgi 45021	REVERSED annexin A5 [Homo sapiens] mitochondrial inner membrane organizing	1						
1.77	10.26	gi 73912720	system protein 1 isoform a [Homo sapiens] coiled-coil domain-containing protein 87 [Homo sapiens] heterogeneous nuclear	1	1.21962	0.9844	0.784586	0.64946	1.253601	1.76032
1.76	1.531	gi 157388967	ribonucleoprotein U isoform b [Homo sapiens] glial fibrillary acidic protein isoform 3 [Homo sapiens]	2	0.85902	0.99372	1.045406	0.93941	1.111446	0.61127
1.7	35.73	gi 14141161	transcription elongation factor B polypeptide 2 isoform a [Homo sapiens]	34	1.76342	1.10382	1.33401	1.0886	1.327369	1.53358
1.7	11.64	gi 334688844	glial fibrillary acidic protein isoform 3 [Homo sapiens] replication protein A 14 kDa subunit [Homo sapiens]	7	0.91713	0.81444	1.222358	1.12989	1.145062	1.32143
1.7	5.932	gi 6005890	ATP synthase lipid-binding protein, mitochondrial isoform A precursor [Homo sapiens]	1						
1.7	11.64	gi 334688844	glial fibrillary acidic protein isoform 3 [Homo sapiens] replication protein A 14 kDa subunit [Homo sapiens]	7	0.91713	0.81444	1.222358	1.12989	1.145062	1.32143
1.69	19.01	gi 4506587	ATP synthase lipid-binding protein, mitochondrial isoform A precursor [Homo sapiens]	1						
1.68	4.93	gi 50659074	ATP synthase lipid-binding protein, mitochondrial isoform A precursor [Homo sapiens]	1	0.92016	0.90905	0.935273	1.02621	1.145511	0.92555

		tRNA							
1.66	11.2	gi 7705477 methyltransferase 112 homolog [Homo sapiens] gem-associated	1						
	1.229	gi 122939157 protein 4 [Homo sapiens]	2						
1.62	4.93	gi 4504347 hemoglobin subunit alpha [Homo sapiens]	1	1.59508	0.66166	1.879694	0.99311	1.061659	0.51581
	5.797	gi 6678271 TAR DNA-binding protein 43 [Homo sapiens]	2						
	1.143	gi 116256464 uncharacterized protein C2orf55 [Homo sapiens]	2						
	2.105	gi 28178838 isocitrate dehydrogenase [NAD] subunit gamma,	1						
		mitochondrial isoform b precursor [Homo sapiens]							
	2.256	RRRgi 166235 REVERSED DNA damage-regulated autophagy modulator protein 2 [Homo sapiens]	1						
1.57	0.5336	gi 297207099 AT-rich interactive domain-containing protein 1B isoform 2 [Homo sapiens]	1						
1.55	3.918	gi 311893345 copine-1 isoform c [Homo sapiens]	1						
	0.503	gi 61676188 E3 ubiquitin-protein ligase HUWE1 [Homo sapiens]	1	1.09776	1.27215	0.877703	1.14276	0.851826	0.89419

7.469	gi 4506193	proteasome subunit beta type-1 [Homo sapiens] acetyl-CoA acetyltransferase,	1	1.43887	2.04849	1.395369	1.22527	1.514252	1.1148
3.981	gi 4557237	mitochondrial precursor [Homo sapiens] AP-2 complex	1	1.24819	1.1585	1.084654	0.95572	0.973047	1.16623
3.233	gi 68799814	subunit mu isoform b [Homo sapiens] dolichyl-diphosphooligosacch	1						
1.5	0.8475 gi 30578410	aride--protein glycosyltransferase subunit STT3B [Homo sapiens] pre-rRNA-processing	1						
1.5	0.8706 gi 39780588	protein TSR1 homolog [Homo sapiens]	1	0.90888	1.05537	0.932494	0.94253	1.05303	1.22672
1.5	1.675 gi 333360851	serpin H1 precursor [Homo sapiens] deoxyuridine 5'-triphosphate	1	0.72935	0.7743	0.915738	0.72061	0.754026	0.75084
4.762	gi 70906441	nucleotidohydrolase, mitochondrial	1	2.0039	0.45709	1.823647	0.98667	1.09756	1.21117
1.48	4.02 gi 312596881	isoform 1 precursor [Homo sapiens] 26S protease	1						
1.47	1.849 gi 18426915	regulatory subunit 8 isoform 2 [Homo sapiens] drebrin isoform a [Homo sapiens]	1						

1.47	1.98	gi 4503915	trifunctional purine biosynthetic protein	1	1.39568	1.34603	0.916473	0.99879	1.676535	1.02895
			adenosine-3 isoform 1 [Homo sapiens]							
1.44		gi 296841091	protein kinase C and casein kinase substrate in neurons	1						
			protein 2 isoform A [Homo sapiens]							
1.626		gi 139394599	hypermethylated in cancer 2 protein	1	1.13664	1.05848	0.96557	1.0482	1.011859	0.96627
			[Homo sapiens]							
1.559		gi 8051636	exportin -T [Homo sapiens]	1						
1.241		gi 359279861	dihydropyrimidinase-related protein 5	1						
			[Homo sapiens]							
1.44	3.081	gi 4503519	eukaryotic translation initiation factor 3	1						
			subunit F [Homo sapiens]							
7.634		gi 4757926	RNA-binding protein 39 isoform b [Homo sapiens]	2						
4.233		gi 115430112	receptor expression-enhancing protein 5	1	0.81179	1.07698	1.398986	0.48126	1.126422	1.05482
			[Homo sapiens]							
1.31	59.91	gi 14389309	tubulin alpha-1C chain [Homo sapiens]	53						
1.31	3.704	gi 52426743	luc7-like protein 3	1						
			[Homo sapiens]							

1.3	3.965	gi 8923390	coiled-coil-helix- coiled-coil-helix domain-containing protein 3, mitochondrial precursor [Homo sapiens]	1	0.85987	0.85484	0.750112	1.52743	0.919463	0.55202
-----	-------	------------	--	---	---------	---------	----------	---------	----------	---------